# ASTRONAUTICA ACTA

OFFIZIELLES ORGAN DER INTERNATIONALEN ASTRONAUTISCHEN FÖDERATION

OFFICIAL JOURNAL OF THE INTERNATIONAL ASTRONAUTICAL FEDERATION

ORGANE OFFICIEL DE LA FÉDÉRATION INTERNATIONALE D'ASTRONAUTIQUE

HERAUSGEGEBEN VON / EDITORIAL BOARD / COMITÉ DES RÉDACTEURS

W. v. BRAUN - Huntsville/Ala. • A. EULA - Roma
B. FRAEIJS DE VEUBEKE - Liége • J. M. J. KOOY - Breda
F. I. ORDWAY III - Huntsville/Ala. • E. SÄNGER - Stuttgart • K. SCHÜTTE - München
L. I. SEDOV - Moskva • L. R. SHEPHERD - Chilton • J. STEMMER - Baden/Schweiz

SCHRIFTLEITUNG / EDITOR-IN-CHIEF / RÉDACTEUR EN CHEF

F. HECHT - Wien

Vol.
4
1958

VOL. IV

MIT 102 ABBILDUNGEN / WITH 102 FIGURES / AVEC 102 FIGURES

SPRINGER-VERLAG · WIEN

I. R. MAXWELL & CO. LTD. · LONDON / PARIS / NEW YORK

1958

Vol.
4
1958

## Inhalt — Contents — Sommaire

**Benedikt, E. T.**, siehe **Klemperer, W. B.**

**Boni, A.:** Observation of a Satellite Near its Culmination (With 12 Figures) . 188

**Cavoti, C. R.**, siehe **Miele, A.**

**Fraeijs de Veubeke, B.:** Le problème du maximum de rayon d'action dans un champ de gravitation uniforme . . . . . 1

**Gerathewohl, S. J., O. L. Ritter,** and **H. D. Stallings, Jr.:** Producing the Weightless State in Jet Aircraft (With 6 Figures) . . . . . 15

**Haviland, R. P.:** The Communication Satellite (With 12 Figures) . . . . . 70

**Klemperer, W. B.,** and **E. T. Benedikt:** Selenoid Satellites (With 2 Figures) . 25

**Kooy, J. M. J.:** On Relativistic Rocket Mechanics (With 1 Figure) . . . . 31

— — Erratum . . . . . 234

**Lawden, D. F.:** Optimal Escape from a Circular Orbit (With 2 Figures) . . 218

**Miele, A.:** General Variational Theory of the Flight Paths of Rocket-Powered Aircraft, Missiles and Satellite Carriers (With 6 Figures) . . . . . 264

— and **C. R. Cavoti:** Optimum Thrust Programming along Arbitrarily Inclined Rectilinear Paths (With 6 Figures) . . . . . 167

**Ordway, F. I., III:** Instrumentation of Artificial Satellites (With 21 Figures) . 90

**Perkins, F. M.:** An Analytical Solution for Flight Time of Satellites in Eccentric and Circular Orbits (With 10 Figures) . . . . . 113

**Ritter, O. L.**, siehe **Gerathewohl, S. J.**

**Singer, S. F.:** Interplanetary Ballistic Missiles — A New Astrophysical Research Tool . . . . . 59

**Stallings, H. D., Jr.**, siehe **Gerathewohl, S. J.**

**Strubell, W.:** Über Erwärmung von in die Atmosphäre eintauchenden Raketenkörpern (Mit 3 Abbildungen) . . . . . 182

**Vertregt, M.:** Die Bahnbestimmung aus dem Vektor der Bahngeschwindigkeit (Mit 1 Abbildung) . . . . . 135

**Winterberg, F.:** Besondere Brennstoffverteilungen und Kühlungsprobleme in Reaktoren von Kernraketen (Mit 9 Abbildungen) . . . . . 138

— Kernverbrennungsplasmen und magnetische Kernbrennkammern für Strahltriebwerke (Mit 11 Abbildungen) . . . . . 235

## Buchbesprechungen — Book Reviews — Comptes rendus

Advances in Geophysics (Edited by H. E. LANDSBERG), Volume 3 (Besprochen von F. HECHT) . . . . . 111

DORFNER, K.-R.: Dreidimensionale Überschallprobleme der Gasdynamik (Besprochen von H. STÜMKE) . . . . . 111

History of German Guided Missiles Development (Herausgegeben von TH. BENECKE und A. W. QUICK) (Besprochen von W. PILZ) . . . . . 234

MCVITTIE, G. C.: General Relativity and Cosmology (Besprochen von L. HALPERN) . . . . . 166

SÄNGER, E.: Zur Strahlungsphysik der Photonen-Strahlantriebe und Waffenstrahlen (Besprochen von J. M. J. KOOY) . . . . . 290

THURING, B.: Einführung in die Methoden der Programmierung kaufmännischer und wissenschaftlicher Probleme fur elektronische Rechenanlagen. 1. Teil: Die Logik der Programmierung (Besprochen von K. SCHÜTTE) . . . . . 112

ZWICKY, F.: Morphological Astronomy (Besprochen von K. SCHÜTTE) . . . 289

Vol.
4
1958

# Le problème du maximum de rayon d'action dans un champ de gravitation uniforme

Par

**B. Fraeijs de Veubeke**[1]

(*Reçu le 29 août 1957*)

**Résumé — Zusammenfassung — Abstract**

**Le problème du maximum de rayon d'action dans un champ de gravitation uniforme.** Le problème du maximum de rayon d'action dans un champ de gravitation uniforme est traité, suivant la voie indiquée par CICALA [1], comme un problème de MAYER du calcul des variations.

Cependant l'emploi du temps comme variable indépendante a été écarté au profit d'une représentation paramétrique qui facilite le choix du système différentiel assurant les calculs numériques les plus compacts [2].

Diverses approximations sont envisagées et une attention particulière a été portée à la prolongation balistique de la trajectoire et à son raccordement à la phase propulsive.

L'emploi des critères classiques, dont celui de WEIERSTRASS, permet de décider si la solution stationnaire fournie par les équations d'EULER donne un maximum véritable. Cependant le critère quantitatif de JACOBI n'est guère susceptible que d'une vérification par calcul numérique.

**Das Problem des maximalen Wirkungsbereiches in einem gleichförmigen Schwerefeld.** Es wird das Problem der maximalen Reichweite in einem gleichförmigen Schwerefeld, dem von CICALA [1] angegebenen Weg folgend, als eine Aufgabe der Variationsrechnung nach MAYER behandelt.

Indessen wurde die Verwendung der Zeit als unabhängige Variable zugunsten einer Parameterdarstellung verlassen, welche die Wahl des Differentialsystems erleichtert, das die zweckmäßigsten numerischen Rechnungen gewährleistet.

Verschiedene Annäherungen wurden ins Auge gefaßt; besondere Aufmerksamkeit wurde der ballistischen Verlängerung der Bahn und ihrer Verbindung mit der Antriebsphase gewidmet.

Die Verwendung der klassischen Kriterien, darunter derjenigen von WEIERSTRASS, gestattet die Entscheidung, ob die durch die Gleichungen von EULER gelieferte stationäre Lösung ein wirkliches Maximum gibt. Hingegen ist das quantitative Kriterium nach JACOBI nur für eine Verifizierung durch numerische Integration geeignet.

**The Problem of Maximum Range in a Uniform Gravitational Field.** The problem of maximum range in a uniform gravitational field is treated, after a method indicated by CICALA [1], as a MAYER problem of the calculus of variations.

However, the use of time as independent variable has been discarded in favour of a parametric representation which facilitates the selection of a differential system ensuring the most compact numerical calculations [2].

[1] Laboratoire d'aéronautique, 75, rue du Val-Benoit, Liége, Belgique.

Various approximations are examined and particular attention is given to the ballistic extension of the trajectory and its junction with the propulsive phase.

The use of classical criteria, such as that of WEIERSTRASS, makes it possible to decide if the stationary solution provided by the EULER equations gives a true maximum. However, the quantitative criterion of JACOBI cannot be verified otherwise than by numerical integration.

## 1. Introduction

Nous nous proposons d'analyser la trajectoire assurant un maximum de distance horizontale parcourue aux engins munis de surfaces portantes évoluant dans un champ de gravitation uniforme.

Dans une note remarquable mais très condensée CICALA [1] a exposé l'application de la technique de MAYER au problème général des performances optimales. Cette optimisation portait à la fois sur la distribution de la portance (ou de l'angle d'incidence aérodynamique) et sur la distribution de la force propulsive.

Nous avons montré par ailleurs comment la représentation paramétrique, outre sa souplesse, évite la nécessité d'un traitement séparé pour les problèmes brachistochrones et permet d'inclure rationnellement les impulsions dans les trajectoires décrites avec moteur fusée [2]. Nous avons aussi donné une synthèse de la trajectoire doublement optimale pour le problème du minimum de consommation avec rayon d'action prescrit [3]. Le maximum de rayon d'action sous consommation donnée est un problème équivalent et, quoique le traitement précédent soit restrictif, dans ce sens qu'il néglige par exemple la traînée induite, nous ne croyons pas utile d'y revenir. En effet la formulation générale de ce problème n'est qu'une petite extension de l'analyse présentée dans [2] et il y a peu d'éléments nouveaux à joindre à la discussion des résultats.

Nous nous placerons plutôt dans le cas où le réglage intentionnel de la force propulsive est abandonné. Plus précisément le débit de consommation et par voie de conséquence la masse totale de l'engin seront supposés être des fonctions connues du temps. Les problèmes brachistochrones de ce type, qui ne comporte donc que l'optimisation de la portance, ont fait l'objet d'une note intéressante de CICALA et MIELE [4].

Notre but est ici d'examiner spécialement les possibilités de prolongation balistique après épuisement du combustible et les conditions précises du raccordement de cette phase avec la phase propulsive.

Plusieurs types d'approximation sont examinés non seulement dans l'idée de dégager des propriétés intéressantes de la trajectoire, qui autrement sont masquées par la généralité de la formulation, mais aussi de jeter un pont entre la théorie variationnelle moderne des performances et les théories anciennes quasi-statiques.

## 2. Équations du mouvement

Le rayon d'action est mesuré suivant un axe horizontal $Ox$, l'axe $Oz$ étant opposé à la direction de la pesanteur. Soit $\sigma$ le paramètre à croissance monotone entre des limites fixes $\sigma_1$ et $\sigma_2$. La trajectoire est caractérisée par les fonctions suivantes:

$V(\sigma)$ la vitesse de vol,
$\theta(\sigma)$ l'angle du vecteur vitesse avec l'horizontale,
$z(\sigma)$ l'altitude,
$x(\sigma)$ la distance horizontale parcourue,
$t(\sigma)$ le temps de vol.

Les dérivées par rapport au paramètre seront dénotées par un exposant $^0$; par exemple

$$dt/d\sigma = t^0 \geqslant 0.$$

Les équations intrinsèques du mouvement suivant la tangente et la normale à la trajectoire s'écrivent respectivement

$$[F]_\alpha = MV^0 - (T - D - Mg \sin\theta)\, t^0 = 0 \tag{1}$$

$$[F]_\lambda = MV\theta^0 - (L - Mg\cos\theta)\, t^0 = 0 \tag{2}$$

où $M$ est la masse totale instantanée de l'engin; elle est liée au débit de consommation $m(t)$ par la relation

$$\frac{dM}{dt} = -m(t) \qquad \text{et donc} \qquad M(t) = M_1 - \int_0^t m(t)\, dt. \tag{3}$$

$T$ est la poussée du propulseur, supposée dirigée suivant la tangente à la trajectoire; c'est une fonction déterminée du débit de consommation, de la vitesse et de l'altitude

$$T = T(m(t), V, z). \tag{4}$$

La traînée $D$ est une fonction connue de la forme

$$D = D_0(z, V) + L^2 D_1(z, V), \tag{5}$$

$L$ étant la portance.

L'altitude et la distance horizontale parcourue sont liées à la vitesse et à sa direction par les relations cinématiques

$$[F]_\beta = z^0 - Vt^0 \sin\theta = 0 \tag{6}$$

$$[F]_\xi = x^0 - Vt^0 \cos\theta = 0. \tag{7}$$

La trajectoire peut être modifiée en agissant sur la variable $L$. Dès que celle-ci est connue en fonction du paramètre ou des autres variables la trajectoire est déterminée; on peut donc l'appeler une variable de guidage. Notre problème est de la déterminer de telle façon que la distance horizontale parcourue soit un maximum.

Si $m$ n'était pas une fonction connue du temps on pourrait s'en servir comme d'une deuxième variable de guidage (problème de la double optimisation).

### 3. Les équations d'Euler, traînée induite négligée

L'approximation consistant à négliger l'effet de la traînée induite s'exprime en posant $D_1 = 0$. On observe alors que la portance n'intervient plus que dans la seule équation (2). Celle-ci n'intervient plus dans le problème variationnel de la trajectoire optimale mais nous sert a posteriori pour le calcul de la portance requise dans la description de cette trajectoire. En d'autres termes $L$ devient une variable ignorable; son rôle de variable de guidage est repris par l'angle $\theta$. En effet, l'équation (2) écartée, ce dernier n'intervient plus dans sa dérivée ce qui est une caractéristique essentielle d'une variable de guidage [2].

Formons alors avec des multiplicateurs de LAGRANGE variables $\alpha(\sigma)$, $\beta(\sigma)$ et $\xi(\sigma)$ la fonction

$$F = \alpha[F]_\alpha + \beta[F]_\beta + \xi[F]_\xi. \tag{8}$$

Si la trajectoire respecte les équations du mouvement cette fonction est toujours nulle ainsi que son intégrale

$$I = \int_1^2 F\, d\sigma$$



Vol. 4 1958

et il en sera de même de la variation première de $I$ qui s'écrit

$$\delta I = [\alpha M\,\delta V + \beta\,\delta z + \xi\,\delta x - U\,\delta t]_1^2 + \int_1^2 ([F]_V\,\delta V + [F]_z\,\delta z + [F]_x\,\delta x + [F]_\theta\,\delta\theta + [F]_t\,\delta t)\,d\sigma = 0 \qquad (9)$$

où

$$[F]_V = -[\alpha M]^0 - \alpha t^0 \frac{\partial}{\partial V}(T - D_0) - \beta t^0 \sin\theta - \xi t^0 \cos\theta$$

$$[F]_z = -\alpha t^0 \frac{\partial}{\partial z}(T - D_0) - \beta^0$$

$$[F]_x = -\xi^0$$

$$[F]_\theta = t^0(\alpha Mg\cos\theta - \beta V\cos\theta + \xi V\sin\theta)$$

$$[F]_t = U^0 - \alpha m(V^0 + g t^0 \sin\theta) - \alpha t^0 \frac{dm}{dt}\frac{\partial T}{\partial m}$$

$$U = \alpha(T - D_0 - Mg\sin\theta) + \beta V\sin\theta + \xi V\cos\theta.$$

Les équations d'EULER d'une trajectoire stationnaire sont donc

$$[F]_V = 0, \qquad [F]_z = 0, \qquad [F]_x = 0, \qquad [F]_\theta = 0, \qquad [F]_t = 0.$$

En vertu de la représentation paramétrique on sait [5, 2] qu'elles ne sont pas indépendantes mais liées par l'identité

$$\alpha^0[F]_\alpha + \beta^0[F]_\beta + \xi^0[F]_\xi + V^0[F]_V + z^0[F]_z + x^0[F]_x + \theta^0[F]_\theta + t^0[F]_t \equiv 0. \qquad (10)$$

Ceci permet en général d'écarter comme superflue l'équation la plus difficile à manipuler.

La troisième équation d'EULER s'intègre directement en fournissant une constante (constante isopérimétrique)

$$\xi = X \text{ (constante)}$$

ce qui permet, supposant les équations d'EULER vérifiées, de mettre (9) sous la forme

$$X\,\delta[x(\sigma_2) - x(\sigma_1)] = -[\alpha M\,\delta V + \beta\,\delta z - U\,\delta t]_1^2. \qquad (11)$$

Pour donner au rayon d'action $x(\sigma_2) - x(\sigma_1)$ un caractère stationnaire (maximum) il est donc indispensable d'avoir $X \neq 0$ et d'annuler encore les termes aux limites figurant au second membre de (11). En fait, les relations entre multiplicateurs étant homogènes il est permis de choisir arbitrairement la valeur d'un des multiplicateurs en un point arbitraire de la trajectoire. Il n'y a donc pas de restriction à poser

$$\xi = X = 1. \qquad (12)$$

L'annulation du second membre de (11) doit préciser les conditions aux limites du problème. Nous annulons à priori les variations d'extrémité

$$\delta V(\sigma_1) = 0, \qquad \delta V(\sigma_2) = 0, \qquad \delta z(\sigma_1) = 0, \qquad \delta z(\sigma_2) = 0$$

en imposant l'altitude et la vitesse aux extrémités de la trajectoire

$$V(\sigma_1) = V_1, \qquad V(\sigma_2) = V_2, \qquad z(\sigma_1) = z_1, \qquad z(\sigma_2) = z_2. \qquad (13)$$

Il subsiste alors la condition

$$[U\,\delta t]_1^2 = 0$$

qui, en raison de notre exigence de prolongation balistique, demande un examen particulier.

Nous supposons que la durée de la phase propulsive est connue; elle s'étend depuis $t(\sigma_1) = 0$ jusqu'à $t(\sigma_3) = \Delta t$. A partir de cet instant la réserve de combustible est épuisée et la phase balistique se poursuit avec les conditions

$$m = 0 \qquad M = M_2 = M_1 - \int_0^{\Delta t} m(t)\, dt. \tag{14}$$

Il découle de (14) que pendant la phase balistique l'équation $[F]_t = 0$ est intégrable et donne

$$U = C \text{ (constante)} \qquad \sigma \geqslant \sigma_3.$$

La condition qui reste à vérifier devient alors la suivante

$$C\,\delta[t(\sigma_2) - t(\sigma_3)] + U(\sigma_3)\,\delta t(\sigma_3) - U(\sigma_1)\,\delta t(\sigma_1) = 0$$

et, puisque la durée de la phase propulsive est fixée,

$$\delta t(\sigma_1) = 0, \qquad \delta t(\sigma_3) = 0$$

et la condition se réduit à

$$C\,\delta t(\sigma_2) = 0.$$

Vol. 4 1958

Si la durée totale du vol était prescrite on aurait $\delta t(\sigma_2) = 0$ et on ne pourrait rien conclure quant à la valeur de la constante $C$. Cette inconnue du problème serait précisément à déterminer par la condition isopérimétrique que nous imposons sur la durée. Sans limitation de durée, cas qui sera le seul envisagé par la suite, la variation $\delta t(\sigma_2)$ est libre et exige

$$U = C = 0, \qquad \sigma \geqslant \sigma_3. \tag{15}$$

### 4. Intégration des équations d'Euler, traînée induite négligée

Pendant la phase propulsive nous utilisons (10) et le fait que $t^0 \neq 0$ pour écarter la nécessité de considérer l'équation d'EULER $[F]_t = 0$. L'élimination de $\beta$ entre les autres équations d'EULER donne, eu égard à (12), les deux équations

$$M\,V\,\varepsilon^0 + \varepsilon\,t^0 \frac{\partial}{\partial V}\,[V(T - D_0)] + \frac{M\,t^0}{\cos\theta} = 0 \tag{16}$$

$$M\,[\tan\theta + \varepsilon\,g]^0 + \varepsilon\,t^0 \frac{\partial}{\partial z}\,[V(T - D_0)] = 0 \tag{17}$$

où l'on a posé $\varepsilon = \alpha\,M/V$.

Ces équations jointes à (1) et (6) déterminent la phase propulsive de la trajectoire. La distance horizontale parcourue s'obtient à partir de (7) par une quadrature. Le choix de la variable indépendante est dans une certaine mesure arbitraire. Le temps étant une variable à croissance monotone et la durée de la phase propulsive étant connue, le choix $\sigma = t$ est assez naturel. On peut alors poser

$$t^0 = 1 \qquad V^0 = dV/dt \quad \text{etc.}$$

Le système différentiel (1), (6), (16) et (17) détermine alors ($z$, $V$, $\varepsilon$ et $\theta$) comme fonctions du temps.

Un autre choix possible, mais qui n'est guère pratique que si $m$ est une constante, est

$$\sigma = -\log_e \frac{M}{M_1} \qquad \text{ou} \qquad M = M_1\,e^{-\sigma} \qquad (\sigma_1 = 0)$$

avec alors $t^0 = M/m$.

Pour l'intégration de la phase balistique l'équation (15) sous la forme suivante obtenue en éliminant $\beta$ par $[F]_\theta = 0$ et utilisant (12)

$$\varepsilon(T - D_0)\cos\theta = -M \qquad \sigma \geqslant \sigma_3 \tag{18}$$

remplace avantageusement une des équations (16) ou (17). Ce remplacement se justifie de nouveau en vertu de l'identité (10). Pendant la phase balistique la masse $M$ reste égale à $M_2$ et la poussée $T(0, z, V)$ devient en général négative.

Tandis que dans la partie propulsive une élimination du multiplicateur $\varepsilon$ n'offre aucun intérêt, cette élimination se fait au contraire ici sans difficulté. Le plus simple est d'éliminer $\varepsilon^0$ entre (16) et (17) puis $\varepsilon$ dans l'équation résultante par (18); on trouve finalement

$$\frac{\theta^0}{\cos\theta} + \frac{g\,t^0}{T - D_0}\left[\frac{\partial}{\partial V}(T - D_0) - \frac{V}{g}\frac{\partial}{\partial z}(T - D_0)\right] = 0. \tag{19}$$

Jointe à (1) et (6) elle détermine entièrement la phase balistique. Dans une intégration pas à pas du problème complet il y a deux valeurs initiales $\varepsilon(\sigma_1)$ et $\theta(\sigma_1)$ qui ne sont pas connues à priori. Elles dépendent, comme nous allons le voir, de deux conditions à respecter l'une en début de phase balistique, l'autre en fin de trajectoire. Leur détermination ne pourra donc se faire que par corrections successives.

A la transition entre phases propulsive et balistique les variables $M$, $z$ et $V$ doivent, sous peine de perdre le sens physique de la solution, rester continues. Les conditions de transition de WEIERSTRASS et ERDMANN [5, 2] demandent alors que les multiplicateurs $\alpha$ et $\beta$ (et donc aussi $\varepsilon$) restent aussi continus. Il en découle finalement par $[F]_\theta = 0$ et (12) que $\theta$ ne peut non plus subir de discontinuité. L'équation (18) doit donc se trouver vérifiée en début de phase balistique par les valeurs $m = 0$, $M = M_2$ et les valeurs $\varepsilon(\sigma_3)$, $V(\sigma_3)$, $z(\sigma_3)$ et $\theta(\sigma_3)$ obtenues en terminaison de phase propulsive.

C'est la première des conditions fixant le choix des inconnues $\varepsilon(\sigma_1)$ et $\theta(\sigma_1)$. La seconde est simplement qu'à l'instant où l'altitude prescrite $z_2$ est atteinte en fin de trajectoire, la vitesse atteigne aussi sa valeur demandée $V_2$.

Il n'est pas sans intérêt d'utiliser le résultat (19) pour examiner quelle loi suit la portance idéale en vol balistique alors que la traînée induite a été négligée. Substituant (19) dans (2) il vient en général

$$L = Mg\cos\theta\left[1 - \frac{V}{(T - D_0)}\left(\frac{\partial}{\partial V} - \frac{V}{g}\frac{\partial}{\partial z}\right)(T - D_0)\right].$$

Dans le cas particulier

$$T = 0 \qquad \text{et} \qquad D_0 = R\,\varrho(z)\,V^n$$

cela donne

$$L = -Mg\cos\theta\left[n - 1 + \left(\frac{V}{V_a}\right)^2\right] \qquad \text{où} \qquad V_a = \sqrt{-\varrho\,g\,dz/d\varrho} \tag{20}$$

est une vitesse caractérisant le gradient (négatif) de la densité atmosphérique, que nous avons déjà introduit antérieurement [3] et qui, pour une atmosphère type, est à toute altitude jusque 25 000 mètres légèrement inférieure à la célérité du son. Par conséquent en régime subsonique, où la loi de traînée admise est très approximativement réalisée avec $n = 2$, la portance est négative. Pour peu qu'on se rapproche de la célérité du son elle peut atteindre en valeur absolue deux fois la composante de la pesanteur. A première vue ce résultat est paradoxal; on s'attendrait plutôt à une portance positive tendant à réduire la chute d'énergie potentielle aux dépens de l'énergie cinétique. Ce paradoxe s'éclaire quand l'application des tests de maximum suggère que la solution obtenue n'est

valable que pour une vitesse terminale imposée suffisamment élevée et que le fait d'avoir négligé la traînée induite entraîne l'existence possible de trajectoires plus ou moins arbitraires avec rayon d'action infini, quand la vitesse terminale imposée n'est pas trop grande (voir section 8).

On peut aussi obtenir une expression de la portance en phase propulsive. Eliminant $\varepsilon_0$ entre (16) et (17) et introduisant le résultat dans (2) il vient

$$L = Mg\cos\theta\left[2 + \frac{\varepsilon\cos\theta}{M}\left(\frac{\partial}{\partial V} - \frac{V}{g}\frac{\partial}{\partial z}\right)V(T - D_0)\right].$$

Au passage de la phase propulsive à la phase balistique la portance subit une discontinuité égale à

$$\Delta L = \frac{M_2\, g\cos\theta(\sigma_3)}{T(0, z_3, V_3) - D_0(z_3, V_3)}\,[0(\sigma_3 - 0) - 0(\sigma_3 + 0)]$$

où

$$0(\sigma) = \left(\frac{\partial}{\partial V} - \frac{V}{g}\frac{\partial}{\partial z}\right)(VT).$$

Vol. 4 1958

Si, pour fixer les idées, la poussée $T$ est une constante $T_0$ avant et est nulle après

$$\Delta L = -M_2\, g\cos\theta(\sigma_3)\,\frac{T_0}{D_0(z_3, V_3)} < 0.$$

Il est donc très possible d'avoir une portance positive dans la partie propulsive.

Quand le problème est modifié par suppression de la phase balistique ($\sigma_3 = \sigma_2$), le maximum de rayon d'action ne dépend que de l'intégration de la première partie. Les inconnues initiales $\varepsilon(\sigma_1)$ et $\theta(\sigma_1)$ sont ici déterminées par la condition que lorsque $t = \Delta t$ on ait à la fois $z(\sigma_2) = z_2$ et $V(\sigma_2) = V_2$.

On peut aussi s'abstenir de spécifier $V(\sigma_2)$; la variation de cette quantité étant libre (11) exige alors la condition terminale

$$\alpha(\sigma_2) = 0 \qquad \text{ou} \qquad \varepsilon(\sigma_2) = 0$$

qui remplace celle que l'on a supprimé. La vitesse terminale qui en résulte est alors celle qui assure le plus grand rayon d'action parmi toutes celles qui pourraient être prescrites. On notera que dans ce cas la portance terminale prend la valeur

$$L(\sigma_2) = 2\, M_2 g\cos\theta(\sigma_2).$$

Il est évident que certaines complications peuvent surgir par suite de limitations physiques qu'il est difficile d'introduire à priori dans la formulation analytique. Ainsi quand les coefficients de portance requis dépassent la capacité aérodynamique de la voilure. La trajectoire est alors à modifier par des segments décrits à portance maximum (positive ou négative).

D'autre part une analyse de ce genre dans le stade d'avant-projet est précisément utile pour délimiter l'importance de la voilure.

### 5. Le problème quasi-statique avec traînée induite

Avant d'accumuler toutes les difficultés provenant de l'introduction de la traînée induite il semble utile de rendre compte du domaine de validité de la théorie quasi-statique, ainsi appelée parce qu'elle suppose les termes d'inertie négligeables dans les équations (1) et (2) et les remplace par les équations d'équilibre

$$T - D = Mg\sin\theta \tag{1'}$$

$$L = Mg\cos\theta. \tag{2'}$$

La portance s'élimine facilement du problème en écrivant (5) comme

$$D = D_0(z, V) + D_1(z, V)\, M^2 g^2 \cos^2\theta. \tag{21}$$

Les équations d'EULER deviennent alors les suivantes:

$$[F]_v = t^0\left[-\alpha\frac{\partial}{\partial V}(T-D) - \beta\sin\theta - \cos\theta\right] = 0$$

$$[F]_z = -\alpha\, t^0\frac{\partial}{\partial z}(T-D) - \beta^0 = 0$$

$$[F]_\theta = t^0\left[(\alpha M g - \beta V)\cos\theta + V\sin\theta - 2\alpha D_1 M^2 g^2 \sin\theta\cos\theta\right] = 0$$

$$[F]_t = U^0 - \alpha\, t^0\left[m g\sin\theta + \frac{dm}{dt}\frac{\partial T}{\partial m} + 2\, m\, D_1\, M\, g^2\cos^2\theta\right] = 0$$

avec $U = V(\beta\sin\theta + \cos\theta)$.

L'élimination des multiplicateurs ne donne guère de résultat simple à interpréter sauf pendant la phase balistique. Durant celle-ci on a toujours $U = 0$, c'est à dire le résultat simple

$$\beta = -\cot\theta$$

et par l'équation $[F]_v = 0$ la condition fondamentale

$$\frac{\partial}{\partial V}(T-D) = 0. \tag{22}$$

Celle-ci jointe à (1') et (2') détermine complètement $L$, $\theta$, et $V$ en fonction de l'altitude. Elle s'interprète aussi par le raisonnement classique du vol plané à meilleure finesse, c'est à dire à partir de la relation

$$dx = \cot\theta\, dz = \frac{L}{T-D}\, dz$$

en cherchant à rendre le rapport de la portance à la traînée complète aussi grand que possible. En effet on ne peut plus se servir que de l'énergie potentielle acquise pendant la phase propulsive. Dans la recherche du maximum l'angle $\theta$ doit être considéré comme une fonction de la vitesse à altitude constante. On a donc la condition

$$\frac{\partial\cot\theta}{\partial V} = -\frac{1}{\sin^2\theta}\frac{\partial\theta}{\partial V} = 0$$

mais en différenciant (1') à altitude constante, $D$ étant donné par (21)

$$\frac{\partial}{\partial V}(T-D)\, dV + D_1 M^2 g^2 \sin\theta\cos\theta\, d\theta = M g\cos\theta\, d\theta$$

et comme le coefficient de $d\theta$ ne peut s'annuler ($\sin\theta$ est négatif) la condition (22) est bien celle qui assure $\partial\theta/\partial V = 0$.

L'intégration complète de la trajectoire se présente comme suit. Les grandeurs initiales $M_1$ et $z_1$ étant données, les quatre autres valeurs $V(\sigma_1)$, $\theta(\sigma_1)$ $\alpha(\sigma_1)$ et $\beta(\sigma_1)$ sont liées par trois relations algébriques à savoir (1'), $[F]_v = 0$ et $[F]_\theta = 0$. On ne dispose donc que d'une seule inconnue initiale pour modifier la forme de la trajectoire pendant la phase propulsive. Pendant la phase balistique toutes les grandeurs sont irrémédiablement fixées en fonction de l'altitude et par conséquent la valeur de $\beta$ est connue en début de phase balistique par la relation

$$\beta(\sigma_3) = -\cot\theta(z_3).$$

Or les conditions de WEIERSTRASS et ERDMANN lient la continuité de $z$ à celle de $\beta$. Par conséquent l'unique inconnue initiale est fixée par la condition que $\beta$

prenne la valeur précédente en fin de phase propulsive. Comme il fallait s'y attendre par suite de la disparition des variations d'extrémité sur la vitesse, on ne peut plus imposer les valeurs initiale et terminale de celle-ci; elle sera même généralement discontinue à la transition. Une fois la solution déterminée il est en principe possible de vérifier à posteriori la validité des hypothèses initiales. Pour la phase propulsive cette vérification n'est guère possible que par calcul numérique. Par contre en phase balistique une conclusion théorique est parfois possible.

Ainsi en régime subsonique pas trop élevé, où les effets du nombre de MACH sont encore négligeables, le rapport de la portance à la traînée totale ne dépend pratiquement que de l'angle d'attaque aérodynamique. La descente en vol plané se fait alors au meilleur angle d'attaque;

$$\cot\theta = \left(\frac{L}{T-D}\right)_{\text{op.}} = \text{constante}$$

$$q = \frac{1}{2}\varrho V^2 = \frac{M g\cos\theta}{c_L S} = \text{constante}$$

car, le coefficient de portance $c_L$ reste constant avec l'angle d'attaque. Derivons alors logarithmiquement la dernière relation par rapport à l'altitude

$$\frac{1}{\varrho}\frac{d\varrho}{dz} + \frac{2}{V}\frac{dV}{dz} = -\frac{g}{V_a{}^2} + \frac{2}{V^2}\frac{dV}{dt}\frac{1}{\sin\theta} = 0.$$

Le terme négligé dans (1) prend donc la valeur

$$M\frac{dV}{dt} = M g\sin\theta\,\frac{1}{2}\left(\frac{V}{V_a}\right)^2$$

et n'est réellement petit devant la composante de la pesanteur que si

$$\frac{1}{2}(V/V_a)^2 \ll 1.$$

Rappelons que la vitesse $V_a$ définie par (20) est presque assimilable à la célérité du son. La condition trouvée s'accorde donc exactement avec celle qui postule l'absence d'effets du nombre de MACH. En conclusion générale on peut affirmer que le terme d'inertie tangentielle ne peut être négligé que pour les engins lents. De plus la descente planée sans effets du nombre de MACH se fait réellement sans force centrifuge.

De toute façon les discontinuités dans la vitesse et l'angle de montée à la transition sont en violation flagrante avec les approximations consenties et demandent une solution de raccord qui n'est pas prévue par le calcul des variations.

Avant de quitter cette section il nous parait utile d'examiner un cas très particulier sur lequel est basé l'ancienne formule du rayon d'action proposée par BRÉGUET. Il s'agit des systèmes propulsifs pour lesquels on peut admettre que dans le domaine des vitesses de vol réalisées sur la trajectoire

$$\frac{T V}{m g} = K \qquad \text{une constante.} \tag{23}$$

La puissance utile développée par unité de débit de combustible est indépendante de la vitesse et de l'altitude. (Cette constance de rendement n'est plus réalisée dans les propulseurs modernes et notamment dans le moteur-fusée où $T$ est indépendant de la vitesse.) L'élimination du temps par (3) permet d'écrire

$$dx + \frac{L}{D}dz = -\frac{V\,dM}{m}\left[\cos\theta + \frac{L}{D}\sin\theta\right]$$

Vol. 4 1958

puis l'élimination du cosinus par (2') et du sinus par (1')

$$dx = -\frac{L}{D}\,dz - \frac{T\,V}{m\,g}\,\frac{L}{D}\,\frac{dM}{M}.$$

Enfin la constance du second membre de (23) permet de mettre cette relation sous la forme

$$dx = -\frac{L}{D}\,d\left(z + K\log_e\frac{M}{M_1}\right). \tag{24}$$

S'il faut tenir compte des effets de compressibilité la simplicité du résultat (24) n'est qu'apparente et il vaut mieux intégrer le problème à partir du système d'équations d'EULER précédemment décrit; mais si le rapport $L/D$ ne dépend que de l'angle d'attaque il est évident que le plus grand rayon d'action s'obtient en volant à la meilleure finesse. Sans détailler la trajectoire la distance horizontale parcourue est immédiatement calculable

$$\Delta x = -\left(\frac{L}{D}\right)_{\text{op}}\left(\Delta z + K\log_e\frac{M}{M_1}\right).$$

En fin de phase propulsive l'altitude atteinte est bien déterminée. Si l'on admet encore que dans la phase balistique $T = 0$ et donc $K = 0$ on obtient finalement pour le rayon d'action

$$x(\sigma_2) - x(\sigma_1) = +\left(\frac{L}{D}\right)_{\text{op}}\left[K\log_e\frac{M_1}{M_2} - (z_2 - z_1)\right]. \tag{25}$$

Cette formule, qui généralise un peu celle de BRÉGUET, ne suppose donc nullement que le vol soit horizontal. Elle reste même vraie si le réglage intentionnel du débit (utilisation de la deuxième variable de guidage) ne modifie pas la propriété (23). On peut alors varier l'angle de montée en réglant la puissance de la propulsion et, pour autant qu'on revienne à la même altitude finale, ceci ne change en rien le rayon d'action.

### 6. Le problème avec traînée induite, force centrifuge négligée

Si on tient compte de l'accélération tangentielle mais que l'on continue à négliger l'accélération centripète il suffit de suivre l'analyse initiale en prenant (21) comme expression de la traînée. On trouve ainsi que les équations (16), (17) et (18) sont à remplacer par

$$M\,V\,\varepsilon^0 + \varepsilon\,t^0\left[\frac{\partial}{\partial V}\,V(T - D) - 2\,D_1\,M^2\,g^2\sin^2\theta\right] + \frac{M\,t_0}{\cos\theta} = 0 \tag{16''}$$

$$M\,[\tan\theta + \varepsilon\,g\,(1 - 2\,M_1\,g\sin\theta)]^0 + \varepsilon\,t^0\,\frac{\partial}{\partial z}\,V(T - D) = 0 \tag{17''}$$

$$\varepsilon\,[T - D - 2\,D_1\,M^2\,g^2\sin^2\theta]\cos\theta = -\,M. \tag{18''}$$

L'équation correspondant à (19) est trop compliquée pour être pratiquement utilisable, mais la transformation du dernier terme de (16'') par (18'') fournit toujours la relation simple

$$M\,\varepsilon^0 + \varepsilon\,t^0\,\frac{\partial}{\partial V}\,(T - D) = 0$$

qui, conjuguée à (18''), permet un calcul numérique plus facile de la partie balistique de la trajectoire.

Comme $\partial D_1/\partial V$ est négatif, la croissance de $\varepsilon$ est moins rapide que sans traînée induite et la décroissance de $\theta$ avec le temps est aussi diminuée. Ceci

tend à justifier l'approximation faite en négligeant la force centrifuge, quoique seul un calcul numérique permettrait une vérification quantitative.

Rien n'est à modifier dans la structure des valeurs initiales et des conditions qui les déterminent.

Pour les propulseurs vérifiant l'hypothèse (23) l'équation (24) se transforme en

$$dx = -\frac{L}{D}\, d\left[z + \frac{V^2}{2g} + K \log_e \frac{M}{M_1}\right] \tag{24'}$$

et la formule de BRÉGUET, sous la forme modifiée que lui a donné RUTOWSKI [6] en découle

$$x(\sigma_2) - x(\sigma_1) = \left(\frac{L}{D}\right)_{\text{op}} \left[K \log_e \frac{M_1}{M_2} + z_1 + \frac{V_1^2}{2g} - z_2 - \frac{V_2^2}{2g}\right]. \tag{25'}$$

### 7. Le problème exact avec traînée induite

Pour traiter le problème exact la fonction $F$ est complétée par l'addition du terme $\lambda[F]_\lambda$. La nouvelle équation d'EULER

$$[F]_L = t^0 (2\,\alpha\, L\, D_1 - \lambda) = 0 \tag{26}$$

permet l'élimination du nouveau multiplicateur $\lambda$, le multiplicateur $\xi$ restant assimilé à l'unité.

La phase propulsive s'obtient en intégrant les équations différentielles (1), (2) et (6) avec l'expression (5) de la traînée et les équations d'EULER suivantes, obtenues après élimination de $\lambda$

$$-[\alpha M]^0 - \alpha t^0 \frac{\partial}{\partial V}(T - D) - \beta t^0 \sin\theta - t^0 \cos\theta + 2\,\alpha\, L\, D_1 M\, \theta^0 = 0$$

$$\beta^0 + \alpha t^0 \frac{\partial}{\partial z}(T - D) = 0 \tag{27}$$

$$(\alpha M g - \beta V)\, t^0 \cos\theta + V t^0 \sin\theta - [2\,\alpha\, L\, D_1 M V]^0 - 2\,\alpha\, L\, D_1 t^0 M g \sin\theta = 0.$$

L'équation $[F]_t = 0$ est écartée comme identiquement satisfaite par (10). L'apparition des nouveaux termes aux limites $[\lambda\, M\, V\, \delta\theta]_1^2$ indique qu'on peut soit imposer l'angle de montée initial $\theta(\sigma_1)$, soit laisser la variation $\delta\theta(\sigma_1)$ libre et dans ce cas on fait en principe choix de l'angle initial assurant le plus grand rayon d'action en prenant $\lambda(\sigma_1) = 0$. Eu égard à (26) ceci pose l'alternative $\alpha(\sigma_1) = 0$ ou $L(\sigma_1) = 0$. Cependant l'examen des équations d'EULER montre que la première alternative lie les valeurs initiales de $\theta$ et $\beta$ si bien que l'ordre du système différentiel ne serait plus en correspondance avec le nombre de conditions aux limites imposables. De plus la variation $\delta V(\sigma_1)$ deviendrait libre alors que nous imposons la vitesse initiale. Il faut donc prendre $L(\sigma_1) = 0$. La même situation se présente en fin de trajection où on peut soit imposer l'angle d'arrivée soit choisir le meilleur en faisant $L(\sigma_2) = 0$.

Le système de valeurs initiales nécessaires à l'intégration numérique pas à pas comporte donc trois valeurs prescrites $V_1$, $z_1$, et $\theta_1$ [ou $L(\sigma_1) = 0$] et trois inconnues (au lieu de deux précédemment) $\alpha(\sigma_1)$, $\beta(\sigma_1)$ et $L(\sigma_1)$ [ou $\theta(\sigma_1)$].

Pendant la phase balistique l'équation $[F]_t = 0$ est de nouveau intégrable sous la forme $U = 0$ qui est ici explicitement

$$\alpha(T - D - M g \sin\theta) + \beta V \sin\theta + V \cos\theta + 2\,\alpha\, L\, D_1 (L - M g \cos\theta) = 0 \tag{28}$$

et remplace avantageusement l'une des équations (27).

Vol. 4 1958

En fait tout le système (27) est réductible au suivant, plus simple

$$\left.\begin{aligned} M\,\beta^0 + \varepsilon\, t^0 \frac{\partial}{\partial z}(T-D) &= 0 \\ M\,\varepsilon^0 + \varepsilon\, t^0 \frac{\partial}{\partial V}(T-D) - 4\,M\,L\,D_1\,\varepsilon\,\theta^0 &= 0 \end{aligned}\right\} \tag{29}$$

où, comme auparavant, $\varepsilon = \alpha\, M/V$.

L'équation (28) doit être vérifiée en début de phase balistique par les valeurs trouvées pour les variables et multiplicateurs en fin de phase propulsive. C'est la première des conditions déterminant les inconnues initiales. Les deux autres demandent que la vitesse atteigne sa valeur prescrite et que $\theta$ atteigne une valeur prescrite (ou que $L$ s'annule) quand l'altitude finale est obtenue.

Observons enfin que (28) est une équation algébrique du second degré en $L$, qu'il est en fait logique d'utiliser comme telle pour le calcul de la portance au cours de l'intégration numérique par intervalles. Si on fait choix de la condition finale $L(\sigma_2) = 0$ la valeur de la racine appropriée de (28) montre que durant la phase balistique

$$L < M\,g\cos\theta$$

et que par conséquent la trajectoire tournera encore sa concavité vers le bas.

### 8. Les conditions pour un maximum véritable

Utilisant d'emblée $\xi = 1$, mettons l'expression du rayon d'action sous la forme de la fonctionnelle

$$x(\sigma_2) - x(\sigma_1) = \int_1^2 G(y, y^0)\, d\sigma$$

où

$$G(y, y^0) = V\cos\theta\, t^0 - \alpha[F]_\alpha - \beta[F]_\beta - \lambda[F]_\lambda$$

qui donne les mêmes équations d'EULER.

Le test de la variation forte de WEIERSTRASS [5] demande que pour un maximum

$$E = G(\overline{y}, \overline{y}^0) - G(y, y^0) - \sum (\overline{y}^0 - y^0)\frac{\partial}{\partial y^0} G(y, y^0) \leqslant 0.$$

Dans cette expression $y^0$ désigne successivement les dérivées $V^0$, $z^0$, $\theta^0$ et $t^0$ intervenant dans l'expression de $G$; les valeurs surlignées sont celles provenant d'une discontinuité *finie et arbitraire* dans la valeur de la variable de guidage mais qui restent compatibles avec les équations de liaison (1), (2) et (6).

Nous devons distinguer les cas suivants

1°) Le problème exact avec traînée induite.

Dans ce cas le changement fini de la valeur $L$ à la valeur $\overline{L}$, laisse $V$, $\theta$, $z$ et $t$ continus

$$\overline{V} = V \qquad \overline{\theta} = \theta \qquad \overline{z} = z \qquad \overline{t} = t$$

mais les dérivées prennent des nouvelles valeurs $\overline{V}^0$, $\overline{z}^0$, $\overline{\theta}^0$ et $\overline{t}^0$, compatibles avec les liaisons.

Le calcul de $E$ fournit le résultat

$$E = \alpha\, D_1\, \overline{t}^0 (L^2 - \overline{L}^2) + \lambda\, \overline{t}^0 (\overline{L} - L).$$

Mais, le long de la trajectoire satisfaisant aux équations d'EULER on a (26)

$$\lambda = 2\alpha L D_1 \text{ et il vient finalement}$$

$$E = -\alpha D_1 \bar{t}^0 (\bar{L} - L)^2. \tag{30}$$

Comme $D_1 > 0$ et $\bar{t}^0 > 0$, le test de WEIERSTRASS est satisfait tant que $\alpha \geqslant 0$.

2°) Le problème avec traînée induite mais force centrifuge négligée.

Ici la disparition de $\theta^0$ des équations entraîne la discontinuité de $\theta$ avec celle de $L$. En fait on peut faire $\lambda \equiv 0$, adopter l'expression (21) de la traînée et considérer $\theta$ comme la variable de guidage dont la discontinuité de la valeur de $\theta$ à $\bar{\theta}$ donne des discontinuités en $V^0$, $z^0$ et $t^0$ liées par (1) et (6). Le calcul de $E$ donne dans ces conditions

$$E = \bar{t}^0 [V(\cos\bar{\theta} - \cos\theta) - (\alpha M g - \beta V)(\sin\bar{\theta} - \sin\theta) - \alpha D_1 M^2 g^2 (\cos^2\bar{\theta} - \cos^2\theta)].$$

Usant de l'équation d'EULER

$$[F]_\theta = t^0 [(\alpha M g - \beta V)\cos\theta + V \sin\theta - 2\alpha D_1 M^2 g^2 \sin\theta \cos\theta] = 0$$

on peut modifier cette expression en

$$E = 2\bar{t}^0 \sin^2 \frac{\bar{\theta} - \theta}{2} \left[ -\frac{V}{\cos\theta} + 2\alpha D_1 M^2 g^2 \cos^2 \frac{\theta + \bar{\theta}}{2} \right]. \tag{31}$$

Vol. 4 1958

Pour une valeur négative de $\alpha$ le critère est vérifié. Pour une valeur positive, l'inégalité

$$\frac{\alpha \cos\theta}{V} \leqslant [2 D_1 M^2 g^2]^{-1}$$

doit être vérifiée.

Nous rapportant à (18'') cette condition demande en phase balistique que la traînée parasite soit supérieure à la traînée induite.

$$D_0 - T \geqslant D_1 M^2 g^2 \cos^2\theta = D_1 L^2.$$

Rappelons que l'égalité correspond à la valeur optima du rapport portance à traînée effective quand celui-ci ne dépend que de l'angle d'attaque; il est donc assez naturel que l'inégalité précédente soit observée quand on tient compte de l'inertie tangentielle.

3°) Le problème avec traînée induite négligée.

Il suffit de faire $D_1 = 0$ dans le résultat (31) pour voir que le critère de WEIERSTRASS est satisfait.

4°) Le problème quasi-statique avec traînée induite.

La disparition de $V^0$ entraîne pour $V$ même une discontinuité liée à celle de $\theta$ de telle façon que (1') reste vérifiée

$$\bar{T} - \bar{D} = M g \sin\bar{\theta}$$

où $\bar{T}$ et $\bar{D}$ sont calculés à partir de $\bar{V}$ et $\bar{\theta}$. On trouve ici

$$E = \bar{t}^0 [\bar{V}\cos\bar{\theta} - V\cos\theta + \beta(\bar{V}\sin\bar{\theta} - V\sin\theta)].$$

En principe les équations $[F]_V = 0$ et $[F]_\theta = 0$ de la section 5 permettent l'élimination de $\beta$ dans cette expression, mais le résultat semble difficile à discuter. En régime balistique on a plus simplement

$$\beta = -\cot\theta$$

et

$$E = \bar{t}^0 \bar{V} \frac{\sin(\theta - \bar{\theta})}{\sin\theta}.$$

Le critère est alors vérifié du fait que l'angle de montée réel de la trajectoire est négatif tout en étant maximum, l'angle surligné ne pouvant alors que lui

être encore inférieur. De l'ensemble de ces résultats il ressort que, moyennant d'éventuels contrôles numériques sur la valeur d'un multiplicateur, le critère de WEIERSTRASS est vérifié de façon forte pour une discontinuité non-nulle de la variable de guidage (exclusion de l'égalité). Il en est alors de même du critère renforcé de LEGENDRE, si bien qu'on est assuré d'un maximum véritable pour une certaine extension de la trajectoire. La limite d'extension est fournie éventuellement par le critère quantitatif de JACOBI, qui ne se prête guère ici à une discussion théorique. La seule remarque que nous voudrions faire à ce propos est d'établir l'existence possible de solutions non-eulériennes quand la traînée induite est négligée. Il suffit pour cela d'observer qu'en vol horizontal on peut évaluer la distance parcourue par

$$dx = \frac{V\,dV}{T - D}.$$

En régime balistique et traînée induite négligée, $T - D$ tend vers zéro avec la vitesse et il suffit qu'il y tende assez rapidement pour que $V = 0$ devienne une singularité non-intégrable. Ainsi si nous posons

$$T - D = - R\,\varrho(z)\,V^n$$

l'intégrale

$$\int_1^2 dx = -\frac{1}{R\,\varrho(z)} \int_1^2 \frac{dV}{V^{n-1}}$$

est divergente pour $V_2 \to 0$, quand $n \geqslant 2$ (bien entendu la solution théorique ignore toute limitation sur le coefficient de portance). Imaginons alors une trajectoire qui soit d'abord purement verticale et que l'on rende horizontale en phase balistique un peu avant d'atteindre l'altitude maximum $z_{\max}$ (où la vitesse s'annulerait). Aussi faible que soit la vitesse résiduelle, la divergence de l'intégrale précédente montre qu'on peut encore obtenir un rayon d'action aussi grand qu'on veut. Le retour à l'altitude prescrite $z_2$ permet de retrouver une vitesse terminale dont la limite supérieure est celle produite par une chute verticale de $z_{\max}$ à $z_2$.

Le problème sans traînée induite est alors sans maximum véritable si la vitesse terminale prescrite est inférieure à cette limite. Par contre, si elle lui est supérieure, il est plausible que le maximum véritable soit celui donné par la solution eulérienne.

Dès qu'on introduit la traînée induite le rayon d'action fourni par n'importe quelle trajectoire est borné et l'intuition physique suggère que le maximum existe et correspond à une trajectoire eulérienne. Le seul cas où l'on puisse imaginer que le critère quantitatif de JACOBI ne soit pas satisfait est celui où il existerait une deuxième solution eulérienne satisfaisant aux mêmes conditions aux limites. Il suffirait alors de choisir celle qui a le plus grand rayon d'action.

## Bibliographie


1. P. CICALA, Le Evoluzioni Ottime di un Aereo. Atti Accad. Sci. Torino **89** (1954–55).
2. B. FRAEIJS DE VEUBEKE, Méthodes Variationnelles et Performances Optimales en Aéronautique. Bull. Soc. Math. Belgique **2**, 136 (1957).
3. B. FRAEIJS DE VEUBEKE, Balistique Externe. Trajectoires optimales. Chap. XII de "La Propulsion par Fusées", Sciences et Lettres, Liége 1957.
4. P. CICALA et A. MIELE, Brachistocronic Manoeuvres of a Variable Mass Aircraft in a Vertical Plane. J. Aeronaut. Sci. **22**, 577 (1955).
5. G. BLISS, Lectures on the Calculus of Variations. Chicago: University of Chicago Press, **1946**.
6. E. S. RUTOWSKI, Energy Approach to the General Aircraft Performance Problem. J. Aeronaut. Sci. **21**, 187 (1954).

Vol.
4
1958

# Producing the Weightless State in Jet Aircraft[1]

By

**S. J. Gerathewohl[2], O. L. Ritter[3], and H. D. Stallings, Jr.[4,5]**

(With 6 Figures)

**Abstract — Zusammenfassung — Résumé**

**Producing the Weightless State in Jet Aircraft.** Simple functions were used for computing the most interesting and important characteristics of the parabolic flights. The results, based upon certain flying characteristics of the T-33, F-94C, and F-104 in subsonic and transsonic flight, are in good agreement with the data obtained for the first two aircraft types during actual zero-gravity maneuvers. Certain flying safety hazards were noticed in the T-33 but remedied through appropriate measures. The F-94C Starfire proved to be superior to the T-33 with regard to safety and duration of the weightless state. If the F-104 would be made available for aeromedical research, weightlessness could be produced for more than one minute.

**Herstellung des gewichtslosen Zustandes in Flugzeugen mit Strahlantrieb.** Für die Berechnung der interessantesten und wichtigsten Charakteristika parabolischer Flüge wurden einfache Funktionen benützt. Die Ergebnisse stützten sich auf bestimmte Flugcharakteristika der Flugzeugtypen T-33, F-94C und F-104 im Unterschall- und Überschallflug. Sie stimmen gut mit den Daten überein, die für die beiden erstgenannten Flugzeugtypen während der tatsächlichen Nullschwere-Manöver erhalten wurden. Gewisse Gefahren für die Flugsicherheit wurden in der T-33-Maschine bemerkt, jedoch durch geeignete Maßnahmen behoben. Die F-94C-Starfire-Maschine erwies sich hinsichtlich Sicherheit und Dauer des gewichtslosen Zustandes als der T-33 überlegen. Falls die F-104 für die aeromedizinische Forschung zur Verfügung stände, könnte Gewichtslosigkeit für eine Zeitdauer von mehr als 1 Minute erzeugt werden.

**Annulation du Champ de la Pesanteur dans les Avions à Réaction.** Des fonctions simples ont été utilisées pour calculer les paramètres les plus importants des trajectoires paraboliques. Les résultats, basés sur certaines caractéristiques de vol des avions T-33, F-94C et F-104 en régime subsonique et transsonique, sont en bon accord avec les données expérimentales obtenues pour les deux premiers types d'avions durant des manoeuvres destinées à annuler le champ de la pesanteur. Certains dangers propres au T-33 ont été évités par l'emploi de remèdes appropriés. Le F-94C Starfire s'est révélé supérieur au T-33 du point de vue sécurité et durée de la période de vol sans pesanteur. Si le F-104 était disponible pour les recherches aéromédicales, l'absence de pesanteur pourrait être réalisée pendant plus d'une minute.

---

[1] Presented at the VIIIth International Astronautical Congress at Barcelona, Spain, October 6—12, 1957.

[2] Principal Investigator.

[3] Department of Radiobiology.

[4] Major USAF, Chief, Flight Operations and Pilot of T-33A and F-94C aircraft.

[5] All authors: School of Aviation Medicine USAF, Randolph Air Force Base, Texas, USA.

In studies of human behavior under conditions of virtual weightlessness, the reduction or elimination of gravity has become an important problem of aeromedical research [1, 2, 3]. The following means were suggested or employed for producing the weightless state: Dropping a capsule from an airplane, the elevator, the "gravitron", the "sub-gravity tower", and the aircraft [4, 5, 8]. From the most practical point of view of those mentioned, only the aircraft seems to be promising for use because of its availability, safety, realism, and the longer periods and various amounts of reduced gravity that can be produced in it.

In order to appreciate the use of modern aircraft for accomplishing the weightless or "agravic" state, some of the mechanical principles of gravity and acceleration are defined below. As expressed in NEWTON's Universal Law of Gravitation, all bodies exert mutual forces of attraction upon one another. In accelerated motion, gravity is the vectorial sum of the forces of gravitation and inertia acting on a body. According to the NEWTONian relation:

$$F = m \cdot a \tag{1}$$

the force of gravity is measured most conveniently in terms of acceleration; with the acceleration due to the terrestrial gravitation 32.17 ft/sec$^2$ as the unit. Normally, with an object being in a state of rest, the forces of inertia are absent and the object finds itself in the "normal state of gravity" of $G = 1$.

If a body is allowed to fall freely, it is subjected to a downward acceleration of 1 $g$. In this case, the forces of inertia compensate the forces of gravity and the body finds itself in the state of "zero-gravity" [6]. If the body is subjected to a downward acceleration smaller than 1 $g$, the forces of inertia are subtracted from the gravitational force. In this case, the body is in a sub-gravity state. In both cases, a second force is superimposed upon the force of gravitation [7].

Within the gravisphere of the earth a body derives its weight from the counterforce that resists its free fall. On the other hand, a body can be defined as weightless if it is allowed to move freely under the influence of gravitation and its inertia only[1]. This is the case when the object is moving along a KEPLERian trajectory. According to the D'ALEMBERT Principle, every body — whether accelerated or not — finds itself in a state of equilibrium under the combined effects of the actual forces exerted on it, i.e., forces of gravity, forces of inertia, and external forces like propulsion, lift, drag, and support. Eq. (1) thus may be written:

$$F - m \cdot a = 0. \tag{2}$$

Now, since $F$ represents the gravitational forces and $m \cdot a$ the "reactive effects", we write:

$$F_g - F_r = 0 \tag{3}$$

where $F_r$ represents the reactive forces, i.e., the inertial effect associated with the acceleration of gravity. In the free fall situation in a vacuum, $F_r$ is a quantity equal in magnitude and opposite in direction of $F_g$, and can be identified as the sole effect of inertia. When an airplane flies along a KEPLERian trajectory, $F_r$ represents the inertial and external forces superimposed on $F_g$. In other words, the aircraft then simulates the motion of a missile cruising in a vacuum. In order to obtain lack of appression in flight through air, the craft must be guided along a parabolic arc, thereby utilizing the inertial forces for counterbalancing $F_g$.

[1] Although the terms "zero-gravity" and "weightlessness" designate the same condition, "zero-gravity" is used here to refer to the physical state, and "weightlessness" to the psychophysiological condition of the individual.

A flight maneuver of this type requires that all accelerations, except the one caused by gravitation which constantly acts downward at a magnitude of 1 $g$, be eliminated completely. This can be accomplished by the pilot by flying the plane through a so-called pushover, holding the needle of his accelerometer precisely between plus and minus 1 $g$ at the zero-mark of the instrument. A push-over is a vertical-planar maneuver in which the angle of climb changes continuously from a plus to a minus value. During the maneuver the air speed decreases uniformly from an initial value $v_0$ to a minimum at the top of the curve, and then increases uniformly back to the initial value shortly before the pull-out. However, the horizontal component of the velocity remains constant during the entire maneuver. It is determined by the minimum speed at which the aircraft is fully controllable and stable during the push-over. Hence, the horizontal component of velocity or "minimum controlling speed" of the airplane is always somewhat higher than the stalling speed. It depends mainly upon the amount and arrangement of control-surface area built into the aircraft.

Throughout the maneuver, the plane moves at considerable air speed. Therefore, a power output of the engines ranging from an appreciable fraction to full power must be maintained to overcome drag although no lift is required. This holds for the downward as well as the upward leg of the maneuver.

Vol. 4 1958

The characteristics of the trajectory described above reveal that it is a parabola with vertical axis. Strictly speaking, the intended trajectory is one described by an unpropelled body in ideally frictionless space subjected to a centrally symmetric gravitational field. Generally, such a trajectory is a conic, one focal point of which always coincides with the center of attraction around which the body revolves. For sufficiently small velocities, such as are achievable by present day aircraft, the conic is a very elongated ellipse with one focal point at the center of the earth. The small section near the apex of the ellipse, emerging from the surface of the earth, can well be represented by a parabola. The condition for good approximation is that the dimensions of the section are small compared to the radius of the earth, or alternately, that the part of earth surface arched over by the section can be considered as flat instead of spherical.

It should be emphasized that the flight path is not necessarily parabolic or elliptic if a state of reduced rather than zero gravity is intended. In this case, the characteristics of the trajectory are determined by additional requirements concerning the direction of the resulting subgravity force with respect to the aircraft. If, for instance, the force is to be directed perpendicularly toward normally positioned seats regardless of the instantaneous orientation of the plane, a rather complicated functional form of the flight profile is obtained which resembles a parabola only superficially [4]. On the other hand, if the subgravity is to be directed vertically toward the surface of the earth irrespective of the orientation of the plane, the resulting trajectory is always parabolic.

For the mathematical analysis of a parabolic flight pattern, an orthogonal coordinate system can be employed having a horizontal $x$-axis and a vertical $y$-axis. The angle of climb is determined by the direction of the aircraft at the beginning of the appressionless state, i.e., at the point 0 in Fig. 1. The interesting and important information to be obtained from an analysis of the flight parabola concerns the duration of the weightless state, and its dependency upon other flight parameters.

In ballistics, the duration of the trajectory is defined as the time required for the projectile to again reach the level of its initial projection. In the flight pattern described in this paper, $T$ is the duration of the weightless state. From Fig. 1 it

can be seen that the vertical location of any point of the parabola can be expressed by:

$$y = v_0 t \sin \varepsilon - \frac{g}{2} t^2; \qquad (4)$$

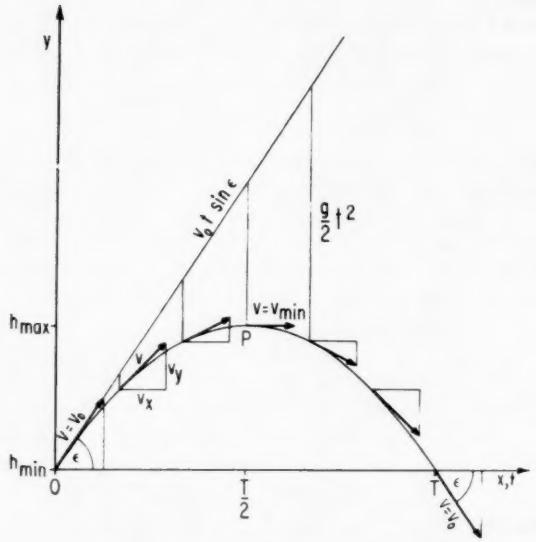


Fig. 1. Schematic of parabolic arc.
In the absence of gravity, a craft starting from point 0 at an angle $\varepsilon$ would follow the straight line $v_0 t \sin \varepsilon$. Gravity causes the craft to fall. The vertical line segments between the straight line and the parabola represent the height of fall at the corresponding points of the trajectory. Also shown are directions and relative magnitudes of the velocity and its horizontal and vertical components. The velocity reaches its minimum at the peak $P$ of the parabola where the vertical component vanishes. The magnitudes of the speed at begin and end of the parabolic arc are equal. The same holds for the angles $\varepsilon$

where $v_0$ = the initial velocity of the aircraft, and $\varepsilon$ = the initial angle of climb. In order to find the duration of the flight, we determine the value $t$ for which $y$ again becomes 0:

$$T = \frac{2}{g} v_0 \sin \varepsilon. \qquad (5)$$

Eq. (5) shows that $T$ depends upon the value of $g$, the velocity $v_0$, and the angle of climb $\varepsilon$, the latter two quantities measured at the point 0. At a given $v_0$ the longest duration is obtained when $\varepsilon = 90^0$, i.e., when the projectile is propelled straight up. However, the airplane cannot rotate about $180^0$ at zero speed on top of a straight line ascent, nor can it maneuver safely below or at its stalling speed. For reasons of good maneuverability we have to stay within the limitations of our flight pattern, i.e., the controlability on the one hand, and the maximum permissible velocity shortly before pull-out, on the other. The controlability speed is always somewhat higher than the stalling speed of the aircraft, and can be determined by flight tests. In a similar manner, the maximum permissible speed is not utilized in parabolic maneuvers but $v_0$ instead, which is the airspeed (IAS) available by the excess thrust for propelling the aircraft upward from the preceding pullout. If an object is hurled upward with a certain initial velocity $v_0$ it will, neglecting air friction, rise to its maximum height in the same time it takes to fall from that height to the ground. The same principle is true for the parabolic maneuver in which case, then, the speed at the end of the trajectory also equals $v_0$. Hence, our problem boils down to finding the optimal value of $\varepsilon$ with respect to the initial velocity $v_0$ and the minimum maneuvering or controlability speed $v_{min}$ of the airplane.

The optimal angle of climb can be found by considering the velocity diagram at point $P$ in Fig. 1. Since the horizontal component of the velocity must be

constant through the entire maneuver, $v_x$ is of the same magnitude as $v_{min}$. Thus we write:

$$v_x = v_{min} = v_0 \cos \varepsilon, \tag{6}$$

$$\cos \varepsilon = \frac{v_{min}}{v_0}. \tag{7}$$

Eq. (7) shows that the optimal angle of climb depends upon the ratio of excess thrust and minimum controlability speed.

Finally, we want to know what relationship exists between the duration of the weightless state and the peak altitude of the maneuver. The maximum height $h_{max}$ is defined as the greatest vertical distance reached by the aircraft as measured from the ground. In Fig. 1 the maximum height is that of the peak $P$ of the parabola:

$$h_{max} = h_{min} + \frac{{v_0}^2}{2g} \sin^2 \varepsilon. \tag{8}$$

Another simple representation results if the peak of the parabola is chosen as origin of the coordinate system. In this system, the altitude at any time is

$$y = h_{max} - \frac{g}{2} t^2, \tag{9}$$

the downward vertical component of the velocity is

$$v_y = g\, t. \tag{10}$$

From the total velocity

$$v = \sqrt{{v_x}^2 + g^2 t^2} \tag{11}$$

the duration of one leg of the parabola is found

$$\frac{T}{2} = \frac{1}{g} \sqrt{{v_0}^2 - {v_x}^2} \tag{12}$$

where

$$v_{0y} = \sqrt{{v_0}^2 - {v_x}^2} \tag{13}$$

is the vertical component of the velocity at the endpoints of the parabola. In terms of maximal and minimal altitudes, this vertical component and the total duration can be represented by

$$v_{0y} = \sqrt{2g\,(h_{max} - h_{min})} \tag{14}$$

$$T = \sqrt{\frac{8}{g}\,(h_{max} - h_{min})}. \tag{15}$$

Finally, the optimal angle of climb is again given by formula (7) of the last section.

The flight path characteristics for producing weightlessness of maximum duration using three different types of airplanes available today in the United States are shown in Table I. The data concerning minimum controlability speed, entry and pull-out speed, and operational altitude, which served for the computation of the optimal angle of climb, peak altitude, and duration of the weightless state, were obtained through parabolic flights involving states of decreased or entirely abolished appression. Table I shows that longer periods of weightlessness can be produced when higher performance aircraft are employed.



Vol. 4 1958

Table I. *Characteristics of optimal flight parabola for three different aircraft*

| Aircraft | Minimum controllability speed | Entry speed $v_0$ | Starting altitude | Maximum height over ground | Angle of climb $\varepsilon$ | Duration of virtual weightlessness |
|---|---|---|---|---|---|---|
| T-33A | 180 knots | 320 knots | 18,000 feet | 20,600 feet | 55° | 28 seconds |
| F-94C | 195 knots | 425 knots | 18,000 feet | 24,400 feet | 63½° | 40 seconds |
| F-104B | 200 knots | 800 knots | 40,000 feet | 66,800 feet | 75½° | 82 seconds |

In Fig. 2, 3, and 4, the total duration $T$ of the maneuver, the height $h_{max} - h_{min}$ of the parabolic arc, and the optimal angle of climb $\varepsilon_{opt}$ are given in the range of maximal speeds between 400 and 2000 knots for three values of the minimal speed.

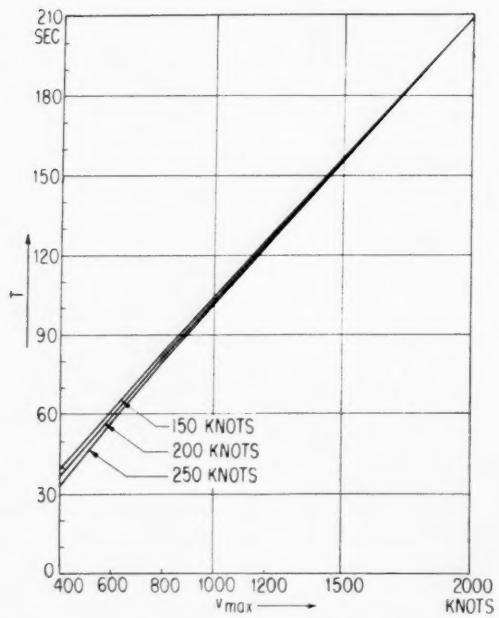


Fig. 2. Duration $T$ of parabolic maneuver in dependence on maximal and minimal speed. The duration is approximately proportional to the maximal speed the craft can achieve. The minimal controllable speed has little influence unless it amounts to an appreciable fraction of the maximal speed

Prominent test and research pilots such as Major (CHUCK) YEAGER, Major ARTHUR MURRAY, SCOTT CROSSFIELD, BILL BRIDGEMAN, Capt. IVEN KINCHELOE, just to mention a few, have on several occasions experienced weightlessness; but very little has been published concerning the practical realization of this state. However, there is a need for the dissemination of information already available, because more and more research organizations become involved in the problem of fact-finding. Now, after we have had the opportunity to try it out ourselves, and after having accomplished more than 200 parabolic flights in the T-33 and F-94 type aircraft encompassing a total of about 2,000 individual parabolas, we feel encouraged to present our practical experiences to the interested organizations and individuals. The presentation will also show how the practical results agree with the figures given in Table I.

Since jet fighters are in great demand by many research units of the U.S. Air Force, preliminary investigation was not begun until 1955 when the School of Aviation Medicine, USAF, had assigned a Lockheed T-33A type jet aircraft

powered by a J-33A-35 engine developing 4,600 lb. thrust. Inasmuch as we had no information to work with it was agreed that the exact flight patterns and working altitudes would have to be determined by a "hit and miss" method. Numerous flights were made using different altitudes, entry airspeeds, angles of attack, and power settings. From the data gathered, the most acceptable flight pattern was selected: Although attempts were made at altitudes that varied from 10,000 to 30,000 feet, the best starting altitude was found to be about 20,000 feet. Therefore, this altitude was considered the optimum working altitude because of usual lack of clouds and turbulance at this height, and because this altitude provided the requirements of safety in the event of emergency. At this altitude the parabola can be flown utilizing the maximum performance of this particular aircraft with the maximum amount of safety; i.e., we could at this level effect corrective action in case of engine trouble that would enable us either to return to the base or eject successfully.

At 20,000 feet, a sharp dive was started at 96 percent engine r.p.m. As the indicated air speed (IAS) built up to 350 knots, an altitude of 17,500 feet was usually reached. Now, a sharp pull-out was begun resulting in a "positive" 3$G$

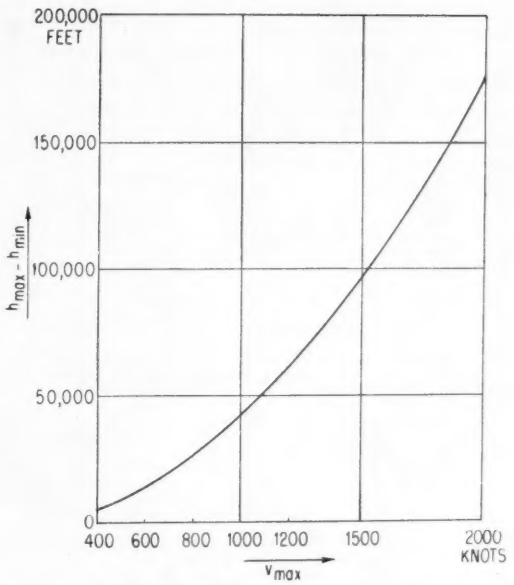


Fig. 3. Height of the parabolic arc vs. maximal speed, for a minimal speed of 200 knots. The height increases approximately with the square of the maximal speed. For minimal speeds of 150 and 250 knots, the curve is shifted up or down, respectively, by approximately 1000 feet

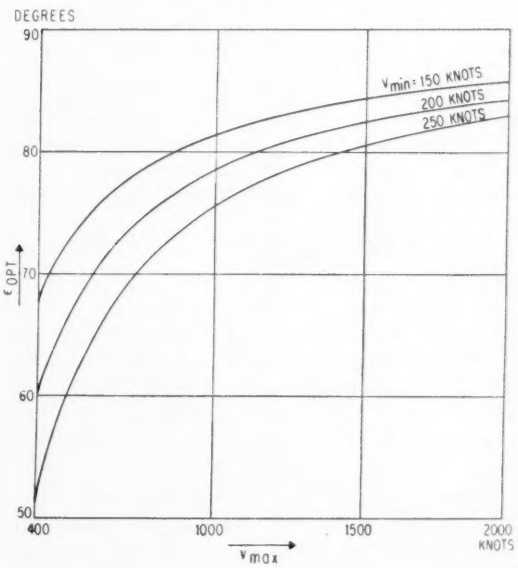


Fig. 4. Optimal value of the initial angle of climb in dependence on maximal and minimal speed. The optimal angle steepens with increasing maximal speed and approaches 90° for very large speeds

condition, and the aircraft was put into an angle of climb of about 60 degrees from the horizontal at full throttle. As the IAS dropped off to 300 knots, forward pressure was applied to the control stick and thus the push-over initiated. At this point of the maneuver, a slight and momentary yawing of the aircraft occurred but was easily controlled by aileron movements. Slight changes in forward pressure were also required to control the attitude of the plane and to maintain the zero-gravity state.

Air speed at the top of the parabola was about 180 knots, and altitude ranged from 20,000 to 20,500 feet. As the apex was reached, forward stick pressure was continued until the plane was diving at an IAS of 350 knots. When the angle of dive was approximately 75 degrees, a pull-out was started early enough to prevent the aircraft from passing its MACH limit and avoiding an excessive radial acceleration during recovery. Usually at this point, the maneuver was repeated again using the pull-out speed for the upswing into the next parabola (see Fig. 5).

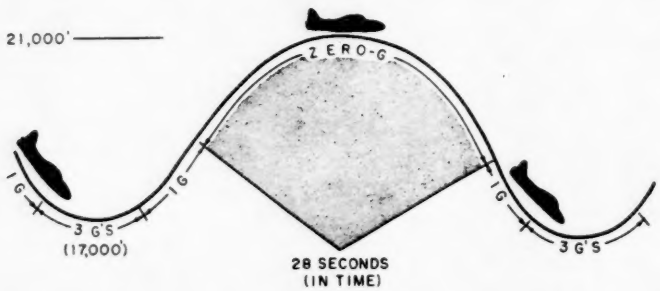


Fig. 5. T-33 "zero-*g*" flight pattern: The maneuver starts at an altitude of about 18,000 feet, reaches almost 21,000 feet at the top of the parabola, and yields about 28 seconds of virtual weightlessness

Theoretically, the IAS is not an important factor for producing the weightless state; in actual flying, however, it is of utmost importance. Yaw and roll movements of the T-33 during parabolas produced undesirable accelerations in all three axes owing to the sensitive aileron boost at low air speeds and rolling motions exaggerated by tip fuel. This was not the case in the F-94C which was used in later experiments.

The standard *g*-meter installed in all U. S. Air Force fighter aircraft was employed as a primary reference. Furthermore, the weightless state was indicated by the release of some small object, usually a cigarette lighter, a glove or in several instances a flashlight in the cockpit. When the object was stationary or floated in space before the subject's eyes, there was little doubt that zero-gravity was present. The parabolic arcs obtained in this fashion varied from 25 to 28 seconds, but the actual state of zero-gravity lasted for a few seconds only; while during the other part, the gravitational force was drastically reduced. For this reason, we call the entire condition the state of virtual weightlessness.

These T-33 flights were not without incident, however. During the sub-gravity state at altitude, fuel in the main tank had a tendency to vaporize, resulting in an overflow from the tank out through the vent drain line. This vaporization prevented the fuel pump from supplying enough fuel to the engine to maintain the required engine r.p.m. Fuel pressure was constantly observed during the run, and as soon as a reduction occurred, the parabola was discontinued and application of "positive" *g*'s usually brought engine operation back to normal.

The few power reductions that occurred during zero-gravity were corrected immediately by reducing throttle and applying "positive" *g*-forces. Complete loss of oil pressure also took place but was of little concern because of the known ability of this engine to run long periods with no lubrication whatsoever. The aircraft's hydraulic system was unaffected.

As the experiments progressed it was felt that extended parabolas were necessary in order that future research concerning man's reaction to zero-gravity could be successfully continued. Since the T-33's capabilities had been exploited to their limits, and since the power loss that had repeatedly occurred during flight was certainly not consistent with safe aircraft operation, a request was forwarded to Headquarters, United States Air Force, for assignment of a two-place jet fighter capable of high thrust and high MACH performance with a pressurized fuel system to be used in the study of weightlessness. In May 1956, an F-94C Starfire was assigned for this purpose.

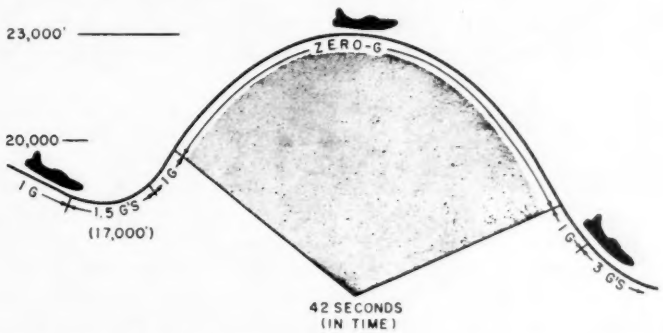


Fig. 6. F-94C "zero-*g*" flight pattern: The maneuver starts at an altitude of about 18,000 feet, reaches about 23,000 feet at the top of the parabola, and yields about 40 seconds of virtual weightlessness

Once again various patterns were attempted using different entry air speeds and altitudes. For the same reasons as given above, the most satisfying altitude was about 20,000 feet. A dive was entered, engine r.p.m. at 100 percent, and as the IAS reached 425 knots a climb of 65 degrees to 70 degrees from the horizontal was executed. With airspeed dropping off, forward stick pressure produced a stable and lengthy parabola yielding almost 40 seconds of practical weightlessness. Since the F-94C has a pressurized fuel system, the treacherous power loss was absent and the 6 degree dihedral present in the Starfire's short but able wings produced a parabola free of rock and roll that had previously presented severe control problems. The F-94C's variable elevator boost made small aft and forward control changes both easy and instantaneous, allowing small corrections to be made without varying the *G*-conditions appreciably. The high MACH rating eliminated the necessity of a too early dive recovery. In short, this ship now performed with both a high degree of efficiency and safety so necessary in our experimental flights (see Fig. 6).

The afterburner of the Starfire was also used to produce the longest period of weightlessness ever recorded, namely, 43 seconds. In this maneuver at 20,000 feet with elevator boost ratio at 11 : 1, engine, r.p.m. was increased to 100 percent and the afterburner actuated. IAS was increased to 430 knots, and the aircraft eased up into a climb of 75 degrees from the horizontal. The afterburner was used until this angle was reached in order to obtain an IAS of

Vol. 4 1958

somewhat over 400 knots. At that time the afterburner was cut off and the parabola begun. Because of the high rate of fuel consumption, the afterburner was not used thereafter unless an extended period of weightlessness was required.

Since we still lack an accurate instrument for indicating and recording sub- and zero-gravity, and the conventional *g*-meter registers accelerations in the vertical only, an auxiliary indicator of *g*-forces in the three axes was introduced. A golf ball, painted black and white for better visual reference, was fastened to the end of a fourteen inch long nylon cord. This contraption was hung in the center top of the windshield inside the pilot's portion of the cockpit. Entry into the zero-state was determined by the conventional device. Then, as weightlessness was achieved, the pilot tapped the ball slightly from below, lifting it just enough to allow it to float. This primitive but revealing device portrayed any acceleration in the three space axes by moving in the opposite direction because of its inertia. Through practice, these movements could be kept at a minimum, and corrections were made by the pilot by simply "flying the ball" so-to-speak. Moreover, a zero-accelerograph has been installed in the F-94C registering the vertically and longitudinally acting accelerations within the range of $\pm$ 0.5 *g* during the weightless phase.

Both parabola patterns, described with the T-33 and the F-94C, had their advantages and their shortcomings. The first one with the sharp dive produces longer states of weightlessness after preceding states of markedly increased acceleration. The second one with the shallow dive before being practically weightless, yields a shorter zero-state, but the preceding acceleration of 1.25 *g* generally remains unnoticed because of the slow rate of change. Hence, the second maneuver seems to be appropriate for determining the effects of weightlessness on the body without preceding increase of weight, which also affects the human organism. The pilot has flown all zero-gravity research flights at the School of Aviation Medicine, USAF, and — assuming an accumulated weightlessness of about 3 minutes during each flight — has been weightless for almost eleven hours with no apparent untoward effects. However, this figure does not mean too much because of the short periods of exposure during each individual parabola.

Vo
4
19

## References

1. F. DIXON and J. L. PATTERSON, JR., Determination of accelerative forces acting on man in flight and in the human centrifuge. U. S. Naval School of Aviation Medicine, Naval Air Station, Pensacola, Fla., July 1953.
2. S. J. GERATHEWOHL, Personal experiences during short periods of weightlessness reported by sixteen subjects. Astronaut. Acta 2, 203 (1956).
3. S. J. GERATHEWOHL, H. STRUGHOLD, and H. D. STALLINGS, JR., Sensomotor performance during weightlessness: Eye-hand coordination. J. Aviat. Med. 27, 7 (1957).
4. F. HABER, Study of subgravity states. School of Aviation Medicine, USAF, Project No. 21—34—003, Report No. 1, April 1952.
5. F. HABER and H. HABER, Possible methods of producing the gravityfree state for medical research. J. Aviat. Med. 21, 395 (1950).
6. H. HABER, Gravity, inertia and weight. In: Physics and Medicine of the Upper Atmosphere. (Edit. by C. S. WHITE and O. O. BENSON, JR.) Albuquerque, N. M.: The University of New Mexico Press, 1952.
7. H. HABER, The physical environment of the flyer. Air University, School of Aviation Medicine, USAF, 1954.
8. T. LOMONACO, M. STROLLO, and L. FABRIS, Behavior of motor coordination in subjects exposed to 3 to 0 *g* acceleration values. Proceedings of the VIIth International Astronautical Congress, Rome, Italy, 17—22 September 1956, p. 825. Roma: Associazione Italiana Razzi, 1956.

Vol.
4
1958

# Selenoid Satellites[1]

By

**W. B. Klemperer** and **E. T. Benedikt**[2]

(With 2 Figures)

(*Received May 14, 1957*)

**Abstract — Zusammenfassung — Résumé**

**Selenoid Satellites.** Discussion of the LAGRANGEian solution of the restricted three-body-problem of constant configuration. The five possible positions are the inferior and superior conjunction, the opposition and two "trojan" positions or sextiles. These positions are computed for a symperiodic Moon companion of the Earth and an Earth companion of the Sun.

**Selenoid-Satelliten.** Es wird die LAGRANGEsche Lösung des vereinfachten Dreikörperproblems konstanter Konfiguration behandelt. Die fünf möglichen Positionen sind die untere und obere Konjunktion, die Opposition und zwei „Trojaner"-Stellungen oder Sextile. Diese Positionen werden für einen symperiodischen Begleiter des Erdmondes und einen zu Sonne und Erde „trojanischen" Erdbegleiter berechnet.

**Satellites sélénoides.** Discussion de la solution lagrangienne du problème simplifié des trois corps dans le cas particulier d'une configuration constante. Les cinq positions possibles sont la conjonction supérieure et inférieure, l'opposition et deux positions "trojanes" ou sextiles. Ces positions sont calculées pour un compagnon lunaire de la terre et un compagnon terrestre du soleil.

With the advent of artificial satellites traveling around the Earth, and in view of the interest evoked by several serious papers on artificial satellites circling the Moon which have been presented before previous International Astronautical Congresses and published in astronautical magazines, the question may well be of interest: Under what conditions should it be possible to establish an artificial "SELENOID" or Moon Companion on such an orbit that it remains in a constant configuration relationship with Earth and Moon? Such a space station would have interesting properties which could become useful in any lunar satellite system telecommunication network, and, conceivably, in a project of checking the Moon and Earth mass ratio.

The kinematics of such Selenoid orbits belong, of course, in the so-called Three-Body-Problem which is notorious for the difficulties with which the treatment of the general case is fraught. However, the present specific problem

---

[1] Presented at the VIIIth International Astronautical Congress at Barcelona, Spain, October 6—12, 1957.

[2] Missiles Engineering Department, Santa Monica Division, Douglas Aircraft Comp., Inc., Santa Monica, Calif., USA.

is a special case, which has been shown by the eminent mathematician, J. L. LAGRANGE, as early as 1772, to be soluble in closed form, in a celebrated treatise [1] which was awarded a prize by the then Royal French Academy of Sciences in Paris.

In that paper — with a great deal of mathematical exercise and without the benefit of a single illustrating figure — he proved that three celestial bodies can travel in constant constellation with respect to each other around their common barycenter if they are situated either on a straight line or at the corners of an equilateral triangle lying in the plane of their mutual revolution. If the Moon were traveling in a circle around the Earth-Moon barycenter, then such a Selenoid would also have to travel in a coplanar circle around it, and the three distances, Earth-Moon-Selenoid, would stay constant. However, with the Moon traveling, as it does, in an elliptical orbit, the Selenoid companion would travel in a coplanar ellipse of the same numerical eccentricity and so that the ratios of the distance between the three bodies remain constant; in other words, so that the configuration formed by them remains similar.

These conclusions were derived by LAGRANGE with great rigor and considerable apparatus of algebra. The solutions have also been derived by LAPLACE, CARATHEODORY, and BRENDEL; the latter's proof is contained in Chapter X of a textbook for students of Celestial Mechanics, by Professor H. HAPPEL, Breslau [2]. What prompted us to take another look at the problem was a desire to present the fundamentals of it in concise form and to discuss its implications for any practical establishment of a Selenoid Satellite.

We contented ourselves with simplifying the general problem by several theoretical assumptions: 1. The satellite is assumed to be a true "planetoid", that is to say, it is so small and light that it does not perceptibly influence or distort the gravity field in which it moves; also the satellite has no propulsion — it travels on a ballistic trajectory. 2. The Sun, though large and massive, is assumed too far away to influence the satellite movement perceptibly as compared to the influence of Earth and Moon. 3. Other astral bodies, such as neighboring planets, even Jupiter, are also considered as of negligible influence. 4. No tidal force nor any other energy-dissipating forces are deemed to be of sufficient influence to warrant taking them into account. 5. Only gravitational and inertial forces are taken into account, none due to electricity, magnetism, radiation, or cosmic dust. 6. We also confined our observations to the hypothetical case of a circular rather than elliptic Moon orbit.

It is at once clear that constant configurations can only exist in a plane coplanar with the Moon's orbit around the Earth. Even a small departure from the lunar revolution plane would evoke a restoring component of the lunar and terrestrial attraction of the Selenoid which would tend to bring it back to the lunar revolution plane. So long as the departure is very small it will merely cause the plane of the new orbit to appear tilted against the lunar orbit. Any large initial departure is likely to lead to an aperiodic motion and eventual loss of constellation.

The conditions of constancy of constellation in the plane of revolution are, obviously, that the forces of gravitational attraction by Moon and Earth must exactly balance the inertial force in an orbit in step with the Moon. For circular orbits traveled at constant velocity, the only inertial force present is the centrifugal force directed away from the barycenter $B$ of the system. The equilibrium condition is therefore most logically expressed in two components, one circumferential, the other radial. The geometry of the general situation is illustrated by Fig. 1, in which the Moon-Earth distance is assigned the value of unity so

that all other distances are expressed in non-dimensional terms of fractions or multiples of it, viz.:

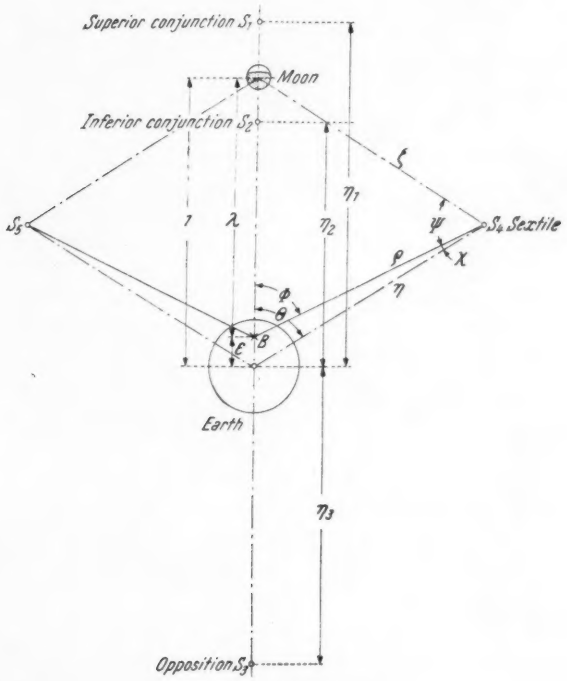


Fig. 1. Geometry

$\varepsilon$ = the relative distance from barycenter to Earth center.
$\lambda$ = the relative distance from barycenter to Moon center.
$\varrho$ = the relative distance from barycenter to Selenoid.
$\eta$ = the relative distance from Earth center to Selenoid.
$\zeta$ = the relative distance from Moon Center to Selenoid
while the angles occurring in the two triangles are:
$\phi$ = the angle encompassed at the barycenter between Moon and Selenoid
$\chi$ = the angle encompassed at Selenoid between Earth center and barycenter.
$\psi$ = the angle encompassed at Selenoid between Moon center and barycenter.
$\theta$ = the angle encompassed at Earth center between Moon and Selenoid.

It will be noted that $\lambda + \varepsilon = 1$ and that the ratio of the two sections, viz., $\varepsilon/\lambda$, is the inverse of the mass ratio of Earth and Moon. (This is readily verified by considering that the centrifugal forces of the two bodies, which are balanced by their mutual attraction, must be equal; these centrifugal forces are proportional to their respective masses and their respective radii of revolution, the angular velocity being common.)

Considering first the circumferential equilibrium of forces (per unit mass) at the Selenoid Satellite, it can be expressed, in non-dimensional terms, by merely equating the sine components of the two NEWTONian attractions, cancelling all constants common to both sides, viz.:

$$\frac{\sin\chi}{\eta^2} = \frac{\varepsilon}{\lambda}\frac{\sin\psi}{\zeta^2}. \qquad (1)$$

Vol. 4 1958

However, as can be gleaned from Fig. 1,

$$\sin\chi = (\varepsilon \sin\phi)/\eta$$

and

$$\sin\psi = (\lambda \sin\phi)/\zeta$$

so that eq. (1) becomes

$$\frac{\varepsilon \sin\phi}{\eta^3} = \frac{\varepsilon \sin\phi}{\zeta^3}$$

which can be fulfilled by $\eta = \zeta$. Hence one locus of points of circumferential equilibrium is the bisecant of the Earth-Moon distance, independently of the Earth-Moon mass ratio. Another such locus is the Earth-Moon axis itself, because for it $\sin\chi = \sin\psi = 0$ in eq. (1). These two straight lines are indicated dot-dashed in Fig. 2.

Now the radial equilibrium of the forces (per unit mass) is expressed by equating the sum of the cosine components of the two attractions to the centrifugal force on the Selenoid, cancelling identical factors which express, on the left side of the equation, the mutual Earth-Moon attraction and, on the right side, the centrifugal force of either body; viz.:

$$\lambda \frac{\cos\chi}{\eta^2} + \varepsilon \frac{\cos\psi}{\zeta^2} = \varrho. \tag{2}$$

As can also readily be gathered from Fig. 1:

$$\cos\chi = (\varrho^2 + \eta^2 - \varepsilon^2)/2\,\varrho\,\eta$$
$$\cos\psi = (\varrho^2 + \zeta^2 - \lambda^2)/2\,\varrho\,\zeta$$

and

$$\varrho^2 = \lambda\,\eta^2 + \varepsilon\,\zeta^2 - \varepsilon\lambda.$$

Inserting these in (2) yields

$$\frac{1 - \eta^2\,(1+\lambda)/\varepsilon - \zeta^2}{\eta^3} + \frac{1 - \zeta^2\,(1+\varepsilon)/\lambda - \eta^2}{\zeta^3} = 2\left(1 - \frac{\eta^2}{\varepsilon} - \frac{\zeta^2}{\lambda}\right) \tag{3 a}$$

or the quintic between $\eta$ and $\zeta$:

$$\frac{2}{\varepsilon}\eta^5\zeta^3 + \frac{2}{\lambda}\eta^3\zeta^5 - 2\,\eta^3\zeta^3 - \eta^5 - \zeta^5 - \frac{1+\varepsilon}{\lambda}\eta^3\zeta^2 - \frac{1+\lambda}{\varepsilon}\eta^2\zeta^3 + \eta^3 + \zeta^3 = 0. \tag{3 b}$$

The locus of all points compatible with this equation is a curve whose main branch departs but little from the lunar orbit path except where it bulges out to loop around the Moon, while another short loop swings inside from the Moon center, as shown on Fig. 2 [1].

The only places where the satellite could be in omnidirectional equilibrium, and hence capable of following the constellation constantly, are those where both eqs. (1) and (2) are fulfilled, i.e. where the curves cross the dot-dashed axes on Fig. 2. These are the five points marked $S_1$, $S_2$, $S_3$, $S_4$, and $S_5$. Their astronomical constellation names, their coordinates as distances from Earth ($\eta$), Moon ($\zeta$) and barycenter ($\varrho$) (all referred to unit Moon-Earth distance), and their bearing angle from the Earth against the Moon are listed in the following table:

[1] If the barycenter were not inside the Earth, then a third branch of the curve would exist; it would very closely follow the Thales circle constructed between the Earth center and the barycenter, as far as it lies outside of the Earth, because at these points the Earth's attraction is normal to the radius vector and the Moon's influence is comparatively weak.

| | | $\eta$ | $\zeta$ | $\varrho$ | $\theta$ |
|---|---|---|---|---|---|
| $S_1$ | Superior Conjunction | 1.1676 | .1676 | 1.1555 | 0 |
| $S_2$ | Inferior Conjunction | .8590 | .1510 | .8369 | 0 |
| $S_3$ | Opposition | .993 | 1.993 | 1.005 | 180° |
| $S_4$ or $S_5$ | Sextile[1] | 1.000 | 1.000 | .994 | $\pm 60°$ |

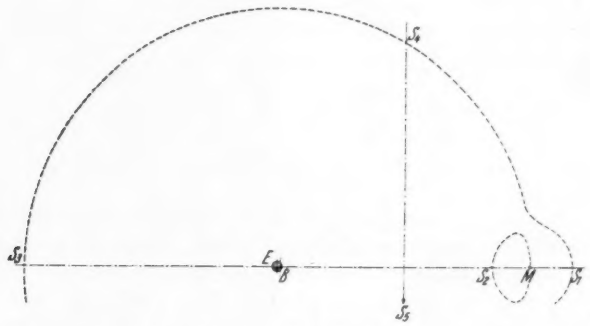

Fig. 2. Loci of peripheral and radial component equilibrium

The common quintic equation for the collinear points reads

$$\overset{+}{\pm}\eta^5\overset{-}{\mp}(2+\varepsilon)\eta^4\overset{+}{\pm}(1+2\varepsilon)\eta^3-(1\overset{\pm}{+}\varepsilon)\eta^2+2(1-\varepsilon)\eta=1-\varepsilon. \qquad (4)$$

This follows from eq. (2) by letting $\overset{+}{\pm}\eta=\overset{\mp}{+}\zeta=1$ and observing that $\varepsilon+\lambda=1$, also $\eta-\varrho=\overset{+}{\pm}1$, and $\cos\chi=1$, $\cos\psi=\overset{\pm}{+}1$. That the sextile point is also a solution is readily verified by trying $\eta=\zeta=1$ in eq. (3 a) or (3 b), with $\cos\theta=1/2$.

In general, all five possible constant constellations are kinematically unstable, except that, as ROUTH has shown, the sextile is stable when $\varepsilon/\lambda<1/25$; small orbits around the libration points are then possible. In the conjunction constellations (the only ones where the Moon is close enough to exert a restoring influence which would be perceptible as a small periodic oscillation superimposed upon the Selenoid orbit motion), the frequency $\omega$ of such oscillation would bear a relationship to the lunar orbit frequency $\Omega$, viz., $\omega/\Omega=\sqrt{\lambda/\eta^3+\varepsilon/\zeta^3}$ for perturbations normal to the orbital plane and slightly different for perturbations tangential to the orbit. The numerical values of those frequency ratios for the mass ratio of the real Moon would be:

| | Normal to Orbital Plane | Tangential to the Orbit |
|---|---|---|
| Superior conjunction | 1.79 | 1.87 |
| Inferior conjunction | 2.27 | 2.33 |

Against radial perturbations the conjunction positions are unstable. In the opposition case, the Moon's influence is so weak that the effect of a perturbation cannot be interpreted as manifesting itself in an oscillation about the old orbit; it simply establishes a new one which is not in permanence of constellation. Any perturbation of the Selenoid in the orbital plane would entail a change in orbital period. Any perturbation out of the plane would cause an ecliptic inclination of the new

[1] Also called Trojan constellation after some planetoids named after Trojan heroes discovered to be in apparently permanent nearly equilateral triangle arrangement with respect to Sun and Jupiter.

Vol. 4 1958

orbit element against the old, which implies a continued oscillation at lunar frequency.

If any real selenoid vehicle were to be placed in space, it would presumably first have to be brought into one of the five libration points and then given a reactive impulse to match its velocity vector to that required to stay in permanence in this constellation. To be sure, the orbit of the Selenoid would have to be not circular but elliptical, geometrically similar to that of the real Moon. This ellipticity is not great so that the behavior would not differ very much from that described under the hypothetical simplifying assumptions. The real path and time table of the artificial Selenoid could readily be computed by reference to the Moon. From a practical viewpoint the constellation of inferior conjunction would probably be the most interesting, inasmuch as the Selenoid should be directly visible in front of the Moon and distinguishable either against the lighted or the dark part of it.

Perhaps it is worth mentioning that in the sextile and, particularly, in the opposition constellations the equilibrium of the Selenoid is much less precarious in peripheral than in radial direction. In fact, anywhere in the arc of the locus of radial equilibrium between these positions the Moon's influence is so weak that an error in bearing would create only a very slow departure from the initial constellation. For instance, in a position of quadrature, i.e., at $90^0$ from the Moon, the peripheral pull component of the Moon would be only of the order of a millionth of a $g$. Hence it may be possible to counteract it for an appreciable period by the thrust of a very weak gas jet after the manner of a Satelloid.

## Appendix

### Symperiodic Earth Companions

Some day it might also become of interest to navigate a space vehicle into a position where it can remain in a fixed constellation with respect to the Earth and Sun. Again there will be — aside from perturbations — five equilibrium positions. Three of these, the sextiles and the opposition, would be two and six months, respectively, ahead or behind the Earth in its annual orbit around the Sun, practically at the same distance from Sun as Earth. The other two are the superior and inferior conjunction which are both located very close to 1% of the Sun's mean distance from the center of the Earth, approximately 1.5 million km, assuming a mass ratio of Earth to Sun of $3.037 \times 10^{-6}$.

This mass ratio is so small that it becomes permissible in eq. (4) to anticipate that $\eta = 1 + \delta$ is very close to 1, so that when the powers of $\eta$ are developed, all terms higher than $\delta^3$ or $\varepsilon\,\delta^2$ can be dropped for a first approximation. Hence eq. (4) reduces to $3\,\delta^3 - \varepsilon\,(1 + \delta)^2 = 0$ and within 2/3% accuracy: $\delta = \sqrt[3]{\varepsilon/3}$.

This approximation gives a good idea of the distances involved, viz., almost 4 times that of the Moon from the Earth. For any practical navigation purposes the ellipticity of the Earth's orbit would have to be taken into account and also the perturbations due to occasional passages of the Moon, and perhaps Venus and Jupiter. The perturbation caused by the Moon's motion is of an amplitude of the order 1/140 of the Earth's attraction; that of Venus in closest constellation comes to about 1/900, that of Jupiter to 1/570.

### References

1. J. L. LAGRANGE, Les Oeuvres de LAGRANGE (The Works of LAGRANGE). J. A. SERRET, Editor. Paris: Gauthier-Villars, 1873.
2. H. HAPPEL, Das Dreikörperproblem. Leipzig: K. F. Koehler, 1941.

Vol.
4
1958

# On Relativistic Rocket Mechanics[1]

By

**J. M. J. Kooy[2]**, NVR

(With 1 Figure)

**Abstract — Zusammenfassung — Résumé**

**On Relativistic Rocket Mechanics.** Most authors, treating rectilinear rocket flight in non gravitational space, consider the rocket plus exhausted masses as *one* mechanical system, and apply the relativistic law of conservation of momentum. In this article, only the rocket plus still included fuel is considered as the mechanical system and the differential equation of rectilinear motion, and also of curvilinear motion in non gravitational space, is directly derived from the basic equation of relativistic mechanics. Further the astronautical aspect of the relativistic time dilatation is discussed. The acceleration of the vehicle with respect to a general metric field is of paramount importance. In order to define this general metric field, the space time structure of the universe as a whole may play a fundamental part.

**Über relativistische Raketenmechanik.** Die meisten Autoren gehen bei der Behandlung der geradlinigen relativistischen Raketenbewegung im schwerefreien Raum von dem relativistischen Impulssatz aus, und betrachten dabei die Rakete und die bereits ausgestoßene Masse als *ein* mechanisches System. In dieser Arbeit wird nur die Rakete und die noch darin befindliche Stoßmasse als das mechanische System betrachtet und die Bewegungsgleichung der geradlinigen und auch der allgemeinen Raketenbewegung im schwerefreien Raum direkt aus der Grundgleichung der relativistischen Mechanik hergeleitet.

Weiter wird der astronautische Aspekt der Zeitdilatation diskutiert. Die fundamentale Bedeutung der Beschleunigung des Fahrzeuges in Beziehung auf ein allgemeines metrisches Feld wird hervorgehoben. Zur näheren Bestimmung dieses allgemeinen metrischen Feldes wird der weltumfassende Raum-Zeit-Zusammenhang herangezogen.

**Sur la Mécanique Relativiste des Fusées.** Pour appliquer la loi relativiste de la conservation de la quantité de mouvement, la plupart des auteurs conçoivent l'ensemble de la fusée et des gaz expulsés comme *le* système mécanique. Dans le présent article le système mécanique ne comporte plus que la masse de la fusée à l'instant considéré et l'équation du mouvement, même non rectiligne, est dérivée directement de l'équation fondamentale de la mécanique relativiste. La dilatation relative du temps est alors discutée du point de vue de l'astronautique. L'accélération du véhicule par rapport à un champ métrique général joue un rôle particulièrement important. La structure spatio-temporelle de l'univers est essentielle dans la définition de ce champ.

---

[1] Presented at the VIIIth International Astronautical Congress at Barcelona, Spain, October 6—12, 1957.

[2] Lector K. M. A., St. Ignatiusstraat 99 a, Breda, Holland.

In classic mechanics we have as fundamental equation:

$$\overline{K} = m \frac{d\overline{v}}{dt}. \tag{1}$$

In (1) $\overline{K}$ is the force by which the particle with mass $m$ is acted upon, whereas $\overline{v}$ denotes the speed of the particle and $t$ the time coordinate. Now it is very essential to observe that the force $\overline{K}$ does not formally follow from (1), but must be *defined* in each physical case. Without such an independent definition of force, it has no sense to speak about the mass $m$, for no method could be indicated in order to measure $m$. In relativistic mechanics we have as fundamental equation:

$$\overline{K} = \frac{d}{dt} \frac{m_0 \overline{v}}{\sqrt{1 - v^2/c^2}} = m_0 \frac{d}{dt} \left( \frac{\overline{v}}{\sqrt{1 - v^2/c^2}} \right), \tag{2}$$

in which $m_0$ is the rest mass of the particle, acted upon by the force $\overline{K}$. Again we can observe that it is very essential that the force $\overline{K}$ does not follow formally from (2), but must again be *defined* in each physical case. For otherwise no method can be indicated to measure $m_0$.

Following this natural line of thought, let us try to derive in direct way the differential equation of rectilinear motion of a rocket in non gravitational space, assuming constant fuel consumption and constant exhaust speed, controlled by the crew. In that case $\overline{K} // \overline{v}$, so that then the corresponding general eq. (2) reduces to:

$$K = m_0 \frac{d}{dt} \left( \frac{v}{\sqrt{1 - v^2/c^2}} \right) = m_0 \frac{\dot{v}}{(\sqrt{1 - v^2/c^2})^3}. \tag{3}$$

In order to apply the general eq. (3) in the case of a rectilinear rocket motion, we can consider the rocket + still included fuel as the mechanical system coming into play. The rest mass of this system then varies with time, so that then in the general eq. (3) $m_0$ represents the *instantaneous rest mass*. The force $K$ by which the system is acted upon must now be defined in this special case, independent on eq. (3). Therefore let us firstly imagine that the rocket is *at rest* on a proofstand, while the rocket motor works (see Fig. 1).

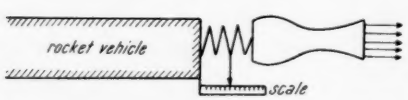

Fig. 1

Let the force by which the rocket vehicle is acted upon be directly measured by the compression of a spring (dynamometer), indicated by a pointer sliding along a scale.

By definition, the force by which the rocket vehicle is acted upon *is* then this pointer reading. Now in this case of the rocket at rest on the proofstand, we may be quite sure of it that the force, as defined in this way, will be equal to the momentum generated per second by expansion of the gases in the nozzle. If $a_0$ be the exhaust speed, $\Delta m_0^*$ the rest mass of the expelled matter per second and $c$ the speed of light, this momentum generated per second becomes:

$$\frac{\Delta m_0^* a_0}{\sqrt{1 - a_0^2/c^2}} = \mu_0 a_0.$$

If the corresponding pointer reading of the dynamometer be $P$, we may then write:

$$P = \mu_0 a_0.$$

Let us now indicate the time coordinate by $t_0$ and assume that at $t_0 = 0$ the rest mass of the rocket vehicle + included fuel be $M_0$. The total quantity of energy expelled per second, *energy of rest mass included*, becomes:

$$\frac{\Delta m_0^* c^2}{\sqrt{1 - a_0^2/c^2}},$$

and the rest mass of this total energy (= rest mass energy + kinetic energy) becomes:

$$\frac{\Delta m_0^*}{\sqrt{1 - a_0^2/c^2}} = \mu_0.$$

Hence the rest mass of the rocket vehicle + still included fuel at any time $t_0$ becomes:

$$M_0 - \mu_0 t_0.$$

Let us now, as next stage in our line of thought, consider our rocket vehicle in rectilinear flight in non gravitational space. Let us thereby assume — for sake of simplicity — that the mass of the rocket motor + content is still very small in comparison to the instantaneous mass of rocket vehicle + still included fuel. We can then again *define* as magnitude of the thrust the *pointer reading* of the dynamometer. (This pointer reading may be conveyed to the terrestrial observer by telemetering.) Then we have to substitute in (3) for $K$ the quantity:

$$\frac{\Delta m_0^* a_0}{\sqrt{1 - a_0^2/c^2}} = \mu_0 a_0,$$

in which now $\Delta m_0^*$ and $a_0$ are the corresponding quantities *as measured by the crew of the rocket vehicle*, that is as to the system of reference at rest as to the rocket vehicle, and with a corresponding clock, at present in the rocket vehicle. The time coordinate, as measured by this astronautical clock, will now be indicated by $t_0$, whereas the terrestrial time will be denoted by $t$. Hence, applying the general eq. (3) we obtain in this way as differential equation of motion:

$$(M_0 - \mu_0 t_0) \frac{dv/dt}{(1 - v^2/c^2)^{3/2}} = \mu_0 a_0. \tag{4}$$

Eq. (4) is quite in accordance with the result of KRAUSE [1], who considered rocket + exhausted fuel as the mechanical system coming into play and applied accordingly the relativistic law of conservation of momentum. Further following KRAUSE, we can multiply (4) by $dt_0 = \sqrt{1 - v^2/c^2}\, dt$, so that then:

$$\frac{dv}{(1 - v^2/c^2)} = \frac{\mu_0 a_0 dt_0}{M_0 - \mu_0 t_0}.$$

If the times $t = 0$ and $t_0 = 0$ coincide, and at $t = 0$, $v = 0$, we obtain by integration [1] the well known formula of ACKERET [2]:

$$\left(\frac{1 + v/c}{1 - v/c}\right)^{c/2a_0} = \frac{M_0}{M_0 - \mu_0 t_0}, \tag{5}$$

by which the mass ratio can be computed required for obtaining a speed $v$. From (5) we find:

$$M_0 - \mu_0 t_0 = M_0 \left(\frac{1 - v/c}{1 + v/c}\right)^{c/2a_0}. \tag{6}$$

Substituting (6) in (4) we obtain:

$$M_0 \left(\frac{1 - v/c}{1 + v/c}\right)^{c/2a_0} \frac{dv/dt}{(1 - v^2/c^2)^{3/2}} = \mu_0 a_0,$$



Vol. 4 1958

whence follows:

$$\frac{M_0}{\mu_0\, a_0}\int_0^v \left(\frac{1-v/c}{1+v/c}\right)^{c/2a_0} \frac{dv}{(1-v^2/c^2)^{3/2}} = t. \tag{7}$$

In (7) the integral can always be evaluated numerically. By (7) we can compute the time required for obtaining the final speed $v$ or any speed $v$ during the powered rectilinear flight.

If in this way $v = v(t)$ is found numerically, the way passed through at time $t$ becomes:

$$s = \int_0^t v(t)\, dt. \tag{8}$$

In case of a photon rocket no matter, but photons are expelled. If $E$ be the energy expelled per second astronautical time, the mass of this energy is equal $E/c^2$, and the momentum $E/c$, so that then: $P = E/c$.

In that case the differential equation of motion for rectilinear flight and constant thrust in non gravitational space becomes:

$$\left(M_0 - \frac{E}{c^2}\, t_0\right) \frac{dv/dt}{(1-v^2/c^2)^{3/2}} = \frac{E}{c}. \tag{9}$$

Hence in this case eq. (5) becomes:

$$\left(\frac{1+v/c}{1-v/c}\right)^{1/2} = \frac{M_0}{M_0 - (E/c^2)\, t_0}, \tag{10}$$

and eq. (7) reduces to:

$$\frac{c\, M_0}{E}\int_0^v \left(\frac{1-v/c}{1+v/c}\right)^{1/2} \frac{dv}{(1-v^2/c^2)^{3/2}} = t. \tag{11}$$

Now the expression under the integral sign can be transformed to:

$$\sqrt{\frac{1-v/c}{(1+v/c)\,(1-v/c)^3\,(1+v/c)^3}}\, dv =$$

$$= \frac{dv}{\sqrt{(1+v/c)^4\,(1-v/c)^2}} = \frac{dv}{(1-v/c)\,(1+v/c)^2}.$$

Hence we may write for (11):

$$\frac{c\, M_0}{E}\int_0^v \frac{dv}{(1-v/c)\,(1+v/c)^2} = t. \tag{12}$$

Now we can split up the integral in (12) in partial fractions, by writing

$$\frac{1}{(1-v/c)\,(1+v/c)^2} = \frac{A}{1-v/c} + \frac{B}{1+v/c} + \frac{C}{(1+v/c)^2}.$$

Hence:

$$1 = A\,(1+v/c)^2 + B\,(1-v/c)\,(1+v/c) + C\,(1-v/c).$$

Or:

$$1 = A\,(1+2\,v/c+v^2/c^2) + B\,(1-v^2/c^2) + C\,(1-v/c).$$

Thus:

$$1 = A + B + C + v/c\,(2\,A - C) + v^2/c^2\,(A - B).$$

This relation must avail for all possible values of $v$, from which follows:

$$\left.\begin{aligned} A + B + C &= 1 \\ 2A - C &= 0 \\ A - B &= 0 \end{aligned}\right\} \quad \text{thus } A = 1/4, \quad B = 1/4, \quad C = 1/2.$$

Hence by (12):

$$\frac{c M_0}{E} \int_0^v \left( \frac{1/4}{1 - v/c} + \frac{1/4}{1 + v/c} + \frac{1/2}{(1 + v/c)^2} \right) dv = t,$$

so that:

$$\frac{c M_0}{E} \left\{ \frac{c}{4} \ln \frac{1 + v/c}{1 - v/c} + \frac{v}{2(1 + v/c)} \right\} = t. \tag{13}$$

By means of (13) we can find for any $v$ the corresponding value for $t$, so that also $v = v(t)$ can be determined numerically. The way passed through at any time $t$ then again follows from (8).

Further by (10) and (13) we can find the rest mass of photon rocket and still included fuel at any terrestrial time $t$ during the powered flight. For by (13) we can find for any speed $v$ the corresponding terrestrial time $t$, and then the corresponding value of $M_0 - (E/c^2)\, t_0$ follows from (10). In case of the rocket expelling matter, we can find in similar way by (6) and (7) the rest mass of rocket vehicle + still included fuel at any time $t$ of the powered flight.

Vol. 4 1958

Now by (5) we can already conclude that the exhaust speed must be at least of the order of magnitude of the speed of light, if we like to obtain a speed $v$ comparable with $c$. Of course the most advantageous case is the photon rocket, but we have to bear in mind that we have today no idea how to obtain a concentrated photonbeam giving a thrust of some technical importance. As well known a large exhaust speed can be obtained by acceleration of charged particles (ions) in an electric field. If $V$ be the electric potential passed through, $e$ the charge and $m_0$ the restmass of each particle, the exhaust speed $a_0$ follows from:

$$e V = m_0 c^2 \left( \frac{1}{\sqrt{1 - a_0^2/c^2}} - 1 \right).$$

If $n$ be the number of particles jettisoned per second, the corresponding jet power becomes

$$n e V = n m_0 c^2 \left( \frac{1}{\sqrt{1 - a_0^2/c^2}} - 1 \right), \qquad \text{in which} \qquad n m_0 = \Delta m_0^*.$$

Of course an equal number of particles of opposite charge must be expelled, in order to keep the vehicle neutral.

It would be very advantageous if this acceleration of electric particles could be combined in some way by applying atomic energy obtained by fusion of nucleons, being the most powerful source known today.

Let us imagine we have a gaseous mixture of $^1_2\mathrm{H}$ and $^1_3\mathrm{H}$ nucleons, through which an electric discharge occurs. Let us indicate the particle charge by $e$ and the masses of the $^1_2\mathrm{H}$ and $^1_3\mathrm{H}$ nucleons by $2\, m_0$ and $3\, m_0$. If then $v_1$ be the speed of a $^1_2\mathrm{H}$ nucleon after having passed through a potential drop $V$, we obtain:

$$e V = 2 m_0 c^2 \left( \frac{1}{\sqrt{1 - v_1^2/c^2}} - 1 \right)$$

whence follows:

$$v_1 = c\sqrt{1 - \frac{4\,m_0^2\,c^4}{(e\,V + 2\,m_0\,c^2)^2}} = c\sqrt{\frac{e^2\,V^2 + 4\,e\,V\,m_0\,c^2}{e^2\,V^2 + 4\,e\,V\,m_0\,c^2 + 4\,m_0^2\,c^4}} \tag{14}$$

and similar as to ${}_3^1\mathrm{H}$:

$$v_2 = c\sqrt{\frac{e^2\,V^2 + 6\,e\,V\,m_0\,c^2}{e^2\,V^2 + 6\,e\,V\,m_0\,c^2 + 9\,m_0^2\,c^4}}. \tag{15}$$

Hence after having passed through a potential drop $V$, the relative speed of the accelerated ${}_2^1\mathrm{H}$ nucleon as to the accelerated ${}_3^1\mathrm{H}$ nucleon becomes:

$$v_{\mathrm{rel}} = \frac{v_1 - v_2}{1 - v_1\,v_2/c^2}. \tag{16}$$

Substituting (14) and (15) in (16) we obtain:

$$v_{\mathrm{rel}} = F(V). \tag{17}$$

By means of (17) we can determine the potential drop $V_{\min}$ in order to obtain the required fusion:

$${}_2^1\mathrm{H} + {}_3^1\mathrm{H} = {}_5^2\mathrm{He} \rightarrow {}_4^2\mathrm{He} + {}_1^0n. \tag{18}$$

From (16) it follows that $v_{\mathrm{rel}}$ tends to the speed of light if $V$ increases, for if we write $v_1 \approx c$, we obtain by (16):

$$\lim_{v_1 \to c} v_{\mathrm{rel}} = \frac{c - v_2}{1 - v_2/c} = c.$$

Of course only fusion occurs in case of an encounter. If the density of the mixture is small, such encounters will be rare and the fusion energy which will be gained will only be a small fraction of the energy required for maintaining the current. By increasing this density a value will be attained at which the gain of fusion energy will cancel the loss of energy required for current maintenance. On the other hand, the density of the mixture may only be increased to such an extent, that the fusion heat development remains below a certain value. In this way it seems possible to come to a controlled employ of fusion energy, which could be used for driving the turbo generators maintaining the current. The ${}_2^1\mathrm{H}$ and ${}_3^1\mathrm{H}$ nucleons and also the formed ${}_4^2\mathrm{He}$ particles can then be used as propulsion material. The quantity of expelled ${}_4^2\mathrm{He}$ particles however must necessarily be small and their contribution to the jet can be disregarded. Thereby, as a consequence of the special theory of relativity, the scattering influence of the COULOMB repulsion tends to zero, if the exhaust speed tends to $c$. Also in the gaseous mixture, by the magnetic field of the convection current, the charged particles will be acted upon by a LORENTZ force, causing a tendency to keep these particles in stream direction, thereby protecting the walls of the vessel. On the other hand, the neutron radiation due to the disintegration

$${}_5^2\mathrm{He} \rightarrow {}_4^2\mathrm{He} + {}_1^0n$$

will give rise to serious difficulties. For the walls a material must be used which can endure this neutron bombardment.

Further, as already stated above, always an equivalent number of electrons must be emitted in order to keep the space ship neutral and maintain the thrust. The ejection of these electrons can further contribute to the thrust.

If $\Delta m_0^*$ be the total rest-mass of $^1_2$H and $^1_3$H nucleons expelled per second astronautical time, the total thrust due to these nucleons becomes:

$$S = \frac{2/5\,\Delta m_0^* v_1}{\sqrt{1 - v_1^2/c^2}} + \frac{3/5\,\Delta m_0^* v_2}{\sqrt{1 - v_2^2/c^2}}, \tag{19}$$

in which $v_1$ and $v_2$ follow from (14) and (15). For simplicity let us neglect the contribution of the expelled electrons to the thrust, as well as their mass. If we then assume $S$ [formula (19)] as constant, and write:

$$\frac{2/5\,\Delta m_0^*}{\sqrt{1 - v_1^2/c^2}} + \frac{3/5\,\Delta m_0^*}{\sqrt{1 - v_2^2/c^2}} = \mu_0' \tag{20}$$

we obtain instead of (4):

$$(M_0 - \mu_0' t_0)\frac{dv/dt}{(1 - v^2/c^2)^{3/2}} = S. \tag{21}$$

Hence again multiplying by $dt_0 = dt\sqrt{1 - v^2/c^2}$ we obtain:

$$\frac{dv}{1 - v^2/c^2} = \frac{S\,dt_0}{M_0 - \mu_0' t_0} = -\frac{S}{\mu_0'}\frac{d(M_0 - \mu_0' t_0)}{M_0 - \mu_0' t_0},$$

or after integration:

$$\frac{c}{2}\ln\frac{1 + v/c}{1 - v/c} = \frac{S}{\mu_0'}\ln\frac{M_0}{M_0 - \mu_0' t_0}.$$

Or:

$$\left(\frac{1 + v/c}{1 - v/c}\right)^{c\mu'_0/2S} = \frac{M_0}{M_0 - \mu_0' t_0}.$$

Hence:

$$M_0 - \mu_0' t_0 = \left(\frac{1 - v/c}{1 + v/c}\right)^{c\mu_0'/2S} M_0.$$

This introduced in (21) gives:

$$M_0\left(\frac{1 - v/c}{1 + v/c}\right)^{c\mu_0'/2S}\frac{dv/dt}{(1 - v^2/c^2)^{3/2}} = S.$$

Or:

$$\frac{M_0}{S}\int_0^v \left(\frac{1 - v/c}{1 + v/c}\right)^{c\mu_0'/2S}\frac{dv}{(1 - v^2/c^2)^{3/2}} = t,$$

whence follows again $v = v(t)$ and $s = \int_0^t v(t)\,dt$. For the rest it may be observed that in the discharge vessel also neutral hydrogen or another neutral medium could be brought, which is heated up by the fusion heat and exhausts through a nozzle. In this way however, assuming a temperature of about $3000^0$ C in the discharge vessel, only exhaust speeds of the order of 10 km/sec. can be obtained.

Vol. 4 1958

Now let us generalize (4) by assuming that $\mu_0$ and $a_0$ are not constant, but prescribed functions of $t_0$. We then obtain:

$$\left(M_0 - \int_0^{t_0} \mu_0(t_0)\, dt_0\right) \frac{\dot{v}}{(1 - v^2/c^2)^{3/2}} = \mu_0(t_0)\, a_0(t_0).$$

Then again multiplying by $dt_0 = \sqrt{1 - v^2/c^2}\; dt$ we find:

$$\frac{dv}{1 - v^2/c^2} = \frac{\mu_0(t_0)\, a_0(t_0)\, dt_0}{M_0 - \int_0^{t_0} \mu_0(t_0)\, dt_0},$$

so that

$$c \int_0^v \frac{d(v/c)}{1 - v^2/c^2} = \int_0^{t_0} \frac{\mu_0(t_0)\, a_0(t_0)\, dt_0}{M_0 - \int_0^{t_0} \mu_0(t_0)\, dt_0}. \tag{22}$$

Or:

$$\frac{c}{2} \ln \frac{1 + v/c}{1 - v/c} = \varphi(t_0). \tag{23}$$

In (22) the right member $\varphi(t_0)$ can be numerically evaluated for any value of $t_0$, so that $v = v(t_0)$ becomes known. Then further:

$$\frac{dt_0}{dt} = \sqrt{1 - 1/c^2\, [v(t_0)]^2},$$

so that:

$$\int_0^{t_0} \frac{dt_0}{\sqrt{1 - 1/c^2\, [v(t_0)]^2}} = t. \tag{24}$$

By numerical integration of (24) we find $t_0 = t_0(t)$, so that then also $v(t_0) = v(t_0(t)) = v(t)$ becomes known. Then further the way passed through at any time $t$ during the powered rectilinear flight again follows from:

$$s = \int_0^t v(t)\, dt.$$

Let us now consider the more restricted case that $a_0(t_0) = a_0 = \text{const}$, whereas $\Delta m_0^* = \Delta m_0^*(t_0)$ is variable and prescribed. In that special case (22) simplifies to:

$$\frac{c}{2} \ln \frac{1 + v/c}{1 - v/c} = a_0 \int_0^{t_0} \frac{\mu_0(t_0)\, dt_0}{M_0 - \int_0^{t_0} \mu_0(t_0)\, dt_0}.$$

Or writing

$$M_0 - \int_0^{t_0} \mu_0(t_0)\, dt_0 = M(t_0),$$

we obtain:

$$\frac{c}{2}\ln\frac{1+v/c}{1-v/c} = -\,a_0\int_{M_0}^{M(t_0)}\frac{dM(t_0)}{M(t_0)},$$

so that:

$$\frac{c}{2\,a_0}\ln\frac{1+v/c}{1-v/c} = \ln\frac{M_0}{M(t_0)},$$

or:

$$\left(\frac{1+v/c}{1-v/c}\right)^{c/2a_0} = \frac{M_0}{M(t_0)} = \frac{M_0}{M_0 - \int_0^{t_0}\mu_0(t_0)\,dt_0}. \tag{25}$$

(25) is again the well known formula of ACKERET which avails for all cases of rectilinear flight in non gravitational space, as long as $a_0$ is kept constant. (For the rest, as soon as we think in terms of the speed of light, ordinary gravitational forces practically do not count.) The formulae above not essentially alter if we consider the more general case that different types of particles are simultaneously emitted with different exhaust speeds.

Vol. 4 1958

As example let us consider a space ship emitting positive and negative particles (the normal case of ion propulsion).

Let $\Delta\, m_{0_1}{}^*$ be the rest mass of the positive particles and $\Delta\, m_{0_2}{}^*$ the rest mass of the negative particles emitted per second astronautical time $t_0$ and let $a_{0_1}$ and $a_{0_2}$ be the corresponding exhaust speeds as to the rocket system of reference. Let $\Delta\, m_{0_1}{}^*$, and thus also $\Delta\, m_{0_2}{}^*$, and further $a_{0_1}$ and $a_{0_2}$ be prescribed as functions of $t_0$. Then for rectilinear motion we obtain:

$$\left.\begin{aligned}\frac{dv/dt}{(1-v^2/c^2)^{3/2}} &= \frac{\mu_{0_1}(t_0)\,a_{0_1}(t_0)+\mu_{0_2}(t_0)\,a_{0_2}(t_0)}{M_0-\int_0^{t_0}\left(\mu_{0_1}(t_0)+\mu_{0_2}(t_0)\right)dt_0}\\ \text{in which}\qquad \mu_{0_1} &= \frac{\Delta\, m_{0_1}{}^*(t_0)}{\sqrt{1-\frac{[a_{0_1}(t_0)]^2}{c^2}}},\qquad \mu_{0_2} = \frac{\Delta\, m_{0_2}{}^*(t_0)}{\sqrt{1-\frac{[a_{0_2}(t_0)]^2}{c^2}}}.\end{aligned}\right\} \tag{26}$$

Again by multiplying with $\sqrt{1-v^2/c^2}\,dt = dt_0$ and subsequent integration we obtain:

$$c\int_0^{v}\frac{d(v/c)}{1-v^2/c^2} = \frac{c}{2}\ln\frac{1+v/c}{1-v/c} = \int_0^{t_0}\frac{\mu_{0_1}(t_0)\,a_{0_1}(t_0)+\mu_{0_2}(t_0)\,a_{0_2}(t_0)}{M_0-\int_0^{t_0}\left(\mu_{0_1}(t_0)+\mu_{0_2}(t_0)\right)dt_0}\,dt_0. \tag{27}$$

The right member of (27) can be integrated numerically, so that $v = v(t_0)$ can be determined. Then further we obtain:

$$\int_0^{t_0}\frac{dt_0}{\sqrt{1-\frac{1}{c^2}\,[v(t_0)]^2}} = t \to t_0 = t_0(t),$$

so that:

$$v(t_0) = v\big(t_0(t)\big) = v(t),\ s = \int_0^t v(t)\,dt.$$

If $a_{0_1}$ and $a_{0_2}$ are maintained at constant value, and for the rest $\Delta m_{0_1}{}^* = \Delta m_{0_1}{}^*(t_0)$ and $\Delta m_{0_2}{}^* = \Delta m_{0_2}{}^*(t_0)$ be prescribed, we may write (27):

$$\frac{c}{2}\ln\frac{1+v/c}{1-v/c} = a_{0_1}\int_0^{t_0}\frac{\mu_{0_1}(t_0)\,dt_0}{M(t_0)} + a_{0_2}\int_0^{t_0}\frac{\mu_{0_2}(t_0)\,dt_0}{M(t_0)}.$$

Now let us write:

$$\frac{1}{\sqrt{1-\frac{a_{0_1}{}^2}{c^2}}} = \beta_1, \qquad \frac{1}{\sqrt{1-\frac{a_{0_2}{}^2}{c^2}}} = \beta_2.$$

We then obtain:

$$\frac{c}{2}\ln\frac{1+v/c}{1-v/c} = a_{0_1}\beta_1\int_0^{t_0}\frac{\Delta m_{0_1}{}^*(t_0)\,dt_0}{M(t_0)} + a_{0_2}\beta_2\int_0^{t_0}\frac{\Delta m_{0_2}{}^*(t_0)\,dt_0}{M(t_0)}.$$

Let us further write:

$$a_{0_2} = k_1 a_{0_1}, \qquad \Delta m_{0_2}{}^*(t_0) = k_2\,\Delta m_{0_1}{}^*(t_0).$$

Then:

$$\frac{c}{2}\ln\frac{1+v/c}{1-v/c} = a_{0_1}(\beta_1 + k_1 k_2 \beta_2)\int_0^{t_0}\frac{\Delta m_{0_1}{}^*(t_0)\,dt_0}{M(t_0)}.$$

Now:

$$-dM(t_0) = [\mu_{0_1}(t_0) + \mu_{0_2}(t_0)]\,dt_0 =$$
$$= [\beta_1\,\Delta m_{0_1}{}^*(t_0) + \beta_2\,\Delta m_{0_2}{}^*(t_0)]\,dt_0 = (\beta_1 + \beta_2 k_2)\,\Delta m_{0_1}{}^*(t_0)\,dt_0,$$

so that we may write:

$$\frac{c}{2}\ln\frac{1+v/c}{1-v/c} = a_{0_1}\frac{\beta_1 + k_1 k_2 \beta_2}{\beta_1 + k_2\beta_2}\int_0^{t_0}\frac{(\beta_1 + k_2\beta_2)\,\Delta m_{0_1}{}^*(t_0)\,dt_0}{M(t_0)}.$$

Hence if we write:

$$\frac{\beta_1 + k_1 k_2 \beta_2}{\beta_1 + k_2\beta_2} = \alpha,$$

we get:

$$\frac{c}{2}\ln\frac{1+v/c}{1-v/c} = -a_{0_1}\alpha\int_{M_0}^{M(t_0)}\frac{dM(t_0)}{M(t_0)}.$$

Hence:

$$\frac{c}{2\,\alpha\,a_{0_1}}\ln\frac{1+v/c}{1-v/c} = \ln\frac{M_0}{M(t_0)}. \qquad \text{Or:} \qquad \left(\frac{1+v/c}{1-v/c}\right)^{c/2\,\alpha\,a_{0_1}} = \frac{M_0}{M(t_0)}. \qquad (28)$$

(28) is then again the formula of ACKERET for this special case. Let us now proceed to the general case of relativistic curvilinear motion of the same rocketship, emitting positive and negative particles, moving in non gravitational

space. In this case the directions of speed and thrust will be different. The rest masses of the positive and negative particles jettisoned per second astronautical time and the corresponding exhaust speeds are again indicated as above. Further the magnitude of the thrust (= the force by which rocket vehicle + still included fuel is acted upon) is again equal to the dynamometer pointer reading as imagined before, and therefore becomes

$$\mu_{0_1} a_{0_1} + \mu_{0_2} a_{0_2} \qquad \text{[compare eq. (26)]}.$$

The *direction* of this thrust now depends on the instantaneous position of the axis of the rocket, and will be different for terrestrial observer and occupant of the vehicle, on account of the LORENTZ contraction of the space of the latter. Therefore in order to avoid mathematical complications, let us prescribe $\Delta m_{0_1}{}^*$ and $\Delta m_{0_2}{}^*$, being the rest masses of the positive and negative particles jettisoned per second astronautical time as well as the magnitudes $a_{0_1}$ and $a_{0_2}$ of the corresponding astronautical exhaust speeds, as functions of $t_0$, whereas the common direction (thrust direction) of the vector quantities $\overline{a}_{0_1}$ and $\overline{a}_{0_2}$, coinciding with the instantaneous axial direction of the rocket, at any astronautical time $t_0$, *be prescribed with respect to the terrestrial system of reference.* (The numerical values of the vector quantities $\overline{a}_{0_1}$ and $\overline{a}_{0_2}$ are $a_{0_1}$ and $a_{0_2}$.)

Vol. 4 1958

Hence in accordance with the fundamental eq. (2) we then obtain as differential equations of motion:

$$\left.\begin{aligned} \left\{M_0 - \int_0^{t_0} [\mu_{0_1}(t_0) + \mu_{0_2}(t_0)]\, dt_0\right\} \frac{d}{dt}\left(\frac{\overline{v}}{\sqrt{1 - v^2/c^2}}\right) &= \mu_{0_1}(t_0)\, \overline{a}_{0_1}(t_0) + \mu_{0_2}(t_0)\, \overline{a}_{0_2}(t_0) \\ \frac{dt_0}{dt} &= \sqrt{1 - v^2/c^2}. \end{aligned}\right\} \quad (29)$$

Then in (29) the force on the right of the vector equation, as prescribed function of astronautical time $t_0$, refers to the terrestrial system of reference $xyz$, as to magnitude *and* direction. (This terrestrial system of reference may be chosen with the earth center as origin, and does not rotate with respect to the celestial sky.) (29) is a system of 4 simultaneous differential equations of first order, with $t$ as independent variable, and $v_x$, $v_y$, $v_z$ and $t_0$ as dependent variables. (The vector equation stands for 3 component equations corresponding with $x$, $y$ and $z$ direction.) Starting from the initial state:

$$t = 0 \rightarrow t_0 = 0 \rightarrow v_x = 0, \qquad v_y = 0, \qquad v_z = 0,$$

this system can be solved numerically, whether by the method of RUNGE-KUTTA, or by the method of successive approximations. Let us write:

$$\left.\begin{aligned} &\frac{\mu_{0_1}(t_0) a_{0_{1_x}}(t_0) + \mu_{0_2}(t_0)\, a_{0_{2_x}}(t_0)}{M_0 - \int_0^{t_0} [\mu_{0_1}(t_0) + \mu_{0_2}(t_0)]\, dt_0} = p_x(t_0) \\ &\text{and similar } p_y(t_0) \text{ and } p_z(t_0). \end{aligned}\right\} \quad (30)$$

Carrying out the differentiations

$$\frac{d}{dt}\left(\frac{v_x}{\sqrt{1 - (v_x{}^2 + v_y{}^2 + v_z{}^2)/c^2}}\right), \text{ etc.,}$$

we then obtain the following set of equations:

$$\left.\begin{aligned}
&\frac{1-(v_y^2+v_z^2)/c^2}{\left(1-(v_x^2+v_y^2+v_z^2)/c^2\right)^{3/2}}\frac{dv_x}{dt}+\frac{v_x v_y/c^2}{\left(1-(v_x^2+v_y^2+v_z^2)/c^2\right)^{3/2}}\frac{dv_y}{dt}+\\
&\qquad+\frac{v_x v_z/c^2}{\left(1-(v_x^2+v_y^2+v_z^2)/c^2\right)^{3/2}}\frac{dv_z}{dt}=p_x(t_0)\\
&\frac{v_y v_x/c^2}{\left(1-(v_x^2+v_y^2+v_z^2)/c^2\right)^{3/2}}\frac{dv_x}{dt}+\frac{1-(v_x^2+v_z^2)/c^2}{\left(1-(v_x^2+v_y^2+v_z^2)/c^2\right)^{3/2}}\frac{dv_y}{dt}+\\
&\qquad+\frac{v_y v_z/c^2}{\left(1-(v_x^2+v_y^2+v_z^2)/c^2\right)^{3/2}}\frac{dv_z}{dt}=p_y(t_0)\\
&\frac{v_z v_x/c^2}{\left(1-(v_x^2+v_y^2+v_z^2)/c^2\right)^{3/2}}\frac{dv_x}{dt}+\frac{v_z v_y/c^2}{\left(1-(v_x^2+v_y^2+v_z^2)/c^2\right)^{3/2}}\frac{dv_y}{dt}+\\
&\qquad+\frac{1-(v_x^2+v_y^2)/c^2}{\left(1-(v_x^2+v_y^2+v_z^2)/c^2\right)^{3/2}}\frac{dv_z}{dt}=p_z(t_0)\\
&\frac{dt_0}{dt}=\sqrt{1-\frac{v_x^2+v_y^2+v_z^2}{c^2}}.
\end{aligned}\right\}\tag{31}$$

The first three eqs. (31) are linear in the differential quotients $dv_x/dt$, $dv_y/dt$ and $dv_z/dt$, so that we can solve these quantities from these equations. Then we can write (31):

$$\left.\begin{aligned}
&\frac{dt_0}{dt}=\sqrt{1-\frac{v_x^2+v_y^2+v_z^2}{c^2}}=F_1(v_x,v_y,v_z)\\
&\frac{dv_x}{dt}=F_2(t_0,v_x,v_y,v_z)\\
&\frac{dv_y}{dt}=F_3(t_0,v_x,v_y,v_z)\\
&\frac{dv_z}{dt}=F_4(t_0,v_x,v_y,v_z).
\end{aligned}\right\}\tag{32}$$

Starting from the initial state $t=0\rightarrow t_0=0$, $v_x=0$, $v_y=0$, $v_z=0$, let us integrate (32) by the method of RUNGE-KUTTA. We then obtain the scheme:

$$\left.\begin{aligned}
&t\rightarrow h,\ t_0\rightarrow k,\ v_x\rightarrow l,\ v_y\rightarrow n,\ v_z\rightarrow q.\\
&k=\frac{1}{6}k_1+\frac{1}{3}k_2+\frac{1}{3}k_3+\frac{1}{6}k_4 \qquad n=\frac{1}{6}n_1+\frac{1}{3}n_2+\frac{1}{3}n_3+\frac{1}{6}n_4\\
&l=\frac{1}{6}l_1+\frac{1}{3}l_2+\frac{1}{3}l_3+\frac{1}{6}l_4 \qquad q=\frac{1}{6}q_1+\frac{1}{3}q_2+\frac{1}{3}q_3+\frac{1}{6}q_4\\
&k_1=F_1(v_x,v_y,v_z)\,h \qquad l_1=F_2(t_0,v_x,v_y,v_z)\,h\\
&k_2=F_1\left(v_x+\frac{l_1}{2},v_y+\frac{n_1}{2},v_z+\frac{q_1}{2}\right)h \qquad l_2=F_2\left(t_0+\frac{k_1}{2},\right.\\
&\qquad\qquad\left.v_x+\frac{l_1}{2},v_y+\frac{n_1}{2},v_z+\frac{q_1}{2}\right)h
\end{aligned}\right\}\tag{33}$$

$$\left.\begin{aligned} k_3 &= F_1\left(v_x + \frac{l_1}{2}, v_y + \frac{n_1}{2}, v_z + \frac{q_1}{2}\right) h \qquad l_3 = F_2\left(t_0 + \frac{k_2}{2}, \right. \\ &\qquad\qquad \left. v_x + \frac{l_2}{2}, v_y + \frac{n_2}{2}, v_z + \frac{q_2}{2}\right) h \\ k_4 &= F_1\,(v_x + l_3, v_y + n_3, v_z + q_3)\, h \qquad l_4 = F_2\,(t_0 + k_3, v_x + l_3, \\ &\qquad\qquad v_y + n_3, v_z + q_3)\, h \end{aligned}\right\} \tag{33}$$

and similar $n$ and $q$.

The computation according to the scheme (33) must be carried out in the sequence $k_1\, l_1\, n_1\, q_1\, k_2\, l_2\, n_2\, q_2\, k_3\, l_3\, n_3\, q_3\, k_4\, l_4\, n_4\, q_4$, and is suitable for a digital electronic computer. Repeating the procedure with half the number of steps, the difference in result is about 15 $\times$ the order of magnitude of the remaining inaccuracy of the result of the first computation.

By this step by step integration, we then find:

$$t_0 = t_0(t), \qquad v_x = v_x(t), \qquad v_y = v_y(t), \qquad v_z = v_z(t). \tag{34}$$

Vol. 4 1958

Then further the coordinates of the rocket vehicle at any terrestrial time $t$ become:

$$x = \int_0^t v_x(t)\, dt + x_0, \qquad y = \int_0^t v_y(t)\, dt + y_0, \qquad z = \int_0^t v_z(t)\, dt + z_0. \tag{35}$$

The integrals in (35) must again be computed numerically. In connection with the first eq. (34) we can then further determine:

$$\begin{aligned} v_x &= v_x(t_0), \qquad v_y = v_y(t_0), \qquad v_z = v_z(t_0) \\ x &= x(t_0), \qquad y = y(t_0), \qquad z = z(t_0). \end{aligned} \tag{36}$$

After having carried out the computation, we can arrange the program of navigation for the crew, in terms of astronautical time $t_0$. The required consecutive directions of navigation (directions of rocket axis) can be indicated by remote celestial objects (spiral nebulae).

We can also proceed in different way by *prescribing* the orbit in space and time, and determine the required program of navigation. In that case the functions

$$x = x(t), \qquad y = y(t), \qquad z = z(t) \tag{37}$$

are given, so that the functions:

$$v_x = v_x(t), \qquad v_y = v_y(t), \qquad v_z = v_z(t) \tag{38}$$

are known.

We have again to start from the system (29). Let us write:

$$\left.\begin{aligned} \frac{d}{dt}\left(\frac{\overline{v}}{1 - v^2/c^2}\right) &= \frac{\mu_{0_1}(t_0)\, \overline{a}_{0_1}(t_0) + \mu_{0_2}(t_0)\, \overline{a}_{0_2}(t_0)}{M_0 - \int_0^{t_0} [\mu_{0_1}(t_0) + \mu_{0_2}(t_0)]\, dt_0} \\ \frac{dt_0}{dt} &= \sqrt{1 - \frac{v^2}{c_2}}\,. \end{aligned}\right\} \tag{29'}$$

If $\overline{v} = \overline{v}(t)$ (hence (38)) is prescribed, the left member of the first eq. (29′) as vector function of $t$ is known. Let us indicate this left member by $\overline{p}(t)$. Further by the last eq. (29′) we obtain:

$$t_0 = \int_0^t \sqrt{1 - \frac{[v_x(t)]^2 + [v_y(t)]^2 + [v_z(t)]^2}{c^2}}\, dt.$$

The integral must be computed numerically. In this way we find $t = t(t_0)$. Then $\overline{v} = \overline{v}(t) = \overline{v}(t(t_0)) = \overline{v}(t_0)$, so that also $\overline{p} = \overline{p}(t_0)$ as function of $t_0$ becomes known.

Then the first eq. (29) is equivalent with the three component equations:

$$\left.\begin{aligned} p_x(t_0) &= \frac{\mu_{0_1}(t_0)\, a_{0_{1_x}}(t_0) + \mu_{0_2}(t_0)\, a_{0_{2_x}}(t_0)}{M_0 - \int_0^{t_0} (\mu_{0_1}(t_0) + \mu_{0_2}(t_0))\, dt_0} \\ &\text{and similar for } y \text{ and } z. \end{aligned}\right\} \tag{39}$$

We may now write the first eq. (39):

$$M_0 - \frac{\mu_{0_1}(t_0)\, a_{0_{1_x}}(t_0) + \mu_{0_2}(t_0)\, a_{0_{2_x}}(t_0)}{p_x(t_0)} = \int_0^{t_0} [\mu_{0_1}(t_0) + \mu_{0_2}(t_0)]\, dt_0.$$

Hence:

$$\left.\begin{aligned} &-\frac{d}{dt_0}\left(\frac{\mu_{0_1}(t_0)\, a_{0_{1_x}}(t_0) + \mu_{0_2}(t_0)\, a_{0_{2_x}}(t_0)}{p_x(t_0)}\right) = \mu_{0_1}(t_0) + \mu_{0_2}(t_0) \\ &\text{and similar for } y \text{ and } z. \end{aligned}\right\} \tag{40}$$

Now let us assume $\Delta m_{0_1}{}^*$ and $\Delta m_{0_2}{}^*$ constant with time, and let us write again: $a_{0_2} = k_1\, a_{0_1}$, $\Delta m_{0_2}{}^* = k_2\, \Delta m_{0_1}{}^*$. We then obtain:

$$-\frac{d}{dt_0}\left(\frac{\Delta m_{0_1}{}^* \dfrac{a_{0_{1_x}}}{\sqrt{1 - (a_{0_{1_x}}{}^2 + a_{0_{1_y}}{}^2 + a_{0_{1_z}}{}^2)/c^2}} + k_2 \Delta m_{0_1}{}^* \dfrac{k_1\, a_{0_{1_x}}}{\sqrt{1 - k_1{}^2 (a_{0_{1_x}}{}^2 + a_{0_{1_y}}{}^2 + a_{0_{1_z}}{}^2)/c^2}}}{p_x(t_0)}\right) =$$

$$= \frac{\Delta m_{0_1}{}^*}{\sqrt{1 - (a_{0_{1_x}}{}^2 + a_{0_{1_y}}{}^2 + a_{0_{1_z}}{}^2)/c^2}} + \frac{k_2 \Delta m_{0_1}{}^*}{\sqrt{1 - k_1{}^2 (a_{0_{1_x}}{}^2 + a_{0_{1_y}}{}^2 + a_{0_{1_z}}{}^2)/c^2}}$$

Hence carrying out a stage further, the system (40) becomes:

$$\left.\begin{aligned} &\left(\Delta m_{0_1}{}^* \frac{a_{0_{1_x}}}{\sqrt{1 - (a_{0_{1_x}}{}^2 + a_{0_{1_y}}{}^2 + a_{0_{1_z}}{}^2)/c^2}} + \right. \\ &\left. + k_2 \Delta m_{0_1}{}^* \frac{k_1\, a_{0_{1_x}}}{\sqrt{1 - k_1{}^2 (a_{0_{1_x}}{}^2 + a_{0_{1_y}}{}^2 + a_{0_{1_z}}{}^2)/c^2}}\right) p_x'(t_0) + \\ &- p_x(t_0) \left\{ \Delta m_{0_1}{}^* \frac{d}{dt_0}\left(\frac{a_{0_{1_x}}}{\sqrt{1 - (a_{0_{1_x}}{}^2 + a_{0_{1_y}}{}^2 + a_{0_{1_z}}{}^2)/c^2}}\right) + \right. \end{aligned}\right\} \tag{41}$$

$$+ k_1 k_2 \Delta m_{0_1}{}^* \frac{d}{dt_0}\left(\frac{a_{0_{1_x}}}{\sqrt{1 - k_1{}^2 (a_{0_{1_x}}{}^2 + a_{0_{1_y}}{}^2 + a_{0_{1_z}}{}^2)/c^2}}\right)\Bigg\} =$$

$$= \frac{\Delta m_{0_1}{}^*}{\sqrt{1 - (a_{0_{1_x}}{}^2 + a_{0_{1_y}}{}^2 + a_{0_{1_z}}{}^2)/c^2}} + \tag{41}$$

$$+ \frac{k_2 \Delta m_{0_1}{}^*}{\sqrt{1 - k_1{}^2 (a_{0_{1_x}}{}^2 + a_{0_{1_y}}{}^2 + a_{0_{1_z}}{}^2)/c^2}}$$

$$\text{and similar for } y \text{ and } z.$$

In (41),

$$p_x'(t_0) = \frac{dp_x(t_0)}{dt_0} = \frac{dp_x(t)}{dt}\frac{dt}{dt_0} = p_x'(t) \cdot \sqrt{1 - \frac{[v(t)]^2}{c^2}},$$

in which again $t = t(t_0)$ must be substituted, and similar $p_y'(t_0)$ and $p_z'(t_0)$. The quantities $p_x'(t)$, $p_y'(t)$ and $p_z'(t)$ are obtained by differentiation of the left members of (31), whereas $\dot{v}_x$, $\dot{v}_y$, $\dot{v}_z$ and $\ddot{v}_x$, $\ddot{v}_y$, and $\ddot{v}_z$, appearing in the expressions, are again known functions following from (38). Further carrying out the differentiation in (41), we obtain a system of 3 simultaneous differential equations, which are linear in $da_{0_{1_x}}/dt_0$, $da_{0_{1_y}}/dt_0$ and $da_{0_{1_z}}/dt_0$, so that the equations can be solved with respect to these three differential quotients. We then obtain the system

$$\left.\begin{aligned} \frac{da_{0_{1_x}}}{dt_0} &= F_1 (a_{0_{1_x}}, a_{0_{1_y}}, a_{0_{1_z}}, t_0) \\ \frac{da_{0_{1_y}}}{dt_0} &= F_2 (a_{0_{1_x}}, a_{0_{1_y}}, a_{0_{1_z}}, t_0) \\ \frac{da_{0_{1_z}}}{dt_0} &= F_3 (a_{0_{1_x}}, a_{0_{1_y}}, a_{0_{1_z}}, t_0). \end{aligned}\right\} \tag{42}$$

Let us again assume that at $t = 0$, $t_0 = 0$, $v_x = 0$, $v_y = 0$, $v_z = 0$. Then at the time of start $t_0 = 0$ (coinciding with $t = 0$), we obtain:

$$M_0 \sqrt{(\dot{v}_x)_{t_0=0}^2 + (\dot{v}_y)_{t_0=0}^2 + (\dot{v}_z)_{t_0=0}^2} =$$

$$= \frac{\Delta m_{0_1}{}^* (a_{0_1})_{t_0=0}}{\sqrt{1 - (a_{0_1})_{t_0=0}^2/c^2}} + \frac{k_1 k_2 \Delta m_{0_1}{}^* (a_{0_1})_{t_0=0}}{\sqrt{1 - k_1{}^2 (a_{0_1})_{t_0=0}^2/c^2}}$$

from which $(a_{0_1})_{t_0=0}$ can be solved numerically [because the functions (38) are prescribed, also the functions $\dot{v}_x = \dot{v}_x(t)$, $\dot{v}_y = \dot{v}_y(t)$, $\dot{v}_z = \dot{v}_z(t)$ are determined, so that also the quantities $(\dot{v}_x)_{t_0=0} = 0$, $(\dot{v}_y)_{t_0=0} = 0$, $(\dot{v}_z)_{t_0=0} = 0$ are known]. We then further obtain:

$$[(a_{0_1})_{t_0=0}]_x = (a_{0_1})_{t_0=0} \frac{(\dot{v}_x)_{t_0=0}}{\sqrt{(\dot{v}_x)_{t_0=0}^2 + (\dot{v}_y)_{t_0=0}^2 + (\dot{v}_z)_{t_0=0}^2}}$$

and similar

$$[(a_{0_1})_{t_0=0}]_y \qquad \text{and} \qquad [(a_{0_1})_{t_0=0}]_z.$$

Vol. 4 1958

[At $t_0 = 0$ (coinciding with $t = 0$) the directions of $\overline{a}_{0_1}$ with respect to the terrestrial system and rocket system of reference are identical.]

Now, starting from the initial state

$$t_0 = 0 \rightarrow [(a_{0_1})_{t_0=0}]_x,\ [(a_{0_1})_{t_0=0}]_y,\ [(a_{0_1})_{t_0=0}]_z,$$

we can integrate the system (42) by the method of successive approximations, or by the method of RUNGE-KUTTA. Again choosing the last one, we obtain the scheme:

$$\left.\begin{array}{l} t_0 \rightarrow h \qquad a_{0_{1_x}} \rightarrow k, \qquad a_{0_{1_y}} \rightarrow l, \qquad a_{0_{1_z}} \rightarrow n \\ k = \frac{1}{6} k_1 + \frac{1}{3} k_2 + \frac{1}{3} k_3 + \frac{1}{6} k_4 \\ l = \frac{1}{6} l_1 + \frac{1}{3} l_2 + \frac{1}{3} l_3 + \frac{1}{6} l_4 \\ n = \frac{1}{6} n_1 + \frac{1}{3} n_2 + \frac{1}{3} n_3 + \frac{1}{6} n_4 \end{array}\right\}$$

Then:

$$\left.\begin{array}{l} k_1 = F_1 (a_{0_{1_x}}, a_{0_{1_y}}, a_{0_{1_z}}, t_0)\, h \\ k_2 = F_1 \left(a_{0_{1_x}} + \frac{k_1}{2}, a_{0_{1_y}} + \frac{l_1}{2}, a_{0_{1_z}} + \frac{n_1}{2}, t_0 + \frac{h}{2}\right) h \\ k_3 = F_1 \left(a_{0_{1_x}} + \frac{k_2}{2}, a_{0_{1_y}} + \frac{l_2}{2}, a_{0_{1_z}} + \frac{n_2}{2}, t_0 + \frac{h}{2}\right) h \\ k_4 = F_1 (a_{0_{1_x}} + k_3, a_{0_{1_y}} + l_3, a_{0_{1_z}} + n_3, t_0 + h)\, h \end{array}\right\}$$

and similar $n$ and $l$.

The computation must be carried out in the sequence $k_1\, l_1\, n_1\, k_2\, l_2\, n_2\, k_3\, l_3\, n_3\, k_4\, l_4\, n_4$. The accuracy can again be estimated as above.

[After having determined:

$$a_{0_{1_x}} = a_{0_{1_x}}(t_0), \qquad a_{0_{1_y}} = a_{0_{1_y}}(t_0), \qquad a_{0_{1_z}} = a_{0_{1_z}}(t_0)$$

in this way, we obtain:

$$a_{0_{1_x}} = a_{0_{1_x}}(t_0(t)) = a_{0_{1_x}}(t) \text{ and similar } a_{0_{1_y}}(t) \text{ and } a_{0_{1_z}}(t).]$$

These quantities $a_{0_{1_x}}$, $a_{0_{1_y}}$, $a_{0_{1_z}}$, determined as functions of $t_0$, refer to the terrestrial system of reference.

Further the coordinates of the spaceship with respect to the terrestrial system of reference, as functions of $t_0$ become:

$$x(t) = x(t(t_0)) = x(t_0) \text{ and similar } y(t_0) \text{ and } z(t_0),$$

so that by these results of computation a program of navigation can be indicated, using different remote celestial objects as consecutive directive points. The required numerical value $a_{0_1}$, at any astronautical time $t_0$, then becomes:

$$a_{0_1} = \sqrt{[a_{0_{1_x}}(t_0)]^2 + [a_{0_{1_y}}(t_0)]^2 + [a_{0_{1_z}}(t_0)]^2}.$$

After these pure theoretical considerations, let us turn to the question what the formulae have to tell us about the prospects of interstellar space flight in a remote future. Firstly let us consider the power required. Let us call the quantity of kinetic energy per second astronautical time, for maintaining the jet, $J$ (jetpower).

Then:

$$J = \Delta m_0^* c^2 \left( \frac{1}{\sqrt{1 - a_0^2/c^2}} - 1 \right). \tag{43}$$

The corresponding thrust then becomes:

$$P = \frac{\Delta m_0^* a_0}{\sqrt{1 - a_0^2/c^2}}. \tag{44}$$

Expanding in (43) $(1 - a_0^2/c^2)^{1/2}$, we obtain:

$$J = \Delta m_0^* c^2 \left[ \frac{1}{2} \frac{a_0^2}{c^2} + \frac{3}{8} \frac{a_0^4}{c^4} + \text{etc.} \right].$$

Hence if $a_0 \ll c$, (43) and (44) reduce to:

$$J = \frac{1}{2} \Delta m_0^* a_0^2 \qquad \text{and} \qquad P = \Delta m_0^* a_0,$$

so that then:

$$J = \frac{1}{2} P a_0. \tag{45}$$

If we take as example $a_0 = 10{,}000$ km/sec $= 10^7$ m/sec, $(a_0/c)^2 = 1/900$, so that we can use the last formula (45). If we further assume for $P$ the very small value of 15 kg we then obtain:

$$J = 7.5 \times 10^7 \text{ kg/sec} = 10^6 \text{ metric H.P.}$$

*Hence for $a_0 = 10{,}000$ km/sec, we require for any 15 kg thrust a million H.P.* If our interstellar space ship has a weight of 150,000 kg, we should obtain an acceleration of 0.0001 $g$ if $g$ = acceleration due to gravity at the terrestrial surface. This acceleration may be sufficient for an interplanetary electric space ship, for an interstellar space ship that must reach a final speed comparable with $c$, it is uttermost inapplicable. By the very long acceleration period all profit of relativistic time dilatation would be excluded. Further with this exhaust speed, we obtain according to (5) a mass ratio of astronomical magnitude. The space ship would have to jettisone itself completely. On the other hand, if we increase the acceleration to $g$, the jet power becomes $10^{10}$ metric H. P. Even if our propulsion instalment would have a thermal efficiency of 99% the space ship would at once be destroyed by the waste heat. And meanwhile the required mass ratio still remains the same: If we increase the exhaust speed $a_0$, the energy situation becomes still more severe. If we increase the initial mass of the space ship, maintaining the same acceleration and exhaust speed, the situation remains the same. We must confess that we are confronted with insurmountable difficulties.

*Only if mankind succeeds in generating the enormous jet powers required practically without any waste heat development, interstellar space flight with a speed comparable with c will have a chance. Further fusion of nucleons will be insufficient. A complete conversion of matter in jet energy, without intermediate heat stage, will be necessary.*

The solution of this formidable problem is perhaps not for ever excluded, but in every case it seems to be far beyond our technical range for the first ages to come.

And even if this problem will have been solved in a remote future, still enormous mass ratios will be required, as soon as we leave the stellar neighbourhood of the solar system.

Vol. 4 1958

In order to pass *in free flight* through a distance of about 100 lightyears — as measured by the terrestrial observer — in an *astronautical* time lapse of about 10 years, we require a time dilatation:

$$\frac{dt_0}{dt} = \sqrt{1 - \frac{v^2}{c^2}} \approx \frac{1}{10},$$

whence follows a travel speed

$$v = c\sqrt{1 - \frac{1}{100}} \approx 0{,}99\,c.$$

Hence with this speed a distance of 99 lightyears (as measured by the terrestrial observer) is passed through in an *astronautical* time lapse of 10 years. If $a_0 = c$ (photon rocket), the required mass ratio in order to obtain this speed becomes by (5):

$$\sqrt{\frac{1 + 0.99}{1 - 0.99}} \approx \sqrt{200} \approx 14.$$

If we like again to reduce this speed to zero at the end of the voyage, the required mass ratio becomes $(\sqrt{200})^2 = 200$. This simple consideration already shows that the nearest stars can then be reached within the range of a human life.

Now let us contemplate which mass ratio will be required in order to pass through *in free flight*, after a period of acceleration, a distance of $1.5 \times 10^6$ lightyears (= distance of nearest galaxy) in about 15 years astronautical time. Then the required time dilatation becomes:

$$\frac{dt_0}{dt} = \sqrt{1 - \frac{v^2}{c^2}} = \frac{15}{1.5 \times 10^6} = 10^{-5}.$$

Hence

$$\frac{v}{c} = \sqrt{1 - 10^{-10}} \approx 1 - \frac{1}{2} \cdot 10^{-10}.$$

By (5) the required mass ratio then becomes, if $a_0 = c$:

$$\sqrt{\frac{2 - \frac{1}{2} \cdot 10^{-10}}{\frac{1}{2} \cdot 10^{-10}}} \approx \sqrt{\frac{2}{\frac{1}{2} \cdot 10^{-10}}} = 2 \cdot 10^5.$$

If we should like not only to attain the travel speed $v = c\,(1 - \frac{1}{2} \cdot 10^{-10})$, but also again to reduce this speed to zero in order to visit the remote object, a mass ratio of $4 \cdot 10^{10}$ will be required:

From these figures it already follows that whatever may be our technical achievements in the remote future, still intergalactic distances will be inconvincible — at least if we like to pass through the way in one human life of today and base on the rocket as principle of locomotion. In fact SÄNGER comes to the same conclusion [3].

But why only to base our hope on the rocket principle? The mighty astronautical barrier: *gravitation*, is in itself still a complete mystery. Why is gravitation always attractive? Is there any interdependence between gravitation and electrodynamic forces? Is perhaps "gravitation" some weak mean effect of an internuclear state of motion? If so, it seems in principle probable to attack gravitation directly on the atomic level, by influencing this internal state, perhaps converting gravitational attraction into gravitational repulsion, with

simultaneous neutralisation of all stresses due to inertia. Here we are scarcely at the very beginning of scientific research. But whatever may be the ultimate way according to which interstellar spaceflight will once be realized despite all obstructions (including the obstruction of interstellar matter), the application of the *time dilatation* will remain an essential independent feature. Therefore let us now turn to this point.

The time dilatation, as well as the LORENTZ contraction, which are fundamental features of the special theory of relativity, will be well known to the reader. The special theory of relativity is strongly confirmed by experiment, so that there can be no doubt about the real appearance of the time dilatation when the travel speed tends to the speed of light. However, by the reciprocity of these phenomena, as a consequence of the formulae describing the space and time interdependence, it seems at first view that the astronaute cannot have, *at the return*, any real advantage of the time dilatation as to the terrestrial inhabitant who was still staying at home. For by this reciprocity, from the astronaute's point of view the physical processes on earth slow down in the same ratio. However, these reciprocal relations are only valid for observers in free flight, moving with respect to each other with constant speed. As soon as the space ship accelerates with respect to the terrestrial observer, this reciprocity is disturbed. At the end of this paper we return to this point.

Vol. 4 1958

Further we have to bear in mind that the paradoxical reciprocity is only a consequence of our restricted outlook in terms of separated space and time. The physical world however is not a world of instantaneous objects, but a world of events. Events, which are simultaneous for one observer may have different time coordinates for another observer, so that the point events, constituting for one observer an object at a given time, will not constitute at all an object at a given time for another observer.

Hence an "instantaneous object" has no absolute existence, it is a product of pure mindspinning corresponding with our conventional restricted outlook on the world in terms of separated space and time, a result of our preference of permanence in the structure of events. The *events* are the basic constituents of the physical world. This world is neither static nor dynamic, but only *is*, in non temporal sense. Hence comparing the worldlines of the astronaute and the terrestrial inhabitant between the intersection points corresponding with the start and the return of the space ship, we have only to count the number of clock beats (point events) along each world line. (The clocks concerned are supposed to be physically quite similar.) We have then all reason to expect that the number of clock beats along the terrestrial world line will be the larger one, and that the gain of time for the astronaute will be practically in accordance with the result obtained by using the formulae of the special theory of relativity, the system of the terrestrial observer thereby considering as "the system at rest". Of course we now surpass the special theory of relativity, by adding — also independent on the general theory of relativity — the hypothesis that there must be a general metric field, defined by the total space time structure of the universe by which "the system at rest" can be defined in each special region. Is there any reason for such a supposition? In this connection it must be emphasized that in the special theory of relativity no explanation is given of the space and time interdependences, as described by the formulae. Now in cosmical respect, there is an enormous difference between the state of the terrestrial inhabitant and the astronaute, travelling with a speed nearly to $c$. The last one has not only this enormous speed with respect to the earth, but also with respect to all other masses, at least, of the cosmical neighbourhood. This last fact may have a predominant

influence on the rate of all physical processes going on in the space ship and may ultimately be also responsible for the time dilatation and LORENTZ contraction as described by the formulae of the special theory of relativity.

According to the conceptions of MACH and EINSTEIN, the mass of any particle can be conceived as a function of its interdependence upon all other masses throughout the universe. This conception is strongly emphasized by modern quantum statistics.

However, we have already advanced above that the objective world of physics is not a world of material objects, but a world of events, not only extending in space, but also in time. In connection with this insight the principle of MACH must not be applied to a spatial conception "mass", but to the more general four-dimensional conception "action" (energy $\times$ time). From this a kind of four-dimensional causality emerges, which can be expressed as follows in mathematical terms.

The action density $F(x, y, z, t)$ at any point $xyzt$ of space time, in which $x$, $y$ and $z$ are space coordinates and $t$ a cosmical time coordinate, must be a function of the distribution of action throughout all space time. In symbols, we then obtain:

$$F(x, y, z, t) = \int \psi(x, y, z, t, x', y', z', t')\, F(x', y', z', t')\, \sqrt{g'}\, dx'\, dy'\, dz'\, dt' \qquad (46)$$

in which $\psi$ represents the type of (unknown) interconnection, while the integral must be extended throughout space time, which may be curved and closed. $\sqrt{g'}$ is a function of $x'$, $y'$, $z'$ and $t'$, depending on the metric structure of space time.

For an intellect knowing the function $\psi$ in specialized form, it is theoretically possible to solve this integral equation, by which all events throughout space time would be known.

For the rest, eq. (46) can be conceived in such a way that the action density $F(x, y, z, t)$ at any point $xyzt$ of space time can be considered, to some extent, as the superposition of the action densities at all other points $x'y'z't'$, any term of the summation being multiplied by a certain factor:

$$\psi(x, y, z, t, x', y', z', t')\, \sqrt{g'}\, dx'\, dy'\, dz'\, dt'$$

dependent on the nature of this interconnection. Hence, to some extent, we can say that at any point of space time, all other events throughout space time are represented.

An integral equation of the type (46) has in general no solution, unless the function $\psi$ is of special form. If we write more generally $\psi = \lambda^{-1}\, \psi'$, in which $\lambda$ is a parameter, we can find an approximate solution by putting:

$$F(x,y,z,t) = \sum_{i=1}^{n} c_i\, \gamma_i(x,y,z,t), \qquad (47)$$

the $\gamma_i$ being functions chosen in a suitable way, and the $c_i$ unknown constants. Substituting (47) in the integral eq. (46) we find, after arranging:

$$\sum_{i=1}^{n} c_i\, [\lambda\, \gamma_i(x,y,z,t) - \xi_i(x,y,z,t)] = 0, \qquad (48)$$

in which:

$$\xi_i = \int \psi'(x,y,z,t,x',y',z',t')\, \gamma_i(x',y',z',t')\, \sqrt{g'}\, dx'\, dy'\, dz'\, dt'. \qquad (49)$$

The integral in (49) must be extended throughout space time. Determining the constants $c_i$ in such a way that (47) satisfies (46) at $n$ points scattered

throughout space time, we obtain by (48) $n$ homogeneous equations in the $c_i$, from which the unknown quantities $c_i/c_j$ can be solved, after determination of $\lambda$ from the equation:

$$D = 0, \tag{50}$$

$D$ being the determinant of the system.

For the rest, the method of least squares can also be applied. Writing (48) in abbreviated form:

$$\sum_{i=1}^{n} c_i \eta_i = 0,$$

we then obtain for the $c_i$ the set of equations:

$$\frac{d}{dc_j} \int \left[ \sum_{i=1}^{n} c_i \eta_i \right]^2 \sqrt{g}\, dx\, dy\, dz\, dt = 0, \qquad (j = 1, 2 \ldots n),$$

in which $\sqrt{g}$ is a function of $x,y,z$, and $t$.

Or:

$$\sum_{i=1}^{n} c_i \int \eta_i \eta_j \sqrt{g}\, dx\, dy\, dz\, dt = 0, \qquad j = 1, 2 \ldots n, \tag{51}$$

the integral being extended throughout space time. $\lambda$ then follows from the equation:

$$D' = 0, \tag{52}$$

$D'$ being the determinant of the system (51).

If the metric structure of space time is conceived as dependent on $F(x,y,z,t)$, the integral eq. (46) becomes an equation of non linear type. Further it may be of some interest to observe that, if space time were flat and infinite, and the action density finite throughout space time, and if further the function $\psi$ were only dependent on the interval, the convergence of this function would necessarily be stronger than the convergence of the reciprocal of the fourth power of the interval.

Further the reversed problem, to determine the function $\psi$, if $F(x,y,z,t)$ throughout space time would be known, is of interest. We can then assume as approximation of $\psi$:

$$\psi = \sum_{i=1}^{n} c_i \gamma_i'(x,y,z,t,x',y',z',t') \tag{53}$$

in which the $\gamma_i'$ are functions, chosen in a suitable way.

Substituting (53) in (46), we find:

$$F(x,y,z,t) = \sum_{i=1}^{n} c_i\, \alpha_i(x,y,z,t), \tag{54}$$

in which:

$$\alpha_i(x,y,z,t) = \int F(x',y',z',t')\, \gamma_i'(x,y,z,t,x',y',z',t') \sqrt{g'}\, dx'\, dy'\, dz'\, dt', \tag{55}$$



Vol. 4 1958

in which the integral must be extended throughout space time. Applying the method of least squares, the $c_i$ can be computed from the equations:

$$0 = \frac{d}{dc_j}\int\left[F(x,y,z,t) - \sum_{i=1}^{n} c_i \alpha_i\right]^2 \sqrt{g}\,dx,\,dy,\,dz,\,dt \Bigg\}, \qquad j = 1, 2 \ldots n \tag{56}$$

in which $\sqrt{g}$ again is a function of $x,y,z$, and $t$, the integral being extended throughout space time. Carrying out (56), we then obtain the system:

$$\int F(x,y,z,t)\,\alpha_j(x,y,z,t)\,\sqrt{g}\;dx\,dy\,dz\,dt = \sum_{i=1}^{n} c_i \int \alpha_i(x,y,z,t)\,\alpha_j(x,y,z,t)\,\sqrt{g}\;dx\,dy\,dz\,dt \Bigg\} \tag{57}$$

$$j = 1, 2 \ldots n$$

from which the $c_i$ can be solved.

For the rest it may be observed that, if we confine our attention to the distribution of action on a cosmical scale, disregarding the fluctuations of smaller order of magnitude, it is very well possible that the corresponding function $\psi$ obtains a less complicated form, suitable for mathematical treatment.

From the foregoing it follows that no event exists on itself; an event is only real by its relations with all other events. Now we have to emphasize that the cosmical time coordinate $t$ in eq. (46) may not be identified with the time coordinate in the special theory of relativity. It will be obvious that the system of coordinates $xyzt$ in (46), embracing the whole universe in space and time, must be chosen in such a way that thereby the "function of universal interdependence" $\psi$ becomes as simple as possible. In order more nearly to determine this most suitable system $xyzt$, we must know something more of the space time structure of the universe as a whole.

Now the conception "universe" implies in the very first place the feature of *completeness*, so that the geometrical representation of the universe ought to express this feature. Now the plain idea of a time endless in past and future and of space of infinite extent, that is the conception of a universe infinite in space and time, has essentially the characteristic of non completeness. For whatever extension it may be thought to have, it always has to surpass its own limits in order to embrace more without ever becoming all embracing. But just the conception "universe" is equivalent with "all embracing existence". Hence if we really believe in the universe (= "all embracing existence"), we have to accept that it is of finite extent. Or better said: we must try to represent it in geometrical terms by an image of finite extent, because only in doing so an infinite regression of "all embracing" existence is avoided.

Further there must be with respect to any event, past and future, and with respect to any body, a surroundings of other bodies, so that the image may not be bounded, neither in time, nor in space. Hence space time must be not bounded and nevertheless finite, in the same way as a closed surface is not bounded in itself, although finite in extent. Another general point of interest is, that the physical properties of material systems vary if all dimensions are increased or decreased in the same ratio. Hence the geometry of space time has also to reflect this general feature, and must therefore be *not* invariant as to conformal transformation.

Going on, it seems a reasonable hypothesis that everywhere in the universe, throughout a region of sufficient large dimensions the general (over all) structure of interdependence of the events, that is the general structure of space time, is the same. In this way we come to the idea of a hyperspherical space time model, in which space time is represented by a four dimensional spherical surface.

Let us now turn — after these reflections — to the physical world as it appears to our senses. This visible world then appears to us as an enormous system of clusters of galactic systems (spiral nebulae) which are on a large scale evenly distributed in space.

Now the most remarkable feature of this gigantic system of clusters of galaxies is that it expands, in such a way that all the mutual distances increase with time, and every galactic cluster can be considered as the center of expansion. It is this universal tendency of scattering, by which we can really speak of a universe, instead of a mere haphazard aggregate of masses. According to HUBBLE, taking into account the newest estimates, the speed of recession increases at a rate of about 55 km/sec per million light years.

Hence assuming in first approximation this expansion as linear with time "since the beginning" (in which now time is a cosmical time coordinate), this beginning must be some 5500 million years ago. In our spherical space time, this "beginning" is no absolute birth of the universe, but only a radiant of worldlines of galactic clusters. In other words on the cosmical scale we have to do with a system of galactic worldlines, radiating from a point. These world lines will be geodesics (large circles on the four dimensional spherical surface). Then, in order to account for an approximate linear expansion "since the beginning", we must assume that the radius of space time is very large in comparison to the geodesic distance of the radiant. If we accept in this model for space and time the same natural units as in the special theory of relativity (which seem to express a still mysterious feature of the absolute world), this geodesic distance (in four dimensional sense) would be 5500 million light years.

Vol. 4 1958

The way in which this hyperspherical model of space time can be tested by an astronomical program of observation has already been indicated in a B.I.S. article [4]. The interesting question, if the galacted radiant observed be the only radiant of space time or not, will not be discussed here. If there were only one radiant, we should obtain an elliptical space time model, a slightly modified kind of spherical continuum in which opposite points are considered as identical.

Accepting the cosmical space time structure indicated above as a rough approximation of the truth, we are now enabled to specify our natural reference system $x,y,z,t$ in eq. (46).

As expression of the squared line element of spherical space time we obtain:

$$ds^2 = r^2 \left[dT^2 + \sin^2 T \left\{dX^2 + \sin^2 X \left(d\vartheta^2 + \sin^2 \vartheta \, d\varphi^2\right)\right\}\right] \tag{58}$$

in which $r$ denotes the radius of space time and $X$, $\vartheta$ and $\varphi$ are the coordinates of instantaneous spherical space. The time $T$ (expressed in arc measure) is *cosmical time*; the cosmical time direction in any small and therefore practically flat region of hyperspherical space time is prescribed; it is the direction of the worldline of a point with respect to which the distribution of the speeds of the spiral nebulae is radial symmetric, the radial speeds increasing with the distance. For the rest the choice of the space coordinates $X$, $\vartheta$ and $\varphi$ is not prescribed.

The center of gravity of the Milky Way system can practically be considered as such a point, and in connection with this, also the earth. (Thereby we assume that the speeds of the spiral nebulae are only due to the expansion of space; small superimposed motions are disregarded.)

From the above it follows that in the model advanced, *only by orientation with respect to the radiant of galactic cluster worldlines, the cosmical time coordinate can be defined.* This is in accordance with the remark advanced above, that the "cosmical expansion" is the first physical evidence that we can really speak of a universe and not only of a haphazard aggregate of events. If there would be more galactic radiants in space time, cosmical time comparable with our ordinary conception of time can only have physical significance in the neighbourhood of a radiant. Of course we can then mathematically extend our cosmical time (with "our" radiant as base of orientation) throughout spherical space time, in the same way as we can imagine meridians subdividing the terrestrial surface. But this extrapolated cosmical time will then only correspond with our sense of time in the neighbourhood of our radiant. If we split up the four dimensional world in space and time as defined by (58) we obtain a harmonically oscillating spatial world of which the intergalactic world space is spherical. The radius of space curvature then becomes in connection with (58):

$$R = r \sin T. \tag{58'}$$

Then in connection with the natural units of space and time as they appear to give the most simple description in the range of the special theory of relativity, we may expect that the present radius of curvature will be of the order of magnitude of 5500 million light years.

However, we have to bear in mind that the actual world is the hyperspherical world of events, and that the conception of an oscillating spatial world is only a restricted view, approaching our ordinary life conceptions. Further this oscillating spatial world is only the complete counterpart of the whole if the structure of the visible universe (in space and time) can be extrapolated over the whole. In that case of elliptical space time — which in itself only *is*, being neither static, nor dynamic, $T$ only varies from 0 to $\pi/2$. Returning to the integral eq. (46) this equation becomes in case of spherical or elliptical space time, as defined by (58):

$$F(X, \theta, \varphi, T) = r^4 \int \psi(X, \theta, \varphi, T, X', \theta', \varphi', T') \cdot$$

$$\cdot F(X', \theta', \varphi', T') \sin^3 T' \sin^2 X' \sin \theta' \, dX' \, d\theta' \, d\varphi' \, dT', \tag{59}$$

in which the integral must be extended throughout space time.

Now returning to relativistic rocket mechanics, it seems logical to introduce the general metric field defined everywhere (or at least in our cosmical space time neighbourhood) by the observer for which the distribution of the recession speeds of the clusters of galaxies is radial symmetric. In connection with the foregoing considerations it seems very probable that the speed of any vehicle with respect to this general metric field will be of predominant importance as to the processes, going on in the vehicle. The coordinates in (59) also refer to this general metric field.

It will be obvious that a terrestrial system of reference including terrestrial time, with the earth as origin, not rotating with respect to the celestial sky (or better the sky of galaxies) practically coincides with the general metric field as defined above, in the small and therefore flat region of our cosmical neighbourhood.

The function $\psi$ in (59) must be such that the solution $F(X,\theta,\varphi,T)$ of the eq. (59) gives a distribution of action density, defining the events throughout space time in such a way that in any small and therefore flat region also the reciprocal LORENTZ contraction and the reciprocal time dilatation is accounted

for, as described by the formulae of the special theory of relativity, if we compare the measurements of an observer at rest with an observer in uniform motion, with the special addition that "at rest" refers to the general metric field. By this addition we only *seem* to return to the old conception of absolute motion. For there are no instantaneous objects in the four dimensional world "which move", but only *events*.

In our considerations above we have still assumed that the red shift of spectral lines of the distant nebulae must be explained in convential way as DOPPLER-effect, leading to the conception of an expanding universe. However, we have still to bear in mind that in cosmology we have to deal with values of time, of distances and of large scale physical phenomena which far exceed our terrestrial experience.

Considering the latest preliminary results of the investigation of the large scale distribution of matter, it appears that the stellar systems are arranged in *clusters of galaxies*. These clusters appear to be space fillers, so that only by way of exception a galaxy belongs to no definite cluster at all. In case of globular clusters of galaxies, the density distribution appears to be similar as in an isothermic gassphere, satisfying the well-known differential equation of EULER [5]. Hence the tendency of clustering is produced by gravitation. Further the average speed of galaxies in a cluster relative to their neighbours is of the order of magnitude of 100 km/sec. to 5000 km/sec.; on the other hand, no lateral motions of galactic clusters with respect to one another have been observed. This whole dynamical image of the visible world points into the direction of a *static* universe. Moreover, investigating the frequency of clusters of galaxies as a function of their angular diameters, the preliminary results of observation also favour the hypothesis of a *non*-expanding universe, whereas the radius of space curvature (assuming spherical space) obviously appears still to be too large for detection [6]. Therefore ZWICKY suggests that the universal red shift in the spectra of very remote objects may be caused by a transfer of energy from the traveling light quanta to a possible immense background of zero energy of the whole universe.

Vol. 4 1958

Hence, in connection with these newest observational results we have — for sake of completeness — also to consider the possibility that the spatial universe is non-expanding. Thereby also the discordance between the age of the spatial universe and the age of the celestial objects, as required in astrophysical theories, would disappear.

Now in case of a static universe, if intergalactic space is spherical — which again may be assumed in connection with the same general reasons as advanced before — the radius of space curvature must be constant with "time", in which "time" refers to any observer at rest with respect to the galactic cluster centers.

Then as to space time as a whole, assuming homogeneity of metric structure, two main possibilities can be advanced: space time may be either cylindrical, being infinite in time direction, or space time may be spherical.

It seems not to be very probable that the image of a cylindrical space time is in accordance with the actual universe. For if there were an infinite past time, it seems inconceivable that the universe is still in a state of energy far from complete dissipation.

If space time is spherical and the radius of space curvature is constant with time, instantaneous space can only be represented by a largest three dimensional spherical manifold in space time, so that the radius of space curvature and the radius of space time must coincide and be equal every-where. This largest threedimensional spherical manifold is then at the *here-now* in question, perpendicular to the local time direction, which may vary with the local entropy

gradient or direction of worldlines. Hence this instantaneous space must be only considered as an extrapolation of the flat spatial region of this here-now.

The radius of space curvature (identical with the radius of space time) could then be determined in principle by counts of centers of clusters of galaxies in different concentric spherical shells of definite thickness, as follows: let $n$ be the number of centers of galactic clusters per unit of volume in our flat neighbourhood. Then the total number of galactic clusters at distances between $R\,X$ and $R(X + dX)$ (in which $X$ denotes the geodesic distance in arc measure) becomes:

$$4\pi R^2 \sin^2 X \cdot R\,dX \cdot n = 4\pi R^3 \sin^2 X\,dX \cdot n = A.$$

The distance (between $R\,X$ and $R(X + dX)$ can be measured by using the constant of HUBBLE for the red shift, determined within our flat neighbourhood, assuming in first approximation that this quantity is independent on the distance of the clusters. Hence we have to count the number of galactic clusters of which the galaxies have red shifts between the corresponding limits, so that $A$ can be determined observationally. If we only investigate in this way a solid angle $\omega$ of the sky, and denote the corresponding counted number by $A'$, we obtain:

$$A = \frac{4\pi}{\omega} A'.$$

On the other hand, if intergalactic space were flat, the number of galactic clusters at distances $R\,X$ and $R(X + dX)$ would be:

$$n \cdot 4\pi R^2 X^2 R\,dX = n \cdot 4\pi R^3 X^2\,dX = B,$$

so that $B$ can be computed. We then further obtain:

$$\frac{A}{B} = \frac{\sin^2 X}{X^2}, \qquad \text{or} \qquad \sqrt{\frac{A}{B}} = \frac{\sin X}{X}. \tag{60}$$

Further the distance $D = R\,X$, hence

$$R = \frac{D}{X}. \tag{61}$$

Now in (60):

$$\sin X = X - \frac{X^3}{3!} + \frac{X^5}{5!} - \text{etc.},$$

so that:

$$\sqrt{\frac{A}{B}} = 1 - \frac{X^2}{3!} + \frac{X^4}{5!} - \text{etc.}$$

Neglecting $X^4$, etc., we obtain:

$$\frac{X^2}{3!} = 1 - \sqrt{\frac{A}{B}}, \qquad \text{or} \qquad X = \sqrt{6\left(1 - \sqrt{\frac{A}{B}}\right)}. \tag{62}$$

Hence the radius of space curvature the follows from:

$$R = \frac{D}{\sqrt{6(1 - \sqrt{A/B})}}. \tag{63}$$

Of course $R$ may then turn out to be much too large for detection with the telescopic power available for the first time to come.

Concluding, it will be obvious that in our considerations of relativistic rocket motion above, the general metric field will now (in case of a static universe) be determined by all observers everywhere at rest with respect to the general mass of galactic clusters.

If $S_1$, $S_2$ and $S_3$ are the centers of three galactic clusters, we can define $S_1$ as the origin of a rectangular system $xyz$, whereas $S_2$ is situated on the $x$ axis and $S_3$ in the $xz$ plane. We thereby assume that the spatial region embracing $S_1$, $S_2$ and $S_3$ is sufficiently small, so that it can be considered as a flat region. *In case of an expanding universe*, $S_2$ and $S_3$ have only radial speeds with respect to $S_1$, so that as to the system $xyz$ there will be no centrifugal field due to rotation. The system $xyz$ then locally represents the general metric as defined above. Only with respect to this system $xyz$, or as to a system $x'y'z'$ having a *uniform motion* with respect to system $xyz$, the fundamental dynamical eq. (2) may be applied — disregarding gravitational fields.

Hence from the dynamical point of view, only the *acceleration* as to the general metric field (being locally the system $xyz$ mentioned above), or as to any other inertial system $x'y'z'$ as defined above, is of fundamental importance. By this acceleration in general the mass

$$\frac{m_0}{\sqrt{1-(v^2/c^2)}}$$

increases, and remains constant as long as $v$ remains constant. The time dilatation can then be dynamically "explained" as due to this increase of mass.

Vol. 4 1958

Summarizing the interdependence of general metric field and time dilatation we can say: only if the space ship accelerates or decelerates with respect to the general metric field there will be as to the space ship system of reference an inertia field. Also, if the acceleration of the space ship with respect to the general metric field is unless zero, there will be a rate of variation of the rate of the space ship clock as to any system of reference having a uniform motion with respect to the general metric field. This rate of variation will be a deceleration of the rate of the space ship clock if the relative speed of the space ship clock increases and an acceleration of the rate of the space ship clock, if the relative speed of the space ship decreases.

(In mathematical symbols we have:

$$\frac{dt_0}{dt}=\sqrt{1-\frac{v^2}{c^2}}=\left(1-\frac{v^2}{c^2}\right)^{1/2}$$

$$\frac{d^2t_0}{dt^2}=-\frac{(v/c^2)\,(dv/dt)}{\left(1-(v^2/c^2)\right)^{3/2}}$$

in which $v$ denotes the numerical value of the relative speed.
Hence if

$$\frac{dv}{dt}>0,\ \frac{d^2t_0}{dt^2}<0,$$

$$\frac{dv}{dt}<0,\ \frac{d^2t_0}{dt^2}>0.$$

As soon as

$$\frac{dv}{dt}=0,\ \frac{d^2t_0}{dt^2}=0,$$

so that then the rate of the space ship clock with respect to the used inertial system of reference will be constant. In accordance with the rate of the space ship clock, the rate of all physical processes going on in the space ship will be varied.)

## References

1. H. G. L. Krause, Relativistische Raketenmechanik. Astronaut. Acta **2**, 30 (1956).
2. J. Ackeret, Zur Theorie der Raketen. Helvet. Physica Acta **19**, 103 (1946).
3. E. Sänger, Die Erreichbarkeit der Fixsterne; Abbildung 2. Kongreßvortrag Rom, 1956.
4. J. M. J. Kooy, Space Travel and Future Research into the Structure of the Universe. J. Brit. Interplan. Soc. **15**, 248 (1956).
5. F. Zwicky, Morphological Astronomy, p. 135. Berlin-Göttingen-Heidelberg: Springer, 1957.
6. Ibidem, pp. 166—170.

Vo
4
19

Vol.
4
1958

# Interplanetary Ballistic Missiles
# A New Astrophysical Research Tool[1]

By

**S. F. Singer[2]**, ARS

(*Received April 4, 1957*)

**Abstract — Zusammenfassung — Résumé**

**Interplanetary Ballistic Missiles, a New Astrophysical Research Tool.** The idea of exploding an H-bomb on the moon must have occurred to many people and no originality can be claimed for the concept. However, no proposal seems to have been put forward which is at all realistic or indicates a good reason for such an undertaking. Yet an agreement on atomic disarmament may raise the question of how to dispose of the bombs usefully.

The purpose of the present paper is to show that the explosion of an H-bomb carried to the moon by means of a missile is completely feasible and approximately equal in difficulty to the firing of an ICBM (Intercontinental Ballistic Missile) with an H-bomb warhead; to show that it is desirable from the point of view of testing, and worthwhile scientifically. These three factors combined, in the author's opinion, make such a project highly desirable. Most of the paper is devoted to the many astrophysical applications of this new research tool; the legal and geopolitical aspects of this operation are beyond the scope of this paper.

**Interplanetarische ballistische Geschosse, ein neues astrophysikalisches Forschungsgerät.** Der Gedanke, eine Wasserstoffbombe auf dem Mond explodieren zu lassen, muß vielen Leuten gekommen sein; für diesen Plan kann keinerlei Originalität beansprucht werden. Immerhin scheint kein Vorschlag gemacht worden zu sein, der überhaupt realistisch ist oder eine gute Begründung für ein solches Unternehmen gibt. Ein Abkommen über Atomwaffenabrüstung muß aber die Frage aufwerfen, wie man die Bomben nützlich verwenden kann.

Der Zweck der vorliegenden Arbeit ist es, zu zeigen, daß die Explosion einer Wasserstoffbombe, die mittels eines ferngelenkten Flugkörpers auf den Mond gebracht wird, durchaus ausführbar und in ihrer Schwierigkeit annähernd gleich dem Abfeuern eines interkontinentalen ballistischen Flugkörpers mit einem Wasserstoffbomben-Kriegskopf ist. Es soll ferner gezeigt werden, daß dies einerseits vom Standpunkt der Erprobung wünschenswert, anderseits wissenschaftlich lohnend ist. Die Zusammenfassung dieser drei Gesichtspunkte macht nach Ansicht des Verfassers ein solches Projekt äußerst anstrebenswert. Der größte Teil der Untersuchung ist den vielerlei astrophysikalischen Anwendungen dieses neuen Forschungsgerätes gewidmet; die gesetzliche und geopolitische Seite des Unternehmens liegt außerhalb des Gesichtskreises dieser Arbeit.

---

[1] Presented at the VIIIth International Astronautical Congress at Barcelona, Spain, October 6—12, 1957.

[2] Professor of Physics, Physics Department, University of Maryland, College Park, Md., USA.

**Engins Balistiques Interplanétaires, instrument nouvel de recherche de l'astrophysique.** L'idée de faire exploser une bombe H sur la lune doit avoir germé dans plus d'un esprit et ne peut être considéré comme originale. Cependant aucune proposition réaliste ou bien motivée n'a été avancée pour la réalisation d'un tel projet. Et pourtant un accord en matière de désarmement atomique soulèverait le problème d'utiliser à bon escient les bombes existantes.

Le but du présent article est de montrer que l'explosion d'une bombe H, portée jusqu'à la lune par un engin, est une entreprise réalisable, d'une difficulté équivalente au lancement d'une fusée balistique intercontinentale avec tête atomique. De plus cette entreprise, interéssante en tant qu' essai, serait riche d' enseignements scientifiques. Dans l'opinion de l'auteur, ces facteurs combinés rendent la réalisation de ce projet hautement désirable.

L'article est surtout consacré aux nombreuses applications astrophysiques de ce nouvel instrument de recherche. Les aspects légaux et géopolitiques de l'opération sortent du cadre de ces considérations.

## Introduction

It is safe to say that there are probably not very many peaceful applications for thermonuclear explosions. Yet if a general atomic disarmament is agreed upon, some applications must be found for existing bombs.

Certainly exploding such devices far away from the earth is a desirable step. An explosion on the surface of the moon is not only peaceful but also useful and, therefore, worthwhile. In particular, such explosions can provide a new astrophysical tool which can tell us a great deal about the environment of the earth, the properties of the interplanetary medium, and in general deepen our understanding about the nature of the universe.

The transportation of the thermonuclear device to the moon involves rockets and guidance techniques which are of importance for astronautics. It is, therefore, appropriate that this paper be presented at the VIIIth Congress of the International Astronautical Federation. In fact, we as astronautics enthusiasts should take special pride in the fact that astronautics provides at least one peaceful application of thermonuclear weapons.

A project to explode thermonuclear bombs on the surface of the moon raises many problems and questions. Some of them at least will be answered in this paper, e.g.: (1) How difficult is such a program compared, for example, with firing an ICBM; (2) What are the hazards involved in such an operation; (3) Will the flash from the explosion blind us; (4) Will the surface of the moon be destroyed; (5) Will the orbit of the moon be affected; (6) What can we observe about the explosion, in addition to the light flash; (7) What after-effects are likely to be encountered and how will they affect life on the earth; (8) What precisely can we learn about the nature of the interplanetary medium, about the environment of the earth, about the surface of the moon? (9) How could we start, and how soon?

The explosion of H-bombs on the moon is certainly an intermediate goal. A less ambitious proposal, and a necessary first step, would be to explode bombs beyond our atmosphere at varying distances. Such experiments can give us important information about astrophysical quantities, e.g., the density of hydrogen gas in the vicinity of the earth. But there has been something about the moon which has intrigued man for centuries and the idea of creating a permanent crater as a mark of man's work is an appealing one. Also the scientific pay-offs are considerably higher.

The growth potentials of this set of experiments are in two directions. (1) One would be to explode thermonuclear devices on other planets as well, in order to study the composition of their atmospheres, perhaps by studying the selective absorption of the light flash from the explosion or an induced photoluminescence. (2) Once we have learned to explode safely thermonuclear devices away from the earth, we can construct truly cosmic thermonuclear devices resembling stars and we can, therefore, initiate a new experimental field of astrophysics: star making. Much may be learned from such pursuits, perhaps even the secret of carrying on a safe continuous

thermonuclear reaction on the earth for the purpose of producing electric power. Certainly this is one of the most challenging of all problems facing mankind at the present time.

The discussion in this paper will be on a non-mathematical level, although it will be made quite evident how the conclusions are calculated. For those who wish to do so, an appendix is available. The accuracy of calculation is not particularly high and can be improved mainly by using data on H-bomb explosions which are at the present time not openly available. However, order of magnitude results are quite satisfactory for the purpose of the present paper.

The purpose of this paper is to propose the establishment of IPBM's (Interplanetary Ballistic Missiles) which, armed with a hydrogen bomb warhead, could be used to blast craters on the surface of the moon. In this paper we (A) first develop a justification and discuss the many advantages of such a scheme and try to show how this type of weapon testing may promote world peace. We next take up (B) the interesting technical aspects of this operation to establish feasibility, and finally discuss (C) scientific benefits of this kind of operation.

Vol. 4 1958

## A. Advantages of IPBM's

Sending IPBM's to the moon in order to explode H-bomb warheads seems to have several very attractive features, not the least of which is the large distance of the moon from the earth (384,400 km or 240,000 miles). As H-bombs become more powerful, the point will soon be reached where tests on the earth may present a health hazard to the world's population as a whole, including the nation conducting the tests. Our proposal would do away with this hazard by exploding H-bombs on the moon, and measuring their performance from the earth: (1) by means of gamma-ray detectors in the high atmosphere, (2) the light flash from the ground, (3) by carefully scaling the lunar crater produced by the explosion. By these methods (discussed later) one can judge quite easily the effectiveness and power of the H-bomb device. The H-bomb race between the big powers would then be reduced to the much more tractable problem of seeing who could make a bigger crater on the moon.

This scheme has many advantages: (1) First of all it can give a good record of the power of the H-bomb for all to see. By conducting the explosion on the moon and in full view of all nations, any competent scientist will be able to deduce the effectiveness of a similar explosion on the earth.

(2) H-bomb testing on the earth is difficult and expensive, particularly for the larger weapons[1]. It must be difficult also to measure the efficiency of the H-bomb explosion on earth because of the influence of the atmosphere, and terrain. For example, most of the radiant energy of the bomb is absorbed by the atmosphere which takes up momentum and produces a strong pressure wave. A test conducted on the moon in a condition of vacuum would permit a better calculation of the energy output and therefore of the efficiency of the bomb.

(3) The testing of long-range space vehicles is also difficult. There are no test ranges in existence which extend over half the globe, and in any case, it would be difficult to find someone to check the accuracy of the impact point at the other end. This problem does not exist with a moon rocket since there the impact point is clearly in view. However, to make it visible one needs an indicator and an H-bomb explosion does provide such an indicator. It is therefore apparent

[1] Cost of Operation Redwing is quoted as more than $ 150 million (Pegasus, Aug. 1957).

that the combination of an IPBM plus H-bomb makes a nice package for testing both the missile and the warhead. That this test is realistic both from the point of view of propulsion and guidance is discussed later in Section B.

(4) An additional point is that after the test is completed, and the data from the explosion have been reported, one is left with a nice small crater on the moon which is unnamed and therefore provides unique opportunities for perpetuating the names of presidents, primeministers, and party secretaries.

(5) There need be no limit to the size of such a lunar bomb. Since its use as a weapon on the earth is clearly impractical, it had better be termed a "device" instead of a "bomb". From an astrophysical point of view it would be interesting to construct and test truly cosmic fusion devices, to simulate processes in the interior of stars. With larger devices and higher temperatures one may test new types of fusion reactions; or investigate the effects of rapid rotation leading to mixing; or construct such fusion devices in concentric layers of varying composition to investigate the burning of stars where mixing is inhibited.

(6) Finally, we should mention the actual scientific benefits of such tests. The results of an explosion on the moon's surface can be used scientifically in various ways: a) it gives a means of checking the prediction of the theory of meteor craters; by knowing the energy output of the bomb and measuring afterwards the size of the crater. b) The explosion results in the ejection of a great deal of vaporized rock, of fine dust, and of rock in the form of rubble. A large fraction of the material escapes from the gravitational field of the moon and is captured by the earth's gravitational field. In entering the earth's atmosphere it provides a unique opportunity for meteor observations since the fragments will produce light trails and ionization in the upper atmosphere. The very smallest dust particles probably will not be visible in the atmosphere but their optical effects can be studied by means of the sunlight which they scatter. These problems are discussed in Section C. It will be shown there that studies of this artificially produced "cosmic dust" simulates an enhancement of interplanetary dust and can be used to study the motion of the interplanetary gas with respect to the earth, as well as the effect of interplanetary magnetic fields and of the earth's magnetic field on the motion of the interplanetary gas. We can also study the effects of the dust on the earth's weather and climate.

We have here a new type of probe for studying the conditions in the outermost regions of the earth's atmosphere. The prospects for astrophysics and geophysics from such tests are therefore quite exciting. In Section C we calculate the expected effects, their observability, and indicate the type of results which one may obtain and how they will illuminate for us the conditions existing in the earth's environment and in interplanetary space, as well as the properties of our own atmosphere.

## B. Technical Aspects

We want here to compare the technical problems involved in constructing and testing an IPBM as against the conventional ICBM. The three points considered are propulsion, guidance, and the actual testing of the fusion device.

### *1. Propulsion*

For a ballistic rocket one requires a burn-out velocity of orbital magnitude, approximately 25,000 feet per second; for a moon rocket about 35,000 feet per second or an increase of 40%. Offhand, therefore, the IPBM would seem to require a great deal more in the way of propulsion, perhaps one or two more stages. But this is not quite correct, mainly because the IPBM payload can be

made quite light. For the IPBM the problem of re-entry does not exist since the moon has no atmosphere. Therefore, with no need to protect it from the atmospheric heating, all of the weight of the warhead can be given over to the actual H-bomb. Neither is it necessary to include fuzing mechanisms and other complicated bomb devices. For the IPBM, we need only a small clock, which activates the bomb for a short period after a time interval given by the travel time from the earth to the moon along a predetermined trajectory, plus a simple impact or proximity fuse. The resulting saving in weight of the warhead can, of course, be realized in a simplification of the propulsion system. This would seem to make the problem of an IPBM not much more difficult than an ICBM from a propulsion point of view[1].

### 2. *Guidance*

As can be seen from the comparison in Table I, the guidance problem for a moon rocket is simpler than the corresponding problem for an ICBM designed to hit a target at a distance of an earth radius. In order to make this comparison we have used data published by the RAND Corporation on sample trajectories from the earth to the moon; even if a different regime is used, the data in Table I give an approximate idea of the accuracy required. The lower accuracy required in the IPBM guiding system reflects itself, of course, in a reduction in the weight of the last stage and therefore a reduction in the size and complexity of the over-all propulsion system.

Vol. 4 1958

Table I. *Comparison of guidance accuracy for IPBM and ICBM*

| | Nominal Velocity | Velocity Error | Angular Error |
|---|---|---|---|
| IPBM[a] | 35 000 ft/sec | + 35[b]<br>− 25 | ± 0.1° |
| ICBM[c] | 20 800 ft/sec | ± 2[d] | ± 0.02° horizontal plane<br>± 0.3°[d] vertical plane |

a) GEORGE H. CLEMENT, The Moon Rocket, in "Earth Satellites as Research Vehicles". Philadelphia: Franklin Institute, 1956.

b) To hit surface of moon facing the earth.

c) For a range of 1 earth radius (4000 miles) and a range accuracy of ± 1 mile (along a minimum energy trajectory).

d) R. C. WENTWORTH, private communication.

### 3. *Bomb Testing*

If we take a nominal 20 megaton H-bomb[2], we can calculate the size crater produced on the moon. Within the accuracy of available theories and assuming a detonation below the surface layer of the moon, this turns out to be a crater of angular diameter one second of arc, which is just visible. For a comparison of crater sizes see Table II. The release of this energy will produce a light flash corresponding to a luminous intensity as a star of magnitude −16, or 1/10,000 that of the sun. If we assume a visual acuity of one minute of arc, then to a dark adapted eye the point of light from the H-bomb flash will be twice as bright as a point on the sun. The gamma-rays and neutrons from the explosion will not reach the lower atmosphere and present no hazard; measurement

[1] It is unfortunately not possible to supply actual numbers here.

[2] 1 MT (megaton TNT equivalent) = $4.2 \times 10^{22}$ ergs.

of their radiation flux will, however, give considerable information on the operational efficiency of the bomb and on the absorption properties of the interplanetary gas between the moon and the earth (see discussion in Section C). As can be seen, therefore, exploding an H-bomb on the moon allows an unexcelled measurement of its power, efficiency and radiation properties.

Table II. *Observable effects of lunar H-bomb explosions*

| | Diameter of Crater (ft) | Depth (ft) | Angular Diameter at Distance of Moon | Crater Volume (cu mi) |
|---|---|---|---|---|
| (Arizona meteorite) | 4150 | 700 | 0.67″ | |
| 10 MT bomb[1] | 5500 | 950 | 0.9″ | $3 \times 10^{-2}$ |
| (Ungava, Quebec meteorite) | 11,500 | 1,330 | 1.9″ | |
| 100 MT bomb[1] | 12,500 | 1,800 | 2.0″ | $3 \times 10^{-1}$ |
| 1000 MT bomb[1] | 25,000 | 3,000 | 4.0″ | 2.4 |
| Piazzi Smyth (lunar craters) | 6 mi. | 3,500 | 5.1″ | |
| Mädler (lunar craters) | 20 mi. | 7,500 | 17.2″ | |
| Tycho (lunar craters) | 54 mi. | 12,000 | 46″ | |
| Copernicus (lunar craters) | 56 mi. | 11,000 | 48″ | |
| Clavius (lunar craters) | 146 mi. | 16,100 | 125″ | |

[1] Assuming an explosion below the surface of the moon.

### C. Scientific Aspects

The scientific applications of the lunar H-bomb explosion as a new astrophysical research tool are so numerous and of such great variety that it might be best to organize them under various headings. We will discuss, therefore: (1) the visible phenomena seen from the ground, (2) the *X*-ray and gamma-ray phenomena seen from the top of the atmosphere, and (3) the radio phenomena observable at the earth. All of these constitute electromagnetic radiations coming at the instant of the explosion. Shortly after the explosion, there will arrive on the earth corpuscular radiation consisting mainly of neutrons. Their measurement is discussed under *4*. Finally there will arrive on the earth particles from the lunar crater, ranging from tiny dust particles which filter slowly through the earth's atmosphere, to larger drops which become solidified, up to fair-sized boulders which can be recovered and analyzed chemically; they lose little mass in traversing the earth's atmosphere. The rock gas and the extremely fine dust ("smoke") from the explosion will not reach the earth or at least will not be easily detectable as it reaches the earth; but because of its light scattering power it can be seen by its optical effects, as discussed under point *1*.

#### *1. Visible Effects*[1]

We can describe in a non-mathematical way what an observer on earth may see. Let us assume that the impact occurs on the dark side of the moon, just beyond the terminator line; the observer is located on the night side of the earth. Now a nuclear fusion explosion releases a lot of energy per gram of material, $10^7$ times higher than TNT, which releases $4.2 \times 10^{22}$ erg/$10^{12}$ gm

[1] The use of bomb explosions to produce light flashes has been suggested by K. A. EHRICKE and others, to aid in the acquisition and tracking of space vehicles.

while in the transformation $4\,H \rightarrow He$ about 1/1000 of the mass appears as energy according to the EINSTEIN relation $E = MC^2$. Therefore 1 gm of bomb material produces $10^{-3} \times (3 \times 10^{10})^2 \sim 10^{18}$ erg/gm, assuming 100% efficiency. This energy appears mainly in the form of radiation, although a small fraction will undoubtedly go to the kinetic energy of the bomb material and container. One-half of this energy goes outward from the moon and will be visible on the earth as a brilliant flash of light. The ultraviolet portion of the radiation is absorbed in the high atmosphere, but the gamma-rays will be able to penetrate quite deep into the atmosphere and should be detectable at balloon altitudes. After this initial flash is over, we will begin to see the effects of the radiation directed towards the moon. Again the visible radiation will be absorbed by the adjacent rock which will be immediately vaporized. The gamma-rays and neutrons will penetrate deeper and extend the volume of nearly instantaneous vaporization. The rock gas in this deeper layer will be under high pressure which is released in an explosion. It is this explosion which gouges out a large crater. In the immediate vicinity of the explosion the material will be vaporized; at some distance the rock will be molten, and further still it will be pulverized and broken up into rubble. All of this material will be ejected with high velocity. Most of the volume is ejected in the form of rock dust and rock rubble, very similar to the case of a crater produced by the impact of a meteorite.

Vol. 4 1958

The hot rock gas (with a temperature of at least 2200 °K) will be visible as a point of light, of orange-red color; it slowly expands as the hot gas diffuses from the point of explosion. Its rate of cooling is very slow so that the glow will remain visible for many minutes.

Some seconds after the explosion a new phenomenon comes into view. The escape velocity of the moon is only 2.3 km/sec, while the mean thermal velocity of the rock gas is $\sim 1$ km/sec and the rock dust, too, is ejected with high velocities. As the gas and dust rise above the lunar surface, they will enter the region of solar illumination, with spectacular consequences. The gas will scatter sunlight and start to give off a bluish color, almost as bright as the daylight sky, i.e. not much different from the brightness of the illuminated surface of the moon. The dust on the other hand will diffract sunlight and appear as a white dot which slowly expands.

It now becomes possible to study the diffusion and motion of the rock gas and rock smoke, the latter consisting of very fine particles of about optical size 0·5 micron to a few microns in diameter. Its rate of diffusion will indicate the density of the interplanetary gas between the moon and the earth, while its motion will indicate the motion of the interplanetary gas with respect to the earth. This question of the existence of a streaming effect or "interplanetary wind" is one of the most fascinating aspects of the whole investigation and could shed a great deal of light on the properties of the earth's outermost atmosphere, i.e. the region between 20 to 60 earth radii, the latter being the distance to the moon. In particular, we would like to know about the control of magnetic fields over the motion of the interplanetary gas by studying the motion of the rock gas and the rock smoke. Does the earth's magnetic field still predominate at these distances or has the interplanetary field become strong enough to take over? These studies can be closely tied in with such geomagnetic problems as the origin of the *aurora*, the existence of a ring current to explain *magnetic storms*, and the deflection of low energy *cosmic rays* by magnetic fields near the earth. A solution of the geomagnetic question by means of this new technique would therefore illuminate many of these most urgent astrophysical problems and would tie in with a whole range of other astrophysical phenomena.

### *2. Ultraviolet, X-rays and Gamma-rays*

It may be expected that a good percentage of the electromagnetic radiation from the explosion will be in the ultraviolet region of the spectrum and even in the *X*-ray and gamma-ray region because of the high temperatures produced in the explosion and because of various nuclear reactions which go on. Some of the latter are a result of the absorption of neutrons by materials surrounding the point of explosion. In any case these radiations would come to the earth, having been absorbed more or less depending on their wavelength and depending on the nature and amount of interplanetary gas between the moon and the earth. Herein lies the most interesting application of the measurements, namely to find out what types of gas exists between the moon and the earth, i.e. in the earth's outermost atmosphere, what its state of ionization is, and how much of it there is. Probably the best way to tackle this problem is by measuring the spectrum of the ultraviolet and *X*-ray radiation at various levels of the ionosphere with rocket-borne spectrographs. A good fraction of the radiation will, of course, be absorbed only in the earth's atmosphere itself and will produce an enhanced ionization there which might be directly measurable from the ground by noting increased radio reflections, i.e. by ionospheric sounding methods. Once we reach the region of gamma-rays the absorption coefficient becomes small; they will be able to reach the atmosphere down to balloon altitudes so that measurements will be facilitated.

### *3. Corpuscular Radiation*

A large number of neutrons are emitted in the fundamental fusion reactions of an H-bomb. The energies are as high as several Mev and may range down to very low energies depending on the nature of the materials surrounding the bomb. The fastest neutrons will arrive near the earth about 10 seconds after the explosion and those of lower velocity and lower energy will arrive later. The very slow neutrons will not arrive at the earth for two reasons: (1) They will decay along the way since their halflife is only 12 minutes: Then they become protons and will be affected by the earth's magnetic field and deflected away from the atmosphere. (2) Also, low energy neutrons are likely to be scattered very effectively by the hydrogen nuclei between the moon and the earth. Here again we have a means of measuring the amount of material between the moon and the earth provided our detection methods can be refined sufficiently.

### *4. Radiosignal from the Explosion*

A rather new point which should be considered quantitatively is the production of a large radio burst similar to that produced by a stroke of lightning in the atmosphere. This burst of radio energy comes about because there is created suddenly a large amount of ionized material and the differential expansion of positive and negative charges will undoubtedly carry with it some electromagnetic effects. It now remains to be determined which of these can be detected on the earth. Effects of very high frequency, more than 50 megacycles, propagate through the ionosphere and could therefore be viewed from sea level by means of radio telescopes pointed towards the moon. In the interval between 50 down to perhaps 1 megacycle the ionosphere acts as an effective barrier and if observations are desired they would have to be carried out from rocket-borne receivers at altitudes of at least 200 km. Lower frequency radio waves, however, may penetrate through the ionosphere in a manner very similar to that of the so-called "radio whistlers". If so, they will follow the magnetic lines of force. It would be tremendously important to find

out where the radio energy ends up on the earth: in other words, which magnetic line of force does it follow? There exist now many radio whistler receiving stations. They are quite simple to set up and require only a long wire which acts as an antenna and a high gain audio amplifier. Since large geographic coverage is necessary, amateurs could participate in the observations very effectively. The purpose would be mainly to find the impact zones of the radio power on the earth's surface and thereby establish the probable path of the radio signal and, therefore, the trajectory of the magnetic line of force.

### *5. Lunar Material Captured by the Earth*

The lunar material captured by the earth must be massive enough so that the earth's gravitational field overcomes the forces of the interplanetary wind which tend to blow away the very fine particles, the rock smoke. Here we are considering particles of about 100 micron diameter and larger. These micrometeorites will enter the earth's atmosphere some considerable time after the explosion. Depending on their initial velocity, which must be larger than the escape velocity from the moon (about 2.3 km per sec), they will reach the earth with times as short as a few hours up to several days. This means that they will be distributed rather uniformly over the earth's surface. If they are charged by the solar ultraviolet radiation as recent studies indicate, and if the frictional effect on the gas between the moon and the earth is still appreciable, then they will enter the earth's atmosphere with velocities much smaller than the escape velocity of 11.2 km per sec. But long before they approach the earth's atmosphere itself they will be deflected by the earth's magnetic field because of their charge and low momentum. In fact, it is fairly sure that they will be deflected towards the poles and probably be observed only in the auroral zones. Because of their low velocity they will not produce any spectacular effects in the earth's atmosphere but filter down slowly into the atmosphere and be detected by collection methods from balloons or mountain tops. One interesting detection method which is not usually applicable to micrometeorites could be applied here. Since we can be fairly certain that these particles would be radioactive because of the intensity of neutron bombardment from the H-bomb explosion, radioactive or radiochemical techniques can be used to make the detectors much more sensitive.

Vol. 4 1958

One of the most interesting effects which these dust particles could produce are changes of the earth's weather and associated climatic changes. An important school of thought holds that climatic changes are caused by dust particles, either accreted by the earth as it moves through interstellar dust clouds, or due to dust produced in planetary or asteroidal collisions, or dust produced in volcanic eruptions on the earth itself. Here we can produce a controlled influx of dust in large quantities which can be used to verify some of these hypotheses, e.g. will the incoming dust provide additional nucleation centers for water vapor and thus cause increased rain fall as has been suggested by BOWEN. Will this increased rain fall remove water vapor from the atmosphere, decrease the percentage of cloud cover, therefore lower the albedo and therefore increase the earth's mean temperature? Or will the incoming dust act chiefly as a reflector or diffractor of solar visible radiation, its size being too small to affect the infrared radiation emanating from the earth, with the end result that the albedo will increase and the earth's climate will get colder? It is possible that both effects will happen one after the other. It would be fascinating to be able to study this problem in a controlled laboratory type of investigation.

In a number of places on the earth there have been found little glassy objects called tectites which are thought to be of extraterrestrial origin. UREY, the

noted cosmochemist, has suggested that they are lunar material which has been splashed out when meteorites impacted on the moon, that they solidified on the way to the earth and then landed at sea level. This represents another hypothesis which could be verified by a lunar H-bomb explosion.

Particular interest attaches to the larger or faster objects coming from the moon. The faster objects will act as meteors and produce luminous and ionization effects in the upper atmosphere which will provide us with a controlled means of studying the upper atmosphere, almost like artificial meteors. The larger objects, particularly those which enter with very low velocities, corresponding to the escape velocity from the earth, may land without having lost much of their mass and without having been greatly heated[1]. These objects might impact directly on the earth, or could be captured by perturbations, chiefly by the earth's atmosphere. Such braking ellipses will cause eventual entry velocities of less than 11 km/sec. With these samples in hand we have an unequalled opportunity of studying the nature of the lunar surface material long before we have an opportunity of visiting the moon in person. Even a simple measurement of the density of the rock sample will tell us whether there is stratification of rocks (as in the earth) indicating that the moon has been liquid at one time. Very fascinating chemical analyses can be carried out which undoubtedly will tell us more about the origin of the moon by comparing chemical ratios with those of the earth.

Of particular interest to the writer is the question of how long this surface material has formed the surface of the moon. This may be determined by a method which I have termed the "cosmic ray age" method. As cosmic rays bombard the surface of the moon, they will produce many nuclear disintegrations. In these nuclear disintegrations two interesting nuclides are produced in large quantities, tritium and helium-3. Tritium is radioactive with a halflife of about 12 years while helium-3 is stable. In the samples of lunar surface we could measure both the tritium and the helium-3. The tritium concentration would tell us immediately the present level of cosmic ray intensity hitting the moon. By comparing it with the cosmic ray intensity which we know to exist in free space we could, therefore, tell whether the moon possesses a magnetic field which keeps away some of the cosmic radiation. From the helium-3 content of the sample we can tell immediately how long the sample has been exposed to cosmic rays, i.e. how long it has formed part of the surface of the moon, because the cosmic rays will not produce helium-3 in any material which is more than a few centimeters below the surface. We would expect that the helium-3 content of the sample corresponds to a time interval between the time when the particular portion of the moon was hit by meteorites and the present. This method would then allow us to take various points on the lunar surface and establish a time history for the lunar surface and, therefore, for the bombardment of the lunar surface by meteorites. In this manner we might be able to state when various large meteorites hit the moon and we will be able to tell something about the prehistoric frequency of meteorite impacts. One might expect that it is much higher than the present rate of meteorite impacts but by how much? The answer to this question will tell us much about the origin of meteorites and asteroids.

In summary, we see that experiments carried on by H-bombs shot to the moon (and eventually to other planets) by means of IPBM's will touch on many

[1] The possibility of blasting loose portions of the moon and recovering them on the earth for chemical study has also been suggested by UREY in a recent issue of the journal "Observatory".

problems of current interest, only some of which have been mentioned here. Such experiments will open up fascinating prospects for astrophysics, for cosmochemistry and for studies of the origin of the solar system.

We hope to have demonstrated that the project is both feasible and worthwhile, and can therefore look forward to seeing it become reality in the near future.

**Acknowledgements**

The suggestion to think about the effects of H-bomb explosions in space came from FRED C. DURANT III in a conversation about two years ago. I am especially indebted to Dr. E. J. ÖPIK for discussing critically the contents of the present paper, for contributing many important ideas and for making available to me many of his calculations, some of them unpublished, on meteor craters and related topics.

Vol.
4
1958

# The Communication Satellite[1]

By

**R. P. Haviland[2]**, ARS

(With 12 Figures)

**Abstract — Zusammenfassung — Résumé**

**The Communication Satellite.** The interrelations between an artificial satellite and the earth and the characteristics of satellites are reviewed to determine their effect on communication systems. The requirements for typical communication systems are studied. A set of services are proposed for integration into a large communication satellite.

**Der Satellit für Übermittlung von Informationen.** Die gegenseitigen Beziehungen zwischen einem künstlichen Satelliten und der Erde sowie die Charakteristika von Satelliten werden untersucht, um ihre Auswirkung auf Nachrichtenübermittlungs-Systeme zu bestimmen. Die Erfordernisse für typische Übermittlungssysteme werden studiert. Es wird vorgeschlagen, einen Satz von Einzeldiensten in einem großen Informationssatelliten zu vereinigen.

**Le Satellite d'Information.** Les caractéristiques des satellites et de leurs orbites sont passées en revue du point de vue de leurs possibilités comme transmetteurs d'information. Les performances exigées des systèmes de télécommunication sont mises à l'étude. On propose un ensemble de services d'information à intégrer dans un grand satellite artificiel.

The use of the satellite vehicle as a platform or base for communication services has been proposed previously [1, 2, 3]. This paper extends consideration of the requirements for such service in some detail, in order to arrive at the optimum conditions for design and operation of such a service.

The basic factor which makes the satellite attractive is its height. It is equivalent to a radio station having a very high antenna mast. This extends the line-of-sight coverage, and makes the use of very high radio frequencies for long distance communication feasible (as will be seen, it also makes the use of the ultra-high frequencies necessary).

The approach of this paper is to review first those characteristics of satellites, and of the satellite-earth system which affect the communication service. Next some of the aspects of communications are considered. Finally, some of the possible communication services are studied. In all cases the approach is that of the system engineer interested in established the magnitude of the problem rather than a detail solution. This is accomplished by the use of simplified models and approximations, rather than by exact solutions.

---

[1] Presented at the VIIIth International Astronautical Congress at Barcelona, Spain, October 6—12, 1957.

[2] Missile and Ordnance Systems Department, General Electric Company, Philadelphia 4, Pa., USA.

Vol. 4 1958

### A. Coverage

The problem of coverage by the satellite can be divided into three parts:

a) The instantaneous coverage of a single satellite station.

b) The total coverage of a single station.

c) The number of stations required to give continuous coverage to a given point on the earth's surface.

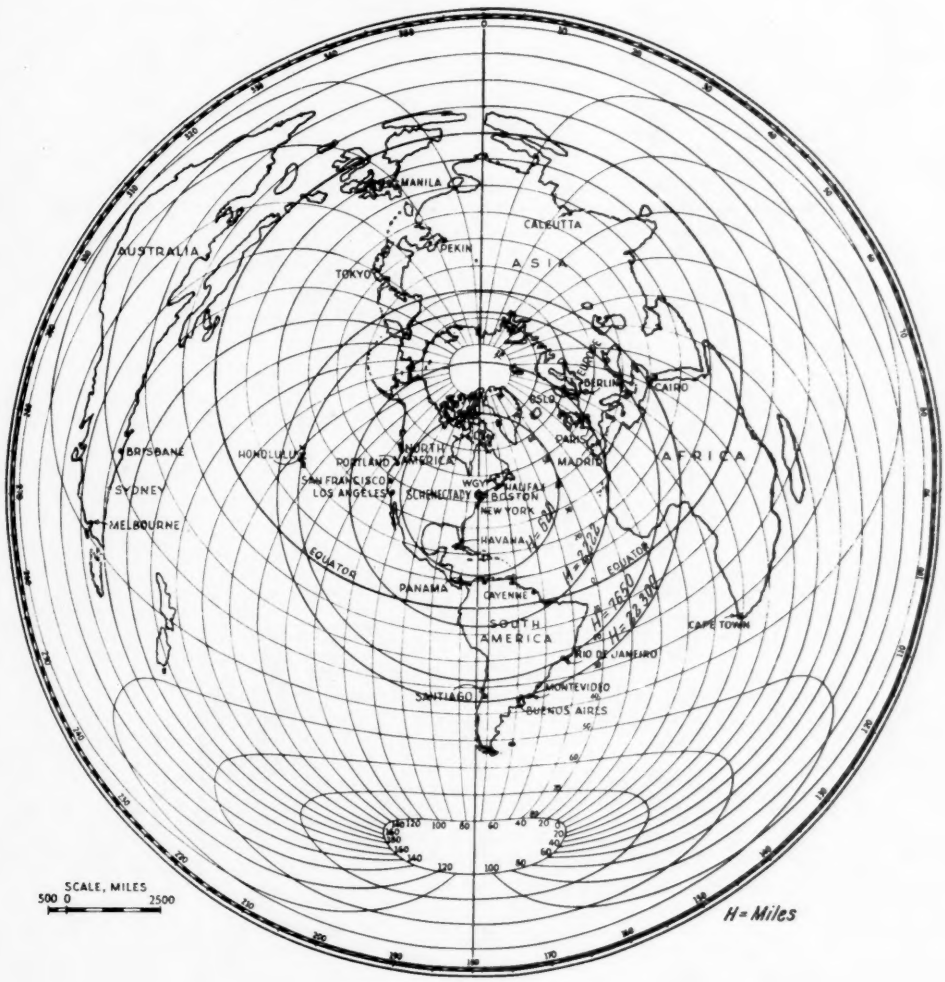


Fig. 1

The instantaneous line-of-sight coverage of a single station is readily calculated from geometrical considerations: these values are shown in Table I. The relative coverage for various heights is shown by the chart of Fig. 1. It is evident that the coverage is large even for modest heights.

The total coverage for a single station is shown in Table II for the three conditions of an equatorial, polar and 45° inclination orbits. It is evident that

Table I. *Instantaneous Coverage of a Satellite*

| Height Miles | Vision Arc Miles | Subtended Angle Degrees | % of Earth |
|---|---|---|---|
| 257 | 2,800 | 140 | 3.0 |
| 620 | 4,200 | 120 | 6.7 |
| 1,210 | 5,600 | 100 | 11.7 |
| 2,222 | 7,000 | 80 | 17.8 |
| 4,000 | 8,400 | 60 | 25.0 |
| 7,650 | 9,800 | 40 | 32.9 |
| 19,000 | 11,200 | 20 | 41.3 |
| 22,300 | 11,800 | 17 | 42.6 |

Table II. *Total Coverage of a Single Satellite*

| Height | Max Latitude of Coverage, Equatorial Orbit | Time to Next Passage, Equatorial Orbit, Hours | Max Latitude of Coverage 45° Inclined Orbit | Max Interval Between Coverage, Hours | |
|---|---|---|---|---|---|
| | | | | Equatorial | Polar |
| 257 | 20° | 1.7 | 65° | 1.51 | 9.35 |
| 620 | 30° | 1.9 | 75° | 1.59 | 8.00 |
| 1,210 | 40° | 2.3 | 85° | 1.79 | 6.66 |
| 2,222 | 50° | 3.0 | 90° | 2.17 | 5.34 |
| 4,000 | 60° | 4.6 | 90° | 3.06 | 4.00 |
| 7,650 | 70° | 9.7 | 90° | 5.92 | 2.66 |
| 19,000 | 80° | 97.5 | 90° | 54.6 | 1.33 |
| 22,300 | 81.5° | (a) | 90° (b) | 0 (a) | 1.13 (c) |

(a) Appears stationary over a point on the equator.
(b) Appears to move from 45° N to 45° S.
(c) Appears to move from 90° N to 90° S.

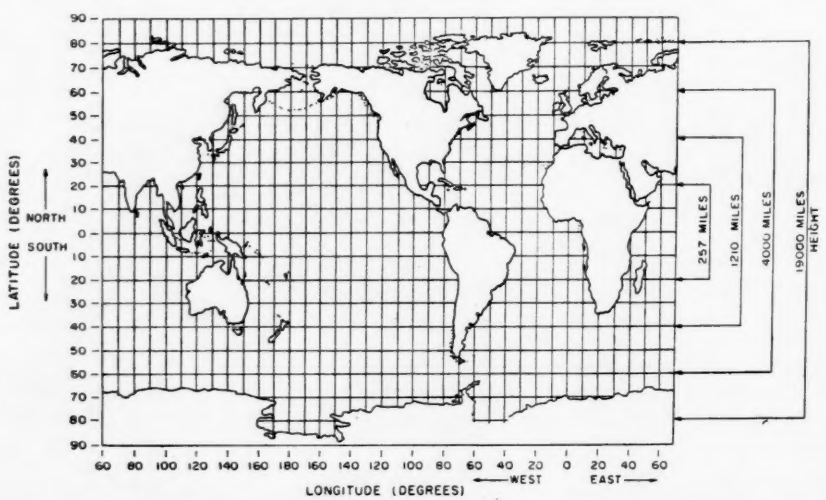


Fig. 2

the polar and inclined orbits are not desirable, since they increase the coverage of uninhabited regions at the expense of more desirable areas, and since the time to return is large compared to the orbital period. For these reasons it does not appear worthwhile to consider them further.

The relative total coverage for various heights and equatorial orbits is shown in Fig. 2. Considering the distribution of population over the earth's surface it appears that any of the orbits above 2220 miles would give satisfactory coverage.

The number of stations in equatorial orbits required to give continuous coverage to a given point is shown in Table III. From 3 to 5 stations are seen to be ample if the stations are above 2200 miles.

Table III. *Number of Satellites to Give Continuous Coverage Equatorial Orbit*

| Station Height | Exact Number | Integral Number No Overlap | 10% Overlap |
|---|---|---|---|
| 257 | 8.8 | 9 | 11 |
| 620 | 5.9 | 6 | 8 |
| 1,210 | 4.4 | 5 | 6 |
| 2,222 | 3.6 | 4 | 5 |
| 4,000 | 3.0 | 3 | 4 |
| 7,650 | 2.6 | 3 | 4 |
| 19,000 | 2.2 | 3 | 3 |
| 22,300 | 2.2 (a) | 3 (a) | 3 (a) |

(a) For worldwide coverage: a single station will give coverage over essentially a hemisphere.

Vol. 4 1958

### B. The Influence of the Satellite Orbit Condition

A factor in the selection of operating condition for the communications service is the effort to be expended for various satellite orbits. This problem cannot be answered in an absolute sense at this time, but it is easy to secure a relative answer.

It is assumed first that continuity of communications is important. As has been seen, this appears to limit consideration to equatorial orbits, and requires use of several stations, except for the special case of the synchronized orbit.

Second, two "limit conditions" may be assumed for the size of the platform: at one extreme, it can be assumed that the size of the system measured by mass is independent of the number of platforms used in the service, and, at the other extreme, that the total mass of the system is independent of the number of stations and their operating conditions. The "point of equality" of mass is assumed to occur with a single station at 22,300 miles.

Finally, it may be assumed that the total effort and expense is measured adequately by the payload energy of operating ($KE$), which is defined by:

$$(KE) = \tfrac{1}{2} M (V_i + V_0 - V_a - V_d - V_g + V_r)^2.$$

Where

$M$ = mass of system or, payload of ascending rockets
$V_i$ = ideal takeoff velocity
$V_0$ = ideal orbital velocity
$V_a$ = ideal velocity of arrival at orbit
$V_d$ = loss due to drag
$V_g$ = loss due to acceleration of gravity
$V_r$ = gain due to rotation of earth.

Values of the first three velocity terms are derived in the Appendix. The sum of the remaining velocity terms is estimated to amount to a loss of 1,000 ft/sec.

The relative kinetic energy calculated on the basis of these assumptions is shown in Fig. 3.

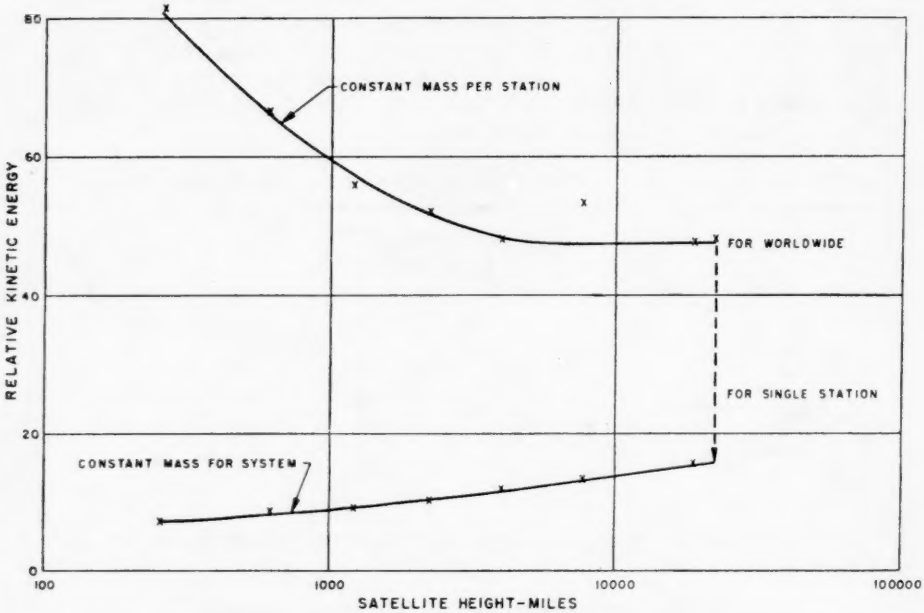


Fig. 3. Relative kinetic energy for satellite system

These curves indicate that:

a) On the basis of the pessimistic assumption of constant station mass the desired service requires less energy if the orbits are high.

b) The more optimistic assumption of constant mass to establish the service favors the lower altitudes. However, the difference between the lowest altitude for good coverage and the higher altitudes is small.

Since it is probable that the true situation is between the limit assumptions, it appears reasonable to conclude that the effort involved in establishing a satellite communication service is essentially independent of the satellite operating conditions chosen. Therefore, these may be selected to give the best grade of service.

### C. The Effect of Satellite Motion

Motion of the satellite with respect to the surface of the earth introduces two problems: first, a Doppler shift is introduced into the radio frequency signals: second, if directive antennas are used on the ground they would have to track the satellite.

The Doppler shift is readily calculated for the equatorial plane and an eastward orbital motion and is found to be:

$$\frac{\Delta F}{F} = \frac{2\pi R_e}{C}\left(\frac{1}{P} - \frac{1}{24}\right)\cos\psi.$$

Where

$\Delta F$ = Doppler shift, mc/s
$F$ = operating frequency, mc/s
$R_e$ = radius of earth, km
$C$ = velocity of light, km/hr
$\psi$ = elevation angle of satellite
$P$ = period of satellite, hours.

The value of this is not particularly large: for example, for the 1200 mile 4 hour orbit the maximum shift amounts to about 900 cycles/sec at an operating frequency of 100 mc/s. This would not be serious for a wide-band system, but would definitely require an automatic frequency control for narrow band-widths.

The amount of Doppler shift decreases with operating altitude, and becomes zero for the 24 hour orbit. This is a definite advantage.

The fact that there is, in general, relative motion of the satellite and earth indicates that any directional earth surface antenna will have to track the satellite. The tracking itself is not a serious limitation, since the maximum tracking rate cannot exceed about 4 degrees per minute, and is much less for satellite heights of 1200 miles or more. However, the acquisition of the next satellite to come into view is much more troublesome, since it will be necessary to have a rapid retrograde motion of the antenna, or to introduce two antennas and the necessary switching. These problems are also eliminated with the synchronized orbit.

Vol. 4 1958

It appears that the importance of these effects depends on the nature of the service. For point-to-point relays the special equipment such as AFC and tracking antennas would not be a serious problem. However, for the broadcast service, with perhaps millions of installations, such equipment would be a major system drawback.

The inverse problem, that of keeping the satellite antenna oriented with respect to earth will have to be solved for any altitude. This may be accomplished with either tracking antennas, or with fixed antennas by controlling the angular motion of the satellite. The fixed antennas appear superior. Controlling the satellite angular motion will certainly be easier with larger satellites, since the effects of personnel movement, rotating machines, etc. will tend to cancel, and in any event will give smaller angular motion for a given momentum change.

### D. Propagation from the Satellite

Any practical satellite will be above at least part of the ionosphere. An estimate of influence of this on communication is made as follows:

a) The minimum useable frequency, by reciprocity, corresponds to the maximum useable frequency of normal transmission, and is

$$MUF = fc \sec \alpha.$$

Where

$MUF$ = Minimum useable frequency
$fc$ = Critical frequency for vertical incidence at layer
$\alpha$ = Angle of arrival at layer.

b) The ionosphere layer is assumed to be very thin, to be located at the virtual height, and to be of constant intensity.

With these assumptions the arrival angle $\alpha$ can be determined geometrically from Fig. 4, which gives

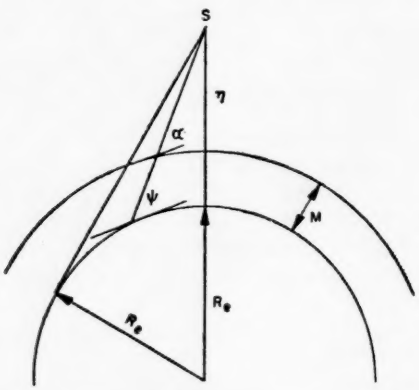


Fig. 4. Geometry of propagation. $S$ satellite, $M$ ionosphere layer height, $\eta$ satellite height $R_e$ radius earth, $\varphi$ elevation angle of satellite, $\alpha$ arrival angle at layer

$$\text{Cos} = \frac{R_e}{R_e + M} \cos \psi$$

$$= \cos \alpha_{max} \cos \psi$$

$M$ = virtual height of layer

$\psi$ = elevation angle of satellite from earth

$R_e$ = radius of earth.

That is, the minimum useable frequency at a given elevation angle is independent of the height of the satellite above the earth.

The value of the $MUF/fc = \sec \alpha$ is given in Fig. 5 as a function of layer height for various values of elevation angle.

The values of known layer heights and critical frequency are time varying quantities, which depend on time of day, solar conditions, and other factors.

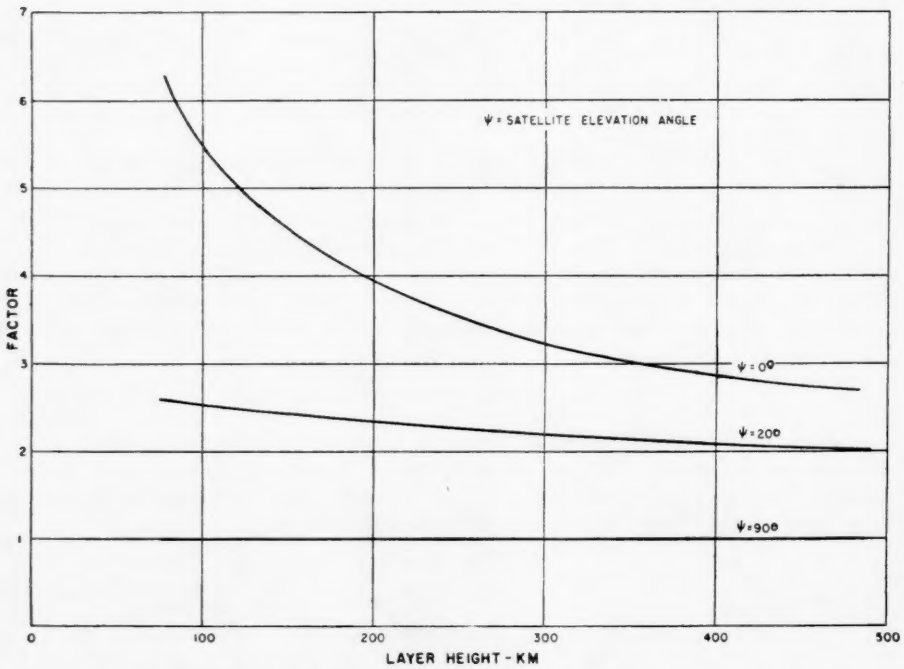


Fig. 5. $MUF$ factor. $\varphi$ satellite elevation angle

Typical values are shown in Table IV A. The corresponding minimum useable frequencies are shown in Table IV B.

Table IV

*A. Typical Values of Ionosphere Critical Frequency Fc and Height*

| Layer Designation | Height km | Sunspot Summer | *Fc*, mc/s, Values For | | |
|---|---|---|---|---|---|
| | | | Maximum Winter | Sunspot Summer | Minimum Winter |
| *E* | 120 | 4 | 4 | 5 | 5 |
| $F_1$ | 210 | 6 | — | 4 | 4 |
| $F_2$ | 400 | 9 | 15 | 5 | 6 |
| *Es* | 120 | 12 | 12 | 12 | 12 |

*B. Typical Values of MUF for Satellite Propagation*

| Layer Designation | Sunspot Summer | *MUF*, mc/s, Values For | | |
|---|---|---|---|---|
| | | Maximum Winter | Sunspot Summer | Minimum Winter |
| *E* | 20 | 20 | 25 | 25 |
| $F_1$ | 24 | — | 16 | 16 |
| $F_2$ | 27 | 45 | 15 | 18 |
| *Es* | 60 | 60 | 60 | 60 |

*Es* — *E* sporadic.

Vol. 4 1958

It is evident that the minimum frequency for complete coverage is around 60 mc/s. Allowing for neglected factors, such as ionospheric and atmospheric bending and absorption, it appears that it is safe to assume that frequencies above 100 mc/s are always useable.

At the other end of the frequency spectrum the maximum useable frequency is determined by atmospheric absorption. The contributions of water vapor and oxygen to this attenuation are shown in Fig. 6. These are the main components. This indicates that frequencies below 10,000 mc/s are useable.

The allowable band of frequencies for the satellite communication service thus covers the range between 100 and 10,000 mc/s. On an absolute basis this is about 10,000 times the bandwidth now available for reliable long range communication, or, on a percentage basis, just double the present spectrum. These factors indicate that there is ample room for the satellite service.

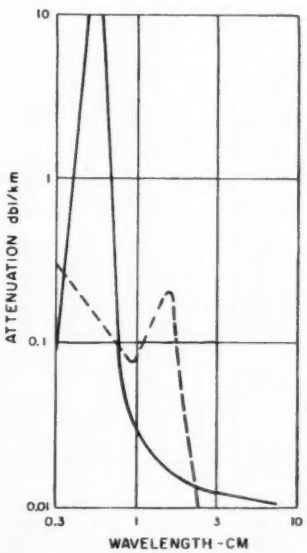


Fig. 6. Atmospheric absorption. – – – – water vapor, ——— oxygen

### E. Basis for Communication Studies [5, 6]

Numerical calculations for the various communication systems will be on:
a) The so-called beacon equation, for one-way transmission:

$$P_t = G - A_t - A_r - K + \frac{S}{N} + F + N + B + Pr.$$

Where

$P_t$ = transmitted power, db referred to 1 watt
$G$ = free space attenuation between isotropic antennas, db
$A_t, A_r$ = gain of transmitting and receiving antennas, db
$K$ = system improvement factor, db
$S/N$ = desired signal to noise ratio, db
$F$ = fading factor, db
$N$ = noise figure of receiver, db
$B$ = line and other loss, db
$Pr$ = theoretical receiver sensitivity, db referred to 1 watt.

b) The so-called radar equation for two-way reflection transmission, written as

$$P_t = 2G - 2A + \frac{S}{N} - K + F - \sigma + N + B + P_r - 28.$$

Where

$\sigma = 10 \log_{10}$ target area in square ft.

c) The energy equation, in appropriate units

$$P_t = A \frac{E^2}{120\pi}$$

$A$ = area to be covered

$E$ = desired signal strength.

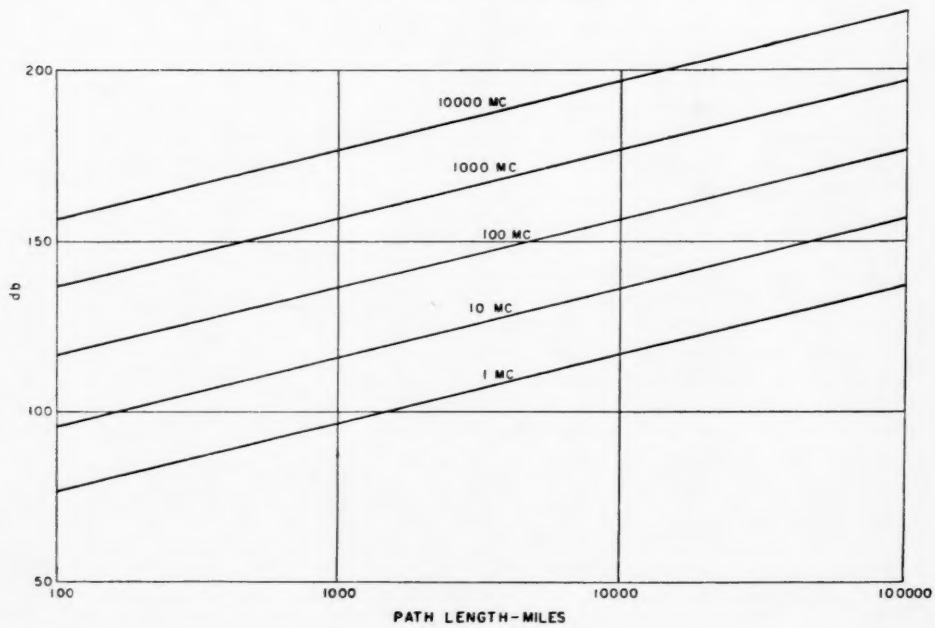


Fig. 7. Free space attenuation

The free space attenuation between isotropic antennas (path attenuation) is given by

$$G = +36.6 + 20 \log_{10} D + 20 \log_{10} fmc.$$

Where

$D$ = distance of transmission, miles

$fmc$ = operating frequency, mc/s.

This factor is shown in Fig. 7.

The gain of a parabolic reflector is given by

$$G = 20 \log fmc + 20 \log_{10} d - 53$$

$d$ = diameter in feet.

The beam width $\theta$ of the parabola is approximately

$$\theta^2 = \frac{27{,}000}{g}.$$

Where

$$g = 10^G$$

= numerical gain.

Vol. 4 1958

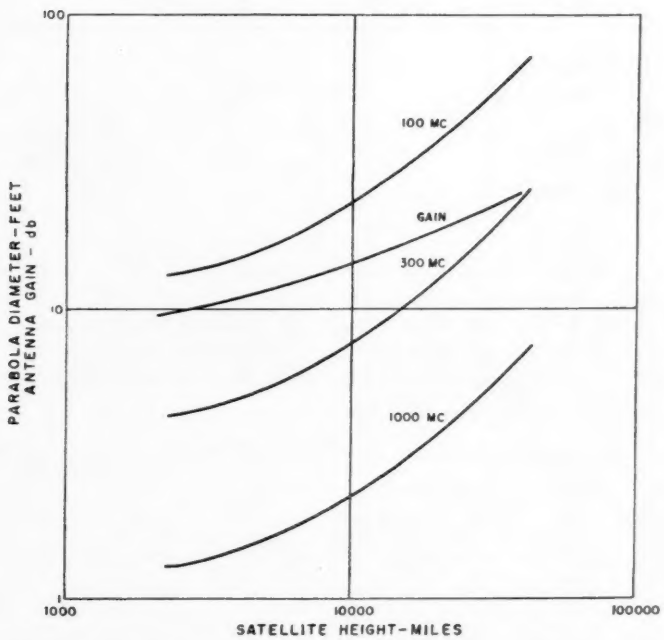


Fig. 8. Size and gain of a parabola illuminating the visible earth

For the special case of an antenna at the satellite which is to illuminate the entire visible sector of the earth's surface, the beam width is determined by geometrical considerations, and is shown in column 3 of Table I. The required antenna size as for various frequencies, and the gain of such antennas are shown in Fig. 8.

The system improvement factor is determined primarily by the type of modulation employed to convey intelligence. Typical values are:

| Modulation System | Improvement Factor $K$ |
|---|---|
| Double sideband telephony | 0 db |
| Single sideband telephony | +3 db |
| FM Broadcast | +15 db |
| AM Telegraphy | +17 db |
| FSK Telegraphy | +21 db |
| Pulse Code Telegraphy (typical) | +28 db |
| Television | 0 db |

The theoretical receiver sensitivity is a function of bandwidth of the receiver, and is 144 db below 1 watt per megacycle of bandwidth. For typical systems the bandwidths and corresponding sensitivities are:

| Modulations System | Bandwidth | Theoretical Sensitivity |
|---|---|---|
| Double Sideband Telephony | 6 kc/s | −166 dbw |
| Single Sideband Telephony | 3 kc/s | −169 dbw |
| FM Broadcast | 75 kc/s | −155 dbw |
| AM Telegraphy | 0.1 kc/s | −184 dbw |
| FSK Telegraphy | 1.7 kc/s | −172 dbw |
| Pulse Code Telegraphy | 3 mc/s | −139 dbw |
| Television Broadcast | 6 mc/s | −136 dbw |

The desirable signal to noise ratio depends on the system and the grade of service desired. For study purposes an average value of 20 db is satisfactory. The fading factor may be assumed to be 10 db, and the lines loss to be 3 db.

In the case of television broadcast services in the USA, the Federal Communication Commission has established the following standards for minimum signal levels, for the peak value of the signal:

| Channel | Freq | Primary | | Signal Levels | | | |
|---|---|---|---|---|---|---|---|
| | | | | Grade *A* | | Grade *B* | |
| | mc/s | db | uv/m | db | uv/m | db | uv/m |
| 2–6 | 54–88 | 74 | 5010 | 68 | 2510 | 47 | 224 |
| 7–12 | 174–216 | 77 | 7080 | 71 | 3550 | 56 | 631 |
| 14–83 | 470–890 | 80 | 10000 | 74 | 5010 | 64 | 1585 |

Relative levels are in db above 1 uv/meter.

There is reason to believe that the requirements for the two higher bands are excessive when applied to the satellite service, since, in part, these were established to permit use of simple dipole antennas. From an overall system view it appears more desirable to assume antennas having an effective area which is independent of frequency. For this reason service levels will be calculated on the basis of those for the low band.

## F. Preliminary Consideration of Communication Systems

Before investigating communication systems in detail it is desirable to determine the effect of height on their feasibility. This can be done by considering a limited number of system types.

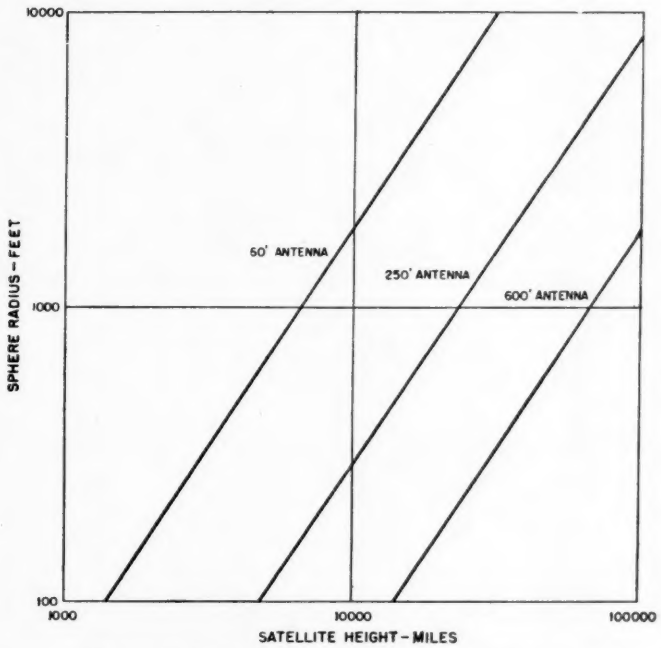


Fig. 9. Effect of height on a passive PCM relay

To secure a wide range of requirements, the systems chosen are:

a) Pulse code passive relay telegraphy
b) FM relay
c) Television area broadcast.

The following assumptions are made as to the operating conditions:

a) The PCM passive system operates on 10 cm, with a 1 megawatt ground transmitter, against a spherical reflector. The reflector size is determined as a function of height for three ground antenna sizes. The system is operative anywhere within the visible area, and provides the $S/N$ ratios of section $E$.

b) The FM relay system operates on 30 cm, with a 60′ dish on the ground, and a satellite dish to completely cover the visible area, with the $S/N$ ratios of Section $E$. Antenna pattern shaping to give uniform signal strength is not used.

c) The TV broadcast system is calculated to give FCC signal levels on channels 2—6 over the visible area. Antenna pattern shaping is used to give uniform power density over the illuminated area.

The effect of height on the three systems is shown in Figs. 9 to 11 inclusive. The following conclusions appear justified.



Vol. 4 1958

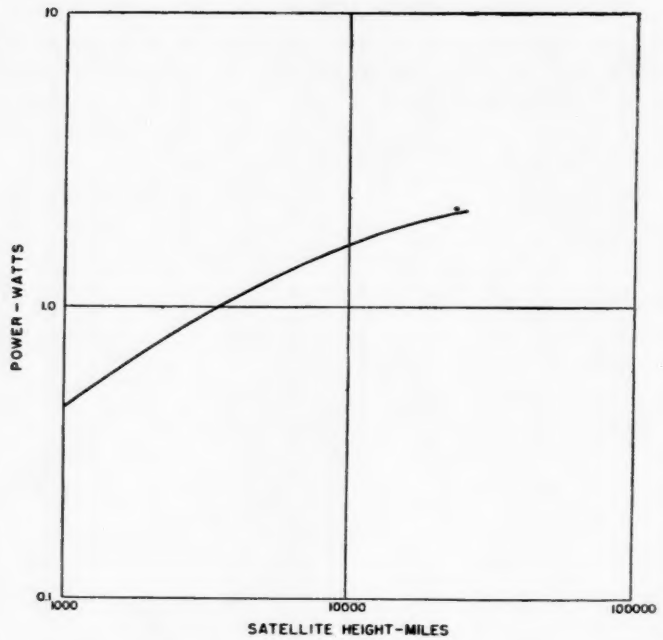


Fig. 10. Effect of height on a FM relay

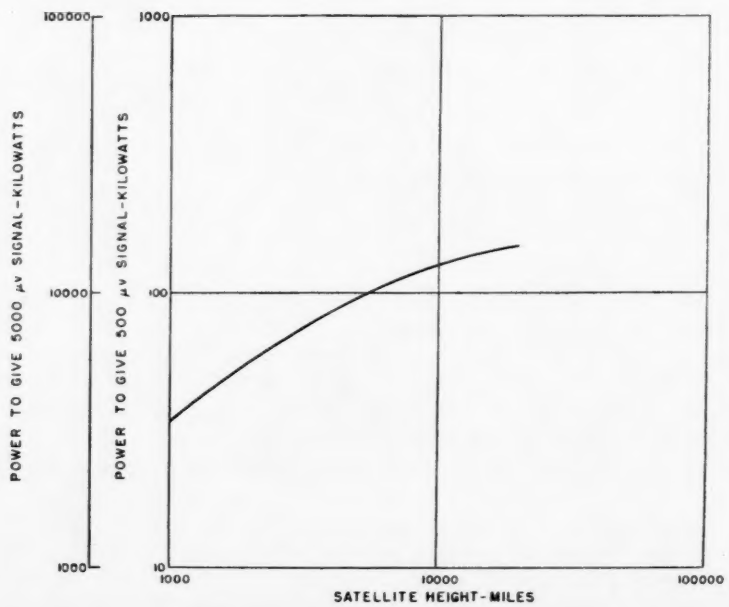


Fig. 11. Effect of height on TV broadcast

Assuming a 100′ radius sphere or equivalent as the practical limit for the satellite, the passive relay system would be useable to an altitude of about 1400 miles with a 60 foot dish, which does not appear unreasonable. At greater altitudes either the power or dish size would have to be increased. Tracking dishes of large size are probably not practical, but a stationary one might be. This indicates that the use of passive communication with the synchronized 22,300 mile satellite may be feasible, and should be studied further.

The power requirement for FM relay service is modest, and is essentially independent of satellite height. The system chosen is probably out of balance in terms of cost, since increasing the transmitted power will permit reduction in antenna size.

The power requirement in the TV broadcast service also changes slowly with altitude. Provision of the FCC Grade B signal over the visible part of the earth can be accomplished with present techniques, but the primary coverage signal level requirements appear excessive. However, it appears possible to provide the primary coverage over smaller areas of the earth surface.

Comparison of the requirements for active and passive systems shows that the power and antenna requirements are more modest for the active system. However, this may not be true if the economics of the system are considered, since equipment at the satellite will be the most expensive to install and operate.

Vol. 4 1958

### G. The Optimum Orbit for Communication Service

The following factors, developed in the previous sections, are of importance in selection of the optimum orbital height:

a) The equatorial orbit appears to be superior in all cases.

b) The coverage of a single satellite obviously increases with altitude, but appears to be entirely adequate for any altitude of 2220 miles or greater.

c) The number of stations required to give continuous coverage to a given point decreases somewhat with increasing altitude, but not by an important factor.

d) The synchronized 22,300 mile satellite permits establishment of a "partial" service, giving continuous coverage to wide areas with a single satellite. All other cases give world wide coverage when continuous coverage is established.

e) The cost of establishing world wide service measured in terms of payload energy appears to be essentially independent of orbital altitude. The cost of continuous coverage to a point or moderate area is probably less for the synchronized orbit, since a single satellite is adequate.

f) The effects of orbital motion are smaller at great altitude, and become zero for the synchronized orbit. This is probably not important for limited communication service, but is important for the broadcast service.

g) Propagation problems are independent of orbital altitude.

h) When used as a passive reflector in the PCM relay service the system requirements are less severe at the lower altitudes. For the synchronized orbit the elimination of tracking requirements may be more important than other system factors.

i) In the FM relay service the system requirements are quite modest, and are essentially independent of altitude.

j) In the TV broadcast service the requirements appear attainable for acceptable wide area coverage, and are essentially independent of altitude. Wide area high quality coverage does not appear feasible at any altitude considered.

k) Small area high quality TV broadcast coverage problems are essentially independent of altitude.

Since only two of these factors favor the lower altitude orbits, and since the synchronized 24 hour orbit appears to be the best of the high altitude orbits, it appears reasonable to conclude that the communication satellite will be based on the use of a platform at 22,300 mile altitude.

### H. Further Consideration of the Television Broadcast Service

The provision of several communication systems from the 22,300 synchronized satellite is now considered in more detail. Because of its more severe technical requirements, the Television Broadcast service is considered first.

It should be noted that the television power levels quoted previously are peak powers, measured at the synchronization level of the USA standard signal. The carrier power is smaller than this, by a factor of 0.66. However, in practice the actual radiated power must be greater than that calculated by area alone, since practical antennas do not have "ideal" patterns. Further, an aural transmitter of 50—70% of the power of the video transmitter is also required. For this study it is assumed that peak power and pattern effects compensate, so that the calculated values are the carrier level, and that the aural and video transmitters have equal power.

To review, the power requirements for illumination of the visible part of the earth are:

| Service Level | Kilowatts Power Required |
|---|---|
| Primary | 14,400 |
| *A* | 3,600 |
| *B* | 35 |

The first two of these are clearly excessive, so that it will be necessary to restrict the coverage area when the best grades of service are to be provided.

If it is assumed that a 50 kw transmitter represents a practical limit, and that the "*A*" grade coverage is desired, the total area coverage possible is $1.15 \times 10^6$ square miles, an area about equal to that part of the USA which lies east of the Mississippi River, or to about that of Western Europe. This coverage appears to be entirely ample, and does have the additional desirable feature of limiting the coverage on the earth to a span of about two time zones.

The antenna pattern needed for this limited area coverage depends on the geographical location of the area, and on the longitude of the satellite. For a satellite of $100^0$ west, to give good coverage at the Americas, the beam required to cover the eastern third of the USA is approximately $2.7^0$ in width and $3.3^0$ in heigth. At a frequency of 100 mc/s the reflector would need to be about 270 feet in width by 200 feet in height.

Considered on a world-wide basis, it appears that the major features of the TV broadcast service would include the following:

a) A network of three satellite stations. A station for the Americas would be located at $100^0$ west, one for Europe/Africa at $30^0$ east, and one for Asia/Australia at $120^0$ east. This nonuniform spacing is indicated by the nonuniform distribution of land masses and population.

b) Each satellite would include a general coverage channel, to furnish a "*B*" level signal to the entire visible part of the earth. The transmitter would have a power of 35—50 kw. The antenna, from Fig. 7, would have a beam width of $17^0$, and a diameter, for 100 mc/s, of 45 feet.

c) Each station would have two larger antenna systems, one for high level coverage to northern industrial areas, the other to southern areas. (It is assumed that the present acceleration of industrial development in the southern latitudes will continue.) Each of these will consist of a single large reflector, about $200 \times 300$ feet in size, with multiple feeds. Three transmitters per large dish appear to give ample coverage.

d) Overall, the equipment at each satellite amounts to a total of seven video transmitters, and seven aural transmitters, amounting to a total power output of 700 kw.

e) The system described lends itself to development in stages. The initial stage could consist of the single general coverage transmitter. The second stage could be achieved by adding one of the limited coverage antennas, with one or more of its transmitters, and so on.

f) The system also lends itself to expansion. This may be accomplished by increasing the number of transmitters, or by increasing the power of a transmitter. For example, megawatt transmitters are technically feasible, which would permit better service levels over wide areas.

g) It would appear that the satellite service and the more restricted coverage surface transmitters would complement each other, with the satellite service being primarily used for network-type programs, and the surface transmitters for local-interest programs.

h) Considering the demonstrated appeal of television programs, particularly for children, it is interesting to speculate on the lingual and sociological impact of the world-wide coverage possible. These speculations are not pursued here.

Vol. 4 1958

## I. Reconsideration of Passive Relay System

It has been found that the passive relay system working against a 1000 foot radius spherical satellite of 22,300 miles requires an excessively large earth antenna.

A major factor in this lies in the nature of the assumed reflector since a sphere reflects isotropically. In the satellite application this means that all energy lying outside a $17^0$ wide cone is wasted. A means of concentrating this energy is needed.

The first thought is a corner reflector. However, an ideal reflector returns all of its energy to the source, whereas the desired system scatters this energy across the visible segment of the earth. What is needed is a diffusing system: that is, a convex reflector. This suggests using a segment of a sphere, which is permissible in this application, since other antennas will require stabilization in any event.

The geometry of the problem requires that the reflection lie in a $17^0$ wide cone, approximately $2\pi/100$ steradians. Since the radar cross section is defined as

$$\sigma = 4\pi \frac{\text{Power scattered per unit solid angle}}{\text{Power incident per unit area}}$$

the cross section in such a case is approximately $200\pi a^2$, where $a$ is the radius of the segment base. Since the required cross section is $10^8$ square feet, for the system previously assumed, the required base radius is 400 feet. This still appears large. Therefore it appears necessary to increase the size of the ground antenna.

A reasonable balance in requirements appears to be a ground antenna of 150′ diameter. This decreases the required cross section to $2.5 \times 10^6$ square feet, and the base radius of the reflecting segment to 65 feet.

This system may not require a special satellite reflector. The area of the television antenna suggested for limited coverage in the preceding section is very nearly the same as that required for the passive link. If the energy incident on it were reflected at the feed point it would be returned to earth. However, with normal feeds the energy would be concentrated into a narrow beam, so that a special design is needed.

It should be noted that the passive system is inherently broad-band, since addition channels do not require additional satellite equipment, and since the system requirements do not change as the frequency changes, providing the antenna and reflector sizes are maintained. Therefore, the system is capable of a large degree of expansion, by adding earth surface transmitter and/or receiver stations.

However, because of the power requirement, it appears that it is best limited to the relay of telegraphic signals. In this service, using PCM modulation, each transmitter is capable of handling around 100 simultaneous messages. These can be received at any point on the visible segment of the earth. In practice, it appears that the system could be made automatic, by the use of destination codes, which would allow the receiving point to select the messages directed to it.

Vo
4
19

### J. Reconsideration of FM Relay Systems

The FM relay system previously discussed was based on the transmission of high fidelity music. It was found that system was not in balance, since antenna size appeared to be excessive.

By increasing the radiated power from 2 watts to 20 watts the ground antenna can be reduced to a diameter of 20 feet. This appears to be a better balance for a limited number of channels. A further increase in power is possible: if this is sufficient the system becomes attractive for the broadcast service. For example, with a 2 kw of power, the required ground antenna is a parabola slightly over 2 feet in diameter, or alternately, a corner reflector antenna of nearly the same dimension. The cost of such an antenna is sufficiently low to be attractive.

Another type of relay service in which FM techniques are useable is long distance telephone communication. By multiplexing, a system capable of carrying high fidelity music can carry 5 simultaneous speech circuits. This gives a power requirement of 0.4 watts per channel if the 60′ antenna is used.

It appears that a 5 channel link would be grossly inadequate for the relaying of telephone signals. For example, the capacity of a coaxial cable is about 600 channels. In the satellite service, since the power required is porportional to bandwidth, this would require a total power of about 250 watts.

This system is probably not the optimum for this service, since the satellite antenna covers the visible segment of the earth. By limiting the coverage to smaller areas on the earth the required power can be reduced. However, it does not appear profitable to pursue this optimization further at this time, since the requirements are modest.

### K. Interstation Relays

To provide world wide service the communication system must provide for communication and relaying between the three satellite stations. Since directive

antennas will be needed, this service could be on the same frequencies as are used for earth coverage. However, to avoid interference problems within the station it appears desirable to use frequencies outside the earth coverage band. This suggests use of the centimeter band.

Since the proposed satellite stations are not uniformily located about the earth, the transmission distance varies with the stations, from around 30,000 to around 40,000 miles. Assuming that 30′ dish antennas are used, that the relayed signal is 6 mc/s wide, corresponding to television signals, and that the allowance for signal/noise ratio, fading, etc. amounts to 53 db, the required power is 2.5 watts per channel. This appears to give a satisfactory system balance. For other types of relaying the same value may be used: for example such a channel could accomodate about 600 voice channels.

### L. The Influence of the Communication Service on the Satellite

By now, it seems obvious that the communications satellite will have two major features: a large power supply, and a number of antenna reflectors. To arrive at the extent of these, the following assumptions are made concerning the services provided by each of the satellite stations:

Vol. 4 1958

a) The television service includes 2 general coverage channels, plus a total of six limited area channels, divided into a northern set and a southern set of three each.

b) There is a passive relay reflector.

c) The system includes 100 relay transmitter links, each having a capacity equivalent to 600 one way voice channels.

d) The system also includes the capacity of 100 relay receiving links.

e) Two FM broadcast transmitters are provided.

f) Interstation links are provided to each of the other two satellite stations. The total capacity of these is equivalent to 100 FM relay links.

For such a system the power requirements are:

| System | Power/Transmitter | Number of Transmitters | Total |
|---|---|---|---|
| TV Broadcast | 50 kw | 16 | 800 kw |
| FM Relay | 0.25 | 100 | 25 |
| FM Broadcast | 2 | 2 | 4 |
| Interstation | .0025 | 100 | .25 |

It is assumed that the efficiency including receiving, terminal and modulation equipment will be 50%. The total demand on the power supply is therefore about 1600 kilowatts.

The antenna requirements for this system would be, assuming maximum utilization of each antenna:

| System | Antenna |
|---|---|
| TV Broadcast | 1—45′ dish<br>2—200′ × 270′ dish |
| Passive Relay | 1—65′ convex reflector |
| FM Relay and Broadcast | 1—4.5′ dish |
| Interstation Relay | 2—30′ dishes |

All antennas would be stabilized with respect to earth.

It appears evident that a system as large as this would have to be designed for manned operation on a long term basis. This, in turn, appears to require a synthetic gravity, obtained by rotation of the station. However, the antennas cannot be allowed to rotate, since they must remain fixed with respect to earth, and must also maintain the direction of antenna polarization constant.

The solution to these opposing requirements is to mount the rotating part of the station as a wheel on an axle which carries the nonrotating parts. The axle would be oriented parallel to the axis of the earth. There would be some friction, so the axle and wheel would require torque jets, to maintain constant angular velocity. Additional jets would be needed to bring the rotational period of the assembly to 24 hours, so that the antennas always point to earth, and to make corrections.

A reasonable arrangement would place the limited coverage antennas at each end of the axle, with the rotating wheel at the center. The passive reflector could bridge the ends of the axle, outside of the wheel on one side.

To avoid slip ring problems it appears desirable to keep all communication equipment in the non-rotating part, probably without air. This introduces the problem of servicing while weightless, and in a space suit, but these problems are probably less important than the possibility of perfect vacuum in tubes, the lack of dust and moisture, and so on. The communication equipment would need to be enclosed in metal, for shielding, and protection against photo-electric emission.

The power supply for such a station appears to be a much larger problem than the communication equipment itself. Solar energy does not appear feasible with the efficiencies possible at present, although a 500 kw unit has been proposed. The size and weight of a nuclear reactor is negligible, but the shielding and generation equipment would be massive. However, nuclear propulsion systems for aircraft are being seriously studied. The problems appear solvable in this application, and since the power rating is orders of magnitude larger than needed here, it appears safe to assume that a solution for the satellite is feasible.

The space requirements for the communication service have not been detailed. It appears that the 400 ton, 250 foot diameter ring of VON BRAUN [7] is too small in some respects: on the other hand the $1000' \times 3000'$ station of ROMICK [8] appears oversize. Probably a station which is between VON BRAUN's and ROMICK's 1500 ton $40' \times 500'$ "Second Phase" in size and mass would be satisfactory.

In any event the station would represent a major undertaking, and is clearly beyond the reach of present rocket technology. With nuclear fuels it should be straightforward: with advances in fuel energy it may become feasible. The question of desirability is separate: this depends on complex economic factors, and on sociological and political factors. These will have to be considered later.

## Appendix

The velocity for establishing a satellite may be derived by assuming that the total energy required is the sum of that needed under "ideal" conditions plus that needed for "practical" considerations.

Assuming that the rocket is of the two period burning type, it can be shown that the optimum "ideal" trajectory is that shown in Fig. 12.

For this letting

$$k = \frac{R_0}{R_e},$$

if can be shown that the orbital velocity is

$$V_0^2 = \frac{V_e^2}{2k}$$

$V_e$ = velocity of escape.

The velocity of takeoff, which must be developed to rise to orbital height, is:

$$V_t^2 = V_e^2 \frac{k}{k+1}.$$

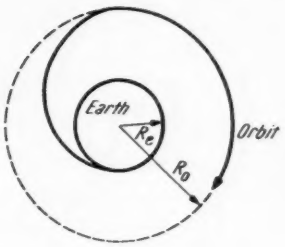


Fig. 12

The rocket arrives at orbital height with an arrival velocity

$$V_a^2 = V_e^2 \frac{1}{k(k+1)}.$$

Correction terms must be added for practical effects. These are:

$V_d$ = The equivalent velocity due to atmospheric drag.
$V_g$ = The equivalent velocity due to gravity action during finite burning periods.
$V_r$ = The velocity of rotation of the earth.

The total velocity required to establish the rocket in the orbit is accordingly:

$$Vi = V_t + V_0 - V_a - V_d - V_g + V_r.$$

Vol. 4 1958

**References**

1. A. C. Clarke, Extra-Terrestrial Relays. Wireless World, October, 1945, pp. 305—308.
2. ARS Space Flight Committee, On the Utility of an Artificial Unmanned Earth Satellite. Jet Propulsion **25**, 71 (1955).
3. R. P. Haviland, On Applications of the Satellite Vehicle. Jet Propulsion **26**, 360—363 (1956).
4. F. E. Terman, Radio Engineers Handbook. New York: McGraw Hill.
5. J. A. Webb, Interplanetary Communications: J. Astronautics **3**, 29 (1956).
6. Federal Telephone and Radio Corp., Reference Data for Radio Engineers, IT and T, New York, 4th Ed., 1956.
7. C. Ryan, ed., Across the Space Frontier. New York: The Viking Press, 1952.
8. D. C. Romick, Preliminary Study of a Satellite Station Concept, presented at ARS Annual Meeting, Chicago, November 14—18, 1955.

# Instrumentation of Artificial Satellites

By

**F. I. Ordway, III**[1], ARS

(With 21 Figures)

## 1. Introduction

In a previous report[2] a number of proposed I.G.Y. satellite experiments were listed. Since that time four instrumentation packages have been tentatively accepted as final for on-board experimentation. These involve satellite environmental measurements, Lyman-alpha measurements; cosmic ray observations, measurements of interplanetary matter; geomagnetic measurements; investigations of the radiation balance of the Earth and the measurement of cloud cover and albedo of the planet. In addition, a number of other on-board experiments may be carried out, but at this time their inclusion is not definite.

Geodetic measurements, studies of the ionosphere, and air density measurements, experiments not requiring active instrumentation, will also be conducted. There are also plans to use minimal and sub satellites to facilitate the carrying out of some experiments.

This report can only be considered as preliminary, since instrumentation design and operating criteria have yet to be frozen, and, indeed, some instrumentation is still in a relatively early developmental stage. In the case of the fourth instrumentation package, it is not yet known (October 1957) whether the radiation balance or the cloud distribution and albedo experiment will be carried out: as it stands, one or the other, and not both, will be flown.

When the instrumentation packages have been fully designed and checked out, and when final figures are released, a more complete technical summary can be given.

## 2. Progress Towards Satellite Launching

Vanguard's engines have now reportedly passed qualification tests. The third stage solid propellant motor, about which little was known until recently, passed pre-qualification and static tests, and reportedly flew on the *Viking 14* Vanguard Test Vehicle. The spring-loaded ejecting mechanism that separates the satellite from the rocket (differential velocity: about two miles per hour) has passed tests. Separation techniques for the first and second stages (six explosive bolts) and second and third stages (rocket powered turntable plus retro rockets) are satisfactory. Development of the Minitrack, gyro-reference system, and launching equipment schedules are reportedly progressing well.

---

[1] Project Director, General Astronautics Corp., 11 W. 42nd St., New York 36, N. Y., USA. (Now, Huntsville Field Office, Box 656, Huntsville, Ala., USA.)

[2] F. I. Ordway, III, Astronaut. Acta **3**, 67 (1957).

Test vehicles *TV—0* and *TV—1* (*Viking 13* and *14* rockets) have been fired from Patrick Air Force Base. *Viking 13* was reported previously; *Viking 14* flew on 1 May and rose to 120 miles when the Grand Central Rocket Company's second stage solid rocket detached for a successful continuing flight.

On the 23rd of October *TV—2* was fired, rising to 109 miles and recording a range of 328 miles. Top speed was 4250 mph and the flight time was 140 seconds. Dummy second and third stages were used with the full scale first stage powered by the General Electric engine.

The next test will be *TV—3*, which will incorporate General Electric powered first and Aerojet-General powered second stages. The third stage will be a dummy. In the following *TV—4* test, a Grand Central Rocket Co. third stage will be substituted for the dummy. Finally, tests *TV—5* and *TV—6* will represent essentially the full Vanguard system.

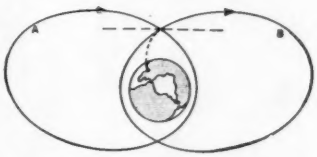


Fig. 1. Orbits produced by projecting satellite not horizontally. *A* downward projection case, *B* upward projection case. (By courtesy of: U.S. Naval Research Laboratory)

The thrusts and firing times of the three stages have now been released as follows:

| | First Stage | Second Stage | Third Stage |
|---|---|---|---|
| Thrust, lb. | 27 000 | 7500 | 2350 |
| Firing time, sec. | 146 | 120 | 30 |

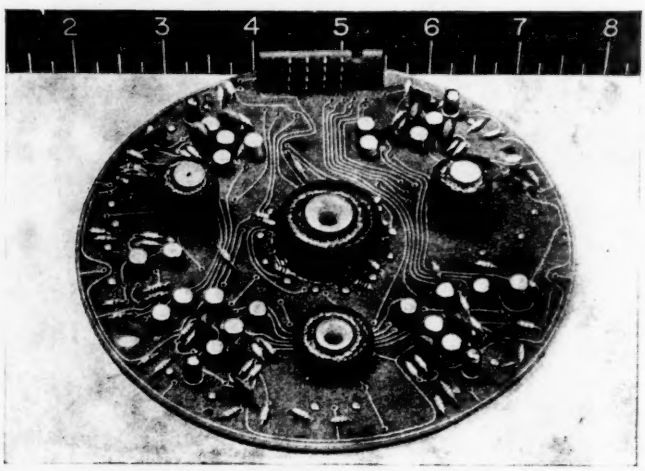


Fig. 2. Basic 48-channel telemetering system. (By courtesy of: U.S. Naval Research Laboratory)

At the conclusion of the *TV—0* and *TV—1* Viking and the five Vanguard or Vanguard-type tests, it is hoped the six scheduled firings, which are currently planned, will be largely successful, and that four satellite vehicles will be established in orbit around the Earth within the 200 mile perigee, 1400 mile apogee limits.

Vol. 4 1958

Fig. 3. Small light-weight Minitrack transmitter. (By courtesy of: U.S. Naval Research Laboratory)

The last four test firings will carry small "minimum" satellites of somewhat more than six inch diameter, and weighing about four pounds. They will carry two radio transmitters, and will incorporate six radio antennae. One transmitter will operate from chemical batteries allowing ten milliwatts of continuous radio frequency output for some two weeks, while the other will employ six exterior-mounted solar cells (permitting the transmitter to radiate at more than five milliwatts). The transmitters will operate, respectively, on 108.00 mc and 108.03 mc.

Fig. 4. Plastic foam incased electronic package is inserted into its gold plated container. (U.S. Navy Photo)

### 3. Pre-Satellite Instrumentation Checkouts

All instrumentation has been, and will continue to be, laboratory tested. Some equipment has been flight tested in Aerobee rockets, including satellite-type thermistors, differential pressures gages, microphones to record micrometeorite incidence, Lyman-alpha ion chambers, solar aspect cells, and transmitting equipment.

### 4. Listing of Tentatively Accepted Experiments

| Satellite Package No. | Description of Experiment | Agency |
|---|---|---|
| 1 | Measurement of Solar Ultra-violet Intensity in the Lyman-alpha Region | Naval Research Laboratory |
| | Satellite Environmental Measurements (pressure, temperature, meteoric incidence, skin erosion) | Naval Research Laboratory |
| 2 | Cosmic Ray Observations | State University of Iowa |
| | Measurements of Interplanetary Matter (meteoric detection experiment) | Air Force Cambridge Research Center |
| 3 | Satellite Geomagnetic Measurements | Naval Research Laboratory |
| 4a | Investigation of Radiation Balance of Earth | University of Wisconsin |
| 4b | Measurement of the Earth's Cloud Cover and Albedo | Army Signal Engineering Laboratories |

Note: The size of satellite instrumentation compartment is 5-1/2 inches in diameter by 7-1/2 inches high. Therein are all electronic circuitry, Minitrack transmitter, batteries. Circuits are mounted on 5-1/2 inch round cards, 3/4 inch high, encapsulated in foam plastic forming shallow wafer.

### 5. Listing of Three Additional Experiments

| Description of Experiment | Agency |
|---|---|
| Measurement of Ionospheric Structure | Ballistic Research Laboratories, Aberdeen |
| Measurement of Meteoric Dust Erosion of a Satellite's Skin[1] | University of Maryland |
| Determination of Flux of Primary Cosmic Ray Nuclei with Atomic Number Larger than Eight | Research Institute for Advanced Study, Martin Co.; Bartol Research Foundation |

[1] With slight modifications this experiment can be used for solar photon, or ultra-violet studies, and cosmic ray studies.

Vol. 4 1958

## 6. Instrumentation Packages

### A. Package No. 1

#### (1) *Lyman-alpha Measurements*

The major experiment of the Group 1 Package consists of small ionization chambers designed to measure 1215.7 Å (Lyman-alpha) radiation from the Sun. This is the strongest emission line of the atomic hydrogen spectrum, responsible for most or all of D-layer ionization.

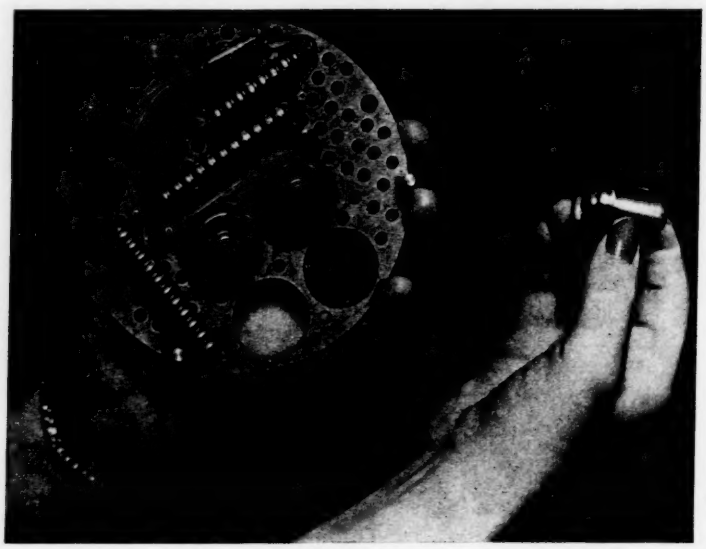

Fig. 5. Tube at right is ionization chamber for measurement of Lyman-alpha radiation. Card contains electrometer tube, resistor, and batteries comprising circuit for measuring ionization chamber current. (By courtesy of: U.S. Naval Research Laboratory)

The window area of the ion chambers is about one square centimeter. The chamber can withstand wide temperature fluctuations, high accelerations, and long-period operation. It is made of copper free of oxygen, and is about an inch long, 0.8 inch in diameter. NRL reports that it will give a current of approximately $5 \times 10^{-9}$ amp when exposed to a normally incident flux of an erg/cm$^2$/sec of Lyman-alpha radiation.

Lithium fluoride was chosen for the window because of its transparent qualities in the far ultraviolet regions of the solar spectrum. Inside the chamber is nitric oxide gas with an ionization threshold of 1340 Å.

The experiment consists of two of these ion chambers almost entirely sensitive to the subject wavelength, a solar aspect cell, two magnetic memory circuits, an orbital switch, and a resetting circuit. The second sensing chamber permits the experiment to have a large degree of aspect freedom[1]. Ion chamber development is considered complete.

[1] A detector has a 120° field of view and will be equatorially mounted. This will allow a solar signal to be obtainable for approximately a third of each spin period. The solar aspect is the angle between the Sun and the normal to the chamber window.

One of the memory cores stores data as the second modulates the Minitrack transmitter with the peak signal stored during the period of the immediately preceding orbit. As the satellite moves from the shadow to the sunlit zone, orbital switching occurs (upon signal from the silicon photoconductive solar cell).

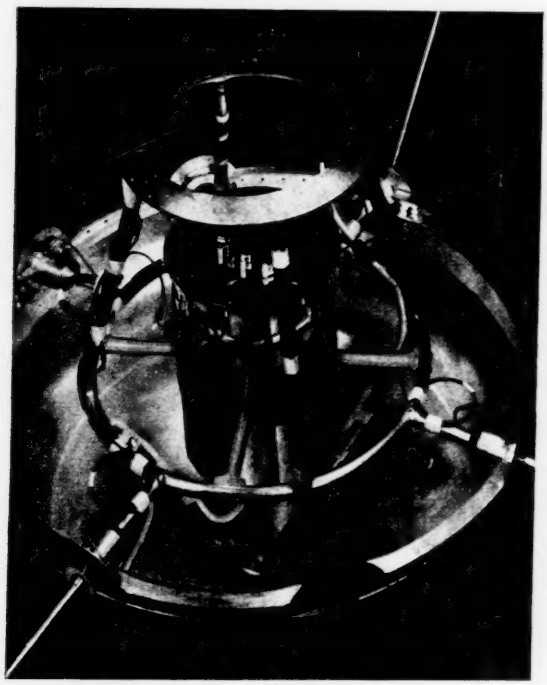

Fig. 6. View of interior of partially assembled satellite with upper half shall removed. Cylinder containing circuit packages is mounted on spin axis. Four antenna rods project radially through equator of sphere. Lyman Alpha ion chamber is shown mounted on shell with window exposed through surface in lower foreground. (By courtesy of: U.S. Naval Research Laboratory)

The total weight of the ion chambers, solar cell, memory circuits, switch, resetting circuits and general circuitry is 1.7 pounds. A pre-prototype model has been low-pressure tested at several temperatures. It is expected that the experiment will detect variations in absolute intensity of better than five percent from normal.

### (2) *Satellite Environmental Measurements*

Measurements will be made of environmental conditions of the satellite, such as temperature, pressure, skin erosion and micrometeoric incidence.

Thermistors will be employed to determine the temperature[1] of the internal instrument package and of two points on the skin of the satellite, namely at one

[1] It is desired that temperatures be carefully regulated to keep values within the efficient operating range of batteries and transistors, i.e. $0^0 - 10^0$ C and $60^0$ C as outside limits. To control the internal energy absorption and radiation balance, a special optical covering has been developed for the satellite, which, it is felt, will provide an average temperature of $20^0$ C.

Vol. 4 1958

pole and at a position at the equator. The thermistors will be about the size of a pinhead, and are composed of a mixture of metal oxides. As environmental temperatures change, resistances will change, and it is resistance that will be measured in the experiment.

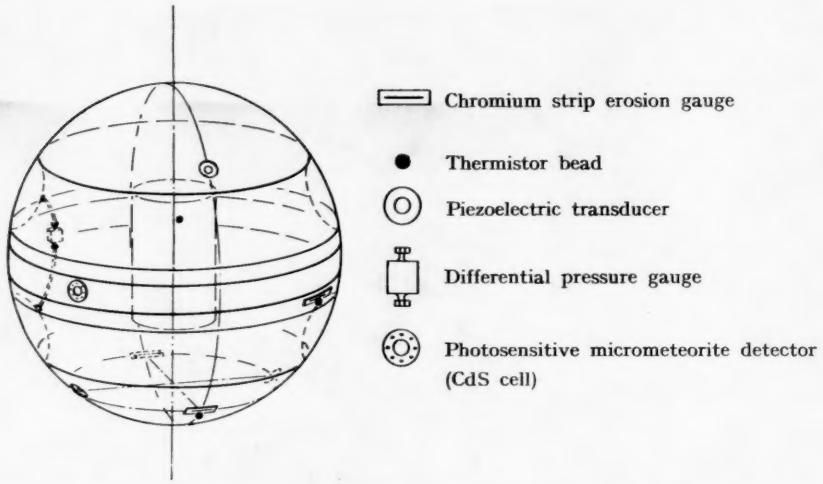


Fig. 7. Location of environmental detectors. (By courtesy of: U.S. Naval Research Laboratory)

The *pressure* inside the satellite will be carefully "observed" by simple aneroid pressure gauges, located inside the pressure-tight chambers that will be incorporated within the shell (weight of these chambers is $2^3/_4$ pounds). When and if a meteor punctures a chamber, a pressure drop will immediately follow, and this will be recorded. To provide for knowledge of one or multiple punctures, simultaneous punctures, and steady leakage it is expected that a bellow-actuated potentiometer will be utilized to determine pressure variations between two puncture zones. One zone will be monitored by a pressure switch.

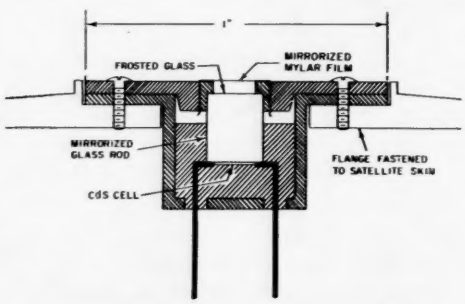


Fig. 8. Photosensitive micrometeorite detector. (By courtesy of: U.S. Naval Research Laboratory)

In order to measure *skin erosion* three thin chromium resistance strips (metallic film evaporated on pyrex glass) and a single cadmium sulfide shell will be placed at four points on the shell. The film resistance erosion gauges will be cemented at positions near the poles (two) and at the equator (two). It is expected that changes in electrical resistance (increased by continued particle impingements) of ten per cent will provide useful data.

Very sensitive microphones will count impinging micrometeoric matter, yielding information on *micrometeoric incidence*. All impact counts will be stored on a magnetic core. Barium titanate type microphones will be used sensitive to

impacts by micrometeorites of $2 \times 10^{-5}$ ergs of energy. Counts up to 1000 can be made and stored on saturable magnetic cores.

## B. Package No. 2

### (1) *Cosmic Ray Observations*

The cosmic ray experiment will attempt to measure the total intensity as a function of both time and position. In two parts, it will effect a continuous transmission of the instantaneous intensity and will permit the storage of intensity on a magnetic tape. Readout will occur by command when the satellite passes over the telemetering fence. Knowledge of cosmic ray intensity distribution, geomagnetic field orientation, cosmic ray albedo, and relative strengths of the terrestrial and interplanetary magnetic fields should be increased.

A GEIGER-MÜLLER tube and a tape recorder are the essential components of the experiment. The experiment will, it is hoped, provide important data on both temporal and positional variations of primary cosmic ray intensity. The counts will be totalled during a complete cycle and, upon command, readout will occur to be followed by erasure of the tape and the commencement of a new counting series. A ratchet system, actuated each second by a time base channel, will drive the tape forward step by step (0.005 inch each). Recording can continue for 120 minutes.

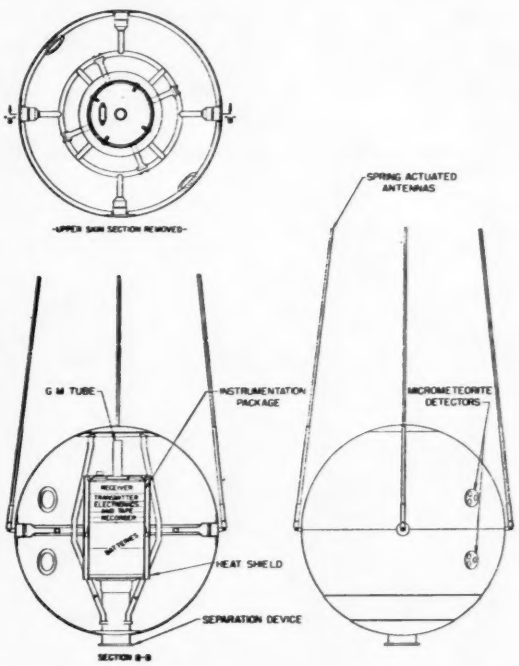


Fig. 9. 20 inches diameter cosmic ray satellite. (By courtesy of: U.S. Naval Research Laboratory)

A scaling circuit records the $G-M$ tube pulses, reducing the rate of operation. The scaler's output is one pulse each five to twenty seconds. A 512 cps tuning fork, in a parallel channel, drives a scale of 512, producing a pulse per second. These channels supply an anti-coincidence circuit (except when a pulse is seen at the $G-M$ tube scaler output) the output of which is tape recorded.

In conducting this experiment it is essential that data be stored representing the whole orbital track, and that it is known at exactly what point on the track a specific counting rate occurred. Therefore, a highly accurate internal time standard had to be incorporated into the device.

The counter will fit into a 5—1/2 inch package, largely occupied by foam and batteries. The plate, $G-M$ tube, and connectors weigh 0.36 lb., while the tape recorder weighs 0.52 lb. The batteries weigh nearly nine pounds. Other items



Vol. 4 1958

include the receiver (nearly half a pound), transmitter (0.38 lb, with HV power supply, fork circuits), modulator and scalers.

*(2) Measurement of Interplanetary Matter*

The micrometeorite bombardment experiment employs thin resistance strips on the skin of the artificial satellite. There will be four groups of three detectors... twelve in all... of which eleven will consist of square patches laid side by side approximately a centimeter on an end. These will be wound by a continuous layer of enamelled wire 17 $\mu$ in diameter. The remaining detection element will be a thin layer of strontium between flared platinum connecting terminals. All will be wired in parallel.

The net resistance of the detectors is part of the frequency determining element of the free-running multivibrator, subcarrier modulation generator. When a meteor hits the detectors the circuit will open to alter the modulation frequency. Assuming a heavy micrometeoric flux, all detectors will open rather quickly and the strontium element will become abrazed. The extent of this abrasion will determine the degree of shift in the modulation frequency.

Unfortunately, few technical details of this experiment have been made available at the time of this writing.

## C. Package No. 3

*Geomagnetic Measurements*

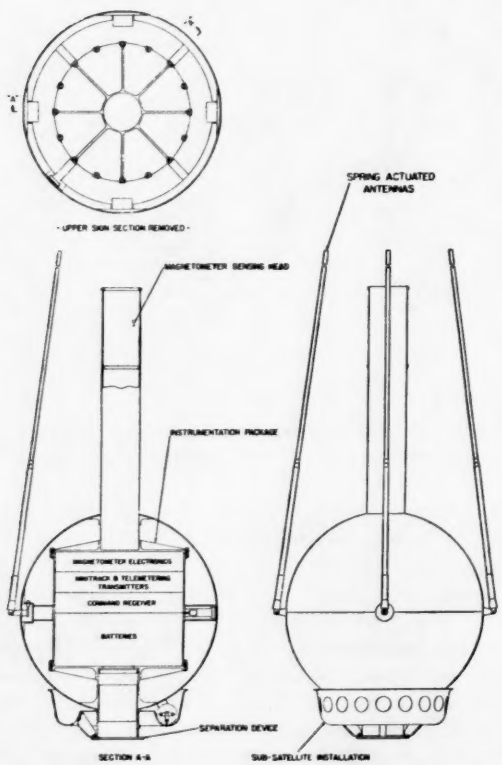


Fig. 10. Magnetometer satellite. (By courtesy of: U.S. Naval Research Laboratory)

It is planned to investigate both diurnal and irregular variations occuring in the magnetic field of the Earth caused by ionospheric currents, and to determine the existance or non-existance of the extraterrestrial ring-current. The effects of magnetic storms on the field and changes caused by the supposed ring-current of streams of charged particles will be carefully studied. Equally important will be the improvement of our knowledge of the main magnetic field of the Earth, and not merely of disturbances.

A proton precession magnetometer under development by Varian Associates will be used, weighing some three to four pounds. Devices of this type have seen considerable experience in high altitude research rockets, and are relatively simple and free from errors. An accuracy of better than ten gammas is assumed. The unit of intensity

of the Earth's magnetism is the gauss, being the intensity of a magnetic field acting with a force of one dyne upon a magnetic pole. The gamma is 1/100,000th of a gauss, and is used in magnetic surveying. The magnetometer used derives its operation from the magnetic moments exhibited by protons. These are aligned and released following which they precess about the Earth's magnetic field at a rate which depends on the scalar value of that field (i.e. independent of aspect).

Vol. 4 1958

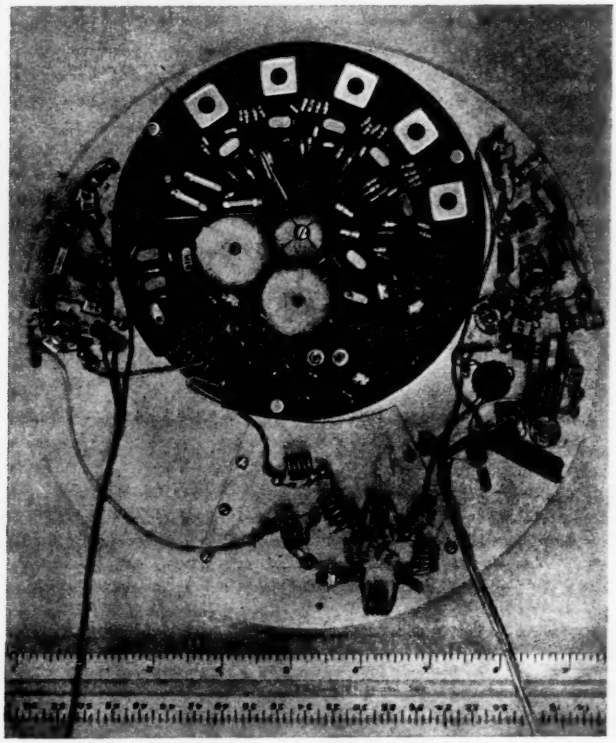

Fig. 11. Magnetic field satellite: Minitrack transmitter (left), telemetering transmitter (right), command receiver (center, top), antenna matching networks (bottom). (By courtesy of: U.S. Naval Research Laboratory)

A magnetic field of about 100 gauss is created by passing a current through a coil placed in a substance rich in protons. The proton's magnetic moment is now polarized, and when the polarizing field is rapidly withdrawn proton precession occurs. The moment induces a voltage in the coil which has been switched to a measuring circuit. The signal is audio-amplified and passed to the telemetering transmitter.

To begin a measurement, a relay in the command receiver is closed upon interrrogation from a Minitrack station. Telemetering and magnetometer circuitry are then on, and within half a second the command receiver relay will open. It becomes possible to apply a polarizing current to the sensing coil for a period of two seconds. Following the switching of the coil to the amplifier, the amplified precession signal can be transmitted to the telemeter for from one and a half to two seconds. Circuits then go off, pending a new interrogation.

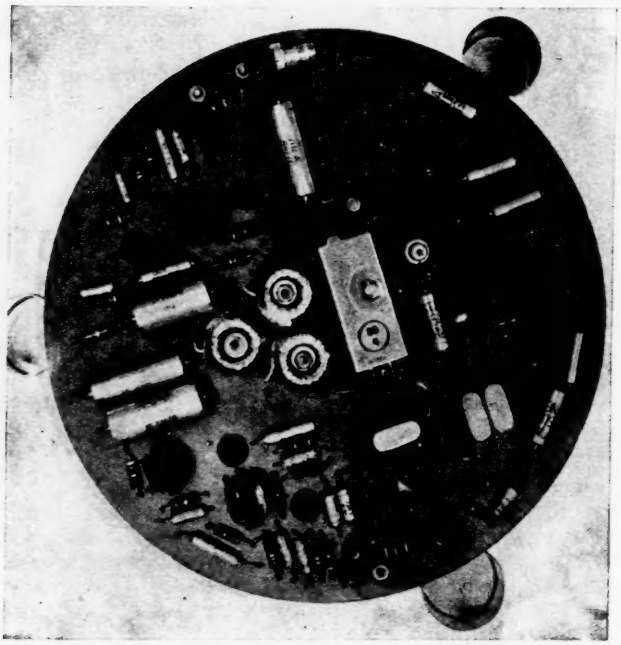

Fig. 12. Magnetic field satellite: module containing the magnetic amplifier and switching circuits. Diameter: $8^1/_2$ inches, weight: 15 ounces. (By courtesy of: U.S. Naval Research Laboratory)

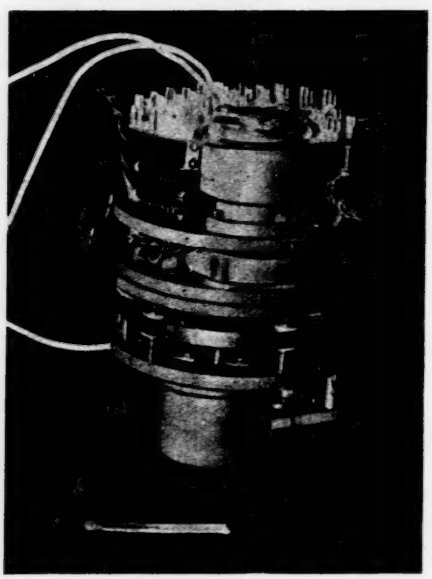

Fig. 13. Miniature tape recorder with cover removed. Programming switches are in center section; magnetic tape in bottom section. (By courtesy of: University of Wisconsin)

Both the signal and a 100 kc standard are magnetic tape recorded at the ground station. It is with reference to this standard that the precession frequency is counted.

It is pointed out that data storage will not be used, but rather measurements will be accomplished when the satellite is within range of Minitrack stations. There are two reasons for this: firstly, it is felt that there

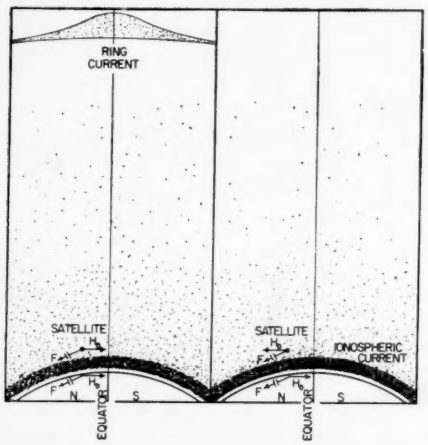


Fig. 14. This figure, prepared by the Naval Research Laboratory, illustrates how the cause of magnetic disturbances may be solved, i.e. are they caused by the postulated ring-current or by ionospheric disturbances? It is not known if ionospheric currents can cause the major disturbance field, or if they merely cause irregularities. The following description is given: If the current lies solely in the ionosphere the disturbance field, $H_D$, at the satellite should add to the Earth's main field, $F$, as illustrated. If the disturbance is created instead by a ring current, its field at the satellite will subtract from the Earth's main field. In both cases the disturbance field at the Earth's surface subtracts from the main field. Thus, through comparison of simultaneous measurements at the satellite and at the Earth's surface the location of the disturbing current is found. During the initial phase of a storm the $H_D$ vectors are all reversed and the same arguments apply. $H_D$ disturbance field, $F$ Earth's main field. (By courtesy of: U.S. Naval Research Laboratory)

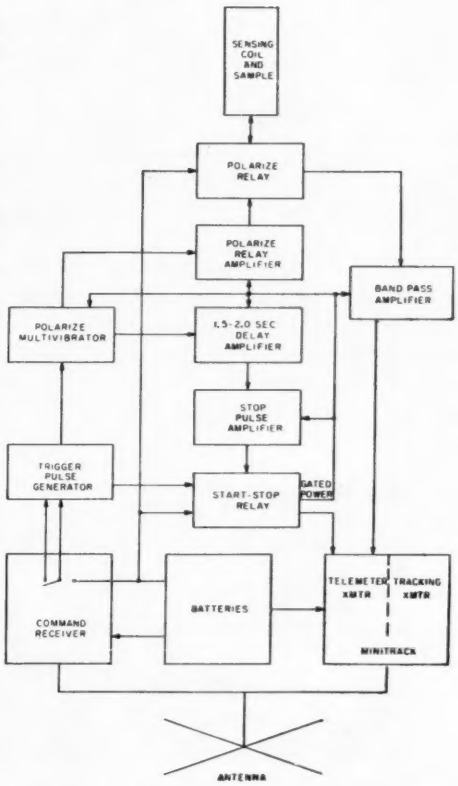


Fig. 15. Magnetometer satellite instrumentation. (By courtesy of: U.S. Naval Research Laboratory)

are too few magnetic observatories in existence to provide good surface reference for comparison with satellite measurements, and secondly "as the disturbance field is found by subtracting the undisturbed main field from the measured intensity", knowledge of the magnitude of the main field would be essential. Now, to determine the main field, measurements must not only be obtained during periods of magnetic calm but on a very wide-spread, dense basis all over the globe. This has not been accomplished.

It is expected that about 50 measurements a day will be achieved, and that the active life of the satellite will be between 70 and 100 days. Each time the

Vol. 4 1958

satellite comes within range of a Minitrack station a few measurements will be taken. While there will be 16 orbits daily, station overlap will permit some 24 passes.

## D. Package No. 4

A decision has yet to be made as to which of the following two experiments will be conducted on-board an Earth satellite vehicle. Both programs are progressing rapidly, and it is expected that a decision will be reached before this Winter.

### (1) *Investigation of the Radiation Balance of the Earth*

Researchers working on this experiment have likened the Earth's atmosphere to an enormous heat engine, with the net incoming solar radiation representing the heat input at the boiler and outgoing long wave energy representing the condenser heat sink. Because of the variable nature of cloud masses, both as to geographic coverage and density, the atmospheric heat engine must function with a nonconstant input of short wave energy. It was therefore decided that an experiment should be devised to determine accurately the changing input and loss relationship.

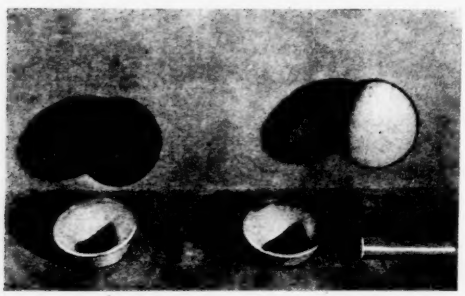

Fig. 16. White and black spherical sensors. Dissembled unit shows KEL-F thermal isolating support. (By courtesy of: University of Wisconsin)

Measurements will be made of the magnitude of radiation currents, including solar radiation, Earth-reflected solar radiation, and energy radiated out by the planet as a whole. The first two supply energy at shorter than 2.5 $\mu$ wavelengths and the latter is in the greater than 2.5 $\mu$ region. Sensors enjoying wavelength discrimination can separate the long from the short wave radiation. For example, to detect the reflected shortwave radiation, a sensor would be used that responds only to this and not to direct shortwave or terrestrial radiation.

Specially surfaced spheres will be employed as sensors (two are 1.25 inch coated spheres; the remaining two are smaller and are fitted with sunshades). In the above example it would be necessary to shield the sphere from the Sun and employ a surface almost black in the shortwave region and with very low absorptivity characteristics in the longwave region.

It has been reported that the sphere has such a sensitivity that a change of 0.001 cal/cm$^2$/min will produce a temperature change of approximately 0.2 $^0$C. It follows that if we use three spherical sensors responding to selective radiation currents it will be possible to measure the resulting temperatures and temperature changes. It should be noted that the temperatures will be affected by altitude changes of the orbiting vehicle.

Small pingpong ball size spheres will be placed on the ends of radio antennae. Temperatures would be measured every half minute, representative of about 150 miles of satellite track. Three simultaneous equations will be solved to obtain incoming solar radiation, reflected solar radiation and outgoing planetary infrared radiation. Once values have been obtained we shall be in a position of

knowing the energy balance and how it varies with position and time. The data storage and telemetering system should be of sufficient capability to read 0.2 °C changes.

The basic elements of the instrumentation for this experiment include four thermistors (to measure the average fourth power temperature of the sensing elements), a coding oscillator (its PRF is controlled by the resistance value of each thermistor in sequence), a time standard (a 512 cps tuning fork is counted down to form 1/2 second pulses, providing precise time intervals for gating the coding oscillator and ratchet drive), a "temporary" storage element, which is a ten binary digit counter (two used), and a "permanent" storage element, namely a small magnetic tape recorder.

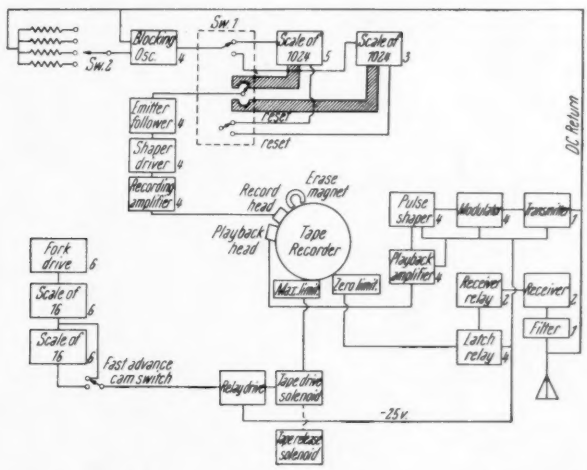


Fig. 17. Block diagram of radiation balance satellite. (By courtesy of: University of Wisconsin)

If the instrumentation operates over the 80 day period, 230,000 sets of observations will be made, figuring on 180 sets per orbit (a set consisting of five numbers between 0 and 1024). The magnetic tape received from the telemetering posts will be directly fed to an electronic digital computer.

Electronics and the tape recorder weigh less than three pounds. Assuming nearly eight pounds of batteries for 80 days operation, the package comes to about 11-1/2 pounds. Power requirements are less than 200 mw. All items are to fit inside a six-inch cylinder.

### (2) *Measurement of Cloud Cover and Albedo of the Earth*

This experiment is also designed to contribute to knowledge of the Earth's energy budget. Optical techniques will be employed and observations from the satellite will be based on contrasting reflections from land, sea and cloud formations. Radiation reflected from many parts of the planet will be scanned, and, when tied to knowledge of precise satellite orientation in terms of the Earth, will yield data on cloud cover distribution.

Two photocells (photoelectric telescopes) observing in opposed directions form the basic detection system. One telemetering channel is needed. Signals generated are mixed with a 300 cps subcarrier, and stored on a magnetic tape

Vol. 4 1958

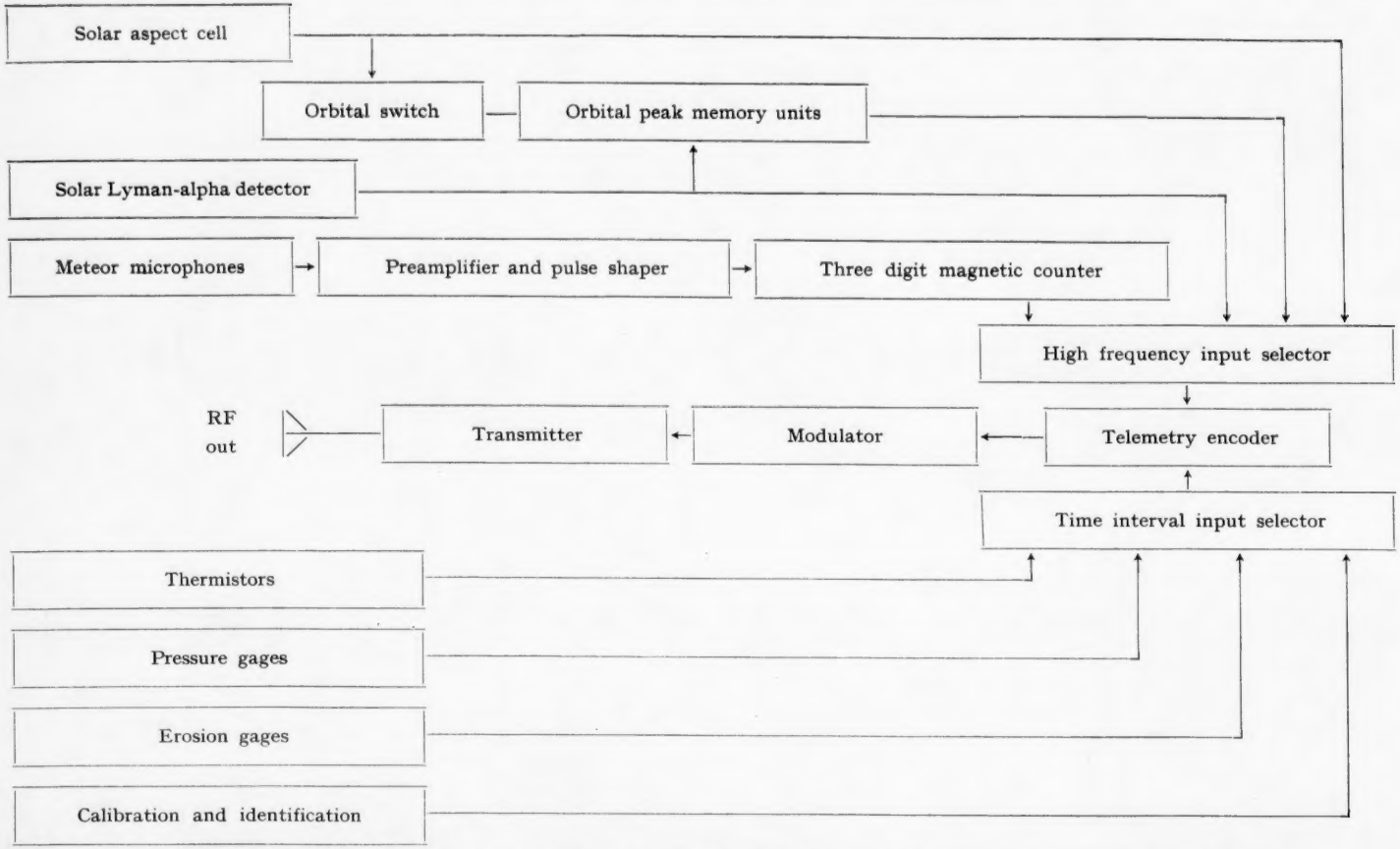


Fig. 18. Block diagram of telemetering system for the first satellite. (By courtesy of: U. S. Naval Research Laboratory)

recorder. Upon command, playback occurs for a one minute period presenting 50 minutes of data. The photocell will sweep the horizons in its view. At perigee (200 miles) the path will be some 15 miles wide and 2500 miles long.

### 7. Experiments Requiring Non-Instrumented Satellites

Other experiments will involve geodetic measurements, ionospheric research and air density studies.

Geodetic advantages derive from both optical and radio tracking of the satellite vehicle, and it is hoped that not only will greater knowledge of the Earth's gravitational anomalies be obtained (by observing perturbations of the orbit) but that ground stations throughout the world will be more accurately linked.

As for the ionosphere, angular errors accruing from 108 mc radio direction measurements will depend on the integrated ion density along the radio transmission path and the zenith angle. The orbital characteristics must be precisely known and radio measurements must be taken over a wide arc. Computations following the basic measurements should give us a good value of integrated ion density over the ground direction-finding station. It is also planned to determine the ionospheric effects on radio signals emanating from the satellite.

Vol. 4 1958

This experiment is being carried out by the Army Ordnance Ballistic Research Laboratories. The use of the Minitrack transmitter as the signal source has been finally decided upon, although BRL earlier desired to use lower frequencies emanating from a specially designed transistorized crystal controlled transmitter. By comparing the reference frequency with the received satellite frequency the Doppler frequency results, and can be compared with theoretical values depending on the exact orbital parameters. Not only will the integrated ion density be determined along the radio path, but local ion density along the satellite track will be obtainable. BRL is interested in the magnitude of and the variation in, ionization and will carefully watch data obtained during the period of satellite transition into or out of darkness.

BRL will Doppler track the 108 mc Minitrack signal from a station in the vicinity of the White Sands Proving Ground. Specially modified super DOVAP receivers are now being prepared to measure the Doppler shift.

The N.A.C.A. will perform an expandable plastic sphere experiment with the Third Instrumentation Package (Magnetometer) firing. It will gain knowledge of air density by noting the relationship between satellite drag and density of the air at extreme altitude. Orbital perturbations will result from air drag on the large, lightweight, inflatable plastic and aluminum foil sphere. Its high drag-to-weight ratio should be of great help in getting the required data.

This sub-satellite experiment is a 30 inch diameter sphere and features 0.000 25 inch thick polyester plastic film bonded to the aluminum foil (itself 0.005 inch thick). It folds into a package which fits inside an annular shaped container. The assemblage is located between the main satellite and the Vanguard third stage rocket.

Once the main satellite is placed into orbit, the sub-satellite is pneumatically-erected by compressed nitrogen gas at 2000 psi pressure. The sub-satellite is now ejected from its container, and, under a pressure of about 0.2 psi, it has the wrinkles formed from folding taken out. Next, it is de-pressurized, but because of its inherant stiffness it maintains itself as a sphere under loadings up to one g, far greater than those to be expected.

The full installation weighs 0.69 pounds, composed as follows:

| | |
|---|---|
| sub-satellite | 0.25 pound |
| pneumatic erection tank | 0.19 pound |
| annular container | 0.25 pound |

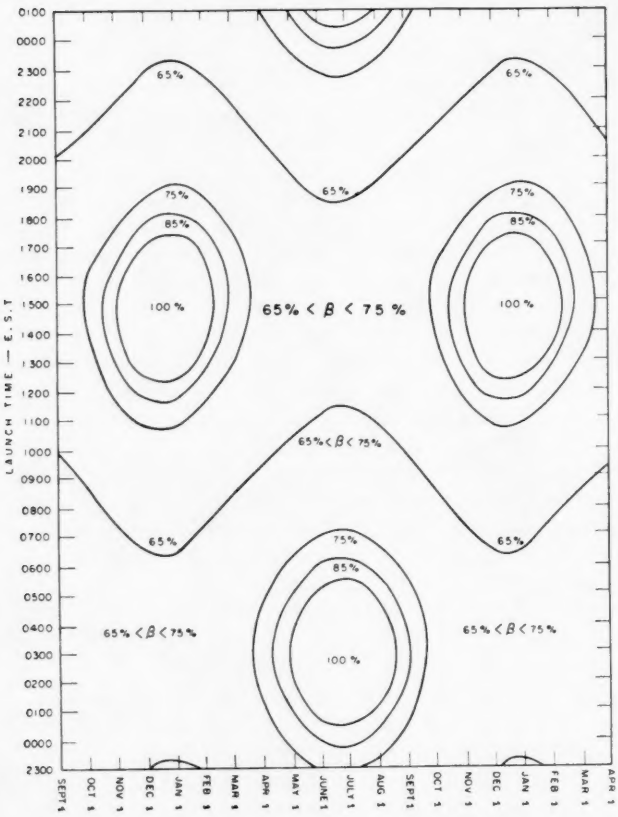


Fig. 19. Percent time in sunlight for 200—1500 mile orbit. Apogee away from Sun. (By courtesy of: U.S. Naval Research Laboratory)

## 8. Other Experiments

There are a number of other experiments still under more or less active consideration. These include a radioactive meteor erosion gauge experiment proposed by the University of Maryland Physics Dept., and a proposal from RIAS (The Martin Co.) on the determination of the flux of primary cosmic ray nuclei with atomic number larger than eight.

Recent reports suggest that the last named experiment will be performed, with support coming from the National Science Foundation. Heavy nuclei components of primary radiation will be observed by the ionization bursts formed while traversing a defined particle length in a gas. An ionization chamber similar to ones previously used in upper air balloon tests will

be tried, properly modified to adhere to satellite requirements, missile acceleration, etc. A linear amplifier has been designed to respond to individual ionization bursts, and pulses will be transmitted during each satellite transit (it should be noted that this refers only to pulses corresponding to atomic number greater-than-eight particles traversing the chamber).

It is expected that the following information will be gained: (a) number of heavy nuclei, (b) spectral distribution of heavy nuclei, (c) diurnal effects, and (d) time variations (due to solar activity). The counting rate will vary according to geomagnetic latitude.



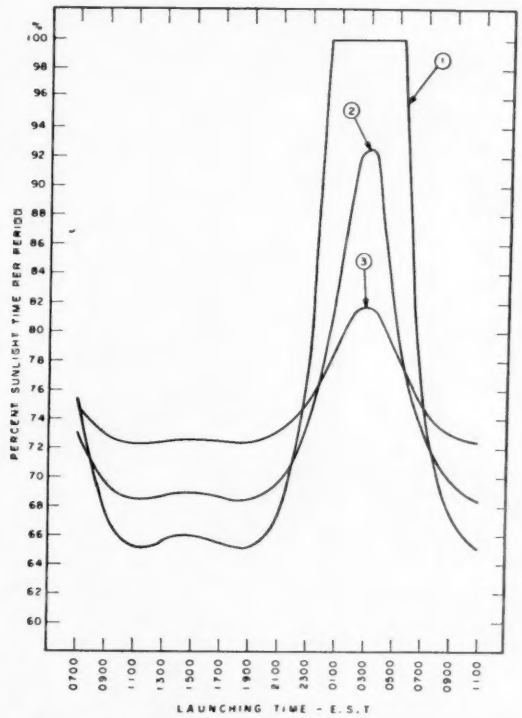


Fig. 20. Percent time in sunlight for 200—1500 mile orbit. Summer solstice ($\delta_{\odot} = +23{,}5^{0}$) June 22. For two week future conditions: add $4^{h}\,50^{m}$. Apogee: *1* away from Sun, *2* $90^{0}$ from Sun, *3* toward Sun. (By courtesy of: U.S. Naval Research Laboratory)

The meteoric erosion experiment would involve the use of a radioactive material coating a portion of the outside surface of the satellite with a detector at a corresponding position inside. As incoming meteoric matter erodes the surface, the radioactive material will be removed, causing a decrease in the counting rate. Microminiaturization techniques keep the gauge weight to about 3/4 of an ounce. The University of Maryland reports three ways in which the radioactive method can be adapted:

(a) as a surface erosion gauge,

(b) as a volume erosion gauge to measure the total amount of material carried away,

(c) in a sandwich form as a penetration gauge.

The radioactive source is strontium-90. Germanium transistors are used in the reduced size circuits. The experiment operates well within the Vanguard-ESVP temperature limits, will operate from the Minitrack 22 volt system, and draws 40 milliwatt. All environmental checks (acceleration, temperature, etc.) have been completed.

### 9. Miscellaneous

All experiments are undergoing, or will undergo, rigid environmental tests, including vibration testing and thermal-vacuum testing.

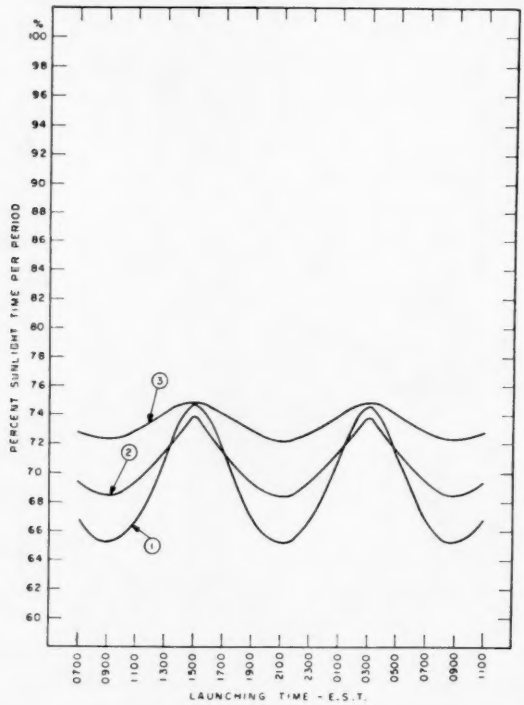


Fig. 21. Percent time in sunlight for 200—1500 mile orbit. Vernal equinox (March 21): add 7 min. ($\delta_\odot = 0^0$), autumnal equinox (September 23): subtr. 7 min., for two week future conditions: add $4^h\ 50^m$. *1* away from Sun, *2* $90^0$ from Sun, *3* toward Sun. (By courtesy of: U.S. Naval Research Laboratory)

A considerable amount of work is being performed to obtain the best batteries, and rather definite battery selection criteria have been established. Miniature silver-cadmium storage cells and mercury cells are presumably to be used. The Signal Engineering Labs have a four ounce solar battery program under way which can fit into a space 3 × 3-1/2 × 1/2 inches. It furnishes three volts at 20 ma. Life cycle, reliability, temperature, vacuum load and vibration tests are being carried out on all batteries.

**Acknowledgement**

The compilation of this material on satellite instrumentation would have been impossible without the excellent cooperation of the U.S. Naval Research Laboratory, the U.S. National Committee for the International Geophysical Year, and of the several agencies working on various aspects of the instrumentation program. The majority of the photographs and illustrations are due to the courtesy of the U.S. Naval Research Laboratory and the Department of the Navy.

**References**

*Five general books* on satellites are available, the first giving the most professional coverage of Vanguard and the second detailing much little-known historical background to the project. The third describes some 30 possible experiments.

1. A. C. CLARKE, The Making of a Moon. New York: Harper, **1957**.
2. E. BERGAUST and W. BELLER, Satellite. Garden City: Hanover House, **1956**.
3. J. A. VAN ALLEN (ed.), Scientific Uses of Earth Satellites. Ann Arbor: University of Michigan, **1956**.
4. P. MOORE, Earth Satellites. New York: Norton, **1956**.
5. M. CAIDEN, Vanguard. New York: Dutton, **1957**.

Vol. 4 1958

*The following papers are the most recent on the subject of instrumentation,* having been presented at the Rocket and Satellite Conference, CSAGI-USNC/IGY, 30 September—5 October, **1957**, Washington, D.C., U.S.A.

W. J. O'SULLIVAN, JR., The USNC-IGY-NACA Earth Sub-Satellite Experiment.
H. FRIEDMAN, The Lyman-Alpha Experiment.
R. TOUSEY, Visibility of the Vanguard Satellite.
R. W. PORTER, Summary Report on United States Satellite Program for the International Geophysical Year.
J. A. VAN ALLEN, Scientific Instrumentation of the Satellite.
V. E. SUOMI, The Radiation Balance of the Earth From a Satellite.
H. E. LAGOW et al., Experiments for Satellite Environmental Measurements.
J. P. HEPPNER et al., A Review of Instrumentation for the Magnetic Field Satellite Experiment.
W. MATTHEWS, Telemetering in Earth Satellites.
R. C. BAUMANN, Satellite Structures and Engineering Testing.
J. P. HAGEN, The Satellite Launching Vehicle-Placing the Satellite in Orbit.

*Other recent papers on satellite instrumentation include:*

J. T. MENGEL, Ear to the Sky (Minitrack). Astronautics **2**, 28 (1957).
A. L. BLOOM and L. E. JOHNSON, A Magnetometer for the Satellite. Electronic Ind. Tele-Tech. **16**, 76 (1957).
H. E. NEWELL, JR., Scientific Uses of an Artificial Earth Satellite. J. Amer. Rocket Soc. **12**, 712 (1955).
H. HABER, Space Satellites, Tools of Earth Research. Nat. Geogr. Mag., April **1956**.
G. H. LUDWIG and J. A. VAN ALLEN, Instrumentation for a Cosmic Ray Experiment for the Minimal Earth Satellite. J. Astronautics **3**, 59 (1956).
S. F. SINGER, Radioactive Meteor Erosion Gauge for Earth Satellites. Physics Dept., Univ. Maryland Quart. Progr. Rep. II (31 March **1957**); Meteorological Measurements from a Minimum Satellite Vehicle. Trans. Amer. Geophysic. Union **38**, 469 (1957); The Application of an Artificial Satellite to the Measurement of the General Relativistic "Red Shift". Physic. Rev. **104**, 11 (1956); Measurements of the Earth's Magnetic Field from a Satellite Vehicle. Univ. Maryland Techn. Rep. No. 32 (March **1956**); Earth Satellites as Research Vehicles. Proceedings of Symposium. Franklin Institute, Monograph No. 2 (June **1956**); Minimum Satellites as "Storm Patrol". Sci. Monthly **85**, 95 (1957); Earth Satellite Instrumentation. Electr. Engng. **76**, 562 (1957).

R. P. HAVILAND, What the Future Holds for the Earth Satellite. Gen. Electr. Rev. (Sept. **1956**).

H. K. KALLMANN and W. W. KELLOGG, Use of an Artificial Satellite in Upper Air Research. RAND P-760 (15 Feb. **1956**).

ARS Space Flight Committee, On the Utility of an Artificial Unmanned Earth Satellite. J. Amer. Rocket Soc. **25**, 71 (1955).

E. C. WHITE et al., Power Supplies and Telemetry for an Instrumented Artificial Satellite. J. Brit. Interplan. Soc. **15**, 177 (1956).

H. E. CANNEY and F. I. ORDWAY, The Uses of Artificial Satellite Vehicles. Astronaut. Acta **2**, 147 (1956); **3**, 1 (1957).

D. T. GOLDMAN and S. F. SINGER, Studies of a Minimum Orbital Unmanned Satellite of the Earth: Radiation Equilibrium and Temperature. Astronaut. Acta **3**, 110 (1957).

M. SUBOTOWICZ, Satellites for Checking Einstein's Relativity Theory. Missiles and Rockets **2**, 57 (1957).

W. A. BAUM, A Fundamental Cosmological Experiment for the Artificial Satellite. Astronom. J. **61**, 171 (1956).

R. P. HAVILAND, On Applications of the Satellite Vehicle. Jet Propulsion **26**, 360 (1956).

H. WEXLER, The Satellite and Meteorology. J. Astronautics **4**, 1 (1957).

C. C. FURNAS, The Vanguard Satellite. Ordnance **41**—220, 596 (1957).

J. KAPLAN, Rocket and Satellite Studies During the I.G.Y. Aeronaut. Engng. Rev. **15**, 64 (1956).

H. E. NEWELL, JR., The Satellite Project. Sci. American **193**, 29 (1955).

J. A. O'KEEFE, Geodesy Comes of Age With Vanguard. Astronautics **2**, 71 (1957).

H. FRIEDMAN, The Vanguard Instrument Package. Astronautics **2**, 66 (1957).

T. A. CHUBB and H. FRIEDMAN, Photon Counters for the Far Ultraviolet. Rev. Sci. Instruments **26**, 493 (1955).

R. W. ROCHELLE, Earth Satellite Telemetry Coding System Using Transistors and Magnetic Cores. Amer. Instn. Electr. Engng., C.P. 57—352, Jan. 1957.

D. H. SCHAEFER, Magnetic Core Event Counter for Earth Satellite Memory. Amer. Instn. Electr. Engng., C.P. 57—359.

W. MATTHEWS, Telemetering in Earth Satellites. Amer. Instn. Electr. Engng., C.P. 57—322.

C. B. HOUSE and R. L. VAN ALLEN, Commutation and Nondestructive Read-Out of Magnetic Memorary Cores in Earth Satellites. Amer. Instn. Electr. Engng., C.P. 57—374.

W. MATTHEWS, Earth Satellite Instrumentation Program. Amer. Instn. Electr. Engng., C.P. 57—323.

H. FRIEDMAN, Scientific Instrumentation in I.G.Y. Satellites. Amer. Instn. Electr. Engng., C.P. 57—213.

J. P. HAGEN, The Exploration of Outer Space With an Earth Satellite. Proc. Inst. Radio Engrs. **44**, 744 (1956).

D. G. MAZUR, Telemetering and Propagation Problems of Placing the Earth Satellite in Orbit. Proc. Inst. Radio Engrs. **44**, 752 (1956).

J. A. VAN ALLEN, The Scientific Value of the Earth Satellite Program. Proc. Inst. Radio Engrs. **44**, 764 (1956).

## Buchbesprechungen — Book Reviews — Comptes rendus

**Dreidimensionale Überschallprobleme der Gasdynamik.** Von K.-R. DORFNER. (Ergebnisse der angewandten Mathematik: Heft 3.) Mit 44 Textabb., VII, 150 S. Berlin-Göttingen-Heidelberg: Springer-Verlag. 1957. DM 26.—.

Die nichtlinearisierte (und erst recht die linearisierte) Theorie der ebenen und rotationssymmetrischen Überschallströmung wird seit langem in der Lehrbuchliteratur ausführlich dargestellt. Dagegen sind Ansätze für eine nichtlinearisierte Theorie bei allgemeineren dreidimensionalen Strömungen kaum vorhanden; auch die zugehörige linearisierte Theorie hat noch nicht eine so eingehende lehrbuchmäßige Darstellung gefunden, wie es dem gegenwärtigen Interesse an diesem Gegenstand entsprechen würde; das gilt insbesondere für die Umströmung von Tragflügeln. — Unter diesen Umständen vermag die vorliegende Monographie, die einen Überblick über die bisher entwickelten linearen Methoden zur Berechnung dreidimensionaler Überschallströmungen an flachen Körpern gibt, eine fühlbare Lücke zu schließen. Grundlegend ist hier das allgemeine Singularitätenverfahren, das keine zusätzlichen Bedingungen an die Flügelform stellt und einen Einblick in die Struktur des Strömungsfeldes vermittelt (Kap. II). Praktisch wichtiger sind jedoch die Verfahren der kegelsymmetrischen, bzw. der verallgemeinerten kegelsymmetrischen (homogenen) Strömung (Kap. III, bzw. IV); hierbei reduziert sich das räumliche Problem durch die Einführung zusätzlicher Bedingungen auf ein leichter zu behandelndes Problem mit nur zwei unabhängigen Variablen. Der rollende Dreieckstragflügel ist eines der Beispiele, für welche die Lösung nach dieser Methode hergeleitet wird. — Die Regeln für das immer wiederkehrende Operieren mit Unstetigkeitsfunktionen werden im Kap. I vorweg behandelt; um so mehr Platz bleibt für die Diskussion der eigentlichen gasdynamischen Fragen. Ferner werden die wichtigsten Formeln jeweils am Schluß des Kapitels zusammengestellt, wodurch das Nachschlagen erleichtert wird. Das klare und inhaltsreiche Werk wird daher dem Aerodynamiker und Luftfahrtingenieur zur Ergänzung der vorhandenen Lehrbücher über Gasdynamik sehr willkommen sein.

H. STÜMKE, Stuttgart

Vol. 4 1958

**Advances in Geophysics.** Edited by H. E. LANDSBERG. Volume 3. Mit 135 Textabb., X, 378 S. New York: Academic Press Inc., Publishers. 1956. $ 8.80.

Die vorliegende Sammlung von Einzelbänden aus dem Bereich der Geophysik wird, sobald sie vollständig vorliegt, ein sehr umfassendes Bild des heutigen Wissens und der Probleme dieser Wissenschaft geben. Der hier besprochene 3. Band bringt unter anderem einen Beitrag von S. F. SINGER, dessen Verdienste um die Verwirklichung künstlicher Erdsatelliten weltbekannt sind. Dieser Beitrag behandelt folgende Probleme: das magnetische Erdfeld, Gestalt der Erde und Schwereanomalien; die Albedo der Erde in Beziehung zum Wetter; Infrarotemission und Temperatur von Atmosphäre, Erdboden und Ozeanen; die Ozonschicht; Nachthimmelsleuchten und Polarlichter; Elektronendichte und elektrische Ströme in der Ionosphäre sowie deren Beziehung zu magnetischen Stürmen; Ableitung atmosphärischer Dichten aus beobachteten Satellitenbahnen, Dichtemessungen und Bestimmung von Zusammensetzung und Elektronendichte der Atmosphäre, Ermittlung von Windströmungen, Temperatur und Turbulenz mit Hilfe künstlicher Meteore; Messungen im ultravioletten und Röntgenbereich des Sonnenspektrums; Lyman-$\alpha$-Strahlung des interplanetaren Wasserstoffes; Teilchenströme und Polarlichtentstehung; kosmische Strahlung (Höhenstrahlung): geomagnetische Effekte, Energiespektrum, Zusammensetzung, Ansteigen im Zusammenhang mit Sonnenfackeln, Abnahme im Zusammenhang mit solarer Korpuskelstrahlung; Messung von Größe und Frequenzverteilung meteoritischer Teilchen, Erosion durch Aufprall; Energiebilanz der Erde und atmosphärische Zirkulation im Großraum; mögliche Satellitenbahnen, Satellit mit und ohne Sendeeinrichtung, Satellit mit Lagekontrolle.

SINGERS Ausführungen nehmen 67 Seiten mit 37 Abbildungen ein. Der Rezensent kennt keine anderen Beispiele für eine ebenso gut durchdachte, knappe und trotzdem im besten Sinn wissenschaftliche Darstellung der Satellitenforschung in einem Einzelbeitrag, die jedem Leser ein gründliches Verständnis der angestrebten Forschungsziele ermöglicht.

Wenngleich der Rezensent sich nicht vermessen darf, über die übrigen, außerhalb seiner Kompetenz liegenden Kapitel ein Urteil zu fällen, hat er darin doch viele Einzeltatsachen gefunden, die in Vorlesungen über Geochemie und Kosmochemie Platz gefunden haben, und daraus großen Nutzen gezogen. Es sind folgende Verfasser und Beiträge zu nennen: A. P. CRARY, Erforschung arktischer Eisinseln; Z. SEKERA, Polarisation des Himmelslichtes; P. BYERLEY, Subkontinentale Struktur im Licht seismologischer Beweise; E. C. BULLARD, A. E. MAXWELL und R. REVELLE, Wärmefluß durch den Tiefseeboden; J. A. JACOBS, Das Erdinnere; P. H. JONES und H. E. SKRIBITZKE, Grundwasserhydrologie. F. HECHT, Wien

**Einführung in die Methoden der Programmierung kaufmännischer und wissenschaftlicher Probleme für elektronische Rechenanlagen.** 1. Teil: Die Logik der Programmierung. Von B. THÜRING. Mit 100 Textabb. 217 S. Baden-Baden: R. Göller Verlag. 1957. Geb. DM 45.—.

Der Verfasser hat sich mit dem ersten systematischen Buch über die Methoden der Programmierung zweifellos ein großes Verdienst erworben.

Die große Bedeutung der Rechenautomaten für die Volkswirtschaft, die Statistik und viele andere Gebiete wird immer mehr erkannt. Nicht zuletzt wird auch die Astronautik bei den jetzt wichtig werdenden Bahnrechnungen nicht auf sie verzichten können.

Rechenautomaten können aber nur eine Vielzahl einfacher arithmischer (und logistischer) Operationen ausführen. Die Maschine bedarf daher sehr genauer Richtlinien für die Reihenfolge der Operationen. Diese Richtlinien müssen aber für jede Aufgabenart nur einmal aufgestellt werden. Man nennt dies die „Programmierung".

Der vorliegende Teil 1 des Werkes will die für alle Aufgaben gemeinsamen Grundzüge der Programmierung erstmalig in systematischer Form darstellen. Darin liegt ohne Zweifel der große Wert dieses Buches, das sich in vier Kapitel gliedert.

*Kapitel 1* (Zahlen-Darstellung und Wortdarstellung; Grundrechenoperationen) erklärt zunächst die Grundzüge des dualen Zahlensystems und befaßt sich sodann mit dem Wesen der Programmanalyse und dem Aufstellen des Ablaufdiagramms, das den Hauptanteil der ganzen Programmierung bedeutet.

Im *Hauptkapitel 2* folgen kaufmännische Rechenpläne (Programme) mit systematischen Darlegungen über die Ablaufdiagramme und die algorithmischen Darstellungen von Plänen. Zahlreiche Aufgaben und Zeichnungen von der einfachsten Addition von Zahlen bis zum Unterplan einer Lohnabrechnung werden bis zur algorithmischen Darstellung durchgeführt und tragen so sehr zur Veranschaulichung bei.

Das *Kapitel 3* enthält wissenschaftliche Rechenpläne, wobei vor allem die Lösungen von Gleichungen (bis zur Lösung einer algebraischen Gleichung vierten Grades) und von linearen Gleichungssystemen durchgeführt werden.

Das *Kapitel 4* behandelt grundsätzliche Dinge, die nicht vergessen werden dürfen, wie etwa „Eingabe" und „Ausgabe", Methoden der Sortierung von „Informations-Einheiten", sowie von Gruppen und Listen solcher.

Gerade die allgemeine Behandlung gibt diesem Buch für jeden, der sich der elektronischen Rechenanlagen bedienen will, seinen besonderen Wert. Mit größtem Interesse darf man den zweiten Band erwarten, der schon angekündigt ist, und der der Rechenanlage der Univac Factronic in Frankfurt am Main (Firma Remington Rand) gewidmet ist, die als die größte zur Zeit in Europa öffentlich zur Verfügung stehende, Daten-verarbeitende elektronische Rechenanlage anzusehen ist.

K. SCHÜTTE, München

Herausgeber, Eigentümer und Verleger: Springer-Verlag, Wien I, Mölkerbastei 5. — Für den Inhalt verantwortlich: Prof. Dr. Friedrich Hecht, Wien VIII, Alserstraße 69. — Druck: Berger & Schwarz, Zwettl, N.-Ö.

# An Analytical Solution for Flight Time of Satellites in Eccentric and Circular Orbits

By

**F. M. Perkins**[1]

(With 10 Figures)

(*Received November 12, 1957*)

Vol. 4 1958

**Abstract — Zusammenfassung — Résumé**

**An Analytical Solution for Flight Time of Satellites in Eccentric and Circular Orbits.** Analytical solutions for the altitude-time relationships for both circular velocity and eccentric satellite orbits are derived and presented. A comparison is made of results from an analytical closed solution with accurate detailed stepwise integrated trajectory computations from a high speed digital computer. The analytical results are sufficiently accurate for most engineering purposes. Furthermore, the analytical approach makes possible the rapid inexpensive solution of large families of trajectories. It also yields an insight into the problem and illustrates general principles of satellite orbital behavior. Use of the generalized curves for the analytical solutions (Figs. 8, 9 and 10) is not limited to any one set of atmospheric density versus altitude data. Furthermore, these plots are completely dimensionless and hence equally applicable to metric and English units of measure.

**Eine analytische Lösung für die Lebensdauer von Satelliten in exzentrischen und Kreisbahnen.** Analytische Lösungen für das Höhe-Zeit-Verhältnis sowohl für Kreisbahngeschwindigkeit als auch für exzentrische Satellitenbahnen werden abgeleitet und vorgeschlagen. Zum Vergleich werden die Resultate einer analytisch geschlossenen Lösung angegeben, die mit Hilfe einer elektronischen Rechenmaschine unter Benützung genauer, stufenweise integrierter Bahnberechnungen erhalten wurde. Die analytischen Ergebnisse sind für die meisten technischen Zwecke ausreichend genau. Außerdem ermöglicht die analytische Annäherung die rasche und billige Lösung großer Familien von Bahnen. Sie gestattet auch einen Einblick in das Problem und illustriert allgemeine Prinzipien des Verhaltens von Satellitenbahnen. Die Benützung verallgemeinerter Kurven für die analytischen Lösungen (Abb. 8, 9 und 10) ist nicht auf irgendeine Annahme der atmosphärischen gegenüber Höhendaten beschränkt. Außerdem sind diese Diagramme völlig dimensionslos und deshalb in gleicher Weise für das metrische wie auch für das englische Maßsystem anwendbar.

**Une solution analytique au problème des durées de vol des satellites sur des trajectoires circulaires ou elliptiques.** Des solutions analytiques pour la relation altitude-temps dans les orbites circulaire et elliptique de satellites sont déduites et présentées. La comparaison d'une solution analytique sous forme finie avec les résultats d'un calcul précis de trajectoire par intégration à pas fin sur une machine digitale montre que les résultats analytiques ont une précision suffisante pour la plupart des applications techniques.

---

[1] Preliminary Design Engineer and Head of Mechanics Section, Preliminary Design and Systems Analysis Group, Astronautics Division, Convair, San Diego, Calif., USA.

L'approche analytique fournit une solution peu couteuse à l'établissement d'une famille étendue de trajectoires. Elle met aussi en évidence les aspects principaux du comportement orbital du satellite. L'utilisation des courbes généralisées (Figs. 8, 9 et 10) pour les solutions analytiques n'est pas limitée à une relation déterminée entre l'altitude et la densité atmosphérique. De plus, étant sans dimensions, les graphiques sont également applicables à tout système d'unités.

### Symbols

$C_D$ = drag coefficient $= \dfrac{D}{S\ (\frac{1}{2}\ \varrho\ V^2)}$

$D$ = drag

$f(\ )$ = a function of

$g$ = gravity constant

$K = g_{oo}\left(\dfrac{C_D\,S}{W}\right)\varrho_0\, r_0^2$ = a constant

$m$ = a constant

$r$ = radius distance from center of earth

$S$ = reference area

$t$ = time

$\bar{t}$ = $\lambda\, t$ = dimensionless expression for time

$V$ = velocity

$W$ = weight

$Y$ = altitude

$\beta$ = a constant

$\Delta$ = an increment of

$\lambda$ = $V_0/r_0$

$\mu$ = universal gravity constant = $gr = 1.404\ 24 \times 10^{16}$ ft$^3$/sec$^2$

$\varrho$ = atmospheric mass density

$\sim$ = proportional to

$\cong$ = approximately equals

$\triangleq$ = equals by definition

### Subscripts

$o$ = initial

$oo$ = at surface of earth

$C$ = circular

$D$ = due to drag

$g$ = due to gravity

## Introduction

Man made satellites are the next step forward in man's conquest of space. Their immediate application is for military reconnaissance and to achieve a greater knowledge of the upper atmosphere. The time which these satellites remain in flight is of primary importance in their efficient design.

In this paper the fundamental equations for the orbital lifetime and the altitude-time relationship of satellites in both circular and eccentric orbits are derived. In the case of eccentric (elliptic) orbits, equations are developed for the rate of fall of perigee and apogee and the rate of approach to circular flight.

The generalized solutions for orbital lifetime and the altitude-versus-time relationships are compared with accurate results obtained from stepwise integration of the trajectory equations of motion by high speed digital computing machines.

## Summary

The following general equation for orbital lifetime of circular velocity satellites was derived.

$$\bar{t} = \frac{\varrho_0}{K}\int_{Y}^{Y_0}\frac{dY}{\varrho}. \tag{21}$$

If density, $\varrho$, is not readily available as an analytical function of altitude, $Y$, the above equation may be graphically integrated by plotting $1/\varrho$ versus $Y$.

Frequently the density at the initial altitude and for some distance below may be expressed by an equation of one of the following two forms.

$$\varrho \sim e^{mY} \tag{22}$$

$$\varrho \sim Y^{\beta}. \tag{23}$$

Substituting of eqs. (22) and (23) respectively into eq. (21) and integrating yields the following orbital lifetime equations.

$$\bar{t} = \frac{1}{-mK}\left[1 - e^{m(Y_0 - Y)}\right] \tag{25}$$

$$\bar{t} = \left(\frac{1}{1-\beta}\right)\frac{Y_0}{K}\left[1 - \left(\frac{Y}{Y_0}\right)^{1-\beta}\right]. \tag{26}$$

Depending upon the atmospheric data used, eq. (25) does not usually apply over a sufficient region of altitude to permit total lifetime determination on one step. Eq. (26), however, does yield an approximate total lifetime expression by setting $Y$ equal to zero.

$$\bar{t} = \left(\frac{1}{1-\beta}\right)\frac{Y_0}{K}. \tag{27}$$

Vol. 4 1958

Eq. (27) is plotted in Fig. 4 using the atmospheric data of Fig. 1. Superimposed upon Fig. 4 are points obtained by an accurate stepwise integration from a high speed digital computing machine using various ratios of weight-to-drag frontal area $W/C_D S$.

A plot of altitude versus time from the theory [eq. (26)] is compared for a sample trajectory to accurate results from machine trajectory computation in Fig. 5.

In the case of eccentric orbits two analytical solutions are described in the text. One involves a single graphical integration for the entire trajectory for each initial perigial velocity and altitude combination chosen. The other involves reading a few points from generalized parametric curves and multiplying by suitable constants. Results of total satellite lifetime from this method are graphically compared with accurate results from a high speed digital computer in Fig. 6. Also presented is a comparison of perigee altitude versus time for two sample trajectories in Fig. 7.

The methods of solution presented herein are applicable to any standard variation of density with altitude. For illustrative purposes only the atmospheric data of Figs. 1 and 2 were employed. These consist of the yet unpublished data of E. O. HULBURT of the Naval Research Laboratory for the lower altitudes connected by a fairing to the GRIMMINGER Model III atmosphere [1] at the higher altitudes.

## Circular Trajectories

A satellite launched into a circular orbit would remain there indefinitely were it not for aerodynamic drag. With circular velocity the centrifugal acceleration away from the center of the earth is just balanced by the gravity acceleration toward the earth so that the rate of curvature of the flight path is the same as that of the earth's surface (assuming a spherical earth) and the vehicle remains at a constant altitude and velocity. The application of a small drag force tends to decrease momentarily the satellite's velocity and thus reduce its centrifugal acceleration without affecting the opposing gravity acceleration. The result is

that the flight path becomes slightly less than horizontal and the vehicle spirals gradually toward the earth. The work done by gravity upon the vehicle as it loses altitude causes it to accelerate and actually gain in velocity even though opposed by aerodynamic drag. In other words: the decreasing of the altitude results in a conversion of potential energy to kinetic energy so that the velocity remains very close to the local circular value. This type of descent continues until the atmospheric density has increased to the point that the deceleration due to drag is so great that the accelerating force due to gravity can no longer maintain circular velocity. The vehicle then decelerates rapidly and commences

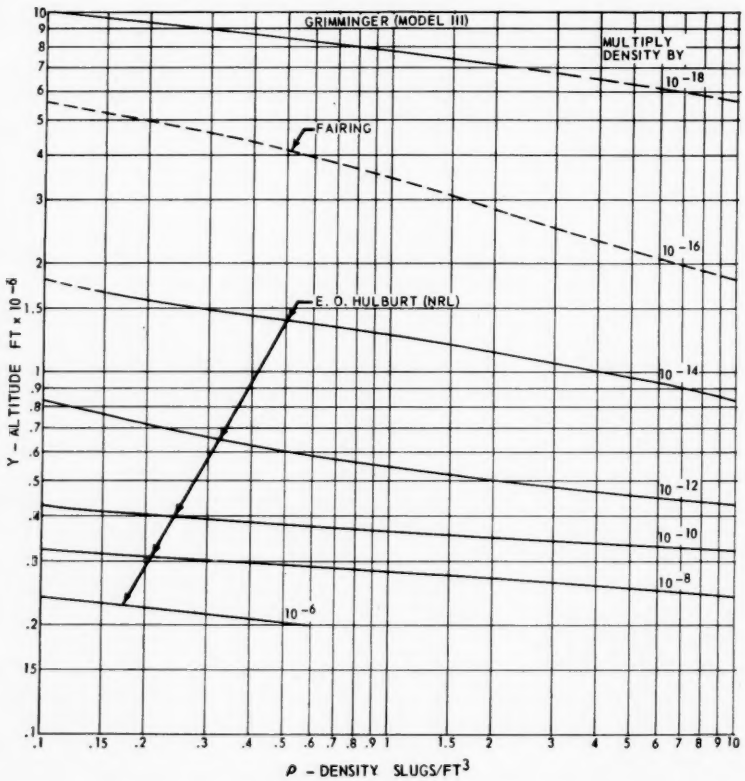


Fig. 1. Altitude vs density on double log scale

a dive into the earth. If the satellite remains intact, the terminal phase of this dive is vertical flight at a very low velocity with the drag approximating the weight.

In establishing the equations of flight it may be assumed that the flight path angle is approximately horizontal so that its cosine is about 1.0. The vertical acceleration is then the sum of the centrifugal and gravity terms.

$$\ddot{r} = \frac{V^2}{r} - \frac{\mu}{r^2}. \tag{1}$$

Starting at circular velocity the vertical acceleration would remain at zero were it not for drag. Assuming the changes in velocity and radius vector are very small, i.e.,

$$\frac{\Delta V}{V} \lll 1.0 \qquad \frac{\Delta r}{r} \lll 1.0 \tag{2}$$

the above equation may be written as follows:

$$\ddot{r} = \frac{V_0^2}{r_0}\left(1 + 2\frac{\Delta V}{V_0} - \frac{\Delta r}{r_0}\right) - \frac{\mu}{r_0^2}\left(1 - 2\frac{\Delta r}{r_0}\right). \tag{3}$$

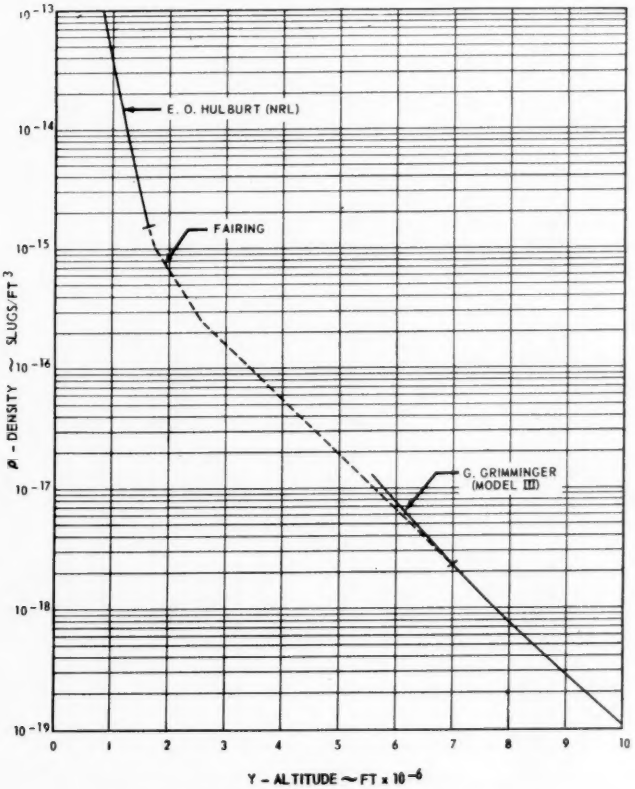


Fig. 2. Density vs altitude on single log scale

Since the initial centrifugal acceleration equals the gravity acceleration,

$$\frac{V_0^2}{r_0} = \frac{\mu}{r_0^2}, \tag{4}$$

eq. (3) simplifies as follows:

$$\ddot{r} = \frac{V_0^2}{r_0}\left(2\frac{\Delta V}{V_0} + \frac{\Delta r}{r_0}\right) \tag{5}$$

Vol. 4 1958

or

$$\Delta\ddot{r} = 2\lambda\Delta V + \lambda^2\Delta r \tag{6}$$

where

$$\lambda = \frac{V_0}{r_0}. \tag{7}$$

The change in velocity, $\Delta V$, is caused by drag and the conversion of potential energy into kinetic energy as altitude changes:

$$\Delta V = \Delta V_D + \Delta V_g \tag{8}$$

$$\Delta V_D = \frac{-g}{W}\int_0^t D\,dt. \tag{9}$$

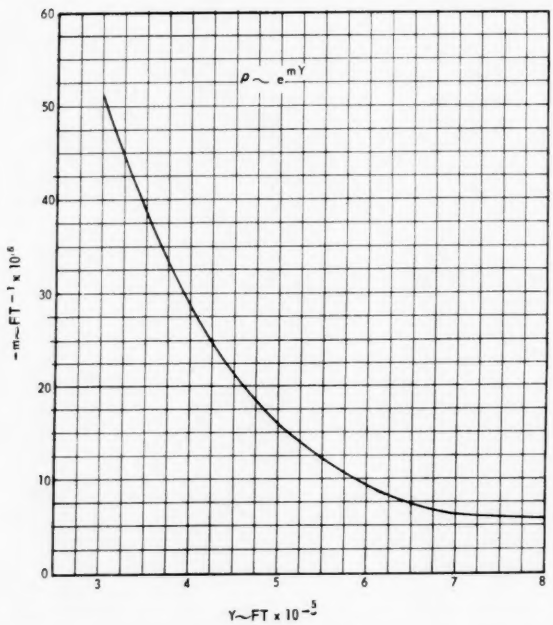


Fig. 3. Logarithmic slope of density curve vs altitude

Assuming the velocity change is small, this reduces to:

$$\Delta V_D = -\frac{K\lambda^2}{2\varrho_0}\int_0^t \varrho\,dt \tag{10}$$

where

$$K = g_{00}\left(\frac{C_D S}{W}\right)\varrho_0 r_0^2. \tag{11}$$

The velocity change due to gravity is

$$\Delta V_g = -\lambda\Delta r. \tag{12}$$

Substitution of these velocity increments from eqs. (10) and (12) into (8) and this in turn into (6) yields an equation for vertical acceleration

$$\Delta\ddot{r} = \frac{-K\lambda^3}{\varrho_0}\int_0^t \varrho\, dt - \lambda^2 \Delta r. \tag{13}$$

Assuming, for the moment, constant density and changing the independent variable from $t$ to $\bar{t}$, where

$$\bar{t} = \lambda t \tag{14}$$

we have

$$\Delta\ddot{r} = -K\bar{t} - \Delta r. \tag{15}$$

$\bar{t}$ is measured in radians and approximates the range angle subtended at the center of the earth when the changes in $r$ and $V$ are small.

The solutions of eq. (15) are:

$$\Delta r = -K(\bar{t} - \operatorname{Sin}\bar{t}) \tag{16}$$

$$\Delta\dot{r} = -K(1 - \operatorname{Cos}\bar{t}). \tag{17}$$

Examination of eqs. (16) and (17) shows that the altitude diminishes at a constant rate plus an oscillation of constant amplitude. It further shows that the rate of descent is a maximum at a half revolution ($\bar{t} = \pi$) about the earth and the vehicle returns to horizontal flight at the end of each revolution. These equations also show that the altitude loss is proportional to $(C_D S/W)$ for constant density.

Vol. 4 1958

For a large number of revolutions the trigonometric term of eq. (16) becomes negligible.

$$\Delta r \cong -K\bar{t}. \tag{18}$$

Differentiating with respect to $\bar{t}$ we have,

$$\Delta\dot{r} = -K \tag{19}$$

where

$$K = g_{00}\left(\frac{C_D S}{W}\right)\varrho_0 r_0^2. \tag{11}$$

It may now be possible to extend the analysis to the case of variable density by substituting $K\,\varrho/\varrho_0$ for $K$ in eq. (19).

$$\frac{d\Delta r}{d\bar{t}} = -K\frac{\varrho}{\varrho_0}; \tag{20}$$

or

$$\bar{t} = \frac{\varrho_0}{K}\int_{Y}^{Y_0}\frac{dY}{\varrho}. \tag{21}$$

Eq. (21) is the fundamental equation for circular orbital stay time. Regardless of what variation of density with altitude is chosen, this equation could be graphically integrated by plotting the reciprocal of density against altitude.

Substitution of a suitable mathematical expression for density as a function of altitude into eq. (21) will result in a closed solution over the region of altitude where the density equation is applicable. Depending upon what standard atmosphere is used, it may be necessary to break the altitude into several regions and obtain closed solutions to eq. (21) over each region. Two simple equations for density are:

$$\varrho \sim e^{mY} \tag{22}$$

and

$$\varrho \sim Y^{\beta} \tag{23}$$

where $m$ and $\beta$ are negative constants. The former equation is a straight line on single logarithm paper and the latter a straight line on double log paper. We now substitute eq. (22) into (21).

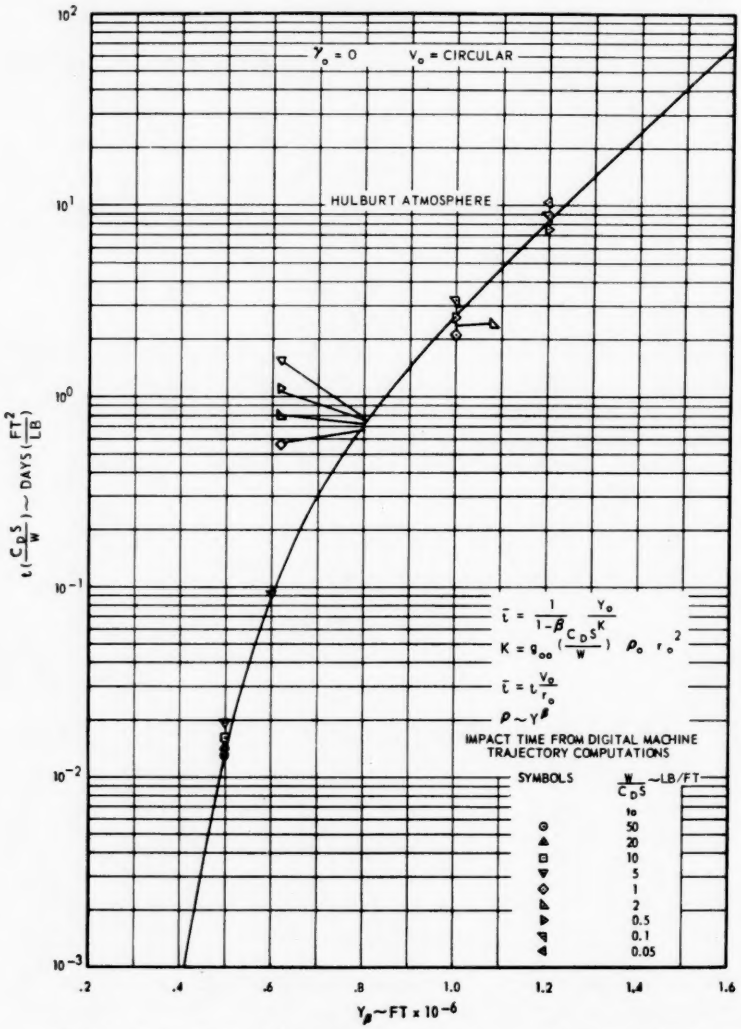


Fig. 4. Generalized plot approximate stay time vs burnout altitude

$$\bar{t} = \frac{e^{mY_*}}{K} \int_{Y}^{Y_*} e^{-mY} dY. \tag{24}$$

Performing the integration, we obtain

$$\bar{t} = \frac{1}{-mK} [1 - e^{m(Y_* - Y)}]. \tag{25}$$

The density relation [eq. (22)] assumed for eq. (25) does not in general permit use of this equation for finding total stay time from initial altitude to ground impact in one step. The density relation of eq. (23) generally applies with greater accuracy over a greater region of altitude than eq. (22). Substitution of eq. (23) into (21) and integration results in:

$$\bar{t} = \left(\frac{1}{1-\beta}\right)\frac{Y_0}{K}\left[1 - \left(\frac{Y}{Y_0}\right)^{1-\beta}\right]. \tag{26}$$

In the case of ground impact, $Y = 0$.

$$\bar{t} = \left(\frac{1}{1-\beta}\right)\frac{Y_0}{K}. \tag{27}$$

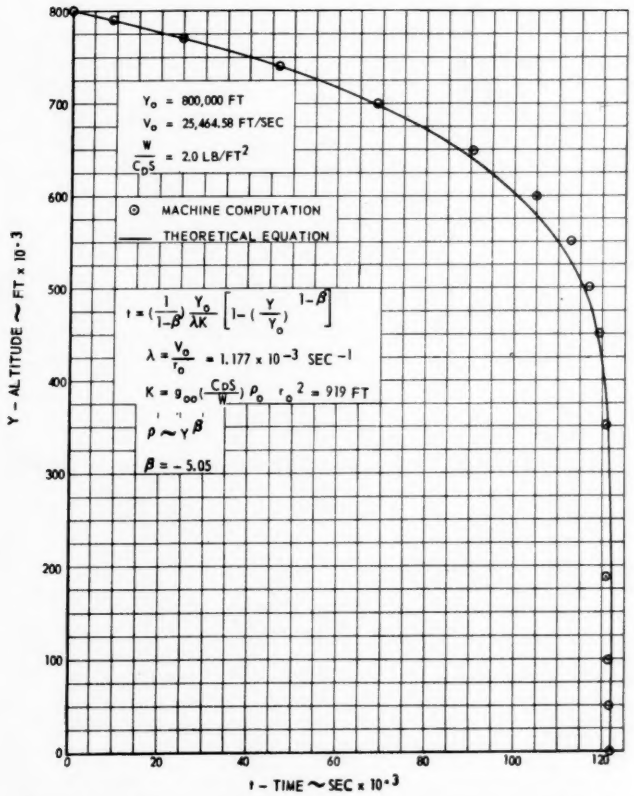


Fig. 5. Altitude vs time of descent for circular velocity satellite

Using the density data by E. O. HULBURT of the Naval Research Laboratory, presented in Fig. 1, an example of a specific trajectory starting at 800 000 feet and using a constant ratio of satellite weight to drag frontal area of 2 lb/ft$^2$ is presented in Fig. 5. The curve from eq. (26) is a reasonable approximation of the more accurate circled points obtained by stepwise integration of the differential equations of motion on a high speed digital computer. It may be noted that when the satellite has fallen out of the region of applicability of the constant $\beta$

used in the density equation, most of the flight time has elapsed and the trajectory has been fairly well determined.

The total time to ground impact presented in eq. (27) is plotted in generalized form in Fig. 4. It may be noted that the time of flight is theoretically proportional to $W/C_D S$. Superimposed upon this plot are total flight times obtained by means of a high speed digital computer for various assumed $W/C_D S$.

## Eccentric Trajectories

A satellite launched into horizontal flight at a supercircular velocity in a vacuum would follow an elliptic trajectory with the perigee (closest point to the earth) at its point of origin and the apogee (furthest point from the earth) at one-half revolution about the earth from the point of origin. The presence of a small amount of aerodynamic drag will cause the altitude to continuously, but not uniformly, fall below this theoretical vacuum ellipse. Since the velocity and atmospheric density are both higher at the perigee than at the apogee, the energy consumed by drag is much higher in the vicinity of the perigee. This causes each successive apogee altitude to drop more than its corresponding perigee as the satellite revolves about the earth. Thus the trajectory becomes more circular as the satellite continues its lop-sided spiralling toward the earth. Of course, due to continuous falling of the satellite below each vacuum ellipse, the points of horizontal flight (apogee and perigee) occur a little sooner than in a vacuum and thus slowly shift their positions about the earth.

The trajectory equations may be formulated in a somewhat similar manner to those of the circular case. Starting with eq. (3), the initial centrifugal acceleration is not equal to the gravity acceleration and, therefore, does not disappear from part of the equation: In other words:

$$\frac{V_0^2}{r_0} \neq \frac{\mu}{r_0^2}. \tag{28}$$

Carrying this through the analysis and using the definition of circular velocity,

$$V_c^2 = \frac{\mu}{r} \tag{29}$$

the equivalent of eq. (13) for eccentric orbits is as follows:

$$\Delta\ddot{r} = \lambda^2 A - \lambda^2 \Delta r - \frac{K\lambda^3}{\varrho_0} \int_0^t \varrho \, dt \tag{30}$$

where

$$A = r_0 \left[ 1 - \left( \frac{V_c}{V} \right)_0^2 \right]. \tag{31}$$

For a small increment of initial velocity above circular,

$$A \cong 2 r_0 \left( \frac{\Delta V_c}{V_c} \right)_0. \tag{32}$$

The independent variable is next changed from $t$ to $\bar{t}$ in eq. (30).

$$\Delta\ddot{r} = A - \Delta r - \frac{K}{\varrho_0} \int_0^{\bar{t}} \varrho \, d\bar{t}. \tag{33}$$

At the point of origin $\bar{t}$ and $\Delta r$ are both zero so the constant $A$ is obviously the initial value of the vertical acceleration $\Delta \ddot{r}_0$ with respect to $\bar{t}$.

The solution of (33) depends upon the form of the density equation used. For mathematical simplicity, eq. (22) is employed.

$$\Delta \ddot{r} = A - \Delta r - K \int_0^{\bar{t}} e^{m \Delta r} \, d\bar{t}. \tag{34}$$

This equation does not readily lend itself to a closed solution. The integral of eq. (34) may be solved if a suitable approximation of the solution $\Delta r$ as a function of $\bar{t}$ were substituted into the exponent. This integral term represents the change in centrifugal acceleration caused by the velocity lost to drag. Therefore, the approximation used for $\Delta r$ must be sufficient to determine density with reasonable accuracy. For one revolution of a high altitude satellite the vacuum flight trajectory will do for this purpose. By solving eq. (34) for only one revolution about the earth we will obtain an expression for the rate of fall of the perigee which might in turn be extended to a solution for total satellite life time.

The vacuum flight equation is obtained by first setting the density equal to zero in eq. (33).

$$\Delta \ddot{r} = A - \Delta r. \tag{35}$$

Solving this equation by a LAPLACE transformation yields the approximate vacuum elliptic equation:

$$\Delta r = A \, (1 - \operatorname{Cos} \bar{t}). \tag{36}$$

It may be observed from eq. (36) that $A$ is half of the altitude change between perigee and apogee.

Eq. (36) is next substituted into the exponent of eq. (34) and one differentiation performed to remove the integral sign.

$$\Delta \dddot{r} + \Delta \dot{r} = - K e^{m A (1 - \operatorname{Cos} \bar{t})} = - K e^{-c} e^{c \operatorname{Cos} \bar{t}} \tag{37}$$

where

$$C = - m A. \tag{38}$$

The last exponential term in eq. (37) may be expanded into an infinite series of powers of the cosine, thusly:

$$\Delta \dddot{r} + \Delta \dot{r} = - K e^{-c} \left[ 1 + c \operatorname{Cos} \bar{t} + \frac{c^2 \operatorname{Cos}^2 \bar{t}}{2!} + \frac{c^3 \operatorname{Cos}^3 \bar{t}}{3!} + \ldots \right]. \tag{39}$$

In order to make this into a first degree equation, each cosine raised to a digital power is replaced by a *finite* series of cosines of digital multiples of the angle $\bar{t}$. These series are found by use of the definition of the cosine.

$$\operatorname{Cos}^n \bar{t} \triangleq \left[ \frac{e^{i\bar{t}} + e^{-i\bar{t}}}{2} \right]^n \tag{40}$$

$$\operatorname{Cos}^n \bar{t} = \frac{1}{2^{n-1}} \cdot \left[ \frac{e^{ni\bar{t}} + n \, e^{(n-2) i\bar{t}} + \left( n \, (n-1)/2! \right) e^{(n-4) i\bar{t}} + \ldots \{ [n \, (n-1) \, (\,) \ldots 1]/n! \} e^{-ni\bar{t}} }{2} \right]. \tag{41}$$

Vol. 4 1958

Summing the first and last exponential term, then the next to the first with the next to the last, etc.;

$$\mathrm{Cos}^n \bar{t} = \frac{1}{2^{n-1}}\left[\mathrm{Cos}\, n\bar{t} + n\,\mathrm{Cos}\,(n-2)\bar{t} + \frac{n(n-1)}{2!}\mathrm{Cos}\,(n-4)\bar{t} + \ldots\right]. \tag{42}$$

If $n$ is *ODD*, end the series at $\mathrm{Cos}\,\bar{t}$ term.

If $n$ is *EVEN*, end the series at Cos 0 term and divide the last term by 2.

Substitution of the appropriate series from eq. (42) into each of the cosine terms of eq. (39) and summing the coefficients of similar terms yield the following equation which is readily solvable:

$$\dot{\Delta}\ddot{r} + \Delta\dot{r} = -K e^{-c}\left[a + b\,\mathrm{Cos}\,\bar{t} + d\,\mathrm{Cos}\,2\bar{t} + f\,\mathrm{Cos}\,3\bar{t} + \ldots\right] \tag{43}$$

where

$$x = \left(\frac{C}{2}\right)^2, \tag{44}$$

$$a = 1 + \frac{x}{(1!)^2} + \frac{x^2}{(2!)^2} + \frac{x^3}{(3!)^2} + \frac{x^4}{(4!)^2} + \ldots$$

$$= \sum_{n=0}^{\infty} \frac{x^n}{(n!)^2}, \tag{45}$$

$$b = 2x^{1/2}\left[1 + \frac{x}{2\,(1!)^2} + \frac{x^2}{3\,(2!)^2} + \frac{x^3}{4\,(3!)^2} + \ldots\right]$$

$$= c\sum_{n=0}^{\infty} \frac{x^n}{n!^2(n+1)}, \tag{46}$$

$$d = 2x\left[\frac{1}{0!\,2!} + \frac{x}{1!\,3!} + \frac{x^2}{2!\,4!} + \frac{x^3}{3!\,5!} + \ldots\right]$$

$$= 2x\sum_{n=0}^{\infty} \frac{x^n}{n!\,(n+2)!} \tag{47}$$

Eq. (43) is solved by means of a LAPLACE transformation, where

$$\mathscr{L}\,[f(\bar{t})] \triangleq \int_0^{s=\infty} e^{-s\bar{t}} f(\bar{t})\, d\bar{t} \tag{48}$$

and

$$\mathscr{L}\,[\Delta r_{\bar{t}}] = F_s \tag{49}$$

where $S$ is a complex number.

Transforming eq. (43),

$$s^3 F - A + sF = -K e^{-c}\left[\frac{a}{s} + \frac{bs}{s^2+1^2} + \frac{ds}{s^2+2^2} + \ldots\right] \tag{50}$$

and solving for the transformed function, $F$,

$$F = \frac{A}{s(s^2+1)} - K e^{-c}\left[\frac{a}{s^2(s^2+1)} + \frac{b}{(s^2+1^2)^2} + \frac{d}{(s^2+1^2)(s^2+2^2)} + \right.$$

$$\left. + \frac{f}{(s^2+1^2)(s^2+3^2)} + \frac{g}{(s^2+1^2)(s^2+4^2)} + \ldots\right]. \tag{51}$$

The final equation for altitude change is obtained by performing the inverse transformation:

$$\Delta r = A\,(1 - \operatorname{Cos} \bar{t}) - K\,e^{-c}\left[a\,(\bar{t} - \operatorname{Sin} \bar{t}) + \frac{b}{2}\,(\operatorname{Sin} \bar{t} - \bar{t} \operatorname{Cos} \bar{t}) + \right.$$
$$\left. + \frac{d}{2^2 - 1}\left(\operatorname{Sin} \bar{t} - \frac{\operatorname{Sin} 2\bar{t}}{2}\right) + \frac{f}{3^2 - 1}\left(\operatorname{Sin} \bar{t} - \frac{\operatorname{Sin} 3\bar{t}}{3}\right) + \ldots\right]. \qquad (52)$$

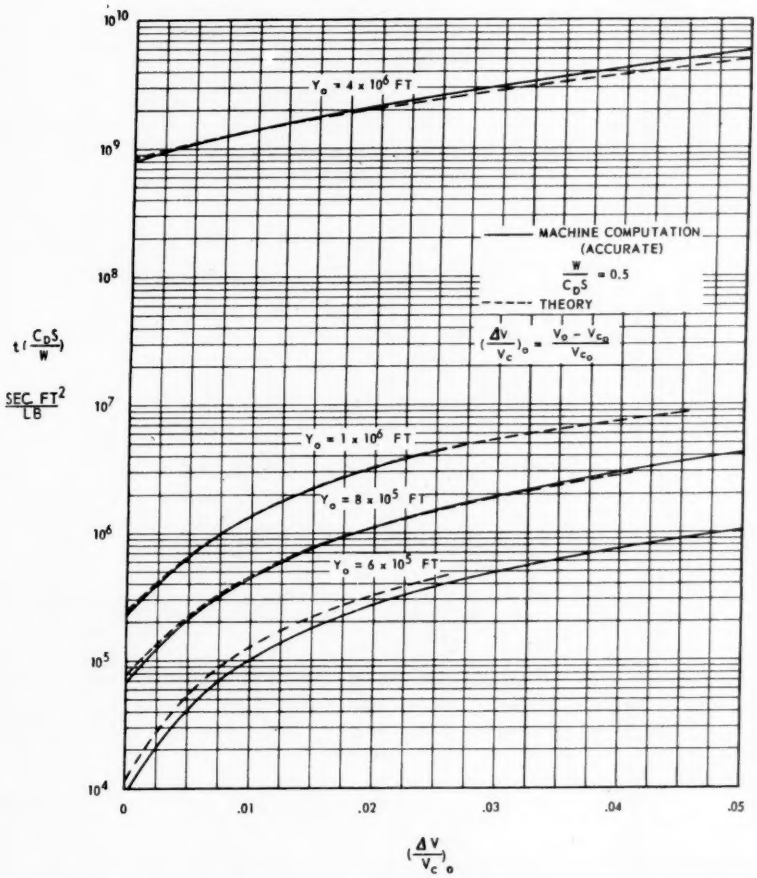


Fig. 6. Total satellite life-time from completely analytical solution and digital machine integration vs initial velocity

At apogee and perigee the sine of $\bar{t}$ or any digital multiple of $\bar{t}$ is zero. Therefore, all terms in the above series with coefficients of $d$ or higher disappear at these points. Further, at perigee the cosine of $\bar{t}$ is unity and at apogee it is minus unity. Making these substitutions into eq. (52) and differentiating with respect to $\bar{t}$ yields the apogee and perigee rates of fall:

$$\dot{r}_p = -\,K\,e^{-c}\left(a - \frac{b}{2}\right) \qquad (53)$$

$$\dot{r}_A = -\,K\,e^{-c}\left(a + \frac{b}{2}\right). \qquad (54)$$

Vol. 4 1958

The rate of closure of apogee and perigee as the trajectory tends to become more circular is

$$\dot{r}_A - \dot{r}_p = -K e^{-c b}. \tag{55}$$

Since the preceding three equations were derived for only one revolution about the earth their constants must be evaluated at the local perigee.

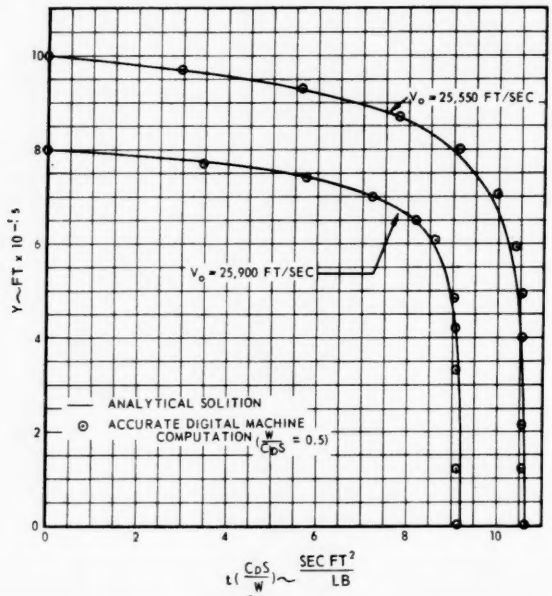


Fig. 7. Comparison of perigee altitude vs time from theory and machine integration for two eccentric trajectories

We may now proceed to derive a relationship between $Y_p$ and $C$. As pointed out earlier, the difference between apogee and perigee radius distance is twice the constant $A$. Making this substitution and the definition of $C$ from eq. (38) results in

$$r_A - r_p = 2A = -\frac{2C}{m}. \tag{56}$$

If we assume that $m$ remains constant, the differential of this equation is

$$\dot{r}_A - \dot{r}_p = -\frac{2}{m_0}\dot{C}. \tag{57}$$

This is next equated to (55) and solved for $\dot{C}$:

$$\dot{C} = \frac{m_0 K}{2} e^{-c b}. \tag{58}$$

The relationship between $Y$ and $C$ may now be found by dividing eq. (53) by (58) and remembering that $r$ differs from $Y$ by a constant amount, the earth radius $r_{00}$.

$$\frac{dY_p}{dC} = -\frac{1}{m_0}\left(2\frac{a}{b} - 1\right). \tag{59}$$

An arbitrary but convenient point of integration for this equation is $C = 1$ because at this point $a/b$ is finite.

$$-m_0 (Y_p - Y_{p_{C=1}}) = \int_1^C \left(2\frac{a}{b} - 1\right) dC. \tag{60}$$

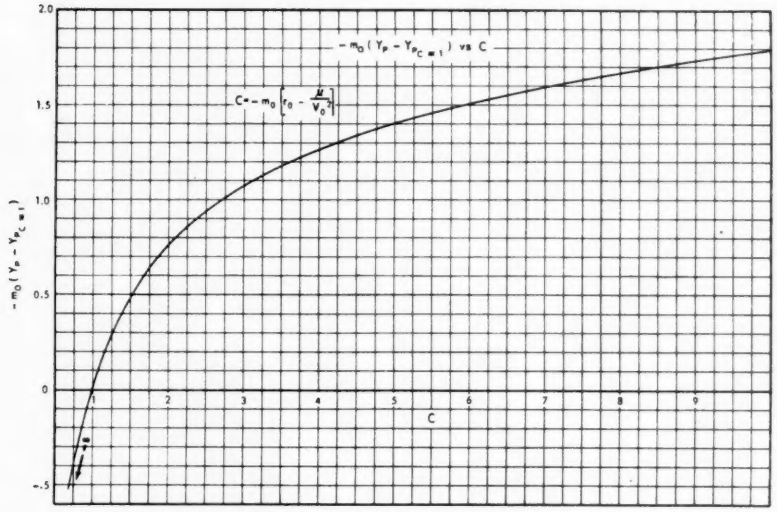


Fig. 8 *a*. Eccentric trajectory altitude parameter vs $C$

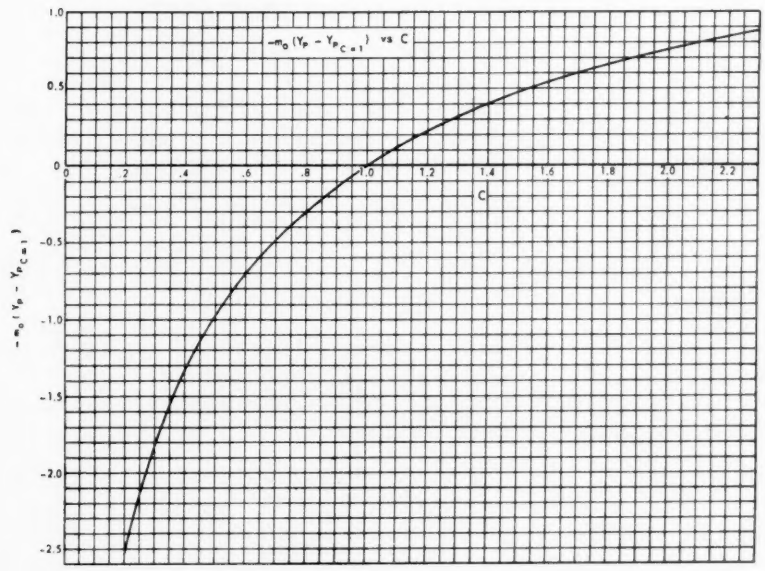


Fig. 8 *b*. Eccentric trajectory altitude parameter vs $C$

The integration was performed graphically and the relationship plotted in Fig. 8 *a*, *b* and *c*.

Vol. 4 1958

As shown in Fig. 8 *a*, as $C$ approaches zero (circular velocity) the perigee altitude decreases without limit. This means that perfect circular flight is approached asymptotically and is never really achieved. This in fact is the case, for even in the so called "circular flight", an oscillation of small amplitude exists, eqs. (16) and (17), and the periodic return to horizontal flight corresponds to successive perigees.

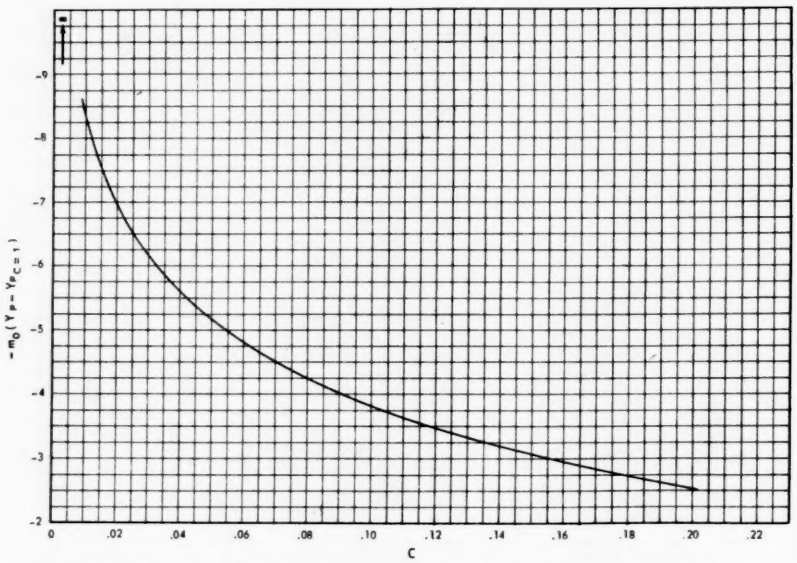


Fig. 8 *c*. Eccentric trajectory altitude parameter vs $C$

Although of no direct application in the solution of orbital lifetime, it may be of passing interest to point out the rate of change with respect to $\bar{t}$ of perigee velocity due to gravity and due to drag.

$$\dot{V}_g \cong -\left(\frac{V_C}{V_p}\right)_0^2 \lambda \dot{r}_p \tag{61}$$

$$\dot{V}_D \cong -\frac{K\lambda}{2} e^{-c} a. \tag{62}$$

These equations are the equivalent of eqs. (12) and (10) respectively for the circular orbits.

The next step is the development of the relationship between perigee altitude $Y_p$ and the dimensionless time or range angle $\bar{t}$.

$$\bar{t}_2 - \bar{t}_1 = \int_1^2 \frac{dY_p}{\dot{Y}_p}. \tag{63}$$

## Solution With One Graphical Integration

If it is desired to use the exact density at the perigee points the following solution requiring one graphical integration results.

Vol. 4 1958

First Fig. 9 is constructed as follows: $-K\varrho/\varrho_0\dot{Y}_p$ from re-arranging eq. (53), is available as a function of $C$. The altitude parameter $-m_0(Y_p - Y_{p_{c=1}})$ is also available as a function of $C$ from Fig. 8. These data are combined in Fig. 9. to present $-K\varrho/\varrho_0\dot{Y}_p$ versus $-m_0(Y_p - Y_{p_{c=1}})$.

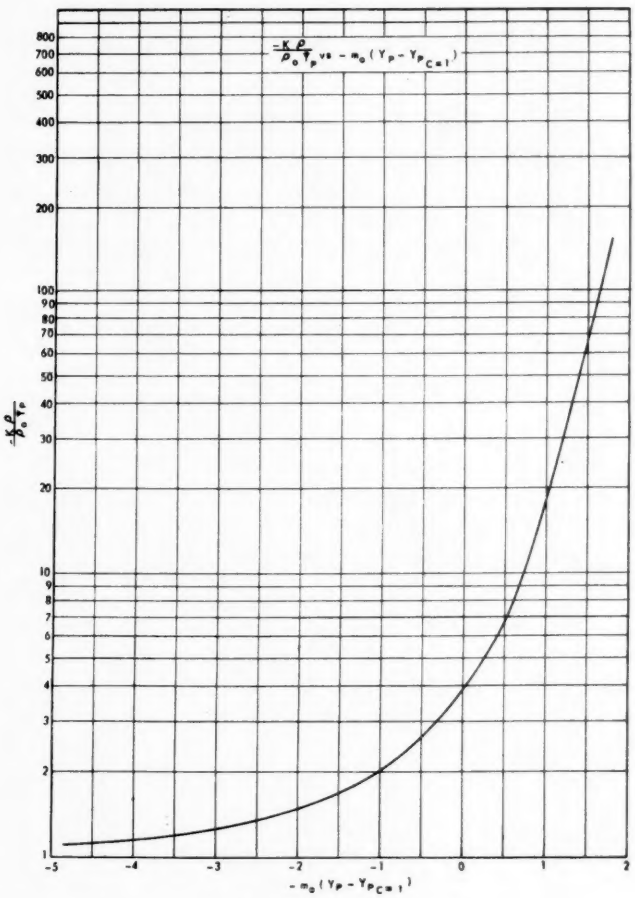


Fig. 9. Eccentric trajectories

Eq. (63) is multiplied by suitable constants

$$\frac{K}{\varrho_0}\bar{t} = \int_{\dot{Y}_p}^{Y_{p_0}} \left[\frac{-\varrho K}{\varrho_0 \dot{Y}_p}\right]_c \frac{dY_p}{\varrho}. \tag{64}$$

Next $C_0$ is obtained from eqs. (31) and (38):

$$C_0 = -m_0\left(r_0 - \frac{\mu}{V_0^2}\right). \tag{65}$$

The initial value of the altitude parameter is obtained from Fig. 8 at this $C_0$. Various values of $Y_p$ from $Y_{p_0}$ to 0 are next assumed and the corresponding values of $-m_0 (Y_p - Y_{p_{c=1}})$ obtained by taking differences along the curve of Fig. 9.

Values of $-K \varrho/\varrho_0 \dot{Y}_p$ from this curve and the correct densities from the atmospheric data employed are substituted into eq. (64) which is then solved by one graphical integration.

It is interesting to note that in the case of circular velocity ($C_0 = 0$) the value of $-\varrho K/\varrho_0 \dot{Y}_p$ is unity and eq. (64) reduces to eq. (21) already derived for circular flight.

## Complete General Solution

If it is considered sufficiently accurate to use the algebraic density relation of eq. (22) all the way to impact, a completely generalized solution is possible.

This is accomplished by substituting $dY_p$ from eq. (59) and $\dot{Y}_p$ from (53) into (63). Integration takes place from the arbitrary point of $C = 1$; as before

$$\left(\frac{\varrho_{c=1}}{\varrho_0}\right) m_0 K (\bar{t} - \bar{t}_{c=1}) = -2 \int_1^c \left(\frac{\varrho_{c=1}}{\varrho}\right) \frac{e^c}{b} dC. \tag{66}$$

The density ratio in eq. (66) is obtained from eq. (22).

$$\frac{\varrho_{c=1}}{\varrho} = e^{-m_0 (Y_p - Y_{p_{c=1}})}. \tag{67}$$

The exponent of this eq. is presented as a function of only $C$ in eq. (60) and Fig. 8. Thus the entire right hand side of eq. (66) is a function of only $C$ and may be graphically integrated. It may be put in several forms by first substituting eq. (60) into (67) and this in turn into the right hand side of (66):

$$-2 \int_1^c e^{\int_1^c (2(a/b) - 1)\, dC} \frac{e^c}{b} dC. \tag{68}$$

This is equivalent to

$$e^{\int_1^c (2(a/b) - 1)\, dC} \int_1^c \frac{e^c}{a - (b/2)} d\left[e^{\int_1^c (2(a/b) - 1)\, dC}\right], \tag{69}$$

or

$$\int_1^{\varrho_{c=1}/\varrho} \left(\frac{-K}{\dot{Y}}\right)_c d\left(\frac{\varrho_{c=1}}{\varrho}\right)_c. \tag{70}$$

Since the right hand side of both eqs. (60) and (66) are functions of $C$ only, the left hand side of these equations may be plotted against each other. This is done in Fig. 10 *a*, *b* and *c* which contain the principal curve for the completely analytical general solution and present

$$\left(\frac{\varrho_{c=1}}{\varrho_0}\right) m_0 K (\bar{t} - \bar{t}_{c=1}) = \oint [-m_0 (Y_p - Y_{p_{c=1}})]. \tag{71}$$

The procedure for the generalized solution is as follows:

1. Determine $C_0$ from eq. (65).

2. Enter Fig. 8 at this $C_0$ to find the initial altitude parameter; $-m_0 (Y_p - Y_{p_{c=1}})$.

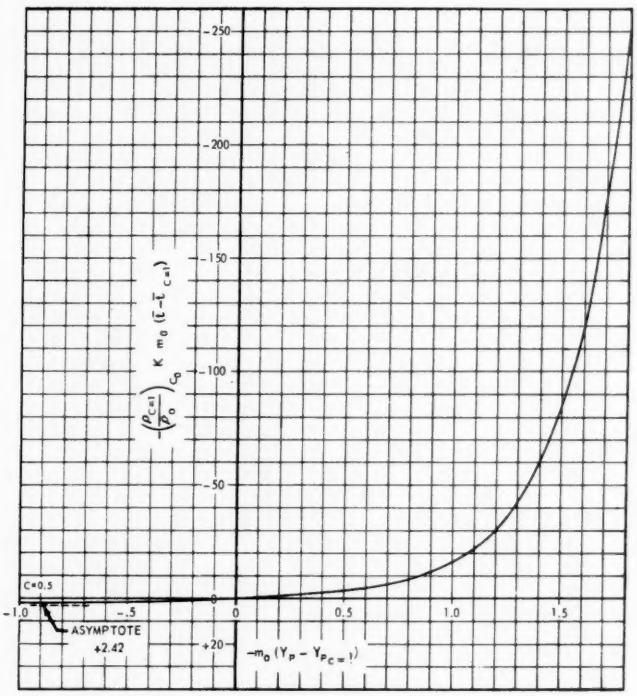


Fig. 10 *a*. Eccentric trajectory time parameter vs altitude parameter

3. Subtract $-m_0 Y_0$ from the initial altitude parameter to find the impact altitude parameter. Fig. 3 contains $m_0$ as a function of $Y_0$.

4. Enter Fig. 10 at both the initial and impact values of the altitude parameter, $-m_0 (Y_p - Y_{p_{c=1}})$, to find the initial and impact values of the time parameter, $-(\varrho_{c=1}/\varrho_0)\, m_0 K (\bar{t} - \bar{t}_{c=1})$.

5. Subtract the initial from the impact value of the time parameter to find the total orbital lifetime parameter

$$\Delta \bar{t}_{\text{PARAM}} = -\left(\frac{\varrho_{c=1}}{\varrho_0}\right) K m_0 \bar{t}. \tag{72}$$

6. Using the expressions for $\varrho_{c=1}/\varrho_0$ and $K_0$ already derived, the time in generalized form is

$$t\left(\frac{C_D S}{W}\right) = \frac{F}{V_0} \frac{\Delta \bar{t}_{\text{PARAM}}}{(\varrho_{c=1}/\varrho_0)} \tag{73}$$

where

$$F = \frac{1}{g_{00}\, m_0\, r_0\, \varrho_0}$$

$$\frac{\varrho_{c=1}}{\varrho_0} = e^{-m_0 (Y_p - Y_{p_{c=1}})_0}.$$

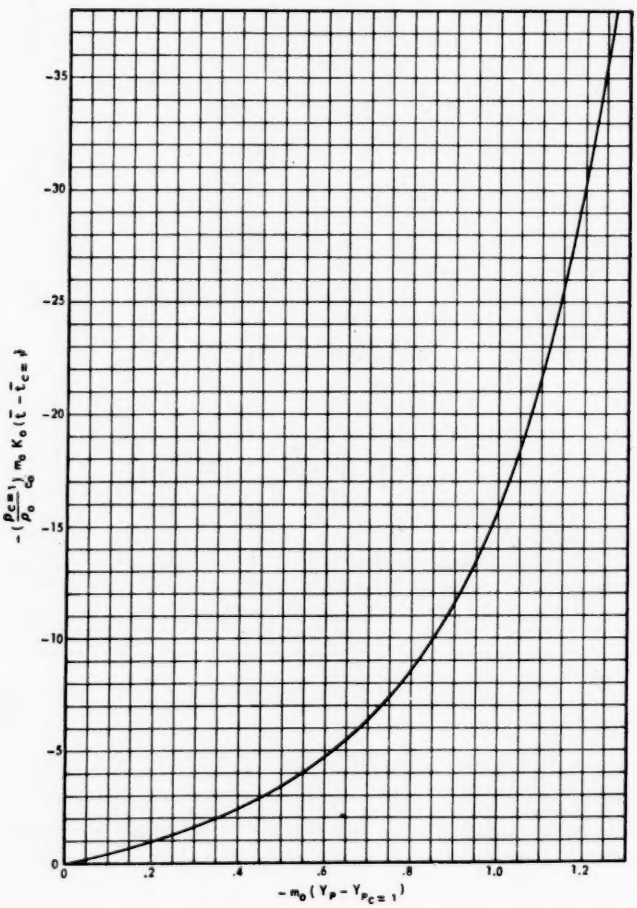


Fig. 10 *b*. Eccentric trajectory time parameter vs altitude parameter

In the case of circular velocity satellites, it may be shown that eq. (73) reduces to

$$t_c \left(\frac{C_D\, S}{W}\right) = \frac{F}{V_0} (1 - e^{m_0 Y_0}). \tag{74}$$

A plot of perigee altitude versus time may be obtained by modifying the above procedure in Step **3** to subtract intermediate values of $-m_0 (Y_0 - Y)$ instead of the total impact value of $-m_0 Y_0$. This has been accomplished in

Fig. 6 where total satellite lifetime from this analytical solution and from detailed integration of the trajectory equations of motion by a digital computer are compared for a variety of initial altitudes and velocities.

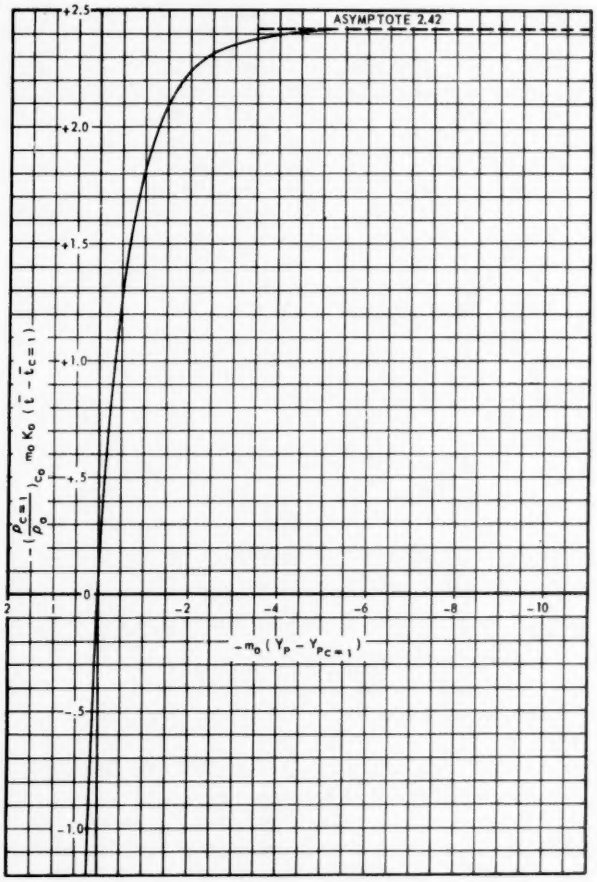


Fig. 10 *c*. Eccentric trajectory time parameter vs altitude parameter

## Example of Generalized Solution

Given

$$Y_0 = 800{,}000 \text{ ft}$$
$$V_0 = 25{,}900 \text{ ft/sec.}$$

At this altitude,

$$\varrho_0 = 1.23 \times 10^{-13} \text{ slugs/ft}^3 \quad \text{(Fig. 1)}$$
$$m_0 = -5.82 \times 10^{-6} \text{ ft}^{-1} \quad \text{(Fig. 3)}$$
$$r_0 = r_{00} + Y_0 = 2.165\,55 \times 10^7 \text{ ft.}$$

From eq. (65),

$$C_0 = -m_0 \left( r_0 - \frac{\mu}{V_0^2} \right) = 4.202.$$

Vol. 4 1958

Enter Fig. 8 at $C_0$ to find initial altitude parameter. Subtract total change in this parameter to find its impact value:

$$\begin{aligned} -m_0\,(Y_0 - Y_{c=1}) &= \quad 1.295 \\ -(-m_0\,Y_0) &= -4.656 \\ \hline m_0\,Y_{c=1} &= -3.361 \end{aligned}.$$

Enter Fig. 10 at these final and initial values of the altitude parameter to find the corresponding values of the time parameter. Subtract this initial from the final (impact) value.

$$\begin{aligned} \text{IMPACT } t_{\text{PARAM}} &= 2.4 \\ -\text{ INITIAL } t_{\text{PARAM}} &= 41.0 \\ \hline \Delta t_{\text{PARAM}} &= 43.4 \end{aligned}$$

Eq. (67)

$$\frac{\varrho_{c=1}}{\varrho_0} = e^{-m_0(Y_0 - Y_{c=1})} = e^{1.295} = 3.65;$$

Eq. (73)

$$t\left(\frac{C_D\,S}{W}\right) = \frac{\Delta t_{\text{PARAM}}}{g_{00}\,(-m_0)\,r_0\,\varrho_0\,V_0\,(\varrho_{c=1}/\varrho_0)}$$

$$= \frac{43.4}{(32.174)\,5.82 \times 10^{-6}\,(2.1655 \times 10^7)\,1.23 \times 10^{-13}\,(2.59 \times 10^4)\,3.65}$$

$$t\left(\frac{C_D\,S}{W}\right) = 920{,}000\,\frac{\text{sec. ft}^2}{\text{lb}}.$$

Theoretical perigee altitude versus time for this entire trajectory is plotted and compared with accurate results from a digital computer in Fig. 7.

### Comparison of Methods of Solution for Eccentric Trajectories

Stepwise integration by a high speed digital computer of the classical equations of motion furnishes the most accurate method of satellite trajectory computation. This was used as a basis of comparison to the completely analytical approach in Figs. 6 and 7.

The completely analytical solution assumes that the density is a straight line function of altitude when plotted on semi-log paper all the way to impact [Eq. (22)]. At the lower altitudes this assumes an unrealistically low density and would hence tend to increase the predicated satellite lifetime. The error due to this effect would be greatest in the case of initial circular velocity because these satellites spend a greater proportion of their lifetime at the lower altitudes. In the case of supercircular initial velocity the assumed increase in altitude to first apogee, $2A$, [Eq. (31)] is lower than actually exists. The density in the vicinity of apogee used in the analysis is, therefore, a little high and this tends to reduce the predicted stay time.

The graphical integration method described, but not illustrated herein, uses the correct densities at perigee throughout, but assumes the original exponential density slope, $m_0$, as the vehicle moves around each distorted ellipse. This method, therefore, always yields a lower predicted lifetime than the completely analytical procedure. In the case of circular velocity satellites, however, it should predict very close to the correct answer.

### Reference

1. G. GRIMMINGER, Analysis of Temperature, Pressure and Density of the Atmosphere Extended to Extreme Altitudes. RAND Corporation, November, 1948, Report No. R-105.

# Die Bahnbestimmung aus dem Vektor der Bahngeschwindigkeit

Von

**M. Vertregt**[1], NVR

(Mit 1 Abbildung)

(*Eingegangen am 13. November 1957*)

**Zusammenfassung — Abstract — Résumé**

**Die Bahnbestimmung aus dem Vektor der Bahngeschwindigkeit.** Eine einfache Ableitung wird gegeben, um die Bahnelemente aus Richtung und Größe des Vektors der Bahngeschwindigkeit zu bestimmen.

**Derivation of the Orbit from the Vector of the Orbital Velocity.** A simple derivation is given to calculate the elements of an elliptic orbit from the direction and the magnitude of the vector of the orbital velocity.

**Dérivation de l'orbite par le vecteur de la vitesse orbitale.** Une méthode est donnée pour dériver les éléments d'une orbite elliptique á partir de la direction et de la grandeur du vecteur de la vitesse orbitale.

Vol. 4 1958

Dieses Problem wurde von Professor Dr. K. SCHÜTTE auf dem IV. Astronautischen Kongreß in Zürich behandelt[2].

Die Aufgabe ist die folgende (siehe Abb. 1):

Ein Körper $m$ beschreibt eine elliptische Bahn um den Körper $M$.

Bekannt sind in einem bestimmten Augenblick:

$r$ der Radius-Vektor des Körpers $m$;
$V$ die lineare Geschwindigkeit des Körpers $m$;
$\beta$ der Winkel, welchen der Geschwindigkeitsvektor mit dem Radiusvektor bildet.

Weiter ist bekannt:
$K$ die Konstante des Schwerefeldes des Körpers $M$.

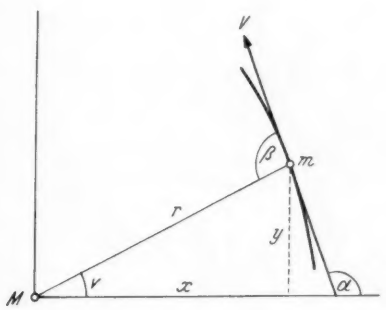


Abb. 1

[1] Mozartlaan 73, Den Haag, Holland.

[2] K. SCHÜTTE, Die Bahnbestimmung aus dem Vektor der Bahngeschwindigkeit und der Einfluß einer Änderung desselben auf die Bahnelemente. (Mit dem ERNST-HEINKEL-Preis der Astronautik für 1953 ausgezeichnete Arbeit.) In: Probleme der Weltraumforschung, S. 89. Biel-Bienne: Laubscher & Cie., 1953.

Mit diesen Bekannten sind zu bestimmen die Unbekannten:

$a$ die halbe große Achse der Ellipse;
$e$ die Exzentrizität der Ellipse;
$v$ der Winkel des Radiusvektors mit der großen Achse der Ellipse.

Die Ableitung, welche der Verfasser in diesem Artikel gab, war sehr kompliziert; es ist jedoch eine einfachere Ableitung möglich, die hier gegeben werden soll.

Aus dem bekannten Satz für die elliptische Bewegung

$$V^2 = K^2\left(\frac{2}{r} - \frac{1}{a}\right) \text{ (Energieintegral)}$$

folgt:

$$a = \frac{1}{(2/r) - (V^2/K^2)}, \tag{1}$$

womit $a$ bestimmt ist.

Aus Abb. 1 folgt:

$$\begin{aligned} x &= r\cos v & dx &= \cos v \cdot dr - r \cdot \sin v \cdot dv \\ y &= r\sin v & dy &= \sin v \cdot dr + r \cdot \cos v \cdot dv; \end{aligned}$$

oder:

$$\frac{dy}{dx} = \frac{\sin v \cdot dr + r\cos v \cdot dv}{\cos v \cdot dr - r\sin v \cdot dv} = \frac{\operatorname{tg} v + r\,(dv/dr)}{1 - r\,(dv/dr)\cdot \operatorname{tg} v}. \tag{2}$$

Nun ist aber:

$$\frac{dy}{dx} = \operatorname{tg}\alpha,$$

wobei $\alpha = v - \beta + 180^0$ ist.

Also folgt:

$$\frac{dy}{dx} = \operatorname{tg}\alpha = \operatorname{tg}(v-\beta) = \frac{\operatorname{tg} v - \operatorname{tg}\beta}{1 + \operatorname{tg}\beta \cdot \operatorname{tg} v}. \tag{3}$$

Aus (2) und (3) folgt somit durch Vergleich:

$$\operatorname{tg}\beta = -\,r\frac{dv}{dr}. \tag{4}$$

Aus der bekannten Gleichung für die Länge des Radiusvektors

$$r = \frac{a\,(1-e^2)}{1 + e\cos v} \tag{5}$$

folgt:

$$\cos v = \frac{a\,(1-e^2) - r}{r \cdot e}, \tag{6}$$

woraus sich

$$\frac{dv}{dr} = \frac{a\,(1-e^2)}{r^2 \cdot e \cdot \sin v} \tag{7}$$

ergibt.

Aus (4) und (7) folgt weiter:

$$\operatorname{tg}\beta = -\frac{a\,(1-e^2)}{r \cdot e \cdot \sin v}. \tag{8}$$

Aus den Gln. (6) und (8) sind nun $e$ und $v$ leicht zu finden.

Denn aus

$$\sin v = \sqrt{1 - \cos^2 v} \tag{9}$$

folgt durch Substitution von (6) in (9):

$$\sin v = \sqrt{1 - \left\{\frac{a\,(1 - e^2) - r}{r \cdot e}\right\}^2}. \tag{10}$$

Wird Gl. (10) in Gl. (8) substituiert, so bekommt man nach Quadrieren und einiger Umrechnung:

$$\operatorname{tg}^2 \beta = \frac{1 - e^2}{e^2 - (1 - (r/a))^2}, \tag{11}$$

woraus:

$$e^2 = \cos^2 \beta + \left(1 - \frac{r}{a}\right)^2 \cdot \sin^2 \beta, \tag{12}$$

womit $e$ gefunden ist.

Die entsprechende quadratische Gleichung bei K. SCHÜTTE [Gl. (22)] gibt $e$ in Abhängigkeit von $v$.

Aus (8) folgt:

$$\sin v = -\frac{a\,(1 - e^2)}{r \cdot e \cdot \operatorname{tg} \beta}. \tag{13}$$

Aus (13) und (6) ergibt sich dann:

$$\operatorname{tg} v = -\frac{1}{\operatorname{tg} \beta \{1 - (r/a\,(1 - e^2))\}}. \tag{14}$$

Gl. (12) wird in (14) substituiert und gibt nach einiger Umrechnung:

$$\operatorname{tg} v = -\frac{1}{\operatorname{tg} \beta \left\{1 - \dfrac{1}{\sin^2 \beta\,(2 - (r/a))}\right\}}. \tag{15}$$

Wir setzen jetzt, wie in SCHÜTTES Arbeit:

$$2 - \frac{r}{a} = f.$$

Damit wird:

$$\operatorname{tg} v = -\frac{1}{\operatorname{tg} \beta \{1 - (1/f \sin^2 \beta)\}}$$

$$= -\frac{\operatorname{tg} \beta}{\operatorname{tg}^2 \beta - (1/f \cos^2 \beta)}.$$

Oder:

$$\operatorname{tg} v = \frac{f \operatorname{tg} \beta}{1 + (1 - f) \operatorname{tg}^2 \beta}. \tag{16}$$

Diese Gleichung ist identisch mit der von K. SCHÜTTE abgeleiteten Gl. (47).

Vol. 4 1958

# Besondere Brennstoffverteilungen und Kühlungsprobleme in Reaktoren von Kernraketen

Von

**F. Winterberg**[1], DGRR

(Mit 9 Abbildungen)

(*Eingegangen am 19. November 1957*)

**Zusammenfassung — Abstract — Résumé**

**Besondere Brennstoffverteilungen und Kühlungsprobleme in Reaktoren von Kernraketen.** Es werden besondere Leistungsverteilungen in Reaktoren von Kernraketen diskutiert, die eine möglichst günstige Kühlung gestatten, und die zugehörigen Brennstoffverteilungen für einige einfache Geometrieverhältnisse berechnet. Günstige Brennstoffverteilungen sind solche, die zu einer konstanten Leistungsdichte im Reaktorkern führen, und solche, bei denen die Oberflächentemperatur der Kühlkanäle konstant bleibt.

**Special Fuel Distributions and Cooling Problems in Reactors of Nuclear Energy Rockets.** Special distributions of the heat production in reactors of nuclear energy rockets are discussed, which allow the most favourable heat transfer. The appropriate fuel distributions are calculated for some simple geometric conditions. Favourable fuel distributions are those that result in a constant density of expended energy in the core of the reactor, and others where the surface temperature of the cooling channels remains constant.

**Répartitions spéciales de combustibles et problèmes de refroidissement dans les réacteurs nucléaires pour fusées.** Des distributions spéciales de la production de chaleur dans les réacteurs nucléaires sont envisagées pour l'optimisation du refroidissement. Les répartitions correspondantes du combustible sont calculées pour quelques modes simples de disposition géométrique. Les répartitions optimales conduisent à une répartition constante de la production de chaleur dans le réacteur, ou sont telles que la température superficielle des canaux de refroidissement soit constante.

## 1. Einleitung

Bei Kernraketen wird das Arbeitsmedium durch die Kühlkanäle eines Reaktors geleitet, hocherhitzt und anschließend in einer Düse expandiert.

Werden zur Aufheizung des Arbeitsmediums Reaktoren verwandt, bei denen der Brennstoff über den Reaktorkern gleichmäßig verteilt ist, so wird das Profil des Neutronenflusses im Reaktor cos-funktionsähnlich sein. Durch den Zusammenhang zwischen Neutronenfluß $\phi$ und Leistungsdichte $Q$

$$Q = E \Sigma_f \phi, \tag{1}$$

[1] Gesellschaft für Kernenergie, Hamburg, Bundesrepublik Deutschland, Reaktorstation Geesthacht.

wo $E$ die pro Spaltung freiwerdende Energie und $\Sigma_f$ der makroskopische Wirkungsquerschnitt für Spaltung ist, wird daher nach Gl. (1) auch die Leistungsverteilung im Reaktorkern die Form einer cos-ähnlichen Funktion besitzen. Im Innern des Reaktors werden deshalb sehr viel größere Temperaturen auftreten als in den Randpartien. Der Anteil des Arbeitsmediums, der durch die Kühlkanäle der Randzonen des Reaktors strömt, wird weit weniger gut aufgeheizt als das durch das Zentrum des Reaktors strömende Kühlmittel.

Die Form der Leistungsverteilung führt außerdem zu höheren Temperaturen im Innern des Reaktors als in den Randzonen. Die höchste dem Material zumutbare Temperatur wird daher nur im Innern des Kerns erreicht, während die Randzonen nicht voll ausgelastet werden können. Es ist daher anzustreben, andere, nicht mehr gleichförmige Spaltstoffverteilungen einzuführen, die eine gleichmäßige thermische Belastung des gesamten Reaktorkerns sicherstellen und bei größtmöglicher Kühlung den besten Wirkungsgrad gewährleisten.

Bei Gl. (1) ist noch zu bemerken, daß für thermische und schnelle Reaktoren das Produkt $\Sigma_f \phi$ nahezu temperaturunabhängig ist. Für thermische Neutronen beobachtet man eine $1/v$-Abhängigkeit von $\Sigma_f$. Da der Neutronenfluß der Gleichung $\phi = n\,v$ gehorcht, wo $n$ die Neutronendichte (Anzahl der Neutronen pro cm$^3$) ist, wird das Produkt $\Sigma_f \phi$ geschwindigkeitsunabhängig und damit auch unabhängig von der Temperatur. Bei schnellen Reaktoren wiederum hat die Reaktortemperatur keinen Einfluß auf das Neutronenspektrum. Die Folge davon ist, daß auch bei schnellen Reaktoren $\Sigma_f \phi$ temperaturunabhängig ist und damit der Gültigkeitsbereich von (1) für alle in Frage kommenden Reaktoren sichergestellt ist.

Vol. 4 1958

## 2. Die Grundgleichungen der Reaktorkühlung

Der Einfachheit halber soll ein zylindrischer Reaktor betrachtet werden. Die $z$-Richtung falle dabei mit der Achse des Zylinders zusammen. Die Kühlkanäle verlaufen parallel zueinander in Richtung der Zylinderachse.

Die Leistungsverteilung über den Reaktor gehorcht dann im Fall einer radialsymmetrischen Brennstoffanordnung der Gleichung

$$Q(v, z) = q(r) \cdot f(z). \tag{2}$$

Auf Grund des Zusammenhangs von Fluß und Leistung nach Gl. (1) folgt aus (2)

$$Q(r, z) \sim \phi(r, z). \tag{3}$$

Die Wärmeentwicklung im Kühlkanal verläuft wegen (2) allgemein nach der Gleichung:

$$dQ = q(r)\, f(z)\, dz. \tag{4}$$

Die erzeugte Wärme $dQ$ muß dabei an das Kühlmittel übertragen werden und wärmt dieses auf, was durch zwei weitere Beziehungen zum Ausdruck kommt (vgl. z. B. [1], S. 668 ff.):

$$dQ = \alpha\, U(t - \vartheta)\, dz \tag{5}$$

$$dQ = M\, c_p\, d\vartheta. \tag{6}$$

In (5) und (6) sind $t$ die Oberflächentemperatur, $\vartheta$ die Kühlmitteltemperatur, beide in $^0$K, $\alpha$ die Wärmeübergangszahl in cal/cm$^2$ s $^0$K, $M$ der Durchsatz in g/s, $c_p$ die spezifische Wärme des Kühlmittels bei konstantem Druck in cal/g $^0$K und $U$ der Umfang des Kühlkanals in cm. Gl. (5) bringt zum Ausdruck, wie die erzeugte Wärme an das Kühlmittel übertragen wird, während Gl. (6) angibt, um welchen Betrag die Temperatur des Kühlmittels durch die aufgenommene Wärme ansteigt.

Aus (4) und (6) folgt:

$$d\vartheta = \frac{q(r)}{M\, c_p} f(z)\, dz \tag{7}$$

$$\vartheta - \vartheta_1 = \frac{q(r)}{M\, c_p} \int_0^z f(z)\, dz. \tag{8}$$

(6) und (7) liefern:

$$t - \vartheta = \frac{q(r)}{\alpha\, U} f(z). \tag{9}$$

Aus (8) und (9) errechnet sich der Verlauf der Wandtemperatur des Kühlkanals zu

$$t - \vartheta_1 = \frac{q(r)}{\alpha\, U} f(z) + \frac{q(r)}{M\, c_p} \int_0^z f(z)\, dz. \tag{10}$$

### 3. Der Reaktor mit gleichförmiger Brennstoffverteilung

Für einen zylindrischen Reaktor ohne Reflektor vom Radius $R$ und der Höhe $H$ mit einer gleichförmigen Brennstoffverteilung gilt (vgl. z. B. [1], S. 173):

$$\phi(r, z) = \phi_0 J_0\left(2{,}405\, \frac{r}{R}\right) \cdot \cos\left(\frac{\pi z}{H}\right). \tag{11}$$

$\phi_0$ ist der maximale Fluß im Zentrum des Kerns und $J_0$ die BESSELsche Zylinderfunktion nullter Ordnung. Weiter gilt für diesen Fall:

$$q(r) \sim J_0\left(2{,}405\, \frac{r}{R}\right) \tag{12 a}$$

$$f(z) \sim \cos\left(\frac{\pi z}{H}\right) \tag{12 b}$$

und nach (10):

$$t - \vartheta_1 = \frac{q(r)}{\alpha\, U} \cos\left(\frac{\pi z}{H}\right) + \frac{q(r)}{M\, c_p}\left[1 - \sin\left(\frac{\pi z}{H}\right)\right]. \tag{13}$$

Ist $M$ sehr groß, so folgt aus (13)

$$t - \vartheta_1 \simeq \frac{q(r)}{\alpha\, U} \cos\left(\frac{\pi z}{H}\right)$$

$$= \frac{1}{\alpha\, U} q(r)\, f(z). \tag{13 a}$$

Aus (13 a) entnimmt man, daß die Verteilung der Oberflächentemperatur bei hohem Durchsatz in der $z$-Richtung cos-förmig ist. Aus Gl. (4) findet man durch Mittelbildung das Verhältnis vom mittleren zum maximalen Fluß (vgl. z. B. [1], S. 643):

$$\frac{\bar{\phi}}{\phi_0} = \frac{1}{\pi R^2 H} \int_0^R \int_{-H/2}^{+H/2} \phi \cdot 2\pi r\, dr\, dz$$

$$= \frac{4\, J_1(2{,}405)}{2{,}405 \cdot \pi} = 0{,}275. \tag{14}$$

Das Verhältnis von maximaler zu mittlerer Leistung ergibt sich aus (14):

$$\frac{Q_{\max}}{\bar{Q}} = \frac{\phi_0}{\bar{\phi}} = \frac{1}{0{,}275} = 3{,}64. \tag{15}$$

Wegen (13 a) gilt weiter für die mittlere Oberflächentemperatur $\bar{t}$

$$\frac{t_{\max} - \vartheta_1}{\bar{t} - \vartheta_1} \simeq 3{,}64. \tag{15 a}$$

Nach Gl. (15) ist auch das Verhältnis von maximaler zu mittlerer Oberflächentemperatur, bezogen auf die Anfangstemperatur des Kühlmittels, sehr groß. Setzt man näherungsweise als Eingangstemperatur des Kühlmittels $\vartheta_1 \approx 0\ ^0\mathrm{K}$ (z. B. flüssiger Wasserstoff) und nimmt als obere, maximale, dem Material gerade noch zumutbare Temperatur $t_{\max} = 3000\ ^0\mathrm{K}$ an, so liegt die mittlere zulässige Oberflächentemperatur bei

$$\bar{t} = \frac{3000}{3{,}64} = 825\ ^0\mathrm{K}.$$

Aus diesem Beispiel ist ersichtlich, wie wichtig es ist, andere Brennstoffverteilungen zu wählen, die eine höhere mittlere Oberflächentemperatur bringen. Das Beispiel zeigt, daß es für wirkungsvolle Kernraketen sogar unerläßlich ist, nach anderen Brennstoffverteilungen zu suchen, um die Temperatur der Arbeitsgase wesentlich über 1000 $^0$K zu bringen. Bevor die in Frage kommenden Möglichkeiten ungleichförmiger Brennstoffverteilungen diskutiert werden, soll jetzt eine Formulierung von Reaktoren mit Integral- und Differentialgleichungen gebracht werden, die es erlaubt, solche ungleichförmigen Brennstoffverteilungen zu berechnen.

Vol. 4 1958

## 4. Allgemeine Formulierung thermischer Reaktoren mit Integral- und Differentialoperatoren

Ein kritischer thermischer Reaktor läßt sich ganz allgemein durch eine Gleichung der Form [2]

$$\phi = H \Sigma_a \phi \tag{16}$$

darstellen.

In Gl. (16) ist $\phi$ der thermische Neutronenfluß, $\Sigma_a$ der Absorptionsquerschnitt des Brennstoffs für thermische Neutronen und $H$ ein Operator, der im Fall der Formulierung durch eine Integralgleichung ein Integraloperator, im Fall einer Vielgruppendiffusionsgleichung ein Differentialoperator ist. Liegt ein unter- oder überkritischer Reaktor vor, so tritt, wie weiter unten noch näher begründet werden soll, anstelle von (16) die Gleichung

$$k_{\mathrm{eff}}\, \phi = H \Sigma_a \phi. \tag{16 a}$$

Gl. (16 a) ist insofern von Bedeutung, als für alle Leistungsreaktoren ein $k_{\mathrm{eff}} > 1$ verlangt wird, um über eine genügend große Reaktivitätsreserve zu verfügen, die durch den Abbrand des Spaltstoffs kontinuierlich abnimmt und durch Kontrollstäbe auf $k_{\mathrm{eff}} = 1$ ausgeglichen wird.

### a) Die Integralgleichung thermischer Reaktoren

Es soll jetzt zuerst die Formulierung des Problems durch eine Integralgleichung gegeben werden. Diese Integralgleichung läßt sich allgemein auf die Form

$$\phi(\mathfrak{r}) = \int K(|\mathfrak{r} - \mathfrak{r}'|)\, \Sigma_a(\mathfrak{r}')\, \phi(\mathfrak{r}')\, d\mathfrak{r}' \tag{17}$$

bringen.

Gl. (17) bringt anschaulich zum Ausdruck, daß alle in den Volumenelementen stattfindenden Ereignisse $\Sigma_a(\mathfrak{r}')\,\phi(\mathfrak{r}')$ zum Flusse $\phi(\mathfrak{r})$ an der Stelle $\mathfrak{r}$ beitragen, wobei der Einfluß dieser Beiträge nur von der Entfernung $|\mathfrak{r}-\mathfrak{r}'|$ abhängt.

In den Raumelementen $d\mathfrak{r}'$ finden nun einerseits Absorptionsprozesse thermischer und andererseits Emissionsprozesse schneller Neutronen statt. Die Absorptionsprozesse thermischer Neutronen in den Volumenelementen $d\mathfrak{r}'$ wirken an der Stelle $\mathfrak{r}$ im Sinne einer Flußverminderung. Die Emissionsprozesse schneller Neutronen in den Volumenelementen $d\mathfrak{r}'$ erhöhen nach Durchlaufen eines Abbremsprozesses dagegen den thermischen Fluß an der Stelle $\mathfrak{r}$. Daher läßt sich der Kern $K(|\mathfrak{r}-\mathfrak{r}'|)$ der Integralgleichung (17) in zwei Bestandteile zerlegen, in einen Neutronenerzeugungs- und einen Neutronenvernichtungskern. Wir schreiben diese Zerlegung hin und diskutieren sie danach:

$$K(|\mathfrak{r}-\mathfrak{r}'|)=\eta\,K_1(|\mathfrak{r}-\mathfrak{r}'|)-K_0(|\mathfrak{r}-\mathfrak{r}'|). \tag{18}$$

$K_1(|\mathfrak{r}-\mathfrak{r}'|)$ ist der Erzeugungskern und $K_0(|\mathfrak{r}-\mathfrak{r}'|)$ der Vernichtungskern.

Da pro vernichtetem Neutron im Mittel $\eta$ schnelle Neutronen entstehen, ist der Erzeugungskern mit diesem Faktor zu multiplizieren, wenn die Kerne vereinbarungsgemäß auf 1 normiert sind.

Unter Voraussetzung der Gültigkeit der Diffusionstheorie erlaubt der Erzeugungskern eine einfache Darstellung. Er ergibt sich aus der Überlegung, daß die Absorption eines punktförmigen Raumelements dem Vorzeichen nach umgekehrt wie eine Quelle thermischer Neutronen wirken muß. Damit erhält man für den Vernichtungskern (vgl. z. B. [1], S. 142):

$$K_0(|\mathfrak{r}-\mathfrak{r}'|)=\frac{e^{-\varkappa(|\mathfrak{r}-\mathfrak{r}'|)}}{4\pi\,D(|\mathfrak{r}-\mathfrak{r}'|)}. \tag{19}$$

In Gl. (19) ist $\varkappa$ die Diffusionskonstante und $D$ der Diffusionskoeffizient.

Wesentlich komplizierter dagegen stellt sich der Erzeugungskern dar. Bei ihm muß berücksichtigt werden, daß die emittierten schnellen Neutronen eine keineswegs mehr punktförmige Abbremsdichte bilden, die dann zum Ausgangspunkt einer thermischen Diffusion wird.

Um einen analytischen Ausdruck für den Erzeugungskern zu gewinnen, soll angenommen werden, daß die Anwendung der FERMIschen Alterstheorie erlaubt ist. Um unter dieser Voraussetzung den Erzeugungskern zu gewinnen, geht man aus von der thermischen Bremsdichte der an der Stelle $\mathfrak{r}'$ entstehenden schnellen Neutronen. Die Anzahl der Ereignisse im Volumenelement $d\mathfrak{r}'$ beträgt $\Sigma_a(\mathfrak{r}')\,\phi(\mathfrak{r}')\,d\mathfrak{r}'$ und gibt anschaulich die Quellstärke schneller Neutronen an. Nach der FERMIschen Alterstheorie wird nun die Bremsdichte thermischer Neutronen an einer Stelle $\mathfrak{r}_0$ (s. Abb. 1) durch den Ausdruck wiedergegeben:

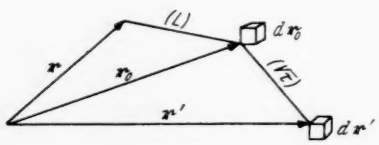


Abb. 1. Zur Ableitung des Erzeugungskerns

$$dQ(\mathfrak{r}_0,\tau)=\frac{e^{-(|\mathfrak{r}_0-\mathfrak{r}'|)^2/4\tau}}{(4\pi\,\tau)^{3/2}}\,\Sigma_a(\mathfrak{r}')\,\phi(\mathfrak{r}')\,d\mathfrak{r}'. \tag{20}$$

In Gl. (20) ist $\tau$ das FERMI-Alter thermischer Neutronen.

An der Stelle $\mathfrak{r}$ ergibt sich jetzt der durch schnelle Neutronen erzeugte thermische Fluß durch nachfolgende thermische Diffusion aus allen sekundären Volumenelementen $d\mathfrak{r}_0$ zu

$$d\phi_1(\mathfrak{r})=\int_{\mathfrak{r}_0}\frac{e^{-\varkappa(|\mathfrak{r}-\mathfrak{r}_0|)}}{4\pi\,D(|\mathfrak{r}-\mathfrak{r}_0|)}\,dQ(\mathfrak{r}_0,\tau)\,d\mathfrak{r}_0. \tag{21}$$

Wird der in (20) angegebene Wert für die Bremsdichte in Gl. (21) eingesetzt, so ergibt sich:

$$d\phi_1(\mathfrak{r}) = \int_{\mathfrak{r}_0} \frac{e^{-\varkappa(|\mathfrak{r}-\mathfrak{r}_0|)}}{4\pi D(|\mathfrak{r}-\mathfrak{r}_0|)} \frac{e^{-|\mathfrak{r}_0-\mathfrak{r}'|^2/4\tau}}{(4\pi\tau)^{3/2}} d\mathfrak{r}_0 \Sigma_a(\mathfrak{r}')\,\phi(\mathfrak{r}')\,d\mathfrak{r}'. \tag{22}$$

Gl. (22) bringt anschaulich zum Ausdruck, daß die in $d\mathfrak{r}'$ entstehenden schnellen Neutronen nach der FERMIschen Alterstheorie zunächst zur Bildung sekundärer, über den ganzen Raum verteilter Quellen thermischer Neutronen $dQ(\mathfrak{r}_0, \tau)$ im Volumenelement $d\mathfrak{r}_0$ führen. Dieser Sachverhalt wird durch das in Abb. 1 in Klammer zwischen $d\mathfrak{r}'$ und $d\mathfrak{r}_0$ stehende $\sqrt{\tau}$ veranschaulicht.

Im zweiten Schritt werden dann diese Quellen thermischer Neutronen zum Ausgangspunkt einer nach $\mathfrak{r}$ hinführenden Diffusion, was in Abb. 1 durch $L$ (in einer Klammer stehend) zum Ausdruck kommen soll. Da alle Volumenelemente in dieser Darstellung als thermische Neutronenquellen aufzufassen sind, ist über $\mathfrak{r}_0$ zu integrieren. Der Beitrag zum Fluß $\phi_1(\mathfrak{r})$ durch die schnellen Neutronen ergibt sich schließlich durch Integration von Gl. (22) über alle primären Volumenelemente:

$$\phi_1(\mathfrak{r}) = \int_{\mathfrak{r}'} \int_{\mathfrak{r}_0} \frac{e^{-\varkappa(|\mathfrak{r}-\mathfrak{r}'|)}}{4\pi D(|\mathfrak{r}-\mathfrak{r}'|)} \frac{e^{-|\mathfrak{r}_0-\mathfrak{r}'|^2/4\tau}}{(4\pi\tau)^{3/2}} d\mathfrak{r}_0 \Sigma_a(\mathfrak{r}')\,\phi(\mathfrak{r}')\,d\mathfrak{r}'. \tag{23}$$

Vol. 4 1958

Für den Erzeugungskern gilt nun die Definitionsgleichung

$$\phi_1(\mathfrak{r}) = \int_{\mathfrak{r}'} K_1(|\mathfrak{r}-\mathfrak{r}'|)\,\Sigma_a(\mathfrak{r}')\,\phi(\mathfrak{r}')\,d\mathfrak{r}', \tag{24}$$

wo $\phi_1(\mathfrak{r})$ der Beitrag der erzeugten Neutronen zum Fluß ist. Damit folgt durch Vergleich von (23) und (24)

$$K_1(|\mathfrak{r}-\mathfrak{r}'|) = \int_{\mathfrak{r}_0} \frac{e^{-\varkappa(|\mathfrak{r}-\mathfrak{r}_0|)}}{4\pi D(|\mathfrak{r}-\mathfrak{r}_0|)} \frac{e^{-|\mathfrak{r}_0-\mathfrak{r}'|^2/4\tau}}{(4\pi\tau)^{3/2}} d\mathfrak{r}_0. \tag{25}$$

Im Fall der Platten- und Kugelsymmetrie sind die Kerne $K_1(x)$ und $K_0(x)$, bzw. $K_1(r)$ und $K_0(r)$ in [2] angegeben:

$$K_1(x) = \frac{e^{\varkappa^2\tau}}{4\varkappa D}\left\{e^{-\varkappa x}\left[1 + F\frac{x}{2\sqrt{\tau}} - \varkappa\sqrt{\tau}\right] + e^{\varkappa x}\left[1 - F\left(\frac{x}{2\sqrt{\tau}} + \varkappa\sqrt{\tau}\right)\right]\right\} \tag{26}$$

$$K_0(x) = \frac{e^{-\varkappa x}}{2\varkappa D} \tag{27}$$

$$K_1(r) = \frac{1}{8\pi D r}\left\{e^{-\varkappa r}\left[1 - F\left(\varkappa\sqrt{\tau} - \frac{r}{2\sqrt{\tau}}\right)\right] - e^{\varkappa r}\left[1 - F\left(\varkappa\sqrt{\tau} + \frac{r}{2\sqrt{\tau}}\right)\right]\right\} \tag{28}$$

$$K_0(r) = \frac{e^{-\varkappa r}}{4\pi D r}. \tag{29}$$

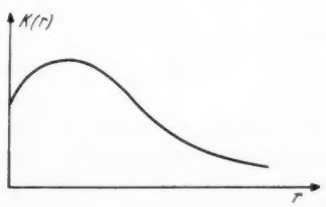


Abb. 2. Der Kern $K(r) = \eta K_1(r) - K_0(r)$

Mit diesen Resultaten läßt sich der Verlauf des gesamten Kerns im Ortsraum darstellen.

Er ergibt sich anschaulich aus der Fragestellung, was geschieht, wenn ein Stückchen spaltbares Material in einen Neutronenfluß gebracht wird. An der Stelle des Stückchens Spaltmaterial wird sich eine Senke des thermischen Flusses infolge thermischer Absorption ergeben. Im Abstand der Bremslänge schneller,

im Stückchen freiwerdender Spaltneutronen wird dagegen eine Überhöhung des thermischen Flusses zu erwarten sein, die mit größerer Entfernung wieder abfällt.

b) Die Vielgruppen-Differentialgleichung thermischer Reaktoren

Für einen thermischen Reaktor ist die Vielgruppen-Diffusionsgleichung in einer Arbeit von GOERTZEL [3] angegeben:

$$\phi = \frac{1}{\Sigma_1}\left(\eta \prod_{i=0}^{n} K_i - K_0\right)\Sigma_a \phi,$$

das heißt

$$H = \frac{1}{\Sigma_1}\left(\eta \prod_{i=0}^{n} K_i - K_0\right). \tag{30}$$

In Gl. (30) bedeutet $\Sigma_1$ den makroskopischen Absorptionsquerschnitt des Moderators (und Strukturmaterials) für thermische Neutronen, $\eta$ die im Mittel pro Absorption im Brennstoff freiwerdenden schnellen Neutronen, $n$ ist die Anzahl der Gruppen vermindert um die thermische Gruppe, für die $n = 0$ festgelegt ist. Die Operatoren $K_i$ sind mit Operatoren $L_i$ verknüpft durch:

$$L_i K_i = 1, \tag{31}$$

wobei die Operatoren $L_i$ der Gleichung

$$L_i = -\alpha_i^2 \Delta + 1 \tag{31 a}$$

gehorchen und die Größen $\alpha_i$ die Gruppendiffusionslängen im Moderator bedeuten. In einer Zweigruppentheorie z. B. ist

$$\alpha_0 = L_0$$
$$\alpha_1 = \sqrt{\tau}$$

die thermische Diffusionslänge und die Bremslänge schneller Neutronen.

In Gl. (30) ist $H_1 = \prod_{i=0}^{n} K_i/\Sigma_1$ der Neutronen-Erzeugungsoperator und $H_0 = K_0/\Sigma_1$ der Neutronen-Vernichtungsoperator.

In Gl. (30) beschreibt der Erzeugungsoperator die Diffusion der Neutronen von einer Gruppe zur anderen, wobei die jeweils höhere Gruppe die Quellenverteilung für die darunter liegende gibt.

Um Gl. (30) auf eine für unsere Zwecke geeignetere Gestalt zu bringen, wird auf sie von links der Operator $\prod_{i=0}^{n} L_i$ angewendet.

Dadurch ergibt sich wegen des Bestehens der Gl. (31) an Stelle von (30):

$$\prod_{i=0}^{n} L_i \phi = \frac{1}{\Sigma_1}\left(\eta - \prod_{i=1}^{n} L_i\right)\Sigma_a \phi. \tag{32}$$

In dieser Form werden wir die Vielgruppen-Diffusionsgleichung in den Rechnungen verwenden.

c) Berücksichtigung der Resonanzabsorption und schnellen Spaltung

Besteht der Reaktor aus einem Gemisch von Spaltmaterial und z. B. Uran 238, das heißt liegt angereichertes Material vor, so muß der Einfluß der Resonanzabsorption und der schnellen Spaltung berücksichtigt werden. Bei schwacher Resonanzabsorption kann bekanntlich die Lösung der FERMI-Alters-Gleichung $q(\mathfrak{r}, \tau)$ durch $p \cdot q(\mathfrak{r}, \tau)$ ersetzt werden, wo $p$ die Resonanz-Entkommwahrscheinlichkeit ist.

Die schnelle Spaltung in Uran 238 findet Berücksichtigung durch den schnellen Spaltfaktor $\varepsilon$. Damit tritt an die Stelle von $\eta$ in den Gln. (18), (30) und (32) $\varepsilon p \eta$.

Diese Feststellung ist insofern problematisch, als bei ungleichförmigen Brennstoffverteilungen die Größe $\varepsilon\, p$ selbst wieder eine Funktion des Ortes sein kann, wenn z. B. die Ungleichförmigkeit der Brennstoffverteilung etwa durch Variation der Anreicherung erzielt wird.

Ist das der Fall, so darf diese Größe nicht als konstant angesehen, sondern muß vielmehr in Abhängigkeit von $\Sigma_a(\mathfrak{r})$ angegeben werden.

Setzt man

$$\varepsilon\, p = f\{\Sigma_a(\mathfrak{r})\}, \tag{33}$$

so geht die Reaktorgleichung (16) über in:

$$\begin{aligned}\phi &= (\eta\, \varepsilon\, p\, H_1 - H_0)\, \Sigma_a \phi \\ &= [\eta\, f(\Sigma_a)\, H_1 - H_0]\, \Sigma_a \phi,\end{aligned} \tag{34}$$

wobei $H_1$ und $H_0$ die Erzeugungs- und Vernichtungsoperatoren sind, als Integral- oder Differentialoperatoren.

In der Schreibweise als Integralgleichung geht (20) über in

$$\phi(\mathfrak{r}) = \int \{\eta\, f\,[\Sigma_a(\mathfrak{r}')]\, K_1(|\mathfrak{r} - \mathfrak{r}'|) - K_0(|\mathfrak{r} - \mathfrak{r}'|)\}\, \Sigma_a(\mathfrak{r}')\, \phi(\mathfrak{r}')\, d\mathfrak{r}'. \tag{34 a}$$

In der Schreibweise als Vielgruppendifferentialgleichung dagegen:

$$\phi = \frac{1}{\Sigma_1}\left(\eta\, f(\Sigma_a) \prod_{i=0}^{n} K_i - K_0\right) \Sigma_a \phi. \tag{34 b}$$

Die Funktion $f[\Sigma_a(\mathfrak{r})]$ ist von Reaktor zu Reaktor verschieden und berechnet sich in bekannter Weise nach den in der Literatur angegebenen Verfahren (vgl. [4], S. 250 ff.). Streng genommen ist auch diese Darstellung unzulässig, da die Resonanzabsorption im Erzeugungsoperator selbst mit berücksichtigt werden müßte. Sie gilt nur dann, wenn die Funktion $f[\Sigma_a(\mathfrak{r})]$ als schwach veränderlich genommen über den Reaktor angesehen werden kann, was meistens der Fall ist. Aber schon die in dieser Näherung gemachte Berücksichtigung der Variation von $\varepsilon\, p$ über den Reaktor schließt eine analytische Behandlung ungleichförmiger Brennstoffverteilungen aus. Glücklicherweise kann in erster Näherung für viele Reaktoren diese Funktion als nahezu konstant angesehen werden, was dazu führt, daß die konstante Größe in Gl. (18), (30) und (32) einfach durch die neue konstante Größe

$$\bar{\eta} = \varepsilon\, p\, \eta$$

ersetzt werden muß.

### d) Die Zeitabhängigkeit der Reaktorgleichung. Die Kritikalität und Reaktivität

Die angegebenen Reaktorgleichungen sowohl in Integral- als auch Differentialform gelten streng für den Fall eines kritischen Reaktors. Ihre Lösungen geben bei vorgegebenen Reaktorabmessungen die benötigten kritischen Mengen für spaltbares Material an. Wie schon betont, wird man aber im allgemeinen von einem Reaktor die Bereitstellung einer bestimmten Reaktivität fordern, um eine gewisse Reserve zu haben.

In diesem Fall ist der Reaktor nicht mehr zeitlich stationär, vielmehr steigt der Neutronenfluß mit der Zeit exponentiell an. Unter der Voraussetzung, daß der Reaktor nur einen kleinen Reaktivitätsüberschuß hat, schreibt sich die zeitabhängige Reaktorgleichung:

$$\psi(\mathfrak{r}, t) + l\, \frac{\partial \psi(\mathfrak{r}, t)}{\partial t} = H\, \Sigma_a(\mathfrak{r})\, \psi(\mathfrak{r}, t). \tag{35}$$



Vol. 4 1958

In Gl. (35) ist $l$ die mittlere Lebensdauer eines Neutrons. Zur Lösung von (35) geht man mit dem Ansatz:

$$\psi(\mathfrak{r}, t) = \phi(\mathfrak{r})\, e^{[(k_{\text{eff}} - 1)/l]t} \tag{36}$$

von (30) ein und erhält:

$$k_{\text{eff}}\, \phi(\mathfrak{r}) = H\, \Sigma_a(\mathfrak{r})\, \phi(\mathfrak{r}). \tag{16 a}$$

Damit hat man an Stelle der weiter unten geforderten Beziehung zwischen

$$\Sigma_a \text{ und } \phi,\ \Sigma_a(\mathfrak{r}) = \frac{c}{\phi(\mathfrak{r})}$$

$$\Sigma_a(\mathfrak{r}) = \frac{k_{\text{eff}} \cdot c}{\phi(\mathfrak{r})}. \tag{37}$$

### 5. Besondere Formen der Wärmequellenverteilung

Um eine besonders günstige Form der Wärmequellenverteilung zu erhalten, sind zwei Fälle besonders ausgezeichnet.

Der erste Fall $A$ ist dadurch gekennzeichnet, daß in ihm

$$Q_{\max}/\bar{Q} = 1 \tag{38}$$

ist. Dieser Fall ist gleichbedeutend mit einer konstanten Wärmequellenverteilung über den Reaktorkern.

Für hohe Durchsätze folgt aus (38) und (10)

$$\frac{t_{\max} - \vartheta_1}{\bar{t} - \vartheta_1} = 1. \tag{39}$$

Setzt man wie im Beispiel des Abschnitts 3 $\vartheta_1 \simeq 0$ und die höchste zulässige Temperatur $t_{\max} = 3000\ ^0\text{K}$, so erhält man als mittlere Oberflächentemperatur der Reaktorkühlkanäle

$$\bar{t} = t_{\max} = 3000\ ^0\text{K},$$

was eine überall gleiche Oberflächentemperatur bedeutet.

Der zweite Fall B ergibt sich aus der Forderung konstanter Kühlkanal-Oberflächentemperaturen bei beliebigen Durchsätzen. Eine Wärmequellenverteilung, welche dieser Forderung genügt, stellt sich noch etwas günstiger als diejenige des Falls A, hat aber für jeden einzelnen Durchsatz eine verschiedene räumliche Verteilung. Man erhält diese Wärmequellenverteilung für einen zylindrischen Reaktor aus Gl. (10) durch partielles Differenzieren von $(t - \vartheta_1)$ nach $r$ und $z$ und darauffolgendes Nullsetzen:

$$\frac{\partial(t - \vartheta_1)}{\partial r} = \left[\frac{f(z)}{\alpha\, U} + \frac{1}{M\, c_p} \int_0^z f(z)\, dz\right] \cdot \frac{\partial q(r)}{\partial r} = 0. \tag{40}$$

Da $f(z)$ überall positiv sein muß, kann die eckige Klammer von (40) nicht verschwinden; daraus folgt:

$$\frac{\partial q(r)}{\partial r} = 0$$

oder

$$q = \text{const.}; \tag{40 a}$$

und wegen

$$\frac{\partial(t - \vartheta_1)}{\partial z} = \frac{q}{\alpha\, U} f'(z) + \frac{q}{M\, c_p} f(z) = 0 \tag{41}$$

oder

$$\frac{f'(z)}{f(z)} = -\frac{\alpha U}{M c_p} \tag{41 a}$$

folgt durch Integration:

$$f(z) = \text{const} \cdot e^{-(\alpha U/Mc_p)z}. \tag{42}$$

Weiter gilt wegen des Zusammenhangs von Neutronenfluß und Leistung für den Fall A konstanter Leistungsdichte im Reaktorkern

$$\Sigma_f \phi = c \quad \text{(im Kern)} \tag{43}$$

und für den Fall B konstanter Kühlkanal-Oberflächentemperatur:

$$\Sigma_f \phi = c \cdot e^{-(\alpha U/Mc_p)z} \quad \text{(im Kern)}. \tag{44}$$

Die Konstante $c$ in Gl. (43), bzw. (44) ist eine willkürliche Konstante, die später nicht mehr benötigt wird.

Durch Verbindung von (40), bzw. (41) mit der Integral- oder Differentialgleichung des Neutronenflusses erhält man die gesuchten Brennstoffverteilungen, die eine Wärmequellenverteilung der beiden genannten Eigenschaften gewährleisten.

Vol. 4 1958

### 6. Fall A: Das Produkt $\Sigma_a \phi$ im Reaktorkern ist konstant

Es soll jetzt berechnet werden, wie der Brennstoff in dem Reaktor bei vorgegebener Geometrie verteilt werden muß, damit die Größe $\Sigma_a(\mathfrak{r})\, \phi(\mathfrak{r})$ im Kern konstant bleibt. Es ist dabei zu beachten, daß $\Sigma_a$ proportional $\Sigma_f$ ist.

Weiter soll angenommen werden, daß der Reaktorkern von einem unendlich großen Reflektor umgeben ist, der dieselbe Beschaffenheit wie der Moderator des Kerns aufweist. Danach kann man auch das Problem dahingehend formulieren, daß man eine endliche Brennstoffverteilung vorgegebener Geometrie in einem unendlich ausgedehnten Moderatorgebiet sucht, für welche die Größe $\Sigma_a(\mathfrak{r})\, \phi(\mathfrak{r})$ in dem vorgegebenen endlichen Gebiet eine räumliche Kastenfunktion ist, so daß diese Größe $= c$ für Ortsvektoren innerhalb des Gebietes $= 0$ für solche außerhalb des Gebietes ist.

Es soll nun gezeigt werden, wie sich die Methode zur Berechnung ungleichförmiger Brennstoffverteilungen im allgemeinsten Fall unter den bereits genannten Voraussetzungen gestaltet. Das Problem ist dabei nur einer einfachen mathematischen Behandlungsweise zugängig, wenn ein Reaktor in einem unendlichen Gebiet gleichartigen Moderators ausgebreitet ist. Die Ergebnisse bringen aber auch ein qualitatives Bild darüber, wie man in anderen Fällen vorzugehen hat. Aus methodischen Gründen soll zuerst der Gang für die Berechnung der gesuchten ungleichförmigen Brennstoffverteilung mit der Reaktordifferentialgleichung erläutert werden. Diese Gleichung lautet:

$$\phi(\mathfrak{r}) = H\, \Sigma_a(\mathfrak{r})\, \phi(\mathfrak{r}). \tag{16}$$

Man macht für die Kastenfunktion $\Sigma_a(\mathfrak{r})\, \phi(\mathfrak{r})$ einen FOURIER-Ansatz:

$$\Sigma_a(\mathfrak{r})\, \phi(\mathfrak{r}) = \int_{\mathfrak{t}}^{\infty} B(\mathfrak{t})\, e^{i\mathfrak{t}\mathfrak{r}}\, d\mathfrak{t} \tag{45 a}$$

mit

$$B(\mathfrak{t}) = \frac{1}{(2\pi)^3} \int_{\mathfrak{R}}^{\infty} \Sigma_a(\mathfrak{r})\, \phi(\mathfrak{r})\, e^{-i\mathfrak{t}\mathfrak{r}}\, d\mathfrak{r}. \tag{45 b}$$

Es soll nun gelten

$$\Sigma_a(\mathfrak{r})\,\phi(\mathfrak{r}) = c$$

innerhalb des in Frage kommenden Gebiets $G$; dann gilt

$$B(\mathfrak{k}) = \frac{c}{(2\pi)^3}\int_G e^{-i\mathfrak{k}\mathfrak{r}}\,d\mathfrak{r}. \tag{45 c}$$

Das in (45 c) stehende Integral ist im Gegensatz zu (45 b) nur über das endliche Gebiet $G$ zu erstrecken. Für den Fluß wird ebenfalls ein FOURIER-Ansatz der Form

$$\phi(\mathfrak{r}) = \int_{\mathfrak{k}} A(\mathfrak{k})\,e^{i\mathfrak{k}\mathfrak{r}}\,d\mathfrak{k} \tag{46}$$

gemacht. Wird (45 a) und (46) in (16) eingesetzt, so erhält man als FOURIER-transformierte Gleichung unseres Problems

$$A(\mathfrak{k}) = H\,B(\mathfrak{k}). \tag{47}$$

Die Anwendung des Operators $H$ im Bildraum der FOURIER-Transformation ist gleichbedeutend mit der Multiplikation einer im allgemeinen algebraischen Funktion $f(\mathfrak{k})$ mit $B(\mathfrak{k})$ auf der rechten Seite von (47):

$$A(\mathfrak{k}) = f(\mathfrak{k})\,B(\mathfrak{k}). \tag{48}$$

Ausführlicher geschrieben läßt sich dies, wie folgt, kurz begründen:

$$\begin{aligned}\int A(\mathfrak{k})\,e^{i\mathfrak{k}\mathfrak{r}}\,d\mathfrak{k} &= H\int B(\mathfrak{k})\,e^{i\mathfrak{k}\mathfrak{r}}\,d\mathfrak{k}\\ &= \int B(\mathfrak{k})\,H\,e^{i\mathfrak{k}\mathfrak{r}}\,d\mathfrak{k}\\ &= \int B(\mathfrak{k})\,f(\mathfrak{k})\,e^{i\mathfrak{k}\mathfrak{r}}\,d\mathfrak{k};\end{aligned}$$

letzteres durch Anwendung von $H$ auf $e^{i\mathfrak{k}\mathfrak{r}}$, wodurch (45) bewiesen ist.

Wird (48) in (46) eingesetzt, so erhält man:

$$\phi(\mathfrak{r}) = \int_{\mathfrak{k}} f(\mathfrak{k})\,B(\mathfrak{k})\,e^{i\mathfrak{k}\mathfrak{r}}\,d\mathfrak{k}. \tag{49}$$

Unter Berücksichtigung, daß $\Sigma_a(\mathfrak{r})\,\phi(\mathfrak{r})$ im Innern des Reaktors $= c$ sein soll, folgt für die Abhängigkeit von $\Sigma_a(\mathfrak{r})$ aus (49):

$$\Sigma_a(\mathfrak{r}) = \frac{c}{\int_{\mathfrak{k}} f(\mathfrak{k})\,B(\mathfrak{k})\,e^{i\mathfrak{k}\mathfrak{r}}\,d\mathfrak{k}}. \tag{50}$$

Gl. (50) ist bereits die Lösung der gestellten Aufgabe im Fall der Beschreibung des Reaktors durch eine Vielgruppen-Differentialgleichung.

Für den Fall einer Integralgleichung läßt sich das Rechenschema auch sofort in geschlossener Form angeben. Dazu gehen wir von der Reaktorintegralgleichung

$$\phi(\mathfrak{r}) = \int K(|\mathfrak{r}-\mathfrak{r}'|)\,\Sigma_a(\mathfrak{r}')\,\phi(\mathfrak{r}')\,d\mathfrak{r}' \tag{17}$$

aus.

In dieser allgemeinen Form läßt sich der auf der rechten Seite von (17) stehende Ausdruck mit dem Faltungssatz für dreidimensionale FOURIER-Transformationen umformen:

$$\phi(\mathfrak{r}) = \int_{\mathfrak{k}} \varkappa(\mathfrak{k})\, B(\mathfrak{k})\, e^{i\mathfrak{k}\mathfrak{r}}\, d\mathfrak{k}. \tag{51}$$

Dabei ist $\varkappa(\mathfrak{k})$ die FOURIER-Transformierte des Kerns von (17); $B(\mathfrak{k})$ die FOURIER-Transformierte der räumlichen Kastenfunktion $\Sigma_a(\mathfrak{r})\,\phi(\mathfrak{r})$, die im Gebiet des Reaktorkerns $G$ den Wert $c$ haben soll:

$$\varkappa(\mathfrak{k}) = \frac{1}{(2\pi)^{3/2}} \int_{R} K(|\mathfrak{r}|)\, e^{-i\mathfrak{k}\mathfrak{r}}\, d\mathfrak{r} \tag{52}$$

$$B(\mathfrak{k}) = \frac{1}{(2\pi)^{3/2}} \int_{R} \Sigma_a(\mathfrak{r})\, \phi(\mathfrak{r})\, e^{-i\mathfrak{k}\mathfrak{r}}\, d\mathfrak{r} \tag{53}$$

$$= \frac{c}{(2\pi)^{3/2}} \int_{G} e^{-i\mathfrak{k}\mathfrak{r}}\, d\mathfrak{r}. \tag{53 a}$$

Gl. (51) in Verbindung mit Gln. (52) und (53 a) stellt bereits die gesuchte Lösung unseres Problems dar. Durch eine der von (49) und (50) folgenden analoge Umformung erhält man daraus für die Abhängigkeit $\Sigma_a(\mathfrak{r})$:

$$\Sigma_a(\mathfrak{r}) = \frac{c}{\int_{\mathfrak{k}} \varkappa(\mathfrak{k})\, B(\mathfrak{k})\, e^{i\mathfrak{k}\mathfrak{r}}\, d\mathfrak{k}}. \tag{54}$$

Damit ist man in der Lage, für Reaktoren beliebiger Geometrie die Brennstoffverteilungen anzugeben.

Trotz der scheinbaren Gleichartigkeit der Ausdrücke (50) und (54) ist jedoch die Berechnung der ungleichförmigen Brennstoffverteilung im Fall der Integralgleichung ungleich schwieriger, da sich die Integrale (51) und (52) sehr viel schwerer auswerten lassen als das einzige bei der Integration der Differentialgleichung auftretende Integral (49).

Es sollen jetzt für die Integralgleichung und Differentialgleichung Lösungen angegeben werden. Während für die Integralgleichung nur die Lösungen analytisch so weit vorbereitet werden, wie sie für das Eingeben in Rechenmaschinen vorliegen sollten, lassen sich für die Differentialgleichung explizit Lösungen in geschlossener Form angeben.

## Die Lösung der Integralgleichung für Platte, Kugel und Zylindersymmetrie

### *a) Platte*

Für einen unendlich großen plattenförmigen Reaktor läßt sich die Integralgleichung auf die Form bringen:

$$\phi(x) = \int K(|x - x'|)\, \Sigma_a(x')\, \phi(x')\, dx'. \tag{55}$$

$K(|x - x'|)$ ist der Kern im eindimensionalen Fall in Gl. (26). Umformung nach dem Faltungssatz ergibt:

$$\phi(x) = \int_{-\infty}^{+\infty} \varkappa(k)\, B(k)\, e^{ikx}\, dk \tag{56}$$



Vol. 4 1958

mit

$$\varkappa(k) = \frac{1}{(2\pi)^{1/2}} \int_{-\infty}^{+\infty} K(|x|)\, e^{-ikx}\, dx \tag{57}$$

und

$$B(k) = \frac{1}{(2\pi)^{1/2}} \int_{-\infty}^{+\infty} \Sigma_a(x)\, \phi(x)\, e^{-ikx}\, dx$$

$$= \frac{c}{(2\pi)^{1/2}} \int_{-R}^{+R} e^{-ikx}\, dx = \sqrt{\frac{2}{\pi}}\, \frac{c}{k} \sin(k R). \tag{58}$$

Die Funktion $\Sigma_a(x)$ im Kern ist dann wegen $\Sigma_a(x)\, \phi(x) = c$:

$$\Sigma_a(x) = c \left[ \int_{-\infty}^{+\infty} \varkappa(k)\, B(k)\, e^{ikx}\, dk \right]^{-1}. \tag{56 a}$$

*b) Kugel*

Im kugelsymmetrischen Fall gilt, wenn der Anfang des Vektors $\mathfrak{r}$ in den Kugelmittelpunkt gelegt wird, unter Verwendung sphärischer Polarkoordinaten:

$$\phi(\mathfrak{r}) = \phi(r) = \int_{\mathfrak{k}} \varkappa(\mathfrak{k})\, B(\mathfrak{k})\, e^{i\mathfrak{k}\mathfrak{r}}\, d\mathfrak{k}. \tag{59}$$

Mit

$$\left.\begin{aligned} d\mathfrak{k} &= 2\pi k^2\, dk\, d\mu \\ \mathfrak{k}\mathfrak{r} &= k r \mu \\ \mu &= \cos\vartheta \end{aligned}\right\} \tag{59 a}$$

schreibt sich (59):

$$\phi(r) = 2\pi \int_{k=0}^{\infty} \varkappa(\mathfrak{k})\, B(\mathfrak{k})\, k^2 \int_{-1}^{+1} e^{ikr\mu}\, d\mu\, dk; \tag{60}$$

somit

$$\phi(r) = \frac{4\pi}{r} \int_{k=0}^{\infty} \varkappa(\mathfrak{k})\, B(\mathfrak{k}) \sin(k r)\, k\, dk. \tag{61}$$

Die Größen $\dot{\varkappa}(\mathfrak{k})$ und $B(\mathfrak{k})$ müssen jetzt noch auf Kugelsymmetrie umgerechnet werden.

Im Dreidimensionalen gilt die Gl. (53)

$$B(\mathfrak{k}) = \frac{1}{(2\pi)^{3/2}} \int_{\mathfrak{R}} \Sigma_a(\mathfrak{r})\, \phi(\mathfrak{r})\, e^{-i\mathfrak{k}\mathfrak{r}}\, d\mathfrak{r}, \tag{53}$$

die sich bei Kugelsymmetrie vereinfachen läßt:

$$B(\mathfrak{k}) = \frac{1}{(2\pi)^{3/2}} \int \Sigma_a(r)\, \phi(r)\, e^{ikr\mu}\, 2\pi r^2\, dr\, d\mu$$

$$= \frac{1}{(2\pi)^{1/2}} \int_0^\infty \Sigma_a(r)\, \phi(r)\, r^2 \int_{-1}^{+1} e^{ikr\mu}\, d\mu\, dr$$

$$= \frac{1}{(2\pi)^{1/2}} \int_0^\infty \Sigma_a(r)\, \phi(r)\, r\, \frac{2 \sin(k r)}{k}\, dr. \tag{62}$$

Damit:

$$k\, B(\mathfrak{k}) = \sqrt{\frac{2}{\pi}} \int_0^\infty r\, \Sigma_a(r)\, \phi(r) \sin(k r)\, dr. \tag{63}$$

Oder, wenn die rechte Seite von (63) als $B(k)$ definiert wird, gilt

$$B(\mathfrak{k}) = \frac{B(k)}{k}. \tag{64}$$

Analog ergibt sich

$$\varkappa(\mathfrak{k}) = \frac{\varkappa(k)}{k} \tag{65}$$

mit

$$\varkappa(k) = \sqrt{\frac{2}{\pi}} \int_0^\infty r\, K(r) \sin(k r)\, dr. \tag{66}$$

$K(r)$ ist der Punktkern [Gl. (28) und (29)].

Man erhält schließlich

$$r\, \phi(r) = \int_{k=0}^\infty \frac{\varkappa(k)\, B(k) \sin(k r)}{k}\, dk. \tag{67}$$

Die Funktion $\Sigma_a(r)$ im Kern ergibt sich dann wegen $\Sigma_a(r)\, \phi(r) = c$ zu:

$$\Sigma_a(r) = c \cdot r \left[ \int_{k=0}^\infty \frac{\varkappa(k)\, B(k) \sin(k r)}{k}\, dk \right]^{-1}. \tag{67 a}$$

*c) Zylinder*

Im zylindersymmetrischen Fall ergibt sich unter Verwendung von Polarkoordinaten:

$$\phi(\mathfrak{r}) = \phi(r) = \int_{\mathfrak{k}} \varkappa(\mathfrak{k})\, B(\mathfrak{k})\, e^{i\mathfrak{k}\mathfrak{r}}\, dk \tag{68}$$

$$\left.\begin{aligned} d\mathfrak{k} &= k\, dk\, d\varphi \\ \mathfrak{k}\mathfrak{r} &= k\, r \cos\varphi \end{aligned}\right\}. \tag{68 a}$$



Vol. 4 1958

Damit:

$$\phi(r) = \int_{k=0}^{\infty} \varkappa(\mathfrak{k})\, B(\mathfrak{k})\, k \int_{0}^{2\pi} e^{ikr\cos\varphi}\, d\varphi\, dk.$$

Da

$$\int_{0}^{2\pi} e^{ikr\cos\varphi}\, d\varphi = 2\pi\, J_0(k\,r)$$

ist, wo $J_0(z)$ die BESSELsche Zylinderfunktion nullter Ordnung ist, folgt:

$$\phi(r) = 2\pi \int_{k=0}^{\infty} \varkappa(\mathfrak{k})\, B(\mathfrak{k})\, J_0(k\,r)\, k\, dk. \tag{69}$$

Es verbleibt noch die Transformation der $\varkappa(\mathfrak{k})$ und $B(\mathfrak{k})$ auf Zylindersymmetrie: Es gilt

$$\begin{aligned} B(\mathfrak{k}) &= \frac{1}{2\pi} \int \Sigma_a(\mathfrak{r})\, \phi(\mathfrak{r})\, e^{-i\mathfrak{k}\mathfrak{r}}\, d\mathfrak{r} \\ &= \frac{1}{2\pi} \int_{0}^{\infty} \Sigma_a(r)\, \phi(r)\, r \int_{0}^{2\pi} e^{-ikr\cos\varphi}\, d\varphi\, dr; \end{aligned} \tag{70}$$

wegen

$$\int_{0}^{2\pi} e^{-ikr\cos\varphi}\, d\varphi = 2\pi\, J_0(-k\,r) = 2\pi\, J_0(k\,r)$$

folgt:

$$B(\mathfrak{k}) = \int_{0}^{\infty} r\, \Sigma_a(r)\, \phi(r)\, J_0(k\,r)\, dr, \tag{71}$$

ebenso

$$\varkappa(\mathfrak{k}) = \int_{0}^{\infty} r\, K(r)\, J_0(k\,r)\, dr. \tag{72}$$

Der in (72) stehende Kern ist der für die Zylindersymmetrie zuständige Kern. Die Funktion $\Sigma_a(r)$ im Reaktorkern ergibt sich zu

$$\Sigma_a(r) = c\left[2\pi \int_{0}^{\infty} \varkappa(\mathfrak{k})\, B(\mathfrak{k})\, J_0(k\,r)\, k\, dk\right]^{-1}. \tag{72 a}$$

## Die Lösung der Differentialgleichung für Platte, Kugel und Zylindersymmetrie

### *a) Platte*

Für die Reaktordifferentialgleichung

$$\prod_{i=0}^{n} L_i\, \phi = \frac{1}{\Sigma_1}\left(\eta - \prod_{i=1}^{n} L_i\right) \Sigma_a \phi \tag{32}$$

mit

$$L_i = -\alpha_i^2 \Delta + 1$$

gilt im eindimensionalen Fall

$$\Delta = \frac{d^2}{dx^2}.$$

Für den Fluß macht man den FOURIER-Ansatz

$$\phi = \frac{1}{(2\pi)^{1/2}} \int_{-\infty}^{+\infty} A(\omega)\, e^{i\omega x}\, d\omega. \tag{73}$$

Ebenso für die Kastenfunktion $\Sigma_a \phi$:

$$\Sigma_a \phi = \frac{1}{(2\pi)^{1/2}} \int_{-\infty}^{+\infty} B(\omega)\, e^{i\omega x}\, d\omega\ ; \tag{74 a}$$

$$B(\omega) = \frac{1}{(2\pi)^{1/2}} \int_{-\infty}^{+\infty} \Sigma_a(x)\, \phi(x)\, e^{-i\omega x}\, dx \tag{74 b}$$

$$= \frac{c}{(2\pi)^{1/2}} \int_{-R}^{+R} e^{-i\omega x}\, dx = \frac{i\,c}{(2\pi)^{1/2}} \frac{e^{i\omega R} - e^{-i\omega R}}{\omega}.$$

Vol. 4 1958

$2R$ ist der Durchmesser des Reaktors.

Wird (61) und (62) in (32) eingesetzt, so erhält man als Beziehung für die FOURIER-Komponenten

$$A(\omega) \prod_{i=0}^{n} (1 + \alpha_i^2 \omega^2) = \frac{B(\omega)}{\Sigma_1} \left( \eta - \prod_{i=1}^{n} (1 + \alpha_i^2 \omega^2) \right), \tag{75}$$

und damit erhält man für den Fluß:

$$\phi(x) = \frac{1}{(2\pi)^{1/2} \Sigma_1} \int_{-\infty}^{+\infty} \frac{B(\omega) \left( \eta - \prod_{i=0}^{n} (1 + \alpha_i^2 \omega^2) \right)}{\prod_{i=0}^{n} (1 + \alpha_i^2 \omega^2)}\, e^{i\omega x}\, d\omega \tag{76}$$

und

$$\Sigma_a(x) = \frac{c}{\phi(x)}. \tag{76 a}$$

Das Integral (76) läßt sich unter Benutzung von (74 b), wie im Anhang gezeigt wird, durch Integration im Komplexen geschlossen auswerten, und man erhält dafür:

$$\phi(x) = \frac{c}{\Sigma_1} \left[ (\eta - 1) - \sum_{i=0}^{n} e^{-R/\alpha_i} \frac{\left[ \eta - \prod_{j=1}^{n} \left( 1 - \left( \frac{\alpha_j}{\alpha_i} \right)^2 \right) \right]}{\prod_{j \neq i=0}^{n} \left( 1 - \left( \frac{\alpha_j}{\alpha_i} \right)^2 \right)} \cosh \left( \frac{x}{\alpha_i} \right) \right]. \tag{77}$$

Die Funktion $\Sigma_a(x)$ ist dann gegeben durch

$$\Sigma_a(x) = \Sigma_1 \left[ (\eta - 1) - \sum_{i=0}^{n} e^{-R/\alpha_i} \frac{\eta - \prod_{j=1}^{n} \left( 1 - \left( \frac{\alpha_j}{\alpha_i} \right)^2 \right)}{\prod_{j \neq i=0}^{n} \left( 1 - \left( \frac{\alpha_j}{\alpha_i} \right)^2 \right)} \cosh \left( \frac{x}{\alpha_i} \right) \right]^{-1}. \tag{78}$$

Für eine Eingruppentheorie $\alpha_0 = L_0$; $\alpha_i = 0$, $i > 0$ ergibt sich:

$$\Sigma(x) = \frac{\Sigma_1}{\eta - 1}\left[1 - e^{-R/L_0}\cosh\left(\frac{x}{L_0}\right)\right]^{-1}. \tag{79}$$

Besser ist es, für $L_0$ die Migrationslänge $M = \sqrt{L_0^2 + \tau}$ zu setzen, wie es der modifizierten Eingruppentheorie entspricht:

$$\Sigma_a(x) = \frac{\Sigma_1}{\eta - 1}\left[1 - e^{-R/M}\cosh\left(\frac{x}{M}\right)\right]^{-1}. \tag{79 a}$$

Bei zwei Gruppen mit $\alpha_0 = L_0$ und $\alpha_1 = \sqrt{\tau}$ erhält man aus (60):

$$\Sigma_a(x) = \Sigma_1\left[(\eta - 1) - e^{-R/L_0}\frac{\eta - (1 - (\tau/L_0^2))}{1 - (\tau/L_0^2)}\cosh\left(\frac{x}{L_0}\right)\right.$$
$$\left. - e^{-R/\sqrt{\tau}}\frac{\eta}{1 - (L_0^2/\tau)}\cosh\left(\frac{x}{\sqrt{\tau}}\right)\right]^{-1}. \tag{80}$$

*b) Kugel*

Bei Kugelsymmetrie hat in (32) der Deltaoperator die Form

$$\Delta = \frac{1}{r^2}\frac{\partial}{\partial r}\left(r^2\frac{\partial}{\partial r}\right). \tag{81}$$

Die Eigenfunktionen des Deltaoperators

$$\Delta\phi = -\omega^2\phi \qquad \text{sind}$$
$$\phi = \frac{e^{i\omega r}}{r}. \tag{82}$$

Es ist daher zweckmäßig, bei Kugelsymmetrie den mit $r$ multiplizierten Fluß einzuführen und ihn einer FOURIER-Transformation zu unterwerfen:

$$r\,\phi(r) = \frac{1}{(2\pi)^{1/2}}\int_{-\infty}^{+\infty} A(\omega)\, e^{i\omega r}\, d\omega; \tag{83}$$

ebenso die mit dem Faktor $r$ multiplizierte Kastenfunktion:

$$r\,\Sigma_a\phi = \frac{1}{(2\pi)^{1/2}}\int_{-\infty}^{+\infty} B(\omega)\, e^{i\omega r}\, d\omega. \tag{84}$$

Auf diese Weise wird $r\,\phi(r)$ und $r\,\Sigma_a(r)\,\phi(r)$ für negative $r$ antisymmetrisch fortgesetzt, was bei der Bildung des FOURIER-Integrals zu berücksichtigen ist.

Die FOURIER-Transformierte von Gl. (84) lautet dann:

$$B(\omega) = \frac{1}{(2\pi)^{1/2}}\int_{-\infty}^{+\infty} r\,\Sigma_a(r)\,\phi(r)\, e^{-i\omega r}\, dr$$
$$= \frac{c}{(2\pi)^{1/2}}\int_{-R}^{+R} r\, e^{-i\omega r}\, dr \tag{85}$$
$$= \frac{c}{(2\pi)^{1/2}}\left[\frac{i\,R\,(e^{i\omega R} + e^{-i\omega R})}{\omega} - \frac{1}{\omega^2}\,(e^{i\omega R} - e^{-i\omega R})\right].$$

In (85) ist $R$ der Radius des Reaktors. Durch Einsetzen von (83) und (84) in (32) ergibt sich für die FOURIER-Komponenten

$$A(\omega) \prod_{i=0}^{n} (1 + \alpha_i^2 \omega^2) = \frac{B(\omega)}{\Sigma_1} \left( \eta - \prod_{i=1}^{n} (1 + \alpha_i^2 \omega^2) \right). \tag{86}$$

Damit erhält man:

$$r\,\phi(r) = \frac{1}{(2\pi)^{1/2} \Sigma_1} \int_{-\infty}^{+\infty} \frac{B(\omega) \left( \eta - \prod_{i=1}^{n} (1 + \alpha_i^2 \omega^2) \right)}{\prod_{i=0}^{n} (1 + \alpha_i^2 \omega^2)} e^{i\omega r}\, d\omega. \tag{87}$$

Das Integral (87) läßt sich unter Verwendung von Gl. (85), wie im Anhang gezeigt wird, ähnlich wie im Fall der Plattensymmetrie mit dem Residuensatz durch Integration im Komplexen leicht auswerten, und man erhält:

$$\phi(r) = \frac{c}{\Sigma_1} \left[ (\eta - 1) - \sum_{i=0}^{n} e^{-R/\alpha_i} \cdot (R + \alpha_i) \frac{\left[ \eta - \prod_{j=1}^{n} \left( 1 - \left( \frac{\alpha_j}{\alpha_i} \right)^2 \right) \right]}{\prod_{j \neq i=0}^{n} \left( 1 - \left( \frac{\alpha_j}{\alpha_i} \right)^2 \right)} \frac{\sinh \left( \frac{r}{\alpha_i} \right)}{r} \right]. \tag{88}$$

Für eine Eingruppentheorie ergibt sich damit für die Funktion $\Sigma_a(r) = (c/\phi(r))$

$$\Sigma_a(r) = \frac{\Sigma_1}{\eta - 1} \left[ 1 - e^{-R/L_0} (R + L_0) \frac{\sinh (r/L_0)}{r} \right]^{-1}. \tag{89}$$

In der modifizierten Eingruppentheorie ist wieder in (79) an Stelle von $L_0$ die Migrationslänge $M$ zu setzen.

Für eine Zweigruppentheorie mit $\alpha_0 = L_0$, $\alpha_1 = \sqrt{\tau}$ hat man

$$\Sigma_a(r) = \Sigma_1 \left[ (\eta - 1) - e^{-R/L_0} (R + L_0) \frac{\eta - \left( 1 - (\tau/L_0^2) \right)}{1 - (\tau/L_0^2)} \frac{\sinh (r/L_0)}{r} - e^{-R/\sqrt{\tau}} (R + \sqrt{\tau}) \frac{\eta}{1 - (L_0^2/\tau)} \frac{\sinh (r/\sqrt{\tau})}{r} \right]^{-1}. \tag{90}$$

*c) Zylinder*

Bei Zylindersymmetrie hat der zweidimensionale Deltaoperator die Form:

$$\Delta = \frac{d^2}{dr^2} + \frac{1}{r} \frac{d}{dr} \tag{91}$$

mit den Eigenfunktionen

$$\Delta J_0(\omega r) = -\omega^2 J_0(\omega r). \tag{92}$$

Daher ist es zweckmäßig, den Fluß einer FOURIER-BESSEL-Transformation zu unterziehen:

$$\phi(r) = \int_0^{\infty} A(\omega) J_0(\omega r)\, \omega\, d\omega; \tag{93}$$

Vol. 4 1958

ebenso die zweidimensionale Kastenfunktion:

$$\Sigma_a \phi = \int_0^\infty B(\omega)\, J_0(\omega r)\, \omega\, d\omega \tag{94}$$

$$B(\omega) = \int_0^\infty \Sigma_a \phi\, J_0(\omega r)\, r\, dr$$

$$= c \int_0^R J_0(\omega r)\, r\, dr = \frac{c R}{\omega} J_1(\omega R). \tag{94 a}$$

Durch Einsetzen von (83) und (84) in die Differentialgleichung erhält man:

$$A(\omega) = \frac{B(\omega)}{\Sigma_1} \frac{\eta - \prod_{i=1}^{n} (1 + \alpha_i^2 \omega^2)}{\prod_{i=0}^{n} (1 + \alpha_i^2 \omega^2)}, \tag{95}$$

und damit unter Berücksichtigung von Gl. (93) und (94 a) schließlich:

$$\phi(r) = \frac{c R}{\Sigma_1} \int_0^\infty \frac{\eta - \prod_{i=1}^{n} (1 + \alpha_i^2 \omega^2)}{\prod_{i=0}^{n} (1 + \alpha_i^2 \omega^2)} J_0(\omega r)\, J_1(\omega R)\, d\omega. \tag{96}$$

Eine geschlossene Darstellung von (98) ist hier schwieriger und soll deshalb nicht gebracht werden.

Für die Funktion $\Sigma_a(r)$ ergibt sich:

$$\Sigma_a(r) = \frac{\Sigma_1}{R} \left[ \int_0^\infty \frac{\eta - \prod_{i=1}^{n} (1 + \alpha_i^2 \omega^2)}{\prod_{i=0}^{n} (1 + \alpha_i^2 \omega^2)} J_0(\omega r)\, J_1(\omega R)\, d\omega \right]^{-1}. \tag{96 a}$$

### 7. Fall B: Die Oberflächentemperatur der Kühlkanäle ist konstant

Es ist jetzt zu berechnen, wie der Brennstoff über den Reaktorkern zu verteilen ist, damit im Kern die Bedingung

$$\Sigma_a \phi = c \cdot e^{-(\alpha U / M c_p) z} \tag{97}$$

erfüllt ist. Für Ortsvektoren außerhalb des Reaktors hingegen soll wieder $\Sigma_a \phi = 0$ sein. Das allgemeine Rechenschema läßt sich für diesen Fall wieder für die Differential- als auch Integralgleichung angeben. Man kann im allgemeinsten Fall dazu die Formeln (50) und (54) verwenden, indem man in ihnen die FOURIER-Transformierte $B(\mathfrak{k})$ durch den Ausdruck

$$B(\mathfrak{k}) = \frac{c}{(2\pi)^3} \int_G e^{-(\alpha U / M c_p) z} e^{-i \mathfrak{k} \mathfrak{r}}\, d\mathfrak{r} \tag{98}$$

ersetzt.

Der Einfachheit halber soll die Rechnung auf einen unendlich ausgedehnten Plattenreaktor beschränkt werden und der praktisch wichtige Fall eines endlichen Zylinders in einer späteren Arbeit behandelt werden. Die Ergebnisse werden sich dabei qualitativ nicht und quantitativ nur sehr wenig ändern.

Zu diesem Zweck soll angenommen werden, daß die Kühlkanäle den Plattenreaktor senkrecht durchsetzen. Diese Richtung sei die $z$-Richtung, so daß in den bisherigen Gleichungen für die Platte die Variable $x$ durch $z$ zu ersetzen ist.

Um gleich zu konkreten Resultaten zu kommen, soll die Verteilung mit der Reaktordifferentialgleichung

$$\prod_{i=0}^{n} L_i \phi = \frac{1}{\Sigma_1}\left(\eta - \prod_{i=1}^{n} L_i\right)\Sigma_a \phi \tag{32}$$

behandelt werden.

Mit dem FOURIER-Ansatz für den Fluß

$$\phi = \frac{1}{(2\pi)^{1/2}} \int_{-\infty}^{+\infty} A(\omega)\, e^{i\omega z}\, d\omega \tag{99}$$

und mit der Abkürzung

$$a = \frac{\alpha\, U}{M\, c_p}$$

und dem FOURIER-Ansatz für die Leistungsverteilung

$$\Sigma_a \phi = \frac{1}{(2\pi)^{1/2}} \int_{-\infty}^{+\infty} B(\omega)\, e^{i\omega z}\, d\omega \tag{100 a}$$

$$\begin{aligned} B(\omega) &= \frac{1}{(2\pi)^{1/2}} \int_{-\infty}^{+\infty} \Sigma_a(z)\, \phi(z)\, e^{-i\omega z}\, dz \\ &= \frac{c}{(2\pi)^{1/2}} \int_{-R}^{+R} e^{-(i\omega + a)z}\, dz \\ &= \frac{c}{(2\pi)^{1/2}} \frac{1}{(i\,\omega + a)} \left[e^{aR}\, e^{i\omega R} - e^{-aR}\, e^{-i\omega R}\right] \end{aligned} \tag{100 b}$$

folgt durch Einsetzen in (32)

$$A(\omega) \prod_{i=0}^{n} (1 + \alpha_i^2\, \omega^2) = \frac{B(\omega)}{\Sigma_1}\left(\eta - \prod_{i=1}^{n} (1 + \alpha_i^2\, \omega^2)\right); \tag{101}$$

somit

$$\phi(z) = \frac{1}{(2\pi)^{1/2}\Sigma_1} \int_{-\infty}^{+\infty} \frac{B(\omega)\left(\eta - \prod_{i=1}^{n} (1 + \alpha_i^2\, \omega^2)\right)}{\prod_{i=0}^{n} (1 + \alpha_i^2\, \omega^2)}\, e^{i\omega z}\, d\omega. \tag{102}$$

Das Integral (102) läßt sich, wie im Anhang gezeigt wird, wieder leicht durch Integration im Komplexen auswerten und man erhält:

$$\begin{aligned} \phi(z) = \frac{c}{\Sigma_1} \sum_{i=0}^{n} \Bigg[ &\frac{1}{2} \frac{\eta - \prod_{j=1}^{n} \left(1 - \left(\frac{\alpha_j}{\alpha_i}\right)^2\right)}{\prod_{j \neq i = 0}^{n} \left(1 - \left(\frac{\alpha_j}{\alpha_i}\right)^2\right)} \left( \frac{e^{R/\alpha_i (a\alpha_i - 1)}}{a\,\alpha_i - 1}\, e^{-z/\alpha_i} - \frac{e^{-R/\alpha_i (a\alpha_i + 1)}}{a\,\alpha_i + 1}\, e^{z/\alpha_i} \right. \\ &\left. + \frac{\eta - \prod_{i=0}^{n} (1 - \alpha_i^2\, a^2)}{\prod_{i=0}^{n} (1 - \alpha_i^2\, a^2)}\, e^{-az} \right] \end{aligned} \tag{103}$$

Vol. 4 1958

und

$$\Sigma_a(z) = \frac{c \cdot e^{-az}}{\phi(z)} = \Sigma_1 e^{-az} \left\{ \sum_{i=0}^{n} [\ldots] \right\}^{-1}. \tag{103 a}$$

Die Summe in Gl. (106) hat für eine Eingruppentheorie den Wert:

$$\sum_{i=0}^{n} [\ldots] = \frac{\eta - 1}{2} \left( \frac{e^{R/L_0(aL_0-1)}}{a L_0 - 1} e^{-z/L_0} - \frac{e^{-R/L_0(aL_0+1)}}{a L_0 + 1} e^{z/L_0} \right) + \frac{\eta - 1 + L_0^2 a^2}{1 - L_0^2 a^2} e^{-az}. \tag{104}$$

Besser ist es, wieder an Stelle von $L$ die Migrationslänge $M$ zu setzen. Für eine Zweigruppentheorie hat die Summe den Wert:

$$\sum_{i=0}^{n} [\ldots] = \frac{\eta - (1 - (\tau/L_0^2))}{2(1 - (\tau/L_0^2))} \left( \frac{e^{R/L_0(aL_0-1)}}{a L_0 - 1} e^{-z/L_0} - \frac{e^{-R/L_0(aL_0+1)}}{a L_0 + 1} e^{z/L_0} \right) + \frac{\eta}{2(1 - (L_0^2/\tau))} \left( \frac{e^{R/\sqrt{\tau}(a\sqrt{\tau}-1)}}{a\sqrt{\tau} - 1} e^{-z/\sqrt{\tau}} - \frac{e^{-R/\sqrt{\tau}(a\sqrt{\tau}+1)}}{a\sqrt{\tau} + 1} e^{z/\sqrt{\tau}} \right) + \frac{\eta - (1 - L_0^2 a^2)(1 - \tau a^2)}{(1 - L_0^2 a^2)(1 - \tau a^2)} e^{-az}. \tag{105}$$

An die Formel (103) schließt sich noch eine wichtige Bemerkung an. Für $a = 1/\alpha_i$ wird die rechtsstehende Summe singulär. Andererseits ist für den Fall sehr großen Kühlmitteldurchsatzes $a = 0$ zu setzen, wodurch (105) in den ebenen Fall konstanter Leistungsdichte übergeht. Man wird daher vernünftigerweise $a < 1/\alpha_i$ für alle $\alpha_i$ fordern müssen. Im übrigen führt der Fall $a > 1/\alpha_i$ zu negativen Werten des Neutronenflusses und scheidet daher von vornherein aus, da er zu keinem kritischen Reaktor führt.

### 8. Einige konkrete Zahlenbeispiele

Abschließend sollen einige konkrete Zahlenbeispiele zusammengestellt werden. Mit den Werten für den mikroskopischen Absorptions-Wirkungsquerschnitt $\sigma_a$ für Uran 235 läßt sich die Größe $\Sigma_a(\mathfrak{r})$ in eine Abhängigkeit $\varrho(\mathfrak{r})$ umformen.

Wegen

$$\Sigma_a(\mathfrak{r}) = N(\mathfrak{r})\, \sigma_a$$

und

$$N(\mathfrak{r}) = \frac{L\, \varrho(\mathfrak{r})}{A},$$

wo $N$ die Anzahl der Atome des Spaltstoffs pro cm³, $\varrho$ seine Dichte in g/cm³, $A$ sein Atomgewicht und $L$ die LOSCHMIDTsche Zahl ist, folgt

$$\varrho(\mathfrak{r}) = \frac{A}{L\, \sigma_a} \Sigma_a(\mathfrak{r}). \tag{106}$$

Es wurden vier Beispiele durchgerechnet. Im ersten Beispiel wurde für den Fall A konstanter Leistungsdichte als Moderator Graphit angenommen, in dem reines Uran 235 eingebettet ist. Dem zweiten Beispiel wurde ein stärker absorbierender Moderator zugrunde gelegt, der z. B. aus einer hitzebeständigen Legierung von keramischen Stoffen und Graphit besteht und einen höheren Absorptionsquerschnitt und damit kleinere Diffusionslänge hat als Graphit. Dieselben Voraussetzungen wurden auch beim dritten und vierten Beispiel gemacht.

Als Reaktivität wurde für alle Beispiele der Wert $k_{\text{eff}} = 1,5$ gewählt.

Zwischen Diffusionslänge $L_0$, dem makroskopischen Absorptionsquerschnitt $\Sigma_1$ des Moderators und der Diffusionskonstanten $D$ besteht der Zusammenhang:

$$L_0^2 = \frac{D}{\Sigma_1} \cdot \qquad (107)$$

$D$ ist in vielen Fällen von der Größe 1 cm, was in allen Beispielen angenommen wird.

In den Abb. 3 bis 6 ist das Ergebnis dieser Rechnungen niedergelegt.

Die von Ort zu Ort veränderliche Spaltstoffdichte ist auf die im Ursprung herrschende Dichte bezogen.

Für die beiden ersten Beispiele, denen der Fall A konstanter Leistungsdichte zugrunde liegt, wurden kugelförmige Reaktoren gewählt, deren Radius 50 cm beträgt.

Die Rechnung wurde jeweils für die Ein- und Zweigruppentheorie durchgeführt. Aus den Abb. 3 bis 6 entnimmt man ein sehr unterschiedliches Verhalten beider Näherungen. Die allgemeine Aussage, daß man immer mindestens mit der Zweigruppentheorie rechnen sollte, wird an diesen Beispielen deutlich.

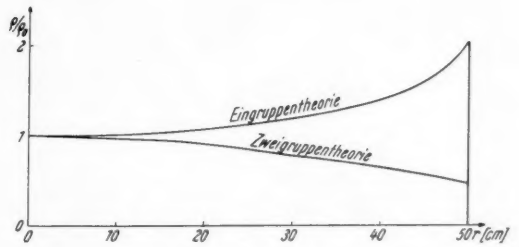


Abb. 3. Kugelförmiger Reaktor konstanter Leistungsdichte. $L_0 = 50$ cm; $\tau = 350$ cm$^2$; $\Sigma_1 = 3,6 \cdot 10^{-4}$ cm$^{-1}$; $R = 50$ cm; $k_{\text{eff}} = 1,5$; Eingruppentheorie $\varrho_0 = 1,18 \cdot 10^{-3}$ g/cm$^3$; Zweigruppentheorie $\varrho_0 = 2,03 \cdot 10^{-3}$ g/cm$^3$

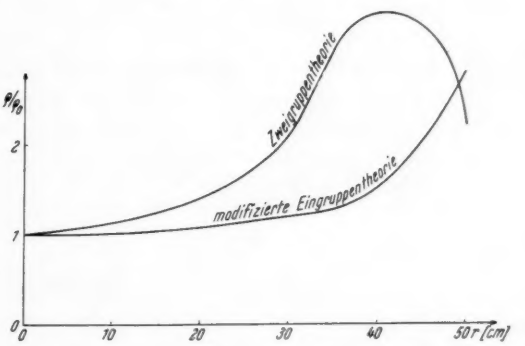


Abb. 4. Kugelförmiger Reaktor konstanter Leistungsdichte. $L_0 = 10$ cm; $\tau = 400$ cm$^2$; $\Sigma_1 = 10^{-1}$ cm$^{-1}$; $R = 50$ cm; $k_{\text{eff}} = 1,5$; Eingruppentheorie $\varrho_0 = 0,682$ g/cm$^3$; Zweigruppentheorie $\varrho_0 = 1,27$ g/cm$^3$

In den meisten Fällen kann man sagen, daß zur Erreichung einer konstanten Leistungsdichte in den Randzonen des Reaktors eine höhere Spaltstoffkonzentration als im Innern hergestellt werden muß.

Für den Fall konstanter Kühlkanal-Oberflächentemperatur wurde ein Beispiel mit demselben Moderator wie in Beispiel 2 durchgerechnet. Der Reaktordurchmesser soll dabei 100 cm betragen. Für die thermodynamische Größe $a$, welche die Dimension (Länge)$^{-1}$ hat, soll gelten

$$a = \frac{1}{2R} \cdot$$

Diese Festlegung ist gleichbedeutend mit der Aussage, daß die Abfallbreite der Wärmequellenverteilung im günstigen Fall von derselben Größenordnung sein wird wie die Reaktordimension.

Um einen Vergleich dieser Rechnung mit dem Fall A konstanter Leistungsdichte zu haben, ist als viertes Beispiel für einen Reaktor derselben Beschaffen-

Vol. 4 1958

heit wie im Beispiel 3 die Rechnung für den Fall A außerdem noch durchgeführt worden.

Das Ergebnis dieser beiden letzten Beispiele ist in Abb. 5 und Abb. 6 aufgetragen.

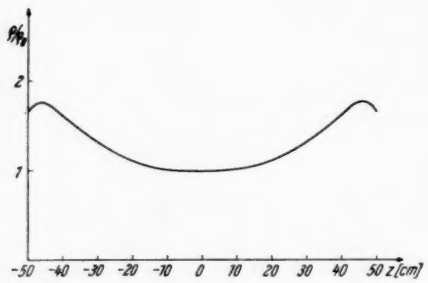


Abb. 5. Plattenförmiger Reaktor konstanter Oberflächentemperatur. $L_0 = 10$ cm; $\tau = 400\,\mathrm{cm}^2$; $a = 10^{-2}\,\mathrm{cm}^{-1}$; $\Sigma_1 = 10^{-1}\,\mathrm{cm}^{-1}$; $R = 50$ cm; $k_{\mathrm{eff}} = 1{,}5$; $\varrho_0 = 1{,}06 \cdot 10^{-1}\,\mathrm{g/cm}^3$

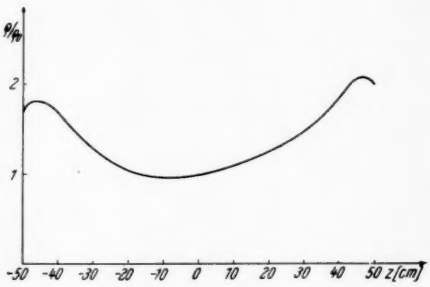


Abb. 6. Plattenförmiger Reaktor konstanter Leistungsdichte. $L_0 = 10$ cm; $\tau = 400\,\mathrm{cm}^2$; $\Sigma_1 = 10^{-1}\,\mathrm{cm}^{-1}$; $R = 50$ cm; $k_{\mathrm{eff}} = 1{,}5$; $\varrho_0 = 0{,}732 \cdot 10^{-1}\,\mathrm{g/cm}^3$

In Abb. 5 ströme das Kühlmittel in der positiven $z$-Richtung.

Der Vergleich mit Abb. 6 lehrt, daß die Forderung einer konstanten Kühlkanaloberflächentemperatur zu einer in Beziehung auf die Reaktormitte unsymmetrisch verzerrten Spaltstoffdichte führt. In der vom Kühlmittel bis zur Mitte durchströmten ersten Hälfte des Reaktors ist dabei eine im Mittel kleinere Spaltstoffdichte erforderlich als von der Reaktormitte bis zum Kühlkanalaustritt.

## Anhang

### 1. Berechnung des Integrals (76)

$$\phi(x) = \frac{1}{(2\pi)^{1/2}\,\Sigma_1} \int_{-\infty}^{+\infty} \frac{B(\omega)\left[\eta - \prod_{i=1}^{n} (1 + \alpha_i^2\,\omega^2)\right]}{\prod_{i=0}^{n} (1 + \alpha_i^2\,\omega^2)}\, e^{i\omega x}\, d\omega$$

mit

$$B(\omega) = \frac{i\,c}{(2\pi)^{1/2}} \frac{e^{i\omega R} - e^{-i\omega R}}{\omega}. \tag{74 b}$$

Nach Einsetzen von (74 b) in (76) folgt:

$$\phi(x) = \frac{i\,c}{2\pi\,\Sigma_1} \left[ \int_{-\infty}^{+\infty} \frac{e^{i\omega(x-R)}}{\omega} \frac{\eta - \prod_{i=1}^{n} (1 + \alpha_i^2\,\omega^2)}{\prod_{i=0}^{n} (1 + \alpha_i^2\,\omega^2)}\, d\omega \right.$$

$$\left. - \int_{-\infty}^{+\infty} \frac{e^{i\omega(x+R)}}{\omega} \frac{\eta - \prod_{i=1}^{n} (1 + \alpha_i^2\,\omega^2)}{\prod_{i=0}^{n} (1 + \alpha_i^2\,\omega^2)}\, d\omega \right].$$

Es handelt sich jetzt nur noch um die Berechnung der beiden in der eckigen Klammer stehenden Integrale:

$$I_1 = \int_{-\infty}^{+\infty} \frac{e^{i\omega(x-R)}}{\omega} \frac{\eta - \prod_{i=1}^{n} (1 + \alpha_i^2 \omega^2)}{\prod_{i=0}^{n} (1 + \alpha_i^2 \omega^2)} d\omega$$

$$I_2 = \int_{-\infty}^{+\infty} \frac{e^{i\omega(x+R)}}{\omega} \frac{\eta - \prod_{i=1}^{n} (1 + \alpha_i^2 \omega^2)}{\prod_{i=0}^{n} (1 + \alpha_i^2 \omega^2)} d\omega,$$

die sich leicht mit dem Residuensatz auswerten lassen.

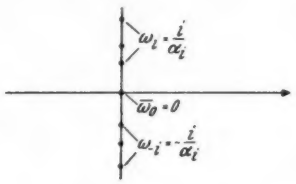


Abb. 7. Lage der Pole in der $\omega$-Ebene

Im Innern des Reaktors ist

$$\left.\begin{aligned} x - R &\leqslant 0 \\ x + R &\geqslant 0 \end{aligned}\right\}, \qquad \text{(a)}$$

im Äußern

$$\left.\begin{aligned} x - R &\geqslant 0 \\ x + R &\leqslant 0 \end{aligned}\right\}. \qquad \text{(b)}$$

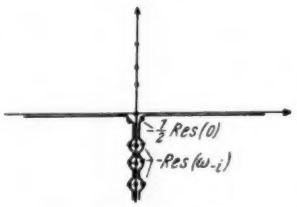


Abb. 8. Integrationsweg zur Berechnung von $I_1$

Wir interessieren uns für den Fall (a).

Die Lagen der Pole $\omega_i$ der Integranden sind

$$\omega_i = \frac{i}{\alpha_i}; \qquad \omega_{-i} = -\frac{i}{\alpha_i} \qquad \text{und} \qquad \bar{\omega}_0 = 0$$

und liegen symmetrisch zur $x$-Achse (s. Abb. 7). Sie ergeben sich durch Nullsetzen von

$$\omega \prod_{i=0}^{n} (1 + \alpha_i^2 \omega^2) = 0,$$

das heißt

$$\bar{\omega}_0 \prod_{i=0}^{n} (\alpha_i \omega_{-i} + i)(\alpha_i \omega_i - i) = 0.$$

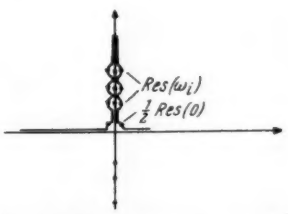


Abb. 9. Integrationsweg zur Berechnung von $I_2$

Wegen der Bedingung (a) konvergiert $I_1$ in der negativ imaginären Halbebene und $I_2$ in der positiv imaginären Halbebene. Der im Nullpunkt gelegene Pol trägt zum Integral mit dem halben Residuum bei. Die auf der reellen Achse laufenden Integrationswege für $I_1$ und $I_2$ werden dann in der in Abb. 8 und 9 dargestellten Weise deformiert.

Die in der negativ gelegenen Halbebene befindlichen Pole haben wegen des rechtsläufigen Umlaufs negative Residuen, die in der positiven Halbebene gelegenen Pole positive Residuen. Der Pol an der Stelle $\omega = 0$ liefert für $I_1$ und $I_2$ je ein halbes Residuum entgegengesetzten Vorzeichens.

Damit ergibt sich für $I_1$:

$$I_1 = -2\pi i \sum_{\omega_{-i}} \text{Res}\,(\omega_{-i}) - \pi i \,\text{Res}\,(0)$$

$$= 2\pi i \sum_{i=0}^{n} \frac{e^{(x-Ri)/\alpha_i}}{2} \frac{\eta - \prod_{j=1}^{n} \left(1 - \left(\frac{\alpha_j}{\alpha_i}\right)^2\right)}{\prod_{j \neq i=0}^{n} \left(1 - \left(\frac{\alpha_j}{\alpha_i}\right)^2\right)} - \pi i (\eta - 1)$$

Vol. 4 1958

und für das Integral $I_2$:

$$I_2 = 2\pi i \sum_{\omega_i} \text{Res}\,(\omega_i) + \pi i\,\text{Res}\,(0)$$

$$= -2\pi i \sum_{i=0}^{n} \frac{e^{-(x+R)/\alpha_i}}{2} \frac{\eta - \prod_{j=1}^{n}\left(1 - \left(\frac{\alpha_j}{\alpha_i}\right)^2\right)}{\prod_{j\neq i=0}^{n}\left(1 - \left(\frac{\alpha_j}{\alpha_i}\right)^2\right)} + \pi i\,(\eta - 1).$$

Daraus folgt für $\phi(x)$:

$$\phi(x) = \frac{c}{\Sigma_1}\left[(\eta - 1) - \sum_{i=0}^{n} e^{-R/\alpha_i} \frac{\eta - \prod_{j=1}^{n}\left(1 - \left(\frac{\alpha_j}{\alpha_i}\right)^2\right)}{\prod_{j\neq i=0}^{n}\left(1 - \left(\frac{\alpha_j}{\alpha_i}\right)^2\right)} \cosh\left(\frac{x}{\alpha_i}\right)\right].$$

## 2. Berechnung des Integrals (87)

$$r\,\phi(r) = \frac{1}{(2\pi)^{1/2}\,\Sigma_1}\int_{-\infty}^{+\infty} \frac{B(\omega)\left(\eta - \prod_{i=0}^{n}(1 + \alpha_i^2\,\omega^2)\right)}{\prod_{i=0}^{n}(1 + \alpha_i^2\,\omega^2)} e^{i\omega r}\,d\omega$$

mit

$$B(\omega) = \frac{c}{(2\pi)^{1/2}}\left[\frac{i\,R\,(e^{i\omega R} + e^{-i\omega R})}{\omega} - \frac{e^{i\omega R} - e^{-i\omega R}}{\omega^2}\right]. \tag{85}$$

Nach Einsetzen von (85) in (87) folgt:

$$\phi(r) = \frac{c}{2\pi\,\Sigma_1 r}\int_{-\infty}^{+\infty} \frac{\eta - \prod_{i=1}^{n}(1 + \alpha_i^2\,\omega^2)}{\prod_{i=0}^{n}(1 + \alpha_i^2\,\omega^2)} \cdot$$

$$\cdot\left[\frac{i\,R}{\omega} e^{i\omega(r-R)} + \frac{i\,R}{\omega} e^{i\omega(r+R)} + \frac{1}{\omega^2} e^{i\omega(r-R)} - \frac{1}{\omega^2} e^{i\omega(r+R)}\right] d\omega.$$

Im Reaktorkern gilt:

$$\left.\begin{aligned} r + R &\geqslant 0 \\ r - R &\leqslant 0 \end{aligned}\right\}.$$

Für $r + R \geqslant 0$ konvergieren die Integranden in der positiv imaginären und für $r - R \leqslant 0$ in der negativ imaginären Halbebene.

Das Integral wird zerlegt in:

$$\phi(r) = \frac{c}{2\pi\,\Sigma_1 r}\,[i\,a\,(I_1 + I_2) + I_3 - I_4],$$

wobei gilt:

$$I_1 = \int_{-\infty}^{+\infty} \frac{e^{i\omega(r-R)}}{\omega} \frac{\eta - \prod_{i=1}^{n}(1 + \alpha_i^2\,\omega^2)}{\prod_{i=0}^{n}(1 + \alpha_i^2\,\omega^2)}\,d\omega$$

$$I_2 = \int_{-\infty}^{+\infty} \frac{e^{i\omega(r+R)}}{\omega} \frac{\eta - \prod_{i=1}^{n} (1 + \alpha_i^2\, \omega^2)}{\prod_{i=0}^{n} (1 + \alpha_i^2\, \omega^2)}\, d\omega$$

$$I_3 = \int_{-\infty}^{+\infty} \frac{e^{i\omega(r-R)}}{\omega^2} \frac{\eta - \prod_{i=1}^{n} (1 + \alpha_i^2\, \omega^2)}{\prod_{i=0}^{n} (1 + \alpha_i^2\, \omega^2)}\, d\omega$$

$$I_4 = \int_{-\infty}^{+\infty} \frac{e^{i\omega(r+R)}}{\omega^2} \frac{\eta - \prod_{i=1}^{n} (1 + \alpha_i^2\, \omega^2)}{\prod_{i=0}^{n} (1 + \alpha_i^2\, \omega^2)}\, d\omega.$$

Die Berechnung der Integrale geschieht wieder mit dem Residuensatz, wobei für die Integrale $I_1$ und $I_3$ der Integrationsweg von Abb. 8, für die Integrale $I_2$ und $I_4$ der Integrationsweg von Abb. 9 zu nehmen ist. Für $I_1$ bis $I_4$ erhält man auf diese Weise

Vol. 4 1958

$$I_1 = 2\pi i \sum_{i=0}^{n} \frac{e^{(r-R)/\alpha_i}}{2} \frac{\eta - \prod_{j=1}^{n} \left(1 - \left(\frac{\alpha_j}{\alpha_i}\right)^2\right)}{\prod_{j \neq i=0}^{n} \left(1 - \left(\frac{\alpha_j}{\alpha_i}\right)^2\right)} - \pi i \operatorname{Res}(0)$$

$$I_2 = -2\pi i \sum_{i=0}^{n} \frac{e^{-(r+R)/\alpha_i}}{2} \frac{\eta - \prod_{j=1}^{n} \left(1 - \left(\frac{\alpha_j}{\alpha_i}\right)^2\right)}{\prod_{j \neq i=0}^{n} \left(1 - \left(\frac{\alpha_j}{\alpha_i}\right)^2\right)} + \pi i \operatorname{Res}(0)$$

$$I_3 = -2\pi \sum_{i=0}^{n} \frac{\alpha_i\, e^{(r-R)/\alpha_i}}{2} \frac{\eta - \prod_{j=1}^{n} \left(1 - \left(\frac{\alpha_j}{\alpha_i}\right)^2\right)}{\prod_{j \neq i=0}^{n} \left(1 - \left(\frac{\alpha_j}{\alpha_i}\right)^2\right)} - \pi i \operatorname{Res}(0)$$

$$I_4 = -2\pi \sum_{i=0}^{n} \frac{\alpha_i\, e^{-(r+R)/\alpha_i}}{2} \frac{\eta - \prod_{j=1}^{n} \left(1 - \left(\frac{\alpha_j}{\alpha_i}\right)^2\right)}{\prod_{j \neq i=0}^{n} \left(1 - \left(\frac{\alpha_j}{\alpha_i}\right)^2\right)} + \pi i \operatorname{Res}(0).$$

Für die Integrale $I_1$ und $I_2$ sind die Residuen für $\omega = 0$ dieselben und heben sich daher in der Summe $I_1 + I_2$ fort. $I_3$ und $I_4$ haben dagegen ein verschiedenes Residuum für $\omega = 0$.

$I_3$ hat für $\omega = 0$ das Residuum:

$$\operatorname{Res}(0) = -2\pi (r - R)(\eta - 1)$$

und $I_4$ an derselben Stelle:

$$\operatorname{Res}(0) = -2\pi (r + R)(\eta - 1).$$

Der in der Differenz von $I_3 - I_4$ von diesem Residuum gelieferte Beitrag ist dann:

$$2\pi r (\eta - 1).$$

Damit ergibt sich schließlich als Resultat nach Einsetzen der Werte aller Integrale $I_1$ bis $I_4$ für $\phi(r)$:

$$\phi(r) = \frac{c}{\Sigma_1}\left[(\eta - 1) - \sum_{i=0}^{n} e^{-R/\alpha_i}(R + \alpha_i) \right.$$
$$\left. \frac{\eta - \prod_{j=1}^{n}\left(1 - \left(\frac{\alpha_j}{\alpha_i}\right)^2\right)}{\prod_{j\neq i=0}^{n}\left(1 - \left(\frac{\alpha_j}{\alpha_i}\right)^2\right)} \frac{\sinh\left(\frac{r}{\alpha_i}\right)}{r}\right].$$

## 3. Berechnung des Integrals (102)

$$\phi(z) = \frac{1}{(2\pi)^{1/2}\Sigma_1}\int_{-\infty}^{+\infty} \frac{B(\omega)\left(\eta - \prod_{i=1}^{n}(1 + \alpha_i^2\omega^2)\right)}{\prod_{i=0}^{n}(1 + \alpha_i^2\omega^2)} e^{i\omega z}\, d\omega$$

mit

$$B(\omega) = \frac{c}{(2\pi)^{1/2}(i\omega + a)}\left[e^{aR}e^{i\omega R} - e^{-aR}e^{-i\omega R}\right] \qquad (100\text{ b})$$

führt auf die Berechnung der Integrale

$$I_1(z) = \int_{-\infty}^{+\infty} \frac{e^{i\omega(z+R)}}{i\omega + a} \frac{\eta - \prod_{i=1}^{n}(1 + \alpha_i^2\omega^2)}{\prod_{i=0}^{n}(1 + \alpha_i^2\omega^2)}\, d\omega$$

$$I_2(z) = \int_{-\infty}^{+\infty} \frac{e^{i\omega(z-R)}}{i\omega + a} \frac{\eta - \prod_{i=1}^{n}(1 + \alpha_i^2\omega^2)}{\prod_{i=0}^{n}(1 + \alpha_i^2\omega^2)}\, d\omega,$$

aus denen sich $\phi(z)$ berechnet:

$$\phi(z) = \frac{c}{2\pi\Sigma_1}\left[e^{aR}I_1(z) - e^{-aR}I_2(z)\right].$$

Für die Berechnung der Integrale sind dieselben Integrationswege zu nehmen wie in Abb. 8 und 9. Auch die Lage der Pole ist dieselbe mit Ausnahme des Pols bei $\omega = 0$, an dessen Stelle ein Pol bei $\omega = i\,a$ auftritt.

### Berechnung von $I_1(z)$

Im Kern ist

$$\left.\begin{aligned} z - R &\leqslant 0 \\ z + R &\geqslant 0 \end{aligned}\right\};$$

außerdem ist aus physikalischen Gründen

$$a > 0.$$

Der Integrand hat Pole bei

$$\omega_i = \frac{i}{\alpha_i} \quad \text{und} \quad \omega_{-i} = -\frac{i}{\alpha_i}, \quad \text{bei} \quad \omega = i\,a,$$

und konvergiert in der positiv imaginären Halbebene; daher tragen nur die Residuen an dieser Ebene zum Integral bei. Daraus folgt:

$$I_1(z) = 2\pi i \sum_{\omega_i} \operatorname{Res}(\omega_i) + 2\pi i \operatorname{Res}(i\,a)$$

$$= 2\pi \sum_{i=0}^{n} \left[ \frac{e^{-(z+R)/\alpha_i}}{2} \frac{1}{a\,\alpha_i - 1} \frac{\eta - \prod_{j=1}^{n} \left(1 - \left(\frac{\alpha_j}{\alpha_i}\right)^2\right)}{\prod_{j \neq i=0}^{n} \left(1 - \left(\frac{\alpha_j}{\alpha_i}\right)^2\right)} + \right.$$

$$\left. + \frac{\eta - \prod_{i=1}^{n} (1 - \alpha_i^2\, a^2)}{\prod_{i=0}^{n} (1 - \alpha_i^2\, a^2)} e^{-a(z+R)} \right].$$

## Berechnung von $I_2(z)$

Der Integrand hat dieselben Pole wie bei $J_1(z)$, konvergiert aber in der negativ imaginären Halbebene, so daß nur die Pole bei

$$\omega_{-i} = -\frac{i}{\alpha_i}$$

einen Beitrag zum Integral bringen.

Daraus folgt:

$$I_2(z) = 2\pi \sum_{i=0}^{n} \frac{e^{(z-R)/\alpha_i}}{2} \frac{1}{\alpha_i\, a + 1} \frac{\eta - \prod_{j=1}^{n} \left(1 - \left(\frac{\alpha_j}{\alpha_i}\right)^2\right)}{\prod_{j \neq i=0}^{n} \left(1 - \left(\frac{\alpha_j}{\alpha_i}\right)^2\right)}.$$

Vol. 4 1958

### Literaturverzeichnis


1. S. Glasstone, Principles of Nuclear Reactor Engineering. New York: D. van Nostrand, 1955.
2. Reactor Handbook: Physics. New York: McGraw Hill, 1954.
3. G. Goertzel, J. Nuclear Energy **2**, 193 (1956).
4. S. Glasstone und M. C. Edlund, The Elements of Nuclear Reactor Theory. New York: D. van Nostrand, 1952.

## Buchbesprechung — Book Review — Compte rendu

**General Relativity and Cosmology.** Von G. C. McVittie. (The International Astrophysics Series: Vol. IV.) X, 198 S. London: Chapman & Hall Ltd. 1956. 42 s.

Das Buch gibt eine Darstellung der auf der allgemeinen Relativitätstheorie beruhenden Modelle des Kosmos im Lichte der mit den 100″- und 200″-Teleskopen gemachten Beobachtungen. Der Autor zeigt, daß keine Widersprüche der Theorie gegenüber den Beobachtungsdaten bestehen.

Das Buch entstand aus mehreren Vorlesungen, die der Verfasser an der University of London, in Harvard und Illinois über Relativitätstheorie gehalten hat.

Nach einem einleitenden Abschnitt über die Entwicklung und Bedeutung der allgemeinen Relativitätstheorie gibt der Verfasser im zweiten Kapitel eine Einführung in die Tensorrechnung und in die Riemannsche Geometrie. In den nächsten zwei Kapiteln folgt eine Zusammenfassung der Prinzipien der Newtonschen Mechanik und der Mechanik der speziellen Relativitätstheorie sowie eine Darstellung der Prinzipien der Mechanik in der allgemeinen Relativitätstheorie. Im fünften Kapitel werden das zentralsymmetrische Feld in Schwarzschildscher Metrik, die Perihelbewegung der Planeten, sowie die Ablenkung und Rotverschiebung des Lichtes behandelt und deren Werte mit neueren Beobachtungsdaten verglichen. In Kapitel VI und VII folgen Näherungslösungen der Einsteinschen Gleichungen und deren Anwendung auf die klassische Gasdynamik, die auch zur Lösung nichtrelativistischer Probleme der Gasdynamik wertvoll sind. In den beiden letzten Kapiteln behandelt der Verfasser Modelle des Kosmos von gleichförmiger Materieverteilung und gibt einen umfassenden Vergleich mit den Beobachtungsdaten; schließlich werden Näherungen zu Modellen nichtgleichförmiger Materieverteilung betrachtet, die den wirklichen Verhältnissen besser entsprechen.

Die mathematische Formulierung der Theorie ist besonders geeignet zur numerischen Berechnung der Parameter, die in den kosmologischen Modellen auftreten. Das Werk schließt mit reichhaltigen Literaturangaben und einem Namen- und Sachverzeichnis.

Der umfassende Vergleich der Ergebnisse der allgemeinen Relativitätstheorie mit neuerem Beobachtungsmaterial dürfte die Darstellung McVitties für die an kosmologischen Theorien interessierten Leser besonders wertvoll erscheinen lassen.

L. Halpern,
Institut für theoretische Physik der Universität Wien

Herausgeber, Eigentümer und Verleger: Springer-Verlag, Wien I, Mölkerbastei 5. — Für den Inhalt verantwortlich: Prof. Dr. Friedrich Hecht, Wien VIII, Alserstraße 69. — Druck: Berger & Schwarz, Zwettl, NÖ.

Vol.
4
1958

# Optimum Thrust Programming along Arbitrarily Inclined Rectilinear Paths[1, 2]

By

**A. Miele[3] and C. R. Cavoti[4]**

(With 6 Figures)

*(Received December 20, 1957)*

**Abstract — Zusammenfassung — Résumé**

**Optimum Thrust Programming along Arbitrarily Inclined Rectilinear Paths.** An analysis of the theory of the thrust programming is presented for the case where a variable mass body is moving along an arbitrarily inclined rectilinear path. The variational problem is treated within the general frame of the problems of MAYER type, i.e., as the problem of minimizing the difference $\Delta G$ between the values which a function $G$ of the generalized coordinates of the missile assumes at the end-points of the trajectory.

By the use of the indirect methods of the Calculus of Variations, it is shown that the totality of extremal arcs is composed of zero-thrust sub-arcs, sub-arcs to be flown with maximum engine output and variable-thrust sub-arcs.

General results are obtained, some of them in a closed form, including as a particular case, previous work developed by HAMEL, TSIEN, EVANS, HIBBS, CICALA, MIELE, LEITMANN and WARD.

The optimum acceleration law is determined and some numerical examples are presented emphasizing the engineering aspects of the present theory in connection with the flight analysis of rockets.

**Optimale Programmierung des Schubes entlang von geradlinigen Bahnen mit willkürlich gewählter Neigung.** Eine Analyse der Theorie der optimalen Programmierung des Schubes wird auf den Fall ausgedehnt, daß ein Körper mit variabler Masse sich auf einer geradlinigen Bahn von willkürlich gewählter Neigung bewegt. Das Problem der Variation wird in dem allgemeinen Rahmen der Probleme der Kategorie von MAYER behandelt; d. h. es soll der Bewegungsverlauf in der Weise vorgeschrieben werden, daß die Differenz von $\Delta G$ zwischen den Werten, die eine Funktion $G$ der verallgemeinerten Koordinaten des Flugkörpers in den Endpunkten der Bahn annimmt, zu einem Minimum gemacht wird.

---

[1] This research was supported by the United States Air Force through the Air Force Office of Scientific Research of the Air Research and Development Command, under Contract No. AF 18(603)—69.

[2] Paper presented at the Fourth Annual Meeting of the American Astronautical Society, January 29—31, 1958, New York, New York; and at the ARS-ASME Joint Aviation Conference, March 17—20, 1958, Dallas, Texas.

[3] Professor of Aeronautical Engineering, Purdue University, Lafayette, Indiana, U.S.A.

[4] Instructor in Aeronautical Engineering, Purdue University, Lafayette, Indiana, U.S.A.

Durch die Anwendung der indirekten Methoden der Variationsrechnung läßt sich zeigen, daß die Gesamtheit der sogenannten „extremen" Kurvenstücke solche enthält, die einem Schub Null, einem Maximalwert des Schubes oder einem variablen Schub entsprechen. Es werden allgemeine Resultate erhalten — zum Teil in geschlossener Form —, als Sonderfälle auch frühere Arbeiten von HAMEL, TSIEN, EVANS, HIBBS, CICALA, MIELE, LEITMANN und WARD umfassend.

Das optimale Beschleunigungsgesetz wird begründet. Einige numerische Beispiele zeigen die praktische Seite dieser Methode beim Studium des Fluges von Raketen.

**Programmation optimale de la poussée le long de trajectoires rectilignes d'inclinaison arbitraire.** La théorie du programme optimum de poussée est étendue au cas où un corps de masse variable se déplace sur une trajectoire rectiligne d'inclinaison arbitraire. Le problème aux variations est traité dans le cadre général des problèmes du type de MAYER, c.a.d. de façon à rendre minimale la différence $\Delta G$ entre les valeurs qu'une fonction $G$ des coordonnées généralisées de ce corps prend aux points extrêmes de sa trajectoire.

En utilisant les méthodes indirectes du Calcul des Variations, on montre que les arcs extremums se composent d'arcs de poussée nulle, de poussee maximum et de poussée variable.

Des résultats généraux sont obtenus, certains d'entre eux sous forme analytique; certains travaux antérieurs de HAMEL, TSIEN, EVANS, HIBBS, CICALA, MIELE, LEITMANN et WARD apparaissent comme cas particuliers.

La loi optimum d'accélération est établie et des exemples numériques font ressortir le caractère pratique de cette méthode dans l'étude du vol des fusées.

Vol. 4 19

## Symbols

| | |
|---|---|
| $a$ | Speed of sound (ft. sec.$^{-1}$) |
| $A$ | Function defined by Eq. (32) |
| $B$ | Function defined by Eq. (33) |
| $C_D$ | Total drag coefficient |
| $C_{D0}$ | Drag coefficient at zero-lift |
| $C_L$ | Lift coefficient |
| $D$ | Drag (lb.) |
| $F$ | Fundamental function, defined by Eq. (6) |
| $g$ | Acceleration of gravity (ft. sec.$^{-2}$) |
| $G(h, m, V)$ | Function whose difference $\Delta G = G_f - G_i$ is to be minimized |
| $h$ | Altitude above sea-level (ft.) |
| $J_k$ ($k$ = 1, 2, 3, 4) | First members of the equations of constraint for the variational problem |
| $K$ | Ratio between induced drag coefficient and square of lift coefficient |
| $L$ | Lift (lb.) |
| $m$ | Instantaneous mass (lb. ft.$^{-1}$ sec.$^2$) |
| $M = V/a$ | MACH number |
| $M_e = V_e/a$ | Ratio of equivalent exit velocity of the rocket engine to atmospheric speed of sound |
| $p$ | Atmospheric pressure at altitude $h$ (lb.ft.$^{-2}$) |
| $P$ | Function defined by Eq. (38) |
| $Q$ | Function defined by Eq. (39) |
| $S$ | Reference surface (ft.$^2$) |
| $t$ | Time (sec.) |
| $V$ | Flight velocity (ft. sec.$^{-1}$) |
| $V_e$ | Equivalent exit velocity of the rocket engine (ft. sec.$^{-1}$) |
| $x$ | Exponent appearing in the drag law defined by Eq. (49) |
| $y$ | Coefficient appearing in the drag law defined by Eq. (49) |
| $\alpha$ | Engine parameter |
| $\beta$ | Engine mass flow (lb.ft.$^{-1}$ sec.) |
| $\gamma$ | Ratio of specific heat at constant pressure to specific heat at constant volume (air) |
| $\delta(\ldots)$ | Variation consistent with the prescribed end-conditions |
| $\varepsilon$ | Variable defined by Eq. (30) |
| $\theta$ | Path inclination with respect to a horizontal plane |
| $\lambda_k$($k$ = 1, 2, 3, 4) | LAGRANGE multipliers |

*Subscripts*

| | |
|---|---|
| $i$ | Denotes initial point |
| $f$ | Denotes final point |

*Superscripts*

| | |
|---|---|
| $\cdot$ | Denotes derivative with respect to time |
| $'$ | Denotes derivative with respect to MACH number |

## I. Introduction

Considerable attention has been devoted, in recent years, to the theory of the thrust programming along particular rectilinear trajectories.

Early analyses have been carried out by HIBBS [1], CICALA and MIELE [2], and MIELE [3] in connection with level paths ($\theta = 0$).

Vertical paths ($\theta = \pi/2$) have been investigated by HAMEL [4], TSIEN and EVANS [5], WARD [6], LEITMANN [7], MIELE [8], and MIELE and CAVOTI [9].

In the present paper a rectilinear trajectory inclined at an arbitrary angle $\theta$ with respect to a horizontal plane is considered. General solutions are derived for the optimizing condition, embodying, as a particular case, the results of [1] to [9]. For the sake of simplicity, the analysis is confined to problems not involving time. The present theory, however, can be immediately extended to cover the case where some time condition is imposed on the flight trajectory.

## II. Fundamental Hypotheses and Equations of Motion

The following hypotheses are used throughout the paper:

(a) the rocket-powered vehicle is ideally regarded as a particle of mass ($m$) variable with the time ($t$);

(b) a rectilinear path inclined at an angle $\theta$ with respect to a horizontal plane is considered;

(c) the thrust vector is parallel to the velocity vector;

(d) the equivalent exit velocity of the rocket engine ($V_e$) is regarded as a constant, independent of the operational condition of the engine;

(e) the engine is capable of delivering all mass flows ($\beta$) bounded between a lower value ($\beta = 0$) and an upper value ($\beta = \beta_{\max}$);

(f) the aerodynamic lag is disregarded, i.e., lift ($L$) and drag ($D$) forces are calculated as in unaccelerated flight;

(g) the acceleration of gravity is a constant.

In view of the above hypotheses, the behaviour of the rocket-powered vehicle is represented with the following set of equations:

$$J_1 \equiv \dot{m} + \beta = 0 \tag{1}$$

$$J_2 \equiv g \cos\theta - \frac{L}{m} = 0 \tag{2}$$

$$J_3 \equiv \dot{V} + g \sin\theta + \frac{D - \beta V_e}{m} = 0 \tag{3}$$

$$J_4 \equiv \dot{h} - V \sin\theta = 0 \tag{4}$$

where $\beta$ is the engine mass flow, $g$ the acceleration of gravity, $\theta$ the path inclination, $V$ the velocity and $h$ the flight altitude. The dot sign denotes derivative with respect to time.

It is assumed that the drag function has the form $D = D(h, V, L)$.

With regard to the thrust function the limitation

$$0 \leqslant \beta \leqslant \beta_{\max} \tag{5}$$

concerning the engine mass flow must be accounted for. Thus, the idea of parametric representation of the variable subject to inequality is introduced, as in



Vol. 4 1958

[3] and [8]. The mass flow $\beta$ is represented as a function of a parameter $\alpha$ having the following properties (Fig. 1):

(a) for $-\infty \leqslant \alpha \leqslant \alpha_1$ : $\beta = 0$

(b) for $\alpha_1 < \alpha < \alpha_2$ : $d\beta/d\alpha \neq 0$

(c) for $\alpha_2 \leqslant \alpha \leqslant +\infty$ : $\beta = \beta_{\max}$

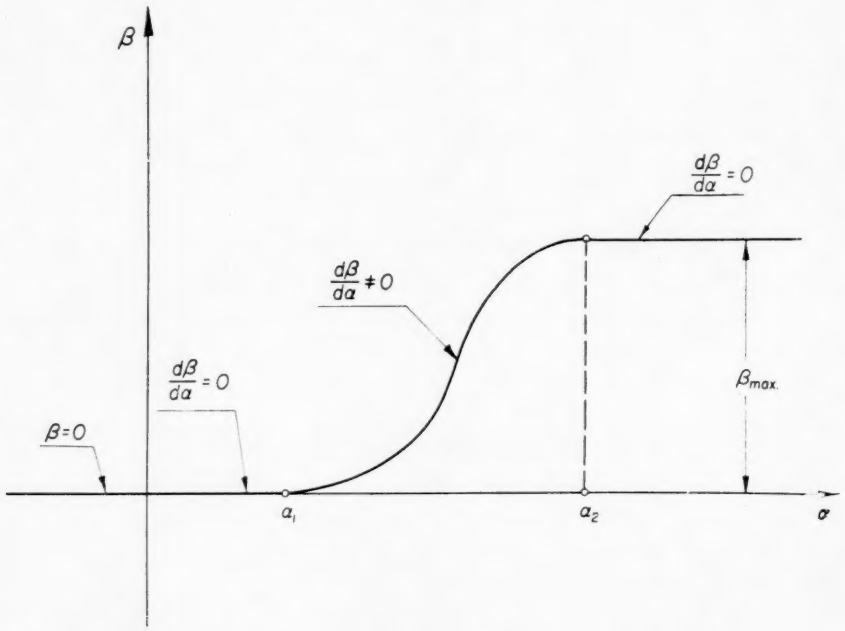


Fig. 1. Parametric representation of the engine characteristics

With the above scheme the independent parameter of the rocket engine becomes $\alpha$, which is allowed to vary between $-\infty$ and $+\infty$; on the other hand, the mass flow $\beta$ becomes a dependent quantity, only varying between 0 and $\beta_{\max}$.

Notice that the condition $d\beta/d\alpha = 0$ represents either a coasting flight or a flight with maximum engine output. On the other hand, $d\beta/d\alpha \neq 0$ represents any other operating condition of the engine intermediate between the two limiting ones. Notice also that $\alpha$ is *only* a parameter and that there is no necessity of attributing to it any special physical meaning.

## III. Variational Formulation

The set of Eqs. (1) to (4) is considered, where $D = D(h, V, L)$ and $\beta = \beta(\alpha)$. The above set involves 4 relations in the five dependent variables $m(t)$, $V(t)$, $h(t)$, $L(t)$ and $\alpha(t)$. One degree of freedom is left and an optimum requirement can be, therefore, imposed. In this connection, the variational problem (of MAYER type) is formulated as follows: "Among all sets of functions $m(t)$, $V(t)$, $h(t)$, $L(t)$ and $\alpha(t)$ satisfying Eqs. (1) to (4) and certain prescribed end-conditions, to determine the special set minimizing the difference $\Delta G = G_f - G_i$, where $G = G(h, m, V)$."

### 1. Euler Equations

A set of variable LAGRANGE multipliers $\lambda_1(t)$, $\lambda_2(t)$, $\lambda_3(t)$, $\lambda_4(t)$ is introduced and the following expression, termed fundamental function, formed:

$$F = \sum_{k=1}^{4} \lambda_k J_k. \tag{6}$$

The unknown functions being five in number, one must write five EULER equations, as follows:

$$\frac{d}{dt}\left(\frac{\partial F}{\partial \dot{z}_j}\right) = \frac{\partial F}{\partial z_j} \qquad (j = 1 \ldots 5) \tag{7}$$

where $z_1 = m$, $z_2 = V$, $z_3 = h$, $z_4 = L$, $z_5 = \alpha$. The explicit form of the EULER equations (7) is indicated below:

$$\dot{\lambda}_1 = \lambda_2 \frac{L}{m^2} + \lambda_3 \frac{V_e \beta - D}{m^2} \tag{8}$$

$$\dot{\lambda}_3 = \frac{\lambda_3}{m}\frac{\partial D}{\partial V} - \lambda_4 \sin\theta \tag{9}$$

$$\dot{\lambda}_4 = \frac{\lambda_3}{m}\frac{\partial D}{\partial h} \tag{10}$$

$$0 = -\frac{\lambda_2}{m} + \frac{\lambda_3}{m}\frac{\partial D}{\partial L} \tag{11}$$

$$0 = \frac{d\beta}{d\alpha}\left[\lambda_1 - \lambda_3 \frac{V_e}{m}\right]. \tag{12}$$

### 2. First Integral

Since the time ($t$) does not explicitly appear in the set of Eqs. (1) to (4) the following first integral holds:

$$-F + \sum_{j=1}^{5} \frac{\partial F}{\partial \dot{z}_j}\dot{z}_j = C \tag{13}$$

where $C$ is an integration constant, i.e.:

$$-\lambda_1 \beta + \lambda_3\left[\frac{V_e \beta - D}{m} - g \sin\theta\right] + \lambda_4 V \sin\theta = C. \tag{14}$$

### 3. Discontinuity of the Eulerian Solution

The EULER equation (12) shows that the extremal arc is discontinuous, being generally composed of:

(a) sub-arcs of equation

$$\frac{d\beta}{d\alpha} = 0 \tag{15}$$

(b) sub-arcs of equation

$$\lambda_1 - \lambda_3 \frac{V_e}{m} = 0. \tag{16}$$

According to the device of parametric representation of the variable subject to inequality, Eq. (15) represents either a coasting flight ($\beta = 0$) or a flight with maximum engine output ($\beta = \beta_{\max}$). Eq. (16), on the other hand, represents a flight condition with a continuously variable thrust, as shown in the following sections.

Vol. 4 1958

Notice that at every corner of the discontinuous extremal solution the ERDMANN-WEIERSTRASS corner conditions must be applied. In this connection, and in analogy with [3] and [8], the following results are immediately obtained:

(a) the multipliers $\lambda_1$, $\lambda_2$, $\lambda_3$ and $\lambda_4$ must be *continuous* at all junction points;

(b) the value of the integration constant $C$ must be the *same* for all sub-arcs forming one extremal arc;

(c) the quantity $\lambda_1 - \lambda_3 V_e/m$ must be *zero* immediately before and immediately after each point of junction.

*4. Boundary Conditions*

For the problem under consideration, the boundary conditions involve a number of fixed end-points conditions plus a number of natural conditions. The latter must be deduced from the general transversality condition:

$$[\delta G + \lambda_1 \delta m + \lambda_3 \delta V + \lambda_4 \delta h - C \delta t]_i^f = 0 \tag{17}$$

which is to be identically satisfied for all systems of variations $\delta(\ldots)$ consistent with the prescribed end-conditions. Notice that if $G$ is independent of the time ($\partial G/\partial t = 0$) and if no time condition is prescribed at one of the two end-points, the transversality condition (17) implies that:

$$C = 0. \tag{18}$$

## IV. Optimizing Condition at Points of the Variable-Thrust Sub-Arc

For problems where $\partial G/\partial t = 0$ and if no time condition is imposed at one of the two end-points, the integration constant of Eq. (14) becomes $C = 0$.

After accounting for Eq. (16), the first integral (14) becomes:

$$\lambda_3 \left[ \frac{D}{m} + g \sin\theta \right] - \lambda_4 V \sin\theta = 0. \tag{19}$$

On the other hand, the time derivative of Eq. (16) yields:

$$\dot{\lambda}_1 - \dot{\lambda}_3 \frac{V_e}{m} - \lambda_3 \frac{V_e}{m^2} \beta = 0 \tag{20}$$

so that Eqs. (8) and (20) imply:

$$\lambda_2 \frac{L}{m} - \lambda_3 \frac{D}{m} - \dot{\lambda}_3 V_e = 0. \tag{21}$$

Consider now the four Eqs. (9), (11), (19) and (21). They can be regarded as forming an algebraic system, linear and homogeneous, in the four unknowns $\lambda_2$, $\lambda_3$, $\dot{\lambda}_3$ and $\lambda_4$. Therefore, an obvious condition for the existence of non-trivial solutions for the multipliers and their derivatives is that the following determinant be zero:

$$\begin{vmatrix} 0 & -\dfrac{1}{m}\dfrac{\partial D}{\partial V} & 1 & \sin\theta \\ 1 & -\dfrac{\partial D}{\partial L} & 0 & 0 \\ 0 & \dfrac{D}{m} + g\sin\theta & 0 & -V\sin\theta \\ \dfrac{L}{m} & -\dfrac{D}{m} & -V_e & 0 \end{vmatrix} = 0. \tag{22}$$

Since the variational problem has one degree of freedom, one extra-relation[1] is needed, in addition to Eqs. (1) to (4), to completely identify the solution. For the variable-thrust sub-arc, this extra relation is represented by Eq. (22), which can also be rewritten as:

$$D(V - V_e) + V V_e \frac{\partial D}{\partial V} - m g \left[ V_e \sin\theta + V \cos\theta \frac{\partial D}{\partial L} \right] = 0. \tag{23}$$

For the particular case of level flight ($\theta = 0$) Eq. (23) simplifies into ([2] and [3]):

$$D(V - V_e) + V V_e \frac{\partial D}{\partial V} - m g V \frac{\partial D}{\partial L} = 0. \tag{24}$$

For the particular case of vertical flight ($\theta = \pi/2$), Eq. (23) yields:

$$D(V - V_e) + V V_e \frac{\partial D}{\partial V} - m g V_e = 0 \tag{25}$$

and, therefore, leads to the first integral (3.1) of [7] and to a particular case of the first integral (29) of [8] (problems where no time condition is imposed).

Vol. 4 1958

*Parabolic Drag Polar*

The particular case of a parabolic drag polar is now considered:

$$C_D = C_{DO}(M) + K(M)\, C_L^2 \tag{26}$$

where $C_D$ is the total drag coefficient, $C_{DO}$ the zero-lift drag coefficient, $C_L$ the lift coefficient and $K$ the ratio of induced drag coefficient to square of lift coefficient. Both $C_{DO}$ and $K$ are assumed to depend on the MACH number ($M = V/a$) only.

Simple manipulations yield the following expression for the drag function and its derivatives:

$$D = \frac{\gamma\, p\, S}{2} \left[ C_{DO} M^2 + \frac{K}{M^2} \varepsilon^2 \cos^2\theta \right] \tag{27}$$

$$\frac{\partial D}{\partial L} = 2 \frac{K}{M^2} \varepsilon \cos\theta \tag{28}$$

$$\frac{\partial D}{\partial V} = \frac{\gamma\, p\, S}{2\, V} \left[ C_{DO} M^2 \left( 2 + \frac{d \log C_{DO}}{d \log M} \right) + \frac{K}{M^2} \varepsilon^2 \cos^2\theta \left( -2 + \frac{d \log K}{d \log M} \right) \right] \tag{29}$$

where

$$\varepsilon = \frac{2\, m\, g}{\gamma\, p\, S}. \tag{30}$$

The optimizing condition (23) is now rewritten as:

$$[A \cos^2\theta]\, \varepsilon^2 + [M_e \sin\theta]\, \varepsilon - B = 0 \tag{31}$$

$$A = \frac{K}{M^2} \left[ M + 3 M_e - M_e \frac{d \log K}{d \log M} \right] \tag{32}$$

$$B = C_{DO} M^2 \left[ M + M_e + M_e \frac{d \log C_{DO}}{d \log M} \right] \tag{33}$$

[1] For the constant-thrust sub-arcs, the extra-relation is either $\beta = 0$ (coasting sub-arc) or $\beta = \beta_{\max}$ (sub-arc flown with maximum engine output).

where $M_e = V_e/a$ is the ratio of equivalent exit velocity of the rocket-engine ($V_e$) to atmospheric speed[1] of sound ($a$). Eq. (31) admits the following solution:

$$\varepsilon = \frac{M_e \sin\theta}{2A\cos^2\theta}\left[-1+\sqrt{1+\frac{4AB}{M_e^2}\cot^2\theta}\right]. \tag{34}$$

For the two limiting cases of level flight ($\theta = 0$) and vertical flight ($\theta = \pi/2$) Eq. (34) becomes indetermined and the solution must be computed through a limiting process.

Concerning level flight ($\theta = 0$) the mass-velocity relationship is supplied by:

$$\varepsilon = \sqrt{\frac{B}{A}} = M^2\sqrt{\frac{C_{DO}}{K}}\sqrt{\frac{M+M_e+M_e\dfrac{d\log C_{DO}}{d\log M}}{M+3M_e-M_e\dfrac{d\log K}{d\log M}}} \tag{35}$$

thus leading, by simple transformation, to Eq. (18) of [2] and to Eq. (58) of [3].

With regard to vertical flight ($\theta = \pi/2$), Eq. (34) leads to:

$$\varepsilon = \frac{B}{M_e} = C_{DO}M^2\left[\frac{M}{M_e}+1+\frac{d\log C_{DO}}{d\log M}\right]. \tag{36}$$

## V. Optimum Acceleration at Points of the Variable-Thrust Sub-Arc

An interesting expression can be derived for the optimum acceleration (and, therefore, for the optimum thrust) at points of the variable-thrust sub-arc if the time derivative of Eq. (23) is calculated. After considering the equations of motion and performing extensive manipulations, the following final result is obtained:

$$\dot{V}/g = P/Q \tag{37}$$

$$P = \frac{V\sin\theta}{g}\left[\frac{\partial D}{\partial h}(V_e - V) - VV_e\frac{\partial^2 D}{\partial V\,\partial h} + mgV\frac{\partial^2 D}{\partial L\,\partial h}\cos\theta\right] +$$

$$+\frac{D+mg\sin\theta}{V_e}\cos\theta\left[-V_e\frac{\partial D}{\partial L}+VV_e\frac{\partial^2 D}{\partial V\,\partial L}-mgV\frac{\partial^2 D}{\partial L^2}\cos\theta - V_e\tan\theta\right] \tag{38}$$

$$Q = D + V\frac{\partial D}{\partial V} + VV_e\frac{\partial^2 D}{\partial V^2} +$$

$$+ mg\left[\sin\theta - 2V\frac{\partial^2 D}{\partial L\,\partial V}\cos\theta + mg\frac{V}{V_e}\frac{\partial^2 D}{\partial L^2}\cos^2\theta\right]. \tag{39}$$

For the particular case of level flight ($\theta = 0$), Eq. (37) yields:

$$\frac{\dot{V}}{g} = \frac{D\left[-\dfrac{\partial D}{\partial L}+V\dfrac{\partial^2 D}{\partial V\,\partial L}-mg\dfrac{V}{V_e}\dfrac{\partial^2 D}{\partial L^2}\right]}{D+V\dfrac{\partial D}{\partial V}+VV_e\dfrac{\partial^2 D}{\partial V^2}+mg\left[mg\dfrac{V}{V_e}\dfrac{\partial^2 D}{\partial L^2}-2V\dfrac{\partial^2 D}{\partial L\,\partial V}\right]}. \tag{40}$$

[1] $M_e$, therefore, *does not* stand for MACH number in the exit section of the rocket.

For the particular case of vertical flight ($\theta = \pi/2$) the optimum acceleration becomes:

$$\frac{\dot{V}}{g} = \frac{\dfrac{V}{g}\left[\dfrac{\partial D}{\partial h}(V_e - V) - V V_e \dfrac{\partial^2 D}{\partial V\, \partial h}\right] - (D + m g)}{D + V \dfrac{\partial D}{\partial V} + V V_e \dfrac{\partial^2 D}{\partial V^2} + m g} \tag{41}$$

i.e., after accounting for Eq. (25):

$$\frac{\dot{V}}{g} = \frac{-D - V_e \dfrac{\partial D}{\partial V} + \dfrac{V_e}{g}(V_e - V)\dfrac{\partial D}{\partial h} - \dfrac{V_e^2}{g} V \dfrac{\partial^2 D}{\partial V\, \partial h}}{D + 2 V_e \dfrac{\partial D}{\partial V} + V_e^2 \dfrac{\partial^2 D}{\partial V^2}}. \tag{42}$$

*Parabolic Drag Polar; Isothermal Atmosphere*

For a drag polar obeying Eq. (26) and for an atmosphere where the speed of sound ($a$) is ideally a constant everywhere, the expression for the optimum acceleration can be simplified to a considerable extent. Either by using Eq. (37) or by computing the time derivative of Eq. (34), the following final result is obtained:

$$\frac{\dot{V}}{g} = \frac{(\gamma M M_e - 1)\varepsilon \sin\theta - \dfrac{K}{M^2}\varepsilon^2 \cos^2\theta - C_{DO} M^2}{\varepsilon + M_e \varepsilon'} \tag{43}$$

where $\varepsilon$ is defined[1] by Eq. (34) and

$$\varepsilon' = \frac{1}{A}\left[-\varepsilon A' + \frac{(A B)'}{M_e \sin\theta + 2 A \varepsilon \cos^2\theta}\right]. \tag{44}$$

The primed quantities appearing in the above equations denote derivatives with respect to MACH number, i.e.:

$$\varepsilon' = \frac{d\varepsilon}{dM} \qquad A' = \frac{dA}{dM} \qquad (A B)' = \frac{d(A B)}{dM}. \tag{45}$$

For level flight ($\theta = 0$), Eq. (43) simplifies into:

$$\frac{\dot{V}}{g} = -\frac{\left]\sqrt{\dfrac{B}{A}}\dfrac{K}{M^2} + C_{DO} M^2\right]\sqrt{\dfrac{A}{B}}}{1 + \dfrac{M_e}{2}\left[\dfrac{B'}{B} - \dfrac{A'}{A}\right]} \tag{46}$$

where

$$B' = \frac{dB}{dM}. \tag{47}$$

With regard to vertical flight ($\theta = \pi/2$), the optimum acceleration is given by:

$$\frac{\dot{V}}{g} = \frac{B(\gamma M M_e - 1) - C_{DO} M^2 M_e}{B + M_e B'}. \tag{48}$$

In particular, if the relationship between zero-lift drag coefficient and MACH number is expressed by:

$$C_{DO} = y M^{x-2} \tag{49}$$

[1] In general, $\varepsilon$ depends on both MACH number and altitude. For the particular case of an isothermal atmosphere, however, $\varepsilon$ has the form $\varepsilon = \varepsilon(M)$.

Vol. 4 1958

(where $y$ and $x$ are appropriate constants), then Eq. (48) reduces to [8]:

$$\frac{\dot{V}}{g} = M \frac{\gamma M^2 M_e + M[\gamma M_e^2 (x-1) - 1] - M_e x}{M^2 + 2 M M_e x + M_e^2 x (x-1)}. \tag{50}$$

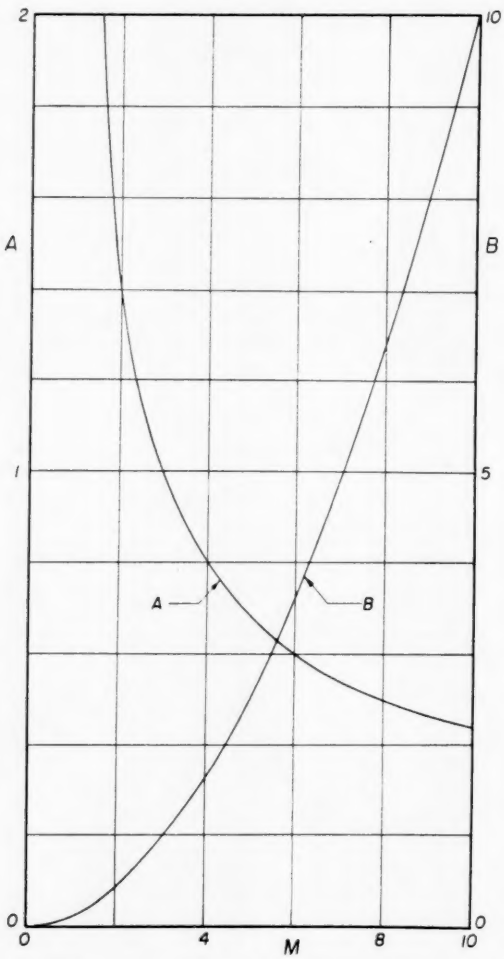


Fig. 2. The functions $A(M)$ and $B(M)$ [hypothetical missile]

## VI. Numerical Results for the Variable-Thrust Sub-Arc

To illustrate the previous theory some numerical computations are carried out, for an isothermal atmosphere and for the all-supersonic region. A hypothetical vehicle is considered. Its propulsion system is such that $M_e = 6$. The drag polar is parabolic and such that:

$$C_{D0} = \frac{0.1}{M} \tag{51}$$

$$K = 0.2\, M. \tag{52}$$

Vol. 4 1958

The two fundamental functions $A(M)$ and $B(M)$ are represented in Fig. 2.

The family of variable-thrust sub-arcs $\varepsilon = \varepsilon(M, \theta)$ is calculated [Eq. (34)] and plotted in Fig. 3 for several values of the path inclination $\theta$ in the MACH number interval $2 < M < 10$. The instantaneous acceleration $\Gamma^*$ at points of the above variable-thrust sub-arcs is indicated in Fig. 4.

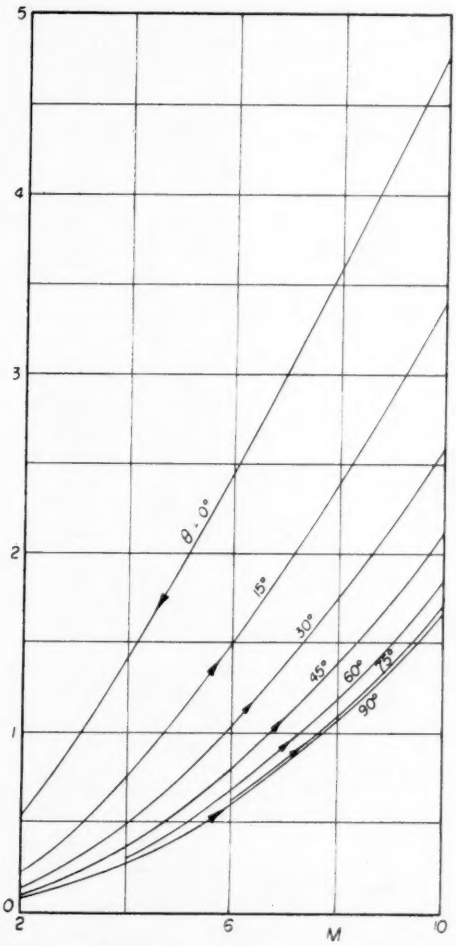


Fig. 3. Representation of the variable-thrust sub-arc in the ($\varepsilon$, $M$) plane for several values of the path inclination [hypothetical missile]

From Figs. 3 and 4 the following concepts are evident:

(a) the optimum operating condition is such that increasing MACH numbers and increasing accelerations are required, for a given $\varepsilon$, as the path inclination increases;

(b) all variable-thrust sub-arcs of Fig. 3 are flown with positive acceleration, except the sub-arc $\theta = 0$ along which the acceleration is negative.

*Vertical Flight*

For the particular case $\theta = \pi/2$ and for a zero-lift drag coefficient satisfying Eq. (51) the instantaneous acceleration $\dot{V}$ [Eq. (50)] is represented in Fig. 5 as a function of the MACH number $M$. Several values are considered for the engine parameter $M_e$, namely $M_e = 6$, $M_e = 8$ and $M_e = 10$.

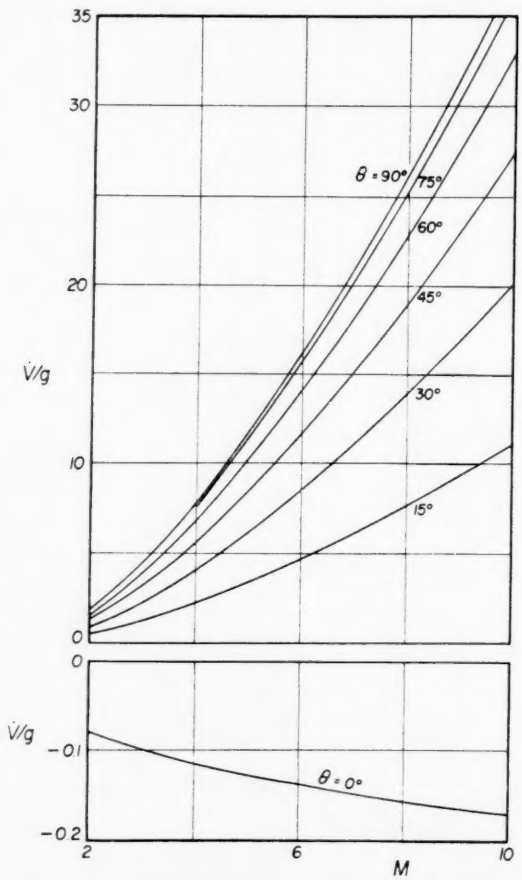


Fig. 4. Acceleration at points of the variable-thrust sub-arc as a function of the MACH number for several values of the path inclination [hypothetical missile]

The above graph shows that the required acceleration at points of the variable-thrust sub-arc rapidly increases as the MACH number increases. For $M_e = 8$ the acceleration is $\dot{V} = 12.8\,g$ at $M = 5$ and $\dot{V} = 42.4\,g$ at $M = 10$. As a consequence, the optimum burning program cannot be followed indefinitely as the MACH number increases, because of limitations of a structural nature (unmanned rockets) or of a physiological nature (manned rockets). This circumstance points out the importance of undertaking a study of the new optimum

burning program for the case where an upper bound is imposed on the modulus of the acceleration vector. This aspect of the research, however, is not considered in the present paper.

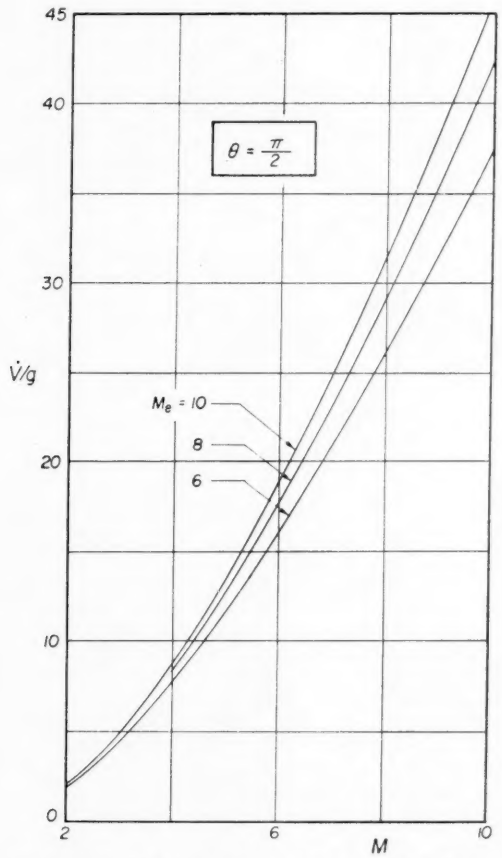


Fig. 5. Acceleration in vertical flight at points of the variable-thrust sub-arc as a function of the MACH number for several values of the engine parameter $M_e$ [hypothetical missile]

## VII. Combination of Sub-Arcs

In the previous sections general solutions have been derived for the problem of extremizing $\Delta G = G_f - G_i$, where $G = G(h, m, V)$. It has been shown that the extremal arc is discontinuous, being generally composed of sub-arcs $\beta = 0$, sub-arcs $\beta = \beta_{\max}$ and sub-arcs flown with variable thrust.

Some brief considerations are now offered on the boundary value problem: it consists of determining that combination of sub-arcs which satisfies a set of prescribed end-conditions. Assuming that the initial MACH number is $M_i = 0$, the extremal path IABF generally starts (Fig. 6) with an initial sub-arc IA flown with maximum engine output, continues with an intermediate sub-arc AB flow with variable thrust and terminates with a final sub-arc BF ([3] and [8]).

The latter can either be travelled with a coasting flight (Case I, Fig. 6) or with maximum engine output (Case II, Fig. 6), depending upon the boundary conditions of the problem.

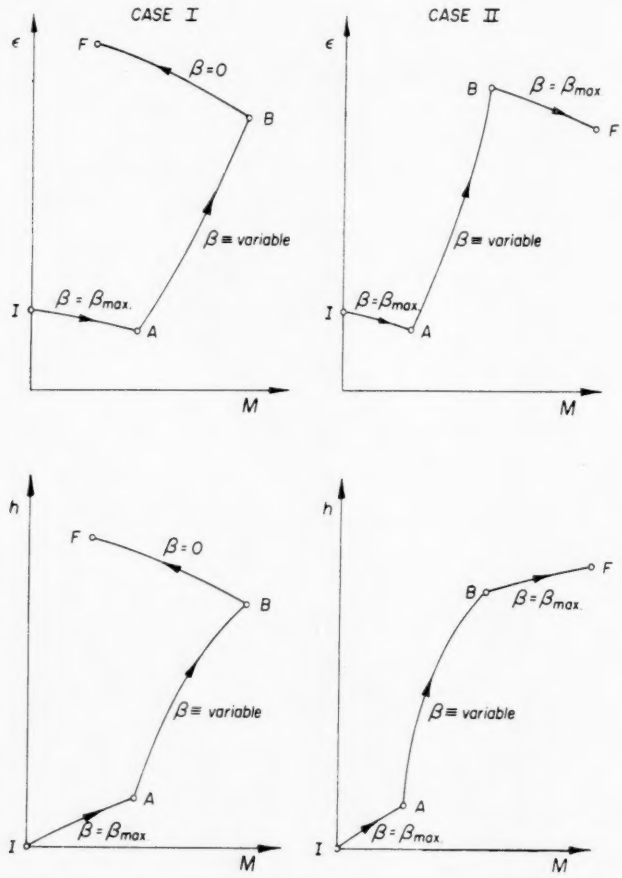


Fig. 6. Possible combinations of sub-arcs for the case where the initial MACH number is zero

The extremal trajectory can be conveniently described by means of either the couple of coordinate planes $(\varepsilon, M)$ and $(m, M)$ or the couple of coordinate planes $(\varepsilon, M)$ and $(h, M)$. With reference to the $(\varepsilon, h, M)$ space (Fig. 6) the boundary conditions are such that, *at most*, only five of the six end coordinates $\varepsilon_i, h_i, M_i, \varepsilon_f, h_f, M_f$ are known. The remaining coordinates are unknown and must be determined from the solution of the variational problem.

The general procedures for solving the boundary value problem are analogous to those described by the senior writer in [2], [3] and [8] and are consequently omitted, for the sake of brevity.

## VIII. Conclusions

A rocket-powered vehicle moving along an arbitrarily inclined rectilinear path is considered in connection with the problem of determining the burning program which minimizes an arbitrarily specified function of the initial and final values for mass, velocity and altitude.

It is shown that the totality of extremal arcs includes zero-thrust sub-arcs, sub-arcs to be flown with maximum engine output and variable-thrust sub-arcs.

General results are obtained, some of them in a closed form, including as a particular case, previous work developed by HAMEL, TSIEN, EVANS, HIBBS, CICALA, MIELE, LEITMANN and WARD. The optimum acceleration law is determined and some numerical examples are presented emphasizing the engineering aspects of the present theory in connection with the flight analysis of rockets.

## References


1. A. R. HIBBS, Optimum Burning Program for Horizontal Flight. J. Amer. Rocket Soc. **22**, 206 (1952).
2. P. CICALA, and A. MIELE, Generalized Theory of the Optimum Thrust Programming for the Level Flight of a Rocket-Powered Aircraft. Jet Propulsion **26**, 443 (1956).
3. A. MIELE, An Extension of the Theory of the Optimum Burning Program for the Level Flight of a Rocket-Powered Aircraft. J. Aeronaut. Sci. **24**, 874 (1957).
4. G. HAMEL, Über eine mit dem Problem der Rakete zusammenhängende Aufgabe der Variationsrechnung. Z. angew. Math. Mechan. **7**, 451 (1927).
5. H. S. TSIEN, and R. L. EVANS, Optimum Thrust Programming for a Sounding Rocket. J. Amer. Rocket Soc. **21**, 99 (1951).
6. L. E. WARD, A Calculus of Variations Problem in Thrust Programming. U.S. Naval Ordnance Test Station, China Lake, California, T.N. 3503/2, August, 1955.
7. G. LEITMANN, Stationary Trajectories for a High-Altitude Rocket with Drop-Away Booster. Astronaut. Acta **2**, 119 (1956).
8. A. MIELE, Generalized Variational Approach to the Optimum Thrust Programming for the Vertical Flight of a Rocket, Part I, Necessary Conditions for the Extremum. Purdue University, School of Aeronautical Engineering, Report No. A-57-1, March, 1957, AFOSR-TN-57-173 [Z. Flugwiss. **6**, 69 (1958)].
9. A. MIELE, and C. R. CAVOTI, Generalized Variational Approach to the Optimum Thrust Programming for the Vertical Flight of a Rocket, Part II, Application of GREEN's Theorem to the Development of Sufficiency Proofs for Particular Classes of Solutions. Purdue University, School of Aeronautical Engineering, Report No. A-57-2, August, 1957, AFOSR-TN-57-652 [Z. Flugwiss. **6**, 102 (1958)].


Vol. 4 1958

# Über Erwärmung von in die Atmosphäre eintauchenden Raketenkörpern

Von

**W. Strubell**[1], DGRR, PTA

(Mit 3 Abbildungen)

*(Eingegangen am 15. Februar 1958)*

**Zusammenfassung — Abstract — Résumé**

**Über Erwärmung von in die Atmosphäre eintauchenden Raketenkörpern.** Die Frage nach den physikalischen Vorgängen, die sich beim Eindringen raketenartiger Flugkörper in die Erdatmosphäre abspielen, ist wiederholt Gegenstand umfangreicher Untersuchungen gewesen [1, 2]. Das Problem hat aber gerade jetzt wieder an Bedeutung gewonnen, als am 6. Dezember 1957 die Trägerrakete des ersten sowjetischen Erdsatelliten möglicherweise in Alaska niederging, ohne zu verdampfen. Bisher waren zwei Anschauungen vertreten; nach der einen sollte der wieder in die Erdatmosphäre eintauchende Körper ähnlich den Meteoren völlig verdampfen, nach der anderen sollte es möglich sein, daß ein solcher Flugkörper ohne Verdampfung die Erdoberfläche erreicht. Der praktische Versuch scheint gezeigt zu haben, daß die letztere Anschauung die richtige ist.

Im folgenden soll an Hand von Ergebnissen aus der Meteorastronomie abgeleitet werden, wann mit einer Verdampfung einer aus dem Weltraum in die Erdatmosphäre eintauchenden Rakete zu rechnen ist und wann nicht.

**On the Heating of Rocket Vehicles Entering into the Earth's Atmosphere.** The problem of determining events which occur as rockets or missiles enter into the earth's atmosphere has been extensively treated several times in the literature [1, 2]. At the present time the problem is of increased importance since the carrier rocket of the first Soviet satellite fell into the earth's atmosphere, possibly in Alaska, on or about 6 December 1957 without being vaporized. Prior to this two concepts existed: firstly, it was thought that a body would entirely vaporize upon entrance into the atmosphere, in a way similar to that of meteors; in accordance with the second conception, such a missile could possibly attain the surface without being totally evaporated. Practical experience seems to have proved this latter view to be true.

This paper attempts to determine, using results of meteor astronomy, which cases would lead to the evaporation of a rocket entering into the earth's atmosphere from space, and in which cases it would not be expected to vaporize.

**Sur l'échauffement des corps de fusée pénétrant dans l'atmosphère.** Plusieurs recherches extensives [1, 2] ont été consacrées à l'investigation des phénomènes physiques qui sont déclanchés lors de la repénétration d'engins dans l'atmosphère terrestre. Ce problème a reçu un regain d'actualité à la suite de la chute, le 6 décembre 1957, de la fusée porteuse du premier satellite russe. Il est possible que cette chute se soit produite en Alaska sans vaporisation. Deux conceptions se confrontent à l'heure

[1] Leipzig O 5, Hermann-Liebmann-Straße 19, Deutsche Demokratische Republik.

actuelle. Selon la première le corps serait intégralement vaporisé lors de la repénétration, comme cela se produit pour les météorites. Selon la seconde l'engin pourrait heurter le sol avant vaporisation complète. L'expérience a confirmé probablement l'exactitude de cette seconde possibilité.

L'article cherche à établir, suivant les données de l'astronomie météoritique, dans quels cas l'évaporation complète d'un engin en repénétration doit ou non être prévue.

**Symbole**

$C_L$ Geschwindigkeit der verdampfenden Luftanteile
$C_R$ Geschwindigkeit der verdampfenden Raketenteile
$\lambda$ Wärmeübergangszahl
$\gamma$ Widerstandsbeiwert
$\mu_R$ mittlere Masse der Rakete
$\mu_L$ mittlere Masse der Luftpartikel
$T_0$ extraterrestrische Temperatur
$T_K$ kritische Temperatur
$k$ BOLTZMANN-Konstante $k = 1{,}38 \cdot 10^{-16}$ erg/grad
$\Delta m$ die Raketenmasse im Verdampfungsherd
$\beta$ Verdampfungsenergie des Raketenkörpers
$\psi$ Verdampfungswert
$v$ Geschwindigkeit der Rakete
$\tau$ Teil des durch Reibung entstandenen Energieverlustes, der zu Leuchterscheinungen führt
$m$ Masse der Rakete
$Q$ Querschnitt der Rakete = Durchmesser
$\varrho_L$ Luftdichte
$W$ Widerstandskraft der Luft
$\delta$ Dichte des Raketenmaterials
$J$ Intensität des Strahlungsanteils vom Gesamtenergieverlust des Eintauchkörpers durch Luftreibung
$v_G$ Grenzgeschwindigkeit des Eintauchkörpers, bei dem gerade keine Verdampfung mehr stattfindet
$T_L$ Lufttemperatur
$M$ Molekulargewicht

Eine Rakete dringt mit einer kosmischen Geschwindigkeit der Größenordnung $8 \cdot 10^5$ bis $1{,}5 \cdot 10^6$ cm/sec in die Erdatmosphäre ein, wobei der untere Grenzwert speziell für eine Satellitenrakete gilt.

Bereits ÖPIK [3], später LINDEMANN und DOBSON [4] sowie HOFFMEISTER [5] nahmen bei ihren Sternschnuppentheorien die Erhitzung der vor dem Körper komprimierten atmosphärischen Luftteilchen zum Ausgangspunkt ihrer Betrachtungen. Eine physikalische Theorie, die etwas über den Eintauchvorgang von Raketen in die Erdatmosphäre aussagen will, muß von Betrachtungen der Wechselwirkung zwischen den Luftpartikeln und dem festen Raketenkörper ausgehen. Ausmaß und Art der stattfindenden Wechselwirkung sind dabei bedingt durch die Größe der Auftreffgeschwindigkeit der Luftteilchen auf die Oberfläche der Rakete. Diese Auftreffgeschwindigkeit ist in großen Höhen, also bei geringer Luftdichte im Höchstfall, gleich der momentanen Geschwindigkeit der Rakete relativ zur Erdatmosphäre. Bei steigender Luftdichte bildet sich vor dem Raketenkörper eine aus Luft, bereits verdampftem Metall und Elektronen bestehende Druckwolke aus. Diese wird an ihrer Stirnseite gegen die ruhende Atmosphäre hin durch einen Verdichtungsstoß abgegrenzt, der dann langsam in einen MACHschen Kegel übergeht.

Auf Grund zahlreicher photographischer Meteorbeobachtungen gelangte CEPLECHA [6, 7] zur Aufstellung von drei sehr wichtigen Postulaten, die, auf unser Raketeneintauchproblem angewandt, folgendes besagen:

1. Die Geschwindigkeit der verdampfenden Raketenteile $C_R$ ist konstant.

2. Die Wärmeübergangszahl $\lambda$ ist nicht geschwindigkeitsabhängig.

3. Der Widerstandsbeiwert $\gamma$ ist eine lineare Funktion der in die Atmosphäre eintauchenden Rakete.



Vol. 4 1958

Die Energie, die beim unelastischen Stoß einer Luftpartikel auf die feste Oberfläche der in die Atmosphäre eintauchenden Rakete übertragen wird, erhitzt nun diese bis zur kritischen Temperatur. Das dadurch gasförmig gewordene Material entweicht zusammen mit Luftpartikeln sofort in den Außenraum. Hieraus ergibt sich nach HOPPE [8], auf unsere Verhältnisse umgerechnet, eine kinetische Energie von

$$\frac{1}{2}\mu_R C_R^2 = \frac{1}{2}\mu_L C_L^2 = \frac{3}{2} k T_K \tag{1}$$

und der Energiesatz für den lokalen Verdampfungsherd

$$\frac{1}{2}\mu_L v^2 = \beta \cdot \Delta m + \frac{1}{2}\Delta m C_R^2 + \frac{1}{2}\mu_L \cdot C_L^2. \tag{2}$$

Nach der Definition der Verdampfungsfunktion $\psi = \Delta m/\mu_L$ erhält man aus (2) und (1)

$$\psi = \frac{v^2}{2\beta} \cdot \frac{1 - \left(\frac{C_R}{v}\right)^2 \cdot \frac{\mu_R}{\mu_L}}{1 + \frac{C_R^2}{2\beta}}. \tag{3}$$

Daraus ergibt sich nach HOPPE [9]

$$\lambda = 2\beta\psi/v^2 \tag{4}$$

und für den Widerstandsbeiwert [10]

$$\gamma = 1 + \frac{1}{3} \cdot \frac{C_R}{v}\left(\psi + \sqrt{\frac{\mu_R}{\mu_L}}\right). \tag{5}$$

Die Kenntnis der bei diesem Problem des Wiedereintauchens von Raketen in die Erdatmosphäre maßgeblichen Größen, wie Geschwindigkeit, Luftdichte und chemische Zusammensetzung des Eintauchkörpers, läßt sich von den drei wesentlichen Koeffizienten $\lambda$, $\gamma$ und $\tau$ ableiten. Die Widerstandskraft der Luft beträgt danach:

$$W = -\gamma Q \cdot \varrho_L \cdot v^2 \tag{6}$$

$$Q = m^{2/3} \cdot \sqrt[3]{9\pi/16\,\delta^2}, \tag{7}$$

und für ein verdrängtes Luftelement $d\mathfrak{M}$ mit der Luftdichte $\varrho_L$, der Raketenmasse $m$ und der zurückgelegten Wegstrecke $ds$ ergibt sich:

$$d\mathfrak{M} = Q\, m^{2/3} \cdot \varrho_L \cdot ds. \tag{8}$$

Aus (6) folgt dann leicht:

$$\dot{m} - \frac{\lambda \cdot v}{2\gamma\beta} \cdot W = 0 \qquad \text{oder} \qquad \dot{m} = \frac{\lambda \cdot v}{2\gamma\beta} \tag{9}$$

und

$$m \cdot \dot{v} - W = 0. \tag{10}$$

Die Geschwindigkeit eines in die Atmosphäre eintauchenden Körpers verändert sich naturgemäß ständig. Der dabei auftretende Energieverlust macht sich in Form von Wärme und sichtbaren Lichtstrahlen geltend. Der Anteil $\tau$ am Gesamtenergieverlust, der sich in sichtbare Strahlung umwandelt, ist mit deren Strahlungsintensität $J$ verknüpft durch:

$$J = -\frac{\tau \cdot v}{2\gamma} \cdot W. \tag{11}$$

Die Geschwindigkeit der Rakete nimmt durch die bremsende Lufthülle ab. Aus dem Widerstandsgesetz (6) läßt sich nun unter Voraussetzung einer konstanten Masse des Eintauchkörpers sofort der Verlauf der Geschwindigkeitsabnahme errechnen.

$$W = m \cdot \frac{dv}{dt} \tag{12}$$

eingesetzt in (6) ergibt

$$m \cdot \frac{dv}{dt} = -\gamma \cdot Q \cdot \varrho_L \cdot v. \tag{13}$$

Durch Integration von (13) ergibt sich

$$v(s) = v_0 \cdot e^{-\gamma Q \cdot \int_0^s \varrho_L \, ds}. \tag{14}$$

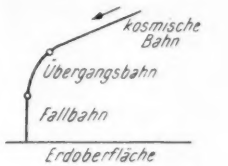


Abb. 1. Schematische Darstellung der Bahnabschnitte, die eine Rakete in der Erdatmosphäre durchläuft

Die Formel (14) gilt um so genauer, je kleiner die Anfangsgeschwindigkeit des in die Atmosphäre eintauchenden Körpers ist, weil dann die Massenkonstanz am besten erfüllt ist. In unserem Falle bedeutet das die Anwendung auf eintauchende Trägerraketen von Satellitenbahnen, bei denen die Geschwindigkeit bei 8 km/sec liegt.

Für den Fall der Massenabnahmen, die bei hohen kosmischen Geschwindigkeiten tatsächlich bis zur Verdampfung des Eintauchkörpers führen, muß der Ablauf des Verdampfungsvorganges bekannt sein, wenn allgemein gültige Aussagen über ihn gemacht werden sollen. Nach HOPPE [10] erfolgt die Bewegung von Meteoren durch die Erdatmosphäre in drei Bahnabschnitten:

1. der kosmischen Bahn, auf der sich der Körper mit geringer Geschwindigkeitsveränderung bewegt;

2. der Übergangsbahn, die unter Abbremsung der kosmischen Geschwindigkeit bis auf eine von der Masse und der Luftdichte abhängige konstante Fallgeschwindigkeit durchlaufen wird, und

3. der Fallbahn, die der Flugkörper in vertikaler Richtung mit einer Geschwindigkeit zurücklegt, die sich aus der Gleichheit von Luftwiderstand und Erdanziehung ergibt.

Kleine Eintauchkörper durchlaufen alle drei Bahnabschnitte, Riesenmeteoriten dagegen erreichen bereits am Anfang der Übergangsbahn den Erdboden.

Bei Eintauchgeräten mit hoher Geschwindigkeit, etwa 11,2 km/sec und mehr, bildet sich am eintauchenden Flugkörper zunächst ein eng begrenzter Verdampfungsherd aus. Dabei wirken drei Prozesse am Abbau der Energiespitze mit, nämlich Ausstrahlung, Wärmeleitung und Verdampfung. Dabei spielen die ersten beiden Punkte, nämlich Ausstrahlung und Wärmeleitung, nur eine untergeordnete Rolle, wie aus Untersuchungen durch Kathodenzerstäubungen [11] festgestellt werden konnte. Durch Reibung mit den Luftteilchen der Atmosphäre wird die mit hoher Geschwindigkeit eintauchende Rakete am Verdampfungsherd, also an der Berührungsstelle Rakete—Luft, bis zur kritischen Temperatur erhitzt. Dadurch gelangt das Material in einen gasförmigen Zustand sehr dichter Packung und entweicht unter Mitreißen von Luftpartikeln. Trägt man nun die nach (3) errechneten Werte für die Verdampfungsfunktion gegen die Geschwindig-



Vol. 4 1958

keit auf, so erhält man die in Abb. 2 dargestellte Kurve. Sie zeigt, daß bei einer Geschwindigkeit $< 10$ km/sec eine Verdampfung nicht stattfindet.

Die von HOPPE [12] berechnete Kurve wurde durch photographische Meteorbeobachtungen von CEPLECHA bestätigt.

Aus dem bisher Dargelegten ergibt sich, daß die Lösung des Problems der Behandlung der atmosphärischen Bahnen von Flugkörpern allgemein auf einen Vorgang der Bewegung einer veränderlichen Masse im widerstehenden Mittel mit veränderlicher Dichte in einem Beschleunigungsfelde zurückzuführen ist. Auf Grund der Geschwindigkeitsabnahme wird aber einmal ein Zustand eintreten, in dem die Verdampfung aufhört. Diese Grenzgeschwindigkeit $v_G$ läßt sich mathematisch erfassen, und zwar tritt dieser Zustand dann ein, wenn beim Aufschlag einer Luftpartikel gerade noch eine Partikel des Eindringkörpers emittiert wird.

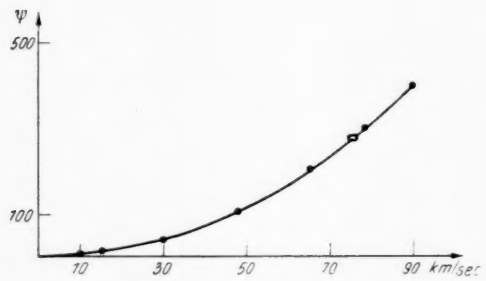


Abb. 2. Der Verdampfungswert $\psi$ in Abhängigkeit von der Geschwindigkeit $v_G$

Diese Grenzgeschwindigkeit läßt sich nach HOPPE [12] wie folgt berechnen: Die Umwandlung der von einer Luftpartikel getroffenen Raketenmasse in den gasförmigen Zustand bewirkt eine Energie, die sich zusammensetzt aus der mittleren kinetischen Energie einer Luftpartikel und der mittleren Schwingungsenergie des getroffenen Flugkörpers, die dieser im ungestörten Zustand besaß. Daraus ergibt sich:

$$\frac{1}{2}\mu_L (v^2 + C^2) + \frac{1}{2} \Delta m\, C_0{}^2 = \beta \cdot \Delta m + \frac{1}{2} \Delta m\, C_R{}^2 + \frac{1}{2} \mu_L\, C_L{}^2. \qquad (15)$$

Weiterhin müssen bekannt sein: die mittlere Temperatur der Luft $T_L$ in verschiedenen Höhen, sowie die extraterrestrische und kritische Temperatur des Flugkörpers. Letztere werden denen von Eisenmeteoriten gleichgesetzt.

Tabelle 1. *Höhe, mittleres Molekulargewicht und mittlere Lufttemperatur nach Nazarek* [13]

| $h$ in km | Molekulargewicht $M$ | mittlere Temperatur $T_L$ in °K |
|---|---|---|
| 5 | 28,97 | 226 |
| 10 | 28,97 | 220 |
| 25 | 28,93 | 224 |
| 40 | 28,79 | 259 |
| 50 | 28,74 | 286 |
| 65 | 28,72 | 256 |
| 80 | 28,72 | 192 |
| 100 | 27,69 | 232 |
| 125 | 25,84 | 284 |
| 280 | 25,23 | 310 |
| 330 | 23,87 | 487 |
| 330 – 1000 | 14,4 | 1500 im Mittel |

Tabelle 2. *Mittleres Molekulargewicht M, extraterrestrische Temperatur $T_0$ °K und kritische Temperatur $T_K$ °K sowie Verdampfungsenergie $\beta$ erg/g für Eisenmeteoriten*

| $M$ | $T_0$ in °K | $T_K$ in °K | $\beta$ |
|---|---|---|---|
| 55,8 | 342 | 8300 | $8{,}6 \cdot 10^{10}$ |

Setzen wir nun in (15) $\Delta m = \mu_R$, so erhält man unter Umformung

$$v_G^2 = 2\frac{\mu_R}{\mu_L} \cdot \left\{\beta + 3\frac{k}{\mu_R}\left[T_K - \frac{1}{2}(T_0 + T_L)\right]\right\}. \tag{16}$$

Die Grenzgeschwindigkeit eines metallischen Eintauchkörpers ist im wesentlichen eine Funktion der Zusammensetzung der Erdatmosphäre und der Temperatur. Diese Funktion ist in Abb. 3 dargestellt und zeigt, daß bei $v_G < 9{,}5$ km/sec keine Verdampfung eines Eintauchkörpers stattfindet, oberhalb dieser Geschwindigkeit aber eine stetig wachsende Verdampfung einsetzt.

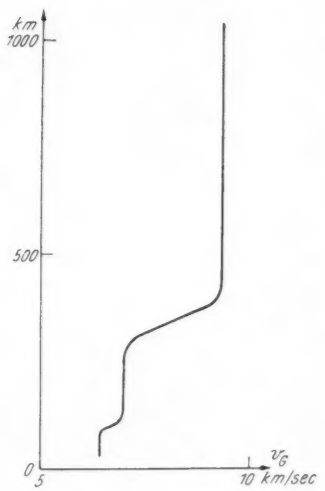


Abb. 3. Die Grenzgeschwindigkeit $v_G$ als Funktion der Höhe

Vol. 4 1958

**Literaturverzeichnis**


1. J. M. J. Kooy und J. W. H. Uytenbogaart, Ballistics of the Future, S. 203 und 401. Haarlem: A. Stam, 1946.
2. H. Ruppe in: Bericht über den V. Internationalen Astronautischen Kongreß, Innsbruck 1954, S. 274. Wien/Innsbruck: Springer, 1955.
3. E. Öpik, Veröff. Sternwarte Dorpat **25**, 1, 29 (1922).
4. F. A. Lindemann und G. Dobson, Proc. Roy. Soc. London **102**, 411 (1923).
5. C. Hoffmeister, Astronom. Nachr. **221**, 353 (1924).
6. Z. Ceplecha, Bull. Astronom. Insts. Czechosl. **6**, 123 (1955).
7. Z. Ceplecha, Bull. Astronom. Insts. Czechosl. **7**, 21 (1956).
8. J. Hoppe, Bull. Astronom. Insts. Czechosl. **7**, 123 (1956).
9. J. Hoppe, Wiss. Z. Univ. Jena, Math. nat. Richtung **3**, 503 (1954).
10. J. Hoppe, Astronom. Nachr. **283**, 95 (1956).
11. R. Seeliger und K. Sommermeyer, Z. Physik **93**, 692 (1935).
12. J. Hoppe, Wiss. Z. Univ. Jena, Math. nat. Richtung **5**, 537 (1956).
13. P. Nazarek, Bull. Amer. Meteorol. Soc. **31**, 46 (1950).

# Observation of a Satellite Near its Culmination[1]

By

**Alessandro Boni[2]**, AIR

(With 12 Figures)

*(Received February 5, 1958)*

**Abstract — Riassunto — Zusammenfassung — Résumé**

**Observation of a Satellite Near its Culmination.** The observation of the angular coordinates of position of a satellite carried out in stations where special photographic equipment is not available, can be made in the best conditions when the satellite passes through the culmination point with respect to the observer. In such a point the altitude angle becomes stationary and the azimuth angular velocity remains almost constant during a short time interval. The equations for the physical parameters necessary to the application of the method are given, assuming that a theodolite is used. However, the process can also be applied to the case of instruments which are equatorially assembled.

**Rilevamento di un satellite presso la culminazione.** Il rilevamento delle coordinate angolari di posizione di un satellite in stazioni che non dispongano di speciali attrezzature fotografiche può essere compiuto nelle migliori condizioni quando il satellite passa per il punto di culminazione rispetto all'osservatore. In questo punto l'angolo di altezza diventa stazionario e la velocità angolare in azimut resta sensibilmente costante durante un breve intervallo di tempo. Vengono date le espressioni delle grandezze che intervengono nell'applicazione del metodo supponendo l'uso di un teodolite, ma il procedimento può essere esteso al caso di strumenti con montaggio equatoriale.

**Beobachtung eines Satelliten in der Nähe seiner Kulmination.** Die Beobachtung der Winkelkoordinaten der Position eines Satelliten in Stationen, wo spezielle photographische Einrichtungen nicht verfügbar sind, kann am besten dann ausgeführt werden, wenn der Satellit durch den Kulminationspunkt (in Beziehung auf den Beobachter) hindurchgeht. In einem solchen Punkt wird der Höhenwinkel stationär und die azimutale Winkelgeschwindigkeit bleibt innerhalb eines kurzen Zeitintervalles fast konstant. Es werden die Gleichungen für die physikalischen Parameter, die für die Anwendung der Methode erforderlich sind, angegeben, vorausgesetzt, daß ein Theodolit benützt wird. Die Methode kann aber auch auf äquatorial montierte Instrumente angewendet werden.

**Relèvement d'un satellite auprès de la culmination.** Les coordonnées angulaires de position d'un satellite peuvent être relevées dans les meilleures conditions par des stations, qui ne sont pas équipées de dispositifs photographiques spéciaux, lorsque le satellite passe par le point de culmination par rapport à l'observateur. À ce point

[1] Presented in a preliminary form at the VIIIth International Astronautical Congress at Barcelona, Spain, October 6—12, 1957.

[2] Via G. Sisco, 7, Roma, Italia.

l'angle d'élévation devient stationnaire et la vitesse angulaire azimutale se maintient sensiblement constante pendant un court intervalle de temps. La note établit les expressions des quantités qui interviennent dans l'application de la méthode. Elle suppose l'emploi d'un théodolite, mais le procédé peut être étendu aux cas où les instruments ont une monture équatoriale.

## I. Method of Observation Near Culmination

### 1. Introduction

In a previous paper[1], I took into consideration several aspects regarding the observation of a satellite, particularly the geophysical type (that is, crossing the atmospheric layer), by optical systems (some aspects are common to the tracking by radio means).

In this paper, I intend to illustrate the characteristics of a *tracking process for the satellite near its point of culmination* with respect to the observer. Under these conditions the angle of altitude remains stationary for a certain time and can be measured with the best accuracy, even if the station has no special equipment available both for cameras and for following up the motion.

Vol. 4 1958

In fact, for other conditions the tracking of the motion relative to the observer, in case of a satellite with an orbit close to the Earth, needs special means to obtain adequate accuracy; this because of the motion being characterized by a high angular velocity of the visual radius[2].

The "classification of tracking stations" may be devised with respect to the scopes, equipment and accuracy. Let us now limit ourselves to the following distinction of *"kinematic tracking stations"*, by which measurements are carried out of both the angular positions and the corresponding satellite transit time:

(a) *Stations for a continuous or almost continuous tracking*, to be provided with special equipment and large phototheodolites in order to photo-record the trajectory and marking the times, the motion being in general referred to the starry sky.

(b) *Stations for a discontinuous or discrete tracking*, where only a limited number of the trajectory fixes are carried out. In this case, equipment having a motion picture system (electronically controlled cinetheodolites) is generally used, to record at given time intervals both the position of a timer hand, and the positions of the azimuth and altitude circles of an optical collimation instrument. By setting devices for a following-up motion, the satellite is kept as long as possible in the middle of the reticle. The picture is now no longer needed; however, as a result less accuracy is obtained.

(c) *Stations for a single tracking*, to carry out only one or very few fixes of the visible arc of the trajectory, which is covered in a very short time. In general, the photo-recording of the position circles and of the watch is avoided. This refers to both the case where the transit of a satellite is expected to occur through one of the spider lines, while the satellite is eventually followed up by the perpendicular spider line, and to the case where one of the spider lines is taken tangent to the trajectory at one or more points.

---

[1] A. Boni, Tracking of a Geophysical Satellite. Paper presented at the VIth Convention of the Italian Geophysical Association, Rome, 9–10 November, 1956.

[2] The tracking conditions of a satellite, apart from some analogies, are generally different from those relating to the tracking of a missile's motion. This is true even in case of a geodetic missile, or a meteor, the trajectory of which (determined by the Sun and perturbed by the Earth) takes an almost rectilinear path, having a very short lifetime.

Included in the latter case is the system taken into consideration in the present paper for tracking a satellite near culmination. Here, the angular velocity of the visual radius has an altitude component which diminishes until it is nullified. Therefore, it is possible to carry out a fairly accurate measurement of the altitude angle.

Thus, a plane tangent to the trajectory is so determined, the position of which is not much influenced by a rough approximation in the azimuth and time measurements.

The accuracy of measurements may be increased by using following-up devices, for which a simplified construction is suggested, due to the fact that even a limited approximation in angular velocities is efficient. The angular velocities may be arranged according to a pre-set programme, the magnitude of the values being generally foreseen.

In successive transits of the satellite near a given station, the azimuth of the culmination point $C$ remains remarkably constant, and in general it deviates only a few degrees from that of the plane taken through the station at right angles with the geocentric projection of the trajectory on the Earth's surface. The altitude angle and the angular velocity at the azimuth near $C$ are essentially a function of the distance taken horizontally between the station and the relative projection of the satellite.

The single tracking stations may perform a useful action, becoming essential during the initial and final revolutions of the satellite, in obtaining control elements of the trajectory to be rapidly supplied to observation centers located in neighbouring zones, as well as in replacing the main stations of continuous (photographic), or discontinuous (cinematographic) tracking, when these stations are unable to operate due to special conditions.

As a matter of fact, each station has a limited operating range, depending on the altitude of the satellite. Moreover, the observations refer only to the same short arc of trajectory, included between two given latitudes, passing near the station during the daily rotation of the Earth. The visibility of said arc requires other conditions, concerning the position with respect to the Sun, both of such an arc and of the station.

It is necessary for the arc at that time not to be located in the Earth's shadow with respect to the Sun, and expecially not to be in opposition, which is the worst condition. There are also to be excluded broad areas around the conjunction with the Sun, leaving as possible only limited zones near the quadratures, relative to Earth's center. More specifically the arc should belong to a special region. The latter is bounded on the one side by the quasi-cylinder formed by the Earth's shadow. From the other side it is limited by the quasi-cone tangential to a non-rotating Earth and passing through the quasi-circle of points in which the Sun appears below the horizon by a sufficient angle (18 degrees in the case of the astronomical twilight).

Moreover, in so far as the position of the station with respect to the sun is concerned, the above arc, extended to latitudes near those of the station and almost in quadrature with the Sun, will be visible, among the many revolutions carried out every day by the satellite, only for the one where the transit occurs when the Sun, in its daily rotation, is sufficiently low, below the local horizon. Namely, in the short time during which the above arc does materialize because of the transit of the satellite, the station should not be too distant from the twilight zones, relative to sunset and sunrise, so that the arc remains above the local horizon.

In conclusion, with regard to visibility it is required that the aforementioned arc be located in the specified approximate quadrature with the sun. Furthermore, the station must reach the above mentioned quadrature in its daily rotation and during the interval of satellite transit.

These conditions require that a set of stations scattered in latitude be prearranged, in order to get a sufficient probability of observation of at least a short arc of the trajectory, which on the other hand is subject to variations. Moreover, in case the observations are not to be limited to only one of the revolutions the satellite performs in a day, the formation of a net extended also in latitude is required.

If the net should be formed only by high-accuracy main stations, the burden would be heavy. Therefore, the advantage is apparent of utilizing also less accurate stations, having however the greatest simplicity, as for example, the above mentioned single tracking stations.

Should the altitude of the satellite decrease, for instance, to under 200 kms, a very great number of stations would be needed, in view of the diminished operating range. This circumstance requires the intervention of a net of voluntary observers, even if the observations imply only a rough approximation.

Vol. 4 1958

It has been mentioned that the single tracking stations near culmination are suitable for giving the fairly accurate position of a plane tangent to the trajectory. Correlating such a datum with other similar data obtained in subsequent days by the same station, or better with other data obtained in the same day by not too distant stations (a few hundreds km at the most), it is possible to obtain a fairly accurate position of the trajectory arc in that interval and, with a less approximation, the different elements of the orbit.

## 2. Tracking Categories Near Culmination

The tracking processes near culmination are related to the degree of accuracy, both of the station and of the data obtained on the orbit at the instant of culmination.

To establish an indicative classification, different accuracy levels may be set forth, viz.: low, mean, high.

The accuracy levels for the stations can be generally laid out as per Table I, with respect to the equipment and the errors $\varepsilon$, in absolute value, allowed in the measurements of the altitude angle $h$, azimuth $A$, and time $t$.

Table 1. *Accuracy of Stations*

| Symbol | Accuracy | $\varepsilon_h$ | $\varepsilon_A$ | $\varepsilon_t$ | Equipment (f.d. = following-up devices) |
|---|---|---|---|---|---|
| SRC. 3 | Low | $1^0-10'$ | $5^0-30'$ | $10^s-1^s$ | Telescope sights with common goniometers |
| SRC. 2 | Mean | $10'-20''$ | $30'-2'$ | $1^s-0^s.1$ | Theodolites: eventual f.d. for $A$ measurements |
| SRC. 1 | High | $20''-1''$ | $2'-10''$ | $<0^s.1$ | Theodolites and cinetheodolites, f.d. for $A$ measurements, and eventually for $h$. |

In so far as the accuracy levels of the data at the moment of culmination are concerned, it is possible to establish in general the classification of Table II,

with reference to the next illustration. The Table concerns the "errors, in absolute value, in the foreseen elements": $t_E$ = time of subsequent transits at the Equator, $T_E$ = period of said transits, $i_E$ = inclination of the orbit plane to the Equator, $\alpha_\Omega$ = right ascension of the ascending node, $b$ = semi-minor axis of the orbit, $\theta_{\Omega p}$ = anomaly of perigee on the orbit starting from $\Omega$.

Table II. *Accuracy of Elements*

| Symbol | Accuracy | $\varepsilon_{tE}$ | $\varepsilon_{TE}$ | $\varepsilon_{iE}$ | $\varepsilon_{a\Omega}$ | $\varepsilon_b$ | $\varepsilon_{\Theta\Omega p}$ |
|---|---|---|---|---|---|---|---|
| ERC. 3 | Low | $1^m$ | $10^s$ | $1^0$ | $1^0$ | 100 km | $45^0$ |
| ERC. 2 | Mean | $<10^s$ | $<1^s$ | $<10'$ | $<10'$ | <10 km | $< 5^0$ |
| ERC. 1 | High | $<1^s$ | $<0^s.1$ | $<1'$ | $<1'$ | <1 km | $<30'$ |

The accuracy levels have been indicated with reference to the values of the elements at the instant of culmination, when it is of interest to know the ensuing values of $h$, $A$, and others, in order to set in advance the stations for the observation.

The prediction of these values at a given time instant requires the knowledge of several other values at previous time instants, so that one may calculate the first and subsequent differences appearing in the extrapolation formulae.

The loss of accuracy in passing from the given data to the extrapolated data depends upon the time intervals to which the data are referred. It also depends upon the regularity and magnitude of the element variations, which may become appreciable when the satellite is orbiting at the lower altitudes, where the motion drag increases together with the air density.

In the case classified as "low accuracy" in Table II, the elements can be derived when there is information available of satellite sightings at a sufficient number of sites, for instance more than ten, in an immediately preceding day and with a magnitude approximation of 1 min.

In fact, in such a case an analysis of the sighting times $t_j$ ($j = 1, 2, \ldots$), in the sites $P_j$, allows one, in general, to determine to which of the subsequent revolutions of the satellite they are referring, and to define an orienting value for the period $T$ and therefore for the average angular velocity $\dot{\theta}_m$ of the satellite, relative to the Earth's center.

Once the longitude $\lambda_j$ of $P_j$ is known, in correspondence to $t_j$ the right ascension $\alpha_j$ of the local zenith is derived, which in connection with the latitude $\varphi_j$ gives the near values of the equatorial coordinates of various points $S_j$ of the satellite trajectory with reference to the fixed stars. The trajectory can be interpolated among the experimental points, carrying out the drawing by one of the cartographic systems. As a result, the inclination $i_E$ of the orbit and the right ascension of the node, $\alpha_\Omega$, are obtained.

Knowing $\dot{\theta}_m$ and $i_E$, a reduction of $t_j$ may be carried out, in the sense of referring the transit times to a same latitude and in particular to the Equator. It will then be possible to achieve a better approximation of the value of $T_E$ and therefore of the corresponding value of the semi-major axis, $a$, of the orbit.

On the basis of $t_j$, indicative values can be derived for the maximum and minimum difference between the angular velocity $\dot{\theta}$ of the satellite along the orbit and the average value $\dot{\theta}_m$. From these differences it is possible to obtain, with a rough approximation only, the values of the semi-minor axis $b$ and of the perigee anomaly, $\theta_{\Omega p}$.

These values can be utilized in predicting the values of some parameters relative to the culmination point $C$, for a given station $P$.

As a matter of fact, owing to the low accuracy of data in such a case, while it is possible to get for the azimuth $A_C$ of $C$ an approximation of the order $\pm 2^0$ and $\pm 2^m$ for the time $t_C$ of transit, appreciable uncertainties will remain about the values at the time $t_C$ of the horizontal distance $D_{\pi,C}$ and of the altitude $Z_C$ of the satellite with respect to $P$, and therefore of the altitude angle $h_C$.

If, for instance, the element errors allow a discrepancy of $\pm 15^0$ in the prediction of $h_C$, this may exceed the field amplitude, which usually is $< 10^0$, of the optical telescope sight of the station. Then, the sighting will be backed by an observer team, sharing the field of uncertainty of $h_C$ on the vertical circle of $A_C$.

Once the tracking has been carried out with the accuracies shown for said stations in Table I, the results in question can be utilized in order to improve the knowledge of the orbit elements. For instance, $\tan h_C$ gives the ratio $Z_C/D_{\pi,C}$, and therefore $Z_C$ will be derived with the same accuracy by which $D_{\pi,C}$ is known; this accuracy is generally greater.

On the other hand, better indications on $D_{\pi,C}$ can be obtained if one measures, from the same station, not only $t_C$ and $A_C$, but also the transit time through a nearby azimuth. As a result, we get an approximate value of the angular velocity $\dot{A}_C$, which can be inserted into the equations relating the $D_{\pi,C}$ to be determined to other already known orbital elements.

The results can be better utilized in case it is possible to dispose of those from a near station, with respect to latitude.

Denoting by $h_C'$ and $h_C''$ the determinations at the two stations, and similarly for $A_C$ and $t_C$, the difference between $A_C'$ and $A_C''$ is particularly small and can be approximately foreseen according to the inclination $i_E$ of the orbit. It is then possible to calculate the arc of the greatest circle on the Earth's surface included between the two culmination points. Hence, knowing the time difference $t_C'' - t_C'$, it is possible to obtain an approximate value of the satellite angular velocity $\dot{\theta}$ on the orbit and subsequently the values of $Z_C$ and $D_{\pi,C}$ are approximated according to the relationships among the different elements.

The processes for the best utilization of the tracking results could vary with regard to the total of data in possession and obtained from different stations, at more or less simultaneous time instants.

The use of stations, classified as of mean and high accuracy in Table I, will be subsequently necessary in order to derive with a better accuracy the orbital elements. The setting of these stations for the culmination conditions will be in general directed by the results obtained from the stations having a lower level of accuracy.

From the previous illustration, the functions to be met by the stations of the various categories in Table I are deduced as follows:

(a) *Low accuracy*: a better approximation for the orbital elements already deduced from simple sighting;

(b) *Mean accuracy*: configuration and positioning of the orbit more accurate with regard to elements of a more difficult determination, such as the eccentricity, the anomaly of perigee, the variation velocities of the orbital plane;

(c) *High accuracy*: differentiation between the predicted values and the observed values, both for control and to separate variations inherent to secondary forces and secular effects.

Hereinafter some problems arising from the tracking near culmination are taken into consideration.

Vol. 4 1958

The order of magnitude of the intervening variables can be obtained by a first approximation analysis, which can be sufficient under certain aspects.

A more accurate evaluation may be required for the solution of some problems. It is then necessary to carry out step-by-step approximations, some of which will be shown.

The characteristic of preference for the tracking method near culmination is the reduced angular velocity in altitude during the observation interval. Particularly when no recording methods of the angular coordinates are employed, the accuracy to be obtained for the measurement of the altitude angle $h$ is for all practical purposes inversely proportional to the slope of the angular velocity versus time diagram.

The usefulness of such a method will be appreciated according to the order of magnitude of accuracy in the measurement of $h$. Some indications will be obtained in determining the function $\dot{h}(t)$, which is one of the first problems to be solved.

Subsequently, it is necessary to determine the azimuth of the culmination point and the relative angular velocity, the duration of sighting, the corrections for step-by-step approximations, and other problems regarding the utilization of the observation results, in order to define the orbital elements and their variations.

## II. Approximate Expressions of Parameters Near Culmination

### 1. Approximate Assumptions in the Analysis of the Problems

Let us designate by $\tau$ a reference system for the coordinates, which can be orthogonal cartesian or spherical. The origin or center will be taken at the Earth's center of gravity $G_T$ (geocentric system), or at the point $P$ where the observer is located (topocentric system); the two cases will be designated by $\tau_G$ and $\tau_P$. The origin may be also chosen in a different way. The orientation of the system can be invariable with respect to fixed stars or rotating jointly with the Earth. Let us call the two references: "absolute" (or with respect to the celestial sphere), and "relative" (or terrestrial), designating them by $\tau_a$ and $\tau_r$ and eventually adding other subscripts, for instance: $\tau_{r,P}$ = relative topocentric system.

We state now the following approximate assumptions, among the others which are to be introduced in connection to particular problems.

$I_1$ = The Earth's surface $\Sigma_T$ can be approximated as a sphere $\Gamma$. Its center can be chosen in two ways, viz.:

(a) $\Gamma = \Gamma_G$, sphere having its center at the center of gravity $G_T$ of the Earth. The radius will be assumed as intermediate between the equatorial and polar radii, $R_e$ and $R_p$, or equal to the geocentric radius of $P$, $R_P = \overline{G_T P}$, specified, for instance by $\Gamma_G(R_P)$.

(b) $\Gamma = \Gamma_P$, sphere which more closely approximates the geoid in the neighbourhood of $P$. The center $G_P$ will be chosen on the vertical passing through $P$, and the radius can be given a value $R_K$ corresponding to the total curvature $K$ of $\Sigma_T$ in $P$.

$I_2$ = The absolute trajectory arc $l_{a,J}$ (with respect to $\tau_a$) followed by the satellite $S_g$ during an interval $J$ for the independent variable (for instance, the time), can be considered as belonging to a plane, $\Pi_{l,a}$, passing through the Earth's center $G_T$. The form of $l_{a,J}$ can be approximated by an ellipse, $\varepsilon_a$.

The time interval $J_t$, during which the form and the orientation of $l_{a,J}$ with respect to the fixed stars are considered as constants, will not be in general greater than the period of revolution $T$.

$I_3$ = The relative trajectory arc $l_{r,J}$ (with respect to $\tau_r$), followed by $S_g$ during $J$, can be considered as belonging to a plane, $\Pi_{l,r}$, passing through $G_T$. The form of $l_{r,J}$ can be approximated by an ellipse, $\varepsilon_r$.

The time interval $J_t$ can be, for instance, established between the instants when $S_g$ reaches a pre-fixed angle of altitude $h$ with respect to $P$, in particular, for $h = 0$, between sunrise and sunset of $S_g$ on the horizon (rational, horizontal plane, $\Pi_P$, through $P$).

$I_4$ = The arc $l_{a,J}$, as per $I_2$, can be approximated by an arc of a circle $\mathcal{C}_a$, having as a center $G_T$, in the interval included between the instants when $S_g$ reaches given values of the angle $h$.

$I_5$ = The arc $l_{r,J}$, as per $I_3$, can be approximated by an arc of a circle $\mathcal{C}_r$, having as a center $G_T$.

$I_6$ = The arc of relative trajectory $l_{r,J}$ and the corresponding arc of absolute trajectory $l_{a,J}$ differ by displacements which can be regarded as negligible (with respect to the length of the above arcs and within a given approximation).

It is to be noted that once assumption $I_6$ is accounted for, one may derive $I_3$ from $I_2$ and $I_5$ from $I_4$; nevertheless, the assumptions in question can also be regarded separately.

Vol. 4 1958

Other assumptions of first approximation, which may be designated as $I_{7,8,9}$ are as follows: The influence of the observer altitude above sea level (with respect to the satellite altitude), the refraction of the rays of light in crossing the Earth's atmosphere, the light aberration, are considered negligible.

## 2. Range of Stations

In analyzing the problems relative to the range of the stations, it is generally sufficient to determine the parameters in a first approximation.

Let us gather together some of relations to be applied hereinafter.

We designate by $P$ the position of the observer and by $S_g$ the satellite (of geophysical type, i.e., orbiting in general at a distance above the Earth's surface of less than 1000 kms).

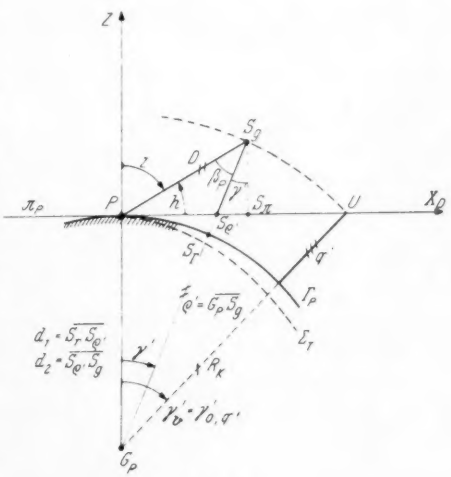


Fig. 1

Assume a system of reference orthogonal axes, having their origin in $P$, Fig. 1, $Z$ vertical, $X_D$ in the vertical plane $\Pi_D$ through $S_g$ and on the same side of the latter. Assume also that the $y_D$ axis is orthogonal to the previous ones and such that the associated trihedral is left-handed.

The horizontal plane through $P$ is designated by $\Pi_P$.

Among the assumptions as per section II, 1, we will now apply $I_1$, that is, we consider the Earth's surface $\Sigma_T$ as a sphere $\Gamma$, namely we apply the form $I_{1,b}$, viz. $\Gamma = \Gamma_P$, a sphere having its center $G_P$ on the vertical through $P$ and radius $R_K$. The Earth's center of gravity $G_T$ is in general to be considered as different from $G_P$.

Other symbols to be used are the following:

$q$ = altitude of satellite with respect to $\Sigma_T$. The symbol $q$ will have subscripts in order to specify the surface by which $\Sigma_T$ is approximated, in particular: $q'$ = altitude of $S_g$ with respect to $\Gamma_P$.

$\varrho$ = distance of $S_g$ from the Earth's center $G_T$. When $\Sigma_T$ is to be approximated by $\Gamma_P$, we have: $\varrho' = \overline{G_P S_g}$.

$h$ = altitude angle of $S_g$, angle formed by $PS_g$ with the horizontal plane through $P$ (already designated by $\Pi_P$). $z$ indicates the zenith distance, a complement of $h$.

$\beta$ = "parallax" of $S_g$, angle under which the radius $PG_T$ is seen from $S_g$. The similar angle relative to $PG_P$ is indicated by $\beta_P$.

$\gamma$ = angle under which $PS_g$ is seen from $G_T$. This angle will be called "radial deflection of $S_g$". The similar angle having its apex $G_P$, instead of $G_T$, is indicated by $\gamma'$ and is called "radial inclination of $S_g$".

$S_\Pi$, $S_\Gamma$, $S_{\varrho'}$ = orthogonal projection of $S_g$ on $\Pi_P$ and points where the radius $G_P S_g$ intersects $\Gamma$ and $\Pi_P$.

$D$, $D_{\varrho'}$ = distances of $S_g$ and $S_{\varrho'}$ from $P$.

$D_H = X_D$ = "horizontal distance" of $S_g$ from $P$. This distance is measured in a horizontal direction.

$d_1$, $d_2$ = lengths of the segments into which $S_{\varrho'}$ divides the segment $S_\Gamma S_G$ (having a length $q'$).

$U$ = point of $\Pi_P$ having a radial distance from $\Gamma_P$ equal to the distance $q'$ which $S_g$ has in the generic position into consideration.

$\gamma'_{0,q'} = \gamma'_U$ = value of $\gamma'$, considered as a function of $h$ and $q'$, for the case $h = 0$, that is a value of $\gamma'$ when $S_g$ is coincident with $U$.

The observations of $S_g$, in order to avoid zones subjected to too strong effects from the atmospheric refraction, will be generally limited to an interval where $h$ is not less than a given value $h_m$ (for instance, $h_m = 30^0$). However, particular observations, even for $h = 0^0$, are not to be excluded.

The range of the stations is conveniently indicated by the great circle arc $PS_\Gamma$ on $\Gamma_P$, expressed by $\gamma'$, measured in radians, degrees, or (for a given $R_K$), in kms.

It is to be noted that:

$$\varrho' = R_K + q' \tag{2.2-1}$$

The angle $\gamma'_{0,q'} = \gamma'_U$, defined above and corresponding to the position $U$ which $S_g$ takes for $h = 0$, and the same $q'$, is derived from:

$$\cos\gamma'_U = R_K/(R_K + q') = 1/(1 + q'/R_K), \tag{2.2-2}$$

or

$$\cos\gamma'_U = 1 - q'/(R_K + q') = 1 - q'/\varrho'. \tag{2.2-2'}$$

By a series expansion of $\cos\gamma'_U$, we have for $\gamma'_U{}^2$ the following approximate expression, neglecting the terms $q'/R_K$ higher than first degree:

$$\gamma'_U{}^2 \cong 2\,q'/(R_K + q') \cdot \qquad [\gamma'_{\text{rad}}]. \tag{2.2-3}$$

To deduce $\gamma'$ in the case of any $h$ (and given $q'$), we must point out:

$$\gamma' = 90^0 - \beta_P - h = z - \beta_P. \tag{2.2-4}$$

Therefore, the calculation of $\gamma'$ is brought back to that of $\beta_P$, as a function of $h$ and $q'$.

Now, taking into consideration the triangle $PG_P S_g$, we have:

$$R_K/\sin\beta = (R_K + q')/\cos h = D/\sin\gamma'. \tag{2.2-5}$$

In particular, we have:

$$\sin\beta = \cos\gamma'_U \cos h = [1/(1 + q'/R_K)]\sin z, \tag{2.2-6}$$

which calls to mind a well-known theorem, particularly used for small values of $\beta_P$, and with the approximation $G_P \equiv G_T$: "The sine of the so-called daily parallax is proportional to the sine of the zenith distance"[1].

From (2.2–4, 6) we obtain the expression of $\gamma'$:

$$\gamma' = \arccos(\cos\gamma'_U \cos h) - h. \tag{2.2–7}$$

Given the altitude $q'$ of $S_g$, two sides of the triangle $PG_PS_g$ are then known and it will suffice to give one of the four elements $D$, $h$, $\beta_P$, $\gamma'$, in order to determine the others, and to such a purpose (2.2–5) can be used jointly with:

$$D^2 = 2R_K(q' + R_K)(1 - \cos\gamma') + q'^2, \tag{2.2–8}$$

$$D^2 + 2DR_K \sin h = 2q'R_K + q'^2, \tag{2.2–9}$$

which give $D$ respectively as a function of $q'$ and $\gamma$, or as an implicit function of $q'$ and $h$.

Some other relations, that can be applied, are those giving $D_r$, $Z$ and $X_D = D_H$, "horizontal distance" of $S_g$:

$$D_r = R_K \tan\gamma' \tag{2.2–10}$$

$$Z = D\sin h = (R_K + q')\cos\gamma' - R_K \tag{2.2–11}$$

$$X_D = D\cos h = (R_K + q')\sin\gamma' = \varrho'\sin\gamma'. \tag{2.2–12}$$

From (2.5–11, 12) we have:

$$X_D/(R_K + Z) = \tan\gamma', \tag{2.2–12'}$$

that can be compared with (2.2–10).

In case that $h = 0$, we have from (2.2–9) a well-known expression:

$$D^2 = 2q'R_K(1 + q'/2R_K) \cong 2q'(R_K + q'), \tag{2.2–13}$$

furthermore, in such a case we have:

$$D = D_r = X_D = R_K \tan\gamma'_U \cong R\gamma'_U. \tag{2.2–13'}$$

For any $h$, from the ratio of (2.2–11, 12) we obtain:

$$\tan h = (\cos\gamma' - \cos\gamma'_U)/\sin\gamma', \tag{2.2–14}$$

and from this, for a small $\gamma'_U$ (and therefore $\gamma'$), we have:

$$\tan h \cong (\gamma'_U{}^2 - \gamma'^2)/2\gamma'. \tag{2.2–15}$$

If $\tan h$ is sufficiently large with respect to unity, that is if the zenith distance $z$ is small, $\gamma'^2$ can be neglected in comparison to $\gamma'_U{}^2$ in eq. (2.2–15), and we may write:

$$\gamma' \cong \gamma'_U{}^2/2\tan h \cong \gamma'_U{}^2 z/2 \cong zq'/(R_K + q'), \tag{2.2–16}$$

which approximates (2.2–7).

In so far as the parameter $d_1 = \overline{S_T S_{\varrho'}}$, is concerned, from Fig. 1 we note that it is a function only of $\gamma'$:

$$d_1 = d_1(\gamma') = R_K(1/\cos\gamma' - 1) \cong R_K\gamma'^2/2, \tag{2.2–17'}$$

while:

$$d_2 = \overline{S_{\varrho'}S_g} = q' - d_1. \tag{2.2–17''}$$

We point out that: "The values of $\gamma'$ and $D$, particularly for $h > h_m$ $(= 30^0)$, and for values of $q'$ of a few hundred kms, are small, having an order of magnitude of a few degrees for $\gamma'$ and of a few hundred kms for $D$".

---

[1] In case $h = 90^0$, the corresponding value of $\beta_P$, called "horizontal parallax", is equal to $90^0 - \gamma'_U$, and we designate it also by $\Pi'_\varphi$, where $\varphi$ is the latitude of $P$. In particular, with the approximation $G_P \equiv G_T$, and for $\varphi = 0$, we have the so-called "equatorial horizontal parallax", $\Pi_0$, such as: $\sin\Pi_0 = R_e/(R_e + q)$, where: $R_e$ = equatorial radius.

Vol. 4 1958

### 3. Relations for a Plane Arc of Trajectory

While in the previous section we have taken into consideration the relations for the parameters in the vertical plane $\Pi_D$, passing through station $P$ and satellite $S_g$, we will now discuss the relations for the parameters in different vertical planes.

As a first approximation, we assume (as per $I_2$ and $I_3$ of section II, 1) that the arc of trajectory may be considered as lying in a plane, $\Pi_l$.

The time interval $J_t$ for which such an assumption applies with a given approximation is longer in the case of an absolute arc of trajectory, $l_{a,j}$, than in the case of a relative arc of trajectory, $l_{r,J}$.

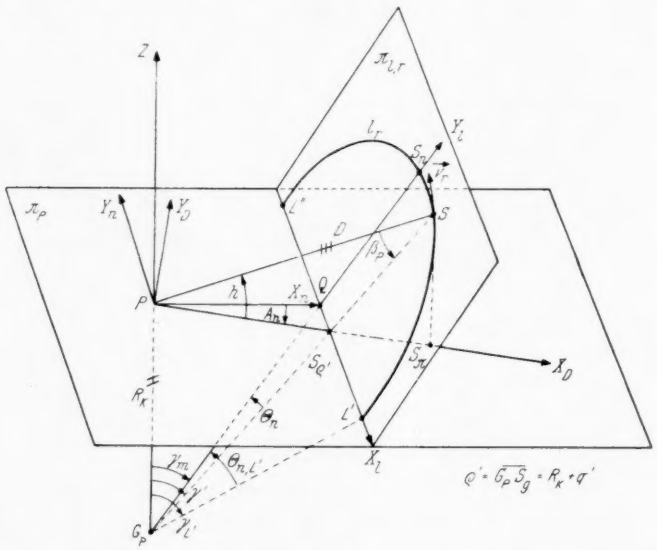


Fig. 2

In order to utilize the results of the previous section, where the Earth's surface $\Sigma_T$ has been taken as a sphere $\Gamma_P$ having its center $G_P$ on the vertical passing through $P$, we will introduce the further assumption that the plane $\Pi_l$ is approximately passing through $G_P$. We will consider separately the corrections to be introduced into the above magnitudes in order to compensate for the errors deriving from the preceding assumptions.

One of these corrections, for instance, must take into consideration the distance $\varrho' = \overline{G_P S_g}$, instead of the radius vector $\varrho = \overline{G_T S_g}$, appearing spontaneously when considering the absolute trajectory of an elliptical form, $\varepsilon_a$, having its focus in $G_T$.

Such a correction will be determined from the vectorial relation:

$$G_T S_g = G_T G_P + G_P S_g. \tag{2.3-1}$$

Similar remarks apply for substituting the altitude $q$, with respect to $\Sigma_T$, with the altitude $q'$, with respect to $\Gamma_P$.

The relative considerations will be given in the next section III, 5, with reference to eqs. (3.5–40, 41).

We will develop the mentioned relations with regard to the arc of relative trajectory $l_{r,J}$, but they can generally be applied also to the absolute trajectory.

Let us introduce the following definitions and symbols, with reference to Fig. 2.

$X_l$ = abscissa axis in the plane $\Pi_{l,r}$ and intersection of the latter with the horizontal plane $\Pi_P$, passing through $P$

$X_n$ = abscissa axis in the plane $\Pi_P$, and perpendicular to the axis $X_l$.

$Q$ = intersecting point of $X_l$ with $X_n$, taken as origin of the coordinates on axes $X_l$, $Y_l$ in $\Pi_l$.

$A_n$ = azimuth of $S_g$ with respect to $X_n$, calculated positively in a clockwise direction (for the observer oriented as the $Z$ axis).

$\theta_n$ = anomaly of $S_g$ in a polar coordinate system in the plane $\Pi_{l,r}$, having its pole in $G_P$, and such an angle being measured starting from $Y_l$, with the positive sign in the counterclockwise direction (for the observer located in $P$).

$\gamma_m$ = inclination of the plane $\Pi_{l,r}$ with respect to the vertical $Z$.

$L$ = one of the points where $S_g$ rises or sets with respect to $\Pi_P$, designated respectively by $L'$ and $L''$, and intersections of the relative trajectory $l_r$ with $\Pi_P$. The distance of said points from $\Gamma_P$ (the sphere by which $\Sigma_T$ is approximated) is indicated with $q'_L$.

The particular positions that $S_g$ takes on the absolute trajectory $l_a$ in correspondence to $L'$ and $L''$ are indicated with $S_{g,L'}$ and $S_{g,L''}$.

The point $Q$ on the axis $X_n$ has the following abscissa:

$$X_{n,Q} = R_K \tan \gamma_m. \tag{2.3-2}$$

In conformity with the axes chosen, the following relations apply, with reference to Fig. 2:

$$X_n = X_{n,Q} + Y_l \sin \gamma_m \tag{2.3-3}$$

$$Y_n = - X_l \tag{2.3-3'}$$

$$Z = Y_l \cos \gamma_m. \tag{2.3-3''}$$

As a function of $\theta_n$, the coordinates $X_l$, $Y_l$ are given by:

$$X_l = - \varrho' \sin \theta_n \tag{2.3-4}$$

$$Y_l = \varrho' \cos \theta_n - R_K / \cos \gamma_m. \tag{2.3-4'}$$

From (2.3-2, 3, 3'') we have for $X_n$:

$$X_n = (R_K + Z) \tan \gamma_m. \tag{2.3-5}$$

On the other hand, with reference to the abscissa $X_D$, defined in the previous section as the horizontal distance of $S_g$ from $P$, we obtain:

$$X_n = X_D \cos A_n. \tag{2.3-6}$$

By writing, now, eq. (2.2-12') in the form:

$$X_D = (R_K + Z) \tan \gamma' \tag{2.3-7}$$

from the comparison of the latter with (2.3-5, 6) we get:

$$\cos A_n = \tan \gamma_m / \tan \gamma'. \tag{2.3-8}$$

Pointing out that:

$$X_l = X_D \sin A_n, \tag{2.3-9}$$

and recalling (2.2-12), which we write in part again:

$$X_D = \varrho' \sin \gamma' \tag{2.3-10}$$

by means of (2.3-4), we obtain:

$$\sin A_n = - \sin \theta_n / \sin \gamma'. \tag{2.3-11}$$

From (2.3-8, 11), squared and added in order to eliminate $A_n$, we have:

$$\sin^2 \gamma' = \sin^2 \gamma_m + \cos^2 \gamma_m \sin^2 \theta_n. \tag{2.3-12}$$

This corresponds to:

$$\cos \gamma' = \cos \theta_n \cos \gamma_m, \tag{2.3-13}$$



Vol. 4 1958

expressing a well-known theorem on the rectangular spherical triangles, Fig. 3, as well as (2.3–8, 11).

Eq. (2.3–13) may also be derived from the two expressions of $R_K + Z$, Fig. 2:

$$R_K + Z = \varrho' \cos\gamma' = \varrho' \cos\theta_n \cos\gamma_m. \qquad (2.3\text{–}14)$$

Taking into consideration any small angle $\alpha$ (a few degrees), the following approximation can be used:

$$\sin\alpha \cong \alpha, \qquad \cos\alpha \cong 1. \qquad (2.3\text{–}15', 15'')$$

These relations can be generally applied to $\gamma_m$, and, with less precision, even to $\theta_n$ and $\gamma'$, but not always to $A_n$.

In such an approximation, we have in particular from (2.3–12) for the angle $\theta_n$ considered as a function of $\gamma'$ and $\gamma_m$:

$$\theta^2_{n,\gamma',\gamma m} \cong \gamma'^2 - \gamma_m{}^2, \qquad (2.3\text{–}16)$$

which may be also obtained taking into consideration the rectangular spherical triangle $PQS_g$ (Fig. 3), assumed as a plane triangle and taking the radian as the length unit.

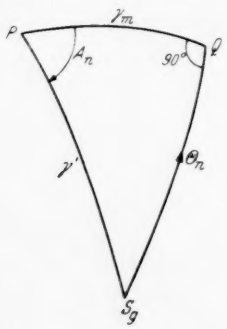


Fig. 3

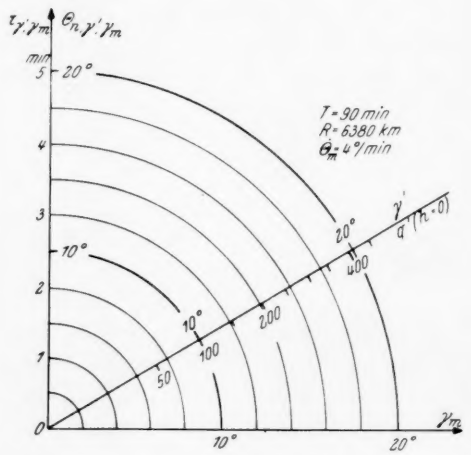


Fig. 4

The plotting of (2.3–16) in a system of cartesian axes $\theta_{\gamma',\gamma m}$ and $\gamma'$, choosing equal measure units for the coordinates, is given by a family of equilateral hyperbolas having as a parameter $\gamma_m$, or, in case the axes are $\theta_{\gamma',\gamma m}$ and $\gamma_m$, we have a family of circles having as a parameter $\gamma'$.

The second plotting given by Fig. 4.

In case a particular value of the altitude $q'$ of $S_g$ is considered, and therefore of $\gamma'_U$, due to (2.2–2), in Fig. 4 we may write, near the values of parameter $\gamma'$, those of $h$, according to (2.2–14), or, if the figure is considered for a particular value of $h$, we may write near the values of $\gamma'$ those of $\gamma'_U$ or of $q'$, as was the case in Fig. 4, where we have considered in particular the case $h = 0$ (then, $\gamma' = \gamma'_U$).

In so far as $A_n$ is concerned, we have moreover from the ratio of (2.3–8, 11) and keeping in mind (2.3–13):

$$\tan A_n = -\tan\theta_n / \sin\gamma_m. \qquad (2.3\text{–}17)$$

The latter in the approximation (2.3–15) for $\theta_n$ and $\gamma_m$ reduces to:

$$\tan A_n \cong -\theta_n/\gamma_m, \tag{2.3–18}$$

or, if we assume that approximation for $\gamma'$, we have from (2.3–11):

$$\sin A_n \cong -\theta_n/\gamma', \tag{2.3–19}$$

which is also deducible from the triangle $PQS_g$ of Fig. 3, considered as a plane triangle, and taking into account the direction assumed as positive for $A_n$ and $\theta_n$.

## 4. Angular Velocity in Altitude Near Culmination for a Circular Arc of Trajectory

We have already mentioned that the stationary condition for the altitude angle $h$ characterizes the tracking method near the "culmination point", $C$. The precision in the measurement of $h_C$ increases as the slope of the angular velocity versus time curve (in the neighbourhood of the culmination instant) decreases.

Consider a point, $S_{g,0}$, where the satellite is on the relative trajectory, $l_{r,J}$, at an instant $t_0$ near the culmination instant, $t_c$. The angle $h(t)$, in a second order neighbourhood of $t_0$, may be expressed by:

$$h(\Delta t) = h_0 + \dot{h}_0 \Delta t + (\ddot{h}_0/2)\,(\Delta t)^2, \tag{2.4–1}$$

where $h_0$, $\dot{h}_0$, $\ddot{h}_0$ are the values that $h(t)$ and its first and second derivatives[1] have in $S_{g,0}$, while:

$$\Delta t = t - t_0. \tag{2.4–2}$$

The angular velocity in altitude in the same neighbourhood has a linear change:

$$\dot{h}(\Delta t) = \dot{h}_0 + \ddot{h}_0 \Delta t, \tag{2.4–3}$$

and for $t = t_C$:

$$\dot{h}_C = 0, \tag{2.4–4}$$

while the slope of the plot is constant, in such an assumption:

$$\ddot{h}(\Delta t) = \ddot{h}_0 = \ddot{h}_C. \tag{2.4–5}$$

A schematic plotting of said functions is given in Fig. 5.

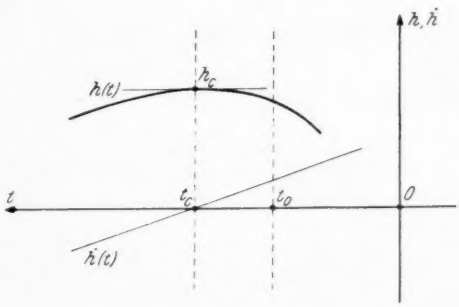


Fig. 5

The maximum variation the function $h(t)$ undergoes in an amplitude interval $2\,\Delta t$, having as a medium point $t_C$, is given by:

$$(\Delta h)_{\max} = (\ddot{h}_C/2)\,(\Delta t)^2, \tag{2.4–6}$$

putting in the previous equations $t_0 \equiv t_C$.

Assuming that, in the measure of $h_C$, the visual observation requires always a same $\Delta t$, the absolute accuracy of the measure will be inversely proportional to the slope $\ddot{h}_C$ of the plot $\dot{h}(\Delta t)$, as indicated by Eq. (2.4–6).

In order to evaluate as a first approximation the function $\dot{h}(\Delta t)$, and the corresponding $\ddot{h}_C$, we will consider the particular case, according to assumption $I_5$

[1] The time derivatives are indicated by dots placed over the symbols of the variables.

Vol. 4 1958

of section II,1, in which the arc $l_{r,J}$ of relative trajectory can be sufficiently approximated by an arc of circle $\mathscr{C}_r$.

In order to utilize the equations of the previous sections II, 2 and II, 3, where the Earth's surface $\Sigma_T$ has been considered approximated by a sphere $\Gamma_P$ having $G_P$ as its center, we will assume, contrary to the above assumption $I_5$, that the center of $\mathscr{C}_r$ can be assumed approximately at $G_P$.

Any eventual correction may be considered apart, for instance in order to take into account that $l_{r,J}$ has with a better approximation an elliptic form, as per assumption $I_3$ of section II, 1.

With reference to Fig. 2, already considered, we have now that the circle $\mathscr{C}_r$, approximating $l_{r,J}$, has the same center $G_P$ as the sphere $\Gamma_P$ approximating $\Sigma_T$, so that all points of $\mathscr{C}_r$ will be at the same distance $q'$ from $\Sigma_T$. In the same way, the points $L'$ and $L''$, where $\mathscr{C}_r$ intersects the horizontal plane $\Pi_P$, passing through $P$, will then be at the same distance from $P$, according to (2.2–9), written for $h = 0$.

In such a case, the triangle $L'PL''$ being isosceles, the median line through $P$ coincides with the axis $X_n$, orthogonal to the base $L'L''$, and the culmination point $C$ coincides, due to symmetry, with the point $S_n$ (Fig. 2), where the axis $Y_l$ intersects $l_{r,j}$. In such a case this point coincides also with the apex $V$ of the arc (point of $Z_{\max}$), while generally these points are different (Fig. 7).

In order to obtain $\dot{h}(t)$, we can start from one of the equations for the trigonometric functions of $h$, for instance:

$$\sin h = Z/D. \tag{2.4–7}$$

By derivation we have:

$$\dot{h}\, D \cos h = \dot{Z} - \dot{D} \sin h. \tag{2.4–8}$$

The term $\dot{D}$ which appears in the above equation may be obtained by derivation of (2.2–9), which we write again in the form:

$$D^2 + 2\, Z\, R_K = \varrho'^2 - R_K{}^2. \tag{2.4–9}$$

For a circular arc ($\varrho' = \text{const}$), we have:

$$\dot{D}\, D = - R_K \dot{Z}. \tag{2.4–10}$$

By this equation, we have from (2.4–8):

$$\dot{h} = \dot{Z}\, K'/D \cos h, \tag{2.4–11}$$

where we have put:

$$K' = K'(D, h) = 1 + R_K \sin h/D. \tag{2.4–12}$$

The factor $K'$, appearing in eq. (2.4–11) of $\dot{h}$, includes two terms, 1 and $R_K \sin h/D$, which correspond respectively to the two terms $\dot{Z}$ and $\dot{D} \sin h$ of (2.4–8).

In place of $\dot{Z}$, in eq. (2.4–11), we may have $\dot{Y}_l$, taking into consideration that, due to (2.3–3''), we get:

$$\dot{Z} = \dot{Y}_l \cos \gamma_m. \tag{2.4–13}$$

On the other hand, by derivation of (2.3–4') we have, for $\varrho' = \text{const.}$:

$$\dot{Y}_l = - \varrho'\, \dot{\theta}_n \sin \theta_n. \tag{2.4–14}$$

This equation and (2.4–13) could be substituted in (2.4–11), thus obtaining for $\dot{h}$ an equation where $\sin \theta_n$ appears.

However, the arc $\theta_n$ being small, it may be substituted for the sine, and may be expressed by:

$$\theta_n = \dot{\theta}_n\, \Delta t, \tag{2.4–15}$$

$\Delta t$ being the time increment with respect to the transit instant through the culmination point $C$, now coinciding with $S_n$, Fig. 2.

It is to be noted how, in case of a circular arc, designating by $v_r$ the velocity (reference is made to the relative trajectory) and by $a_{r,N}$ the centripetal acceleration, we get:

$$v_r = \varrho' \dot{\theta}_n, \tag{2.4-16}$$

$$a_{r,N} = v_r^2/\varrho' \,^1. \tag{2.4-17}$$

By these equations, from (2.4-14) we obtain for $\dot{Y}_l$:

$$\dot{Y}_l \cong - a_{r,N} \Delta t. \tag{2.4-18}$$

The expression of $\dot{h}$, which we are seeking, as a function of $\Delta t$ is obtained by substituting (2.4-13, 18) in (2.4-11); it is similar to (2.4-3):

$$\dot{h}\,(\Delta t) = \ddot{h}_c \Delta t, \tag{2.4-19}$$

with the following expression for $\ddot{h}_c$:

$$\ddot{h}_c \cong - (a_{r,N} K/D)_c, \tag{2.4-20}$$

where the parameters $a_{r,N}$, $D$ are calculated in $C$, and the function $K$ is defined by:

$$K = K\,(D, h, \gamma_m) = (1 + R_K \sin h/D) \cos \gamma_m / \cos h. \tag{2.4-21}$$

As it is seen from (2.4-20), the inversed slope $\ddot{h}_c$ in the plot of $\dot{h}(\Delta t)$, for given $a_{r,N}$ and $K$, increases together with $D$, as well as the accuracy in the measure of $h_c$, due to what has been said.

The centripetal acceleration $a_{r,N}$, appearing in the expression (2.4-20) of $\ddot{h}_c$, presents limited changes (depending essentially on the altitude $q'$) for the satellites having a geophysical use.

In the function $K$, according to eq. (2.4-21), the factor $\cos \gamma_m$ can be replaced by the unity, as was the case in the computation of the values of $\ddot{h}_c$ listed in Table III (it has been assumed $a_{r,N} = 10$ m/sec$^2$).

Table III. $\ddot{h}_C$ (*arc seconds/sec*$^2$)

| $h$ \ $D$ | 500 km | 1,000 | 1,500 | 2,000 |
|---|---|---|---|---|
| 30° | 35.2 | 10.0 | 5.0 | 3.1 |
| 45° | 58.5 | 16.1 | 7.8 | 4.7 |
| 60° | 99.3 | 26.9 | 12.9 | 7.8 |

The above function $K$ can be expressed also in other variables; for instance, once the relationship $R_K/D$ has been obtained from (2.2-5):

$$R_K/D = \cos(\gamma' + h)/\sin \gamma', \tag{2.4-22}$$

[1] It is to be noted that in the absolute motion of $S_g$, with a velocity $v_a$, the corresponding centripetal acceleration $a_{a,N} = v_a^2/\varrho$ equals in the case of a circular motion, the gravitational attraction $H_1(\varrho)$ per unit of mass, which we designate as $g_{p,\varrho}$. Therefore, we have: $g_{p,\varrho} = H_1(\varrho) = g_p\,(R_p/\varrho)^2$, where $g_p$ is the gravitational acceleration at the pole and $R_p$ the relative radius. In assumption $I_6$ of section II, 1, stating that the relative and absolute trajectories differ from each other by a small quantity in the interval $J_t$, we have, at least in the order of magnitude: $a_{r,N} \cong a_{a,N} \cong g_{p,\varrho}$ and (2.4.18) becomes: $\dot{Y}_l \cong - g_{p,\varrho} \Delta t$, as in the fall of weights.

Vol. 4 1958

after substitution into (2.4–21) and some simplifications, we get:

$$K = \cos\gamma_m \sin(\gamma' + h)/\sin\gamma'. \tag{2.4–23}$$

This equation shows that when the values of $h$ approach $90^0$, then $K \to 1/\gamma'$, that is, due to (2.2–16), $K' \to \varrho'/z\,q'$, ($z$ = zenithal distance), while $D \to q'$. Therefore, in such a case:

$$\ddot{h}_c \cong -\,a_{r,N}\,\varrho'/zq'^2. \tag{2.4–24}$$

In particular, if the trajectory is passing through the zenith, then:

$$z \cong -\,(v_r/q')\,\Delta t, \tag{2.4–25}$$

and $\dot{h}(\Delta t)$, bearing in mind (2.4–17, 19), at culmination does not go to zero, but retains the value:

$$\dot{h}_{90^0} = -\,\dot{z}_{90^0} = v_r/q'. \tag{2.4–26}$$

## 5. Azimuth Velocity Near Culmination

By knowing the value, even if with a limited approximation, that the azimuthal angular velocity, $\dot{A}$, reaches near the culmination point $C$, we are able to set in advance the eventual following-up devices, fitted to the collimation instrument.

Subsequently, the value of $\dot{A}$, measured during the observations, can be introduced into the relations connecting it to other parameters, in order to determine them.

With reference to the expression (2.3–8) of $\cos A_n$, by derivation we obtain[1]:

$$\dot{A} = \dot{\gamma}\tan\gamma_m/\sin^2\gamma'\sin A_n. \tag{2.5–1}$$

Here the angular velocity $\dot{\gamma}$ appears. This can be obtained as a function of $\dot{\theta}$ by deriving (2.3–13). Keeping in mind (2.3–11), we have:

$$\dot{\gamma} = \dot{\theta}_n\cos\gamma_m\sin\theta_n/\sin\gamma' = -\,\dot{\theta}_n\cos\gamma_m\sin A_n. \tag{2.5–2}$$

By substituting into (2.5–1), we get:

$$\dot{A}_n = -\,\dot{\theta}_n\sin\gamma_m/\sin^2\gamma'. \tag{2.5–3}$$

In case $A_n = 0$, that is in correspondence to $S_n$, Fig. 2, where $\gamma' = \gamma_m$, we obtain:

$$\dot{A}_{n,0} = -\,\dot{\theta}_n/\sin\gamma_m. \tag{2.5–4}$$

Therefore, we can write:

$$\dot{A}_n = \dot{A}_{n,0}\,K_A \tag{2.5–5}$$

where we have placed, also recalling (2.3–12):

$$K_A = (\sin\gamma_m/\sin\gamma')^2 = 1/(1 + \operatorname{cotg}^2\gamma_m\sin^2\theta). \tag{2.5–6}$$

These equations apply within the assumptions of section II, 3, for a trajectory lying in a plane, passing with a sufficient approximation through the center $G_P$ of the sphere by which the Earth's surface is approximated in the neighbourhood of $P$.

In case the arc of trajectory be approximately circular, as it was described in section II, 4, its apex then coincides with $S_n$, this becoming the culmination point, and the relative angular velocity at the azimuth has the following expression, derived according to (2.5–4) and by (2.2–16) and (2.4–16):

$$\dot{A}_{n,0} = -\,\dot{\theta}_n\,(\varrho'/X_{D,V}) = -\,v_r/X_{D,V}, \tag{2.5–7}$$

where $X_{D,V}$ indicates the horizontal distance from $P$ of the apex $V$ ($\equiv S_n$).

Eq. (2.5–7) shows that $\dot{A}_{n,0}$ is amplified with respect to $\dot{\theta}_n$ in the ratio $\varrho'/X_{D,V}$.

[1] The subscript $n$ for the azimuth points out that we have taken the direction of axis $X_n$ (Fig. 2) as the origin. However, it can be omitted in the derivative, $\dot{A}_n$, which does not depend upon the origin.

When the approximation (2.3–15) is used for $\theta$, $\gamma'$ and $\gamma_m$ eqs. (2.5–5, 6) yield:

$$\dot{A}_{n,0}/\dot{A}_n \cong (\gamma'/\gamma_m)^2 \cong 1 + (\theta_n/\gamma_m')^2, \tag{2.5–8}$$

and also, recalling (2.4–15), (2.5–4):

$$\dot{A}_{n,0}/\dot{A}_n \cong 1 + (\dot{A}_{n,0}\,\Delta t)^2. \tag{2.5–9}$$

When $h \to 90^0$, then $\gamma_m \to 0$, and $\dot{A}_n$ takes very high values. Simultaneously, an indetermination for the azimuths arises in the neighbourhood of the culmination point.

## 6. Duration of the Trajectory Above the Horizon

More generally, we determine the time $\tau$ elapsing between the two transits of $S_g$ at the altitude $h$ with respect to $P$, and in particular, for $h = 0$, we obtain the time between the rise and the setting of $S_g$ on the horizon (rational for $P$).

For the actual visibility of the satellite, it will then be necessary to consider the lighting conditions, as it has already been pointed out.

In the evaluation of $\tau$ as a first approximation, we take into account the assumptions $I_{1,b}$ and $I_5$ of section II, 1, spherical Earth and circular arc of relative trajectory, $l_{r,J}$, with its center taken here approximatively as $G_P$.

Moreover, we assume that the angular velocity $\dot{\theta}$ in the interval $\tau$ takes an almost constant value $\dot{\theta}_\tau$ and therefore, according to (2.4–15):

$$\tau \cong 2\,\theta_n/\dot{\theta}_\tau, \tag{2.6–1}$$

where $\theta_n$ will be calculated in correspondence with $h$.

The order of magnitude of $\dot{\theta}_\tau$ is indicated by the average angular velocity $\dot{\theta}_m$, called also "average motion", during the revolution period $T$:

$$\dot{\theta}_m = 2\pi/T, \tag{2.6–2}$$

and, correspondingly, $\tau$ has, as an order of magnitude, the fraction $\theta_n/\pi$ of $T$.

A more approximate value of $\dot{\theta}_\tau$ is given by the angular velocity $\dot{\theta}_{n,c}$ near the culmination point $C$, which for a circular arc satisfies eq. (2.4–16):

$$\dot{\theta}_\tau \cong \dot{\theta}_{n,c} \cong (v_r/\varrho')_c. \tag{2.6–3}$$

The terms $\tau$ and $\theta_n$ can be expressed as functions of $\gamma_m$ and $h$. In the case of a constant altitude $q'$, $h$ being determined by $\gamma'$ according to (2.2–7), $\tau$ and $\theta_n$ can be expressed as functions of $\gamma'$ and $\gamma_m$. As a consequence, with reference to (2.3–13) we have:

$$\tau_{\gamma',\gamma m} = 2\,\theta_{n,\gamma',\gamma m}/\dot{\theta}_\tau \cong (1/\dot{\theta}_{n,c}) \arccos(\cos\gamma'/\cos\gamma_m). \tag{2.6–4}$$

In case $h = 0$, the variable $\gamma'$ takes, for $q' = \text{const.}$, the value $\gamma'_U$, given by (2.2–2), and correspondingly (2.6–4) gives $\tau_{\gamma' U,\gamma m}$.

If the trajectory passes through the zenith ($\gamma_m = 0$), then $\theta_n$ reduces to $\gamma'$:

$$\theta_{n,\gamma',0} = \gamma', \tag{2.6–5}$$

and when $h = 0$ is further specified, we have according to (2.2–3):

$$\theta_{n,\gamma' U,0} = \gamma'_U \cong (2\,q'/\varrho')^{1/2}. \tag{2.6–6}$$

Consider now the case where $\theta_n$ and $\gamma'$ are small. As a consequence eq. (2.3–16) can be regarded as representative of $\theta_n$ as a function of $\gamma'$ and $\gamma_m$:

$$\theta_{n,\gamma',\gamma m}{}^2 \cong \gamma'^2 - \gamma_m{}^2. \tag{2.6–7}$$

A graph of this equation is represented in Fig. 4, taking as cartesian axes $\theta_{n,\gamma',\gamma m}$ and $\gamma_m$. For a given value of $h$, notice that the values of $\gamma'_U$ and $q'$ are dependent from $\gamma'$ and can be written on side of the parameter $\gamma'$, in Fig. 4. In particular, for $h = 0$, $\gamma' = \gamma'_U$.

The scale of $\theta_{n,\gamma',\gamma m}$ can be arranged with another scale of $\tau_{\gamma',\gamma m}$ on the side, as soon as the value of $\dot{\theta}_\tau$ is established. In Fig. 4 we have taken for $\dot{\theta}_\tau$ the value $\dot{\theta}_m$, obtained from (2.6–2) for $T = 90$ min.

Vol. 4 1958

## III. Further Approximations

### 1. Relative Quasi-Elliptical Trajectory

According to the assumption $I_2$ of section II, 1, the absolute trajectory $l_{a,J}$ of $S_g$ can be considered as an ellipse $\varepsilon_a$, neglecting within the time interval $J_t$ the changes of form and plane $\Pi_{l,a}$ of $\varepsilon_a$ (for instance, for the perturbations due to the Earth's oblateness).

The relative trajectory $l_r$ of $S_g$ with respect to a reference trihedral $\tau_r$, fixed to the Earth, is obtained by compounding the absolute motion with the reciprocal of the tow motion, $M_T$, due to the Earth's rotation.

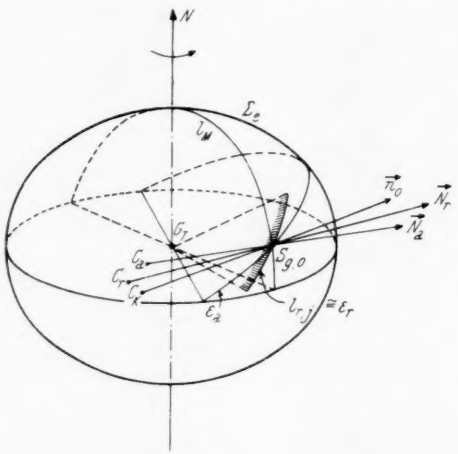


Fig. 6

During the motion $-M_T$, the orbit $\varepsilon_a$ generates a round surface, which we call $\Sigma_e$, on the axis $SN$ of the Earth, Fig. 6. The meridian section of $\Sigma_e$ is indicated in said figure by $l_M$.

Let $S_{g,0}$ be the position of the satellite in a given instant $t = t_0$, and $l_{r,J}$ the relative trajectory arc in a neighbourhood $J_t$ of $t_0$. The arc $l_{r,J}$ is plotted in Fig. 6 in the position it has on $\Sigma_e$ at the instant $t_0$, that is issuing from $S_{g,0}$.

The radii projecting from the center $G_T$ are transformed, due to the motion-$M_T$, into radii $l_r$ projecting from $G_T$.

Bearing in mind that the absolute velocity $\vec{v}_a$ of $S_g$ has an order of magnitude included generally in the interval $7 \div 8$ km/sec, while the tow velocity $\vec{v}_\tau$ is less than 0.5 km/sec for a point located at the Equator, the angle between $\vec{v}_a$ and the relative velocity $\vec{v}_r$ of $S_g$ is small. An amplitude of the same order can be given to the angle between the osculating planes at $\varepsilon_a$ and $l_{r,J}$ in $S_{g,0}$, which we call $\Pi_{a,0}$ and $\Pi_{r,0}$.

Therefore, the plane $\Pi_{r,0}$ intersects the surface $\Sigma_e$ according to a line $l_{r,\pi}$. The latter lies in the neighbourhood of $\varepsilon_a$; furthermore, it represents a second order neighbourhood of $l_{r,J}$ in $S_{g,0}$.

To evaluate the infinitesimal discrepancy of the third order, between $l_{r,\pi}$ and $l_{r,J}$, it should be necessary to carry out the twist calculation of such a line.

Actually, $\varepsilon_a$ and $l_{r,J}$ can be represented in neighbourhoods of second order of $S_{g,0}$ by the respective osculating circles, having as centers $C_a$ and $C_r$ respectively, on the main perpendiculars $\vec{N}_a$, $\vec{N}_r$, belonging to the planes $\Pi_a$, $\Pi_{r,0}$.

The surface $\Sigma_e$ in the neighbourhood of $S_{g,0}$ is approximated by the local sphere $\Gamma_K$, having as center $C_K$, on the perpendicular $\vec{n}_0$ at $\Sigma_e$ in $S_{g,0}$, and radius equal to the inverse of the square root of the total curvature. The above osculating circles are approximately parallels of $\Gamma_K$ and their centers $C_a$, $C_r$, are almost located on the perpendiculars taken from $C_K$ to planes $\Pi_a$ and $\Pi_{r,0}$.

The curvature radius of $\varepsilon_a$ can be determined by the knowledge of $\vec{v}_a$ and of the component according to $\vec{N}_a$ of the absolute acceleration $\vec{a}_a$ (radial, for the

central motions). In a similar way, we can proceed for $l_{r,J}$, computing first the relative acceleration $\vec{a}$, by the Coriolis theorem.

If the orbit $\varepsilon_a$, as is generally the case, has a small eccentricity, then all the curvature centers $C_a$, $C_r$, $C_K$ are not very distant from $G_T$.

## 2. Culmination Point for Elliptical Trajectory

Let us take into consideration some corrections to be applied with respect to the case of a circular arc, considered in section II, 4, when more generally the relative trajectory arc $l_r$ is assumed to be of an elliptical form.

In such a case, as it has already been mentioned, and with reference to Fig. 7, representing a view of the $\Pi_{l,r}$ plane of $l_r$, the culmination point $C$ is generally different both from the apex $V$ of $l_r$ (point of maximum $Z$ and $Y_l$), and from the point $S_n$ (Figs. 2 and 7), where the axis $Y_l$ intersects $l_r$.

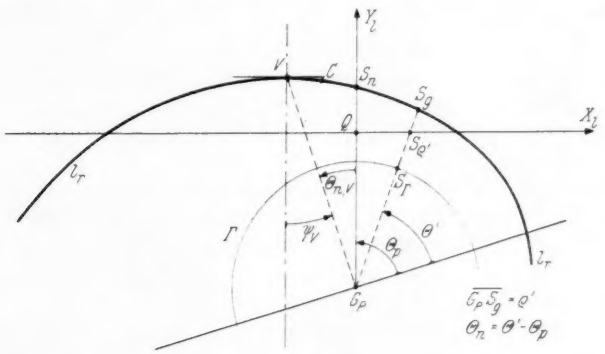


Fig. 7

The culmination point $C$ is defined by the condition $\dot{h} = 0$, which according to (2.4–8) is equivalent to:

$$\dot{Z} - \dot{D} \sin h = 0. \tag{3.2–1}$$

$\dot{D}$ can be obtained by derivation of (2.4–9), and we get in place of (2.4–10), which was valid for $\varrho' = \text{const.}$:

$$D\,\dot{D} = -R_K \dot{Z} + \varrho'\,\dot{\varrho}'. \tag{3.2–2}$$

Substituting into (3.2–1), this condition is written:

$$\dot{Z} = \dot{\varrho}'\,\varrho' \sin h/(D + R_K \sin h). \tag{3.2–3}$$

As in eq. (2.4–13):

$$\dot{Z} = \dot{Y}_l \cos \gamma_m, \tag{3.2–4}$$

while for $\dot{Y}_l$, by derivation of (2.3–4′), we obtain in place of eq. (2.4–14):

$$\dot{Y}_l = -\varrho'\,\dot{\theta}_n \sin \theta_n + \dot{\varrho}' \cos \theta_n. \tag{3.2–5}$$

The apex $V$ of the trajectory is defined by $\dot{Y}_l = 0$, and correspondingly we have for $\theta_n$ from (3.2–5):

$$\tan \theta_{n,V} = (\dot{\varrho}'/\varrho'\,\theta_n)_V \cong \theta_{n,V}, \tag{3.2–6}$$

where $\theta_{n,V}$, being small, can be substituted for its tangent.

In the same approximation, (3.2–5) is written, assuming for $\varrho'$, $\dot{\varrho}'$, $\dot{\theta}_n$ the values in $V$ and recalling (3.2–6):

$$\dot{Y}_l \cong -\varrho'\,\dot{\theta}_n\,\theta_n + \dot{\varrho}' \cong \varrho'_V\,\dot{\theta}_{n,V}\,(\theta_{n,V} - \theta_n). \tag{3.2–7}$$

Vol. 4 1958

In the condition (3.2-3), relative to point $C$, we can take in the right side of the equation the values of the parameters in the apex $V$, which is near $C$, and then by (3.2-4, 7) we have:

$$\theta_{n,V} - \theta_{n,c} = (\dot{\varrho}' \sin h / \dot{\theta}_n X_D K)_V, \tag{3.2-8}$$

where the same expression (2.4-21) holds for $K$, and $X_D = D \cos h$, as in (2.2-12), that is:

$$X_D K = (D + R_K \sin h) \cos \gamma_m. \tag{3.2-9}$$

The following equation for $\theta_{n,c}$ is obtained from (3.2-6, 8):

$$\theta_{n,c} \cong \theta_{n,V} (1 - \varrho' \sin h / X_D K)_V. \tag{3.2-10}$$

The azimuth of the culmination point, $A_{n,c}$, will then be calculated by (2.3-18), or by (2.3-10, 11):

$$\sin A_{n,c} = - (\varrho' / X_D) \sin \theta_{n,c}. \tag{3.2-11}$$

Eq. (3.2-6) can be written:

$$\theta_{n,V} \cong [(1/\varrho') \, d\varrho'/d\theta_n]_V, \tag{3.2-12}$$

allowing the calculation of $\theta_{n,V}$ by step-by-step approximations, considering the values that the right side of the equation takes for an initial value $\theta_n = 0$ and then for the values of $\theta_{n,V}$, subsequently obtained in the left side of the equation.

In the assumption $I_3$ of section II, 1, that the relative trajectory arc $l_{r,J}$ can be approximated in the interval $J$ by an ellipse $\varepsilon_r$, and taking approximately the focus in $G_P$, we have as an expression of $\varrho'$ as a function of $\theta_n$:

$$\varrho' = a_r (1 - e_r^2) / [1 + e_r \cos (\theta_n - \theta_{n,p})], \tag{3.2-13}$$

where: $a_r$ = semi-major axis, $e_r$ = eccentricity, $\theta_{n,p}$ = value of $\theta_n$ for the perigee, variables for which we can take the values inherent to the absolute trajectory, due to the fact that for the calculation of $\theta_{n,V}$ a limited approximation is sufficient in order to pre-set the observation instruments.

From (3.2-13) we get the derivative, $d\varrho'/d\theta_n$:

$$d\varrho'/d\theta_n = [\varrho'^2 / a_r (1 - e_r^2)] \, e_r \sin (\theta_n - \theta_{n,p}), \tag{3.2-14}$$

which can be substituted into (3.2-12). For small values of the eccentricity we have the approximate solution:

$$\theta_{n,V} \cong - e_r \sin \theta_{n,p}, \tag{3.2-15}$$

which shows that $\theta_{n,V}$ has as a maximum $e_r$, in absolute value.

In the limiting case $h = 0$, we have from (2.4-21): $K = \cos \gamma_m \cong 1$, moreover $X_D = D$, while (3.2-10) gives in this case: $\theta_{n,c} = \theta_{n,V}$. For instance, assuming that the distances of $S_g$ from $\Sigma_T$ (Earth's surface) are 300 kms and 2200 kms at the perigee and apogee respectively, we have $e_r \cong 1/8$, the maximum value of $\theta_{n,V}$ is about $7^0$ and assuming $X_D = 2000$ km, we have for $h = 0$ from (3.2-11): $|A_{n,c}|_{\max} \cong 30^0$, a maximum occurring when $|\theta_{n,p}| \cong 90^0$, with an almost sinusoidal change for the intermediate values, according to (3.2-15).

Denote by $\Psi$ the angle formed by the perpendicular to the trajectory with the radius vector $G_T S_g$. The expression calculated for $\tan \Psi$ is identical to the expression computed for $\tan \theta_n$ at $V$. The relationship $\Psi_V = \theta_{n,V}$ stresses (Fig. 7) that the $Y_l$-axis is parallel to the normal to $l_r$ at $V$.

## 3. Relative Velocity

The absolute velocity $\vec{v}_a$ of $S_g$ can be considered as the resultant of the radial $v_{a,\varrho}$ and transversal $v_{a,\theta}$ components:

$$v_{a,\varrho} = \dot{\varrho}, \tag{3.3-1}$$

$$v_{a,\varrho} = \varrho \, \dot{\theta}. \tag{3.3-2}$$

These components are obtained, as it is known, by the knowledge of $\varepsilon_a$.

Let us take as a reference system for the generic position of $S_g$ a geocentric and equatorial system of spherical coordinates. We designate by $\delta$ the declination of $S_g$, and by $\mathscr{P}_\delta$ (Fig. 8) the parallel passing through $S_g$, taking eventually $\varrho$ as a radius of the sphere $\Gamma_G$ of the coordinates.

The relative velocity $\vec{v}_r$ is given by:

$$\vec{v}_r = \vec{v}_a - \vec{v}_\tau, \tag{3.3–3}$$

where $\vec{v}_\tau$ is the tow velocity due to the Earth's rotation motion, $M_T$. We have as a magnitude:

$$v_\tau = \omega_T \varrho \cos \delta \tag{3.3–4}$$

where $\omega_T$ is the angular velocity of the Earth's rotation (see Note 1, p. 213).

Even $\vec{v}_r$ can be considered as compounded of a radial component $v_{r,\varrho}$ according to $G_T S_g$ (we take the same pole in $G_T$) and of a transversal component $v_{r,\theta}$, which is tangent to the sphere $\Gamma_G$ in $S_g$.

Let us designate by $i_{a,\delta}$ and $i_{r,\delta}$, see (3.5–38), the angles formed by $\vec{v}_{a,\theta}$ and $\vec{v}_{r,\theta}$ with the parallel $\mathscr{P}_\delta$ (Fig. 8). While:

$$v_{r,\varrho} = v_{a,\varrho} = \dot{\varrho}, \tag{3.3–5}$$

$v_{r,\theta}$ and $i_{r,\delta}$ satisfy the relations to be obtained projecting (3.3–3) according to the direction of $\mathscr{P}_\delta$, and in an orthogonal direction (on $\Gamma_G$):

$$v_{r,\theta} \sin i_{r,\delta} = v_{a,\theta} \sin i_{a,\delta}, \tag{3.3–6}$$

$$v_{r,\theta} \cos i_{r,\delta} = v_{a,\theta} \cos i_{a,\delta} - v_\tau. \tag{3.3–7}$$

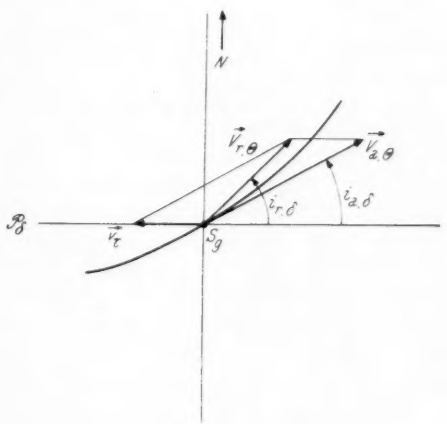


Fig. 8

These equations allow the following approximate solution, $v_\tau$ being small with respect to $v_a$:

$$v_{r,\theta} \cong v_{a,\theta} - v_\tau \cos i_{a,\delta}, \tag{3.3–8}$$

$$i_{r,\delta} = i_{a,\delta} + \Delta i, \tag{3.3–9}$$

$$\Delta i \cong (v_\tau / v_{a,\theta}) \sin i_{a,\delta}. \tag{3.3–9'}$$

Subsequently, we will obtain the magnitude of $\vec{v}_r$ from:

$$v_r^2 = v_{r,\varrho}^2 + v_{r,\theta}^2. \tag{3.3–10}$$

The angle $\psi_a$ that $\vec{v}_a$ forms with $\vec{v}_{a,\theta}$ is given by:

$$\tan \psi_a = v_{a,\theta} / \dot{\varrho}, \tag{3.3–11}$$

and it is small for ellipses having a small eccentricity. The similar angle $\psi_r$ will be almost equal to $\psi_a$, keeping in mind eq. (3.3–5) and $v_{r,\theta}$ being not very different from $v_{a,\theta}$:

$$\psi_r \cong \psi_a, \tag{3.3–12}$$

This means that the eccentricity and the perigee anomaly calculated for the ellipse $\varepsilon_{r,0}$ (which approximates $l_{r,J}$ in the neighbourhood of $S_{g,0}$) are close to the analogous magnitudes calculated for $\varepsilon_a$, as it was said with regard to (3.2–13).

Vol. 4 1958

## 4. Instant of Culmination

In order to predict the instant of culmination with a sufficient approximation, in order to pre-set the observing stations, we can consider the assumption $I_{1,a}$ that is, a spherical Earth $\Gamma_G$, with its center at $G_T$ and radius $R_P$.

Assume now that the right ascension $\alpha_S$ and the instant $t_\delta$ when $S_g$ attains the position $S_\delta$ are known quantities, the position $S_\delta$ being characterized by a declination $\delta_S$, whose value is close or equal to the geocentric latitude ($\varphi_G$) of $P$.

The right ascension $\alpha_P$ of the zenith of $P$ at the same instant $t_\delta$ can be determined by known systems[1]:

Putting:

$$\alpha_r = \alpha_S - \alpha_P, \tag{3.4–1}$$

the arc $\gamma_E$ of the great circle included between $P$ and $S_g$ at the instant $t_\delta$ can be calculated by a known equation of the spherical trigonometry:

$$\cos\gamma_E = \sin\varphi_G \sin\delta_S + \cos\varphi_G \cos\delta_S \cos\alpha_r. \tag{3.4–2}$$

In case $\delta_S = \varphi_G$, particularly considered in Fig. 9, (3.4–2) is simplified to:

$$\cos\gamma_E = 1 - \cos^2\delta_S\,(1 - \cos\alpha_r), \tag{3.4–3}$$

which, for small values of $\alpha_r$, as those generally considered, can be approximated by:

$$\gamma_E \cong \alpha_r \cos\delta_S. \tag{3.4–4}$$

Let us designate by $l_{r,\theta}$ the geocentric projection on $\Gamma_G$ of the relative trajectory $l_{r,J}$ of $S_g$, forming the angle $i_r$ (see the previous section) with the parallel $\mathscr{P}_\delta$.

Actually, the osculating plane in $S_\delta$ to $l_{r,J}$ does not pass through $G_T$; however, as the relative distance is small, we can assume $l_{r,\theta}$ to be a great circle arc in the interval into consideration.

Taking (Fig. 9) from $P_\delta$ an arc of circle at right angles to $l_{r,\theta}$, this is intersected in a point which, with reference to the previous Fig. 2, is the geocentric projection of the origin $S_n$ of the arcs indicated by $\theta_n$.

Designating by $\theta_{n,\delta}$ the arc $S_n S_\delta$ (Fig. 9), and considering $P S_n S_\delta$ to be a rectangular spherical triangle, we have:

$$\tan\theta_{n,\delta} = \tan\gamma_E \cos i_r, \tag{3.4–5}$$

and approximatively, in the limits of applicability of (3.4–4):

$$\theta_{n,\delta} \cong \gamma_E \cos i_r. \tag{3.4–6}$$

The instant $t_n$ of the transit of $S_g$ through $S_n$ is given approximately by:

$$t_n \cong t_\delta - R_P\,\theta_{n,\delta}/v_{r,\theta} \cong t_\delta - \theta_{n,\delta}/\dot{\theta}_\delta. \tag{3.4–7}$$

With an equation similar to the latter, we can calculate the culmination instant $t_c$, keeping in mind the expressions (3.2–6, 10) for the discrepancies $\theta_{n,V}$ and $\theta_{n,c}$ from $S_n$ of the apex $V$ of $l_{r,J}$ and of the culmination point $C$.

The azimuth $A$ of $S_g$ with respect to the meridian is given by:

$$\sin(A - 90^0) = \sin\theta_{n,\delta}/\sin\gamma_E \cong \theta_{n,\delta}/\gamma_E. \tag{3.4–8}$$

While the preceding equations could be considered satisfactory for determining $t_c$, the azimuth could require a better approximation.

To such a purpose, once a first position $S_{n,1}$ of $S_n$ has been established by the above equations, a second more approximate position $S_{n,2}$ will be obtained

---

[1] If $\alpha_S$ and $\delta_S$ are given in dependence of the Greenwich civil average time, $T_m$ (= U.T. = universal time), and $T_s$ is the Greenwich sidereal time corresponding to $T_m$, being $\lambda_P$ = longitude of $P$ (positive to the East of Greenwich), we have: $\alpha_P = T_s + \lambda_P = T_{s,P}$ = sidereal time in $P$.

by imposing the condition at right angles of $P\,S_{n,2}$ to the arc $l_{r,\theta}$, issuing now from $S_{n,1}$, where the new value of $i_r$ is to be calculated. The value of $\gamma_E$ corresponding to $S_{n,1}$ will be obtained from (3.4–2), putting in place of $\delta_S$, and of $\alpha_r = \alpha_S - \alpha_P$, the values $\delta_{S,1}$ and $\alpha_{r,1}$ for the instant $t_{n,1}$ of the transit through $S_{n,1}$ (resulting from the assumed data). Notice that:

$$\delta_{S,1} \cong \delta_S - \theta_{n,\delta} \sin i_r, \tag{3.4–9}$$

where $\delta_S$, $\theta_{n,\delta}$, $i_r$ are the previous values.

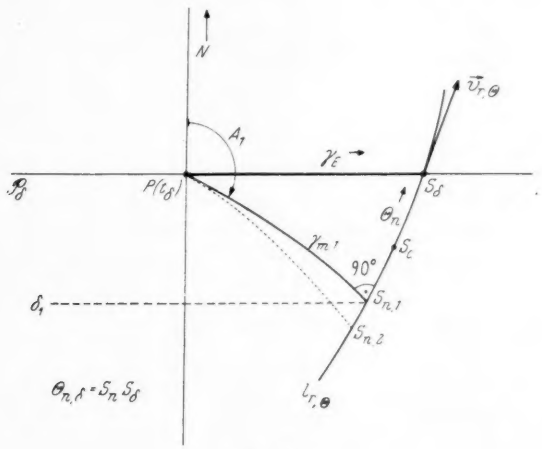


Fig. 9

## 5. Transformations of Coordinates

To study in step-by-step approximations the problems regarding the motion of $S_g$, it is very often required to pass from one system of coordinates to another one, using the corresponding equations of transformation.

We have already introduced (see section II, 1) the symbols $\tau_a$ and $\tau_r$ for the absolute and relative reference systems (the first is valid for an invariable orientation with respect to the fixed stars, the second is fixed to the rotating Earth), specifying by further subscripts $G$ and $P$ whether the origin is in the Earth's center $G_T$, or in the location $P$ of the observer (geocentric and topocentric system).

Let us indicate by $\tau_{a'}$ some reference systems, which, even if they are not rigorously $\tau_a$, have however an orientation, with respect to the fixed stars, varying only slowly, according to the particular problem: for instance, the system of equatorial coordinates, right ascension $\alpha$ and declination $\delta$, receiving well-known corrections due to the phenomena of precession and nutation.

The cartesian coordinates will be indicated as per Table IV, by small Greek letters in the systems $\tau_a$, underlined when the origin is $P$, and by Latin letters in the systems $\tau_r$, small or capital letters respectively, according to the origin in $G_T$ or $P$.

*Table IV*

| System | Origin $G_T$ | Origin $P$ ($P'$, $P''$, ...) |
|---|---|---|
| $\tau_a$, $\tau_{a'}$ | $\xi$, $\eta$, $\zeta$ | $\underline{\xi}$, $\underline{\eta}$, $\underline{\zeta}$ ($\underline{\xi}'$, $\underline{\xi}''$, ...) |
| $\tau_r$ | $x$, $y$, $z$ | $X$, $Y$, $Z$ ($X'$, $X''$, ...) |

Vol. 4 1958

The orientation of the system will be specified by a subscript, for instance $\xi_\omega$, where the letter $\omega$ could vary, according to the special orientation.

The particular point to which the coordinates are referred could be indicated by a further subscript, for instance: $\xi_{\omega,S}$ = coordinate of $S_g$.

In specifying the symbols used, we will have the opportunity to refer to well-known transformation equations of the coordinates.

When two systems differ only in the origin, the following transformation equations hold:

$$\xi_{\omega,Q} = \xi_{\omega,Q} - \xi_{\omega,P}, \tag{3.5-1}$$

giving for $Q \equiv P$ (origin):

$$\xi_{\omega,P} = 0, \tag{3.5-2}$$

and for $Q \equiv G_T$:

$$\xi_{\omega,G} = -\xi_{\omega,P}. \tag{3.5-3}$$

In the case of two systems $\tau_\omega$, $\tau_{\omega'}$, having a different orientation and the same origin, indicating by $x_h$ ($h = 1, 2, 3$) the $x$, $y$, $z$, and by $\varphi_{h,k}$ the directing cosines of the axes, we apply the known equations of transformation ($h = 1, 2, 3$):

$$x_{\omega',h} = \varphi_{h,1}\, x_{\omega,1} + \varphi_{h,2}\, x_{\omega,2} + \varphi_{h,3}\, x_{\omega,3} = \sum_{k=1}^{3} \varphi_{h,k}\, x_{\omega,k}. \tag{3.5-4}$$

Indicating: $\vec{x}_\omega$ = vector of components $x_{\omega,k}$ in the reference $\tau_\omega$, $\Phi_{\omega,\omega'}$ = linear operator characterized by the matrix $||\varphi_{h,k}||$:

$$\Phi_{\omega,\omega'} = ||\varphi_{h,k}||, \tag{3.5-5}$$

eq. (3.5-4) can be synthetized by:

$$\vec{x}_{\omega'} = \Phi_{\omega,\omega'}\, \vec{x}_\omega. \tag{3.5-6}$$

The transfer from $\tau_\omega$ to $\tau_{\omega'}$ sometimes reduces to a rotation around a determined axis. If this is one of the coordinate axes, for instance $Z$, we have for $\Phi$ the particular expression, where $\theta$ is the value of the rotation:

$$\Phi(z;\theta) = \begin{Vmatrix} \cos\theta & \sin\theta & 0 \\ -\sin\theta & \cos\theta & 0 \\ 0 & 0 & 1 \end{Vmatrix}, \tag{3.5-7}$$

Let us consider some particular reference systems, starting from the almost absolute ones.

Let us indicate (Fig. 10):

$\tau_{a',\gamma}$ = equatorial coordinate system with its axis $\xi_\gamma$ oriented towards the vernal equinox $\Upsilon$. The corresponding spherical coordinates are indicated by $\alpha$, $\delta$.

$\tau_{a',l}$ = system where $\xi_l$, $\eta_l$ lie in the orbital plane of $S_g$, $\Pi_{a,l}$. This plane has an inclination $i$ on the equatorial plane, and intersects it in the line of nodes $G_T\Omega$, taken as the axis $\xi_l$.

With regard to the plane $\Pi_{a,l}$ use is made of a polar coordinate system $(\varrho, \theta)$, with center in $G_T$. The angle $\theta$ is measured from the reference line $\xi_l$. The right ascension of $\Omega$ is indicated by $\alpha_\Omega$. For $S_g$ we have:

$$\xi_l = \varrho\cos\theta, \qquad \eta_l = \varrho\sin\theta, \qquad \zeta_l = 0. \tag{3.5-8}$$

$\tau_{a',\nu}$ = equatorial coordinate system, with its axis $\xi_\nu$ directed as $G_T\,\Omega$. The spherical coordinate measured on the equator starting from $\Omega$ is indicated by $\alpha_{\nu,Q}$, for a generic point $Q$:

$$\alpha_{\nu,Q} = \alpha_Q - \alpha_\Omega. \tag{3.5-9}$$

The transfer from $\tau_{a',l}$ to $\tau_{a',\nu}$ is carried out by a rotation operator of the type (3.5–7):

$$\Phi(\xi_l \equiv \xi_\nu; -i) = \begin{Vmatrix} 1 & 0 & 0 \\ 0 & \cos i & -\sin i \\ 0 & \sin i & \cos i \end{Vmatrix}. \qquad (3.5\text{–}10)$$

In the case of $S_g$, the transfer resulting from the polar coordinates $\varrho$, $\theta$ to those in the system $\tau_{a',\nu}$, keeping in mind (3.5–8, 10) is expressed by:

$$\xi_{\nu,S} = \varrho \cos\theta, \qquad \eta_{\nu,S} = \varrho \sin\theta \cos i, \qquad \zeta_{\nu,S} = \varrho \sin\theta \sin i. \qquad (3.5\text{–}11)$$

Denote by $\delta_S$ the declination of $S_g$. Denote also by $\alpha_{\nu,S}$ the difference between right ascension and $\alpha_\Omega$, according to (3.5–9). It follows that:

$$\sin\delta_S = \sin\theta \sin i, \qquad (3.5\text{–}11')$$

$$\tan\alpha_{\nu,S} = \tan\theta \cos i. \qquad (3.5\text{–}11'')$$

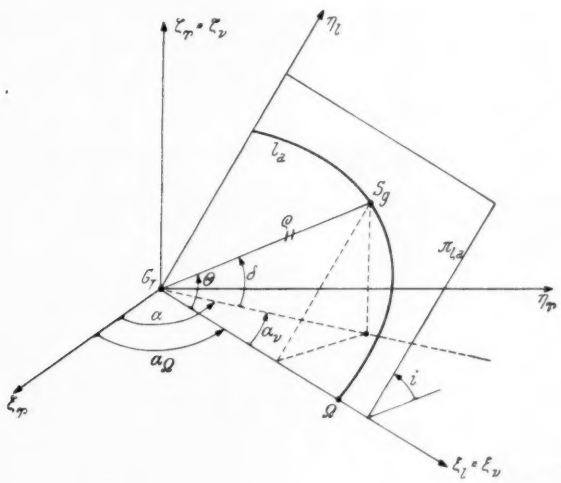


Fig. 10

As in the previous section, we designate for $P$: $\alpha_P$ = right ascension[1] (of the zenith): $R_P, \varphi_G$ = geocentric distance and latitude, $r_P$ = radius of the parallel:

$$r_P = R_P \cos\varphi_G. \qquad (3.5\text{–}12)$$

The coordinates of $P$ with respect to the system $\tau_{a',\nu}$ are, recalling (3.5–9):

$$\xi_{\nu,P} = r_P \cos\alpha_{\nu,P}, \qquad \eta_{\nu,P} = r_P \sin\alpha_{\nu,P}, \qquad \zeta_{\nu,P} = r_P \tan\varphi_G. \qquad (3.5\text{–}12')$$

The direction of the collimation line $P S_g$ is determined with respect to $\tau_{a',\nu}$ by values $\underline{\alpha}_S, \underline{\delta}_S$ of $\alpha$, $\delta$ verifying the following equations:

$$\tan(\underline{\alpha}_S - \alpha_\Omega) = (\eta_{\nu,S} - \eta_{\nu,P})/(\xi_{\nu,S} - \xi_{\nu,P}). \qquad (3.5\text{–}13)$$

$$\tan^2\underline{\delta}_S = (\zeta_{\nu,S} - \zeta_{\nu,P})^2/[(\xi_{\nu,S} - \xi_{\nu,P})^2 + (\eta_{\nu,S} - \eta_{\nu,P})^2]. \qquad (3.5\text{–}13')$$

[1] $\alpha_P$ may be given by the expression: $\alpha_P = \alpha_{P,O} + \dot{\alpha}_T (t - t_0)$, where $\alpha_{P,O}$ = right ascension of $P$ at the instant $t_0$, and $\dot{\alpha}_T$ = Earth's angular velocity with respect to point $\gamma$: $\dot{\alpha}_T = (d_m/d_S)\omega_T$, being: $\omega_T = 2\pi/86400$ rad/sec, the angular velocity of the Earth referred to the mean Sun, and $d_m/d_s = 1 + 1/365.2422$ the ratio between the duration of the mean day and that of the sidereal day.

Vol. 4 1958

The application of these equations occurs when we take into account the motion of $S_g$ with respect to the starry sky, as in some systems of photographic recording of the trajectory of $S_g$ (and in visual observations or without the use of goniometers).

In (3.5–13, 13′) we can shortly put:

$$\xi_{\nu,S} = \xi_{n,S} - \xi_{n,P} \tag{3.5–14}$$

and similar expressions, in agreement with the notations of Table IV.

In the relative reference systems, let us consider the following:

$\tau_{r,G,\lambda}$ = geocentric relative system of equatorial coordinates, with its axis $x_\lambda$ directed towards the Equator point having a longitude equal to the longitude $\lambda_P$ of $P$.

$\tau_{r,G,e}$ = geocentric relative system with its axis $z_e$ parallel to the direction that the vertical $Z$ in $P$ would have, when the Earth's surface $\Sigma_T$ is approximated by the international ellipsoid, to be indicated by $\Sigma_{T,e}$. The axis $x_e$ is parallel to the direction of the meridian of $\Sigma_{T,e}$ passing through $P$ and oriented to South. The positive direction of $y_e$ is such that the system $x_e\ y_e\ z_e$ is left-handed.

We can make use of a system $\tau_{r,G,e'}$, with the coordinates $x_{e'}$, $y_{e'}$ obtained by changing sign to $x_e$, $y_e$, that is with the axis $x_{e'}$, oriented to North and $y_{e'}$, to West.

$\tau_{r,P,\lambda}$ and $\tau_{r,P,e}$, systems similar to the two preceding ones, have their origin in $P$.

For the transfer from $\tau_{a',\nu}$ to $\tau_{r,G,\lambda}$ we employ the equations relative to the rotation operator:

$$\Phi(z_\lambda \equiv \zeta_\nu; \alpha_{\nu,P}) = \begin{Vmatrix} \cos\alpha_{\nu,P} & \sin\alpha_{\nu,P} & 0 \\ -\sin\alpha_{\nu,P} & \cos\alpha_{\nu,P} & 0 \\ 0 & 0 & 1 \end{Vmatrix}. \tag{3.5–15}$$

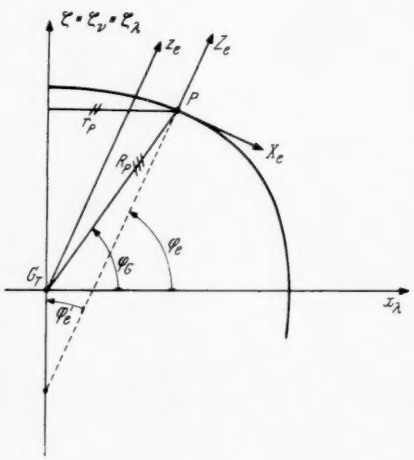


Fig. 11

In the system $\tau_{r,G,\lambda}$ the coordinates of $P$ are:

$$\begin{aligned} x_{\lambda,P} &= r_P, \\ y_{\lambda,P} &= 0, \\ z_{\lambda,P} &= z_{\nu,P} = R_P \sin\varphi_G. \end{aligned} \tag{3.5–16}$$

By applying (3.5–1), we obtain the equations for the transfer with a translation from $\tau_{r,G,\lambda}$ to $\tau_{r,P,\lambda}$, and in particular for $S_g$ we should have for instance, recalling the symbols of Table IV:

$$X_{\lambda,S} = x_{\lambda,S} - x_{\lambda,P}. \tag{3.5–17}$$

By means of the coordinates in the system $\tau_{r,P,\lambda}$, we express the hour angle and the declination of $S_g$.

For the transfer from $\tau_{r,G,\lambda}$ to $\tau_{r,G,e}$ (Fig. 11), we apply the rotation:

$$\Phi(y_e \equiv y_\lambda; -\varphi_e') = \begin{Vmatrix} \cos\varphi_e' & 0 & -\sin\varphi_e' \\ 0 & 1 & 0 \\ \sin\varphi_e' & 0 & \cos\varphi_{e'}, \end{Vmatrix}, \tag{3.5–18}$$

where:

$\varphi_e$, $\varphi_e'$ = geographical latitude and colatitude of $P$, that is with respect to the ellipsoid $\Sigma_{T,e}$.

The transfer from $\tau_{a',\nu}$ to $\tau_{r,G,e}$ is obtained as a product of the transformations defined by the rotations (3.5–15, 18):

$$x_e = (\xi_\nu \cos\alpha_{\nu,P} + \eta_\nu \sin\alpha_{\nu,P}) \cos\varphi_e' - \zeta_\nu \sin\varphi_e', \tag{3.5–19}$$

$$y_e = -\xi_\nu \sin\alpha_{\nu,P} + \eta_\nu \cos\alpha_{\nu,P}, \tag{3.5–19'}$$

$$z_e = (\xi_\nu \cos\alpha_{\nu,P} + \eta_\nu \sin\alpha_{\nu,P}) \sin\varphi_e' + \zeta_\nu \cos\varphi_e'. \tag{3.5–19''}$$

In particular, these equations can be applied to $P$, and recalling (3.5–12'), we obtain by simplification:

$$x_{e,P} = r_P (\cos\varphi_e' - \tan\varphi_G \sin\varphi_e') = R_P \sin(\varphi_e - \varphi_G) \cong R_P (\varphi_G - \varphi_e). \tag{3.5–20}$$

$$y_{e\,P} = 0. \tag{3.5–20'}$$

$$z_{e,P} = r_P (\sin\varphi_e' + \tan\varphi_G \cos\varphi_e') = R_P \cos(\varphi_e - \varphi_G) \cong R_P. \tag{3.5–20''}$$

For the transfer from $\tau_{r,G,e}$ to $\tau_{r,P,e}$ we apply the translation eqs. (3.5–1), and in particular for $S_g$ we have:

$$X_{e,S} = x_{e,S} - R_P \sin(\varphi_e - \varphi_G) \tag{3.5–21}$$

$$Y_{e,S} = y_{e,S} \tag{3.5–21'}$$

$$Z_{e,S} = z_{e,S} - R_P \cos(\varphi_e - \varphi_G). \tag{3.5–21''}$$

These equations are suitable for representing the relative motion of $S_g$ with respect to the reference term $\tau_{r,P,e}$, which, we repeat, has its origin in $P$, and its axes $Z_e$, $X_e$, $Y_e$ are respectively oriented as the vertical (with reference to the Earth's ellipsoid), the meridian (to South), and the parallel (to East).

For the satellite, the coordinates of the type $x_{e,S}$ are calculated by (3.5–19) substituting in place of $\xi_{\nu,S}$ the expressions (3.5–11).

In order to study problems requiring the utmost accuracy, it is necessary to take into account the true direction of the vertical in $P$ and of the meridian. Let us designate:

$\tau_{r,G,g}$ and $\tau_{r,P,g}$ = reference trihedrals with origin $G_T$ and $P$, with their axes $Z_g$, $X_g$, $Y_g$ oriented as the astronomical vertical (with respect to the geoid) of the location, and the astronomical meridian (to South), and the perpendicular to both (to East).

The transfer from $\tau_{r,G,e}$ to $\tau_{r,G,g}$, as well as the transfer from $\tau_{r,P,e}$ to $\tau_{r,P,g}$ are both carried out by the same operator, having a matrix of the type:

$$\Phi_{e,g} = \begin{matrix} 1+\varepsilon_{11} & \varepsilon_{12} & \varepsilon_{13} \\ \varepsilon_{21} & 1+\varepsilon_{22} & \varepsilon_{23} \\ \varepsilon_{31} & \varepsilon_{32} & 1+\varepsilon_{33} \end{matrix} \tag{3.5–22}$$

where $\varepsilon_{h,k}$ are very small coefficients with respect to unity (in general $\varepsilon^2_{h,k} < 10^{-7}$), and in particular $\varepsilon_{11}$, $\varepsilon_{22}$, $\varepsilon_{33}$ can be considered as having gone to zero, being infinitesimals of second order with respect to the other 6 local constants $\varepsilon_{h,k}$, which can be reduced to 3 independents by the perpendicularity conditions:

$$\Phi_{e,g} \cong \begin{matrix} 1 & \varepsilon_1 & -\varepsilon_3 \\ -\varepsilon_1 & 1 & \varepsilon_2 \\ \varepsilon_3 & -\varepsilon_2 & 1 \end{matrix} . \tag{3.5–23}$$

Let us give the expressions for the distance $D$ (of $S_g$ from $P$) and for the ordinate $Z_{e,S}$, and their derivatives, occurring in the study of the culmination problems.



Vol. 4 1958

With reference to $\tau_{r,P,e}$, neglecting the local geodetical corrections, and remarking that:

$$D^2 = X_{e,S}^2 + Y_{e,S}^2 + Z_{e,S}^2, \tag{3.5–24}$$

$$\varrho^2 = x_{e,S}^2 + y_{e,S}^2 + z_{e,S}^2, \tag{3.5–25}$$

from (3.5–21) we obtain:

$$D^2 = \varrho^2 + R_P^2 - 2 R_P [x_{e,S} \sin(\varphi_e - \varphi_G) + z_{e,S} \cos(\varphi_e - \varphi_G)]. \tag{3.5–26}$$

The direction cosines of $G_T S_g$ with respect to $\tau_{r,G,e}$ (and to $\tau_{r,P,e}$):

$$u_{e,x} = x_{e,S}/\varrho, \qquad u_{e,y} = y_{e,S}/\varrho, \qquad u_{e,z} = z_{e,S}/\varrho, \tag{3.5–27}$$

are expressed by (3.5–19) applied to $S_g$, and by (3.5–11). In particular we have:

$$u_{e,z} = (\cos\theta \cos\alpha_{\nu,P} + \sin\theta \cos i \sin\alpha_{\nu,P}) \sin\varphi_e' + \sin\theta \sin i \cos\varphi_e', \tag{3.5–27'}$$

and similar equations for $u_{e,x}$, $u_{e,y}$.

We recall that by $\gamma$ we have indicated (section II, 2) the angle formed by $G_T S_g$ with the axis $z_e$ (and $Z_e$):

$$\cos\gamma = u_{e,z} = z_{e,S}/\varrho. \tag{3.5–28}$$

By calculating the time derivative of the third equation of (3.5–27), one obtains[1]:

$$\dot{z}_{e,S} = \dot{Z}_{e,S} = \dot{\varrho}\, u_{e,z} + \varrho\, \dot{u}_{e,z}, \tag{3.5–29}$$

$$\dot{u}_{e,z} = u_{e,y}\, \dot{\alpha}_{\nu,P} \sin\varphi_e' + \dot{\theta}\, [(-\sin\theta \cos\alpha_{\nu,P} + \cos\theta \cos i \sin\alpha_{\nu,P}) \sin\varphi_e' + \cos\theta \sin i \cos\varphi_e'], \tag{3.5–29'}$$

in which all terms containing $di/dt$ have been neglected.

From (3.5–26) we have by derivation:

$$D\dot{D} = \varrho\,\dot{\varrho} - R_P [\dot{x}_{e,S} \sin(\varphi_e - \varphi_G) + \dot{y}_{e,S} \cos(\varphi_e - \varphi_G)], \tag{3.5–30}$$

with expressions for $\dot{x}_{e,S}$, $\dot{y}_{e,S}$ similar to (3.5–29).

While the altitude angle is given by:

$$\sin h = Z_{e,S}/D, \tag{3.5–31}$$

the culmination point $C$ is defined by the condition:

$$\dot{Z}_{e,S}/\dot{D} = \sin h, \tag{3.5–32}$$

that is by:

$$\dot{Z}_{e,S}\, D^2 = Z_{e,S}\, D\, \dot{D} \tag{3.5–32'}$$

where for $D^2$ and $D\dot{D}$ we apply (3.5–26, 30).

For determining $C$ it is necessary to solve eq. (3.5–32'), which can be done by step-by-step approximations.

A more uniform process consists in tabulating $X_{e,S}$, $Y_{e,S}$, $Z_{e,S}$ for values of the time $t$ having the same interval (e.g. 10 seconds), in a neighbourhood of the meridian transit of $P$ ($\alpha_S = \alpha_P$), or at the parallel ($\delta_S = \varphi_e$), if this is possible ($\varphi_e > i$). Otherwise, the procedure is to be carried out for the maximum value of $\delta_S$ ($= i$).

Designating by $t_E$ the transit instant at the Equator (at the node), by $t_p$ the transit instant at the perigee and by $t_{\Omega p} = t_p - t_E$ the relative interval, it could be convenient to consider the time $t'$ counted starting from $t_p$:

$$t = t_E + t_{\Omega p} + t'. \tag{3.5–33}$$

Moreover, let $\theta'$ be the anomaly counted starting from the perigee:

$$\theta' = \theta - \theta_{\Omega p}. \tag{3.5–34}$$

---

[1] We point out that: $\dot{\alpha}_{\Omega P} = \dot{\alpha}_P - \dot{\alpha}_\Omega$, where with reference to Footnote 1, p. 213: $\dot{\alpha}_P = \dot{\alpha}_T$, while $\dot{\alpha}_\Omega$ is the precession angular velocity of the node $\Omega$.

The functions $\varrho(t')$ and $\theta'(t')$ embody characteristics of quasi-permanence in the subsequent revolutions and their tabulation can be convenient.

We point out that, by putting:

$$K = dt'/dt = 1 - dt_E/dt - dt_{\Omega p}/dt \qquad (3.5\text{–}35)$$

a ratio slowly varying with the time and close to 1, one obtains in general:

$$d/dt = K\, d/dt'. \qquad (3.5\text{–}36)$$

The angle $i_{a,\delta}$, that the absolute velocity of $S_g$ makes with the parallel having the latitude $\varphi_G = \delta_S$, is given by:

$$\tan i_{a,\delta} = (1/\cos \delta_S)\, d\delta_S/d\alpha_{v,S}, \qquad (3.5\text{–}37)$$

where the differentials of $\delta_S$ and $\alpha_{v,S}$ are obtained from eqs. (3.5–11′, 11″). In developing the calculation, we have:

$$\tan i_{a,\delta} = \cos\theta \tan i. \qquad (3.5\text{–}38)$$

Designating by $G_P$ the center of the local sphere through $P$, having as coordinates $Z_{e,G_P} = -R_K$, $X = Y = 0$, we obtain the distance $\varrho'$ of $G_P$ from $S_g$ by:

$$\varrho'^2 = (Z_{e,S} + R_K)^2 + X_{e,S}^2 + Y_{e,S}^2. \qquad (3.5\text{–}39)$$

In a neighbourhood of the point $S_n$ (see Figs. 2 and 12), the difference between the distances $\varrho$ and $\varrho'$ retains an almost constant value, which can be calculated in correspondence with any point $S_{g,1}$ of said neighbourhood by means of (3.5–25, 39):

$$\varrho - \varrho' = \varrho_1 - \varrho_1' \cong \text{const}. \qquad (3.5\text{–}40)$$

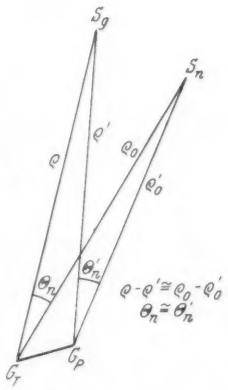


Fig. 12

This equation can be used for the transfer from $\varrho$ to $\varrho'$, in the relations considered in section II, 3. Similar approximate equations could be taken for the transfer from $\gamma$ to $\gamma'$, and from $q$ to $q'$, parameters considered in said section. In so far as the angles $\theta_n$ and $\theta_n'$, having as apices $G_T$ and $G_P$ (Fig. 12), are concerned, we can take:

$$\theta_n \cong \theta_n'. \qquad (3.5\text{–}41)$$

Other approximate relations considered in the previous sections can be verified in their approximation by means of the equations described in the present section and by their series developments, which can be obtained for the different cases.

Vol. 4 1958

# Optimal Escape from a Circular Orbit

By

**D. F. Lawden**[1], BIS

(With 2 Figures)

(*Received June 18, 1958*)

**Abstract — Zusammenfassung — Résumé**

**Optimal Escape from a Circular Orbit.** The general theory of optimal escape of a rocket from a circular orbit about a centre of inverse square law attraction is given and applied to the case of a rocket whose motor thrust causes an acceleration which is of constant magnitude and large by comparison with the gravitational acceleration in the circular orbit. The optimal thrust direction programme is computed. The problem of optimal escape employing a small thrust is also solved by a direct method and it is found that, over the major portion of the escape trajectory, the direction of thrust must bisect the angle between the direction of motion and the perpendicular to the line joining the rocket to the centre of attraction. Ultimately, the directions of thrust and motion are aligned in all cases.

**Günstigstes Verlassen einer Kreisbahn.** Es wird die allgemeine Theorie des günstigsten Ausbrechens einer Rakete aus einer um ein Gravitationszentrum nach dem Gesetz des reziproken Entfernungsquadrates führenden Kreisbahn angegeben. Diese Theorie wird auf den Fall einer Rakete angewendet, deren Motorschub eine Beschleunigung von konstanter Größe bewirkt, die im Vergleich zur Gravitationsbeschleunigung in der Kreisbahn groß ist. Das optimale Programm der Schubrichtung wird berechnet. Mit Hilfe einer direkten Methode wird auch das Problem des günstigsten Ausbrechens unter Verwendung eines kleinen Schubs gelöst. Dabei ergibt sich, daß auf dem größten Teil der Fluchtbahn die Richtung des Schubs jenen Winkel zweiteilen muß, der zwischen der Bewegungsrichtung und der Senkrechten zu jener Linie auftritt, welche die Rakete mit dem Anziehungszentrum verbindet. Zum Schluß sind die Richtungen des Schubs und der Bewegung in allen Fällen gleichgerichtet.

**Libération optimale d'une orbite circulaire.** La théorie générale de la libération optimale d'une fusée d'une orbite circulaire autour d'un centre de gravitation est établie et appliquée au cas d'une fusée, dont l'accélération constante est grande comparée à celle du champ de gravitation. La programmation optimale de la direction de la poussée est calculée. Le problème de la libération optimale, utilisant une faible poussée est aussi résolu par une méthode directe. On trouve que, sur la plus grande partie de la trajectoire de libération, la direction de la poussée doit bissecter l'angle entre la tangente à la trajectoire et la perpendiculaire à la droite joignant la fusée au centre d'attraction. Dans tous les cas la direction de la poussée finit par rejoindre la tangente à la trajectoire.

[1] Professor of Mathematics, University of Canterbury, Christchurch, New Zealand.

Vol. 4 1958

## 1. Introduction

The problem of programming the thrust direction of a rocket to permit its escape from a circular orbit with the minimum expenditure of propellant was considered in an earlier paper [1]. The magnitude of the thrust was assumed to be a given function of the time. It was shown that economy in the expenditure of propellant could be achieved by directing the thrust at a small angle to the direction of motion, this angle being steadily decreased so that at the termination of the manoeuvre the directions of thrust and of motion were aligned. The sense of this angle had to be chosen so that the thrust was thrown off from the direction of motion towards the centre of attraction. However, the precise relationship between this throw-off angle and the time variable was not determined and it is the object of the present paper to carry the investigation one stage further by obtaining this relationship in two extreme cases, (i) when the acceleration due to the motor thrust is large by comparison with gravity in the circular orbit and (ii) when it is small.

Particular escape manoeuvres have been investigated by TSIEN [2] and BENNEY [3]. The former showed that escape is effected economically by directing the thrust along the perpendicular to the straight line joining the rocket to the centre of attraction and the latter that further improvement results when the thrust direction is aligned with the direction of motion.

## 2. General Theory

General equations governing the optimal trajectory of escape have been found in our earlier work [1]. However, it will be convenient to summarise this argument in a somewhat different form in the present paper, so as to provide suitable equations from which our new calculations may proceed.

We shall choose units of length and time such that the radius of the circular orbit from which escape is to be effected and the velocity in this orbit are both unity. Then, assuming an inverse square law of gravitational attraction towards the centre $O$ of the orbit, the gravitational acceleration at distance $r$ from $O$ will be $1/r^2$. Assuming that the trajectory of escape lies in the plane of the orbit, let $(r, \theta)$ be polar coordinates of the rocket $R$ at time $t$ since the commencement of the manoeuvre; we shall take $\theta = 0$ at $t = 0$ (Fig. 1). $f$ is the acceleration caused by the motor thrust and is directed at an angle $\phi$ to the perpendicular to $OR$ as indicated in the figure. $f$ will be regarded as a given function of $t$. $\mathfrak{V}$ is the rocket velocity, making an angle $\psi$ with the perpendicular to $OR$ and hence $\varepsilon = \psi - \phi$ is the throw-off angle. Let $\mathfrak{V}$ have components $(u, v)$ along and perpendicular to $OR$. Then equations for the motion of the rocket are:

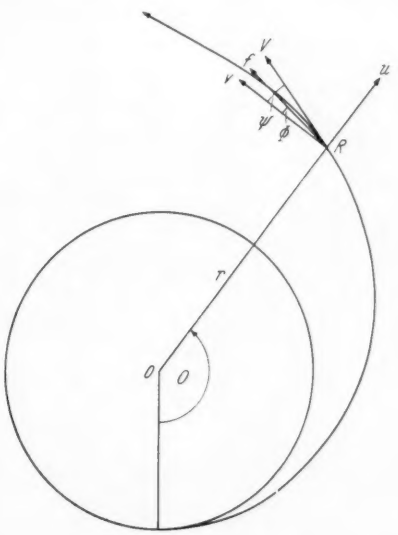


Fig. 1

$$\left.\begin{aligned} \dot{u} - \frac{v^2}{r} + \frac{1}{r^2} &= f \sin \phi, \\ \dot{v} + \frac{uv}{r} &= f \cos \phi, \\ \dot{r} - u &= 0. \end{aligned}\right\} \tag{1}$$

Let $t = T$ when the rocket has acquired sufficient energy to permit its escape and the motors are closed down. Then $\phi$ must be made to vary with $t$ in such a manner that $T$, and hence the propellant expenditure, is minimised. Suppose $\phi = \phi(t)$ specifies this optimal thrust direction programme. Let $\phi = \phi(t) + \delta\phi(t)$ represent any neighbouring programme. If $(r + \delta r,\ \theta + \delta\theta)$ are the coordinates of the rocket and $(u + \delta u,\ v + \delta v)$ are its velocity components at time $t$ when the thrust follows the perturbed programme, by taking the first variation of eqs. (1), we obtain

$$\left.\begin{aligned} \delta\dot{u} - \frac{2v}{r}\delta v + \left(\frac{v^2}{r^2} - \frac{2}{r^3}\right)\delta r &= f\,\delta\phi \cos\phi, \\ \delta\dot{v} + \frac{v}{r}\delta u + \frac{u}{r}\delta v - \frac{uv}{r^2}\delta r &= -f\,\delta\phi \sin\phi, \\ \delta\dot{r} - \delta u &= 0. \end{aligned}\right\} \tag{2}$$

These equations are to be integrated under the initial conditions $\delta u = \delta v = \delta r = 0$ and determine the perturbed trajectory.

Consider the homogeneous linear equations in variables $x, y, z$, viz.

$$\left.\begin{aligned} \dot{x} - \frac{2v}{r}y + \left(\frac{v^2}{r^2} - \frac{2}{r^3}\right)z &= 0, \\ \dot{y} + \frac{v}{r}x + \frac{u}{r}y - \frac{uv}{r^2}z &= 0, \\ \dot{z} - x &= 0. \end{aligned}\right\} \tag{3}$$

Let

$$\begin{pmatrix} x \\ y \\ z \end{pmatrix} = \begin{pmatrix} x^1 \\ y^1 \\ z^1 \end{pmatrix}, \begin{pmatrix} x^2 \\ y^2 \\ z^2 \end{pmatrix}, \begin{pmatrix} x^3 \\ y^3 \\ z^3 \end{pmatrix} \tag{4}$$

be the three solutions of these equations satisfying at $t = T$ the conditions

$$\begin{pmatrix} x^1 \\ y^1 \\ z^1 \end{pmatrix} = \begin{pmatrix} 1 \\ 0 \\ 0 \end{pmatrix}, \begin{pmatrix} x^2 \\ y^2 \\ z^2 \end{pmatrix} = \begin{pmatrix} 0 \\ 1 \\ 0 \end{pmatrix}, \begin{pmatrix} x^3 \\ y^3 \\ z^3 \end{pmatrix} = \begin{pmatrix} 0 \\ 0 \\ 1 \end{pmatrix} \tag{5}$$

respectively. The solutions (4) then form a fundamental linearly independent set of solutions of the eqs. (3).

Employing the method of variation of parameters as in [1], we can now express the solution of eqs. (2) at the instant $t = T$ in the form

$$\delta u(T) = \int_0^T \frac{f}{\Delta} \delta\phi \, (A^1 \cos\phi - A^2 \sin\phi) \, dt,$$

$$\delta v(T) = \int_0^T \frac{f}{\Delta} \delta\phi \, (B^1 \cos\phi - B^2 \sin\phi) \, dt, \tag{6}$$

$$\delta r(T) = \int_0^T \frac{f}{\Delta} \delta\phi \, (C^1 \cos\phi - C^2 \sin\phi) \, dt,$$

where

$$A^1 = y^2 z^3 - y^3 z^2, \qquad A^2 = z^2 x^3 - z^3 x^2,$$
$$B^1 = y^3 z^1 - y^1 z^3, \qquad B^2 = z^3 x^1 - z^1 x^3,$$
$$C^1 = y^1 z^2 - y^2 z^1, \qquad C^2 = z^1 x^2 - z^2 x^1,$$
$$\Delta = \begin{vmatrix} x^1 & x^2 & x^3 \\ y^1 & y^2 & y^3 \\ z^1 & z^2 & z^3 \end{vmatrix}.$$

Vol. 4 1958

In the case of the optimal trajectory, the rocket has sufficient energy to escape along a parabolic arc at $t = T$. Hence its total energy is zero at this instant and thus

$$u^2(T) + v^2(T) - \frac{2}{r(T)} = 0. \tag{7}$$

Suppose that conditions for escape are achieved at $t = T + \delta T$ on the perturbed trajectory. Then

$$\{u\,(T + \delta T) + \delta u\,(T + \delta T)\}^2 + \{v\,(T + \delta T) + \delta v\,(T + \delta T)\}^2 - \frac{2}{r\,(T + \delta T) + \delta r\,(T + \delta T)} = 0. \tag{8}$$

But

$$u\,(T + \delta T) + \delta u\,(T + \delta T) = u(T) + \delta T\,\dot{u}(T) + \delta u(T), \tag{9}$$

to the first order of small quantities. Similar equations can be written down for $v$ and $r$. Hence, eq. (8) yields

$$\delta T \left\{ u(T)\,\dot{u}(T) + v(T)\,\dot{v}(T) + \frac{\dot{r}(T)}{r^2(T)} \right\} + u(T)\,\delta u(T) + v(T)\,\delta v(T) + \frac{\delta r(T)}{r^2(T)} = 0. \tag{10}$$

This last equation determines $\delta T$. If our original trajectory is optimal, $T$ is stationary relative to all small variations of the thrust direction programme. In this case $\delta T = 0$ for all variations $\delta\phi$ and thus

$$u(T)\,\delta u(T) + v(T)\,\delta v(T) + \frac{\delta r(T)}{r^2(T)} = 0. \tag{11}$$

Substituting from eqs. (6), we obtain

$$\int_0^T \frac{f}{\Delta} \delta\phi \, (P \cos\phi - Q \sin\phi) \, dt = 0, \tag{12}$$

where

$$P = A^1 u(T) + B^1 v(T) + \frac{C^1}{r^2(T)}, \tag{13}$$

$$Q = A^2 u(T) + B^2 v(T) + \frac{C^2}{r^2(T)}. \tag{14}$$

But eq. (12) can only be true for all functions $\delta\phi$ if

$$P\cos\phi - Q\sin\phi = 0,$$

i.e. if

$$\tan\phi = \frac{P}{Q}. \tag{15}$$

Eq. (15) determines the optimal thrust direction programme.

At $t = T$, in view of the conditions (5),

$$A^1 = 1, \quad B^1 = 0, \quad C^1 = 0, \quad A^2 = 0, \quad B^2 = 1, \quad C^2 = 0.$$

Hence, at this instant,

$$P = u(T), \qquad Q = v(T),$$

and

$$\tan\phi(T) = \frac{u(T)}{v(T)} = \tan\psi(T).$$

Thus $\phi(T) = \psi(T)$, or $\varepsilon(T) = 0$. We conclude that, at the instant the motors are shut down, the directions of thrust and motion are aligned.

### 3. The Case of Large Thrust

In this section we shall assume that $f$ is constant and large. Then, if $\mu$ is the ratio of the rocket's mass at the instant $t$ to its initial mass and $c$ is the exhaust velocity of its motors,

$$ft = -c\log\mu. \tag{16}$$

We shall put

$$ft = \tau. \tag{17}$$

Then eqs. (1) may be written

$$\left.\begin{aligned} \dot{u} &= \sin\phi + \lambda\left(\frac{v^2}{r} - \frac{1}{r^2}\right), \\ \dot{v} &= \cos\phi - \lambda\frac{u\,v}{r}, \\ \dot{r} &= \lambda\,u, \end{aligned}\right\} \tag{18}$$

where, from this point onwards, dots will denote differentiations with respect to $\tau$ (instead of $t$) and $\lambda = 1/f$ is small.

Similarly, eqs. (3) now take the form

$$\left.\begin{aligned} \dot{x} &= \lambda\left\{\frac{2\,v}{r}\,y + \left(\frac{2}{r^3} - \frac{v^2}{r^2}\right)z\right\}, \\ \dot{y} &= \lambda\left\{-\frac{v}{r}\,x - \frac{u}{r}\,y + \frac{u\,v}{r^2}\,z\right\}, \\ \dot{z} &= \lambda\,x. \end{aligned}\right\} \tag{19}$$

Writing $f T = W$, $W$ is the characteristic velocity of the manoeuvre and, at its termination, $\tau = W$.

We shall now assume that all the quantities $u, v, r, x, y, z, \phi, W$ are regular functions of $\lambda$ for sufficiently small values of this parameter, so that we may write

$$u = u_0 + \lambda u_1 + \lambda^2 u_2 + \ldots, \tag{20}$$

with similar expansions for the remaining variables. Substituting these expansions in the first of eqs. (18) and comparing coefficients of like powers of $\lambda$ in the two members of the equation, we obtain the following equations

$$\dot{u}_0 = \sin \phi_0, \tag{21}$$

$$\dot{u}_1 = \phi_1 \cos \phi_0 + \frac{{v_0}^2}{r_0} - \frac{1}{{r_0}^2}, \tag{22}$$

$$\dot{u}_2 = \phi_2 \cos \phi_0 - \frac{1}{2} \phi_1{}^2 \sin \phi_0 + \frac{2 v_0 v_1}{r_0} - \frac{{v_0}^2 r_1}{{r_0}^2} + \frac{2 r_1}{{r_0}^3}. \tag{23}$$

Treating the second of eqs. (18) in the same manner, we obtain

$$\dot{v}_0 = \cos \phi_0, \tag{24}$$

$$\dot{v}_1 = - \phi_1 \sin \phi_0 - \frac{u_0 v_0}{r_0}, \tag{25}$$

$$\dot{v}_2 = - \phi_2 \sin \phi_0 - \frac{1}{2} \phi_1{}^2 \cos \phi_0 - \frac{u_0 v_1 + u_1 v_0}{r_0} + \frac{u_0 v_0 r_1}{{r_0}^2}. \tag{26}$$

From the third of eqs. (18), we find that

$$\dot{r}_0 = 0, \tag{27}$$

$$\dot{r}_1 = u_0, \tag{28}$$

$$\dot{r}_2 = u_1. \tag{29}$$

Since, for all $\lambda$, $u = 0$ when $\tau = 0$, we deduce from eq. (20) that

$$u_0(0) = u_1(0) = u_2(0) = \ldots = 0. \tag{30}$$

Similarly, since $v = 1$, $r = 1$ when $\tau = 0$,

$$v_0(0) = 1, \qquad v_1(0) = v_2(0) = \ldots = 0, \tag{31}$$

$$r_0(0) = 1, \qquad r_1(0) = r_2(0) = \ldots = 0. \tag{32}$$

Substitution of the expansions in eqs. (19) yields

$$\dot{x}_0 = 0, \tag{33}$$

$$\dot{x}_1 = \frac{2 v_0}{r_0} y_0 + \left( \frac{2}{{r_0}^3} - \frac{{v_0}^2}{{r_0}^2} \right) z_0, \tag{34}$$

$$\dot{y}_0 = 0, \tag{35}$$

$$\dot{y}_1 = - \frac{v_0}{r_0} x_0 - \frac{u_0}{r_0} y_0 + \frac{u_0 v_0}{{r_0}^2} z_0, \tag{36}$$

$$\dot{z}_0 = 0, \tag{37}$$

$$\dot{z}_1 = x_0. \tag{38}$$

Since

$$W = W_0 + \lambda W_1 + \lambda^2 W_2 + \ldots, \tag{39}$$

$$x = x_0 + \lambda x_1 + \lambda^2 x_2 + \ldots,$$

it follows that

$$x(W) = x_0(W_0) + \lambda \{x_1(W_0) + W_1 \dot{x}_0(W_0)\} +$$

$$+ \lambda^2 \{x_2(W_0) + W_1 \dot{x}_1(W_0) + W_2 \dot{x}_0(W_0) + \tfrac{1}{2} {W_1}^2 \ddot{x}_0(W_0)\} + \ldots. \tag{40}$$

Vol. 4 1958

with similar expansions for $y(W)$, $z(W)$. But the three sets of solutions $x^i(\tau)$, $y^i(\tau)$, $z^i(\tau)$ $(i = 1, 2, 3)$ of eqs. (19) must satisfy the conditions (5) at $\tau = W$ for all sufficiently small values of $\lambda$. We accordingly arrive at the conditions

$$\begin{pmatrix} x_0^1 \\ y_0^1 \\ z_0^1 \end{pmatrix} = \begin{pmatrix} 1 \\ 0 \\ 0 \end{pmatrix}, \quad \begin{pmatrix} x_0^2 \\ y_0^2 \\ z_0^2 \end{pmatrix} = \begin{pmatrix} 0 \\ 1 \\ 0 \end{pmatrix}, \quad \begin{pmatrix} x_0^3 \\ y_0^3 \\ z_0^3 \end{pmatrix} = \begin{pmatrix} 0 \\ 0 \\ 1 \end{pmatrix}. \tag{41}$$

$$x_1^i + W_1 \dot{x}_0^i = y_1^i + W_1 \dot{y}_0^i = z_1^i + W_1 \dot{z}_0^i = 0, \tag{42}$$

where $i = 1, 2, 3$, all to be satisfied at $\tau = W_0$.

By the same reasoning as that which led to eq. (40), we can show that

$$u(W) = U_0 + \lambda U_1 + \lambda^2 U_2 + \ldots, \tag{43}$$

where

$$U_0 = u_0(W_0), \tag{44}$$

$$U_1 = u_1(W_0) + W_1 \dot{u}_0(W_0), \tag{45}$$

$$U_2 = u_2(W_0) + W_1 \dot{u}_1(W_0) + W_2 \dot{u}_0(W_0) + \tfrac{1}{2} W_1^2 \ddot{u}_0(W_0). \tag{46}$$

Similar expansions exist for $v(W)$ and $r(W)$. Substituting these in eq. (7), its left hand member may be expressed as a power series in $\lambda$. Equating the coefficients of the powers of $\lambda$ in this series to zero, we obtain the results:

$$U_0^2 + V_0^2 - \frac{2}{R_0} = 0, \tag{47}$$

$$U_0 U_1 + V_0 V_1 + \frac{R_1}{R_0^2} = 0, \tag{48}$$

$$U_1^2 + V_1^2 + 2 U_0 U_2 + 2 V_0 V_2 + \frac{2 R_2}{R_0^2} - \frac{2 R_1^2}{R_0^3} = 0. \tag{49}$$

The first of these equations will determine $W_0$, the second $W_1$ and the third $W_2$.

We shall now obtain a first approximation to the optimal manoeuvre by the neglect of all terms $O(\lambda)$.

From eqs. (33), (35) and (37) and conditions (41), we conclude that for all $\tau$

$$\begin{pmatrix} x_0^1 \\ y_0^1 \\ z_0^1 \end{pmatrix} = \begin{pmatrix} 1 \\ 0 \\ 0 \end{pmatrix}, \quad \begin{pmatrix} x_0^2 \\ y_0^2 \\ z_0^2 \end{pmatrix} = \begin{pmatrix} 0 \\ 1 \\ 0 \end{pmatrix}, \quad \begin{pmatrix} x_0^3 \\ y_0^3 \\ z_0^3 \end{pmatrix} = \begin{pmatrix} 0 \\ 0 \\ 1 \end{pmatrix}. \tag{50}$$

Hence, neglecting terms $O(\lambda)$,

$$A^1 = 1, \quad B^1 = 0, \quad C^1 = 0, \quad A^2 = 0, \quad B^2 = 1, \quad C^2 = 0, \tag{51}$$

for all $\tau$. To the same order of accuracy, eqs. (13) and (14) now give

$$\left.\begin{aligned} P &= u(W) = U_0, \quad [\text{eq. (44)}], \\ Q &= v(W) = V_0. \end{aligned}\right\} \tag{52}$$

To this order, eq. (15) is accordingly

$$\tan \phi_0 = \frac{U_0}{V_0}, \tag{53}$$

i.e. $\phi_0$ is constant for all $\tau$.

We can now integrate eqs. (21), (24), (27) under the initial conditions (30) – (32) to give

$$u_0 = \tau \sin \phi_0, \quad v_0 = \tau \cos \phi_0 + 1, \quad r_0 = 1. \tag{54}$$

Hence

$$U_0 = W_0 \sin \phi_0, \qquad V_0 = W_0 \cos \phi_0 + 1 \tag{55}$$

and eq. (53) is equivalent to

$$\tan \phi_0 = \frac{W_0 \sin \phi_0}{W_0 \cos \phi_0 + 1}. \tag{56}$$

This implies that

$$\phi_0 = 0. \tag{57}$$

Hence

$$u_0 = 0, \qquad v_0 = \tau + 1, \qquad r_0 = 1. \tag{58}$$

Substituting in eq. (47), we find that

$$W_0 = \sqrt{2} - 1. \tag{59}$$

It follows that

$$U_0 = 0, \qquad V_0 = \sqrt{2}, \qquad R_0 = 1. \tag{60}$$

Vol. 4 1958

Our problem has now been solved to zero order in $\lambda$. The value $(\sqrt{2} - 1)$ derived for $W$ is clearly identical with the value appropriate to this quantity when the thrust is impulsive.

Proceeding to the calculation of first order terms, we will first integrate eqs. (34), (36) and (38) under the three sets of conditions (42). These conditions now reduce to

$$x_1^i = y_1^i = z_1^i = 0, \tag{61}$$

to be satisfied at $\tau = \sqrt{2} - 1$. It will be found that the three sets of solutions are

$$x_1^1 = 0, \qquad y_1^1 = 1 - \tfrac{1}{2}(\tau + 1)^2, \qquad z_1^1 = (\tau + 1) - \sqrt{2}, \tag{62}$$

$$x_1^2 = (\tau + 1)^2 - 2, \qquad y_1^2 = 0, \qquad z_1^2 = 0, \tag{63}$$

$$x_1^3 = -\tfrac{1}{3}(\tau + 1)^3 + 2(\tau + 1) - \tfrac{4}{3}\sqrt{2}, \qquad y_1^3 = 0, \qquad z_1^3 = 0. \tag{64}$$

Thus, to the first order in $\lambda$,

$$A^1 = 1, \tag{65}$$

$$B^1 = \lambda\{\tfrac{1}{2}(\tau + 1)^2 - 1\}, \tag{66}$$

$$C^1 = \lambda\{\sqrt{2} - (\tau + 1)\}, \tag{67}$$

$$A^2 = \lambda\{2 - (\tau + 1)^2\}, \tag{68}$$

$$B^2 = 1, \tag{69}$$

$$C^2 = 0. \tag{70}$$

We can now calculate $P, Q$, to $O(\lambda)$ from eqs. (13), (14), viz.

$$P = \lambda\{u_1(W_0) + \tfrac{1}{2}\sqrt{2}(\tau + 1)^2 - (\tau + 1)\}, \tag{71}$$

$$Q = \sqrt{2} + \lambda\{v_1(W_0) + W_1\}. \tag{72}$$

Eq. (15) then yields

$$\phi_1 = \tfrac{1}{2}\sqrt{2}\, u_1(W_0) + \tfrac{1}{2}(\tau + 1)^2 - \tfrac{1}{2}\sqrt{2}(\tau + 1). \tag{73}$$

It is now possible to integrate eqs. (22), (25) and (28) under the initial conditions (30) — (32). The results of these integrations are:

$$u_1 = \tfrac{1}{2}\sqrt{2}\,\tau\, u_1(W_0) + \tfrac{1}{2}(\tau + 1)^3 - \tfrac{1}{4}\sqrt{2}(\tau + 1)^2 - (\tau + 1) + \tfrac{1}{4}(2 + \sqrt{2}), \tag{74}$$

$$v_1 = 0, \tag{75}$$

$$r_1 = 0. \tag{76}$$

Putting $\tau = W_0 = \sqrt{2} - 1$ in eqs. (74) – (76), we find that

$$u_1(W_0) = \tfrac{1}{2}(\sqrt{2} - 1), \qquad v_1(W_0) = 0, \qquad r_1(W_0) = 0. \tag{77}$$

Thus, eqs. (73) and (74) reduce to

$$\phi_1 = \tfrac{1}{2}(\tau + 1)^2 - \tfrac{1}{2}\sqrt{2}(\tau + 1) + \tfrac{1}{4}(2 - \sqrt{2}), \tag{78}$$

$$u_1 = \tfrac{1}{2}(\tau + 1)^3 - \tfrac{1}{4}\sqrt{2}(\tau + 1)^2 - \tfrac{1}{4}(2 + \sqrt{2})(\tau + 1) + \tfrac{1}{2}\sqrt{2}. \tag{79}$$

From eq. (45) and two similar equations for $V_1$ and $R_1$,

$$U_1 = \tfrac{1}{2}(\sqrt{2} - 1), \qquad V_1 = W_1, \qquad R_1 = 0, \tag{80}$$

and hence, substituting in eq. (48), we obtain

$$W_1 = 0. \tag{81}$$

This completes the solution to the first order in $\lambda$.

Since $W_1 = 0$, we find it necessary to compute $W_2$ in order to assess the inferiority of our optimal thrust programme employing a finite thrust when it is compared with escape under an impulsive thrust.

Integrating eq. (26) under the initial condition (31), we compute that

$$v_2 = -\frac{1}{8}(\tau + 1)^5 + \frac{1}{8}\sqrt{2}(\tau + 1)^4 + \frac{1}{8}\sqrt{2}(\tau + 1)^3 - \frac{1}{8}(\sqrt{2} + 1)(\tau + 1)^2$$

$$- \frac{1}{16}(3 - 2\sqrt{2})(\tau + 1) + \frac{1}{16}(7 - 4\sqrt{2}). \tag{82}$$

Similarly, from eq. (29), we obtain

$$r_2 = \frac{1}{8}(\tau + 1)^4 - \frac{1}{12}\sqrt{2}(\tau + 1)^3 - \frac{1}{8}\sqrt{2}(\sqrt{2} + 1)(\tau + 1)^2$$

$$+ \frac{1}{2}\sqrt{2}(\tau + 1) - \frac{1}{24}(7\sqrt{2} - 3). \tag{83}$$

From two equations of the type (46), we now calculate that

$$V_2 = W_2 - \frac{1}{16}(11\sqrt{2} - 15), \qquad R_2 = \frac{1}{24}(19 - 13\sqrt{2}), \tag{84}$$

and hence, from eq. (49) that

$$W_2 = \frac{1}{48}(5\sqrt{2} - 7). \tag{85}$$

To summarise, we have shown that the optimal programme for $\phi$ to the first order in $\lambda$ is

$$\phi = \lambda\{\tfrac{1}{2}(\tau + 1)^2 - \tfrac{1}{2}\sqrt{2}(\tau + 1) + \tfrac{1}{4}(2 - \sqrt{2})\}. \tag{86}$$

To the same order of approximation, the motion of the rocket under this thrust programme is determined by the equations

$$u = \lambda\{\tfrac{1}{2}(\tau + 1)^3 - \tfrac{1}{4}\sqrt{2}(\tau + 1)^2 - \tfrac{1}{4}(2 + \sqrt{2})(\tau + 1) + \tfrac{1}{2}\sqrt{2}\}, \tag{87}$$

$$v = \tau + 1, \tag{88}$$

$$r = 1. \tag{89}$$

Since $\dot{\theta} = \lambda v/r$, we have also

$$\theta = \lambda(\tau + 1). \tag{90}$$

Thus the angular displacement of the rocket during the escape manoeuvre is $\lambda\sqrt{2}$ or $\sqrt{2}/f$ radians.

Also

$$\tan \psi = \frac{u}{v}, \tag{91}$$

and hence

$$\psi = \lambda \{\tfrac{1}{2}(\tau+1)^2 - \tfrac{1}{4}\sqrt{2}(\tau+1) - \tfrac{1}{4}(2+\sqrt{2}) + \tfrac{1}{2}\sqrt{2}(\tau+1)^{-1}\}. \tag{92}$$

It now follows that the throw-off angle is given by

$$\varepsilon = \tfrac{1}{4}\lambda\sqrt{2}(\tau+1)^{-1}(\tau+1-\sqrt{2})^2, \tag{93}$$

and is zero at $\tau = \sqrt{2} - 1$ as expected. The initial value of this angle is $\frac{1}{4}\lambda(3\sqrt{2}-4) = (3\sqrt{2}-4)/4f = 0.061/f$ radians. $\varepsilon/\lambda$ has been plotted against $\tau$ in Fig. 2.

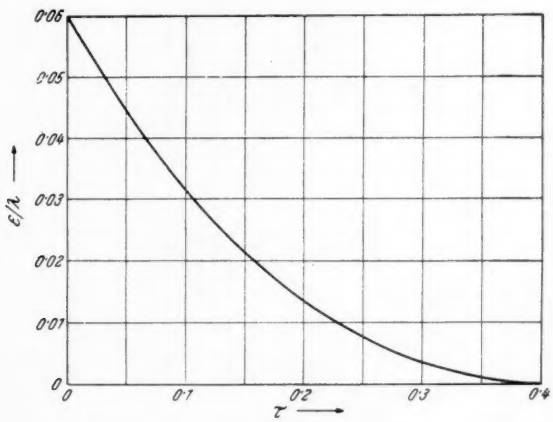


Fig. 2

The characteristic velocity of the manoeuvre is given by

$$W = \sqrt{2} - 1 + \frac{1}{48}\lambda^2(5\sqrt{2}-7), \tag{94}$$

$$= 0.414\,214 + 0.001\,481\,\lambda^2.$$

Comparing this with the corresponding results for the non-optimal manoeuvres of TSIEN and BENNEY, viz.

$$W = 0.414\,214 + 0.002\,349\,\lambda^2,$$

$$W = 0.414\,214 + 0.001\,615\,\lambda^2$$

respectively, we note a small improvement. In terms of the mass ratio, the improvement on TSIEN's manoeuvre is $0.087\,\lambda^2/c\,\%$ and on BENNEY's manoeuvre is $0.013\,\lambda^2/c\,\%$. Thus, if $\lambda = 1$ and $c = \frac{1}{4}$ (i.e. the acceleration due to the motor thrust is equal to the gravitational acceleration at the initial orbit and the exhaust velocity is one quarter of the velocity in this orbit), then the mass ratio improvements are about 0.35% and 0.05% respectively.

### 4. The Case of Small Thrust

It is natural when dealing with this case to seek expansions of the various variables in powers of $f$. However, it is found that, if $t$ is retained as the independ-

Vol. 4 1958

ent variable, these series converge less and less rapidly as we proceed along the escape trajectory and may even diverge over the latter stages. On the other hand, if a change is made to $\tau$, no such expansions exist. This case is accordingly very much more difficult to deal with.

To amplify these statements, we will suppose $f$ constant and the thrust direction programme to be determined by

$$\phi = f\,\phi_1 + f^2\,\phi_2 + \ldots, \tag{95}$$

i.e. $\phi$ is of the first order in $f$. Both TSIEN's and BENNEY's programmes satisfy this condition. We then seek a solution of the form

$$u = u_0 + f\,u_1 + f^2\,u_2 + \ldots, \tag{96}$$

with similar expansions for $v$ and $r$. Substitution of these expansions in eqs. (1) and consideration of coefficients of powers of $f$, leads to the equations

$$\left.\begin{aligned}
&\dot{u}_0 - \frac{{v_0}^2}{r_0} + \frac{1}{{r_0}^2} = 0,\\
&\dot{u}_1 + \frac{{v_0}^2 r_1}{{r_0}^2} - \frac{2\,v_0\,v_1}{r_0} - \frac{2\,r_1}{{r_0}^3} = 0,\\
&\dot{v}_0 + \frac{u_0\,v_0}{r_0} = 0,\\
&\dot{v}_1 + \frac{u_0\,v_1 + u_1\,v_0}{r_0} - \frac{u_0\,v_0\,r_1}{{r_0}^2} = 1,\\
&\dot{r}_0 = u_0,\\
&\dot{r}_1 = u_1,
\end{aligned}\right\} \tag{97}$$

where dots here denote differentiations with respect to $t$. These equations are to be solved under the initial conditions ($t = 0$),

$$\left.\begin{aligned}
&u_0 = u_1 = \ldots = 0,\\
&v_0 = 1, \qquad v_1 = v_2 = \ldots = 0,\\
&r_0 = 1, \qquad r_1 = r_2 = \ldots = 0.
\end{aligned}\right\} \tag{98}$$

It will be found that

$$\left.\begin{aligned}
&u_0 = 0, \qquad v_0 = 1, \qquad r_0 = 1,\\
&u_1 = 2\,(1 - \cos t),\\
&v_1 = 2\sin t - t,\\
&r_1 = 2\,(t - \sin t),
\end{aligned}\right\} \tag{99}$$

for all $t$.

Hence, to the first order in $f$

$$\left.\begin{aligned}
&u = 2\,f\,(1 - \cos t),\\
&v = 1 + f\,(2\sin t - t),\\
&r = 1 + 2\,f\,(t - \sin t).
\end{aligned}\right\} \tag{100}$$

Also, since $\dot{\theta} = v/r$, we have

$$\theta = t + \tfrac{1}{2}\,f\,(8 - 8\cos t - 3\,t^2). \tag{101}$$

Clearly, over the early part of the trajectory, the rocket spirals steadily outwards from the circular orbit, apart from a small oscillation, superposed upon this steady spiral motion, of period approximately that of its motion in the original orbit. It is of interest to note that, when $t = 2\pi$, i.e. after approximately one revolution in the spiral, eqs. (100) give

$$u = 0, \qquad v = 1 - 2\pi f, \qquad r = 1 + 4\pi f. \tag{102}$$

Thus, to the first order at this instant,

$$u = 0, \qquad v^2/r = 1/r^2. \tag{103}$$

These are the conditions that the rocket should be in a circular orbit of radius $r$. It follows that the early motion may be regarded as a sequence of transfers from one circular orbit to another of slightly larger radius via a spiral tangential to both.

If, now, second order terms, viz. $u_2, v_2, r_2$, are calculated, it will be found that expressions of the type $t^2 \sin t$, $t^2 \cos t$ appear. These represent oscillations of steadily increasing amplitude which will eventually become comparable with the non-oscillatory terms. We conclude, therefore, that the latter stages of the escape manoeuvre may be described as successive transfers between ellipses (rather than circles) of increasing eccentricity, the final transfer being to a parabola along which the escape to infinity is made. It is this complexity of the trajectory which is largely responsible for the difficulty experienced in dealing with this case.

It is natural to change the independent variable to $\tau = f t$, as was done in the previous section, for the range of $\tau$-values from the circular orbit to escape will remain finite as $f \to 0$, whereas the range of $t$-values becomes infinite. If this change of variable is made in eqs. (100), the oscillatory terms $\cos t$ and $\sin t$ are replaced by $\cos(\tau/f)$ and $\sin(\tau/f)$ respectively. Neither of these terms possesses an expansion in ascending powers of $f$, since neither is regular in the neighbourhood of $f = 0$. In general, therefore, we cannot expect the equations of motion to possess a solution of the form (96), if $\tau$ is accepted as the independent variable.

Vol. 4 1958

However, it will be found that the oscillatory terms present in eqs. (100), arise from the complementary functions of certain differential equations and hence can be eliminated by appropriate modification of the initial conditions (98). In fact, if we require that at $t = 0$

$$\left.\begin{aligned} u_0 &= 0, \qquad v_0 = 1, \qquad r_0 = 1, \\ u_1 &= 2, \qquad v_1 = -1, \qquad r_1 = 0, \end{aligned}\right\} \tag{104}$$

it will be found that eqs. (100) are replaced by

$$u = 2f, \qquad v = 1 - f t, \qquad r = 1 + 2 f t. \tag{105}$$

Similarly, by appropriate choice of the initial conditions on $u_i, v_i, r_i, (i = 2, 3, \ldots)$, oscillatory terms may be entirely eliminated from the solution. The new set of conditions so obtained differs from the old set only in so far as quantities of the first order and higher orders are concerned. The new conditions assume that the rocket is moving initially in an elliptical orbit of small eccentricity of order $f^2$ instead of a perfect circle. With the object of simplifying the analysis, we shall now suppose that the initial orbit is subjected to this small modification and consider the problem of escape from the modified orbit. The escape trajectory will then be a simple spiral.

Since no oscillatory terms are to appear in the solution of the equations of motion, we may now assume a solution of the form (96) with $\tau$ as the independent variable. Putting $f t = \tau$ in eqs. (1), we obtain

$$\left.\begin{aligned} f(\dot{u} - \sin\phi) &= \frac{v^2}{r} - \frac{1}{r^2}, \\ f(\dot{v} - \cos\phi) &= -\frac{u\,v}{r}, \\ f\dot{r} &= u, \end{aligned}\right\} \tag{106}$$

where dots once again (and for the remainder of this section) denote differentiations with respect to $\tau$. Substituting the expansions (96), etc. together with a corresponding one for $\phi$, viz.

$$\phi = \phi_0 + f\,\phi_1 + f^2\,\phi_2 + \ldots \tag{107}$$

(we shall prove $\phi_0 = 0$ under optimal conditions below), and equating coefficients of like powers of $f$ from the two members of each equation, we obtain

$$\frac{v_0^2}{r_0} - \frac{1}{r_0^2} = 0, \tag{108}$$

$$\frac{u_0\,v_0}{r_0} = 0, \tag{109}$$

$$\dot{v}_0 - \cos\phi_0 = \frac{u_0\,v_0\,r_1}{r_0^2} - \frac{u_1\,v_0 + u_0\,v_1}{r_0}, \tag{110}$$

$$u_0 = 0, \tag{111}$$

$$u_1 = \dot{r}_0. \tag{112}$$

Whence, from eqs. (108), (109) and (111), we obtain

$$u_0 = 0, \qquad v_0 = 1/r_0^{1/2}. \tag{113}$$

Eliminating $u_1$ from eq. (110) by the use of eq. (112) and employing eqs. (113), we find that eq. (110) is equivalent to

$$\dot{r}_0 = 2\,r_0^{3/2}\cos\phi_0. \tag{114}$$

Integrating this equation under the initial condition on $r_0$ from (104), we obtain

$$r_0 = \frac{1}{\left(1 - \int_0^\tau \cos\phi_0\,d\tau\right)^2}. \tag{115}$$

Hence

$$v_0 = 1 - \int_0^\tau \cos\phi_0\,d\tau. \tag{116}$$

This completes the solution to zero order in $f$ for any thrust direction programme. It will be noted that, to this order, all the initial conditions (104) have been satisfied.

Substituting this solution in eq. (7) to calculate a zero order approximation to $W$ (viz. $W_0$), we obtain

$$\left(1 - \int_0^W \cos\phi_0\,d\tau\right)^2 = 0,$$

or

$$\int_0^{W_0} \cos\phi_0\,d\tau = 1. \tag{117}$$

It is now obvious by inspection that this equation for $W_0$ has a minimum solution when $\cos\phi_0$ takes its maximum value of unity for all values of $\tau$. To zero order, therefore, $\phi_0 = 0$ is the optimal programme (TSIEN's) and

$$\left.\begin{aligned} u_0 &= 0, \\ v_0 &= 1 - \tau, \\ r_0 &= (1-\tau)^{-2}, \end{aligned}\right\} \tag{118}$$

$$W_0 = 1. \tag{119}$$

This solution implies that when escape conditions have been achieved, $r_0 = \infty$ and the trajectory is infinitely long. If we try to proceed to the next stage of approximation upon this as a basis, certain terms become infinite and the method fails. We shall accordingly calculate the optimal programme leading to conditions just short of escape, replacing eq. (7) by

$$u^2 + v^2 - \frac{2}{r} = -\eta^2. \tag{120}$$

Ultimately, we shall suppose that $\eta \to 0$.

Substituting from eqs. (118) into eq. (120), we now calculate that

$$W_0 = 1 - \eta. \tag{121}$$

To reduce the labour of calculation, we shall now look for a solution in the form

$$u = f u_1 + f^3 u_3 + \ldots, \tag{122}$$

$$v = (1 - \tau) + f^2 v_2 + \ldots, \tag{123}$$

$$r = (1 - \tau)^{-2} + f^2 r_2 + \ldots, \tag{124}$$

$$\phi = f \phi_1 + f^3 \phi_3 + \ldots, \tag{125}$$

$$W = 1 - \eta + f^2 W_2 + \ldots, \tag{126}$$

where we have omitted terms which, if included, would later be found to vanish. Substituting these expansions in eqs. (106) and equating coefficients of powers of $f$ as before, we obtain the equations

$$\dot{u}_1 - \phi_1 = -(1 - \tau)^6 r_2 + 2(1 - \tau)^3 v_2 + 2(1 - \tau)^6 r_2, \tag{127}$$

$$(1 - \tau)^3 u_1 = 2, \tag{128}$$

$$\dot{v}_2 + \tfrac{1}{2}\phi_1^2 = -(1 - \tau)^3 u_3 - (1 - \tau)^2 u_1 v_2 + (1 - \tau)^5 u_1 r_2, \tag{129}$$

$$\dot{r}_2 = u_3. \tag{130}$$

Putting $s = 1 - \tau$, we can obtain the solution to these equations in the form

$$u_1 = \frac{2}{s^3}, \tag{131}$$

$$v_2 = \frac{95}{14 s^7} - \frac{\phi_1}{s^3} + \frac{1}{2}\int_s^1 \left(\phi_1 - \frac{1}{s^4}\right)^2 ds - \frac{1}{2} K, \tag{132}$$

$$r_2 = \frac{K}{s^3} - \frac{53}{7 s^{10}} + \frac{\phi_1}{s^6} - \frac{1}{s^3}\int_s^1 \left(\phi_1 - \frac{1}{s^4}\right)^2 ds, \tag{133}$$

where $K$ is an integration constant and $\phi_1$ is regarded as a function of $s$. $K$ will be determined by the initial conditions and its existence proves that these are still arbitrary to a limited extent at the level of the second order in $f$.

Now [c. f. eq. (40)],

$$u(W) = u_0(W_0) + f\{u_1(W_0) + W_1 \dot{u}_0(W_0)\} + f^2\{u_2(W_0) + W_1 \dot{u}_1(W_0) + W_2 \dot{u}_0(W_0) + \tfrac{1}{2} W_1^2 \ddot{u}_0(W_0)\} + \ldots$$

$$= \frac{2f}{\eta^3} + O(f^3). \tag{134}$$

Similarly

$$v(W) = \eta + f^2\left\{\frac{95}{14\eta^7} - \frac{\phi_{11}}{\eta^3} + \frac{1}{2}\int_\eta^1 \left(\phi_1 - \frac{1}{s^4}\right)^2 ds - \frac{1}{2} K - W_2\right\}, \tag{135}$$

Vol. 4 1958

$$r(W) = \frac{1}{\eta^2} + f^2\left\{\frac{K}{\eta^3} - \frac{53}{7\eta^{10}} + \frac{\phi_{11}}{\eta^6} - \frac{1}{\eta^3}\int_{\eta}^{1}\left(\phi_1 - \frac{1}{s^4}\right)^2 ds + \frac{2}{\eta^3}W_2\right\}, \tag{136}$$

where $\phi_{11}$ is the value taken by $\phi_1$ at $\tau = W_0 = 1 - \eta$.

Substituting these expressions in eq. (120) and taking account of terms to $O(f^2)$, we calculate that

$$W_2 = -\frac{1}{2}K - \frac{17}{14\eta^7} + \frac{1}{2}\int_{\eta}^{1}\left(\phi_1 - \frac{1}{s^4}\right)^2 ds. \tag{137}$$

$\phi_1$ is, at present, an arbitrary function of $s$. We now choose it so that $W_2$ is minimised. Clearly this will be so if

$$\phi_1 = \frac{1}{s^4} = \frac{1}{(1-\tau)^4}. \tag{138}$$

Thus, the optimal thrust direction programme is given by

$$\phi = \frac{f}{(1-\tau)^4} = \frac{f}{(1-ft)^4}, \tag{139}$$

to the first order in $f$.

To the same order, the trajectory of escape is determined by the equations

$$u = \frac{2f}{(1-\tau)^3}, \tag{140}$$

$$v = 1 - \tau, \tag{141}$$

$$r = \frac{1}{(1-\tau)^2}. \tag{142}$$

Also, since $f\dot{\theta} = v/r$,

$$\theta = \frac{1}{4f}\{1 - (1-\tau)^4\} + O(f). \tag{143}$$

The characteristic velocity of the manoeuvre is given by

$$W = 1 - \eta - f^2\left(\frac{1}{2}K + \frac{17}{14\eta^7}\right) + O(f^3). \tag{144}$$

Since $\tan\psi = u/v$, we have

$$\psi = \frac{2f}{(1-\tau)^4} \tag{145}$$

to the first order. Comparing eqs. (139) and (145), we observe that

$$\phi = \tfrac{1}{2}\psi \tag{146}$$

approximately. Thus our optimal manoeuvre requires that the direction of thrust should bisect the angle between the direction of motion and the perpendicular to the radius vector $r$. This programme is the mean of the programmes of TSIEN and BENNEY.

Clearly, as $\eta \to 0$, $f$ must also approach zero at least as rapidly as $\eta^5$, if the above argument is to remain valid. We shall assume, therefore, that $\eta$ is first fixed to have some small value and the range of values of $f$ then restricted to ensure convergence of our expansions.

The thrust direction programme determined by eq. (146) will ensure optimal achievement of conditions close to escape. These conditions will be reached via

a spiral trajectory never diverging widely from a circle; this follows from eq. (140), where $u$ is seen to be of order $f$. However, over the latter part of the escape trajectory (which we have not considered) the rocket orbit is transformed from an approximately circular one into a parabolic one and this part of the trajectory will accordingly diverge greatly from a circle. In fact, over this portion of the track, the rocket is at such a great distance from the centre of attraction that the thrust is comparable in magnitude with gravity and conditions approximate more closely to those assumed in section 3 than they do to those assumed in this section. It may be expected, therefore, that the thrust direction programme determined by eq. (86) will have to be followed over this final section of the escape trajectory and that the angle between thrust direction and rocket motion will be steadily reduced towards the end of the manoeuvre, so that these directions are aligned at the instant of escape as required by the general theory.

## 5. Conclusion

As a result of this investigation, we are entitled to conclude that, under all circumstances, if escape is effected from a circular orbit by aligning the motor thrust with the direction of motion, the propellant expenditure will be very nearly minimal, and that little advantage is to be gained from a more complex thrust direction programme. However, if escape is to be effected in such a manner that the rocket is to arrive at infinity with a non-zero velocity, this conclusion may be invalidated. This point deserves further investigation.

Vol. 4 1958

## References

1. D. F. Lawden, Optimal Programming of Rocket Thrust Direction. Astronaut. Acta **1**, 41 (1955).
2. H. S. Tsien, Take-off from Satellite Orbit. Jet Propulsion **23**, 233 (1953).
3. D. J. Benney, Escape from a Circular Orbit Using Tangential Thrust. Jet Propulsion **28**, 167 (1958).

## Buchbesprechung — Book Review — Compte rendu

**History of German Guided Missiles Development.** Herausgegeben von TH. BENECKE und A. W. QUICK. Mit zahlreichen Textabb., VIII, 420 S. Braunschweig: Verlag A. Appelhans & Co. 1957. Geb. DM 32.—.

Nach dem Kriege ist eine Reihe oft unvollkommener und mangelhafter Arbeiten erschienen, in denen versucht wurde, eine Übersicht über die Entwicklung ferngelenkter Fluggeräte während des Krieges in Deutschland zu geben. Die vorliegende Zusammenfassung von 26 Vorträgen, die im Rahmen des AGARD-Seminars im April 1956 in München gehalten wurden, hat diese Aufgabe in eindrucksvoller Form erfüllt: Die geschickte Auswahl der Themen sichert dem Leser eine gute Übersicht über die wesentlichen Entwicklungen; allein die Darstellung seitens der berufensten Autoren, die von ihren eigenen Arbeiten berichten, verbürgt Sachlichkeit und hohes Niveau.

Nach einer einführenden Übersicht über die verschiedenen Entwicklungen findet der Leser 14 Arbeiten, die Problemen der Lenkung und Steuerung gewidmet sind. Die Fragen des Lenkverfahrens, der Steuersysteme, der Steuergeräte, der Zündauslösung, ihre Anwendungen und Entwicklung an verschiedenartigen Geräten sind noch heute aktuell, auch wenn die technologische Entwicklung auf den einzelnen Gebieten inzwischen fortgeschritten sein mag. Die Darstellung dieser Probleme in ihrer ersten Entwicklungsform und ihre Zusammenstellung vermitteln einen selten gebotenen Einblick in dieses weite Wissensgebiet.

Die aerodynamische Entwicklung der V 2 kann als Schulbeispiel für die Lösung derartiger Aufgaben gelten. Es sind wohl für kein anderes Gerät so vollständige und korrekte Messungen bekannt geworden.

Neun Arbeiten befassen sich mit Fragen der Triebwerksentwicklung: Treibstoffe, Pulverraketen- und Flüssigkeitsraketentriebwerke, Staustrahl- und Verpuffungsstrahltriebwerke sind die Themen. Bei den Flüssigkeitstriebwerken wird je eine Entwicklung mit Wasserstoffsuperoxyd, mit Flüssig-Sauerstoff und mit Salpetersäure als Sauerstoffträger beschrieben, bei den Staustrahltriebwerken je eine Entwicklung für Unterschall- und Überschallfluggeschwindigkeit. Auch hier erkennen wir die wohlgelungene Absicht, den gesamten Bereich der modernen Triebwerksentwicklung zu erfassen und so dem Leser einen Überblick und eine Gegenüberstellung zu ermöglichen.

Das Buch wird auch bei dem Fachmann großes Interesse finden, dem es manche Anregung vermitteln wird. Es ist ein einzigartiges Dokument deutscher Pionierarbeit, von deutschen Autoren zusammengestellt, und es wäre zu begrüßen, wenn es auch in deutscher Sprache erschiene. W. PILZ, Stuttgart

### Erratum

KOOY, J. M. J.: On Relativistic Rocket Mechanics. Astronaut. Acta **4**, Fasc. **1**, **31** (**1958**).

p. **55**, line 18 read: ... EMDEN [5] for: ... EULER [5].

Herausgeber, Eigentümer und Verleger: Springer-Verlag, Wien I, Mölkerbastei 5. — Für den Inhalt verantwortlich: Prof. Dr. Friedrich Hecht, Wien VIII, Alserstraße 69. — Druck: Berger & Schwarz, Zwettl, NÖ.

# Kernverbrennungsplasmen und magnetische Kernbrennkammern für Strahltriebwerke

Von

**F. Winterberg**[1], DGRR

(Mit 11 Abbildungen)

(*Eingegangen am 13. September 1957*[2])

Vol. 4 1958

**Zusammenfassung — Abstract — Résumé**

**Kernverbrennungsplasmen und magnetische Kernbrennkammern für Strahltriebwerke.** Es werden die Eigenschaften von Kernverbrennungsplasmen der Fusions- und Spaltungsreaktionen im Zusammenhang mit dem Antrieb von Raketen diskutiert.

Um eine Berührung der heißen Plasmen mit den Wänden der Verbrennungskammern zu verhindern, werden bestimmte Anordnungen von Magnetfeldern zum Einschluß der Plasmen vorgeschlagen.

Eine Reihe Möglichkeiten zur direkten Erzeugung von elektrischem Strom aus der Kernenergie zur Aufrechterhaltung der benötigten starken Magnetfelder wird zusammengestellt.

**Nuclear Combustion Plasmas and Magnetic Nuclear Combustion Chambers for Jet Propulsion.** The properties of fusion and fission plasmas are discussed in connexion with rocket propulsion.

To prevent contact of the hot plasmas with the walls of the combustion chambers special arrangements of magnetic fields are proposed for confining the plasmas.

For maintaining the necessary high magnetic fields a variety of methods for direct conversion of nuclear into electrical energy are considered.

**Plasmas nucléaires et chambres de réaction magnétiques pour moteurs-fusée.** Les propriétés de plasmas provenant de réactions nucléaires par fission ou fusion sont discutées en relation avec la propulsion par fusée.

En vue d'empêcher le contact du plasma à haute température avec les parois de la chambre certaines dispositions de champs magnétiques sont proposées pour le pincement du flux.

Plusieurs possibilités d'extraction directe de l'énergie électrique à partir de la réaction nucléaire sont rassemblées en vue de produire les champs magnétiques nécessaires.

## Einleitung

Die Ausströmgeschwindigkeit einer thermischen Rakete ist proportional der Wurzel aus der absoluten Temperatur. Für größenordnungsmäßig höhere Ausströmgeschwindigkeiten sind deshalb größenordnungsmäßig höhere Temperaturen

[1] Forschungsreaktor Geesthacht bei Hamburg, Bundesrepublik Deutschland.

[2] Leider erfolgte aus technischen Gründen eine Verzögerung der Publikation der vorliegenden Arbeit. (Die Redaktion.)

erforderlich. Die bisher zur Diskussion gestellten thermischen Atomraketen, bei denen der Antrieb durch Aufheizung einer Rückstoßmasse erfolgt, sind durch eine obere Grenze der dem Reaktormaterial zumutbaren Temperatur begrenzt. Die maximal theoretisch denkbare Temperatur bei Kernfusions- oder Kernspaltungsprozessen ist jedoch um viele Größenordnungen höher. Die hohe Temperatur der Reaktionsprodukte wird größtenteils zu Gunsten einer Entropievermehrung vernichtet.

Es werden hier neue Wege diskutiert, die bisherige Nachteile ausschließen, dafür aber eine Fülle neuer technischer Probleme bringen.

Es wird zunächst vorgeschlagen, Plasmareaktoren als Raketenbrennkammern zu verwenden. Als Reaktionsplasmen kommen dafür Fusions- und Spaltungsplasmen in Frage.

Wie SÄNGER gezeigt hat, können einige thermonukleare Reaktionen zwischen $10^7$ und $10^9$ °C gezündet werden und die Energieproduktion eines solchen thermonuklearen Plasmareaktors ist von derselben Größenordnung wie bei chemischen Hochdruckfeuerungen.

Wenn statt der bisherigen mit festen oder flüssigen Kernbrennstoffen arbeitenden Spaltungsreaktoren solche mit gasförmigen, etwa mit Uranhexafluorid, verwendet werden, zeigt sich, daß solche Reaktoren selbst bei sehr hohen Temperaturen unter Umständen überkritisch gehalten werden können. Die Energieproduktion ist dabei in günstigsten Fällen, selbst bei Temperaturen oberhalb $10^6$ °C, noch um Größenordnungen höher als bei chemischen Höchstdruckfeuerungen und wird erst oberhalb $10^8$ °C geringer als diese.

Im Vergleich zu den thermonuklearen Kernfeuerungen liegen bei den Spaltungskernfeuerungen die maximalen Energieproduktionsraten um Größenordnungen höher.

Die Ausbrandzeiten liegen im günstigsten Fall in der Größenordnung von Sekunden.

Bei Anwendung solcher Plasmareaktoren als Kernbrennkammern von Raketen muß der zum Abbrand kommende Kernbrennstoff in die gezündete bzw. überkritische Kernbrennkammer gepumpt werden, aus der er in einer Raketendüse expandiert wird. Die nach diesem Prinzip arbeitenden Atomraketen unterscheiden sich von den chemischen Raketen im wesentlichen nur durch die Verwendung von Kernbrennstoffen an Stelle chemischer Treibstoffe.

Die hohe Temperatur der Kernbrandplasmen erlaubt keine Anwendung materieller Wände. Der einzig gangbare Weg, der sich hier eröffnet, ist durch die Möglichkeit, ein Plasma in ein Magnetfeld einzuschließen und damit von seiner materiellen Umgebung zu isolieren, gegeben.

Durch entsprechende Gestaltung des Magnetfeldes lassen sich magnetische Kernbrennkammern fast jeder gewünschten Form, z. B. mit einer LAVAL-Düse versehen, herstellen. Die Zündung der Kernbrandplasmen erfolgt beim thermonuklearen Plasmareaktor durch adiabatische Kompression im Magnetfeld, beim Spaltungsplasmareaktor durch die Bedingung der Überkritikalität des Verbrennungsraumes.

Die Kopplung des Magnetfeldes mit den Reaktionsplasmen bietet außerdem die Möglichkeit einer direkten Umwandlung der Reaktionsenergie in elektrische Energie. Die Gewinnung von Elektrizität ist einmal für die Aufrechterhaltung der magnetischen Kernbrennkammern, zum anderen für die Zündung der thermonuklearen Reaktion erforderlich. Es ist daher eine Kombination der verschiedenen hier vorgeschlagenen Wege voraussichtlich notwendig.

Bei einem anderen, zur Diskussion gestellten Weg ist die Direkterzeugung von Atomenergie in Elektrizität in einem überkritischen Reaktor vorgesehen.

Der Grundgedanke eines solchen überkritischen Reaktors basiert auf der Möglichkeit, die anfänglich hohe Energie (von 90 MeV) der geladenen Spaltprodukte zum Aufbau eines elektrischen Feldes zu verwenden. Es ist dabei denkbar, eine Spannung von $4{,}5 \times 10^6$ Volt zu erreichen. Mit dieser Spannung beschleunigte Ionen haben eine Geschwindigkeit von größenordnungsmäßig $10^9$ cm/s.

Die Direkterzeugung von Elektrizität aus Kernenergie ist auch für eine Aufheizung von Plasmen mit Lichtbögen für Staustrahltriebwerke von Bedeutung.

## 1. Atomtechnik und Raketentechnik

Alle zukünftigen Anwendungsmöglichkeiten der Atomenergie sind durch zwei Tatbestände wesentlich bestimmt.

A. Während den Menschen seit Entdeckung des Feuers nur Umwandlungsgrade der Materie in Energie von $10^{-10}$ technisch greifbar waren, sind durch die Erschließung der Atomenergie Umwandlungsgrade der Materie von $10^{-3}$ zum ersten Male möglich geworden. Zur Veranschaulichung sei daran erinnert, daß 1 kg Steinkohle 8 kWh im Vergleich zu 1 kg Uran 235 mit 25 Millionen kWh liefert.

Vol. 4 1958

B. Die Atomenergie hat zum ersten Mal den Weg eröffnet, sehr hohe Temperaturen künstlich zu erzeugen, wie sie bisher nur im Sterneninneren theoretisch angenommen wurden. Die bei kernchemischen Verbrennungsprozessen auftretenden Partikelgeschwindigkeiten liegen um viele Zehnerpotenzen höher als bei den stärksten chemischen Verbrennungsprozessen. Die Geschwindigkeit z. B. der bei einer Kernspaltung auseinanderfliegenden Spaltstücke entspricht einer Temperatur von $10^{12}$ °C.

Nun zwei für die Raketentechnik maßgebliche Gesichtspunkte.

C. Im Gegensatz zu einem Fahrzeug, das sich auf der Erde fortbewegt und theoretisch beliebig oft auf Zwischenstationen zur Erneuerung seiner Treibstoffvorräte halt machen kann, ist an ein Raketenfahrzeug die Forderung zu erheben, über möglichst große Energiereserven zu verfügen, da über weite Strecken keine Zwischenlandungen erlaubt sein können.

D. Um einer Rakete einen möglichst hohen Antrieb zu verleihen, ist die Forderung nach einer möglichst großen Ausströmgeschwindigkeit zu erheben. Bei thermischen Raketen ist dies gleichbedeutend mit der Forderung nach einer möglichst hohen Brennkammertemperatur.

Wie man sieht, ist die Forderung C durch Tatbestand A grundsätzlich erfüllt und Forderung D durch Tatbestand B.

Alle bisherigen Vorschläge zur Realisierung von Atomraketen laufen darauf hinaus, in einem herkömmlichen Spaltungsreaktor ein Arbeitsmedium aufzuheizen und anschließend in einer Düse zu expandieren.

Allen diesen Vorschlägen sind aber vor allem zwei Argumente entgegenzuhalten. Einmal besteht wenig Aussicht, mit festen Reaktorbrennstoffen über Temperaturen von einigen $10^3$ °C zu gelangen. Dadurch ist es nicht möglich, über wesentlich höhere Temperaturen, als sie schon bei chemischen Raketen üblich sind, hinauszukommen. Die niedere Entropie der Spaltungsstücke wird nutzlos zu einem solchen Aufheizreaktor entwertet und es ist notwendig, viel Schubmasse mitzunehmen. Zum andern besteht aber noch eine weitere Schwierigkeit, auf die zuerst von WIGNER [3] hingewiesen wurde. Diese Schwierigkeit besteht darin, daß der zur Aufheizung des Arbeitsmediums erforderliche Reaktor im abgeschalteten Zustand außerhalb der Erdatmosphäre infolge ungenügender Kühlung zu einem baldigen Zerschmelzen der ganzen Rakete führen würde.

Die hier gemachten Vorschläge umgehen diese Nachteile.

Im Gegensatz zu allen bisherigen Vorschlägen verzichten sie grundsätzlich auf Reaktoren der üblichen Bauart.

Es sollen daher 1. an Stelle fester Kernbrennstoffe gasförmige verwendet werden, die auf hohe Temperaturen gebracht werden, 2. die heißen Plasmen durch magnetische Felder von allen materiellen Gebilden isoliert und 3. die damit eng zusammenhängende Bedeutung von Wegen zur Freisetzung von elektrischer Energie auf damit verbundenem oder anderem Weg diskutiert werden. Die vorliegende Arbeit ist die Weiterentwicklung zweier Arbeiten [1, 2], in denen Spaltungsplasmareaktoren als Raketenbrennkammern erörtert werden.

## 2. Thermonukleare Reaktionen

### *A. Allgemeines*

Während die Kernspaltung eine Kernreaktion ist, die über ungeladene Neutronen abläuft, handelt es sich bei thermonuklearen Prozessen um Kernreaktionen zwischen Atomkernen mit gleicher Ladung. Zur Auslösung einer solchen Kernreaktion müssen daher die beiden Reaktionspartner eine kinetische Anfangsenergie besitzen, die zur Überwindung der gegenseitigen COULOMB-Abstoßung ausreicht.

Erst wenn einander die Kerne genügend nahe gekommen sind, überwiegt der Einfluß der starken, aber nur auf kurze Entfernung wirkenden anziehenden Kernkräfte, die abstoßenden elektrostatischen Kräfte.

Die Möglichkeit der thermonuklearen Reaktion beruht darauf, daß die Bedingung einer kinetischen Mindestenergie der Reaktionspartner bei genügend hohen Temperaturen von selbst gegeben ist. Es genügt daher, die zur Kernreaktion kommenden Stoffe auf eine genügend hohe Temperatur zu bringen, um im makroskopischen Maßstab eine Kernverbrennung durchzuführen. Wegen der notwendigerweise hohen Temperaturen werden die Atome dabei praktisch vollständig ionisiert sein, so daß man von dem zum Abbrand kommenden Kernverbrennungsplasma spricht. Bei technisch beherrschbaren Drucken reicht, wie SÄNGER [3] gezeigt hat, die Energieproduktion thermonuklearer Reaktionen pro $cm^3$ und s bei genügend hohen Temperaturen an jene chemischer Hochdruckfeuerungen heran. Die Ausbrandzeiten des Kernverbrennungsplasmas können dabei so klein werden, wie es für technische Zwecke notwendig ist.

Ein großes Hindernis für thermonukleare Reaktionen bedeuten die erforderlichen hohen Zündungstemperaturen, die ausnahmslos über $10^7$ °C liegen, also um viele Größenordnungen höher als bei chemischen Reaktionen.

### *B. Das Kernverbrennungsplasma*

Um die physikalischen Verhältnisse zu übersehen, soll jetzt etwas über das zum Abbrand kommende Kernverbrennungsplasma gesagt werden.

Jedes im Gleichgewicht befindliche Gas enthält neben der häufigsten, durch die Temperatur $T$ bestimmten Teilchengeschwindigkeit von der Größe

$$v = \sqrt{\frac{3\,k\,T}{M}} \tag{1}$$

auch alle anderen Teilchengeschwindigkeiten zwischen Null und Unendlich, wobei die Verteilung der Teilchen auf diese Geschwindigkeiten durch die MAXWELL-BOLTZMANNsche Geschwindigkeitsverteilung bestimmt ist. Es kommen also schon bei beliebig niederen Temperaturen, wenn auch äußerst selten, Teilchengeschwindigkeiten vor, die ausreichen, das abstoßende COULOMB-Potential der Kerne zu überwinden, und somit zu einer Kernreaktion führen können. Bei

Erhöhung der Temperatur treten solche Teilchenenergien immer häufiger auf, was eine Erhöhung der Energieproduktion zur Folge hat. Außer diesen energiespendenden Reaktionen finden aber auch Verlustprozesse an die Umgebung des Plasmas statt. Erst bei sehr hohen Temperaturen und damit hoher Energieproduktion ist es möglich, die Energieverluste an die Umgebung kleiner als die Energieproduktion des Plasmas zu machen.

Um technisch eine thermonukleare Reaktion in Gang zu bringen, ist es wesentlich, durch eine möglichst starke Aufheizung über den Punkt, von dem ab die Verluste an die Umgebung kleiner werden als die Energieproduktion, möglichst schnell zu gelangen.

### *C. Die Energieproduktionsrate thermonuklearer Reaktionen*

Die Idee der Energieproduktion durch thermonukleare Kernreaktionen ist zum ersten Mal von ATKINSON und HOUTERMANS [4] im Zusammenhang mit der Frage nach der Energieerzeugung in den Sternen ausgesprochen worden. Die Berechnung der Energieproduktionsrate als Funktion von Temperatur und Plasmadichte waren zum damaligen Zeitpunkt des Standes der Theorie der Kernreaktionen noch mit Fehlern behaftet. GAMOW [5] hat diese Mängel beseitigt, und wir folgen seiner Ausarbeitung der Idee von ATKINSON und HOUTERMANS, wobei wir uns an die zweckmäßige Bezeichnungsweise der unter [3] zitierten Arbeit von SÄNGER anschließen.

Vol. 4 1958

Um die Anzahl der stattfindenden Kernreaktionen pro $cm^3$ und Sekunde eines Kernbrandplasmas zu erhalten, muß der Reaktions-Wirkungsquerschnitt $\sigma(v)$ der betrachteten Kernreaktion mit der MAXWELL-Verteilung

$$dN = f(v)\, dv$$

multipliziert und von Null bis Unendlich integriert werden. Die Integration wird dabei mit der Sattelpunktsmethode durchgeführt. Die Energieproduktion pro $cm^3$ und s ergibt sich durch Multiplikation dieses Resultats mit der Wärmetönung der betrachteten Einzelreaktion.

Mit den Bezeichnungen:

$v$ die Teilchengeschwindigkeit,
$R$ der Radius des gebildeten Zwischenkerns,
$A_1, A_2$ die Atomgewichte der reagierenden Kerne,
$A = A_1 A_2/(A_1 + A_2)$,
$M$ die Nukleonenmasse,
$\Gamma$ die Resonanzbreite des angeregten Zwischenkerns,
$Z_1$ und $Z_2$ die Kernladungszahlen der Stoßpartner,
$e$ das elektrische Elementarquantum,
$\hbar$ das PLANCKsche Wirkungsquantum,
$T$ die absolute Temperatur,
$E$ die Wärmetönung der Einzelreaktion,
$\varrho$ die Plasmadichte,
$c_1, c_2$ relative Gewichtskonzentrationen der Reaktionspartner,
$k$ die BOLTZMANN-Konstante,

$$k_1 = \frac{4}{3^{5/2}} \frac{\Gamma \hbar R^2}{M^3 A A_1 A_2 e^2 Z_1 Z_2} \exp 8 \left( \frac{R A M e^2 Z_1 Z_2}{2 \hbar^2} \right)^{1/2} \quad [\mathrm{cm^3\, g^{-2}\, s^{-1}]}$$

$$k_2 = \left( \frac{27 \pi^2 A M e^4 Z_1^2 Z_2^2}{k \hbar^2} \right)^{1/3} \quad [\mathrm{grad^{1/3}}],$$

erhält GAMOW für die Energieproduktion in erg pro g und s den Ausdruck:

$$\Delta E = E \varrho^2 c_1 c_2 k_1 (k_2 T^{-1/3})^2 \exp [- k_2 T^{-1/3}] \, [\mathrm{erg\, g^{-1}\, s^{-1}}]. \qquad (2)$$

Aus Gl. (2) folgt durch Differenzieren das Maximum der Reaktionsrate bei einer Optimaltemperatur von

$$T_{\text{opt}} = \left(\frac{k_2}{2}\right)^3 \tag{3}$$

mit

$$\Delta E_{\max} = (2/e)^2 E \varrho c_1 c_2 k. \tag{4}$$

Die Lage des Maximums ergibt sich anschaulich durch die bestmögliche Überlappung der Kurve des Wirkungsquerschnitts und der MAXWELL-Verteilung.

Mittels der Gasgleichung läßt sich Gl. (2) auf die für technische Verhältnisse interessantere Form

$$\Delta E = E p^2 c_1 c_2 \frac{M^2 k_1 T^{-2}}{k^2 \left(\frac{c_1}{A_1} + \frac{c_2}{A_2}\right)^2} (k_2 T^{-1/3})^2 \exp\left[-k_2 T^{-1/3}\right] [\text{erg cm}^{-3}\,\text{s}^{-1}] \tag{5}$$

bringen. In Gl. (5) wird die Energieproduktion bei festgehaltenem Feuerraumdruck pro $\text{cm}^3$ und s angegeben, wie sie für technische Fragestellungen von Interesse ist. Die Energieproduktion je Volumen- und Zeiteinheit hat bei festgehaltenem Druck über der Temperatur ein Maximum bei der kleineren Temperatur

$$T_{\text{opt}}' = \left(\frac{k_2}{8}\right)^3$$

von der Höhe

$$\Delta E_{\max} = (8/e)^8 E p^2 c_1 c_2 \frac{M^2 k_1}{k_2^6 k^2 \left(\frac{c_1}{A_1} + \frac{c_2}{A_2}\right)^2}. \tag{6}$$

Die Ausbrandzeit des Kernbrandplasmas ist durch die Halbwertzeit des Reaktionsablaufs gemäß

$$\tau = \frac{E}{\Delta E_{\max}} \tag{7}$$

charakterisiert.

Neben den dabei betrachteten Zweierstoßkombinationen sind auch kompliziertere Reaktionsketten denkbar, wie der BETHE-WEIZSÄCKER-Zyklus der Sonne und der vermutliche Wasserstoffbombenprozeß zum Aufbau von Helium aus Lithium und Deuterium:

$$\left.\begin{array}{l} \rightarrow n + {}^6\text{Li} \longrightarrow {}^3\text{H} + {}^4\text{He} \\ {}^3\text{H} + {}^2\text{H} \longrightarrow {}^4\text{He} + n \rightarrow \end{array}\right]. \tag{8}$$

wobei ein Neutron sich in jeder Reaktionskette wieder selbst reproduziert.

Eine Zusammenstellung der Energieproduktionskurven nach dem besten gegenwärtig verfügbaren experimentellen Material findet sich bei POST [6].

### 3. Die Kernspaltungsverbrennung

#### *A. Allgemeines*

In Analogie zur thermonuklearen Verbrennung lassen sich die physikalischen Gesetze der Kernspaltungsverbrennung aufstellen, wie sie in den unter [1, 2] angegebenen Arbeiten entwickelt wurden.

Im Gegensatz zu allen bisherigen Reaktoren mit festen oder flüssigen Kernbrennstoffen sollen solche mit gasförmigen Spaltstoffen verwendet werden und die Reaktion bei solchen Temperaturen ablaufen, daß man mit Recht von

einem Spaltstoffplasma sprechen darf. Als solche Spaltstoffplasmen kommen z. B. Uran und Plutonium bei hohen Temperaturen in gasförmigem Zustand in Frage. Aber auch viele Kombinationen mit anderen Stoffen sind denkbar.

Ein Reaktor dieser Art soll als Plasma-Spaltungsreaktor bezeichnet werden.

*B. Der prompt kritische Plasma-Spaltungsreaktor als Raketenbrennkammer*

In der Atomtechnik unterscheidet man zwischen schnellen, intermediären und thermischen Reaktoren. Bei der ersten Art findet keine Abbremsung der anfänglich mit $10^9$ cm/s fliegenden Neutronen, bei der zweiten Art eine teilweise Abbremsung und bei der dritten Art eine Abbremsung bis auf thermische Energien statt. Die Abbremsung hat bei thermischen Neutronenenergien z. B. den Vorteil, daß der Wirkungsquerschnitt für Spaltung etwa um den Faktor 100 größer ist. Die freien Weglängen und damit die kritischen Abmessungen sind entsprechend kleiner. Von Nachteil bei thermischen Neutronenenergien ist, daß die Reaktionskette für bestimmte Zwecke, wie z. B. für Bomben, nicht schnell genug abläuft. Von Vorteil für die Zwecke der Raketentechnik wäre dabei, daß Wasserstoff als bestes Bremsmittel für Neutronen verwendet werden müßte, der durch seine hohe Ausströmgeschwindigkeit gegenüber allen anderen Stoffen begünstigt ist.

Vol. 4 1958

Die Eigenschaft des Wasserstoffs, bestes Bremsmittel für Neutronen zu sein, ergibt sich bekanntlich aus der Tatsache, daß Protonen und Neutronen etwa dieselbe Masse besitzen, und somit ein Neutron schon bei einem Stoß alle Energie an das Proton abzugeben vermag.

Wesentlich für das Arbeiten eines Plasmareaktors ist, daß die Anordnung überkritisch ist, das heißt, daß die Neutronenverluste an die Umgebung nicht die im Reaktor erzeugten Neutronen übersteigen. In dem hier zur Diskussion gestellten Strahltriebwerk wird, wie schon betont, der Kernbrennstoff in die überkritische Kernbrennkammer gebracht, die den Plasmareaktor bildet und nach Abbrand in einer Raketendüse expandiert. Außerdem erübrigt sich hier eine Zündung, da sie durch die Bedingung der Kritikalität von selbst gegeben ist. Im Gegensatz zu allen anderen Reaktoren soll der Plasmareaktor bei sehr hohen Temperaturen arbeiten, das heißt mit Plasmen, die eine geringe Dichte besitzen. Um die Energieproduktion unter diesen Umständen genügend hoch zu halten, müßte deshalb ein solcher Reaktor, wie bei Atombomben, am besten prompt kritisch gemacht werden. Normalerweise arbeiten die Reaktoren im verspätet überkritischen Bereich. Darunter versteht man bekanntlich, daß die Kettenreaktion durch die von den Spaltstücken nach ungefähr 10 s abgedampften Neutronen gerade in Gang gehalten wird. Im verspätet kritischen Bereich ist die Energieproduktion daher viel geringer. Die lange Lebensdauer der verspäteten Neutronen gewährt dabei eine leicht durchführbare Regelung des Reaktors.

Es wird für viele Fälle genügen, bzw. erwünscht sein, eine geringere Energieproduktion als im prompt kritischen Fall zu erhalten. Die für den prompt kritischen Fall berechneten Energieproduktionsraten geben dann eine obere Grenze der möglichen Energieproduktion des Kernspaltungsplasmas an, da alle Übergänge zwischen prompt und verspätet kritisch möglich sind.

*C. Das Kernspaltungsplasma*

Zum Unterschied von Feuergasen der thermonuklearen Reaktionen und vieler chemischer Verbrennungsprozesse, deren Reaktivität bei konstanter Plasmadichte mit wachsender Temperatur zunimmt, sind die Kettenreaktionsprozesse der Kernspaltung (von extremen Fällen abgesehen) im Vergleich dazu fast temperaturunabhängig. Selbst die an sich kleinen Temperaturkoeffizienten

der Reaktivität von Reaktoren beruhen im wesentlichen auf Dichte-Änderungen mit wachsender Temperatur. Der Unterschied wird verständlich, wenn man berücksichtigt, daß zum Zustandekommen einer thermonuklearen Reaktion die Reaktionspartner eine hohe Geschwindigkeit zur Überwindung des COULOMB-Berges besitzen müssen. Als Folge davon werden die Wirkungsquerschnitte stark temperaturabhängig, im Gegensatz zu den Wirkungsquerschnitten der ungeladenen Neutronen, auf die der COULOMB-Berg keinen Einfluß hat. Die Situation ist hier vielmehr so gelagert, daß für niedere Neutronenenergien ein $1/v$-Gesetz des Wirkungsquerschnitts beobachtet wird, während für hohe Energien der Wirkungsquerschnitt im wesentlichen geschwindigkeitsunabhängig und größenordnungsmäßig durch den geometrischen Wirkungsquerschnitt bestimmt ist. Im Vergleich zu den anderen Reaktionen bleibt jedoch bei Spaltungsreaktionen die Abhängigkeit der Reaktivität von der Dichte, da diese allein den für die Reaktionsgeschwindigkeit maßgeblichen makroskopischen Wirkungsquerschnitt $N\sigma$ bestimmt. Im Kernfeuerungsgas der Kernspaltungsreaktionen wird die Verbrennung in jenen Gebieten um so schneller vor sich gehen, die eine höhere Dichte haben.

Es soll jetzt das Schicksal eines Kernbrennstoffteilchens betrachtet werden. Es werde dabei angenommen, daß das Teilchen in die Brennkammer gelangt und für sich genommen plötzlich überkritisch wird. Als Folge davon findet in diesem Teilchen eine starke Wärmeentwicklung statt, die zu einer starken Ausdehnung des Teilchens und schließlich Ausstoßung durch die Düse führt. Die zu diesem Aufheizprozeß notwendigen Zeiten sind dabei so kurz, daß entsprechend der SÄNGERschen Theorie der Kurzzeitvorgänge [7] nur die translatorischen Freiheitsgrade zu berücksichtigen sind.

Um den geschilderten Vorgang quantitativ zu erfassen, müssen die dafür maßgeblichen Reaktorgleichungen aufgestellt werden, die die Energieproduktion als Funktion von Druck und Temperatur liefern.

### *D. Die Reaktorgleichungen des prompt kritischen Plasmareaktors*

Das zeitliche Verhalten eines Reaktors läßt sich durch zwei Gleichungen beschreiben. Die erste Gleichung liefert den Zusammenhang der Änderung des Neutronenflusses in Abhängigkeit von Fluß und Temperatur und die zweite den Zusammenhang von Fluß und Temperatur. Während die erste Gleichung sich aus reaktorkinetischen Überlegungen ergibt, wird die zweite durch den thermodynamischen Zusammenhang von Neutronenfluß und Leistung gewonnen.

Die erste Reaktorgleichung lautet im prompt kritischen Fall:

$$l_0 \dot{\phi} = (\eta - 1)\, \phi. \tag{9}$$

Dabei bedeuten $l_0$ die Stoßzeit eines Neutrons zwischen zwei Reaktionen, $\phi$ den Neutronenfluß in (n/cm²s) und $\eta$ den Vermehrungsfaktor der Neutronen. $\eta - 1$ ist der Faktor, um den sich die Neutronenzahl nach einer Generation vermehrt, wobei berücksichtigt ist, daß pro Spaltung ein Neutron verbraucht wird.

Die Stoßzeit $l_0$ ist durch die Beziehung

$$l_0 = \frac{1}{N \sigma_a v} \tag{10}$$

festgelegt. $v$ ist die Geschwindigkeit der Neutronen, $\sigma_a$ der Wirkungsquerschnitt des Spaltstoffs für Spaltung und Einfang.

Wegen $p = N k T$ schreibt sich (10)

$$l_0 = \frac{T}{p} \frac{k}{\sigma_a v}. \tag{10 a}$$

Damit schreibt sich Gl. (9):

$$\frac{T}{P}\dot{\phi} = \frac{(\eta - 1)\,\sigma_a\, v}{k}\,\phi. \tag{11}$$

Bei konstantem $l_0$, das heißt, wenn sich mit wachsendem Fluß die Dichte nicht ändert, folgt durch Integration von (9)

$$\phi = \phi_0\, e^{\frac{\eta-1}{l_0}\,t}. \tag{12}$$

In dem uns interessierenden Fall konstanten Plasmadrucks ist aber $l_0$ keineswegs mehr konstant, sondern nach (11) eine Funktion der Temperatur. Um das damit verbundene Problem zu lösen, muß noch die zweite Reaktorgleichung aufgestellt werden, die den Zusammenhang zwischen Fluß und Temperatur liefert.

Die Leistung $Q$ pro cm³ hängt mit der Temperatur bei konstantem Druck gemäß

$$Q = \varrho\, c_p\, \dot{T} \qquad [\mathrm{erg\,cm^{-3}\,s^{-1}}] \tag{13}$$

zusammen. Andererseits ist die Leistung mit dem Fluß durch die Beziehung

$$Q = N\,\sigma_f\,\phi \cdot 3{,}1 \cdot 10^{-4} \qquad [\mathrm{erg\,cm^{-3}\,s^{-1}}] \tag{14}$$

verknüpft, wobei die Größe $3{,}1 \cdot 10^{-4}$ die pro Spaltung freiwerdende Energie in erg angibt. $\varrho$ ist die Plasmadichte. Durch Verbindung von (12) und (13) folgt

$$\varrho\, c_p\, \dot{T} = N\,\sigma_f\,\phi \cdot 3{,}1 \cdot 10^{-4} \qquad [\mathrm{erg\,cm^{-3}\,s^{-1}}]. \tag{15}$$

Mittels der Gasgleichung

$$N = \frac{p}{k\,T}, \qquad \text{bzw.} \qquad \varrho = \frac{p}{R\,T}\,A \tag{16}$$

und der für Kurzzeitvorgänge maßgeblichen spezifischen Wärme der Translation bei konstantem Druck

$$c_p = \frac{5}{2}\,\frac{R}{A}$$

folgt aus (15)

$$\dot{T} = 3{,}1 \cdot 10^{-4}\,\frac{2}{5}\,\frac{\sigma_f}{k}\,\phi. \tag{17}$$

Die Gln. (9) und (17) legen das zeitliche Verhalten des Reaktors fest.

Führt man noch die Abkürzungen

$$a = \frac{(\eta - 1)\,\sigma_a\, v}{k}$$

$$b = 3{,}1 \cdot 10^{-4}\,\frac{2}{5}\,\frac{\sigma_f}{k}$$

ein, so lassen sich (11) und (17) auf die einfache Form

$$T\,\dot{\phi} = a\,p\,\phi \tag{18 a}$$

$$\dot{T} = b\,\phi \tag{18 b}$$

bringen.

Aus (18 a) folgt durch Differentiation

$$\ddot{T} = b\,\dot{\phi}. \tag{19}$$

Wenn man in Gl. (18 a) mittels (18 b) und (19) den Fluß eliminiert, erhält man:

$$T\,\ddot{T} = a\,p\,\dot{T}. \tag{20}$$

Vol. 4 1958

An (20) ist bemerkenswert, daß sich die Größe $b$ herausgehoben hat. Wir kommen darauf noch zurück. Setzt man:

$$\dot{T} = q,$$

so folgt

$$\ddot{T} = \frac{dq}{dT}\dot{T} = q\frac{dq}{dT}.$$

In (20) eingesetzt liefert dies:

$$T\,q\frac{dq}{dT} = a\,p\,q. \tag{21}$$

Gl. (21) hat einmal die nicht interessierende Lösung $q = 0$, das heißt $T = \text{const.}$, und zum anderen die aus der Differentialgleichung

$$T\frac{dq}{dT} = a\,p \tag{22}$$

folgende Lösung:

$$\dot{T} - \dot{T}_0 = a\,p\ln\frac{T}{T_0}. \tag{23}$$

Hierbei bedeuten $T_0$ die Temperatur und $\dot{T}_0$ deren Änderung zur Zeit $t = 0$.

Da auf der linken Seite von (23) ein Ausdruck steht, der proportional der Leistung ist, liefert (23) bereits die Energieproduktion als Funktion von Druck und Temperatur. Zur Beurteilung der zeitlichen Dauer des betrachteten Aufheizprozesses muß Gl. (23) nochmals integriert werden und man erhält

$$t = \frac{1}{a\,p}\int_{T_0}^{T}\frac{dT}{\dot{T}_0 + \ln\dfrac{T}{T_0}}. \tag{24}$$

*E. Die Energieproduktionsrate als Funktion von Druck und Temperatur*

Um die Energieproduktionsrate zu bestimmen, muß man das durch die Gl. (23) bestimmte Schicksal eines Teilchens herausgreifen. Es soll dabei angenommen werden, daß $\dot{T}_0$ klein gegen die übrigen Größen ist, außerdem soll $T \gg T_0$ sein, so daß sich (23) in der Form schreiben läßt:

$$\dot{T} \simeq a\,p\ln T. \tag{25}$$

Mit (18 b) ergibt sich daraus für den Fluß

$$\phi \simeq \frac{a}{b}\,p\ln T \tag{26}$$

bzw.

$$\phi = 0{,}806\cdot 10^4\,(\eta - 1)\,v\ln T. \tag{26 a}$$

Die Leistung berechnet sich aus Gl. (14); wegen $p = N\,k\,T$ folgt mit (26)

$$Q \simeq 2{,}5\,(\eta - 1)\frac{v\,\sigma_f}{k}\,p^2\frac{\ln T}{T} \qquad [\text{erg cm}^{-3}\,\text{s}^{-1}]. \tag{27}$$

An Gl. (27) ist bemerkenswert, daß die pro Spaltung freiwerdende Energie nicht eingeht. Dies scheinbar widerspruchsvolle Ergebnis läßt sich aber verständlich

machen. Bei einer geringeren Kernreaktionsenergie wird nämlich die gleiche Leistung durch die Kettenreaktion bei derselben Temperatur erst zu einem späteren Zeitpunkt erreicht. Dabei ist zu bemerken, daß unsere Ausgangsgleichungen eine Abnahme der Spaltstoffsubstanz durch die voranschreitende Kettenreaktion unberücksichtigt lassen. Bei einer kleineren Reaktionsenergie würde sich eine solche Abnahme schon bei Erreichung niederer Temperaturen bemerkbar machen, indem sie ein weiteres Anwachsen der Kettenreaktion verbietet. Aus diesem Grund ist die Anwendung der Gl. (27) für chemische Kettenreaktionen beispielsweise nur unterhalb dieser Grenze statthaft. Durch diese Einschränkung wird eine obere Grenze für die maximal erreichbare Temperatur festgelegt. Kernkettenreaktionen können im Gegensatz zu chemischen Kettenreaktionen viel weiter voranschreiten und damit zu viel höheren Temperaturen führen, bis sie durch den Ausbrand des Brennstoffs zum Abreißen kommen. Aus (27) entnimmt man, daß die Energieproduktion bei konstantem Druck mit wachsender Temperatur abnimmt im Einklang mit der Tatsache, daß die Anzahl der zur Spaltung pro $cm^3$ verfügbaren Kerne bei konstantem Druck mit wachsender Temperatur geringer wird.

Vol. 4 1958

Gl. (27) gibt streng genommen nicht die richtige Energieproduktion wieder, die sich durch Bildung des Mittelwerts der Energieproduktion eines Teilchens, genommen über den Aufheizprozeß, ergeben würde. Da der Aufheizprozeß von den Anfangsbedingungen abhängt und außerdem außerordentlich schnell durchlaufen wird, kann man mit guter Näherung auf diese Verfeinerung verzichten. Im stationären Betrieb ist darauf zu achten, daß die Kettenreaktion bei Erreichung der gewünschten Energieproduktion nicht weiter ansteigt.

Je nachdem, ob die Spaltneutronen abgebremst werden oder nicht, spricht man von einem thermischen oder schnellen Reaktor. Außerdem ist eine teilweise Abbremsung auf mittlere Neutronenenergien möglich. Reaktoren dieser letzten Art werden als intermediäre Reaktoren bezeichnet. Wir beschränken uns bei der Diskussion der Gl. (27) auf die beiden Grenzfälle schneller und thermischer Reaktoren und stellen die benötigten Werte zusammen.

| | schnell | thermisch |
|---|---|---|
| $\eta$ | 2,5 | $\lesssim 2{,}5$ |
| $v$ | $\sim 2 \cdot 10^{9}$ [cm $s^{-1}$] | $\sim 2 \cdot 10^{5}$ [cm $s^{-1}$] |
| $\sigma_f$ | $\sim 2 \cdot 10^{-24}$ [$cm^2$] | $\gtrsim 2 \cdot 10^{-22}$ [$cm^2$] |

Beim thermischen Reaktor ist für die Neutronengeschwindigkeit der unter thermischen Normalbedingungen geltende Wert und als Spaltquerschnitt der halbe Wirkungsquerschnitt von U 233 genommen worden. Letzteres soll berücksichtigen, daß ein Teil der in der Brennkammer vorhandenen Atomkerne Moderator-Atome sind. Für einen thermischen Reaktor ist das Produkt $\sigma_f v$ temperaturunabhängig, da $\sigma_f$ für niedere Energien ein $1/v$-Gesetz befolgt. Mit den oben angegebenen Werten erhält man für den schnellen Reaktor:

$$Q \simeq 4{,}5 \cdot 10^{6}\, p^2\, \frac{\log T}{T^{10}} \qquad [\text{cal cm}^{-3}\,\text{s}^{-1}] \tag{27a}$$

und für den thermischen Reaktor

$$Q \simeq 4{,}5 \cdot 10^{4}\, p^2\, \frac{\log T}{T^{10}} \qquad [\text{cal cm}^{-3}\,\text{s}^{-1}]. \tag{27 b}$$

Der Druck $p$ ist dabei in atm einzusetzen.

In Abb. 1 sind die Energieproduktionsraten als Funktion der Temperatur beim Druck von 1 und 100 atm aufgetragen. Zum Vergleich ist die Energieproduktion einer V2-Raketenbrennkammer eingetragen. Man sieht, daß bei Feuerraumdrucken, wie sie in chemischen Hochdruckraketen üblich sind, die Energieproduktion erst bei sehr hohen Temperaturen unter diejenige chemischer Hochdruckfeuerungen gelangt.

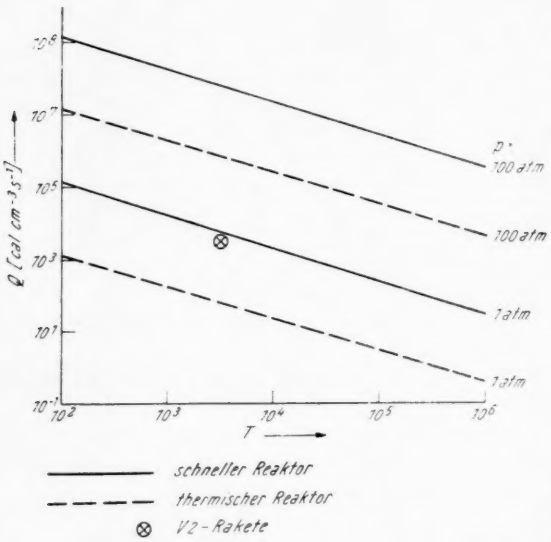


Abb. 1. Grenzkurven für die Energieproduktion von Kernspaltungsplasmen

Der Vergleich von schnellem und thermischem Reaktor lehrt, daß sich der schnelle Reaktor in Beziehung auf die Energieproduktion um den Faktor $10^2$ günstiger stellt. Der Faktor $10^2$ ergibt sich daraus, daß die Neutronengeschwindigkeit beim schnellen Reaktor um den Faktor $10^4$ größer, der Spaltquerschnitt aber um den Faktor $10^2$ kleiner ist.

### *F. Abschätzung des zeitlichen Verlaufs*

Um den zeitlichen Verlauf der Brennstoffaufbereitung abzuschätzen, muß man auf Gl. (24) zurückgreifen. Setzt man in (24) die Größe $(\dot{T}_0 + \ln T/T_0)^{-1}$ als langsam veränderliche Funktion vor das Integral und nimmt dafür einen Mittelwert von der Größenordnung 1 an, so erhält man:

$$T \sim a\, p\, t \tag{28}$$

als Abhängigkeit der Temperatur von der Zeit.

Nach dieser rohen Abschätzung besteht ein zeitlich linearer Temperaturanstieg.

Für schnelle Reaktoren ist $a \simeq 10^1$ und für thermische $a \simeq 10^{-1}$; damit ergibt sich, wenn wir $p$ in atm ausdrücken:

$$T \sim 10^7\, p\, t \qquad \text{(28 a) schneller Reaktor}$$
$$T \sim 10^5\, p\, t \qquad \text{(28 b) thermischer Reaktor.}$$

Aus (28 a) und (28 b) entnimmt man die außerordentliche Schnelligkeit des Aufheizprozesses.

Für die spezifischen Wärmen darf man daher die für Kurzzeitvorgänge maßgeblichen translatorischen Freiheitsgrade zugrunde legen.

### *G. Die Ausbrandzeiten*

Von weiterer Wichtigkeit für die Beurteilung des Reaktionsablaufs sind die Ausbrandzeiten. Sie geben eine Aussage, wie hoch der Ausbrand des Brennstoffs bei gegebener Aufenthaltsdauer in der Brennkammer ist.

Die Abnahme der spaltbaren Kerne pro cm³ durch Kernspaltungen wird durch die Gleichung

$$\frac{dN}{dt} = -N\,\sigma_f\,\phi \tag{29}$$

beschrieben. Man definiert als Ausbrandzeit die Zeit, bei der die Anzahl der spaltbaren Kerne auf den $e$-ten Teil abgesunken ist:

$$\tau = \frac{1}{\sigma_f\,\phi}, \tag{30}$$

oder wenn man $\phi$ aus Gl. (26) einsetzt,

$$\tau = \frac{0{,}825\cdot 10^{-4}}{\sigma_f\,v}\,\frac{1}{p\ln T}. \tag{31}$$

Man erhält ($p$ in atm) für den schnellen Reaktor:

$$\tau \simeq \frac{0{,}5\cdot 10^{3}}{p\log_{10} T} \tag{31 a}$$

und für den thermischen Reaktor:

$$\tau \simeq \frac{0{,}5\cdot 10^{5}}{p\log_{10} T}. \tag{31 b}$$

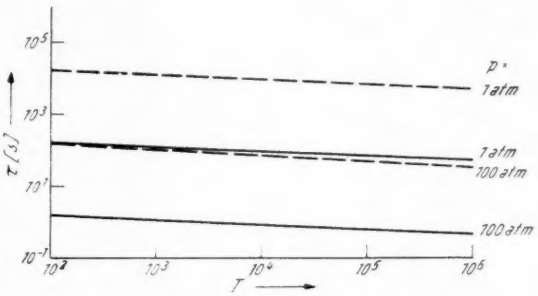


Abb. 2. Ausbrandzeiten von Kernspaltungsplasmen

In Abb. 2 sind die Ausbrandzeiten aufgetragen. Daraus lernt man, daß nur bei schnellen Reaktoren und zugleich hohen Drucken die Ausbrandzeiten auf Werte herunterkommen, die eine Verwendung von Plasmareaktoren in Raketen wirtschaftlich tragbar erscheinen lassen. Andernfalls muß ein großer Verlust an teurem Brennstoff, der unverbrannt abgestrahlt wird, in Kauf genommen werden.

### *H. Der kritische Radius des Plasmareaktors*

Zum Zwecke der Abschätzung soll einfachheitshalber die Gültigkeit der elementaren Neutronendiffusionsgleichung vorausgesetzt werden. Man darf deshalb den gewonnenen Ergebnissen nur den Wert einer ganz rohen Abschätzung beimessen.

Bei der Berechnung des kritischen Radius des Plasmareaktors folgen wir dem bekannten Buch von GLASSTONE und EDLUND [8]. Als Kritik wollen wir dabei vorwegnehmen, daß die im Rahmen dieses Buches abgeleiteten Formeln von der Differentialgleichung der Neutronendiffusion gewonnen sind und deshalb streng genommen nur in dem Maße Gültigkeit besitzen, als die freie Weglänge klein gegen die Dimension des Reaktors ist. Diese Situation ist im Fall des Plasmareaktors sicher nicht gegeben.

Der kritische Radius $R_0$ eines kugelförmigen Reaktors wird durch den Ausdruck

$$R_0 = \frac{\pi L}{\sqrt{\eta - 1}} \tag{32}$$

bestimmt.

Vol. 4 1958

Dabei bedeuten:

$$L = \frac{1}{N\sqrt{3\,\sigma_s\,\sigma_f}}$$

die Diffusionslänge der Neutronen, $\sigma_s$ und $\sigma_f$ die Wirkungsquerschnitte gegenüber Streuung und Spaltung, $N$ die Anzahl der spaltbaren Kerne pro $cm^3$.

Setzt man, wie es größenordnungsmäßig bei schnellen Neutronen der Fall ist,

$$\sigma_s \sim \sigma_f \sim 10^{-23}\,cm^2 = \sigma,$$

so ergibt sich der kritische Radius größenordnungsmäßig zu

$$R_0 \sim \frac{1}{N\sigma}. \tag{33}$$

Wegen $p = N\,k\,T$, wo $p$ der Druck in dyn, $k$ die BOLTZMANN-Konstante und $T$ die absolute Temperatur ist, ergibt sich

$$R_0 \sim \frac{k}{\sigma}\frac{T}{P} \tag{34}$$

oder

$$R_0 \sim 10\,\frac{T}{P}, \tag{34 a}$$

wobei der Druck $p$ in (34 a) in Atmosphären zu messen ist. Bei $T = 10^6$ °C und $p = 10^2$ atm würde das zu einem kritischen Radius von der Größenordnung km führen.

Glücklicherweise sind hier die Verhältnisse insofern doch noch günstiger, als es möglich ist, den Reaktorkern mit einem Neutronenreflektor zu umgeben. Es gibt Neutronenreflektoren, die eine Albedo von nahezu 1 haben, das heißt fast jedes auf den Reflektor treffende Neutron wird in den Reaktorkern rückreflektiert.

Darüber hinaus ist es sogar noch denkbar, den Reaktor mit einem überkritischen Reflektor zu umgeben, der selber aus spaltbarem Material besteht und unter entsprechenden Bedingungen sogar Albedowerte über 1 bringen kann. Bei einem überkritischen Reflektor wird ein auftreffendes Neutron mit einer gewissen Wahrscheinlichkeit eine Kernspaltung auslösen, so daß unter diesen Umständen mehr Neutronen reflektiert werden können, als auf den Reflektor auftreffen. Mit der Anwendung solcher überkritischer Reflektoren sind aber weitere erhebliche Schwierigkeiten verbunden, die in einer starken, durch die Spaltungsprozesse im Reflektor verursachten Erwärmung gegeben sind. Unabhängig davon scheint es nicht ausgeschlossen zu sein, schon bei Anwendung unterkritischer Reflektoren überkritische Anordnungen zu erhalten. Als solche unterkritische Reflektoren eignen sich für schnelle Neutronen besonders schwere Elemente, für thermische Neutronen am besten Stoffe der leichtesten Atomkerne.

Wesentlich für die Güte eines Reflektors ist die Größe seines Streuwirkungsquerschnitts für Neutronen. Besonders geeignet sind bestimmte Isotope, die in gewissen Energiebereichen Resonanzstreuung aufweisen und zu Albedowerten von nahezu 1 in den betrachteten Bereichen führen. Bei Anwendung eines Reflektors beträgt der kritische Radius eines Reaktors

$$R = R_0 - \delta, \tag{35}$$

wo $\delta$ das sogenannte „reflector saving" und $R_0$ der kritische Radius ohne Reflektor ist.

Die Neutronendiffusionstheorie liefert für $\delta$ den Ausdruck:

$$\delta \simeq \frac{D_c}{D_r} L_r. \tag{36}$$

Darin bedeuten $D_c$ und $D_r$ die Diffusionskoeffizienten im Reaktor ($c$) und Reflektor ($r$); $L_r$ ist die Diffusionslänge im Reflektor. Zwischen $D$ und der Streuweglänge besteht der Zusammenhang:

$$D = \frac{1}{3} \lambda_s. \tag{37}$$

Damit erhält man für den kritischen Radius bei Berücksichtigung von Gl. (32)

$$R \simeq \frac{\pi L_c}{\sqrt{\eta - 1}} - \frac{D_c}{D_r} L_r \qquad (L_c = L \text{ gesetzt}). \tag{38}$$

Es soll jetzt gefordert werden $R \leqslant 0$, was mit einer kleinen Abmessung des Reaktors gleichwertig ist. Drückt man $D_c$, $D_r$, $L_c$ und $L_r$ durch die Wirkungsquerschnitte aus, wobei zu beachten ist, daß $\lambda = 1/N\sigma$ ist, so folgt aus G. (38) mit der gestellten Forderung

$$\frac{\pi^2}{\eta - 1} \left(\frac{\sigma_s}{\sigma_f}\right)_c \leqslant \left(\frac{\sigma_s}{\sigma_a}\right)_r. \tag{39}$$

$\sigma_a$ ist der Absorptionsquerschnitt des Reflektormaterials. Die Indizes $c$ und $r$ beziehen sich auf Reaktor und Reflektor. Die Ungleichung (39) ist insofern beachtenswert, als in ihr nicht die Anzahl der Atome pro cm³ von Reaktor und Reflektor eingehen, was streng sicherlich falsch ist und mit unserer rohen Abschätzung in Zusammenhang zu bringen ist. Gl. (39) beinhaltet, daß im gleichen Maße wie der kritische Radius ohne Reflektor mit abnehmender Teilchenzahl pro cm³ bei konstantem Druck, das heißt mit steigender Temperatur wächst, das „reflector saving" zunimmt.

Der kritische Radius mit Reflektor wird deshalb bei konstantem Druck von der Teilchenzahl im Reaktor, und damit von der Temperatur unabhängig.

Für schnelle Neutronen ist $\sigma_s \sim \sigma_f$; daraus folgt als übrig bleibende Forderung an den Streu- und Absorptionsquerschnitt des Reflektors, wenn man noch $\eta = 2{,}5$ setzt:

$$\sigma_s \geqslant 6{,}5\, \sigma_a, \tag{40}$$

eine Bedingung, die sich bei der Wahl geeigneten Reflektormaterials, hohen Streu- und kleinen Absorptionsquerschnitts unter Umständen erfüllen lassen wird. Es scheint danach nicht ausgeschlossen zu sein, selbst bei sehr hohen Feuergastemperaturen und damit kleinen Teilchenzahlen pro cm³ noch überkritische Anordnungen im technisch erlaubbaren Rahmen zu erhalten.

### *1. Verwendung von Gassuspensionen*

Die Nachteile der Verwendung von rein gasförmigen Brennstoffen liegen in der Größe der kritischen Radien. Bei Anwendung eines Neutronen-Reflektors wird dieses ernste Problem nur gemildert, aber wohl noch nicht beseitigt. Es ist also notwendig, nach neuen Möglichkeiten zu suchen, die von den geschilderten abweichen. Solche neuen Möglichkeiten bieten die Suspension fester Kernbrennstoffteilchen in einem Trägergas. Ein solcher Suspensionsreaktor wurde von De Bruyn [9] auf der Genfer Atomkonferenz vorgeschlagen. Bei einer solchen Gassuspension kann es sich beispielsweise um ein Uranstaub-Gasgemisch handeln. Bei diesen Gassuspensionen können pro cm³ mehr Brennstoffatome gebracht werden als in einem Plasmareaktor.

Vol. 4 1958

Haben die festen Brennstoffteilchen einen Durchmesser von $10^{-4}$ cm, so können alle Spaltprodukte unabgebremst aus ihnen heraustreten und ihre Energie zunächst an das Trägergas abgeben, bevor sie wieder auf ein Brennstoffteilchen treffen.

Entscheidend für die Wirkungsweise einer solchen Gassuspension in einem Reaktor ist die Lebensdauer der Teilchen bei der hohen Temperatur. Ist die Lebensdauer nun genügend groß, so kann die Energieproduktion des Plasmas selbst bei hohen Temperaturen beliebig hochgetrieben werden.

### 4. Einschluß des Plasmas in magnetische Wände

Zur Gewährleistung einer stationären Kernverbrennung ist es unbedingt notwendig, zu verhindern, daß das heiße Plasma mit irgendwelchen materiellen Wänden in Berührung kommt. Es ist daher eine unumgängliche Forderung, das heiße Plasma in anderer Weise als in materielle Wände einzuschließen.

Bei der kosmischen Kernverbrennung in Sternen bildet das Gravitationsfeld des Sterns eine Potentialmulde, die ein räumliches Zusammenhalten der Materie bewirkt. Der Gasdruck aller Teilchen einschließlich der Photonen wird in diesem Fall durch den entgegengesetzt wirkenden Gravitationsdruck das Gleichgewicht halten. Der Gravitationsdruck im Innern einer inkompressiblen Kugel der Dichte $\varrho$ und vom Radius $r$ beträgt:

$$p = \frac{2\pi}{3} \varrho G r^2 \tag{41}$$

($G = 6{,}66 \cdot 10^{-8}\,\mathrm{g^{-1}\,cm^3\,s^{-2}}$ Gravitationskonstante).

Soll der Druck von 100 at im Inneren einer Kugel der Dichte 1 g/cm³ erreicht werden, so müßte die Kugel einen Radius von etwa 300 km haben. An diesem Beispiel lernt man, daß Gravitationsfelder für den Einschluß technischer Kernverbrennungsplasmen ungeeignet sind.

Anders verhält sich die Situation bei elektrischen und magnetischen Feldern. Da ein Plasma aus geladenen Teilchen besteht, wirken solche Felder auf Plasmen.

Elektrische Felder bilden keine Potentialmulden und scheiden daher aus. Dagegen ist es möglich, den gewünschten Effekt mit Magnetfeldern zu erreichen.

Die Plasma-Teilchen beschreiben im magnetischen Feld räumliche Spiralen um die Feldlinien. Ein Plasma verhält sich im Magnetfeld wie ein diamagnetischer Körper. Befindet sich ein Plasma im Magnetfeld, so findet eine Diffusion der Teilchen im Gebiete kleinerer Magnetfeldstärke statt.

Anschaulich bewegen sich die geladenen Teilchen im Magnetfeld mit dem Radius

$$r = \frac{m v_\perp c}{Z e H}. \tag{42}$$

In (42) ist $H$ die Magnetfeldstärke, $Z$ die Kernladungszahl und $v_\perp$ die Geschwindigkeit senkrecht zur Richtung von $H$. Kommen die Teilchen in Gebiete von kleinerem $H$, so werden die Krümmungsradien ihrer Bahnen größer, wobei sie durch Stöße noch weiter in die Gebiete kleinerer Feldstärke abwandern. Gelangen sie in Gebiete von größerem $H$, so geschieht das Gegenteil. Die abnehmenden Krümmungsradien ihrer Bahnen stellen sich dem Hineinwandern der Teilchen in Gebiete von größerer Magnetfeldstärke entgegen. Aus dieser anschaulichen Betrachtung ergibt sich, daß es durchaus möglich ist, in inhomogenen Feldern geeigneter Gestalt Plasmen einzuschließen. In einer anderen Betrachtungsweise

läßt sich sagen, daß sowohl das magnetische Feld als auch das elektrische der Feldstärken $H$ bzw. $E$ einen Druck der Größe [10]

$$P = \frac{H^2}{8\pi} \quad \text{bzw.} \quad p = \frac{E^2}{8\pi} \quad [\text{dyn}] \tag{43}$$

auf das Plasma ausüben. Zur Erreichung eines Felddruckes von $10^2$ at z. B. sind daher Magnetfeldstärken von etwa 50 000 Gauß erforderlich.

Um eine stationäre Kernverbrennung durchzuführen, muß das gezündete Plasma in ein solches Feld eingeschlossen werden [6]. Durch diese Forderung scheidet das elektrische Feld, wie schon gesagt, bei alleiniger Verwendung jedenfalls aus.

Es ist aber möglich, das Plasma vollständig in ein Magnetfeld einzuschließen. Solche Feldanordnungen werden als magnetische Flasche bezeichnet.

Ein Beispiel einer solchen magnetischen Flasche ist der sogenannte Pinch-Effekt.

Die durch ein Plasma gehende elektrische Entladung führt zu einem Magnetfeld, das die Entladung und damit das Plasma selbst umschließt. Es zeigt sich jedoch [11], daß der Pinch-Effekt unstabil ist und daher ausscheidet. Um aus dieser Schwierigkeit zu gelangen, hat man vorgeschlagen, magnetische Flaschen durch Felder äußerer Spulenanordnungen herzustellen. Eine solche magnetische Flasche mit einfachen topologischen Eigenschaften ist durch die Torusgeometrie gegeben.

Die Feldlinien einer torusförmigen Spule umschließen im Innern ein zusammenhängendes Gebiet mit großer Feldstärke $H$ und damit magnetischem Druck $p = H^2/8\pi$.

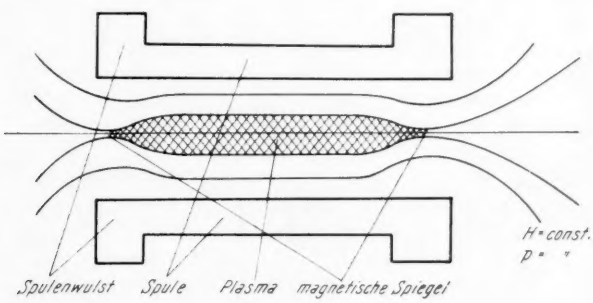


Abb. 3. Magnetische Flasche

Ein anderes Beispiel einer solchen magnetischen Flasche, dem wir unsere besondere Aufmerksamkeit schenken wollen, ist durch eine Längsspule gegeben, bei welcher die Feldstärke an den Enden stark erhöht ist. Das Feldlinienbild einer solchen Spule ist in Abb. 3 aufgetragen.

Die Erhöhung dieser Feldstärke an den Spulen soll in dem gezeichneten Spulenwulst zum Ausdruck kommen. Die Feldlinien $H = \text{const.}$ entsprechen einem magnetischen Druck $P = H^2/8\pi = \text{const.}$ Wie bei SPITZER [10] ausgeführt wird, bildet eine Feldlinienverdichtung der vorliegenden Art für geladene Teilchen einen magnetischen Spiegel von bestimmter Reflexionskraft.

Die Reflexionskraft eines solchen magnetischen Spiegels wird in dem zitierten Werke angegeben.



Vol. 4 1958

Wenn die magnetische Feldstärke an den Spulenenden für alle Abstände zur Spulenachse um einen konstanten Faktor $H/H_0$ größer ist als im Spulenzentrum, dann ist das Reflexionsvermögen des magnetischen Spiegels

$$R = 1 - \frac{H_0}{H}. \tag{44}$$

Gl. (44) bringt zum Ausdruck, daß das Reflexionsvermögen des magnetischen Spiegels für $H \to \infty$ nach 1 strebt, wie es anschaulich zu erwarten ist.

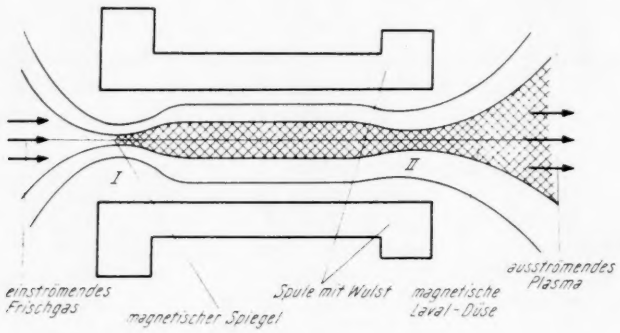


Abb. 4. Magnetische Kernbrennkammer

Für die Zwecke einer magnetischen Kernbrennkammer wird es nun aber von Bedeutung sein, die Feldlinienanordnung so zu treffen, daß die Brennkammer zu einer Seite hin gut verschlossen und zur anderen Seite hin etwa in Form einer LAVAL-Düse geöffnet ist. Beides läßt sich, wie in Abb. 4 angedeutet ist, gut erreichen, in welcher eine magnetische Raketenbrennkammer schematisch angedeutet ist. Das zur Verbrennung bestimmte Frischgas werde auf der linken Seite der Kammer von außen durch ein Gebiet sehr hoher magnetischer Feldstärke (*I*) in die Kammer eingeführt. Da es ungeladen angenommen werden kann, bildet der bei (*I*) gebildete magnetische Spiegel hoher Reflexionskraft für das eintretende Frischgas kein Hindernis. Nachdem das Frischgas in der Kammer aufgeheizt, gezündet und zum Abbrand gekommen ist, strömt es durch die magnetische LAVAL-Düse (*II*) mit hoher Geschwindigkeit aus. Für $T \sim 10^8\,^0\mathrm{K}$ sind dabei für Helium Ausströmgeschwindigkeiten bis zu $10^3$ km/s zu erwarten.

Für unsere Zwecke ist wesentlich, festzustellen, daß sich durch geeignete Spulenanordnungen magnetische Felder konstruieren lassen, die alle gewünschten Eigenschaften besitzen einschließlich derjenigen, beliebige Düsen zu bilden.

## 5. Zündung der thermonuklearen Verbrennung

### *A. Die Bestimmung der Zündungstemperatur*

Die Bestimmung der Zündungstemperatur für thermonukleare Reaktionen ist zuerst von SÄNGER [3] angegeben worden, war aber im Ansatz für das Opazitätsgesetz noch nicht ganz korrekt. Die richtigen Werte dafür finden sich in den Arbeiten von TELLER [12], POST [6] und LINHART [13]. Die Zündungsbedingung für irgendeinen Vorgang gehorcht der Ungleichung

$$\frac{E}{I} \geqslant 1. \tag{45}$$

Dabei bedeutet $E$ die Energieproduktion des zu zündenden Materials und $I$ seine Energieverluste an die Umgebung. Es wird angenommen, daß bei den hohen Temperaturen nur die Strahlungsverluste ins Gewicht fallen. Es wurde bereits gezeigt, daß es möglich ist, diese Voraussetzung mit Hilfe magnetischer Flaschen zu erfüllen.

Strahlt der kugelförmig mit dem Radius $r$ angenommene Körper schwarz, so gilt für die aus der Oberfläche austretende Strahlung

$$I_s = 4\pi r^2 \sigma T^4. \tag{46}$$

In Gl. (2) ist $\sigma$ die STEFAN-BOLTZMANNsche Konstante und $T$ die absolute Temperatur.

Andererseits ist die Energieproduktion einer Plasmakugel vom Radius $r$ durch Gl. (2) bestimmt.

$$E = \frac{4\pi}{3} r^3 \cdot a \varrho^2 T^{-2/3} \exp\left[-b T^{-1/3}\right]. \tag{47}$$

In Gl. (2 a) und $a$ und $b$ sind die die Reaktionen charakterisierenden Konstanten, die sich in ihrer Bedeutung aus (2) ergeben. Setzt man (47) und (46) in (45) ein, so ergibt sich

$$\frac{E}{I} = f_s(T)\, \varrho^2 \cdot r \geqslant 1. \tag{48}$$

$f_s(T)$ ist in dieser Gleichung nur noch eine Funktion von $T$.

Aus (48) entnimmt man, daß für genügend große $r$ die Zündungsbedingung immer erfüllbar ist. Für technisch beherrschbare Drucke und damit Dichten führt (48) auf Radien astronomischer Größenordnung, wie sie uns bei stationären Kernverbrennungen in Sternen bekannt sind.

Glücklicherweise strahlen insbesondere die Wasserstoffe keinesfalls schwarz, so daß eine Einstellung des thermodynamischen Gleichgewichts der Photonen mit den übrigen Teilchen des Plasmas nicht möglich ist.

Die Theorie von KRAMERS zeigt, daß für Plasmen mit wachsender Temperatur die freie Weglänge der Photonen stark zunimmt und für technische Kernverbrennungsplasmen schließlich solche Werte annimmt, die groß gegen deren Abmessungen ist. Die Folge davon ist, daß jedes Photon nach seiner Entstehung ohne weitere Wechselwirkung aus dem Plasma gelangt. Die Abstrahlung ist daher im Gegensatz zur Schwarzstrahlung proportional zum Volumen und nicht zur Oberfläche der strahlenden Körper. Die Photonenausstrahlung ist eine Elektronenbremsstrahlung, die durch Elektron — Kern und Elektron — Elektron frei — frei — Übergänge entsteht.

Diese Abstrahlung gehorcht für eine Kugel vom Radius $r$ theoretisch dem Gesetz

$$I_g = \frac{4\pi}{3} r^3 \cdot 7{,}58 \cdot 10^{20} \varrho^2 T^{0{,}5} \frac{Z^2}{A} \qquad [\mathrm{erg\,s^{-1}}]. \tag{49}$$

Aus Gl. (49) entnimmt man, daß die Wasserstoffe gegenüber allen anderen Stoffen in Beziehung auf ihre kleine Abstrahlung bevorzugt sind. Setzt man (13) und (2 a) in (10) ein, so erhält man

$$\frac{E}{I_g} = f_g(T) \geqslant 1. \tag{50}$$

An Gl. (50) ist bemerkenswert, daß sich der Radius $r$ und die Dichte $\varrho$ herausgehoben haben. Es gibt daher für die Art der Kernverbrennung keinen kritischen Radius. Außerdem ist die Zündungstemperatur unabhängig von der Plasmadichte. Aus der Gleichung $f_g(T) = 1$ berechnet sich die Zündungstemperatur.



Vol. 4 1958

Diese Gleichung hat zwei Wurzeln. Die Zündungstemperatur entspricht der kleineren Wurzel.

Es ist also möglich, eine thermonukleare Reaktion zu zünden, selbst wenn die erforderliche hohe Temperatur nur in einem kleinen Raumbereich erreicht wird. Die Zündungstemperatur für die $T - D$-Reaktion liegt bei $3 \cdot 10^7$ °K und für $D - D$ bei $3 \cdot 10^8$ °K.

Die Ausstrahlung wird von einer bestimmten Temperatur oberhalb der Zündungstemperatur wieder größer als die Energieproduktion, was sich im Auftreten der zweiten Wurzel der Gl. (17) zeigt.

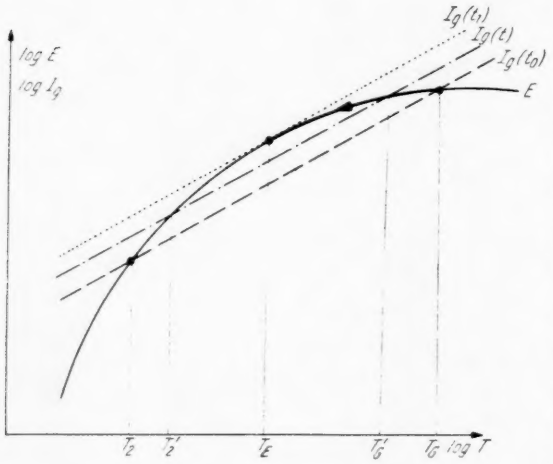


Abb. 5. Zündungstemperatur, obere Grenztemperatur und Erlöschungstemperatur einer Kernverbrennung (schematisch). Der fette Kurvenzug gibt den Gang des stabilen Arbeitspunktes an

In Abb. 5 ist dieser Sachverhalt schematisch wiedergegeben. Auf ihr sind die Energieproduktions- und Abstrahlungskurven in doppellogarithmischer Auftragung qualitativ wiedergegeben. Die thermonukleare Reaktion ist nur in dem Bereich von der Zündungstemperatur bis zur Grenztemperatur $T_G$ selbst erhalten. Die aufgezogene Linie von $\log I_g$ beziehe sich auf den Augenblick der Ingangsetzung der Kernverbrennung. Durch den vorschreitenden Abbrand wird die Ausstrahlung als Funktion der Zeit $t$ größer, was sich in einem parallelen Verschieben der Geraden $\log I_g$ nach oben hin äußert. Dadurch wird die Zündungstemperatur $T_Z'$ hinaufgesetzt und die Grenztemperatur $T_G'$ herabgesetzt. Die Schnittpunkte $T_Z'$ und $T_G'$ treffen einander schließlich nach der Zeit $t_1 - t_0$ bei der Erlöschungstemperatur $T_E$. Der stabile Arbeitspunkt der Kernverbrennung wandert von $T_G$ über $T_G'$ bis zur Erlöschungstemperatur $T_E$. Indem man dem Plasma neuen thermonuklearen Brennstoff zuführt, ist es aber denkbar und wohl auch möglich, die Kernverbrennung über diese Zeit hinaus aufrechtzuerhalten. Die Kernverbrennung wird nach gelungener Zündung zu einer weiteren Erhöhung der Plasma-Temperatur führen, bis der Vorgang bei der Temperatur $T_G$ sich selbst stabilisiert. Diese Selbststabilisierung ist von Vorteil, da sie eine äußere Regelung überflüssig macht.

Sie kann aber auch von Nachteil sein, wenn beide Schnittpunkte nahe beieinander liegen, wie es leider bei der $D - D$-Reaktion der Fall ist. Es genügen dann bereits geringe zusätzliche Energieverluste des Plasmas nach außen, um es zum Erlöschen zu bringen.

Bei der $T - D$-Reaktion liegen die Verhältnisse wesentlich günstiger, jedoch stehen der Verwendung von Tritium wirtschaftliche Gründe entgegen.

Bei der $T - D$-Reaktion ist diese obere Temperaturgrenze $T_G$ der Kernverbrennung wesentlich höher als die Zündungstemperatur und in dem Zwischen-

bereich beider Temperaturen erreicht das Ausstrahlungsverhältnis $E/I_g$ Werte, die weit über 1 liegen.

Bei der Verwendung von Deuterium bildet sich aber glücklicherweise zu etwa gleichen Teilen Tritium und Helium. Das entstandene Tritium kompensiert durch seine viel größere Energieproduktion in der Reaktion mit Deuterium die Ausstrahlung des gebildeten Heliums, so daß die Schnittpunkte von $E(T)$ und $I_g(T)$ zeitlich langsamer zusammenrücken, als es ohne diesen Effekt sonst der Fall wäre.

Für die selbständige Unterhaltung einer thermonuklearen Verbrennung ist es weiterhin erforderlich, daß die Fusionsprodukte ihre Energie an das Plasma abgeben. Nach LINHART [13] folgt die Bedingung dafür aus dem Zusammenhang zwischen Magnetfeldstärke und Lamorfrequenz, der in Gl. (42) angegeben ist.

Beträgt die Energie der Fusionsprodukte $E$, so ist ihr Lamorradius $r$ wegen $v = \sqrt{2\,M\,E}$

$$r = \frac{\sqrt{2\,M\,E}\,c}{Z\,e\,H}. \tag{51}$$

Vol. 4 1958

Die Fusionsprodukte der $D - D$-Reaktion haben etwa eine Energie von 1 MeV. Daraus folgt ein Lamorradius für die He-Kerne zu

$$r = \frac{0{,}7 \cdot 10^5}{H} \qquad [\text{cm}], \tag{52}$$

das sind bei einer Feldstärke von beispielsweise $10^4$ G 10 cm.

Die minimale Größe der Kernbrennkammer $R$ ergibt sich nun aus der Forderung, daß $R > r$ sein muß, um ein Aufschlagen der Fusionsprodukte auf die Wände zu verhindern. Andernfalls würde ihre kinetische Energie dem Plasma nicht zugeführt werden, was zur Aufrechterhaltung der Verbrennung notwendig ist.

### *B. Die Zündung*

Von allen gemachten Vorschlägen, thermonukleare Reaktionen zu zünden, scheint der von LINHART [13] gemachte besonders Erfolg versprechend zu sein.

Er teilt das Zündungsproblem in zwei Stufen ein.

1. Vorwärmung des Plasmas durch elektrische Entladung auf mittlere Temperaturen.

2. Adiabatische Kompression und Zündung des Plasmas im Magnetfeld durch schnelles Erhöhen der Magnetfeldstärke und damit des magnetischen Druckes.

Die erste Stufe vollzieht sich in der Weise, daß die Energie der elektrischen Entladung sich zunächst auf die Elektronen überträgt, die durch Stöße einen Teil ihrer Energie an die Kerne abgeben. Der spezifische Widerstand eines Plasmas wird mit wachsender Temperatur kleiner nach dem Gesetz

$$\varrho = \frac{\text{const}}{T^{3/2}} \qquad [\Omega\ \text{cm}] \tag{53}$$

für ein Deuteriumplasma

$$\varrho = \frac{6{,}5 \cdot 10^4}{T^{3/2}} \qquad [\Omega\ \text{cm}], \tag{54}$$

was für $T = 10^6$ °K auf einen Wert von

$$\varrho = 6{,}5 \cdot 10^{-5} \qquad [\Omega\ \text{cm}]$$

führt.

Von Kupfer beträgt der spezifische Widerstand $1{,}7 \cdot 10^{-6}$. Bei $10^6$ °K hat daher das Plasma bereits Leitfähigkeitswerte, wie sie bei Metallen vorkommen, so daß durch elektrische Entladungen über diese Temperatur hinaus nicht mehr viel Energie dem Plasma zugeführt werden kann.

Die Kompression eines Plasmas kann ein-, zwei- und dreidimensional erfolgen [10]. Die Temperaturerhöhungen sind bei ein- und zweidimensionaler Kompression größer als bei der dreidimensionalen. Die Temperaturerhöhung gehorcht der Formel:

$$T/T_0 = (V_0/V)^{\gamma-1} = (P/p_0)^{\frac{\gamma-1}{\gamma}}, \tag{55}$$

wobei $\gamma = (m+2)/m$ ist und $m$ die Anzahl der Freiheitsgrade. Wegen $P = H^2/8\pi$ schreibt sich Gl. (55)

$$T/T_0 = \left(\frac{H}{H_0}\right)^{2\frac{\gamma-1}{\gamma}}. \tag{56}$$

Im Falle einer zylindrischen Raketenbrennkammer werde das Magnetfeld axial erhöht; dann gilt $m = 2$ und damit $\gamma = 2$, damit

$$\frac{T}{T_0} = \frac{H}{H_0}. \tag{57}$$

Angenommen, das Plasma werde im ersten Schritte bei einer Feldstärke von $H_0 = 30$ Gauß auf $T_0 = 10^6$ °K gebracht und im zweiten Schritt werde die Feldstärke auf $10^4$ Gauß, einem technisch vorstellbaren Wert gebracht, dann beträgt die Temperaturerhöhung

$$\frac{T}{T_0} = \frac{10^4}{3 \cdot 10^1} \simeq 3 \cdot 10^2$$

und für $T_0 = 10^6$ folgt $T = 3 \cdot 10^8$ C°, was der Zündungstemperatur von Deuterium entspricht.

Die Kompression im Magnetfeld muß aus zwei Gründen sehr schnell erfolgen. Einmal steigen die Ausstrahlungsverluste mit wachsender Temperatur rasch an und zum anderen muß die Kompression schneller vonstatten gehen, als der Stoßzeit der Teilchen entspricht. Die stattfindenden Stöße gleichen die rein zweidimensionale Kompression aus, so daß dann eine dreidimensionale Kompression mit einem Wert von $\gamma = 5/3$ zu erwarten ist, wodurch der Exponent in Gl. (56) ungünstiger wird.

### 6. Direkterzeugung von Elektrizität aus Kernenergie

Die große Schwierigkeit, die der Anwendung so starker Magnetfelder in der Raketentechnik im Wege steht, liegt auf der Hand. Es ist nämlich noch nicht die Frage beantwortet, auf welche Weise die benötigten starken elektrischen Ströme hergestellt werden können, mit denen die Spulen zur Erzeugung der Magnetfelder gespeist werden sollen.

Zur Herstellung so starker Magnetfelder sind unter irdischen Bedingungen kraftwerksähnliche Vorrichtungen notwendig, die in einer Rakete nicht mitgeführt werden können.

Der hauptsächlichste Grund hierfür ist nicht einmal in der Größe solcher Kraftwerke zu suchen, da sich mit herkömmlichen Reaktoren, ohne den biologischen Strahlenschutz allerdings, sogar recht kleine wirkungsvolle Kraftwerke herstellen lassen. Vielmehr ist die Schwierigkeit darin zu sehen, daß jede Wärmekraftmaschine über einen Kühler den Teil der wertlos gewordenen Wärme unter Entropievergrößerung an die Umgebung abgeben muß

der bei den schlechten Wirkungsgraden herkömmlicher Wärmekraftwerke den größten Teil ausmacht. Im Vakuum des Weltenraumes kann diese Energieabgabe nur über die Abstrahlung von Photonen geschehen, die bei einem schwarzen Körper nach dem STEFAN-BOLTZMANNschen Gesetz

$$W = F\,\sigma\,T^4 \tag{58}$$

geschieht, wobei $W$ die Leistungsabgabe, $F$ die strahlende Fläche, $\sigma$ die STEFAN-BOLTZMANNsche Konstante und $T$ die absolute Temperatur ist. Daraus ergibt sich bei vorgegebener Leistung und Temperatur des Strahlungskühlers die benötigte Abstrahlungsfläche. Bei einer Leistung von beispielsweise $W = 50$ Megawatt und einer Temperatur von $T = 4 \cdot 10^2$ °K ergibt sich eine benötigte Abstrahlungsfläche von $4 \cdot 10^4$ m$^2$.

Die außerordentlichen Größen der benötigten Abstrahlungsflächen erklären die Schwierigkeiten, die dem Einbau konventioneller Atomkraftanlagen in Raketen entgegenstehen. Es ist daher anzustreben, nach Wegen zu suchen, die es gestatten, ohne den Umweg über die Wärme die Kernenergie direkt in Elektrizität zu verwandeln.

Im folgenden wird hierfür eine Reihe von Möglichkeiten zusammengestellt.

Vol. 4 1958

*A. Direkte Verwandlung der Bremsstrahlung durch Photozellen und der Wärme durch Thermoelemente in Elektrizität*

Wie bereits ausgeführt, strahlt ein Plasma hoher Temperatur seine Energie in Form von Bremsstrahlung ab. Die Abstrahlung erfolgt dabei nach Gl. (49). Es ist nun daran zu denken, einen Teil dieser sehr intensiven Bremsstrahlung durch Photozellen direkt in Elektrizität zu verwandeln. Unter Umständen sind dazu bestimmte Halbleiterphotozellen besonders geeignet, bei denen man bekanntlich hinsichtlich ihres Wirkungsgrades schon erstaunlich gute Werte erzielt hat. Auf diese Weise ist zu hoffen, wenigstens einen Teil der benötigten elektrischen Energie aus dem Plasma direkt wieder zurückzugewinnen.

Auch die immer noch beträchtlichen Wärmemengen, die durch Absorption der auftretenden Strahlungen an unerwünschter Stelle freigesetzt werden, können wenigstens zum Teil wieder als Elektrizität direkt zurückgewonnen werden. Hierzu eignen sich bekanntlich Thermoelemente, deren Wirkungsgrad allerdings schlecht ist.

*B. Direkterzeugung von Elektrizität aus Plasmen durch magnetohydrodynamische Kopplung des Plasmas mit dem Magnetfeld*

Wie von TELLER [12] zuerst im Fall thermonuklearer Reaktionsplasmen gezeigt wurde, besteht eine Möglichkeit, Elektrizität durch die Kopplung des Plasmas mit dem Magnetfeld ohne Umweg über die Wärme zu gewinnen. Die TELLERsche Idee ist von COLGATE und AAMODT [13] auf Kernspaltungsplasmen übertragen und diskutiert worden.

Zwischen Magnetfeld und Plasma besteht eine Wechselwirkung, die in der Gl. (43) ihren Außdruck findet. Jede mit äußerer Energiezufuhr bedingte Erhöhung des Magnetfeldes führt zu einer Kompression des Plasmas. Umgekehrt führt jede durch innere Wirkung des Plasmas verursachte Expansion zu einer Abgabe elektrischer Energie nach außen, die z. B. vom Leitersystem der Feldspulen abgenommen werden kann. Das Plasma wirkt hier wie die Primärwicklung eines Transformators. Die vom Plasma in elektrische Energie verwandelte Arbeit berechnet sich nach der Gleichung

$$A = \int_{V_0}^{V_1} p\,dV = \frac{1}{8\pi}\int_{V_0}^{V_1} H^2\,dV. \tag{59}$$

Bei konstantem äußerem Magnetfeld beträgt die Arbeit

$$A = \frac{H^2}{8\pi}(V_1 - V_0). \tag{60}$$

Nimmt man an, daß $V_1 = 100\, V_0$, $V_0 = 10^4$ cm$^3$ und $H = 10^4$ G ist, so beträgt die geleistete Arbeit

$$A \sim 10^{13}\,\text{erg}.$$

Nimmt man weiter an, daß sich dieser Vorgang in einem geeigneten Kreisprozeß etwa hundertmal in der Sekunde wiederholt, was zu einem Wechselstrom von 100 Hz führt, so beträgt die dabei freiwerdende elektrische Leistung

$$W \sim 100\,\text{Megawatt}.$$

Aus diesem numerischen Beispiel sieht man, was für eine große Bedeutung die Ausnutzung solcher Prozesse für die Raketentechnik einmal erlangen kann.

*C. Kalte Direkterzeugung von Elektrizität in einem Kernspaltungsreaktor*

Es soll jetzt ein anderer Weg gezeigt werden, der es ermöglicht, ohne Umweg über die Wärme Kernenergie direkt in Elektrizität zu verwandeln.

Der Wärmeerzeugungsprozeß in einem Kernspaltungsreaktor herkömmlicher Bauweise geschieht in mehreren Schritten. Zuerst findet durch Einfang eines Neutrons in einem spaltbaren Kern eine Kernspaltung statt. Der Kern wird dabei in zwei etwa gleich große Stücke zerlegt, die mit einer Anfangsgeschwindigkeit von $10^9$ cm/s auseinanderfliegen. Die kinetische Energie dieser Spaltstücke beträgt bei dieser Geschwindigkeit rund 90 MeV.

Die Reichweite der Spaltprodukte in metallischen Schichten ist gemessen worden und beträgt etwa $10^{-3}$ cm. Auf dieser Wegstrecke geben die Spaltprodukte ihre ganze kinetische Energie an die umliegenden Atome ab. Anschaulich läßt sich dieser Vorgang so auffassen, daß die Spaltprodukte eine hohe Temperatur in der engeren Umgebung ihres Bremsweges erzeugen. Durch Wärmeleitung an die weitere Umgebung nimmt diese lokale Temperaturspitze schnell ab. Schließlich findet der Vorgang sein Endstadium in einer Erwärmung des ganzen Reaktors. Die Wärme wird dann in der üblichen Weise durch ein Kühlmittel abgeführt.

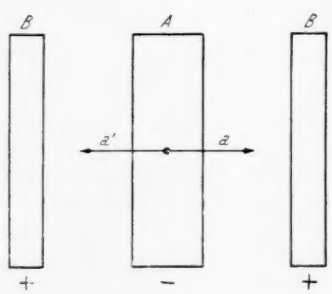


Abb. 6. Zur Direkterzeugung von Elektrizität aus der Kernspaltung

Ein Spaltprodukt ist bei einer Energie von 90 MeV im Mittel 20fach ionisiert. Zur Beschleunigung eines solchen Spaltprodukts auf diese Energie müßte es eine Spannung von $90/20 = 4{,}5$ Millionen Volt durchlaufen.

Daß diese Spaltprodukte auch umgekehrt in der Lage sind, eine Spannung von 4,5 Millionen Volt aufzubauen, ist der Grundgedanke für die Direkterzeugung von Elektrizität aus Kernspaltungsreaktionen.

Abb. 6 ist ein Beispiel einer Anordnung, die dies leistet. $A$ ist eine Platte aus spaltbarem Material, z. B. Plutonium. $B$ ist eine Auffangplatte aus irgend einem Metall oder anderem Leiter. Zwischen den Platten $A$ und $B$ herrscht Hochvakuum. In der Platte $A$ soll eine Kernspaltung stattfinden. Die Pfeile $a$ und $a'$ deuten die Flugbahn der Spaltprodukte an. Bei der Spaltung werden etwa die Hälfte der Hüllen-Elektronen des spaltbaren Atoms durch die momentane Beschleunigung der Spaltprodukte auf $10^9$ cm/s abgestreift. Die abgestreiften Elektronen verbleiben in der Platte $A$ und laden diese negativ auf. Das positiv

geladene Spaltprodukt $a$ trifft auf die Platte $B$ und lädt diese positiv auf. Der geschilderte Vorgang wiederholt sich mit weiteren Spaltprodukten.

Jedes weitere Spaltprodukt hat dabei das Feld der durch Spaltprodukte bereits erfolgten Aufladung der Platte $B$ zu überwinden. Schließlich wird die zwischen $A$ und $B$ herrschende Spannung so groß sein, daß die weiteren Spaltprodukte die Platte $B$ gerade noch erreichen können. Zwischen $A$ und $B$ herrscht dann eine Spannung von 4,5 Millionen Volt unter der Annahme, daß die Mehrzahl der Spaltprodukte beim Austritt aus der Platte $A$ eine Energie von 90 MeV haben und 20fach ionisiert sind. Beides ist streng genommen nicht erfüllt.

Weiters wäre zu wünschen, daß alle Spaltprodukte aus der Platte senkrecht austreten. Leider ist dies aber keineswegs der Fall und setzt daher in erster Linie den Wirkungsgrad der Anordnung in Beziehung auf die Direkterzeugung von Elektrizität herab, was sich in sehr unangenehmer Weise in einer Erwärmung der Platten äußert. Die Spaltung ist im Gegensatz zu dem geäußerten Wunsch isotrop, so daß alle Richtungen gleich wahrscheinlich sind.

Wird die Spannung an den Platten beispielsweise auf 4,5 Millionen Volt festgehalten, so schlagen alle nicht senkrecht austretenden Spaltprodukte in parabelförmigen Bahnen auf die Platte $A$ zurück. Dadurch wird $A$ erwärmt. Man wird daher die zwischen $A$ und $B$ herrschende Spannung herabsetzen, um einer größeren Anzahl von Spaltprodukten zu erlauben, auf der Platte $B$ zu landen. Das führt dazu, daß auch die Platte $B$ erwärmt wird. Bei einer bestimmten unterhalb von 4,5 Millionen Volt liegenden Spannung erreicht der Wirkungsgrad, wie hier nicht näher erläutert werden soll, einen maximalen Wert. Zur Hinaufsetzung dieses Wirkungsgrades ist daran zu denken, zusätzliche Gitter einzubauen, um die Spaltprodukte in andere Bahnen zu lenken, die ein bevorzugt senkrechtes Auftreffen der Teilchen auf die Platte $B$ gewährleisten. Günstiger als Platten würden sich Zylinder stellen, an deren Achse dünne Spaltstoffdrähte ausgespannt sind. Am günstigsten würden sich winzige Spaltstoffkugeln im Zentrum von konzentrischen Kugelschalen stellen. Eine solche Anordnung darf aber als technisch undurchführbar angesehen werden, so daß wir ihr kein weiteres Augenmerk schenken brauchen.

Vol. 4 1958

Da die Spaltprodukte in Metallen eine Reichweite von etwa $10^{-3}$ cm haben, ist dafür zu sorgen, daß die Platte $A$ genügend dünn ist. Anderenfalls würden nur die an der Oberfläche stattfindenden Kernspaltungen zum Aufbau des Spannungsgefälles beitragen.

Eine Dicke der Platte $A$ von $10^{-4}$ cm dürfte genügen, um praktisch alle Spaltprodukte zum Austritt zu bringen.

Der Energieverlust der Spaltprodukte in Materie erfolgt nach einer sogenannten BRAGG-Kurve. Auf dem ersten Teil des Abbremsweges finden wegen der hohen Geschwindigkeit der Spaltstücke praktisch keine Ionisationen im Bremsmittel und damit Energieverluste an die Umgebung statt. Wenn die Platte $A$ dünn genug ist, werden auch Spaltstücke, welche die ganze Platte durchsetzen, noch nicht zu große Energieverluste erlitten haben.

Ein weiteres wesentliches Merkmal dieser Vorrichtung besteht darin, daß eine genügend große, sich periodisch wiederholende Anordnung von Platten $A$ und $B$ einen überkritischen Kernreaktor ergibt. Der Kernreaktor kann dabei als schneller, thermischer oder intermediärer Reaktor arbeiten.

Eine solche überkritische Anordnung ist in Abb. 7 veranschaulicht. Die Platten aus Spaltmaterial werden an eine Sammelschiene angeschlossen, ebenso die Auffangplatten. Zwischen beiden Sammelschienen wird dann durch eine gesteuerte Kettenreaktion eine Spannung von z. B. 3 Millionen Volt aufrechterhalten.

Die Steuerung des Reaktors kann dabei über Strom und Spannung als Meßwertgeber erfolgen. Der Neutronenfluß ist der Stromstärke proportional. Beträgt der Abstand zwischen den Spaltstoffplatten $A$ cm und ist $d$ die Dicke der Platten in cm, so berechnet sich für einen schnellen Plutoniumreaktor einer beispielsweise kugelförmigen Anordnung des ganzen Reaktors der kritische Radius nach der Diffusionstheorie zu

$$R = 8{,}8 \cdot \frac{x}{d} \text{ (cm)}. \tag{61}$$

Dieser Wert gibt aber auch die Größenordnungen von anderen geometrischen Anordnungen wie Zylinder und Kubus richtig wieder. Bei einem Abstand von $x = 1$ cm und einer Plattendicke von $d = 10^{-4}$ cm erhält man einen kritischen Radius von $10^5$ cm. Dieser kritische Radius kann aber durch einen Neutronenreflektor ganz erheblich gesenkt werden.

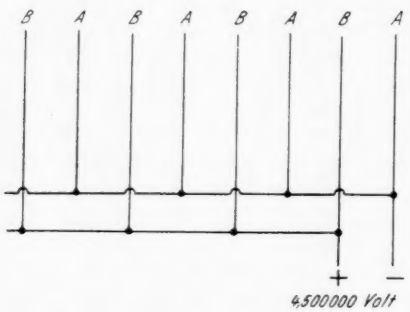


Abb. 7. Zur Direkterzeugung von Elektrizität aus einem überkritischen Kernreaktor

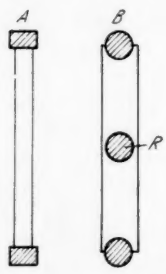


Abb. 8. Zur Anordnung von Moderator und Spaltstoff

Bei einem großen Reaktor und einem großen Reflektor ist die Reflektorsaving durch Gl. (5) gegeben. Die Berechnung in Frage kommender Reflektoren zeigt, daß der kritische Radius des geschilderten Reaktors auf technisch beherrschbare Größenverhältnisse herabgedrückt werden kann.

Günstiger in Beziehung auf den kritischen Radius stellt sich ein thermischer Reaktor. Zu diesem Zweck werden nach dem Beispiel der Abb. 8 die Platten $B$ oder auch $A$ oder beide von Röhren $R$ durchsetzt, bzw. sind jeweils mit Röhren verbunden. Die Röhren werden mit einer Moderatorflüssigkeit, z. B. $H_2O$, angefüllt, oder durchflossen. Aber auch die Anwendung von Graphit oder Beryllium als Moderator ist möglich. Im letzteren Fall ist daran zu denken, die Platten $B$ ganz oder zum Teil aus diesen Stoffen herzustellen. Schon eine geringe Menge von Moderator kann die Verhältnisse grundlegend ändern. Die Neutronenenergien liegen dann im intermediären Bereich. Da mit einer Erwärmung des ganzen Reaktors zu rechnen ist, kann durch Umpumpen der Moderatorflüssigkeit diese Wärme durch die Röhren abgeführt werden. Haben wir z. B. reines Plutonium und leichtes Wasser im Volumenverhältnis 1 : 10 des ganzen Reaktors, so beträgt der kritische Radius ohne Reflektor etwa 2 m. Die hohe zwischen den Platten $A$ und $B$ herrschende Spannung hat zur Folge, daß sich zwischen $A$ und $B$ eine Gasentladung ausbilden wird. Zur Herabsetzung dieser Gasentladung muß der zwischen $A$ und $B$ liegende Raum etwa auf ein möglichst hohes Vakuum gebracht werden. Bei

einem höchsten Vakuum kann dann zwischen $A$ und $B$ nur noch eine Entladung durch Feldemission stattfinden.

In Abb. 9 ist der Feldemissionsstrom als Funktion der Feldstärke aufgetragen. Man entnimmt aus dieser Abbildung, daß selbst bei einem Abstand von

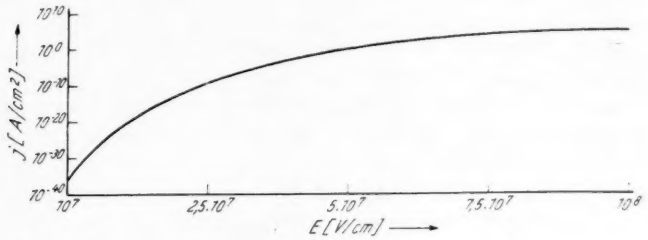


Abb. 9. Feldemissionsströme

Vol. 4 1958

2 mm zwischen $A$ und $B$ und damit einer Feldstärke zwischen $A$ und $B$ von 22 Millionen Volt/cm noch kein nennenswerter Strom auftreten kann. An Kanten und Spitzen hingegen sind erheblich größere Feldstärken zu erwarten, die zu Entladungen Anlaß geben können. Außerdem werden durch geringe Gasreste Kathodenstrahlentladungen von $A$ nach $B$ ausgelöst. Diese Entladungen lassen sich durch Auftragung dünnster Nichtleiterschichten herabdrücken. Auch an die Möglichkeit, zwischen die Platten $A$ und $B$ eine solche nicht-leitende Schicht zu bringen, wäre zu denken. In Abb. 10 wird die Wirkungsweise eines solchen Isolators erläutert. Auf der nach $B$ zugekehrten Seite des Isolators $J$ werden alle Oberflächenelektronen so lange abgesaugt, bis sich ein Gleichgewicht eingestellt hat. Die $B$ zugewandte Oberfläche lädt sich dabei positiv auf. Auf der $A$ zugekehrten Seite passiert das Umgekehrte. Eine starke negative Aufladung wird eintreten. Diese starke negative Ladungsschicht wird dann dem Austritt von Ladungsträgern aus $A$ entgegenwirken, womit der gewünschte Zweck erreicht ist.

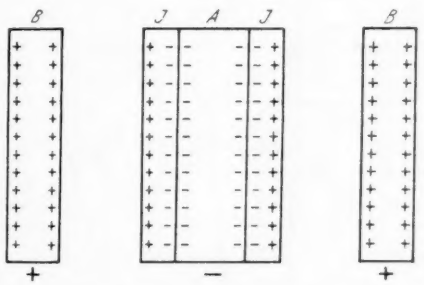


Abb. 10. Zur Direkterzeugung von Elektrizität aus der Kernspaltung

Es ist darauf zu achten, die Isolationsschicht möglichst dünn zu halten, um eine zu starke Abbremsung der Spaltstücke im Isolator zu verhindern.

### 7. Kombination der verschiedenen Anordnungen

Für die praktische Anwendung in Raketen wird es von großer Bedeutung sein, die verschiedenen hier skizzierten Verfahren zu kombinieren. Vor allem ist man genötigt, die großen Magnetfelder wenigstens anfänglich zur Zündung aufzubauen. Für diesen anfänglichen Strom wird man den die Elektrizität direkterzeugenden Spaltstoffreaktor mit Erfolg benützen können. Man kann aber auch direkt mit diesem Spaltstoffreaktor einen Ionenstrahl beschleunigen.

Weiter besteht die Möglichkeit, diesen Reaktor für das Magnetfeld eines Spaltstoffplasmareaktors, der Teilchen abstrahlt, zu verwenden. Dann kann dieser Spaltstoffplasmareaktor Strom liefern, der einen Ionenstrahl unterhält. Die gleichen Möglichkeiten stehen für den Fusionsreaktor offen mit dem Nachteil allerdings, daß sehr starke Magnetfelder und damit ein hoher Stromverbrauch erforderlich sind. Schließlich kann zwischen direkterzeugenden Spaltstoffreaktor und Fusionsreaktor ein Spaltstoffplasmareaktor geschaltet werden, der den Strom für die Magnete des Fusionsreaktors liefert.

Die drei zuletzt genannten Fälle sind insofern von Bedeutung, als man den Spaltstoffplasmareaktor schon mit geringen Feldstärken betreiben kann, wenn man seine Temperatur relativ niedrig hält und auf die Abstrahlung seines Plasmas verzichtet.

Es ist aber auch daran zu denken, den Spaltstoffplasmareaktor primär als Stromquelle zu verwenden. Wird der Spaltungsplasmareaktor bei relativ niederen Temperaturen von einigen $10^3$ °K betrieben, so ist es möglich, das Plasma in einen festen Behälter einzuschließen.

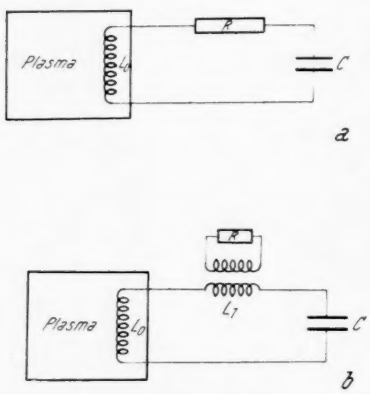


Abb. 11. Schaltungen von Plasma und Schwingungskreis

Wirkt in diesem Behälter das Feld eines Elektromagneten, so findet eine Kompression des Plasmas und damit Erhöhung der Reaktionsrate statt. Diese Erhöhung der Reaktionsrate im Plasma führt zu einer stärkeren Erwärmung und Ausdehnung und damit Arbeit gegen das Magnetfeld, so daß der Magnetspule elektrische Energie entnommen werden kann. Nach einiger Zeit wird eine weitere Ausdehnung des Plasmas aufhören, da ja die mit der Ausdehnung verbundene Abnahme der Reaktivität zu einer Abnahme der Energieproduktion führt. Wird nun die der Magnetspule entnommene elektrische Energie zur Aufladung eines Kondensators verwendet, so kann nach Beendigung der Ausdehnung der Kondensator seine Energie wieder dem Magnetfeld zurückgeben, das dann seinerseits wieder eine Kompression des Plasmas bewirkt, so daß das Spiel von neuem beginnen kann. In dieser Anordnung bildet der Kondensator mit der Magnetspule einen gedämpften Schwingungskreis, der durch die Kopplung mit dem Plasma erregt und zeitlich im stationären Betrieb auf eine feste Frequenz nach Beendigung des Einschwingungsvorganges sich einspielt.

Zur Ingangsetzung des Einschwingvorganges dürfte die schwache in den Spulen eigens vorhandene magnetische Remanenz genügen, so daß die Anordnung selbst-erregend ist. Zur Entnahme von elektrischer Energie aus diesem Schwingungskreis ist erstens daran zu denken, die Energie in einem Arbeitswiderstand im Primärkreis zu verbrauchen oder aber über eine induktive Transformatorkopplung zu jeder gewünschten Spannung zu gelangen und da Energie in einen sekundär geschalteten Arbeitskreis zu schalten. Solche Arbeitswiderstände sind z. B. Lichtbögen, Magnete von Fusionsreaktoren und Ionenquellen.

In Abb. 11 ist die Schaltung von Plasma und Schwingungskreis für beide Möglichkeiten schematisch aufgezeichnet.

**Literaturverzeichnis**


1. F. WINTERBERG, Mitt. Forsch.-Inst. Physik d. Strahlantriebe Nr. 6. Stuttgart: Verlag Flugtechnik, E. v. Olnhausen, 1956.
2. F. WINTERBERG, Fusées et Recherche Aéronautique **2**, 9 (1957).
3. E. SÄNGER, Astronaut. Acta **1**, 61 (1955).
4. R. ATKINSON und F. HOUTERMANS, Z. Physik **54**, 656 (1928).
5. G. GAMOW und C. L. COUTCHFIELD, Theory of Atomic Nucleus and Nuclear Energy Sources. Oxford: At the Clarendon Press, 1947.
6. R. F. POST, Rev. Mod. Physics **28**, 338 (1956).
7. E. SÄNGER, P. GOERCKE und I. BREDT, Z. physik. Chem. **199**, 46 (1952).
8. S. GLASSTONE und M. EDLUND, The Elements of Nuclear Reactor Theory. New York: D. van Nostrand Company, 1952.
9. H. DE BRUYN et al., Genf 1955, Peaceful Uses of Atomic Energy United Nations, P 938.
10. L. SPITZER, The Physics of Fully Ionized Gases. New York: Interscience Publishers, 1956.
11. M. KRUSKAL und M. SCHWARZSCHILD, Proc. Roy. Soc. (London) A **223**, 348 (1954).
12. E. TELLER, Nuclear Sci. Engng. **1**, 313 (1956).
13. S. A. COLGATE und R. L. AAMODT, Nucleonics **15**, Nr. 8, 50 (1957).


Vol. 4 1958

# General Variational Theory of the Flight Paths of Rocket-Powered Aircraft, Missiles and Satellite Carriers[1]

By

**Angelo Miele**[2], ARS, AAS

(With 6 Figures)

(*Received March 3, 1958*)

**Abstract – Zusammenfassung – Résumé**

**General Variational Theory of the Flight Paths of Rocket-Powered Aircraft, Missiles and Satellite Carriers.** General equations are presented for analyzing the optimum flight paths of rocket-powered aircraft, missiles and satellites. The Earth is assumed spherical; the variability of the acceleration of gravity with the altitude is accounted for.

The variational question is investigated within the general frame of the problems of MAYER type, i.e., as the problem of minimizing the difference $\Delta G$ between the final and initial values of an arbitrarily specified function $G(X, h, V, \theta, m, t)$ of range, altitude, velocity, path inclination, mass and time.

A characteristic of the general problem is that it embodies three degrees of freedom. They are, respectively, associated with the simultaneous optimization of the time history of lift, thrust modulus and thrust direction. Special problems involving either one or two degrees of freedom are investigated by the introduction of additional constraining equations.

Excluding a few exceptional cases, the totality of extremal arcs is generally composed of zero-thrust sub-arcs, sub-arcs flown with maximum engine output, and variable-thrust sub-arcs. Thus, discontinuous solutions are found and discussed in the light of the ERDMANN-WEIERSTRASS corner conditions. The results presented here generalize, in a single unified theory, large segments of previous treatments developed by the author and other researchers.

For the case of a flat Earth, particular attention is devoted to some special classes of trajectories, such as: vertical paths associated with problems where $G = G(h, V, m, t)$; level paths associated with functional forms of the type $G = G(X, V, m, t)$; arbitrarily inclined rectilinear paths associated with problems where $G = G(X, h, V, m)$; curvilinear trajectories flown with negligible induced drag; non-lifting paths imbedded in an isothermal medium; and vacuum flight trajectories.

For several of the above particular cases, closed form expressions are derived for the distribution of LAGRANGE multipliers and the optimizing condition. Some

[1] This research was supported by the United States Air Force, through the Air Force Office of Scientific Research of the Air Research and Development Command, under Contract No. AF 18(603)–69 and is a condensed version of the investigation described in [15]. – Presented at the IXth International Astronautical Congress at Amsterdam, Netherlands, August 25–30, 1958.

[2] Professor of Aeronautical Engineering, Purdue University, Lafayette, Indiana, U.S.A.

first integrals are determined for the equations of motion and the set of EULER equations. Furthermore, a complete formulation of the boundary conditions is supplied by means of the general transversality condition; its application is shown to typical flight paths of Earth satellites and intercontinental missiles.

**Allgemeine Variationstheorie der Flugwege von mit Raketenantrieb bewegten Flugzeugen, Flugkörpern und Satellitenträgern.** Es werden allgemeine Gleichungen für die Auswertung der optimalen Flugbahnen von raketenangetriebenen Flugzeugen, Flugkörpern und Satelliten angegeben. Die Erde wird kugelförmig angenommen; die Veränderlichkeit der Schwerebeschleunigung mit der Höhe wird berücksichtigt.

Das Variationsproblem wird untersucht im Rahmen der Probleme vom MAYER-Typ, das ist der Aufsuchung der Mindestdifferenz $\Delta G$ zwischen Anfangs- und Endwert einer willkürlich bestimmten Funktion $G\,(X, h, V, \theta, m, t)$ von Reichweite, Höhe, Geschwindigkeit, Bahnneigung, Masse und Zeit.

Das allgemeine Problem umfaßt drei Freiheitsgrade. Diese sind beziehungsweise verknüpft mit der gleichzeitigen Optimalisierung des zeitlichen Ablaufs der Auftriebskraft, des Schubmoduls und der Schubrichtung. Spezielle Probleme, die nur einen oder zwei Freiheitsgrade betreffen, werden mittels Einführung von zusätzlichen Beschränkungsgleichungen behandelt.

Mit Ausnahme einiger Sonderfälle besteht die Mannigfaltigkeit aller extremen Bahnstreckenteile aus Bögen, die entweder ohne Schub oder mit Maximalschub oder mit veränderlichem Schub durchflogen werden. So werden unterbrochene Lösungen gefunden, die im Lichte der ERDMANN-WEIERSTRASSschen Eckbedingungen besprochen werden. Die Resultate, wie sie hier dargestellt werden, vereinigen in einer einheitlichen Theorie eine Reihe von früheren Arbeiten des Verfassers und anderer Forscher.

Besondere Aufmerksamkeit wird unter der Annahme einer flachen Erde auf einige bestimmte Klassen von Flugbahnen gelenkt, wie z. B. vertikale, wo $G = G\,(h, V, m, t)$; waagrechte, wo $G = G\,(X, V, m, t)$; beliebig geneigte geradlinige, wo $G = G\,(X, h, V, m)$; gekrümmte Flugbahnen mit vernachlässigbarem, induziertem Widerstand; auftriebslose in isothermer Umgebung; und schließlich Flugbahnen im luftleeren Raum.

Für einige dieser speziellen Fälle werden geschlossene Ausdrücke für die Verteilung der LAGRANGEschen Faktoren und die Optimalisierungsbedingung abgeleitet. Einige erste Integrale werden für die Bewegungsgleichungen und die Gruppe von EULER-Gleichungen bestimmt. Ferner wird eine vollständige Formulierung der Grenzbedingungen mittels der allgemeinen Transversalitätsbedingung angegeben und ihre Anwendung auf typische Anflugbahnen von Erdsatelliten und Fernraketen gezeigt.

**Une théorie variationnelle générale pour les trajectoires d'avions propulsés par fusée, de missiles et de satellites.** Des équations générales sont présentées, pour analyser les trajectoires de vol optimum d'avions propulsés par fusée, de missiles et de satellites. On suppose que la Terre est sphérique; on tient compte de la variation de l'accélération de la pesanteur avec l'altitude.

Le problème aux variations est étudié dans le cadre général des problèmes du type de MAYER, c. a. d., comme le problème de minimiser la différence $\Delta G$ entre la valeur finale et initiale d'une fonction $G\,(X, h, V, \theta, m, t)$ arbitrairement définie du rayon d'action, de l'altitude, de la vitesse, de l'inclinaison de la trajectoire, de la masse et du temps.

Le problème général est caractérisé par le fait qu'il comprend trois degrés de liberté, qui sont associés respectivement, avec l'optimisation simultanée de la variation avec le temps de la portance, du module de la poussée, et de la direction de la poussée. Les cas particuliers comprenant un ou deux degrés de liberté sont étudiés en introduisant des équations supplémentaires de liaison.

A part quelques cas exceptionnels, la totalité des arcs extremaux est généralement composée d'arcs partiels parcourus avec une poussée nulle, avec une poussée maximum, et avec une poussée variable. Ainsi, des solutions discontinues sont obtenues et sont discutées à l'aide des conditions de ERDMANN-WEIERSTRASS. Les résultats présentés

Vol. 4 1958

ici généralisent, en une seule théorie, nombre d'études précédentes dues à l'auteur et à d'autres auteurs.

Quelques classes particulières de trajectoires ont été tout spécialement étudiées, dans l'hypothèse d'une Terre plate, ce sont: les trajectoires verticales associées avec les problèmes où $G = G(h, V, m, t)$; les trajectoires à altitude constante associées avec les fonctions de la forme $G = G(X, V, m, t)$; les trajectoires rectilignes arbitrairement inclinées associées avec les problèmes où $G = G(X, h, V, m)$; les trajectoires curvilignes parcourues avec une trainée induite négligeable; les trajectoires à portance nulle dans un milieu isotherme; les trajectoires parcourues dans le vide.

Pour quelques uns des cas particuliers cités ci-dessus, des expressions analytiques sont obtenues pour la distribution des multiplicateurs de LAGRANGE et pour la condition d'optimisation. Quelques intégrales premières des équations du mouvement et des équations d'EULER sont obtenues. De plus, une expression complète des conditions aux limites est donnée grâce à la condition générale de transversalité; son application à des trajectoires typiques de satellites et d'engins intercontinentaux est indiquée.

## Foreword

This article is an attempt to introduce a broad, unified theory of the flight programming for rocket-powered vehicles. Considerations of size have inclined the writer to present only statements of a general engineering nature, with regard to the necessary conditions for the extremum. Detailed topics such as discontinuities arising from staging or methods of solution of special types of boundary value problems have been excluded. For these problems, the interested reader is referred to the continuously growing specialized literature on the subject.

## I. Introduction

When a missile is flying in a vertical plane, several possibilities exist for modifying its trajectory: to control the elevator's position; to control the thrust magnitude; to control the thrust direction. It is in this sense that a missile in symmetrical flight can be thought of as a machine having three degrees of freedom: they are, respectively, associated with the time history of the lift and of the thrust vector.

Thus, for a given set of end-conditions, infinite trajectories exist which are mathematically and physically possible. Among them it is of engineering interest to seek those special paths which meet some *optimum* requirement.

Generally speaking, the problem of the best operational performance in a vertical plane can be stated as the problem of saturating the previously mentioned three degrees of freedom in such a way that the difference $\Delta G = G_f - G_i$ between the final and the initial value of an arbitrarily specified function $G$ of the generalized coordinates of the missile is a minimum. In practical cases the $G$-function can be, for instance, the range, the altitude, the flight velocity, the energy-height, the mass, the time, the dynamic pressure or the skin temperature.

Particular aspects of the above general problem can be originated by *freezing* one or two degrees of freedom and studying the optimization of the remaining one(s). In this connection, the interested reader can find much useful information in the enclosed list of References.

### Description of the Present Research

Under the sponsorship of the Office of Scientific Research of the United States Air Force, an investigation of a wide class of variational problems of interest in the Mechanics of Flight of rockets has been undertaken. Detailed aspects of the theory of the optimum burning program have been considered in the papers of

[1] to [4] and [17], which deal with rectilinear trajectories either horizontal or vertical or arbitrarily inclined. One degree of freedom characterized the problems investigated in [1] to [4], namely the degree of freedom associated with the time history of the modulus of the thrust.

With the present paper all the restrictions introduced in [1] to [4] and [17] are removed. The paths considered are of a general, curvilinear nature; the Earth is spherical; the acceleration of gravity is variable. Furthermore, and more important, three degrees of freedom characterize the broad aspects of the present investigation. The latter is concerned with the simultaneous determination of the time history of modulus of the thrust, direction of the thrust and angle of attack. General equations are presented covering a wide group of variational problems of the Mechanics of Flight. These equations contain, as a particular case, not only previous work developed by the author and his associates [1] to [4] and [17] but also a large segment of the contributions due to several other researchers (see list of References).

Vol. 4 1958

## II. Fundamental Equations

The trajectories considered in the present report are entirely contained in a plane passing through the center of the Earth. The latter is assumed to be spherical. The vector acceleration of gravity is regarded as radially directed; its modulus ($g$) is related to the altitude by the following relationship:

$$g = g_0 \left( \frac{\varrho_0}{\varrho_0 + h} \right)^2 \tag{1}$$

where the sub-index 0 denotes quantity evaluated at sea-level, $\varrho_0$ radius of the Earth, $h$ altitude above sea-level and $\varrho = \varrho_0 + h$ distance between aircraft and center of the Earth.

The airplane is conceived as a particle, on which aerodynamic forces of symmetric type are acting, i.e., lift ($L$) and drag ($D$). These forces are calculated as in unaccelerated flight, i.e., by neglecting the so-called aerodynamic lag. Thus, the relationship between lift ($L$) and drag ($D$) is assumed to have the general form:

$$D = D(h, V, L) \tag{2}$$

where $V$ is the flight velocity, relative to the Earth.

The power plant considered here is an ideal rocket engine, such that its equivalent exit velocity ($V_e$) is a constant. The modulus of the thrust is $V_e \beta$, where $\beta$ is the mass flow. The latter is variable, though bounded between a lower value ($\beta = 0$) and an upper value ($\beta = \beta_{\max}$)

$$0 \leqslant \beta \leqslant \beta_{\max}. \tag{3}$$

### 1. Parametric Representation of the Engine Characteristics

In order to handle the inequality (3) the idea of parametric representation of the engine characteristics is introduced [1] to [3]. The mass flow ($\beta$) is represented as a function of a parameter ($\alpha$) having the following properties:

(a) for $-\infty \leqslant \alpha \leqslant \alpha_1$, $\beta = 0$, $d\beta/d\alpha = 0$

(b) for $\alpha_2 \leqslant \alpha \leqslant +\infty$, $\beta = \beta_{\max}$, $d\beta/d\alpha = 0$

(c) for $\alpha_1 < \alpha < \alpha_2$, $d\beta/d\alpha \neq 0$.

With the above scheme, $\alpha$ is considered the *independent parameter* of the rocket engine and is allowed to vary between $-\infty$ and $+\infty$. The mass flow $\beta$

becomes a *dependent* quantity, varying between 0 and $\beta_{max}$ according to the scheme of Fig. 1. In turn, the thrust $V_e \beta$ is limited between 0 and $V_e \beta_{max}$.

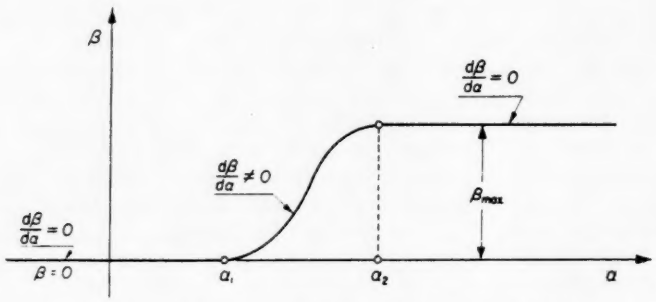


Fig. 1. Parametric representation of the engine characteristics

Notice that the condition $d\beta/d\alpha = 0$ represents either a coasting flight or a flight with maximum engine output. On the other hand, $d\beta/d\alpha \neq 0$ represents any other operating condition of the engine intermediate between the two limiting ones. Notice also that $\alpha$ is *only* a parameter and that there is no necessity of attributing to it any special physical meaning.

## 2. Kinematical Relationships

The following relations tie distance flown ($X$), altitude ($h$), time ($t$), velocity modulus ($V$) and path inclination ($\theta$):

$$J_1 \equiv \dot{X} - \frac{\varrho_0}{\varrho_0 + h} V \cos\theta = 0 \tag{4}$$

$$J_2 \equiv \dot{h} - V \sin\theta = 0. \tag{5}$$

The dot sign denotes time derivative and the $X$-variable curvilinear coordinate measured (Fig. 2) along the circle of radius $\varrho_0$ and positive westward with respect to an observer located at the North Pole; in turn, $\theta$ is the angle which the velocity vector forms with the plane tangent to the spherical surface of radius $\varrho_0 + h$ passing through the aircraft.

## 3. Dynamical Equations

The dynamical behaviour of the aircraft on the two directions tangent ($t$) and on the normal ($n$) to the flight path (Fig. 2) is represented by the below indicated equations:

$$J_3 \equiv \dot{V} + g_0 \left(\frac{\varrho_0}{\varrho_0 + h}\right)^2 \sin\theta + \frac{D(h, V, L) - V_e \beta(\alpha) \cos\omega}{m} = 0 \tag{6}$$

$$J_4 \equiv \dot{\theta} - \frac{V \cos\theta}{\varrho_0 + h} + \frac{g_0}{V} \left(\frac{\varrho_0}{\varrho_0 + h}\right)^2 \cos\theta - \frac{L + V_e \beta(\alpha) \sin\omega}{m V} + 2\,\omega_E \cos\varphi_E = 0 \tag{7}$$

where $\alpha$ is the so-called engine parameter, defined in Section II, 1, $\omega$ the angle between thrust vector and velocity vector (Fig. 2), $m$ the instantaneous mass of the vehicle, $\omega_E$ the modulus of the angular velocity associated with the motion

of the Earth around its polar axis and $\varphi_E$ the smaller of the two angles which the polar axis forms with the perpendicular to the plane of the motion. The last term on the right of Eq. (7) is due to the CORIOLIS acceleration. Furthermore, the relationship between mass, time and engine mass flow is indicated as:

$$J_5 \equiv \dot{m} + \beta(\alpha) = 0. \tag{8}$$

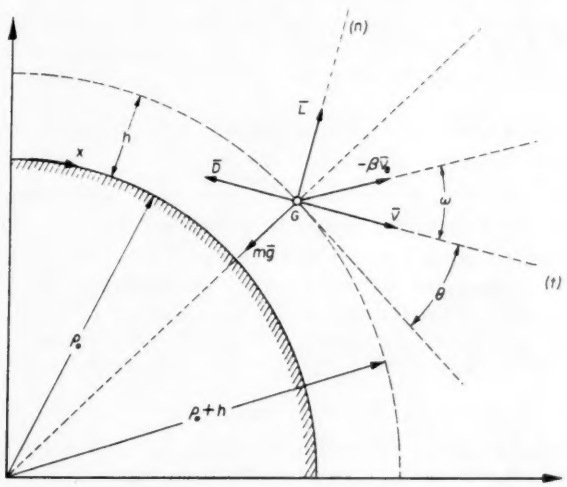


Fig. 2. Illustration of the coordinate system used in the present paper

## 4. Problem with Three Degrees of Freedom

Eqs. (4) to (8) form a set of five differential relationships, where the independent variable is one ($t$) and the dependent variables are eight ($X, h, V, \theta, m, L, \alpha, \omega$).

It follows that the general problem of the optimum trajectory in a vertical plane embodies three degrees of freedom. They are, respectively, associated with the time programming of: lift distribution $L(t)$; engine mass flow $\beta[\alpha(t)]$ and thrust direction $\omega(t)$.

## 5. Problems with Two Degrees of Freedom or One Degree of Freedom

In addition to studying trajectories of a general nature, it is of engineering interest to understand the behaviour of the rocket along special types of flight paths.

Thus, in the present report, the possible presence of either one or two constraining equations of the form[1]:

$$J_6 \equiv \Phi(X, h, V, \theta, m, L, \beta(\alpha), \omega, t) = 0 \tag{9}$$

$$J_7 \equiv \Psi(X, h, V, \theta, m, L, \beta(\alpha), \omega, t) = 0 \tag{10}$$

is accounted for.

[1] Within the context of the present analysis Eqs. (4) to (8) are called *fundamental constraints*; while Eqs. (9) and (10) are termed *additional constraints*.



Vol. 4 1958

## III. Variational Formulation

The set of Eqs. (4) to (10) is now considered. The independent variable is the time ($t$). The dependent variables are the range ($X$), the altitude ($h$), the flight velocity ($V$), the path inclination ($\theta$), the mass ($m$), the lift ($L$), the engine parameter ($\alpha$) and the thrust direction ($\omega$). For $\Phi$ and $\Psi$ not identically zero, one degree of freedom is left[1] and an optimum requirement can be, therefore, imposed. In this connection, the variational problem (of MAYER type) is stated as follows: "Among all sets of functions $X(t)$, $h(t)$, $V(t)$, $\theta(t)$, $m(t)$, $L(t)$, $\alpha(t)$ and $\omega(t)$ satisfying Eqs. (4) to (10) and certain prescribed end-conditions, to determine the special set which minimizes the difference[2] $\Delta G = G_f - G_i$, where $G = G(X, h, V, \theta, m, t)$."

Particular cases of the above general problem are, for instance:

(a) the case $G = -X$, maximizing the range[3];

(b) the case $G = -m$, minimizing the propellant consumption;

(c) the case $G = t$, minimizing the time of flight.

The end-conditions are concerned with the initial and final values for $X$, $h$, $V$, $\theta$, $m$, $t$. Notice that some, *but not all*, of these coordinates can be assigned. Notice also that the end-values for the non-derivated variables $L$, $\beta$ and $\omega$ cannot be prescribed. In fact, they are a mathematical consequence of the set of constraining equations and EULER equations, as shown in the following sections.

### 1. Euler Equations

A set of variable LAGRANGE multipliers $\lambda_1(t) \ldots \lambda_7(t)$ is introduced and the following expression, termed fundamental function, formed:

$$F = \sum_{k=1}^{7} \lambda_k J_k \tag{11}$$

where $J_1 \ldots J_7$ denote, respectively, the first members of Eqs. (4) to (10). Since the unknown functions are eight in number, one must write eight EULER equations. They are written as:

$$\frac{d}{dt}\left(\frac{\partial F}{\partial \dot{z}_J}\right) = \frac{\partial F}{\partial z_J} \qquad (J = 1 \ldots 8) \tag{12}$$

where $z_1 = X$, $z_2 = h$, $z_3 = V$, $z_4 = \theta$, $z_5 = m$, $z_6 = L$, $z_7 = \alpha$, and $z_8 = \omega$. From the above equations, the following explicit form of the EULER equations is obtained:

$$\dot{\lambda}_1 = \lambda_6 \frac{\partial \Phi}{\partial X} + \lambda_7 \frac{\partial \Psi}{\partial X} \tag{13}$$

$$\dot{\lambda}_2 = \lambda_1 \frac{\varrho_0}{(\varrho_0 + h)^2} V \cos\theta + \lambda_3 \left[\frac{1}{m}\frac{\partial D}{\partial h} - 2 g_0 \frac{{\varrho_0}^2}{(\varrho_0 + h)^3} \sin\theta\right] + \\ + \lambda_4 \frac{\cos\theta}{(\varrho_0 + h)^2}\left[V - 2\frac{g_0}{V}\frac{{\varrho_0}^2}{\varrho_0 + h}\right] + \lambda_6 \frac{\partial \Phi}{\partial h} + \lambda_7 \frac{\partial \Psi}{\partial h} \tag{14}$$

---

[1] The problem with two degrees of freedom is generated when *either* $\Phi$ or $\Psi$ is *identically* zero; analogously the problem with three degrees of freedom is obtained when *both* $\Phi$ and $\Psi$ are *identically* zero.

[2] The sub-index $i$ denotes initial point; the sub-index $f$ refers to final point.

[3] Clearly, the problem of *maximizing* $X_f - X_i$ is identical with the problem of *minimizing* $-(X_f - X_i)$.

$$\dot{\lambda}_3 = -\lambda_1 \frac{\varrho_0}{\varrho_0 + h} \cos\theta - \lambda_2 \sin\theta + \frac{\lambda_3}{m}\frac{\partial D}{\partial V} + \\ + \lambda_4 \left[ \frac{L + V_e \beta \sin\omega}{m V^2} - \frac{\cos\theta}{\varrho_0 + h}\left(1 + \frac{g_0}{V^2}\frac{{\varrho_0}^2}{\varrho_0 + h}\right)\right] + \lambda_6 \frac{\partial \Phi}{\partial V} + \lambda_7 \frac{\partial \Psi}{\partial V} \quad (15)$$

$$\dot{\lambda}_4 = \lambda_1 \frac{\varrho_0}{\varrho_0 + h} V \sin\theta - \lambda_2 V \cos\theta + \lambda_3 g_0 \left(\frac{\varrho_0}{\varrho_0 + h}\right)^2 \cos\theta + \\ + \lambda_4 \frac{\sin\theta}{\varrho_0 + h}\left[V - \frac{g_0}{V}\frac{{\varrho_0}^2}{\varrho_0 + h}\right] + \lambda_6 \frac{\partial \Phi}{\partial \theta} + \lambda_7 \frac{\partial \Psi}{\partial \theta} \quad (16)$$

$$\dot{\lambda}_5 = \frac{\lambda_3}{m^2}\left[V_e \beta \cos\omega - D\right] + \frac{\lambda_4}{m^2 V}\left[L + V_e \beta \sin\omega\right] + \lambda_6 \frac{\partial \Phi}{\partial m} + \lambda_7 \frac{\partial \Psi}{\partial m} \quad (17)$$

$$0 = \frac{\lambda_3}{m}\frac{\partial D}{\partial L} - \frac{\lambda_4}{m V} + \lambda_6 \frac{\partial \Phi}{\partial L} + \lambda_7 \frac{\partial \Psi}{\partial L} \quad (18)$$

$$0 = \frac{d\beta}{d\alpha}\left[-\lambda_3 \frac{V_e}{m}\cos\omega - \lambda_4 \frac{V_e}{m V}\sin\omega + \lambda_5 + \lambda_6 \frac{\partial \Phi}{\partial \beta} + \lambda_7 \frac{\partial \Psi}{\partial \beta}\right] \quad (19)$$

$$0 = \lambda_3 \frac{V_e \beta}{m}\sin\omega - \lambda_4 \frac{V_e \beta}{m V}\cos\omega + \lambda_6 \frac{\partial \Phi}{\partial \omega} + \lambda_7 \frac{\partial \Psi}{\partial \omega}. \quad (20)$$

An important mathematical consequence of the set of Eqs. (13) to (20) is that:

$$\frac{d}{dt}\left[\lambda_1 \dot{X} + \lambda_2 \dot{h} + \lambda_3 \dot{V} + \lambda_4 \dot{\theta} + \lambda_5 \dot{m}\right] + \lambda_6 \frac{\partial \Phi}{\partial t} + \lambda_7 \frac{\partial \Psi}{\partial t} = 0. \quad (21)$$

Generally speaking, the set of EULER equations (13) to (20) and constraining Eqs. (4) to (10) must be dealt with by approximate procedures of integration. The main difficulty stems from the circumstance that the variational problems of the Mechanics of Flight are *boundary value problems*, i.e., problems with conditions prescribed in part at the initial point and in part at the final point. Thus, the use of trial-and-error techniques is, in the general case, an unavoidable necessity.

## 2. Discontinuity of the Eulerian Solution

As the EULER equation (19) shows, the extremal arc is discontinuous. In fact it generally embodies[1]:

(a) sub-arcs of equation

$$\frac{d\beta}{d\alpha} = 0, \quad (22)$$

(b) sub-arcs of equation

$$-\frac{V_e}{m}\left[\lambda_3 \cos\omega + \frac{\lambda_4}{V}\sin\omega\right] + \lambda_5 + \lambda_6 \frac{\partial \Phi}{\partial \beta} + \lambda_7 \frac{\partial \Psi}{\partial \beta} = 0. \quad (23)$$

According to the parametric representation illustrated in Section II, 1, Eq. (22) represents either a coasting flight or a flight with maximum engine output. Eq. (23), on the other hand, is representative of a flight condition with a continuously variable mass flow, as shown in the following sections of this article.

[1] An important exception is represented by the case where one of the two additional constraints prescribes that the mass flow is either a constant or a known function of the time. In such a case the aforementioned discontinuity disappears.

Vol. 4 1958

### 3. Erdmann-Weierstrass Corner Conditions

In view of the discontinuous character of the solution, the ERDMANN-WEIERSTRASS corner conditions must be applied. These are continuity conditions to be satisfied at *every corner* of the discontinuous extremal solution. In analogy with [1] to [4], the analysis of the corner conditions yields the following results:

$$(\lambda_k)_- = (\lambda_k)_+ \qquad (k = 1 \ldots 5) \tag{24}$$

$$(\lambda_1 \dot{X} + \lambda_2 \dot{h} + \lambda_3 \dot{V} + \lambda_4 \dot{\theta} + \lambda_5 \dot{m})_- = (\lambda_1 \dot{X} + \lambda_2 \dot{h} + \lambda_3 \dot{V} + \lambda_4 \dot{\theta} + \lambda_5 \dot{m})_+ \tag{25}$$

where the subscript $(-)$ denotes a condition immediately before a corner and the subscript $(+)$ a condition immediately after a corner.

### 4. Boundary Conditions

For the problem under consideration the boundary conditions include a number of fixed end-points conditions plus a number of natural conditions. The latter must be deduced from the following general transversality condition of the Calculus of Variations:

$$[\delta G + \lambda_1 \delta X + \lambda_2 \delta h + \lambda_3 \delta V + \lambda_4 \delta\theta + \lambda_5 \delta m - (\lambda_1 \dot{X} + \lambda_2 \dot{h} + \lambda_3 \dot{V} + \lambda_4 \dot{\theta} + \lambda_5 \dot{m})\, \delta t]_i^f = 0 \tag{26}$$

which is to be identically satisfied for all systems of variations consistent with the prescribed end-conditions. After considering that $G = G(X, h, V, \theta, m, t)$, Eq. (26) generally splits into twelve sub-conditions, namely 6 at the initial point and 6 at the final point.

### 5. Additional Constraints Independent of the Time

If the additional constraints (9) and (10) are independent of the time, i.e., if $\partial\Phi/\partial t = 0$, $\partial\Psi/\partial t = 0$, Eq. (21) admits the first integral

$$\lambda_1 \dot{X} + \lambda_2 \dot{h} + \lambda_3 \dot{V} + \lambda_4 \dot{\theta} + \lambda_5 \dot{m} = C \tag{27}$$

where $C$ is an integration constant. Notice that the corner condition (25) can be rewritten as:

$$(C)_- = (C)_+. \tag{28}$$

The value of the integration constant $C$ is, therefore, the same for all sub-arcs forming one extremal arc. Furthermore, the transversality condition is transformed into:

$$[\delta G + \lambda_1 \delta X + \lambda_2 \delta h + \lambda_3 \delta V + \lambda_4 \delta\theta + \lambda_5 \delta m - C\, \delta t]_i^f = 0. \tag{29}$$

*Particular Case*

If the $G$-function is independent of the time $(\partial G/\partial t = 0)$ and if no time condition is prescribed at one of the two end-points, the transversality condition yields the important result:

$$C = 0. \tag{30}$$

### 6. Additional Constraints Independent of Both the Lift and the Thrust Inclination

If the additional constraints (9) and (10) are independent of both $L$ and $\omega$, i.e., if $\partial\Phi/\partial L = 0$, $\partial\Phi/\partial\omega = 0$, $\partial\Psi/\partial L = 0$, $\partial\Psi/\partial\omega = 0$, the two EULER equations (18) and (20) yield the following result [5]:

$$\omega = \arctan \frac{\partial D}{\partial L}. \tag{31}$$

Implied in Eq. (31) is an elegant graphical interpretation, illustrated in Fig. 3 where $M = V/a(h)$ is the MACH number[1] and $C_L = C_L(C_D, M)$ the drag polar, i.e., the relationship between lift coefficient ($C_L$), MACH number and drag coefficient ($C_D$). If $P$ is the representative point of the aircraft and if $M$ is the instantaneous MACH number, the optimum value of $\omega$ is identical with the angle which the tangent to the $C_L(C_D)$ curve associated with the given MACH number $M$ forms with the $C_L$-axis. The particular case of a drag polar of the form

$$C_D = C_{D_0}(M) + K(M)\, C_L^2 \tag{32}$$

is now considered, where $C_{D_0}$ is the zero-lift drag coefficient and $K$ the induced drag factor. After accounting for the classical definitions of lift and drag, Eqs. (31) and (32) lead to:

$$\omega = \arctan(2\,K\,C_L). \tag{33}$$

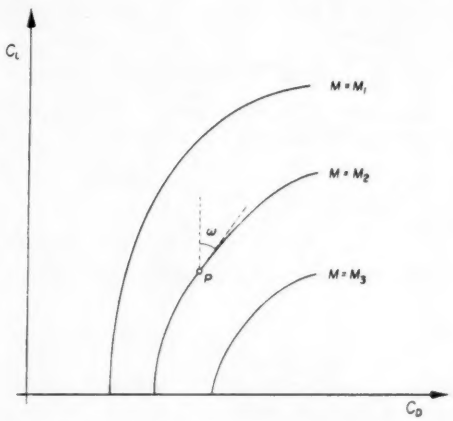


Fig. 3. Optimum inclination of the thrust axis as related to the polar diagram of the vehicle

Vol. 4 1958

## 7. Additional Constraints Independent of the Distance Flown

If the additional constraints are such that $\partial\Phi/\partial X = 0$, $\partial\Psi/\partial X = 0$, the EULER equation (13) admits the first integral

$$\lambda_1 = C_1 \tag{34}$$

where $C_1$ is a constant.

## 8. Problems with Three Degrees of Freedom

If $\Phi \equiv 0$ and $\Psi \equiv 0$, Eqs. (27), (28), (29), (31) and (34) simultaneously hold. The boundary conditions for some important particular cases are now formulated.

### *a) Typical Boundary Conditions for a Satellite Carrier*

The problem of minimum propellant consumption ($G = -m$) is now considered in connection with the following data:

$$\left.\begin{aligned} X_i, h_i, V_i, m_i, t_i &\equiv \text{given} \\ h_f, V_f, \theta_f &\equiv \text{given} \end{aligned}\right\} \tag{35}$$

$$\theta_i, X_f, m_f, t_f \equiv \text{free}. \tag{36}$$

From the general transversality condition, the following consequences are deduced:

$$\left.\begin{aligned} \lambda_{4i} &= 0, \qquad C = 0 \\ \lambda_{1f} &= 0, \qquad \lambda_{5f} = 1 \end{aligned}\right\}. \tag{37}$$

The set of twelve conditions (35) and (37) together with the equations of motion and the EULER equations completely determines the optimum trajectory.

[1] The symbol $a$ denotes speed of sound.

It should be noticed that the first LAGRANGE multiplier is $\lambda_1 = 0$ everywhere. Furthermore, the EULER equation (18) leads to:

$$\left(\frac{\partial D}{\partial L}\right)_i = 0. \tag{38}$$

For a drag polar obeying Eq. (32), the above condition implies that the *initial lift be zero.*

*b) Typical Boundary Conditions for an Intercontinental Missile*

The problem of minimum propellant consumption ($G = -\dot{m}$) is considered here for the following set of data:

$$\left.\begin{aligned} &X_i, h_i, V_i, m_i, t_i \equiv \text{given} \\ &X_f, h_f \qquad\quad \equiv \text{given} \end{aligned}\right\} \tag{39}$$

$$\theta_i, V_f, \theta_f, m_f, t_f \equiv \text{free}. \tag{40}$$

The transversality condition yields:

$$\left.\begin{aligned} &\lambda_{4i} = 0, \qquad C = 0 \\ &\lambda_{3f} = 0, \qquad \lambda_{4f} = 0, \qquad \lambda_{5f} = 1 \end{aligned}\right\}. \tag{41}$$

The set of twelve conditions (39) and (41) together with the EULER equations and the equations of motion completely determines the optimum path.

## IV. Equations for a Flat Earth

The CORIOLIS acceleration is now neglected and the mathematical assumption $\varrho_0 = \infty$ introduced into the set of constraining equations and EULER equations. Nine of the above fifteen equations hold unchanged. For convenience and quick reference, however, both the constraining equations and the EULER equations are now rewritten. The former read as follows:

$$J_1 \equiv \dot{X} - V\cos\theta = 0 \tag{42}$$

$$J_2 \equiv \dot{h} - V\sin\theta = 0 \tag{43}$$

$$J_3 \equiv \dot{V} + g_0\sin\theta + \frac{D(h, V, L) - V_e\beta(\alpha)\cos\omega}{m} = 0 \tag{44}$$

$$J_4 \equiv \dot{\theta} + \frac{g_0}{V}\cos\theta - \frac{L + V_e\beta(\alpha)\sin\omega}{mV} = 0 \tag{45}$$

$$J_5 \equiv \dot{m} + \beta(\alpha) = 0 \tag{46}$$

$$J_6 \equiv \Phi(X, h, V, \theta, m, L, \beta[\alpha], \omega, t) = 0 \tag{47}$$

$$J_7 \equiv \Psi(X, h, V, \theta, m, L, \beta[\alpha], \omega, t) = 0. \tag{48}$$

In turn, the EULER equations take the form:

$$\dot{\lambda}_1 = \lambda_6\frac{\partial\Phi}{\partial X} + \lambda_7\frac{\partial\Psi}{\partial X} \tag{49}$$

$$\dot{\lambda}_2 = \frac{\lambda_3}{m}\frac{\partial D}{\partial h} + \lambda_6\frac{\partial\Phi}{\partial h} + \lambda_7\frac{\partial\Psi}{\partial h} \tag{50}$$

$$\dot{\lambda}_3 = -\lambda_1\cos\theta - \lambda_2\sin\theta + \frac{\lambda_3}{m}\frac{\partial D}{\partial V} - \lambda_4\frac{g_0}{V^2}\cos\theta + \\ + \frac{\lambda_4}{mV^2}[L + V_e\beta\sin\omega] + \lambda_6\frac{\partial\Phi}{\partial V} + \lambda_7\frac{\partial\Psi}{\partial V} \tag{51}$$

$$\dot{\lambda}_4 = \lambda_1 V \sin\theta - \lambda_2 V \cos\theta + \lambda_3 g_0 \cos\theta - \lambda_4 \frac{g_0}{V} \sin\theta + \lambda_6 \frac{\partial \Phi}{\partial \theta} + \lambda_7 \frac{\partial \Psi}{\partial \theta} \tag{52}$$

$$\dot{\lambda}_5 = \frac{\lambda_3}{m^2} [V_e \beta \cos\omega - D] + \frac{\lambda_4}{m^2 V} (L + V_e \beta \sin\omega) + \lambda_6 \frac{\partial \Phi}{\partial m} + \lambda_7 \frac{\partial \Psi}{\partial m} \tag{53}$$

$$0 = \frac{\lambda_3}{m} \frac{\partial D}{\partial L} - \frac{\lambda_4}{m V} + \lambda_6 \frac{\partial \Phi}{\partial L} + \lambda_7 \frac{\partial \Psi}{\partial L} \tag{54}$$

$$0 = \frac{d\beta}{d\alpha} \left[ - \lambda_3 \frac{V_e}{m} \cos\omega - \lambda_4 \frac{V_e}{m V} \sin\omega + \lambda_5 + \lambda_6 \frac{\partial \Phi}{\partial \beta} + \lambda_7 \frac{\partial \Psi}{\partial \beta} \right] \tag{55}$$

$$0 = \lambda_3 \frac{V_e \beta}{m} \sin\omega - \lambda_4 \frac{V_e \beta}{m V} \cos\omega + \lambda_6 \frac{\partial \Phi}{\partial \omega} + \lambda_7 \frac{\partial \Psi}{\partial \omega}. \tag{56}$$

Notice that Eqs. (21) to (41) hold formally unchanged, provided, however, the time derivatives $\dot{X}$, $\dot{h}$, $\dot{V}$, $\dot{\theta}$, $\dot{m}$ be computed from Eqs. (42) to (46).

Vol. 4 1958

## V. Vertical Paths

An important category of trajectories is represented by the class of vertical paths which is now investigated[1] in connection with problems where $G = G(h, V, m, t)$. Under the hypothesis that the thrust direction is vertical, the equations of the two additional constraints (47) and (48) become:

$$\Phi \equiv \theta - \frac{\pi}{2} = 0 \tag{57}$$

$$\Psi \equiv \omega = 0. \tag{58}$$

It should be noticed that the multipliers $\lambda_1$, $\lambda_4$, $\lambda_6$ and $\lambda_7$ are only contained in Eqs. (49), (52), (54) and (56) which have, therefore, a non-essential character. The four remaining EULER equations embody three multipliers ($\lambda_2$, $\lambda_3$ and $\lambda_5$) and are written as follows:

$$\dot{\lambda}_2 = \frac{\lambda_3}{m} \frac{\partial D}{\partial h} \tag{59}$$

$$\dot{\lambda}_3 = - \lambda_2 + \frac{\lambda_3}{m} \frac{\partial D}{\partial V} \tag{60}$$

$$\dot{\lambda}_5 = \frac{\lambda_3}{m^2} [V_e \beta - D] \tag{61}$$

$$0 = \frac{d\beta}{d\alpha} \left[ - \lambda_3 \frac{V_e}{m} + \lambda_5 \right] \tag{62}$$

Clearly Eqs. (59) to (62) suffice to determine both the distribution of LAGRANGE multipliers and the optimizing condition. In view of the constancy of $X$ and $\theta$ the first integral (27) is transformed into:

$$\lambda_2 V + \lambda_3 \left[ \frac{V_e \beta - D}{m} - g_0 \right] - \lambda_5 \beta = C. \tag{63}$$

Furthermore, the transversality condition is written as:

$$[\delta G + \lambda_2 \delta h + \lambda_3 \delta V + \lambda_5 \delta m - C \delta t]_i^f = 0 \tag{64}$$

[1] In the present section as in all the following sections use is made of the hypothesis of flat Earth.

where $G = G(h, V, m, t)$. Notice that, as Eq. (62) points out, the extremal arc is composed of sub-arcs $\beta = 0$, sub-arcs $\beta = \beta_{\max}$ and variable-thrust sub-arcs such that

$$\lambda_5 - \lambda_3 \frac{V_e}{m} = 0. \tag{65}$$

## Variable-Thrust Sub-Arcs

For the sub-arcs defined by Eq. (65) simple manipulations yield the below indicated integral results for the LAGRANGE multipliers [2]:

$$\lambda_2 = C_2 \left( \frac{\partial D}{\partial V} + \frac{D}{V_e} \right) \exp\left( \frac{V + g_0 t}{V_e} \right) \tag{66}$$

$$\lambda_3 = C_2 m \exp\left( \frac{V + g_0 t}{V_e} \right) \tag{67}$$

$$\lambda_5 = C_2 V_e \exp\left( \frac{V + g_0 t}{V_e} \right) \tag{68}$$

where $C_2$ is an integration constant. In turn, elimination of the multipliers from Eq. (63) yields the following holonomic form for the optimizing condition [2]:

$$m g_0 = D\left( \frac{V}{V_e} - 1 \right) + V \frac{\partial D}{\partial V} - \frac{C}{C_2} \exp\left( - \frac{V + g_0 t}{V_e} \right). \tag{69}$$

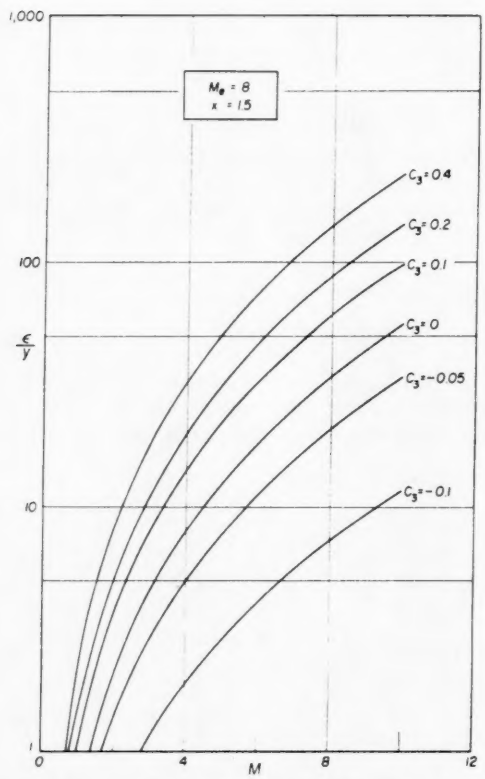


Fig. 4. Family of variable-thrust sub-arcs for vertical flight [$G = G(h, V, m, t)$]

The particular case where the relationship between zero-lift drag coefficient and MACH number is approximated as[1]

$$C_{D_0} = \gamma M^{x-2} \tag{70}$$

is now considered, $x$ and $\gamma$ being appropriate constants. Assuming an isothermal atmosphere, the time—MACH number relationship and the altitude—MACH number relationship can be integrated in a closed form [2], so that the optimizing condition (69) becomes

$$\frac{\varepsilon}{\gamma M^x} = \frac{M}{M_e} + x - 1 + C_3 \left[ M - \frac{1}{\gamma M_e} + M_e (x - 1) - \frac{x}{\gamma M} \right] \tag{71}$$

[1] For the all-supersonic domain the exponent $x$ is, in practice, a number bounded between 1 and 2.

where $M_e = V_e/a$ is the ratio of equivalent exit velocity of the rocket engine to *atmospheric* speed of sound[1], $C_3$ a new constant (*proportional* to $C$) and

$$\varepsilon = \frac{2\, m\, g_0}{\gamma\, p\, S}. \tag{72}$$

In the above equations $p$ is the local atmospheric pressure, $S$ a reference surface for the aerodynamic coefficients and $\gamma$ the ratio of specific heat at constant pressure to specific heat at constant volume. Eq. (71) is plotted in Fig. 4 for $x = 1.5$, $M_e = 8$ and for several values of the constant $C_3$. The particular value of $C_3$ associated with the solution of a given variational problem depends upon the boundary conditions of the problem and upon the analytical expression of the $G$-function whose difference $\Delta G$ is to be minimized [2, 6].

*Problems where No Time Condition is Imposed*

If the $G$-function has the form $G = G\,(h, V, m)$ and if no time condition is imposed at one of the two end-points, the transversality condition yields $C = 0$. As a consequence, the optimizing condition (69) modifies for $C_3 = 0$ into [7, 2]

$$m\, g_0 = D\left(\frac{V}{V_e} - 1\right) + V\frac{\partial D}{\partial V}. \tag{73}$$

Vol. 4 1958

Notice that, after introducing the usual definition of drag, Eq. (73) can be rewritten as:

$$\varepsilon = C_{D_0} M^2 \left[\frac{M}{M_e} + 1 + \frac{d \log C_{D_0}}{d \log M}\right]. \tag{74}$$

In particular, if the relationship between zero-lift drag coefficient and MACH number obeys Eq. (70), the above formula reduces to:

$$\varepsilon = y\, M^x \left[\frac{M}{M_e} + x - 1\right]. \tag{75}$$

## VI. Level Paths

The flight path is now assumed horizontal. Problems of the form $G = G\,(X, V, m, t)$ are analyzed. After assuming the thrust parallel to the vector velocity, the additional constraints are written as:

$$\Phi \equiv \theta = 0 \tag{76}$$

$$\Psi \equiv \omega = 0. \tag{77}$$

Once more, the system of EULER equations (49) to (56) splits into two non-interacting sets. In fact, the multipliers $\lambda_2$, $\lambda_6$ and $\lambda_7$ are only present in Eqs. (50), (52) and (56). The remaining EULER equations are written as

$$\dot{\lambda}_1 = 0 \tag{78}$$

$$\dot{\lambda}_3 = -\lambda_1 + \frac{\lambda_3}{m}\frac{\partial D}{\partial V} \tag{79}$$

$$\dot{\lambda}_5 = \frac{\lambda_3}{m^2}\left[V_e \beta - D\right] + \frac{\lambda_4}{m^2 V} L \tag{80}$$

$$0 = \lambda_3 \frac{\partial D}{\partial L} - \frac{\lambda_4}{V} \tag{81}$$

[1] $M_e$, therefore, *does not* stand for MACH number in the exit section of the rocket engine.

$$0 = \frac{d\beta}{d\alpha}\left[-\lambda_3 \frac{V_e}{m} + \lambda_5\right]. \tag{82}$$

In view of the constancy of $h$ and $\theta$, the first integral (27) is transformed into

$$\lambda_1 V + \frac{\lambda_3}{m}\left[V_e \beta - D\right] - \lambda_5 \beta = C. \tag{83}$$

Furthermore, the transversality condition (29) is written as

$$[\delta G + \lambda_1 \delta X + \lambda_3 \delta V + \lambda_5 \delta m - C\, \delta t]_i^f = 0. \tag{84}$$

As Eq. (82) points out, the extremal arc is composed of sub-arcs $\beta = 0$, sub-arcs $\beta = \beta_{\max}$ and variable-thrust sub-arcs.

## Variable-Thrust Sub-Arcs

For the sub-arcs such that $\lambda_5 - (\lambda_3 V_e/m) = 0$ the distribution of LAGRANGE multipliers can be integrated in a closed form, as follows

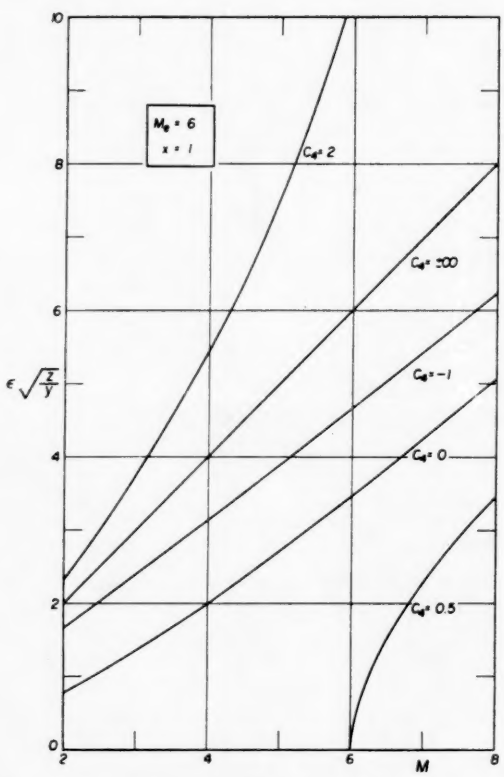


Fig. 5. Family of variable-thrust sub-arcs for level flight $[G = G\,(X, V, m, t)]$

$$\lambda_1 = C_1 \tag{85}$$

$$\lambda_3 = \frac{m}{D}\,(C_1 V - C) \tag{86}$$

$$\lambda_4 = \frac{m V}{D}\,(C_1 V - C)\,\frac{\partial D}{\partial L} \tag{87}$$

$$\lambda_5 = \frac{V_e}{D}\,(C_1 V - C). \tag{88}$$

After further manipulations, the LAGRANGE multipliers can be eliminated, so that the following important form is obtained for the optimizing condition [1]:

$$\left(\frac{V}{V_e} - C_4\right) \times \left(D + V_e \frac{\partial D}{\partial V} - m\, g_0 \frac{\partial D}{\partial L}\right) - D = 0 \tag{89}$$

where

$$C_4 = \frac{C}{C_1 V_e}. \tag{90}$$

For a parabolic drag polar obeying Eq. (32), the optimizing condition (89) can be rewritten as [1]:

$$\varepsilon = M^2 \sqrt{\frac{C_{D_0}}{K}} \sqrt{\frac{A_1 - C_4 A_2}{A_3 - C_4 A_4}} \tag{91}$$

$$A_1 = 1 + \frac{M}{M_e} + \frac{d \log C_{D_0}}{d \log M} \tag{92}$$

$$A_2 = 1 + \frac{M_e}{M}\left[2 + \frac{d \log C_{D_0}}{d \log M}\right] \tag{93}$$

$$A_3 = 3 + \frac{M}{M_e} - \frac{d \log K}{d \log M} \tag{94}$$

$$A_4 = 1 + \frac{M_e}{M}\left[2 - \frac{d \log K}{d \log M}\right] \tag{95}$$

As an example, consider the particularly simple case where the induced drag factor is expressed as $K = z\,M$ ($z$ being an appropriate constant) and the zero-lift drag coefficient obeys Eq. (70). The important relation (91) takes the form $\varepsilon \sqrt{z/y} = f(M)$ and is plotted in Fig. 5 for $M_e = 6$ and $x = 1$.

*Problems where No Time Condition is Imposed*

If the $G$-function has the form $G = G(X, V, m)$ and if no time condition is imposed at one of the two end-points, the transversality condition (84) yields $C = 0$. As a consequence, the optimizing condition (89) modifies into [8]

$$V\left(D + V_e \frac{\partial D}{\partial V} - m\, g_0 \frac{\partial D}{\partial L}\right) - V_e D = 0. \tag{96}$$

In particular, for a drag polar obeying Eq. (32), the optimizing condition is rewritten as

$$\varepsilon = M^2 \sqrt{\frac{C_{D_0}}{K}} \sqrt{\frac{A_1}{A_3}}. \tag{97}$$

## VII. Arbitrarily Inclined Rectilinear Paths

The class of rectilinear trajectories inclined at the arbitrary angle $\theta$ with respect to a horizontal plane is now considered, in connection with problems not involving time. Assuming the thrust tangent to the flight path, the additional constraints take the form

$$\Phi \equiv \theta - \text{const.} = 0 \tag{98}$$

$$\Psi \equiv \omega = 0. \tag{99}$$

Once more, the set of EULER equations (49) to (56) splits into two non-interacting sets. In fact, the multipliers $\lambda_6$ and $\lambda_7$ are present only in Eqs. (52) and (56). The remaining EULER equations are written as

$$\dot{\lambda}_1 = 0 \tag{100}$$

$$\dot{\lambda}_2 = \frac{\lambda_3}{m} \frac{\partial D}{\partial h} \tag{101}$$

$$\dot{\lambda}_3 = -\lambda_1 \cos\theta - \lambda_2 \sin\theta + \frac{\lambda_3}{m} \frac{\partial D}{\partial V} \tag{102}$$

$$\dot{\lambda}_5 = \frac{\lambda_3}{m^2}\,[V_e \beta - D] + \frac{\lambda_4 L}{m^2 V} \tag{103}$$

$$0 = \lambda_3 \frac{\partial D}{\partial L} - \frac{\lambda_4}{V} \tag{104}$$

$$0 = \frac{d\beta}{d\alpha}\left[\lambda_5 - \lambda_3 \frac{V_e}{m}\right]. \tag{105}$$

Vol. 4 1958

The above set admits the first integral

$$\lambda_1 V \cos\theta + \lambda_2 V \sin\theta + \lambda_3 \left[ \frac{V_e \beta - D}{m} - g_0 \sin\theta \right] - \lambda_5 \beta = C. \qquad (106)$$

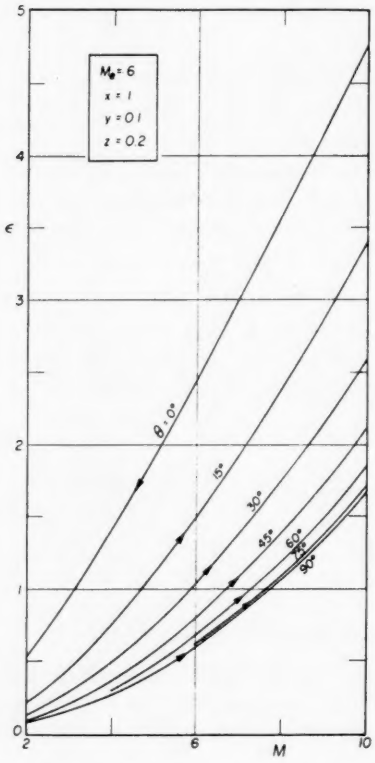


Fig. 6. Family of variable-thrust sub-arcs for arbitrarily inclined straight paths [$G = G(X, h, V, m)$]

## Variable-Thrust Sub-Arcs

As the EULER equation (105) shows, the extremal trajectory includes sub-arcs $\beta = 0$, sub-arcs $\beta = \beta_{\max}$ and variable-thrust sub-arcs such that

$$\lambda_5 - \lambda_3 \frac{V_e}{m} = 0. \qquad (107)$$

Notice that Eqs. (103) and (107) imply that

$$\lambda_3 D V + \dot{\lambda}_3 m V V_e - \lambda_4 L = 0. \qquad (108)$$

The particular case of problems not involving time is now discussed. For these problems $G = G(X, h, V, m)$ and no time condition is prescribed at one of the two end-points. The integration constant is $C = 0$, so that Eqs. (102), (106) and (107) yield

$$\lambda_3 \left[ D + m g_0 \sin\theta - V \frac{\partial D}{\partial V} \right] + m V \dot{\lambda}_3 = 0. \qquad (109)$$

Eqs. (104) and (107) to (109) can be regarded as forming a system linear and homogeneous in $\lambda_3$, $\dot{\lambda}_3$, $\lambda_4$ and $\lambda_5$. As a consequence, non-trivial solutions exist for the multipliers and their derivatives if

$$\begin{vmatrix} V \dfrac{\partial D}{\partial L} & 0 & -1 & 0 \\ V_e & 0 & 0 & -m \\ D V & m V V_e & -L & 0 \\ D + m g_0 \sin\theta - V \dfrac{\partial D}{\partial V} & m V & 0 & 0 \end{vmatrix} = 0. \qquad (110)$$

The development of the above determinant leads to the important result [4]:

$$D(V - V_e) + V V_e \frac{\partial D}{\partial V} - m g_0 \left( V_e \sin\theta + V \cos\theta \frac{\partial D}{\partial L} \right) = 0. \qquad (111)$$

The latter contains, as a particular case, Eq. (73) which refers to vertical flight and Eq. (96) which refers to level flight. For a parabolic drag polar with coefficients depending on the MACH number, Eq. (111) admits the following solution

$$\varepsilon = \frac{M^2}{2\,K\,A_3}\,\frac{\sin\theta}{\cos^2\theta}\,[-1+\sqrt{1+4\,K\,C_{D_0}\,A_1\,A_3\cot^2\theta}]. \tag{112}$$

For $C_{D_0}$ satisfying Eqs. (70) and $K = z\,M$, Eq. (112) is plotted in Fig. 6. The assumed data are as follows: $M_e = 6$, $y = 0.1$, $x = 1$, and $z = 0.2$.

## VIII. Trajectories Flown with Negligible Induced Drag

In several problems of the Mechanics of Flight of rocket-powered aircraft important analytical simplifications may be achieved [9] by neglecting the induced drag $D_i\,(h, V, L)$ with respect to the zero-lift drag $D_0\,(h, V)$. The total drag $D = D_0 + D_i$ is approximated as $D \cong D_0\,(h, V)$. As a consequence, Eqs. (44) and (45) no longer interact. Furthermore, the drag derivative appearing in the EULER equation (54) simplifies into $\partial D/\partial L = 0$.

### 1. Constant Mass Flow (Problem with One Degree of Freedom)

If the rocket engine is operated at constant mass flow and if the thrust vector is parallel to the velocity vector, the equations of the two additional constraints are

$$\Phi \equiv \beta(\alpha) - \text{const.} = 0 \tag{113}$$

$$\Psi \equiv \omega = 0. \tag{114}$$

The set of EULER equations (49) to (56) is such that Eqs. (55) and (56) become ineffectual with regard to the present problem. The remaining equations are written as

$$\dot{\lambda}_1 = 0 \tag{115}$$

$$\dot{\lambda}_2 = \frac{\lambda_3}{m}\,\frac{\partial D}{\partial h} \tag{116}$$

$$\dot{\lambda}_3 = -\lambda_1\cos\theta - \lambda_2\sin\theta + \frac{\lambda_3}{m}\,\frac{\partial D}{\partial V} \tag{117}$$

$$0 = \lambda_1\,V\sin\theta - \lambda_2\,V\cos\theta + \lambda_3\,g_0\cos\theta \tag{118}$$

$$\dot{\lambda}_5 = \frac{\lambda_3}{m^2}\,(V_e\,\beta - D) \tag{119}$$

$$0 = \lambda_4. \tag{120}$$

The first integral for the above system and the transversality condition are respectively formulated as

$$\lambda_1\,V\cos\theta + \lambda_2\,V\sin\theta + \lambda_3\left[\frac{V_e\,\beta - D}{m} - g_0\sin\theta\right] - \lambda_5\,\beta = C \tag{121}$$

$$[\delta G + \lambda_1\,\delta X + \lambda_2\,\delta h + \lambda_3\,\delta V + \lambda_5\,\delta m - C\,\delta t]_i^f = 0 \tag{122}$$

where $G = G\,(X, h, V, m, t)$.

*Problems Not Involving Horizontal Distance*

The particular case where $G = G\,(h, V, m, t)$ is now considered, with the further assumption that no condition is imposed on the $X$-coordinate at one of the two end-points. In view of the fact that $\lambda_1 = 0$ everywhere, the EULER equation (118) shows that the extremal arc splits into the following component sub-arcs [10]

$$\cos\theta = 0 \tag{123}$$

$$\lambda_2\,V - \lambda_3\,g_0 = 0. \tag{124}$$

Vol. 4 1958

Eq. (123) represents either a vertical dive or a vertical zoom; Eq. (124), on the other hand, is representative of a flight condition with a continuously variable path inclination, as shown in the following section.

*Variable Path Inclination Sub-Arcs.* The time derivative of Eq. (124) is now computed yielding

$$\lambda_2 [V_e \beta - D - m g_0 \sin\theta] + \dot{\lambda}_2 m V - \dot{\lambda}_3 m g_0 = 0. \tag{125}$$

Notice that Eqs. (116), (117), (124) and (125) can be regarded (for $\lambda_1 = 0$) as forming a system linear and homogeneous in $\lambda_2$, $\dot{\lambda}_2$, $\lambda_3$ and $\dot{\lambda}_3$. As a consequence, non-trivial solutions exist for the multipliers and their derivatives if

$$\begin{vmatrix} 0 & m & -\dfrac{\partial D}{\partial h} & 0 \\ m\sin\theta & 0 & -\dfrac{\partial D}{\partial V} & m \\ V & 0 & -g_0 & 0 \\ V_e\beta - D - m g_0 \sin\theta & mV & 0 & -m g_0 \end{vmatrix} = 0 \tag{126}$$

i.e., if

$$V_e \beta - D - V \frac{\partial D}{\partial V} + \frac{V^2}{g_0} \frac{\partial D}{\partial h} = 0. \tag{127}$$

Assuming an isothermal atmosphere and accounting for the analytical expression for the zero-lift drag, Eq. (127) can be rewritten as [10]

$$\eta = C_{D_0} M^2 \left[ 3 + \gamma M^2 + \frac{d \log C_{D_0}}{d \log M} \right] \tag{128}$$

$$\eta = \frac{2 \beta V_e}{\gamma p S}. \tag{129}$$

For the particular case of a zero-lift drag coefficient obeying Eq. (70), Eq. (128) becomes

$$\frac{\eta}{y} = M^x [1 + x + \gamma M^2]. \tag{130}$$

## 2. Relaxing of a Condition (Problem with Two Degrees of Freedom)

If the condition of constancy of the mass flow is eliminated, i.e., if Eq. (113) is replaced by $\Phi \equiv 0$, the problem of the optimum trajectory is transformed into one with two degrees of freedom. As a consequence, the system of EULER equations (115) to (120) is to be completed by the further equation:

$$\frac{d\beta}{d\alpha} \left( \lambda_5 - \lambda_3 \frac{V_e}{m} \right) = 0, \tag{131}$$

which defines the optimum mass flow. Once more the solution arc embodies sub-arcs $\beta = 0$, sub-arcs $\beta = \beta_{\max}$ and variable-thrust sub-arcs.

### *Problems Not Involving Both Horizontal Distance and Time*

The particular case where $G = G(h, V, m)$ is now considered, with the further assumption that no condition is imposed on the two coordinates $X$ and $t$ at one of the two end-points. As a consequence, the simultaneous conditions $\lambda_1 = 0$, $C = 0$ must be applied.

*Variable-Thrust Sub-Arcs.* For the variable-thrust sub-arc defined by $\lambda_5 - (\lambda_3 V_e/m) = 0$, the first integral (121) becomes

$$\lambda_2 V \sin\theta - \lambda_3 \left[\frac{D}{m} + g_0 \sin\theta\right] = 0. \tag{132}$$

Furthermore, Eq. (119) yields

$$\dot{\lambda}_3 V_e + \lambda_3 \frac{D}{m} = 0. \tag{133}$$

Notice that (for $\lambda_1 = 0$), Eqs. (117), (132) and (133) are linear and homogeneous in $\lambda_2$, $\lambda_3$ and $\dot{\lambda}_3$. Non trivial solutions for the multipliers and their derivatives exist if

$$\begin{vmatrix} m\sin\theta & -\dfrac{\partial D}{\partial V} & m \\ -mV\sin\theta\ D + mg_0\sin\theta & 0 \\ 0 & D & mV_e \end{vmatrix} = 0 \tag{134}$$

i.e., if

$$D(V - V_e) + V V_e \frac{\partial D}{\partial V} - m g_0 V_e \sin\theta = 0. \tag{135}$$

After accounting for the usual definition of drag Eq. (135) can be rewritten as

$$\varepsilon \sin\theta = C_{D_0} M^2 \left[1 + \frac{M}{M_e} + \frac{d\log C_{D_0}}{d\log M}\right]. \tag{136}$$

If the relationship between zero-lift drag coefficient and MACH number obeys Eq. (70), Eq. (136) yields

$$\frac{\varepsilon \sin\theta}{y} = M^x \left[\frac{M}{M_e} + x - 1\right]. \tag{137}$$

In conclusion, the present problem involves both a discontinuity in the path inclination and a discontinuity in the mass flow. With regard to the lift versus time history, the optimizing condition is expressed by either $\sin\theta = +1$ or $\sin\theta = -1$ or by Eq. (127); with regard to the engine mass flow, the optimizing condition is expressed by either $\beta = 0$ or $\beta = \beta_{\max}$ or by Eq. (135). The way in which the different branches of the solution must be combined in order to satisfy a set of prescribed end-conditions is not analyzed in the present report. The latter, in fact, is rather concerned with statements of a general nature than with the detailed discussion of special technical problems. The interested reader, however, may find considerable information on the solution of boundary value problems involving discontinuous solutions in previous papers by the author and his associates [1 to 4; 8 to 10].

## IX. Non-Lifting Paths

The category of trajectories flown with zero lift is now considered, in connection with the further assumption that the thrust is tangent to the flight path. The additional constraints are written as

$$\Phi \equiv L = 0 \tag{138}$$

$$\Psi \equiv \omega = 0. \tag{139}$$

Once more, the set of EULER equations (49) to (56) splits into two non-interacting sets. In fact, the multipliers $\lambda_6$ and $\lambda_7$ are only present in Eqs. (54) and (56).



Vol. 4 1958

The remaining EULER equations are formulated as follows

$$\dot{\lambda}_1 = 0 \tag{140}$$

$$\dot{\lambda}_2 = \frac{\lambda_3}{m}\frac{\partial D}{\partial h} \tag{141}$$

$$\dot{\lambda}_3 = -\lambda_1 \cos\theta - \lambda_2 \sin\theta + \frac{\lambda_3}{m}\frac{\partial D}{\partial V} - \lambda_4 \frac{g_0}{V^2}\cos\theta \tag{142}$$

$$\dot{\lambda}_4 = \lambda_1 V \sin\theta - \lambda_2 V \cos\theta + \lambda_3 g_0 \cos\theta - \lambda_4 \frac{g_0}{V}\sin\theta \tag{143}$$

$$\dot{\lambda}_5 = \frac{\lambda_3}{m^2}[V_e \beta - D] \tag{144}$$

$$0 = \frac{d\beta}{d\alpha}\left[\lambda_5 - \lambda_3 \frac{V_e}{m}\right]. \tag{145}$$

Implied in the above set is the below-indicated first integral

$$\lambda_1 V \cos\theta + \lambda_2 V \sin\theta + \lambda_3\left[\frac{V_e\beta - D}{m} - g_0 \sin\theta\right] - \lambda_4 \frac{g_0}{V}\cos\theta - \lambda_5 \beta = C. \tag{146}$$

Notice that, as Eq. (145) shows, the extremal arc embodies sub-arcs $\beta = 0$, sub-arcs $\beta = \beta_{\max}$ and variable-thrust sub-arcs, along which

$$\lambda_5 - \lambda_3 \frac{V_e}{m} = 0. \tag{147}$$

## Variable-Thrust Sub-Arcs

The sub-arcs flown with variable engine mass flow are now considered. By means of simple manipulations, the below indicated expressions are derived from Eqs. (141), (142), (144), (146) and (147)

$$\dot{\lambda}_3 = -\lambda_3 \frac{D}{m V_e} \tag{148}$$

$$\lambda_1 \cos\theta + \lambda_2 \sin\theta - \frac{\lambda_3}{m}\left(\frac{D}{V_e} + \frac{\partial D}{\partial V}\right) + \lambda_4 \frac{g_0}{V^2}\cos\theta = 0 \tag{149}$$

$$\lambda_1 V \cos\theta + \lambda_2 V \sin\theta - \lambda_3\left[\frac{D}{m} + g_0 \sin\theta\right] - \lambda_4 \frac{g_0}{V}\cos\theta = C \tag{150}$$

$$\dot{\lambda}_2 + \dot{\lambda}_3 V_e \frac{\partial \log D}{\partial h} = 0. \tag{151}$$

*Isothermal Atmosphere.* The particular case of an isothermal atmosphere is now considered, i.e., of an atmosphere where the speed of sound ($a$) is constant. The drag function is written as

$$D = \frac{\gamma}{2} p_0 S C_{D_0}(M) M^2 \exp\left(-\gamma \frac{g_0}{a^2} h\right) \tag{152}$$

where $S$ is a reference surface, $p_0$ the static pressure at $h = 0$ and $\gamma$ the ratio of specific heat at constant pressure to specific heat at constant volume. Notice that Eq. (151) becomes

$$\dot{\lambda}_2 - \dot{\lambda}_3 \gamma g_0 \frac{M_e}{a} = 0 \tag{153}$$

admitting, therefore, the following first integral

$$\lambda_2 - \lambda_3 \gamma g_0 \frac{M_e}{a} = C_5 \tag{154}$$

where $C_5$ is an integration constant. The above result holds for all problems of the form $G = G(X, h, V, \theta, m, t)$, regardless of the end-conditions[1].

Since the EULER equation (140) implies the other first integral

$$\lambda_1 = C_1. \tag{155}$$

Eqs. (149), (150), and (154) can be regarded as a non-homogeneous, linear algebraic system in the unknown multipliers $\lambda_2$, $\lambda_3$ and $\lambda_4$. In particular, the solution for the multiplier $\lambda_3$ is

$$\lambda_3 = \frac{A}{B} \tag{156}$$

$$A(V, \theta) = 2\, V\, [C_5 \sin\theta + C_1 \cos\theta] - C \tag{157}$$

$$B(V, h, \theta, m) = \frac{D}{m} + g_0 \sin\theta + \frac{V}{m}\left(\frac{D}{V_e} + \frac{\partial D}{\partial V}\right) - 2\,\gamma\, g_0\, M\, M_e \sin\theta. \tag{158}$$

Vol. 4 1958

*Optimum Acceleration.* From Eqs. (148) and (156) the optimum acceleration can be computed at points of the variable-thrust sub-arc. Rather lengthy manipulations yield the following result

$$\dot{V} = \frac{K_1 A + K_2 B}{K_3 A + K_4 B} \tag{159}$$

$$K_1 = -\frac{g_0}{V}\cos\theta \frac{\partial B}{\partial \theta} + V \sin\theta \frac{\partial B}{\partial h} - \frac{m}{V_e}\frac{\partial B}{\partial m}\left[\frac{D}{m} + g_0 \sin\theta\right] \tag{160}$$

$$K_2 = -\frac{A\, D}{m\, V_e} + \frac{\partial A}{\partial \theta}\frac{g_0}{V}\cos\theta \tag{161}$$

$$K_3 = \frac{\partial B}{\partial m}\frac{m}{V_e} - \frac{\partial B}{\partial V} \tag{162}$$

$$K_4 = \frac{\partial A}{\partial V} \tag{163}$$

which generalizes the one obtained in [11] to the case of problems where $\partial G/\partial t \neq 0$ and/or some time condition is prescribed at both end-points.

## X. Trajectories Flown in a Vacuum

The case of a path flown in an ideally vacuum environment is now considered. The drag function is $D = 0$ everywhere. Furthermore, the first additional constraint is written as

$$\Phi \equiv L = 0. \tag{164}$$

[1] An analogous first integral has been indicated in Eq. (29) of [11], limited to problems not involving time. The present first integral (154), on the other hand, has a more general character insofar as it also applies if $(\partial G/\partial t) \neq 0$ and if some time condition is prescribed at both end-points.

## Case where the Mass Flow is a Prescribed Function of the Time

The particular case where the additional constraint has the form

$$\Phi\,[\beta(\alpha), t] = 0 \tag{165}$$

is now considered. The EULER equation (55) becomes ineffectual, while the remaining EULER equations are written as

$$\dot{\lambda}_1 = 0 \tag{166}$$

$$\dot{\lambda}_2 = 0 \tag{167}$$

$$\dot{\lambda}_3 = -\lambda_1 \cos\theta - \lambda_2 \sin\theta + \frac{\lambda_4}{V^2}\left[-g_0 \cos\theta + \frac{V_e \beta \sin\omega}{m}\right] \tag{168}$$

$$\dot{\lambda}_4 = \lambda_1 V \sin\theta - \lambda_2 V \cos\theta + \lambda_3 g_0 \cos\theta - \lambda_4 \frac{g_0}{V} \sin\theta \tag{169}$$

$$\dot{\lambda}_5 = \frac{\lambda_3}{m^2} V_e \beta \cos\omega + \frac{\lambda_4}{m^2 V} V_e \beta \sin\omega \tag{170}$$

$$0 = \lambda_3 \frac{V_e \beta}{m} \sin\omega - \lambda_4 \frac{V_e \beta}{m V} \cos\omega. \tag{171}$$

It should be noticed that a mathematical consequence of Eqs. (168) and (169) is that

$$\frac{d}{dt}\left(\frac{\lambda_4}{V}\cos\theta + \lambda_3 \sin\theta\right) = -\lambda_2 \tag{172}$$

$$\frac{d}{dt}\left(\lambda_3 \cos\theta - \frac{\lambda_4}{V}\sin\theta\right) = -\lambda_1. \tag{173}$$

As a consequence the following first integrals can be written for the system of EULER equations

$$\lambda_1 = C_1 \tag{174}$$

$$\lambda_2 = C_6 \tag{175}$$

$$\frac{\lambda_4}{V}\cos\theta + \lambda_3 \sin\theta = -C_6 t + C_7 \tag{176}$$

$$\lambda_3 \cos\theta - \frac{\lambda_4}{V}\sin\theta = -C_1 t + C_8 \tag{177}$$

where $C_1$, $C_6$, $C_7$ and $C_8$ are integration constants. As a further step, Eq. (171) is solved for the inclination of the vector thrust with respect to the vector velocity

$$\tan\omega = \frac{\lambda_4}{\lambda_3 V}. \tag{178}$$

In turn, the inclination of the vector thrust with respect to the $X$-direction is given by

$$\tan(\theta + \omega) = \frac{\tan\theta + \tan\omega}{1 - \tan\theta \tan\omega} = \frac{\frac{\lambda_4}{V}\cos\theta + \lambda_3 \sin\theta}{\lambda_3 \cos\theta - \frac{\lambda_4}{V}\sin\theta}. \tag{179}$$

After accounting for Eqs. (172) and (173), Eq. (179) is rewritten as

$$\tan(\theta + \omega) = \frac{-C_6 t + C_7}{-C_1 t + C_8}. \tag{180}$$

It is, therefore, concluded that the absolute inclination in space of the vector thrust is a bilinear function of the time [12], a result which holds for all problems of the form $G = G(X, h, V, \theta, m, t)$ regardless of the end-conditions.

*a) Problems of the Form $G = G(X, h, m, t)$ where the Vector Velocity is Free at the Final Point*

If the values of $V_f$ and $\theta_f$ are free at final point and if $G = G(X, h, m, t)$, the transversality condition yields $\lambda_{3f} = 0$, $\lambda_{4f} = 0$. In turn, Eqs. (176) and (177) lead to $C_7 = C_6 t_f$, $C_8 = C_1 t_f$; so that Eq. (180) becomes

$$\tan(\theta + \omega) = \frac{C_6}{C_1} = \frac{C_7}{C_8}. \tag{181}$$

The optimum inclination in space of the vector thrust, therefore, is a constant for all problems of the form $G = G(X, h, m, t)$ such that no condition is imposed on the vector velocity at final point [13].

*b) Problems Not Involving Range*

Vol. 4 1958

If the $G$-function has the form $G(h, V, \theta, m, t)$ and if no condition is imposed on the $X$-variable at one of the two end-points, the transversality condition yields $C_1 = 0$. As a consequence, the inclination in space of the vector thrust becomes

$$\tan(\theta + \omega) = -\frac{C_6}{C_8} t + \frac{C_7}{C_8} \tag{182}$$

i.e., a linear function of the time [14].

## Conclusions

A basic theory is presented for analyzing the optimum flight paths of rocket-powered aircraft, missiles and satellites. A large segment of the existing body of knowledge is generalized.

The problem with three degrees of freedom is considered; it consists of the simultaneous optimization of the time history of lift, thrust modulus and thrust direction.

Special problems involving either one or two degrees of freedom are investigated, within the general frame of the present unified theory, by the introduction of additional constraining equations. Particular attention is devoted to special classes of trajectories, such as: vertical paths; horizontal paths; arbitrarily inclined rectilinear paths; trajectories flown with negligible induced drag; non-lifting paths; and vacuum flight trajectories.

For several of the above particular cases closed form expressions are derived for the optimizing conditions. Furthermore, a complete formulation of the boundary conditions is supplied by means of the general transversality condition of the Calculus of Variations.

## Remarks

The present article is a condensed version of the investigation described in [15] to which the interested reader is referred for more detailed information. In particular, [15] contains the following topics omitted here: (1) a discussion of the flight paths of interceptor missiles subject to a prescribed guidance law; (2) an analysis of the optimizing condition for high speed gliders.

It should be emphasized that, while the general equations of Sections I to III refer to a curved Earth, all successive developments of Sections IV to X have been carried out under the hypothesis of a Flat Earth. In more recent work, however, some closed form solutions have been obtained for motion over a curved Earth. These solutions will be presented in a forthcoming paper by the author and his associates.

## References


1. A. MIELE, An Extension of the Theory of the Optimum Burning Program for the Level Flight of a Rocket-Powered Aircraft. J. Aeronaut. Sci. **24**, 874 (1957). (AFOSR-TN-56-302, June, 1956.)
2. A. MIELE, Generalized Variational Approach to the Optimum Thrust Programming for the Vertical Flight of a Rocket, Part I, Necessary Conditions for the Extremum. Z. Flugwiss. **6**, 69 (1958). (AFOSR-TN-57-173, March, 1957.)
3. A. MIELE and C. R. CAVOTI, Generalized Variational Approach to the Optimum Thrust Programming for the Vertical Flight of a Rocket, Part II, Application of GREEN's Theorem to the Development of Sufficiency Proofs for Particular Classes of Solutions. Z. Flugwiss. **6**, 102 (1958). (AFOSR-TN-57-652, August, 1957.)
4. A. MIELE and C. R. CAVOTI, Optimum Thrust Programming along Arbitrarily Inclined Rectilinear Paths. Astronaut. Acta **4**, 167 (1958). (AFOSR-TN-58-48, December, 1957.)
5. J. V. BREAKWELL, The Optimization of Trajectories. North Amer. Aviat. Inc., Report No. AL-2706, August, 1957.
6. A. MIELE, On the Brachistocronic Thrust Program for a Rocket-Powered Missile Travelling in an Isothermal Medium. Jet Propulsion (in publication).
7. G. LEITMANN, Stationary Trajectories for a High-Altitude Rocket with Drop-Away Booster. Astronaut. Acta **2**, 119 (1956).
8. P. CICALA and A. MIELE, Generalized Theory of the Optimum Thrust Programming for the Level Flight of a Rocket-Powered Aircraft. Jet Propulsion **26**, 443 (1956).
9. A. MIELE, Optimum Climbing Technique for a Rocket-Powered Aircraft. Jet Propulsion **25**, 385 (1955).
10. A. MIELE and J. O. CAPPELLARI, Approximate Solutions to the Optimum Climbing Trajectory for a Rocket-Powered Aircraft. Purdue University, School of Aeronautical Engineering, Report No. A-57-4, July, 1957.
11. A. E. BRYSON and S. E. ROSS, Optimum Rocket Trajectories with Aerodynamic Drag. Jet Propulsion **28**, 465 (1958).
12. D. F. LAWDEN, Optimal Rocket Trajectories. Jet Propulsion **27**, 1263 (1957).
13. B. D. FRIED and J. M. RICHARDSON, Optimum Rocket Trajectories. J. Appl. Physics **27**, 955 (1956).
14. D. B. FRIED, On the Powered Flight Trajectory of an Earth Satellite. Jet Propulsion **27**, 641 (1957).
15. A. MIELE, General Variational Theory of the Flight Paths of Rocket-Powered Aircraft, Missiles and Satellite Carriers. Purdue University, School of Aeronautical Engineering, Report No. A-58-2, January, 1958. (AFOSR-TN-58-246).
16. P. CICALA, Soluzioni discontinue nei problemi di volo ottimo. Atti Accad. Sci. Torino **90** (1955–1956).
17. A. MIELE, Minimality for Arbitrarily Inclined Rocket Trajectories. Jet Propulsion **28**, 481 (1958).

Vol.
4
1958

## Buchbesprechungen — Book Reviews — Comptes rendus

**Morphological Astronomy.** Von F. ZWICKY. Mit 55 Textabb., IV, 299 S. Berlin-Göttingen-Heidelberg: Springer-Verlag. 1957. Geb. DM 49.60.

Schon fast zehn Jahre vor Erscheinen dieses Buches hat der Verfasser, ein in Pasadena lebender sehr bekannter Astronom und Astrophysiker und Fellow Member der American Rocket Society, in seiner Halley Lecture am 12. Mai 1948 in Oxford zu zeigen versucht, welchen Beitrag eine morphologische Astronomie im Rahmen der gesamten morphologischen Forschungsmethode leisten kann. Er ordnete seine Betrachtungen damals unter die folgenden Gesichtspunkte: Beobachtung der Erscheinungen des Himmels, Experimente mit den Erscheinungen des Himmels, theoretische Ergänzungen, Anwendung der gewonnenen Erkenntnisse für konstruktive Zwecke, Verbreitung der gewonnenen Erkenntnisse und ihrer Beziehungen auf alle Gebiete menschlicher Tätigkeit.

Nach vielerlei Hemmungen und Verzögerungen sind die damaligen Ansätze nun zu einem einzigartigen Buch ausgereift. Es ist erstaunlich, was der Verfasser an neuen Erkenntnissen und Übersichten, die natürlich zum großen Teil auf den Beobachtungen der großen amerikanischen Spiegelteleskope beruhen, zusammenzustellen vermag. In einzelnen Punkten mag er hier und da von astronomischer Seite wohl kritisiert werden. Doch unzweifelhaft gelingt ihm der Nachweis, daß die morphologische Methode auch in der Astronomie nützlich ist. Die Probleme der modernen Astronomie gewinnen in dieser kritischen Beleuchtung oftmals ganz neue Perspektiven. Hierin und in der sicher dadurch ausgelösten Diskussion liegt der große Wert dieses ungewöhnlich geistreichen und gehaltvollen Buches.

Wie weit der Verfasser den Rahmen zu spannen vermag, das lassen schon die Überschriften der einzelnen Kapitel erkennen, die bereits einen tiefen Einblick in die Eigenart des Werkes zu geben vermögen:

I. Morphologische Forschung und Erfindung.
II. Wolken und Haufen von Milchstraßen.
III. Die Verteilung der Milchstraßen und Milchstraßenhaufen im Großen.
IV. Kinematische und dynamische Merkmale der großräumigen Anhäufungen der Materie.
V. Dimensionale und dimensionslose Morphologie in der Kosmologie.
VI. Morphologische Hauptzüge der einzelnen Milchstraßen.
VII. Morphologisch-astronomisches Kaleidoskop.
VIII. Die morphologische Methode und eine a priori-Erkenntnis; die magischen Zahlen.

Der Astronom und Astrophysiker wird manchen Abschnitt mit Genuß lesen, auch wenn er dabei ihm vielleicht mehr oder weniger bekannte Dinge findet, die er aber in einer ganz anderen Art betrachten wird. Auch der Astronautiker wird vielerlei Anregung erfahren und Gelegenheit haben, seine Verbindung zu einer der Grundwissenschaften der Astronautik zu vertiefen.

Das Buch regt jedenfalls stark zum Nachdenken an; und wenn der Verfasser in der Einleitung noch zwei oder drei weitere Bücher zum selben Thema in Aussicht stellt, so kann man ihnen nur mit großer Spannung entgegensehen.

K. SCHÜTTE, München

**Zur Strahlungsphysik der Photonen-Strahlantriebe und Waffenstrahlen.** Von E. SÄNGER. (Mitteilungen aus dem Forschungsinstitut für Physik der Strahlantriebe e.V. Stuttgart: Heft 10.) Mit 74 Textabb., 173 S. München: R. Oldenbourg. 1957. DM 52.—.

Es ist kaum möglich, von einer Originalarbeit wie der vorliegenden in einem kurzen Bericht das Wesentliche hervorzuheben. Selbstverständlich darf der Leser nicht erwarten, daß schon jetzt ein Entwurf eines Photonentriebwerkes möglich ist oder ein Photonenstrahl von genügender Stärke technisch erzeugt werden kann, um damit anfliegende Raketengeschosse zu bekämpfen. Trotzdem ist es reizvoll, wenn jemand den Mut hat, über diese zukünftigen Möglichkeiten nachzudenken und die dafür erforderlichen wissenschaftlichen Grundlagen zu sammeln. Dabei kommt man sofort zu grundlegenden Fragen von Raum, Zeit und Materie, die von ungeheurer Bedeutung sind.

Das Hauptthema dieses Buches ist die allgemeine Feldtheorie der theoretischen Physik. Nach dieser quantenmechanischen Feldtheorie werden die anziehenden und abstoßenden Feldkräfte durch Austausch von Feldquanten (Photonen, Gravitonen usw.) erklärt. Beim Aussenden eines Feldquants übt dieses eine Rückwirkung (Impuls) auf das emittierende Massenteilchen aus, und ebenso erfährt das absorbierende Massenteilchen einen Stoß. In dieser Weise kann eine abstoßende Fernkraft unmittelbar verständlich gemacht werden. Für die Erklärung anziehender Feldkräfte ist man gezwungen, Feldquanten negativer Masse (negativer Energie) anzunehmen, deren Vierervektor (MINKOWSKI-Geschwindigkeit) längs der Weltlinie des Quants in die Richtung der Vergangenheit weist. Weiter muß man nach dieser quantenmechanischen Auffassung auch bei statischen Feldern einen fortwährenden Austausch von Feldquanten zwischen den betreffenden Massen annehmen. Das Wesentliche dieser quantenmechanischen Vorstellung ist meines Erachtens darin zu erblicken, daß die eigentlichen Bausteine der Raum-Zeit-Welt durch diese Austauschprozesse dargestellt werden. (Bekanntlich kann dem Begriff „Materieller Körper" in der absoluten Raum-Zeit-Welt keine tiefere Bedeutung zukommen, da die Punktereignisse, die für einen bestimmten Beobachter „einen Gegenstand in einem bestimmten Augenblick" bilden, für einen anderen Beobachter, der sich in Beziehung auf den ersten bewegt, *nicht* gleichzeitig sind.)

Für die lichtschnellen Feldquanten selbst (das heißt in ihrer Eigenzeit) fallen Emission und Absorption zusammen. Vom absoluten Standpunkt haben wir also beim Austausch des Quants in der Emission und Absorption *dasselbe Ereignis* zu erblicken. Die lichtschnellen Feldquanten sind daher das universale Bindeglied alles Geschehens und zugleich die eigentlichen Elemente des universalen Geschehens, das in jedem Hier-Jetzt, also überall in der Raum-Zeit-Welt, hervorgeht, das sozusagen zugleich raumzeitlich ausgedehnt und auch wieder nicht raumhaft und nicht zeithaft ist.

Obige Betrachtung möge genügen, um zu zeigen, wie anregend das vorliegende Buch ist. Man soll es lesen und durchdenken! J. M. J. KOOY, Breda

Herausgeber, Eigentümer und Verleger: Springer-Verlag, Wien I, Mölkerbastei 5. — Für den Inhalt verantwortlich: Prof. Dr. Friedrich Hecht, Wien VIII, Alserstraße 69. — Druck: Berger & Schwarz, Zwettl, NÖ.

Vol.
4
1958

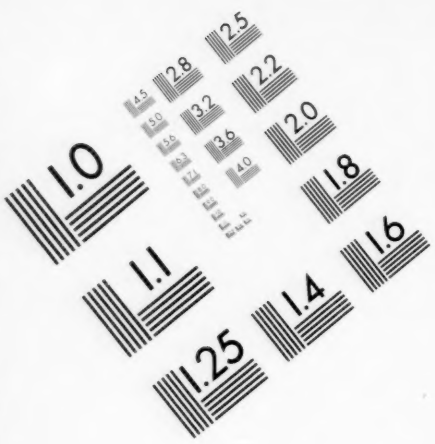


NATIONAL MICROGRAPHICS ASSOCIATION

MS303-1980

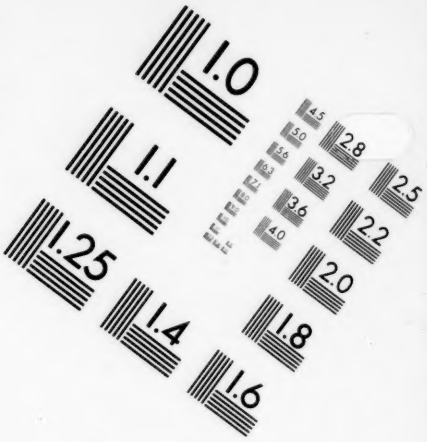

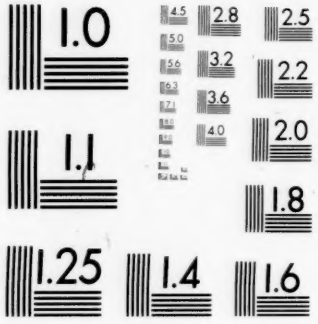


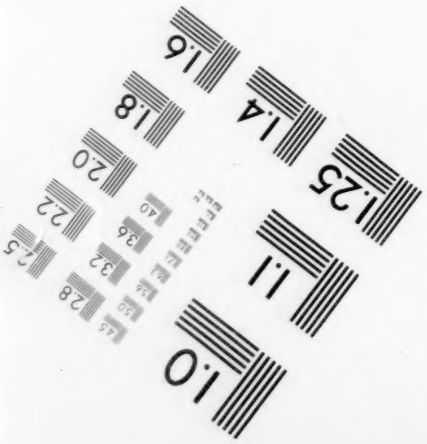


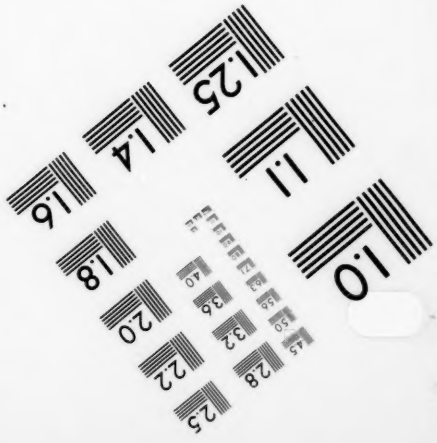

# PERGAMON PRESS INC.

MICROFORMS INTERNATIONAL
MARKETING CORPORATION
FAIRVIEW PARK, ELMSFORD, NEW YORK 10523

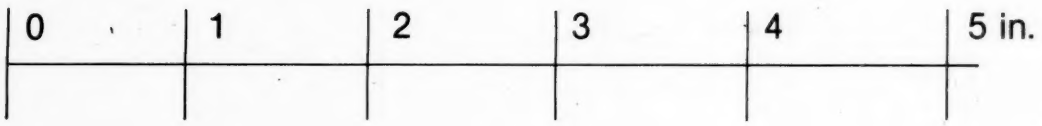


**PRODUCED AT**

**MIMC MICROFORMS LABORATORY
ELMSFORD, NEW YORK**